Nonlinear Truss Analysis of Non-ductile Reinforced Concrete Frames with Unreinforced Masonry Infills

Daniel Ricardo Salinas Guayacundo

Dissertation submitted to the faculty of the
Virginia Polytechnic Institute and State University
in partial fulfillment of the requirements for the degree of

Doctor of Philosophy
In
Civil Engineering

Roberto T. Leon, Co-chair
Ioannis Koutromanos, Co-chair
Finley A. Charney
Matthew R. Eatherton

March 18, 2016
Blacksburg, VA

Keywords: Masonry Infills, Nonlinear Reinforced Concrete Frames, Nonlinear Finite Element Analysis, Truss Analysis.

Nonlinear Truss Analysis of Non-ductile Reinforced Concrete Frames with Unreinforced Masonry Infills

Daniel Ricardo Salinas Guayacundo

Abstract

Non-ductile Reinforced Concrete Frames (RCF) with and without Unreinforced Masonry (URM) infills can be found in many places around the world including the Western United States, Eastern Europe, Asia and Latin America. These structures can have an unsatisfactory seismic performance which may even lead to collapse due to brittle failure modes. Furthermore, the effect of the infills on the seismic response of the structural system is not always accounted for in analysis and design. At present, there is no consensus on whether masonry infills are beneficial (by increasing the resistance of the system) or detrimental (by leading to brittle failure modes) for RCF construction.

This study focuses on the development of a simplified modeling approach for non-ductile RCF with URMI that combines the simplicity of strut-and-tie models with the accuracy of Nonlinear Finite Element Analysis (NLFEA). Despite the fact that NLFEA procedures are the most advanced way to address the structural analysis of RCF with URM infills, their conceptual complexity and computational cost may hinder their widespread adoption as an analysis and design tool. At the same time, simplified methods, such as those based on the equivalent strut concept, may be overly crude and neglect essential aspects of the nonlinear response. To address the need for an adequately accurate, but computationally and conceptually efficient analysis method, this study establishes a novel method for planar RCF with URM infills subjected to lateral loads. The method, which is

based on the Nonlinear Truss Analogy (NLTA) is shown to have an accuracy comparable to that of NLFEA. Specifically, the method is shown to adequately capture the strength and stiffness degradation and the damage patterns while entailing a reduced computational cost (compared to that of NLFEA). The proposed method is expected to bridge the gap between overly crude equivalent strut models and computationally expensive NLFEA.

Acknowledgements

I would like to thank God for giving me the opportunity to become a Hokie. He blessed me with the strength, endurance to go through all difficulties and the passion to achieve this work. In addition, I would especially like to express my sincere gratitude to Dr. Roberto Leon for his encouragement, support, and patience during all these years. Working under his supervision was always an inspiration and honor. I would also like to express my gratitude to Dr. Ioannis Koutromanos who served as co-chair. He is an impressive researcher and professor. I am grateful for all his guidance, expertise, and encouragement.

I am also indebted to my committee, Dr. Finley Charney and Dr. Matthew Eatherton for their constructive comments, suggestions and support throughout this process. I'll always remembered Dr. Finley Charney's approach for solving challenging problems. I am sure my notes from his classes will be valuable for years to come.

I'd like to thank to my first mentor here at VT, Dr. Thomas M. Murray, for his guidance and friendship. I am deeply indebted to him for the rest of my life for bringing me at VT. I'd like to express my appreciation to my first temporal advisor Dr. Eatherton.

In addition, I'd like to express my appreciation to my professors Dr. Wollmann, Dr. Wright, Dr. Moen, Dr. Rojani, Dr Easterling, Dr. Cousins, Dr. Rodriguez-Marek, Dr. Green, Dr. Leon, Dr. Koutromanos, Dr. Charney and Dr. Eatherton.

I am also appreciative of my colleagues Francisco Flores, Johnn Judd, Armen Adekristi, Jeena Jayamon, Miguel Robles, Abraham Lama, Luis de Leon, Mohammadreza Moharrami, Adrian Tola, and Edgardo Marmolejo, my first structural analysis and programming tutor.

I would also like to thank Drs. Maziar Partovi, Kesio Palacio and Hee-Jeong Kang from TNO DIANA for their valuable feedback on my NLFEA models. Also I would like to thank you Dr. Keneth Elwood research team at UBC, especially to Dr. Majid Baradaran Shoraka, who graciously shared his enhanced model of the limit state material. In addition, thank you to Dr. Luis Garcia, Dr. Mete Sozen and Dr. Santiago Pujol for sharing their comments and information through personal communications.

I would also like to acknowledge Colfuturo (2011-2 – 2012-2) and Colciencias (2013-1 – 2015-2) for their scholarship-loan program for funding my education.

This would not be possible without the support of my family, for which I am forever appreciative, especially to my Mother Ana Elvira, my siblings Claudia Patricia and William Alberto, and mi niece Andrea Carolina. Thank you for your unconditional support, patience understanding and love.

Table of Contents

List of Figures

List of Tables

1. Introduction

1.1. Definition of the Problem

Reinforced concrete frames constitute a significant portion of the building inventory in earthquake-prone areas of the United States, Eastern Europe, Asia and Latin America. Many older buildings of this type were not detailed to ensure the ductility required to perform satisfactorily during extreme seismic events. The vulnerability of such structures, hereinafter termed non-ductile frames, to complete collapse and associated human and economic losses may have serious implications for the resilience of built communities. Many earthquakes have exposed the imminent risk associated with non-ductile frames, mostly in developing countries including those in Algeria 1980; Mexico 1985; Ecuador 1987; Colombia 1999; Taiwan 1999; Turkey 1999; Iran 2003; Sumatra 2005; Pakistan 2005; China 2008; and Haiti 2010. The combination of non-ductile concrete frames with brittle masonry infills has been found to be particularly vulnerable, and it is this latter type of structure that will be addressed in this work.

In **Figure 1-1**, the cumulative global earthquake fatalities from 1900 to 1968 for earthquakes with 1000 or more deaths and from 1968–2011 for earthquakes with one or more deaths is presented. It can be appreciated that there is a direct correlation between the number of fatalities and the increase in world population. Furthermore, it is apparent that advances in earthquake engineering procedures, standards, and methods, introduced after the late 1960's, are not appreciably reducing the slope in the cumulative fatality curves. This is due to the fact that growing

urbanization in the third world continues to produce structures designed and built without following any seismic standard.

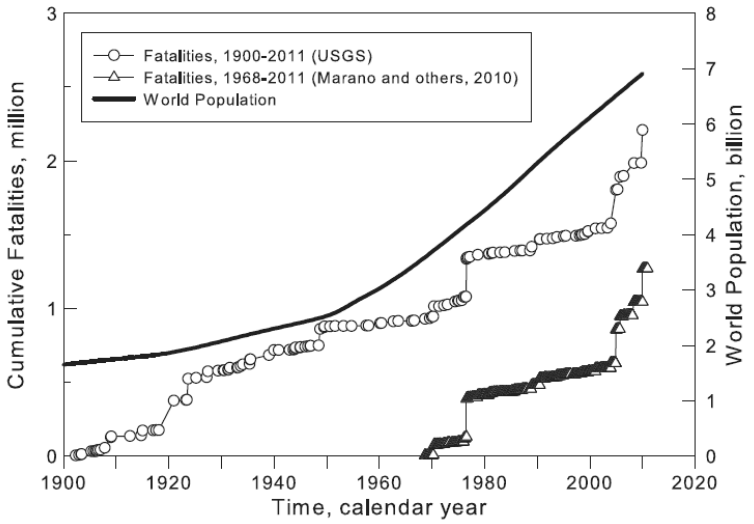

Figure 1-1 Cumulative global earthquake fatalities from 1900 to 2011 for earthquakes with 1000 or more deaths and from 1968–2011 for earthquakes with one or more deaths. Holzer and Savage (2013).

The above facts indicate the need for the systematic, quantitative characterization of the performance and vulnerability of non-ductile reinforced concrete frames. A significant number of previous research efforts have relied on experimental tests to elucidate the hysteretic behavior and failure modes of such structures. While experimental research is always indispensable to provide real-life observations of the physical behavior, the size of the specimens and the range of possible configurations that can be tested are inherently limited by constraints associated with the capabilities of testing equipment and economics. Therefore, computational simulation is deemed necessary to allow systematic parametric studies which can focus on entire structural systems and also examine a sufficient range of possible configurations. Several studies have formulated and

implemented simulation tools which can be applied to the nonlinear response of RCF with URM infills.

This thesis addresses the development of a simplified modeling approach for non-ductile RCF with URMI that combines the simplicity of strut-and-tie models with the accuracy of Nonlinear Finite Element Analysis (NLFEA). In this study, NLFEA techniques are used to evaluate the strength, ductility and damage patterns of infilled frames. The proposed approach, which is based on the Nonlinear Truss Analogy (NLTA) is shown to have an accuracy comparable to that of NLFEA. Specifically, the method is shown to adequately capture the strength and stiffness degradation and the damage patterns while entailing a reduced computational cost (compared to that of NLFEA). The proposed method is expected to bridge the gap between overly crude equivalent strut models and computationally expensive NLFEA.

In this study, special characteristics of the Colombian construction are taken as a case study for two reasons: (1) this country is exposed to a high number of earthquakes and has a large inventory of vulnerable RCF structures; and (2) the Colombian government has granted two scholarship-loans to the author [Colfuturo (2011-2 – 2012-2) and Colciencias (2013-1 – 2015-2)] to support this work. In order to provide an adequate background about Colombia's seismicity, design standards and construction practices, Appendix A is included in this document. Post-earthquake studies have exposed the vulnerability of Colombia's infrastructure. Throughout the years, many studies have been developed in Colombia with the idea of estimating the losses that a seismic event could produce DEPAE. and JICA (2002), Cardona and Yamin (1997), AIS (2009.). Their convergent conclusions point to a high risk for its infrastructure. For instance, The Japan International Cooperation Agency in 2002 DEPAE. and JICA (2002) describes the scenario of a 7.5 magnitude earthquake with an epicenter near Bogota. The result is that Bogota would suffer a

15% loss of the city value. As a reference, the well-known Mexican earthquake of 1985 produced about a 5% loss of the total value of Mexico City. The study was developed for Bogota, mostly characterized by having better procedural controls, materials, and skilled labor than the rest of the country. It can be inferred that other cities in Colombia would have higher negative results in terms of human and economic losses due to poorer construction practices.

Despite the fact that in the past few years some important buildings have been retrofitted, a gross percentage of Colombian buildings still remain without any structural intervention mainly for lack of economic resources and encouragement from government policies. Retrofitting an existing building can be as expensive as building a new building. Most importantly, the above facts indicate the need for a conceptual tool that allows to estimate the performance and vulnerability of RCF with URM infills.

Finally, the reality reflects that thousands of Colombian buildings would collapse under a moderate or higher earthquake. Many buildings have already validated this conclusion in the past (see Appendix A), and there are studies that show the current elevated risk. The above facts indicate the need for a systematic and quantitative way to evaluate the performance and vulnerability of non-ductile frames. It is imperative that the structural analysis model incorporates the sources of nonlinear behavior, in order for the physical model to be adequately described by its analytical counterpart. In this sense, the proposed method is expected to efficiently contribute in the determination of the performance and vulnerability evaluation of RCF with URM infills.

1.2. Motivation and Objectives

The analysis of RCF is challenging because the seismic response is likely to be highly non-linear due to factors such as rebar buckling, concrete cracking, and concrete crushing. The problem gains complexity once the presence of the infill is considered, especially when rigorously considering both the frame infill interaction and the infill modes of failure. Based on the previous information, the methodology proposed for the present work includes:

a) Conducting a survey of key vulnerabilities of RCF structures in Colombia, by examining existing building codes, construction practices and available building data.
b) Carrying out a state-of-the-art review of available analytical models to account for the key vulnerabilities that need to be addressed in assessing RCF construction in Colombia.
c) Surveying methods for accounting the presence of the URM infills, including NLFEA procedures.
d) Developing a novel, practical-oriented methodology that deals with the presence of the infills which (i) overcomes the limitations of the simplified URM infill representation and (ii) have comparable benefits to the results from more non-linear refined FEA.

The main objective of this research is to propose a novel approach which adequately captures the monotonic 2D nonlinear behavior of RCF with URM infills that incorporates: (i) axial-flexure-shear interaction (ii) different failure modes of the URM infills and its effects on the RCF, and (iii) axial load redistribution as the damage evolves. Despite that Colombia's non-ductile RCF are taken as the case study here, the proposed approach is applicable to any RCF worldwide because it relies on material-level calibration. This research will include the following tasks:

- Identify, characterize and model some of the key vulnerabilities presented in the Colombian non-ductile construction.
- Construct NLFEA models of RCF with URM infills and validate their effectiveness by comparing with test results.
- Propose a novel approach for RCF with URM infills that adequately captures the strength and stiffness degradation and the damage patterns at a reduced computational cost when compared to that of NLFEA.
- Validate the effectiveness of the proposed approach by comparing its results with NLFEA simulations and experimental test results.

Three-dimensional models and torsional effects are considered beyond the scope of this proposal.

1.3. Contribution to the Knowledge Base

At the present time, a significant number of structures exist worldwide that were designed and constructed with little or no consideration of lateral load. Colombia, as a case study, reflects this reality. The contribution of the present work is to propose an analytical, practical-oriented approach that elucidates the structural response of the RCF with URM. Its goals are twofold: (a) to provide a rational way to assess the nonlinear behavior of RCF structures through nonlinear pushover analysis models, and (b) to close the gap between simplified and refined NLFEA models that deals with the response of RCF with URM infills. The work is intended to be used not only as a performance assessment tool for existing older or new construction but it can also easily modified

to evaluate the cost-effective of some retrofit schemes such as composite overlays mortars or fiber-based retrofits.

1.4. Organization

This dissertation is organized as follows. Chapter 2 describes important aspects related to vulnerabilities and special characteristics of RCF in Colombia. Chapter 3 introduces the NLFEA procedures applied to RCF with URM infills. In Chapter 4 a novel method based on the Nonlinear Truss Analogy (NLTA) applied to RCF with URM infills is introduced. In Chapter 5 a parametric study of diverse parameters affecting the lateral response of the RCF with URM infills is presented. In Chapter 6, a monotonic nonlinear 2D Nonlinear Truss Analysis of a prototype building in Colombia is presented. In Chapter 7 conclusions and future research needs are presented. Appendix A includes background about Colombia's seismicity, design standards and construction practices. Appendix B introduces practical-oriented approaches to address some of these key vulnerabilities in modeling non-ductile RCF. Appendix C describes the typical masonry properties for Colombia. Appendix D describes the implementation of the proposed methodology in OpenSEES, in a step-by-step-basis. Finally, Appendix E includes the OpenSEES script for one of the specimens analyzed in Chapter 4.

2. Trends and Challenges in Nonlinear Analysis in Non-ductile RCF

As a first step in this study, a comprehensive review of the literature related with some of the most relevant aspects associated with RCF in Colombia is conducted. As consequence, Chapter 2 is divided in two parts. The first part looks at bare frames while the second part incorporates the presence of the URM infills. Subsequently, and based on the previous evidence from post-earthquake studies in Colombia presented in Appendix A, some of these aspects are studied in more detail in order to investigate their current state of the art.

2.1. Key Vulnerabilities Presented in RCF

A very complete list of critical deficiencies contributing to the collapse vulnerability of concrete buildings is found in the document NIST GCR 10-917-7 (2010). The order of deficiencies presented in the document, and presented here in **Figure 2-1**, is not associated with a level of importance or frequency. Note that deficiencies (A) shear-critical columns, (B) unconfined beam-column joints, (C) slab-column connections, (D) splice and connectivity weakness are component or local deficiencies. These can limit the ability of a structure to resist seismic loading without necessarily causing collapse. Deficiencies such as (E) weak-story mechanism, (F) overall weak frames, (G) overturning mechanisms, (H) severe plan irregularity, (I) severe vertical irregularity and (J) pounding, are system-level deficiencies that, alone or in combination with component deficiencies, can elevate the potential for collapse of a structure during strong ground shaking. In fact, the concepts presented in this list are applicable to any RCF system constructed worldwide.

Non-ductile RCF contain one or more of these deficiencies, with each additional deficiency potentially decreasing the structural performance during an earthquake or leading to the structural collapse. This NIST report emphasizes that the main challenge is to be able to identify when these structural deficiencies can lead to building collapse and when they will not.

Because not all old structures can be considered as non-ductile based on the low percentage of collapses reported after some earthquake reconnaissance (Otani (1999)), special attention is required to find the "true" non-ductile buildings that will perform poorly under seismic excitations.

The two most common element deficiencies that can lead to a collapse of a non-ductile RCF are shear-critical columns (Deficiency A), and unconfined beam–column joints (Deficiency B). Based on the fact that a gross percentage of the non-ductile RCF constructed in Colombia were constructed without following any standard and detailing rules, those structures are more likely to present these key vulnerabilities. The following sections discuss in more detail the problems with modeling unreinforced joints and column failures.

Deficiency A: Shear-critical columns	**Deficiency B: Unconfined beam-column joints**
 Shear and axial failure of columns in a moment frame or gravity frame system.	 Shear and axial failure of unconfined beam-column joints, particularly corner joints.
Deficiency C: Slab-column connections	**Deficiency D: Splice and connectivity weakness**
 Punching of slab-column connections under imposed lateral drifts.	 Inadequate splices in plastic hinge regions and weak connectivity between members.
Deficiency E: Weak-story mechanism	**Deficiency F: Overall weak frames**
 Weak-column, strong-beam moment frame or similar system prone to story collapse from failure of weak columns subjected to large lateral deformation demands.	 Overall deficient system strength and stiffness, leading to inadequacy of an otherwise reasonbably configured building.
Deficiency G: Overturning mechanism	**Deficiency H: Severe plan irregularity**
 Columns prone to crushing from overturning of discontinuous concrete or masonry infill wall.	 Conditions (including some corner buildings) leading to large torsional-induced demands.
Deficiency I: Severe vertical irregularity	**Deficiency J: Pounding**
 Setbacks causing concentration of damage and collapse where stiffness and strength changes. Can also be caused by change in material or seismic-force-resisting-system.	 Collapse caused by pounding of adjacent buildings with different story heights and non-coincident floors.

Figure 2-1 Component and system-level seismic deficiencies found in pre-1980 concrete buildings adapted from NIST GCR 10-917-7 (2010).

2.1.1. Unreinforced Beam-Column Joint Models

For many years, the importance of beam column joints (BCJ) was overlooked. This was true because there was little evidence of major damage or collapse that could be attributed to the failure of BCJ. Poor detailing of the columns and beams held the attention of the researchers and the media based on post-earthquake damage surveys. When subjected to large ground motions, many RCF buildings have shown soft story mechanisms from lack of rotational capacity associated with improper detailing of plastic hinges in both columns and beams. After learning from these previous experiences, requirements to produce much better curvature ductility in the beam and column elements were developed and implemented into codes (i.e., Chapter 19 of ACI 318-89). At this stage BCJ became the weak links in the structural system, and their importance was recognized by documents such as ACI-352 (1991).

Figure 2-2 (a) and (b) present a typical idealization for the RCF and BCJ respectively. As can be seen in **Figure 2-2** (b), the response of the joint region will be governed by shear forces, which are transmitted by bearing, bond, and friction. Shear cracking, when not properly controlled, induces brittle failures, as shear failure is related to diagonal tensile behavior in concrete. Today it is understood that beam column joints are key elements in the seismic performance and integrity of RC frames.

When a RCF experiences earthquake force, the joint region is subjected to large additive moments at opposite ends of the columns and beams. As a consequence, the joint region is subjected to vertical and horizontal shears that are typically much larger than those used to size the elements that frame into the joint as shown in **Figure 2-2** (b). The reversal in moments in the joint also means that the beam reinforcement is required to be in compression on one side

and in in tension on the other side. For that reason, high bond stresses are required to sustain this steep gradient bond along the joint and bond failure may occur with corresponding degradation of moment capacity and stiffness that will lead to excessive lateral drifts.

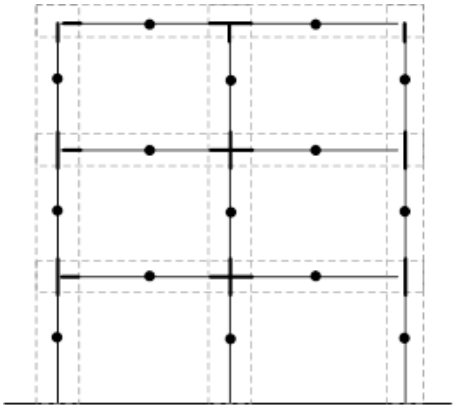

a) Model idealization

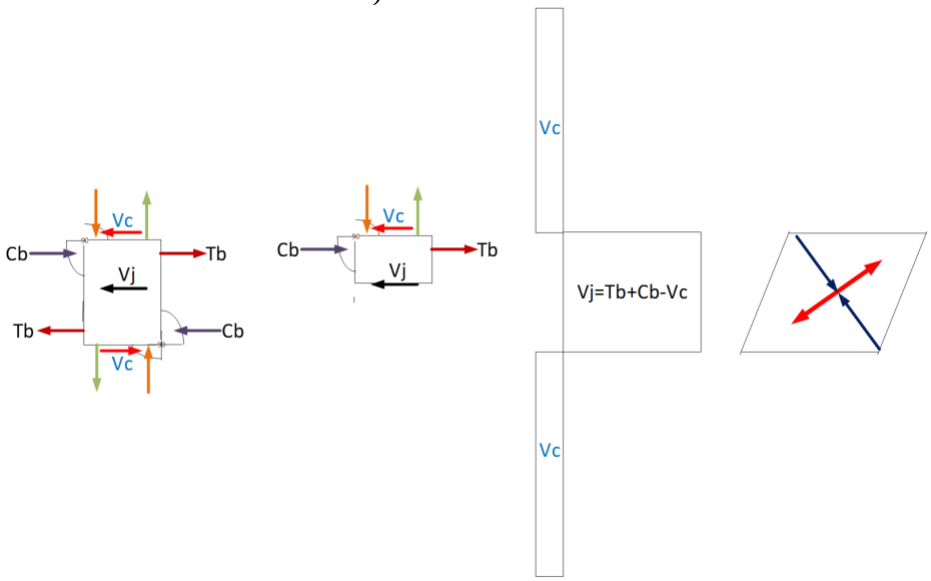

b) Internal forces at BCJ, shear demand, and deformed shape

Figure 2-2 BCJ idealization.

If internal joints are assumed to be rigid in the analyses, the discrepancies from true behavior are mainly that the structure will have a shorter period of vibration. This implies that since the internal joints will actually be more flexible the true displacements will be underestimated. In some cases, for larger drift demands the structure will lose its lateral deformation capacity as a preamble to loss of axial load-carrying capacity.

In **Figure 2-3** some examples of failures of exterior RCBCJ are presented. Some of them are partial collapses **Figure 2-3** (b) and **Figure 2-3** (c) and in some cases, **Figure 2-3**(a), it can be inferred that the BCJ failure triggered the collapse of this structure. The common denominator on these failures is that no plastic hinges formed in the columns or beams. This is not an indication that these elements had an appropriate overcapacity and ductility, as the joint failure precluded their reaching large inelastic deformations. The failure was due to the limited capacity of the joint to transmit the forces and to keep its integrity.

a) Structure collapse Kaiser Permanente Building, Northridge earthquake. (photo credit, G. Edstrom)

b) Partial Building Collapse due to failure of beam-column joints in the Izmit, Turkey earthquake. (photo credit, NISEE)

c) Collapsed building following Izmit, Turkey earthquake. Hassan (2011)

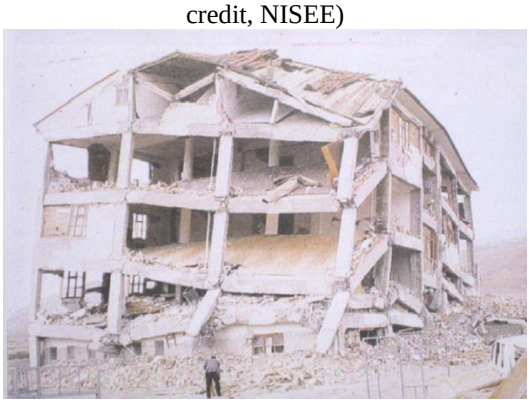

d) Joint failure and partial building collapse Erzincan, Turkey earthquake. Hassan (2011)

Figure 2-3 Photos of failures of BCJ from Hassan (2011).

2.1.1.1. State of the Art Review

Through the years, many researchers have proposed models to represent the nonlinear behavior of BCJ. The early attempts relied on: (i) the lumped plasticity concept applied generally at the end of one elastic element, or/and (ii) the "two component model" concept proposed by Clough et al. (1965) to idealized a steel frame as combination an elasto-plastic element representing the yielding behavior and one elastic element to represent strain hardening behavior. These types of models are referred herein as implicit models because they do not define the joint region physically, and therefore they fail to represent the joint kinematics. Some examples are depicted in **Figure 2-4.** On the other hand, some of the newest approaches are based on the definition of the physical panel zone by using a macro-element and centerline analysis. The macro-element is composed of certain numbered joints, elements and springs that are assembled to represent the nonlinear behavior in the joint through the interrelation of their elements, constitutive relationships and boundary constraints. Concepts of lumped plasticity or distributed plasticity can be used. These type of models are referred here as explicit models. The difference between implicit and explicit models is in the modeling and computational effort required, and, in some cases, on the practicality of such models for everyday design. A general classification of the beam column joint models will be proposed in the following section.

Implicit Models

For about 50 years, extensive research has been done with the intent to model the hysteretic behavior of RC members under reversed cyclic loading. The first step in conducting an analysis of a BCJ, is to define the structural model that represents the nonlinear problem. The challenge is to find a set of rules that represent the hysteretic behavior of RC members under cyclic loading. Many

hysteresis rules and deterioration models have been proposed to date Takeda et al. (1970), Saiidi (1979), Ilki and Kumbasar (2000), Feghali (1999), Clough and Johnston (1966), Ibarra et al. (2005), and most recently the modified Ibarra Lignos and Krawinkler (2011), among others. Many models have been implemented by applying or refining some of the degradation models proposed by the above researchers. Some of the most relevant implicit models are: Giberson (1969), Otani (1973), Anderson and Townsend (1977), Filippou et al. (1983b), El-Metwally and Chen (1988), among others. Some of them are depicted in **Figure 2-4**. Readers are referred to those references for a more detailed discussion.

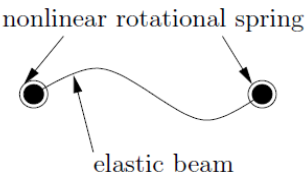

a) Giberson (1969) from Mitra (2007)

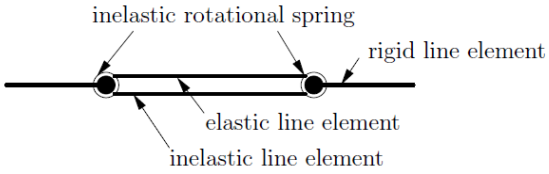

b) Otani (1973) from Mitra (2007)

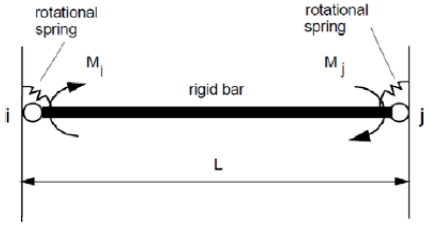

c) Filippou et al. (1983b), from Sharma et al. (2011)

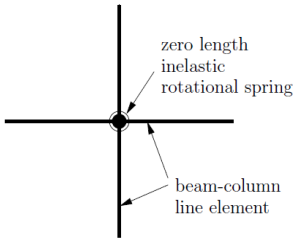

d) El-Metwally and Chen (1988) from Mitra (2007)

Figure 2-4 Examples of implicit BCJ models.

Explicit Models.

With the development of computational techniques, an important number of beam column models and super-elements have been proposed during the last years, **Figure 2-5** and Appendix B.3 depict some of the most relevant explicit models.

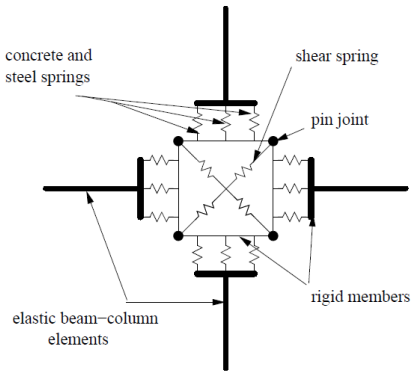

a) Youssef and Ghobarah (2001) from Mitra (2007)

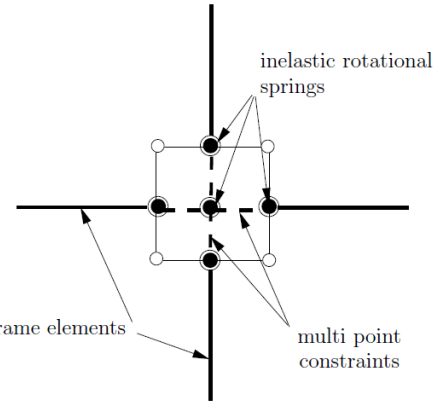

b) Altoontash (2004) from Mitra (2007)

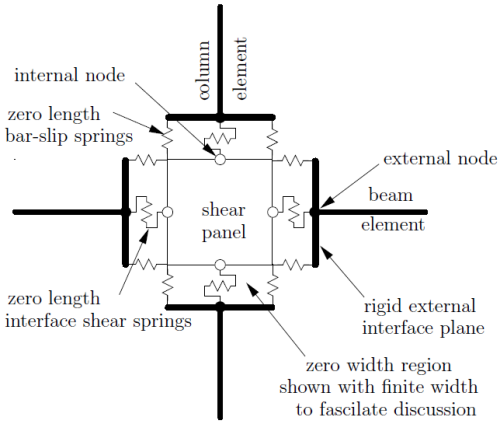

c) Lowes and Altoontash (2003) from Mitra (2007)

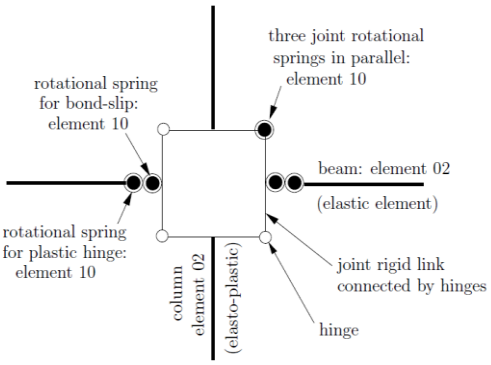

d) Shin and LaFave (2004) from Mitra (2007)

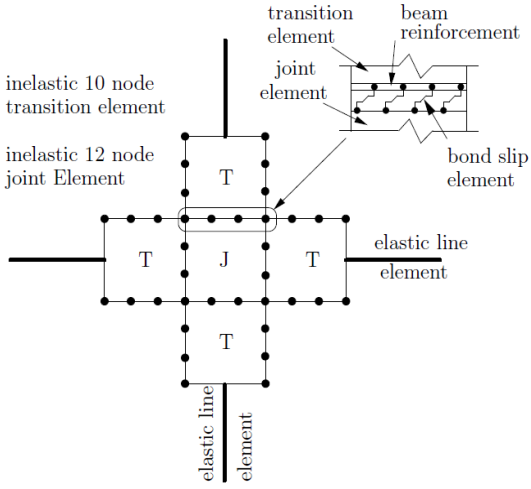

e) Elmorsi et al. (2000) from Mitra (2007)

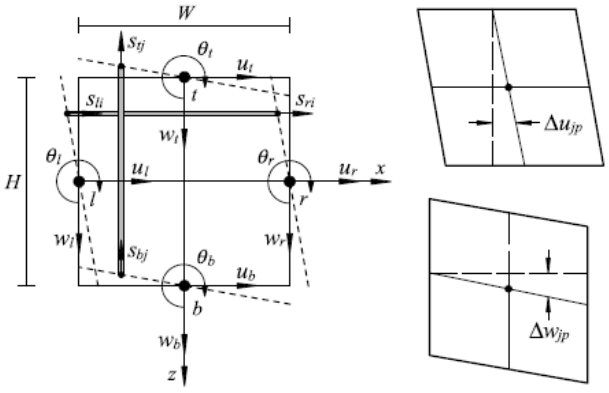

f) Saito and Kikuchi (2012)

Figure 2-5 Examples of explicit BCJ models.

Explicit models have been applied in powerful platforms such as OpenSEES McKenna (2011). Other authors use similar concepts and degradation rules. Some of the most relevant explicit models are: Ghobarah and Biddah (1999), Elmorsi et al. (2000), Youssef and Ghobarah (2001), Lowes and Altoontash (2003), Altoontash (2004), Shin and LaFave (2004), Kusuhara et al. (2006), and Saito and Kikuchi (2012).

For the constitutive relationship of the panel zone, the Ghobarah and Biddah (1999) model uses a tri-linear idealization based on a softening truss model. The Elmorsi et al. (2000) model, in contrast, uses a plane stress element approach. The Saito and Kikuchi (2012) model uses axial springs connecting rigid bodies. The remaining explicit models rely on the Modified Compression Field Theory (MCFT) proposed by Vecchio and Collins (1986) to define the backbone envelope curve for the shear panel. Additional features to include bond deterioration and cyclic degradation are often considered; however, the key parameter is the constitutive model used for the panel zone.

Generally, despite the fact that the explicit models are more complex, mechanistically based and well-elaborated, their calibration depends almost exclusively on test results. Even though the springs are calibrated from test data, due to the difference in reliability, measurements, and overall quality and instrumentation, it is recognized that these springs do not ensure the accuracy of the analysis for either other test results found in the literature or actual BCJ in service. In fact, multi-spring models are more likely to suffer from numerical instability during frame analysis. However, for non-ductile BCJ, all the explicit models that use the MCFT for defining the shear envelope for the panel zone tend to underestimate the shear joint response (Lowes et al. (2005)). In fact, the MCFT is limited to ductile joints, because once the tensile stress in the joint is greater than the cracking stress of the concrete, there is no external mechanism to balance the tensile force that is produced in the joint for the case of non-ductile joints. In other words, MCFT does not account for

the dowel action provided by the longitudinal reinforcement of the columns, and once cracking is present, convergence problems will appear.

Based on the above information, explicit models lack the simplicity, numerical stability and practicality to robustly evaluate RCF performance under cyclic loading. Despite that the validation of a practical-oriented approach to the nonlinear analysis of RCF with unreinforced beam column joint was not an integral part of this study, some studies were conducted along this line of inquiry. The reader is referred to Appendix B where a simplified and practical oriented approach is presented, slightly modified and validated with some test results found in the literature.

2.1.2. Column Failures

Building codes and standards around the world are oriented to establish as good practice the implementation of the premise: “strong column weak beam” design philosophy. The above, with the idea to ensure adequate dissipation of seismic energy at the beam hinge locations. This principle leads to the requirement that the beam failure should be precede column failure to ensure appropriate load distribution and to delay/reduce the possibility of having a soft story collapse mechanism. This section describes typical column failures. These type of failures can be classified into three major categories: shear-critical columns (SCC), flexure-shear-critical columns (FSCC), and flexure-critical columns (FCC). **Figure 2-6** shows a schematic representation of the force-displacement behavior of these three types of columns.

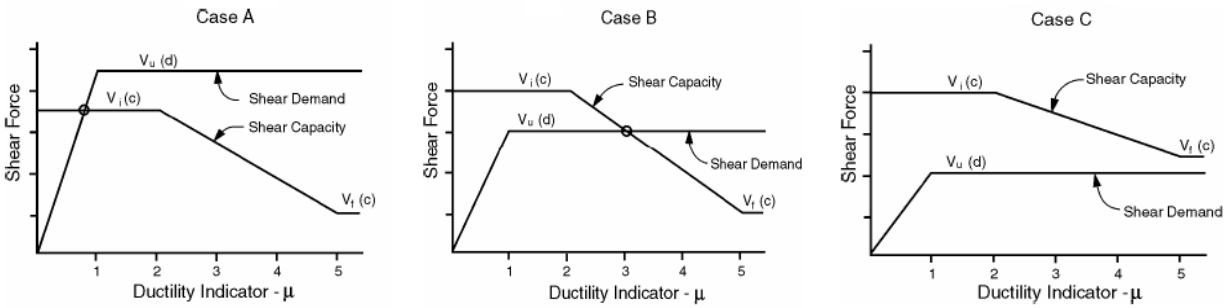

a) shear-critical columns (SCC) b) flexure-shear-critical columns (FSCC) c) flexure-critical columns (FCC)

Figure 2-6 ATC model for shear demand-capacity relation ATC (2006).

SCC (case A on **Figure 2-6**) are characterized by their brittle mode of failure and for having the lowest ductility compared with the other types of columns. They fail initially in shear with the column exhibiting no yielding of the longitudinal reinforcement; axial failure and collapse will occur quickly. FSCC (case B on **Figure 2-6**) behavior is present in those of columns where yielding in flexure occurs before shear capacity is excedded. Those types of columns can sustain considerable ductility demands before failing in shear. For many years their capacity was underestimated, because flexural yielding resulted in an important amout of energy being dissipated throught the hysteretic behavior concentrated in the plastic hinge regions prior the shear failure. These FSCC exhibit strength degradation from both in-cycle and cyclic damage. FCC are characterized as having the greatest ductility. FCC (case C on **Figure 2-6**) yield in flexure without sustaining shear failure. Since this dissertation address nonductile RCF, only a shear-critical column (SCC) model is consider as relevant for this research. For that reason, the following subsections are intended to provide a background information related to SCC.

2.1.2.1. Strength-based vs. Deformation-based Models for SCC

Through the years, numerous analytical and empirical models have been proposed to predict the failure of SCC. For convenience, these models can be classified based on their formulation as either strength-based or deformation-based. Strength-based models calculate the shear capacity as a function of the strength provided by the concrete and the transverse steel. Examples of these models include those by Watanabe and Ichinose (1991), Sezen and Moehle (2004), and Priestley et al. (1994). Within a reasonable approximation, these models are able to predict the shear strength based on the drift demand, but a limitation is that that these models have little success when they are used in reverse to calculate the deformation capacity for a given a shear strength demand. Deformation-based models are intended to predict the value of drift, or rotation at which shear and axial failure will occur. Shear failure is defined when the shear resistance capacity is degraded to 80% of the maximum shear. Examples of this approach can be found in Pujol et al. (1999), Kato and Ohnishi (2002), Elwood and Moehle (2005), and Hossein and Toshimi (2007).

2.1.2.2. Limit State Material (LSM)

The limit state material is a model for shear and axial failures of RC columns with light transverse reinforcement (Elwood (2004)). This model introduces shear and axial nonlinear springs attached in series with a linear (or non-linear) beam column element through a zero-length element as shown in **Figure 2-7**. Each non-linear spring has a pre-defined limiting capacity-curve in terms of a load–deformation relationship. The capacity curve can be defined in terms of axial

or shear forces vs. lateral drift. The general idea is to monitor the lateral displacement for the system. Once the displacement reaches the shear failure surface, the shear spring backbone curve is modified to a degrading hysteretic curve. Strength degradation is activated up to the point where axial failure is presented. According to Nakamura and Yoshimura (2002), this point is reached when the lateral shear capacity is approximately zero. **Figure 2-7** presents a schematic representation of this model. The shear spring backbone curve is modified to a degrading hysteretic curve.

The LSM model is applicable to existing reinforced concrete building columns vulnerable to shear failure during seismic excitations. For defining the axial capacity curve, the LSM assumes that the axial load on a shear-damaged column is to be supported by a combination of compression of the longitudinal reinforcement and force transfer through shear-friction. The latter can be characterized by a model such as the Mattock and Hawkins (1972) on an idealized shear-failure plane. The empirical capacity curve for the axial spring is based on the calibration of 12 full-scale pseudo-static column tests by Lynn (2001) and Sezen (2002). The drift ratio at axial failure for a shear-damaged column is inversely proportional to the magnitude of the axial load and directly proportional to the amount of transverse reinforcement. For defining the shear capacity curve, an empirical equation is given based on the analysis of 50 shear-critical reinforced concrete columns database compiled by Sezen (2002). The LSM model may not be applicable to columns with parameters outside the ranges included in the database.

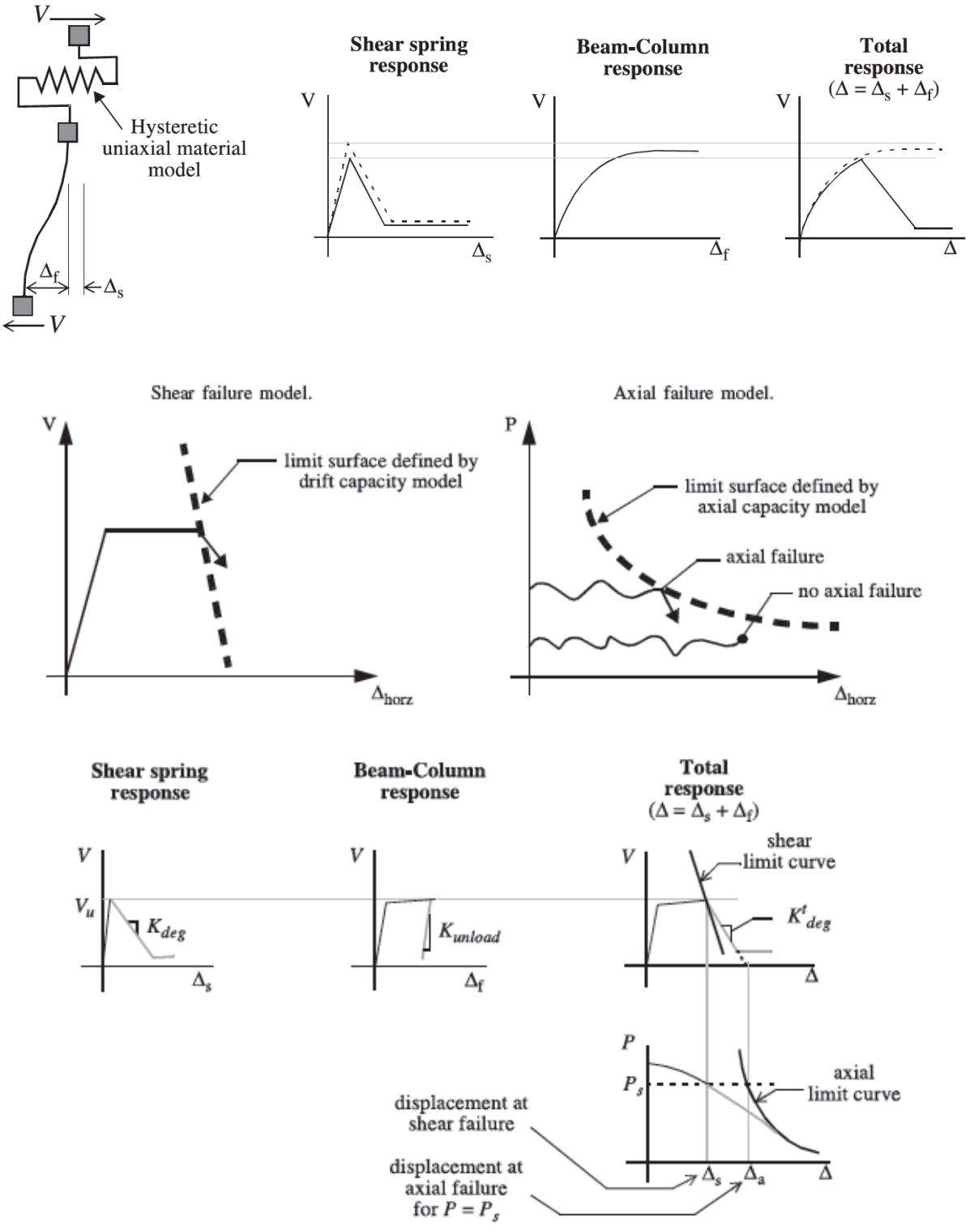

Figure 2-7 Limit state material (Elwood (2004)).

The relationships for the drift ratio at axial failure are as follows:

$$\left(\frac{\Delta}{L}\right)_{Axial} = \frac{4}{100}\frac{1+(\tan(\theta))^2}{\tan(\theta)+P(s/A_{st}f_{yt}d_c\tan(\theta))} \quad (2\text{-}1)$$

$$\left(\frac{\Delta}{L}\right)_{shear} = \frac{3}{100} + 4\rho'' - \frac{1}{40}\frac{v}{\sqrt{f'_c}} - \frac{1}{40}\frac{P}{A_g f'_c} \geq \frac{1}{100} \quad (2\text{-}2)$$

where θ is the angle of the shear failure surface from horizontal (assumed to be 65°), P is the axial load (kN), A_{st} is the transverse reinforcement area (mm^2) at spacing "s" (mm) and with yield strength f_{yt} (in MPa), d_c (in mm) is the depth of the column core between centerlines of the ties, ρ" is the transverse reinforcement ratio, ν is the nominal shear stress (MPa), f_c' is the concrete compressive strength (MPa), and A_g is the gross cross-sectional area (mm^2).

More recently, Ghannoum and Moehle (2012) proposed a slight modification of the LSM model. This proposed model utilizes mainly localized column end-rotations and axial loads to assess column shear capacity and shear failure triggers. Once shear failure is triggered, the analytical model modifies the column response by introducing softening and cyclic degradation in the constitutive properties of a zero-length shear spring element. The zero-length shear spring can be attached in series to any beam-column element.

In essence, LSM is a conceptually simple and practical approach. Unfortunately, there is little information about RCF with SCC details up to collapse that would allow validation of the accuracy of the model. Test such as those carried out by Otani (1973), Bracci (1995), Calvi et al. (2002), and Pinto et al. (2002) did not achieve collapse. Only tests by Hossein and Toshimi (2007), and Elwood and Moehle (2008) reached partial or full collapse.

2.2. Unreinforced Masonry Infills

RCF with unreinforced masonry infills can be found in many places around the world including the Western United States, Eastern Europe, Asia and Latin America. Masonry infills have been widely used as nonstructural elements (partitions, facades), because of their benefits in terms of good thermal and acoustic insulation properties, low cost (especially in developing countries where labor is relatively inexpensive), aesthetics, fire resistance, and waterproofing properties. Even though the importance of the behavior of the infills in the seismic response of the structural system is not always recognized in design, experience has shown that their participation can be decisive. On some occasions the participation may be favorable (Akin (2006), Fardis and Panagiotakos (1997)), and on others it may be adverse (Zarnic and Tomazevic (1985)). At the present time there is no consensus of opinion whether masonry infills are beneficial or harmful when seismic loads are introduced into the RCF. As will be presented in Section 2.2.4, failure mechanisms for masonry infilled frames are complex and depend on many interacting variables. In this section, a brief literature review on masonry infills is presented.

In Colombia, the infills are commonly used for facades and partitions. They are typically built using clay tiles and type M, S or N mortar. Vast majority of infills are not built to be in full contact with the surrounding RC frame, but the gap widths are usually not uniform. As the last part of the construction process, the perimeter wall is usually covered with mortar Bastidas et al. (2002). At the same time, the atypical construction sequence where the infill wall is used as a formwork for casting the RC beams is commonly presented in areas where the evidence of the lack of adequate construction supervision is the common denominator. The Popayan earthquake in 1983 was characterized by having a significant number of soft-story collapse mechanism attributed the

excess of flexibility of the local RCF and due to the presence of the URM infills in non-ductile frames. Moreover, post-earthquake observations after the Quindio earthquake in 1999 confirmed that the failure of clay tile URM walls accounted for a large percentage of the overall damage in the affected civil infrastructure (Sanchez-Silva et al. (2000)). In addition to the presence of the key vulnerabilities discussed in previous sections, it was also noted that during this earthquake that there was evidence of frame-infill interaction which resulted in some out of plane failures and extensive infill damage and collapses. Buildings designed in accordance with the Colombian code performed well structurally (Asfura and Flores (1999)), even though there was widespread damage to masonry infill panels and other non-structural components.

Finally, it is important to introduce a small clarification. Despite the similar appearance between RCF with masonry infill walls and confined masonry, both systems differ in terms of construction sequence and structural behavior, so the deformations and lateral strength of the confined masonry system cannot be considered equal to RCF with masonry infills. Basically, in the RCF with masonry infill walls systems, beams and columns are cast first and then the masonry wall is constructed (Tomaževič (1999)). The connection between the infill and the frame is made only by plaster. For practical purposes, under low lateral demands, the entire system (frame + infill) can be idealized as monolithic. However, as the lateral demand increases, the infill will partially separate from the surrounding frame. This behavior imposes an additional challenge to properly model the frame/infill interaction to account for the contribution of the infill to the lateral force resisting system which is present in reality but commonly is neglected in the initial stages of analysis and design.

The rationale for neglecting infill walls in the design process is partly attributed to incomplete knowledge of the behavior of quasi-brittle materials such as URM, and of the composite behavior

of the frame and the infill, as well as the lack of conclusive experimental and analytical results to substantiate a reliable design procedure for this type of structures. For confined masonry construction, the design relies on strain compatibility generated by the assumption of perfect bond between its elements (bare frame + URM or RM); thus the type of interaction between the infilled masonry and the RCF is different than when the separation must be considered explicitly.

2.2.1. Important Considerations of RCF with URM Infills

Masonry in general is composed of two materials, clay bricks and mortar that exhibit different mechanical properties. Their interaction between the bricks and mortar as a composite material (or masonry unit) will determine the response. If the RCF is added to the analysis, an additional complexity is introduced as the in-plane stiffness of the masonry is higher than the RCF. Despite the fact that the masonry unit is in contact with the frame through the mortar, there is no perfect bond between the frame and masonry. Thus, the fame and infill will deflect in a different manner and interaction stresses will develop. Even now, some standards don't address this behavior, so its effect is typically neglected. As a matter of fact, the forces produced by this interaction can result in an unexpected brittle behavior in the elements of the structural system.

Some of the negative characteristics associated with RCF with masonry infills can be summarized as follows:

- Infills have heavy weight with low ductility (masonry infills can roughly contribute up to the 30% of the seismic mass; according with the Colombian Standard, the recommended partition load is 3.5 KN/m^2 (73 psf)).

- The presence of infills can increase lateral stiffness, which can attract larger seismic inertial forces.
- After ≈0.7% lateral drift, the infills contributions to the strength and stiffness of the system will begin to deteriorate rapidly and/or be exhausted (Akin (2006)).
- Infills have low tensile and shear strength, particularly for poor mortars.
- Infill nonlinear behavior and their interaction with the bare frames are difficult to represent analytically and to be captured by practical or simplified approaches.
- Infills can attract undesired forces to columns and other structural members that had not been designed to resist, so shear failure or captive column behavior can occur.
- Infills have a brittle-type of failure in compression as well as in tension.
- Infills have low out-of-plane stiffness.
- Infills have large stress concentration at corners of windows and doors.
- Due to the interaction between the bare frames and the infill, there is a possibility to produce a soft story mechanism and trigger global collapse.
- There are high overall uncertainties associated with all aspects of the problem (strength, stiffness, deformation capacity, components-interactions, response, and failures types for a given system).

In contrast, some of the above points can also be considered as positive points (i.e., additional strength and stiffness). As was mentioned earlier, there is no consensus whether RCF with masonry infills are beneficial or harmful to resist forces from seismic demand. The proper answer to this question is likely to be "it depends on…" due to the overall uncertainty (input signal, response, interactions, and so on). For instance, on May 1, 2003, a 6.4 (Mw) magnitude earthquake struck Bingöl, Turkey, producing severe damage. Four buildings survived the earthquake with very little

damage in an area where other buildings had significant damage, or collapsed. Preliminary results attributed the good performance to the presence of the masonry infills. A detailed discussion about this particular example is presented in Akin (2006). In the same way, Fardis and Panagiotakos (1997) have demonstrated the overall beneficial effect of masonry infills on seismic performance, especially when the building structure itself was poorly engineered. Thus, in order to provide a better picture, one must consider some of the structural benefits of having masonry infills in RCF construction:

- If the infills are properly confined by the bare frame, the infill walls can be a source of additional lateral stiffness to the building resulting in lower seismic deformation demands on the story and members. This is primarily valid for low drift levels.
- Since the masonry infills will be deformed, cracked, and in some cases destroyed, these elements will contribute to the global energy dissipation capacity of the structural system while they remain confined by the frame.
- Masonry infills are an additional source of overstrength.

2.2.2. Factors Affecting Masonry Strength

Properties such as tensile and shear strength, which are difficult or expensive to measure directly, are commonly correlated to the compressive strength of masonry units by applying a coefficient. For that reason, it is useful to consider those properties that will affect the compressive strength of the masonry infills. A RCF infilled with masonry unit subjected to a lateral force is depicted in **Figure 2-8**, which shows the force path, deflected shape and frame-infill interaction.

It is noted that the resulting infill compressive stresses are inclined at an angle (θ). For that reason, the force transfer mechanisms in the infill are axial stresses which produce (a) inclined compression plus transverse stresses, and (b) shear stresses represented by bond and friction stresses. As it will be discussed in section 2.2.4, the seismic interaction forces produced between the RCF and the masonry infill walls can result in one of several possible failure mechanisms. Those type of failures are a function of the strength and stiffness of the infills as compared to those of the frame.

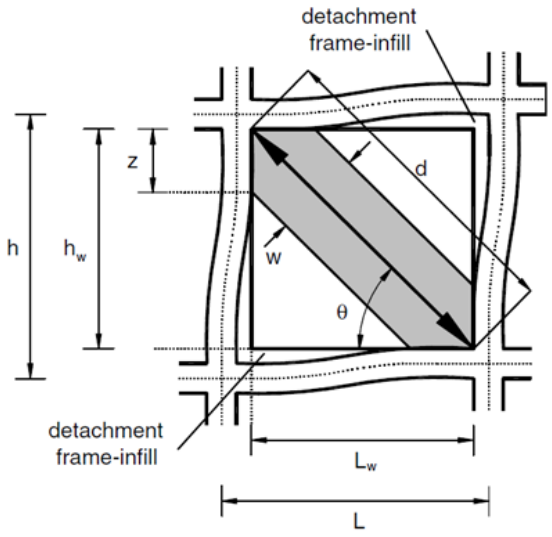

Figure 2-8 Frame-infill interaction. Asteris et al. (2011).

A masonry unit is composed of two materials: the mortar and the filler pieces (bricks, blocks, etc.). Each material has its own different set of stress-strain relationships. **Figure 2-9** depicts possible failure modes from a compression test of a masonry unit. For a pure compression test, the mortar and the filler pieces will try to behave in a different manner, making their interaction complex and resulting in many failure modes.

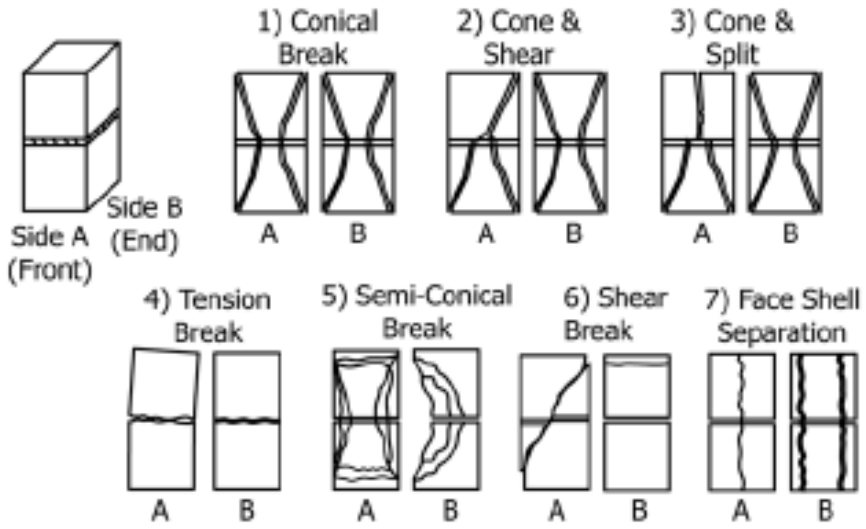

Figure 2-9 Possible failure modes from a compression test of a masonry unit from C1314 (2014).

Under compression loads, the filler pieces and the mortar will have axial and transverse deformations. Due to friction and bond stresses generated between the piece and the mortar, both materials initially will maintain compatibility of deformation. The deformability of the mortar is greater than the filler piece, so the filler piece will restrain the mortar transversely (Kaushik et al. (2007)). Therefore, the mortar will be in a tri-axial compressive strength state, and the filler piece will be subjected to tensile stresses. In general terms, the magnitude of the transverse stresses will be a function of the difference of the deformability (i.e., directly proportional to the modular ratio of the elements), and the thickness of the mortar. This phenomenon is commonly called the joint effect. **Figure 2-10** depicts the schematic representation of the masonry prism under compression.

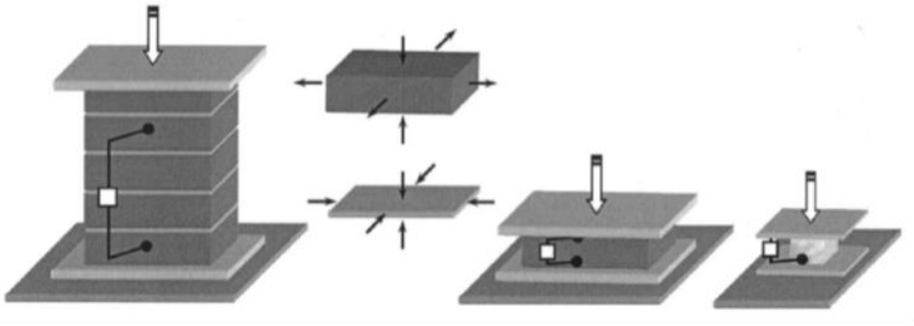

Figure 2-10 Masonry compression test and behavioral component response. Kaushik et al. (2007).

As can be appreciated there are a lot of variables that influence the strength of masonry units. The most relevant are:

- Mechanical properties of the filler piece such as compression strength and tension strength. The ratio of the compressive strength of the masonry unit (f'_m) to the compressive strength of the clay or concrete units (f_p), termed the efficiency (Efficiency=f'_m/f_p), is a good parameter to determine to estimate the compressive strength of the masonry. For clay units the efficiency ranges from 10% to 40%, while for concrete block units it ranges from 50% to 90%.
- For the clay bricks, the initial rate of absorption (IRA) is defined as the number of grams of water absorbed in one minute over 30 square inches of brick bed area (ASTM C67 (2013a)). Acceptable IRA values for the pieces range from 10 to 30 grams. The importance of this property is that a dry brick (IRA above 30) will absorb too much water from the mortar during the construction stage and therefore should be wetted before lying. If the brick is too dry, it will affect the strength of the mortar.

- Mechanical properties of the mortar such as: compression strength, tension strength.
- Mortar thickness.
- Slenderness ratio of the wall, that is, the smaller of the ratio of effective height and effective length of the wall to its thickness. The larger is the slenderness ratio, the lower the strength.
- Eccentricity of the vertical load on the wall. The larger the eccentricity, the smaller the strength.
- Percentage and localization of openings in the wall.
- Defects in construction such as use of substandard materials, unfilled joints between bricks, out-of-plumb walls, etc.
- Age of construction.

2.2.3. Literature Review of RCF with URM Infills

For more than 60 years experimental and analytical attempts have been made to characterize the stiffness, strength, monotonic and cyclic behavior of infills for both in-plane and out-of-plane effects. The efforts can be classified into two major categories: experimental and analytical. Some of the more relevant experimental works are: Benjamin and Williams (1958), Fiorato (1971), Klingner and Bertero (1978), Bertero and Brokken (1983), Zarnic and Tomazevic (1988), Mehrabi et al. (1994), Klingner (1997), Fardis and Panagiotakos (1997), Al-Chaar (1998b), El-Dakhalchni et al. (2004), and Kyriakides and Billington (2008). In terms of analytical contributions, the following can be mentioned: Klingner and Bertero (1978), Mehrabi et al. (1994), Saneinejad and Hobbs (1995), Kodur et al. (1995), Madan et al. (1997), Fardis and Panagiotakos (1997), Al-Chaar (1998b), Buonopane and White (1999), Lee and Woo (2002), El-Dakhalchni et al. (2004), Crisafull

and Carr (2007), Al-Chaar (1998b), Centeno et al. (2008), Stavridis (2009) , Rodrigues et al. (2008), Kyriakides and Billington (2008), and Koutromanos (2011).

The above references cover adequately the research done on infills on RCF and steel frames, lab tests, analysis, and some retrofit schemes that were carried out in the past six decades. An important subset of these researchers have investigated the behavior of the RCF infilled with masonry brick clays, as well as a few who addressed non-ductile RCF with unreinforced masonry infills. This group includes Fiorato (1971), Zarnic and Tomazevic (1988), Mehrabi et al. (1994), Fardis and Panagiotakos (1997), Al-Chaar (1998b), Buonopane and White (1999), Lee and Woo (2002), Centeno et al. (2008). These references are the most relevant for this study because they have a direct correlation with the type of structures that are being addressed in this study. For that reason, additional information related with those, will be briefly discussed next.

Based on the work done on non-ductile RCF with masonry infills, a significant increase in both the strength and stiffness due to the presence of the masonry has been reported by many authors Fiorato (1971), Zarnic and Tomazevic (1988), Pujol and Fick (2010). The above can be attributed to the fact that the non-ductile RCF possesses an excess of flexibility as compared with the in-plane strength of the masonry infill walls. Due to these special characteristics, the advantages and disadvantages of frame-infill interaction can be gleaned. For instance, if the mortar quality is poor, sliding cracks are likely to occur in the infill panel. This can introduce a short-column effect, which in turn may lead to brittle shear failure of the columns (Fiorato (1971), Lee and Woo (2002)). However, if the overall strength of the infill is very low, the infill will not produce significant damage on the bare frame. This observation can be inferred in the work done on non-ductile RCF with masonry infills developed by Buonopane and White (1999).

One of the first and more elaborate and ambitious research related with what we can call today non-ductile RCF with masonry infills was carried out at the labs of the University of Illinois at Urbana Champaign. Fiorato et al. (1970) tested a total of 27 1/8 scaled RCF tests (8 one-story one-bay, 12 five-story one-bay, 6 two-story three-bay with masonry infills, 1 five-story one-bay with no filler walls). The control variables were the number of stories, number of bays, amount, quality, and arrangement of the frame reinforcement, vertical loads on the columns, and wall openings. Fiorato (1971) concluded that the masonry infill walls have profound effects on the strength. Comparing the behavior of the bare frame with and without infill walls, they pointed out that infills produced a considerable increase of strength and stiffness, but at the same time the overall response observed was less ductile. They also observed that the initial lateral response is analogous to the response of a deep beam. However, this analogy fails to describe the load-deformation characteristics of the system (frame + infills), specifically after cracking. At that moment, the contribution of the RCF to the lateral resistant increases. The load-deflection characteristics of the frame-wall systems can be calculated using the knee-braced-frame concept based on the development of a system of columns braced by segments of the cracked walls. The presence of openings in the infill walls resulted in a more flexible system with lower strength and stiffness but with improving ductility. Finally, they recommended that in order to improve the ductility, and possibly the strength of the system, proper transverse reinforcement must be provided in the column.

Mehrabi et al. (1994) tested fourteen half-scale infilled RC frames for monotonic and cyclic loads. The prototype frame was designed for moderate wind loads and severe earthquake loads. The tests had different beam-to-column capacity ratios labeled in the document as weak-frame and strong-frame design, respectively. The frame specimens had aspect ratios of around 1/2 and 2/3,

respectively. Two types of masonry units were used for the infill: hollow concrete blocks and solid concrete blocks, both with type S mortar. In addition, vertical loads were applied onto the specimens with two different distributions. One had vertical loads only on the columns and the other had the loads distributed between the columns and the beam.

In general, the experimental and analytical results have indicated that the addition of infill panels has a profound influence on the behavior of RCF. Infills increase both the lateral strength and stiffness of a bare frame, and improve the energy-dissipation capability of a structure significantly. This is more evident in the case of a strong panel. Specimens subjected to cyclic loadings demonstrated a lower resistance and a faster strength degradation than those subjected to monotonic loadings. The panel aspect ratio, in the range considered in this study, had little influence on the lateral load resistance behavior. This was evident as well for the influence of the distribution of the vertical loads between the top beam and the columns.

In terms of behavior, the damage on the weak infill (hollow units) was dominated by slip failure producing flexural hinges in the columns, and for the solid infill produced brittle-type of failure in the columns for the frame that was designed for moderate wind conditions. Infill crushing was reported for the frame designed for severe earthquake loads. In terms of the analytical models developed, the finite element analyses showed a good agreement for simulating the behavior of infilled frames. Because of the detailed information available from this test series, the Mehrabi specimens (Mehrabi et al. (1994)), will be extensively used in Chapters 3, 4, and 5 for comparisons to the analytical models presented herein.

Another important contribution for non-ductile RCF with masonry infills was carried out by Al-Chaar (1998a). He studied the strength and stiffness behavior, post-yield behavior, and residual strength of non-ductile RCF with masonry infills under in-plane lateral loads through both lab tests

and approximate and non-linear finite element analysis. He tested five half-scale models. One single-bay bare frame, one single-bay with CMU infill, one single-bay with brick infill, one double-bay with CMU infill, and one triple-bay with brick infill. The idea of using different infill materials was to study the influence of different masonry infill strengths as fillers of non-ductile RCF. The failure the bare RCF occurred in the beam-column joint. As expected, for the RCF with infills the cracking was more extensive for the brick-masonry infill than for the concrete masonry infill. Flexural and shear cracks occurred in the concrete columns. About 20% degradation was observed for the case of a concrete masonry infill after the failure, whereas no significant strength degradation was observed for the brick infill.

In terms of older construction it is believed that infills can improve the behavior of Non-ductile RCF (Pujol and Fick (2010)). In addition, despite of the fact that openings indeed reduce the strength and stiffness, they also can help to improve the ductility of an infilled frame (Zarnic and Tomazevic (1988)). Finally, infills can be seen as a second mechanism of defense against induced lateral demands. Since the ductility of the RCF without infills is greater than with the infills (Fiorato (1971), Zarnic and Tomazevic (1988)), for a proper response the frame itself must be able to dissipate the energy imposed by the earthquake and avoid dependence on the additional ductility that the infill can provide.

2.2.4. Failure Mechanisms

The failure mechanisms of the masonry infilled frames are complex because of the reasons exposed in the previous discussions. Mehrabi et al. (1994) defined 24 different in-plane failure mechanisms for infilled frames as presented in **Figure 2-11**.

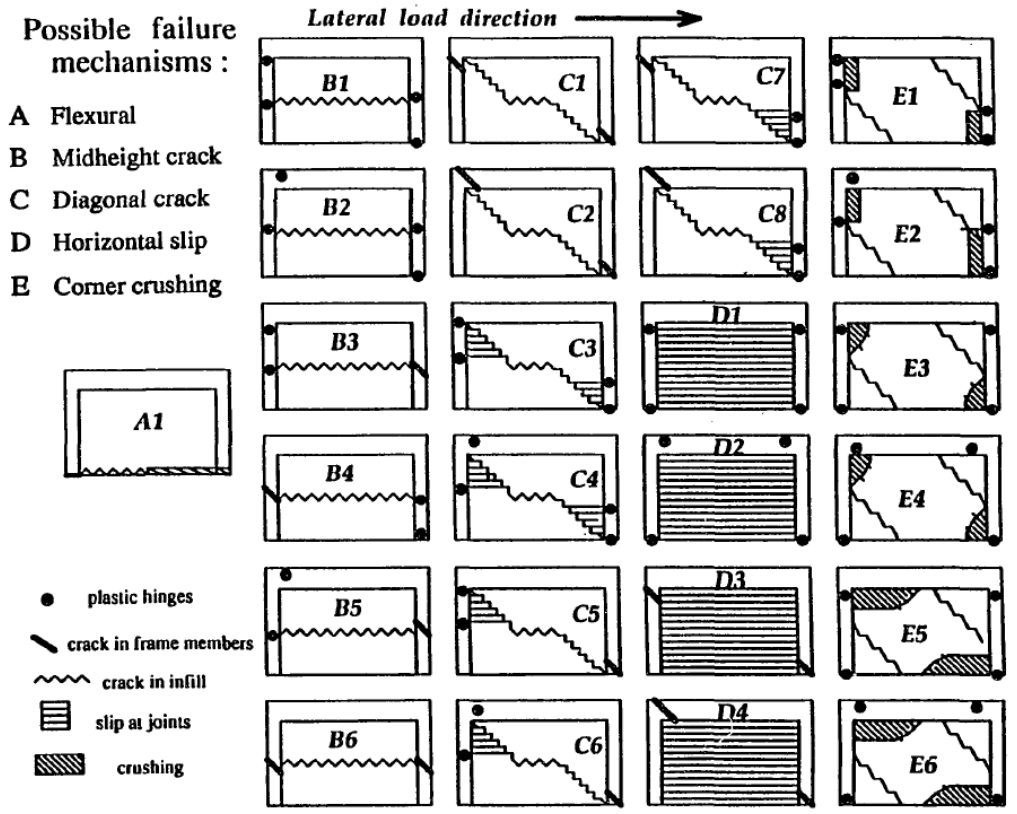

Figure 2-11 Failure mechanisms of infilled frames from Mehrabi et al. (1994).

Stavridis (2009) reduced Mehrabi's list to three main mechanisms **Figure 2-12** with the following characteristics:

1. Horizontal sliding of the masonry with flexural or shear failure of the columns. Infill crushing is sometimes observed in these tests. This failure mechanism was observed in the weak frames with weak panels and also can occur for a strong infill bounded by a relatively strong and ductile RC frame.
2. Diagonal cracking in the infill with column shear failure or, more rarely, plastic hinges in columns. This failure typically occurs in weak/non-ductile frames with strong infill.

3. Infill corner crushing with flexural failure in the columns. This mechanism is most likely in strong and ductile frames with strong infill.

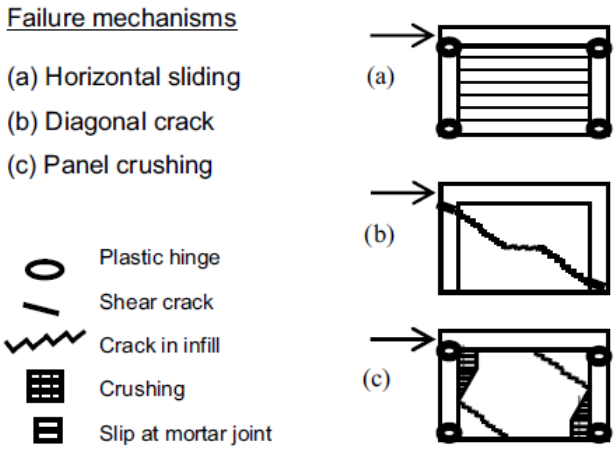

Figure 2-12 Failure mechanisms of infilled frames from Stavridis (2009).

The wide range of failure mechanisms is consistent with the uncertainty of the mechanical properties, differences in strengths and stiffness between the RCF and the infills and reiterative frame infill interaction.

2.2.5. Analytical Approaches

This section addresses some of the most relevant modeling approaches used to RCF with URM infills. These approaches range from simplified **Figure 2-13** (a), to more elaborate and phenomenological-oriented based methods on finite elements analysis **Figure 2-13** (b) and (c). Simplified approaches incorporate a single or multiple struts into the analytical model in order to

represent the effects of the infill wall (Al-Chaar (1998b), Crisafull and Carr (2007), Stavridis (2009), Sattar (2013)). This can be achieved by using truss-type elements with a zero-tension constitutive relationship attached to them, or by using linear or nonlinear springs to model the infill. These choices are made based on the desired objective.

More sophisticated models such as: Lotfi and Shing (1991), Shing and Mehrabi (2002), Stavridis and Shing (2009), Koutromanos and Shing (2012) rely on the finite element techniques to account for the cracking of the frame and the infill, and for the contact stresses generated by the frame-infill interaction. These models are created with more elaborate constitutive relationships and complex elements. It is worth noting that the approximate and elaborate approaches have been calibrated to match some test results in a reasonable way. At the present time and based on the uncertainty associated mainly with the materials and their complex inter-relations, and the frame-infill interaction, a strut based approach adjusted to match some experimental tests can have little success capturing the real behavior for all situations because of the high dispersion associated with the behavior of these types of structures. For these reasons, nonlinear fine elements procedures are the most rational way to address the analysis of RCF and URM infills, unfortunately none of NLFEA procedures meet the requirements for widespread use by practicing structural engineers.

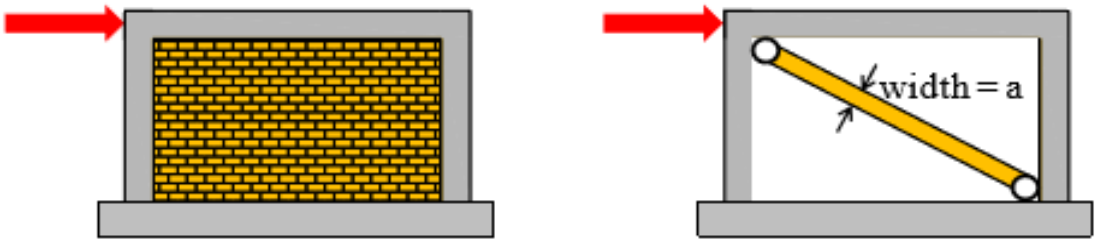

a) Simplified strut idealization Koutromanos and Shing (2013).

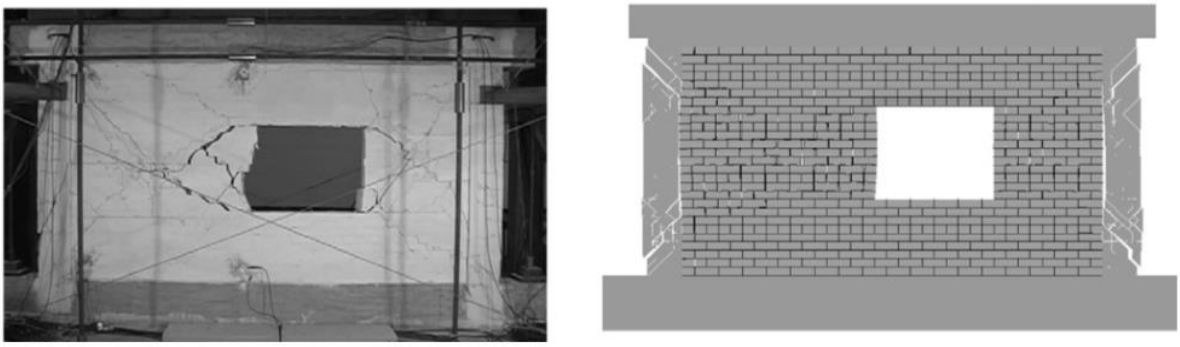

b) Nonlinear Finite Element Analysis. Koutromanos (2011).

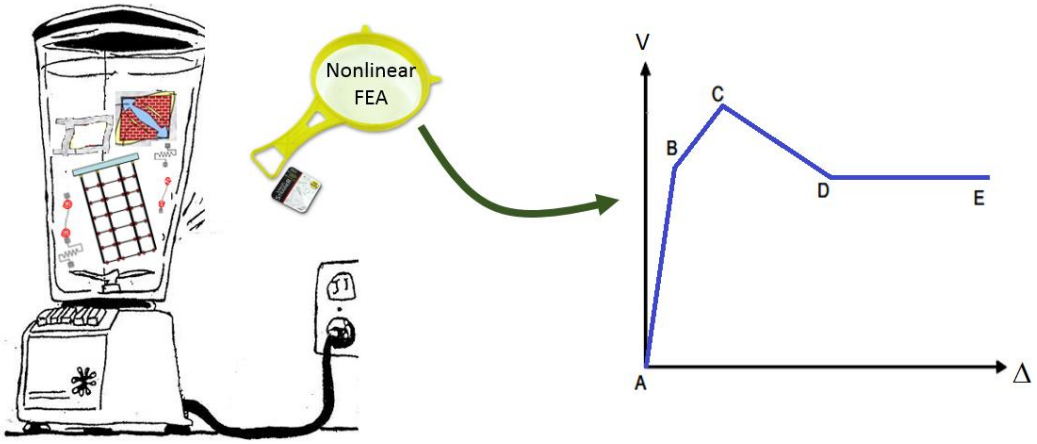

c) Phenomenological approach.

Figure 2-13 Analytical approaches for modeling RCF with URM infills.

Simplified approaches for approximate modeling are based on the representation of the masonry infill through an equivalent strut element. Polyakov (1960), was the first one in introducing this modeling approach. After him, other researchers focused on finding expressions

for the width of the strut with the aim of calibrating the stiffness or strength of the masonry wall (Holmes (1961), Stafford Smith (1967), Mainstone (1971), Zarnic and Gostic (1998)). In addition, Fiorato (1971) proposed an equivalent beam model to estimate the initial stiffness and cracking strength of an infilled frame, and he also proposed a knee-braced frame model to simulate the short-column effect observed in their experiments. Others, idealized the frame-infill as a shear beam (Benjamin and Williams (1958)).

Lateral load demands cause lateral deflection due to shear and flexural deformations. Despite the simplicity of the strut method, for obvious reasons, this method tends to overestimate the stiffness of the specimen at cracking of the panel, but it can be a good predictor for the initial stiffness of the system. Other researchers used plastic analysis methods to calculate the maximum lateral resistances for different failure mechanisms of infilled frames (Wood (1978), and Liauw and Kwan (1985)).

Al-Chaar (1998a), proposed a simplified procedure for evaluating the capacity of infilled frames by using a pushover analysis method. He uses eccentric struts to represent the masonry infill and its interaction with the RCF. The idea is to distribute the nonlinear behavior of the infills to the column directly. This method relies on the development of plastic hinges to capture the nonlinearities of the structural system. The proposed method has been proven by the author to give reliable results when it is compared against some test results and nonlinear finite element analysis. The proposed method can be used for fully infilled frames as well as partially infilled and perforated masonry panels. This method neglects the frame-infill interaction, it fails in adequately describe the possible transfer mechanisms, it induces unrealistic shear demands on the columns and it is not able to capture most of the failure patters presented in **Figure 2-11**.

Stavridis (2009) conducted a series of experimental tests and analytical studies ranging from approximate methods to robust finite element analysis. He performed a sensitivity analysis on the RCF with masonry infills tested by Mehrabi et al. (1994). He also performed a parametric study on the influence of openings (sizes and locations) in the infills frames. Based on that experience, he proposed a simplified backbone curve (shear vs. lateral displacement) as a simplified tool to conservatively predict the global behavior of the RCF when it is filled with solid masonry bricks. Unfortunately, the representation of the complex behavior of RCF with URM by a simplified backbone curve applicable to solid units implies and inherit limitation of its application for different infills strength, and its possible failure modes. It seems as a predefined expected behavior for describing a quite complex structural system which is characterized but the uncertainty of the parameters involved in the analysis, most of them enumerated in Section 2.2.2.

2.3. Challenges in Nonlinear Analysis of Mansonry-infilled RCF

Nonlinear analysis masonry-infilled frames represents a significant challenge due to the possibility of having multiple sources of nonlinearities in a structural analysis including material, geometric and contact nonlinearities.

Material nonlinearity refers to the fact that the response of the materials that comprise the structural system is characterized as being highly nonlinear. In terms of RCF elements, the inelastic behavior is due to concrete crushing, concrete cracking, and buckling and/or fracture of reinforcement. The orthotropic nature of the URMI is characterized by (i) cracking in tension and shear-sliding of the mortar joints (ii) fracture of the mortar joints, and (iii) the possibility of having

cracking, crushing and fracture of the masonry units. As a result, it is obvious that the in the constitutive equations the stress is represented by a nonlinear function of the strain.

Geometric nonlinearity refers to the fact that when a structural element is loaded, it deflects. When calculating equilibrium in the deformed configuration, this leads to secondary actions due to the fact that the ends of the member may no longer be aligned with its original configuration. As a consequence, due to large displacements and/or large deformations, the strains become a nonlinear function of the displacements. In a RCF this phenomenon is especially important in columns members undergoing lateral displacements while carrying gravity loads. For RCF with URMI this can be important for the cases of large openings and ductile behavior of RCF undergoing large displacements. A common approach to calculate this effect is by using the P-Delta analysis that explicitly includes the geometric stiffness matrix which is subtracted from the elastic stiffness matrix.

Nonlinear contact problems allows load transfer and interaction between element components. In RCF with URMI the load transfer is presented at the mortar joint interfaces and the interaction of RCF and URMI might result in several types of failures as presented in **Figure 2-11**. Those problems are very difficult problems to handle, particularly when dealing with frictional effects because of energy dissipation. To account for the contact condition, NLFEA are commonly employed. This approach involves complex formulations such as cohesive crack interface elements with large dummy stiffness values to ensure the contact condition. In most cases the geometry of the contact zone is unknown.

For the present study, the effects of material and contact nonlinearities are assumed to control the nonlinear behavior of non-ductile RCF with URMI. Geometric nonlinearities are not included because it is expected that this structural system cannot reach large drift values (i.e. more than 3%)

without substantial strength deterioration. In addition, as was presented in Section 2.2.1, after ≈ 0.7% lateral drift the infill contributions to the strength and stiffness of the system will begin to deteriorate rapidly and/or be exhausted (Akin (2006)). Thus after the peak response of the system, the concrete alone is being subjected to higher strength values (i.e. 3-5 times) which would not have been possible to reach without the presence of the infill. The combination of this high strength values resisted by the RCF and its non-ductile condition would accelerate the degradation of the lateral response at low drift values where P-Delta effects are assumed to be negligible. Based on this rationale, the non-linear effects were not considered.

2.4. Nonlinear Analysis of Mansonry-infilled RCF in Colombia

Based on the information presented in Sections 2.1 and 2.2, it is evident that: (1) the presence of the infills in the Colombian RCF buildings is a common practice, and (2) experimental and analytical results have indicated that URM infills has a profound influence on the behavior of RCF buildings. Thus, it is clear that the remaining part of this study should be dedicated to the nonlinear analysis of the RCF with URM infills.

Two types of analysis approaches for performing the nonlinear analysis of RCF with URM infills can be presented: (1) simplified based on a strut element representation for the infills, and (2) advanced based on NLFEA models with a continuum representation of the elements that comprise this structural system.

Regarding the single diagonal strut representation, this idealization applied to represent the masonry infill has the following shortcomings:

- It ignores the shear transfer that develops between the beam and the wall.
- It induces unrealistically large shear demands on the columns causing their premature shear failure.
- It ignores the variation of the axial force along the height of each column.
- It does not account for the variation in direction of the compressive forces generated as damage evolves.
- It neglects the axial contribution of the infill generated when the column fails.
- It fails to capture some main failure mechanisms as the depicted on **Figure 2-9**.

The above facts indicate that a comprehensive study of the NLFEA procedure is needed for three main reasons: (1) to understand its effectiveness in overcoming the limitations pointed out for the simplified approach, (2) to take as stating point in the establishment of novel non-continuum version which is intended to help to bridge the gap between overly crude equivalent strut models and the advanced NLFEA, and (3) to use them as comparison tool to validated the proposed methodology. Therefore, Chapter 3 will be dedicated to study the nonlinear finite element analysis of masonry-infilled RC frames. Therefore, Chapter 4 will then look at how truss methods can be used for study this structural system in order to overcome the numerous limitations described above.

3. Nonlinear Finite Element Analysis (NLFEA) of Masonry-infilled RC Frames

As mentioned in the previous chapter, the presence of infill walls in reinforced concrete frame construction may significantly affect the behavior of such structures under lateral loading. The interaction between the frame and the infill walls is complicated and requires models which can capture all the features of the response, such as the contact between the frame members and masonry infills and the localized damage at the mortar joints of the masonry. This chapter focuses on the use of nonlinear finite element models to capture the inelastic lateral response of non-ductile infilled frames. The analyses are conducted with a commercial finite element program, which includes material models and element formulations capable of capturing the physical mechanisms leading to failure of reinforced concrete and masonry components.

3.1. Introduction

In a displacement-based finite element analysis, the structure is subdivided into a number of small parts, or elements, subjected to a constitutive law that describes the material behavior (i.e linear or nonlinear). For linear systems, the equation to be solved is: $[K]\{U\} = \{F^{ext}\}$, where the global displacement vector $\{U\}$ is found by solving the linear system of equations one single time. In the above equation, $[K]$ and $\{F^{ext}\}$ are the global stiffness matrix and global external force vector, respectively. For nonlinear systems, the equation to be solved is: $\{r\} = \{0\}$, where $\{r\}$ is called the residual, and each component of this vector is a nonlinear function of the displacement.

Moreover, $\{r\} = \{F^{ext}\} - \{F^{int}\}$, where $\{F^{ext}\}$, and $\{F^{int}\}$ are the global internal and external force vectors respectively. $\{F^{int}\}$ is an implicit function of the displacement field {U}. Thus in a displacement-based finite element analysis (linear or nonlinear), $\{F^{int}\}$ can be calculated for a given displacement. For the nonlinear case, a trial and error procedure is implemented by "guessing" a nodal displacement vector {U} and checking whether the nonlinear equilibrium equation is satisfied. This equation $\{r\} = \{0\}$ represents a nonlinear system of equations that need to be iteratively followed until the changes in the solution from one step to the next fall below a specified tolerance (Koutromanos (2014)).

The basic difference between elastic and plastic material behavior is that elastic behavior exhibits zero permanent or zero irreversible deformations and thus the only variable needed to determine the stresses is the strain. However, when plastic behavior occurs, permanent deformations can be observed, and knowing the strain is not sufficient information to uniquely determine the stresses. History variables, or so called internal values, need to be provided. Those history variables control the strain hardening or softening behavior by changing the shape of the yield surface (for the case of isotropic hardening/softening) and/or the position of the yield surface (for the case of kinematic hardening) (Koutromanos (2014)).

In the context of small strains theory, the basic assumption in plasticity is that a strain decomposition can be made, where the plastic strain is disaggregated into an elastic and a plastic part. The continuum model used in this study for modeling the RCF, masonry units and the interface adopts an elasto-plastic formulation based on plasticity theory, which requires that the following conditions be satisfied (Koutromanos (2014)):

1. ***Yield function*** (f): This represents a combination of stresses for which plastic flow is initiated. This yield condition can be written as a function of the stress vector and the internal state parameter (q). The evolution of the internal variables controls the strain hardening or softening phenomenon. When the yield function is plotted on the stress space, $f(\{\sigma\},\{q\}) = 0$, it represents a so-called hypersurface. From above, three possibilities exist: (i) the condition $f < 0$ represents the elastic domain (no plastic deformation); (ii) the condition $f = 0$ represents the yield criterion (plastic flow occurs which is governed by a *flow rule*); and, (iii) the condition $f > 0$ cannot occur for a rate-independent elasto-plastic material.
2. ***Flow rule:*** This specifies the inelastic, or plastic strain rate vector as a function of the state of stress. Basically, $\{\dot{\varepsilon}^p\} = \dot{\lambda}\{r\}$ where $\dot{\lambda} \geq 0$ is a scalar quantity. $\dot{\lambda}$ is called the plastic multiplier and $\{r\}$ is a vector that defines the flow direction (i.e. the direction of the plastic strain increment). The components of $\{r\}$ are a function of $\{\sigma\}$ and $\{q\}$. A convenient approach is to define a scalar function $\{g\}$, called the plastic potential function, in such way that $r_{i,j} = \frac{\partial g}{\partial \sigma_{i,j}}$. The surface corresponding to the equation $g(\{\sigma\},\{q\}) = 0$ is called the plastic potential surface. When the yield function is taken as the plastic potential function ($g = f$), the flow rule is called ***associative flow rule***; otherwise, the flow rule is called ***non-associative***. Finally, the plastic multipliers are restricted by the standard Kuhn–Tucker conditions given as: $f \leq 0$; $\dot{\lambda} \geq 0$ and $\dot{\lambda} f = 0$
3. ***Consistency condition:*** This requires that $\dot{f} = 0$, when $f = 0$ and introduces a constraint on the evolution of the stresses and internal variables when plastic flow occur.

Quasi-brittle materials are considered materials whose behavior is affected by cracking (fracture) processes. Materials such as clay, brick, mortar, ceramics, rock or concrete exhibit such behavior. Failure assessment of quasi-brittle materials is mainly dependent on the proper modeling of their constitutive behavior. Nonlinear finite element analysis of RCF with URM infills is very challenging due to the multiple and complex mechanisms that need to be captured including but not limited to flexure or shear dominated behavior in the beam, columns and walls, sliding of bed mortar joints, crushing in compression of concrete and masonry pieces, crack initiation and propagation, frame-infill interaction, and time-dependent effects.

It is important to realize that quasi-brittle materials are heterogeneous materials that typically resists compression relatively well, but can only resist small tensile stresses. During tensile loading, cracks are formed in concrete initially due to stress concentration at the aggregate-paste interface, an inherently weak area due to poor crystalline structure. This phenomenon is accompanied by a fast degradation (i.e softening) after the peak stress has been reached. The failure mechanism in tension is characterized by the presence of localized cracks patterns which result in a full separation of the material. Under compressive loading, quasi-brittle materials exhibit linear behavior approximately until one third of the peak compressive stress followed by a nonlinear response up to the peak strength after which a softening is present. The failure mechanism in compression is mainly isotropic, due to distributed small-scale cracking.

The effect of cracking can be accounted for in computational simulation with either of two approaches, namely, smeared-crack continuum-based approach or discrete-crack approach. In the smeared-crack approach, the effect of cracks is accounted for at the stress-strain level. The effect of the displacement discontinuity introduced by a crack is smeared out over a region whose size can be considered equal to the size of the finite elements. The smeared-crack approach can

adequately describe the average stress-strain response of reinforced materials, when the damage is manifested in the form of multiple, diffuse cracks.

Some examples of continuum models are: Rankine-Hill - Anisotropic model (Lourenco (1996)), smeared crack models (Litton (1974), Borst and Nauta (1985), Rots (1988)), Maekawa damage-plasticity model (Maekawa et al. (2003)). The discrete crack approach explicitly accounts for the displacement discontinuities introduced by cracks, through the use of cohesive-crack interface elements in the mesh. Discrete crack models are better suited for cases where inelastic deformations are manifested in the form of strongly localized displacement discontinuities at locations of cracks or along weak planes, such as the mortar joints in unreinforced masonry components. The material models are based on the discrete concept. For instance, if an unreinforced masonry wall is desired to be modeled by using the continuum approach, the bricks and mortar joints can be modeled together by using a single homogeneous material. In the discrete approach, bricks are modeled with a different material and properties from the mortar. The bricks can be elastic elements or even continuum elements, and the mortar joints can be represented by linear interfaces with a linear or nonlinear material properties ascribed to them.

Depending on the level of accuracy and the simplicity desired, different modeling alternatives can be used in modeling URM infills. **Figure 3-1** presents some alternatives. Furthermore, the failure mechanism presented in quasi-brittle materials is due to a process of progressive internal crack growth in tension, shear or compression.

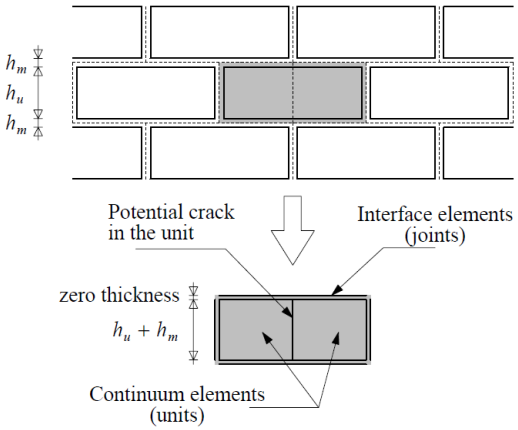

a) Discrete modeling.

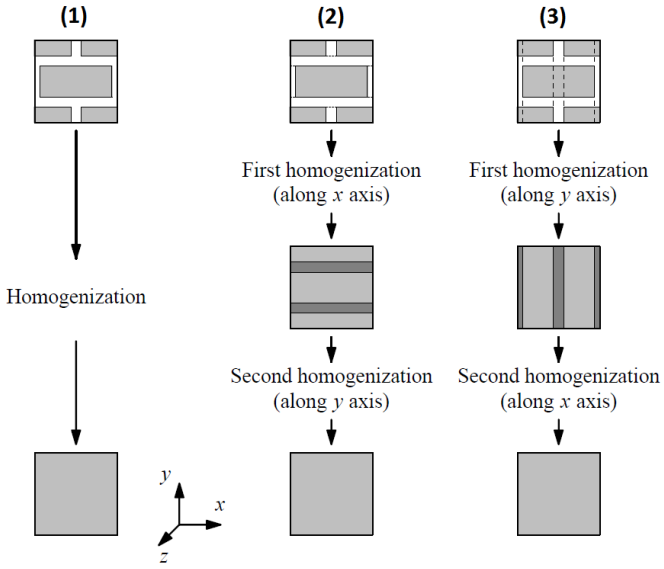

b) Continuum Modeling based homogenization. (1) objective of homogenization, (2) homogenization xy, and (3) homogenization yx.

Figure 3-1. Modeling strategies for masonry structures adapted from Lourenco (1996).

3.2. Smeared Crack Modeling Background

Smeared crack models have been widely used in the analysis of RC structures. The cracked material is treated as an equivalent continuum. In a smeared-crack model, cracking occurs if the

principal tensile stress is greater than the maximum tensile strength defined by the failure surface. The material is considered isotropic until the exceedance of the tensile strength and the cracked material is modeled with a nonlinear orthotropic constitutive model.

The total strain crack model is one type of smeared-crack model. "Total" refers to the fact that the constitutive model is based on total strain representation which describes the stress as a continuous function of the strain. In this model, the unloading and reloading is modeled using the secant modulus, determined by the maximum and minimum strain in each crack direction.

The total strain crack model has different types: including the ***Fixed Crack Model***, in where crack directions are not allowed to change after cracking occurs, and the ***Rotating Crack Model***, in which the crack direction is normal to the principal stress and rotates during the analysis with the principal strain axes such that it always remains perpendicular to the direction of principal strain. As a consequence of that, no shear transfer law needs to be explicitly formulated and used for a rotating crack model.

Rotating crack models have been successfully applied to simulate RCF with URM infills (Including: Shing and Lotfi (1994), Al-Chaar and Mehrabi (2008), Sattar (2013))

Rots and Blaauwendraad (1989), Shing and Lotfi (1994) have pointed out that smeared crack models can overestimate the strength and ductility of members having shear dominated behavior. Moreover, this formulation can be affected by stress locking. In order to overcome that difficulty, interface elements need to be added in the model. **Figure 3-2** depicts the deformed shape of RC shear critical column modeled with smeared crack elements vs smeared crack elements with element interfaces. Note the inherent inability of the smear crack formulation in representing the discontinuity that occurred due the presence of the shear failure. This is due to the fact that

geometrical discontinuities are modeled using the assumption of displacement continuity. On the other hand, the discrete cracking approach allows to capture that discontinuity, with the additional advantage of not being susceptible to stress-locking.

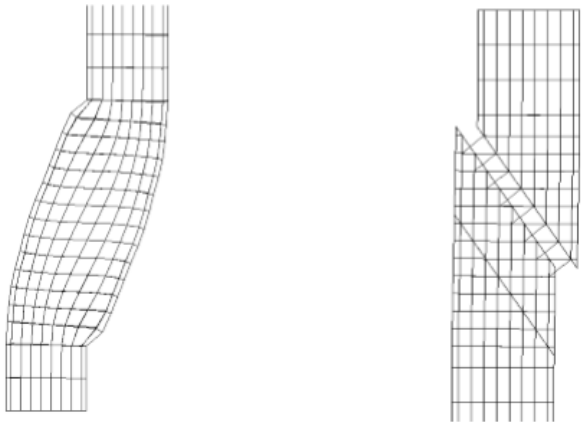

Figure 3-2. Deformed shape of RC shear critical column using a) Smear crack elements and b) Smear crack elements with interface elements (Shing and Spencer (1999)).

In the present study, the inelastic behavior both in tension and compression are described by the integral of the $\sigma - \delta$ diagram. These quantities are known as fracture energy. There are three ways of applying a force to enable a crack to propagate: a) Mode-1 fracture energy – (Opening mode), b) Mode-2 fracture energy (In plane shear mode), and c) Mode-3 fracture energy (Out -of-plane).

3.3. Combination of Smeared-crack Elements and Discrete-cohesive Crack Interface Elements to Describe Damage in Concrete and Masonry

The use of line interface elements, as potential discrete cracks, has been found to be a versatile solution for cases where the fracture path can be pre-assumed by judgment or a preliminary

analysis, and cases where certain fracture tendency can be observed (i.e. mortar joints in URM walls).

The brick-to-mortar interface is considered as the weakest link in masonry structure and can develop a tensile failure, and shear failure. It is well-known that for RCF with URM infills, (a) diagonal and horizontal cracking within the infill and (b) slip of mortar joints are the dominant failure mechanisms. Although other mechanisms can occur, it is the degradation of shear resistance of cracked masonry which defines degradation of lateral stiffness and the resistance of a RCF with URM infills (Al-Chaar and Mehrabi (2008)). In order to determine the values for modeling the brick to mortar interface, Pluijm (1992) proposed a test set-up which keeps constant normal confining pressure during shearing without allowing the application of any tensile stress. Parameters such as the mode-II fracture energy (Gf^{II}), internal friction angle, cohesion, and the dilatancy angle can be obtained from test results or from empirical equations, as also explained in subsequent sections.

There are different NLFEA platforms available that can be used to perform NLFEA of RCF with URM infills using a smeared crack formulation. Al-Chaar and Mehrabi (2008) reviewed the capabilities of different packages including ANSYS, ADINA, ABAQUS, and DIANA. The objective was to review and to understand their capabilities in modeling structural RCF with URM infills. That comparison focused on the capabilities of the four different software studied to model the mortar joints and their shear degradation over time. The conclusion was that DIANA has some built-in material models and elements which can allow the simulation of RCF with URM infills under lateral in-plane loading. For this study, TNO Diana granted a one-year license agreement to be used to perform the NLFEA simulations.

3.4. Constitutive Models for Continuum Elements

The Total Strain Crack Model (TSCM) is one type of smeared-crack model, where the name total is used to indicate that the compressive and tensile behavior is defined by one stress-strain relationship. The TSCM comprises two parts: (1) the basic material properties (Young's modulus, Poisson's ratio, and similar), and (2) the definition of the behavior in tension, shear, compression, and additional effects (i.e., the effect of lateral cracking or lateral confinement).

The basic concept of the TSCM is that the stress is evaluated in the directions which are given by the crack directions. The strain transformation matrix is determined by calculating the eigenvectors of the strain tensor. The deterioration of the concrete material due to cracking and crushing is monitored with internal damage variables which track the normal and transverse strains, including the effect of lateral confinement and lateral cracking. In the Rotating Crack Model, the tangent stiffness is formulated in the cracked coordinate system prior to transformation into a consistent global system. Damage recovery is not possible; therefore degradation of stiffness is an ever-increasing function once damage evolves.

3.4.1. Tensile Behavior

For the Total Strain Crack Model, tensile behavior can be classified into four (4) major categories including: a) Elastic, b) Ideal and brittle, c) Linear tension softening (based on ultimate strain), and d) Tension softening curves (based on fracture energy). The latter has four (3) softening functions, including a linear softening curve, an exponential softening curve, and a nonlinear

softening curve according to Hordijk (1991). These functions are all related to a crack bandwidth as is usual for smeared crack models.

In order to model the softening produced by internal crack growth in tension, the present study uses an exponential function for modeling tensile resistance in concrete and masonry units **Figure 3-3**. Equation 3.1 present the exponential softening relation with an area under the curve equal to G_f^I/h, where "h" is the bandwidth. In this approach, Gf^I is the energy needed to create a crack opening with a unit area (Lourenco (1996)).

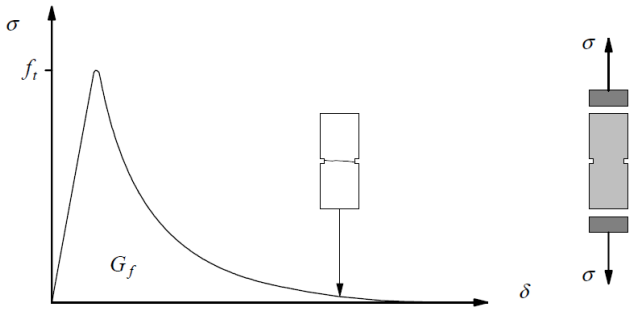

Figure 3-3. Exponential Tensile Behavior. Lourenco (1996).

The numerical model selected in this study is presented in the following equations:

$$\frac{\sigma_{nn}{}^{cr}(\varepsilon_{nn}{}^{cr})}{f_t} = exp\left(-\frac{\varepsilon_{nn}{}^{cr}}{\varepsilon_{nn}{}^{cr}.ult}\right) \tag{3-1}$$

where: sigma $\sigma_{nn}{}^{cr}$ = tensile stresses normal to the crack.

f_t= tensile resistance.

$\varepsilon_{nn}{}^{cr}$= crack strain in the normal direction.

$\varepsilon_{nn}{}^{cr}.ult = \frac{Gf^I}{h*ft}$= ultimate crack strain in the normal direction.

The crack bandwidth "h" is a characteristic length providing mesh objectivity with respect to the fracture energy. For instance, for 2D elements with linear shape functions, "h" is defined as the square root of twice of the element area. For beam and truss elements, the value of "h" is commonly taken as the length of the element.

In the literature several expressions have been proposed for calculating the mode-I fracture energy Gf^I (i.e., Eq. 3-2 Hordijk (1991) and 3-3 (CEB-FIB 1990).

$$G_f{}^I = 0.065 * ln\left(1 + \frac{f'c}{10}\right) \qquad \text{Hordijk (1991)} \qquad (3\text{-}2)$$

$$G_f{}^I = 10^{-3} * \alpha_f (f'c^{0.7}) \qquad \text{(CEB-FIB 1990)} \qquad (3\text{-}3)$$

where α_f is a coefficient which depends on the maximum aggregate size according with CEB-FIB (1990).

Fracture energy values are assumed to be a given function of the material. Pluijm (1992) found that for a tensile bond strength ranging from 0.3 to 0.9 [N/mm^2] the value of Gf^I ranges from 0.005 to 0.02 [N.mm/mm^2]. **Figure 3-4** presents the relation of mode-I fracture energy (in N/m) and compressive strength of the material.

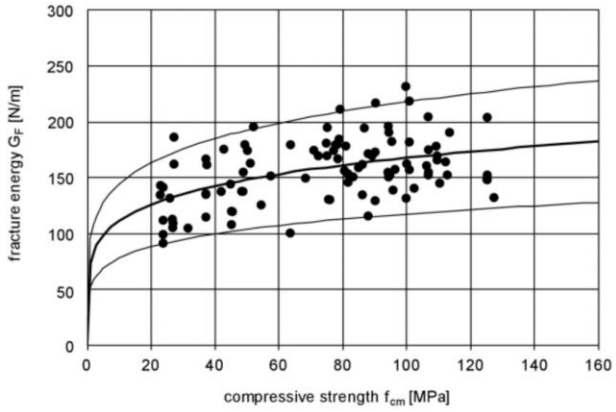

Figure 3-4. First mode fracture energy as function of compressive strength.fib. (2013)

3.4.2. Compressive Behavior

Compressive behavior describes the material within the same concept as the tensile behavior. The compressive behavior of a Total Strain Crack Model is in general a nonlinear function between the stress and the strain, for the present study, a parabolic function is selected for modeling the compressive resistance in concrete and masonry units **Figure 3-5**. This representation facilitates the calibration process for matching test results. Two mandatory parameters need to be defined, including: (i) the maximum compressive strength of the material (f'c), and (ii) the compressive fracture energy, which is defined as the area under the compressive stress-strain curve from strain at maximum stress to the ultimate strain. Equation 3.4 presents the parabolic function. This is based on the definitions according to Feenstra (1993). Up to one-third of the maximum compressive strength (f'c), the strain $\alpha_c/3$ a linear variation is considered. Then a parabolic equation is established with peak strength at α_c strain and residual value at ultimate strain α_u. Eq. 3-4 to 3-7 describe the model.

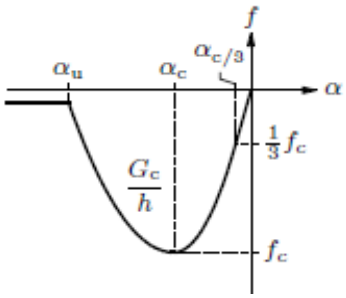

Figure 3-5. Compressive behavior based on Feenstra (1993).

$$f = -f'_c \frac{1}{3}\left(1 + 4\left(\frac{\alpha_j - \alpha_c/3}{\alpha_c - \alpha_c/3}\right) - 2\left(\frac{\alpha_j - \alpha_c/3}{\alpha_c - \alpha_c/3}\right)^2\right) \quad (3\text{-}4)$$

$$\frac{\alpha_c}{3} = -\frac{1}{3}\frac{f'_c}{E} \quad (3\text{-}5)$$

$$\alpha_c = -\frac{5}{3}\frac{f'_c}{E} \quad (3\text{-}6)$$

$$\alpha_u = \alpha_c - \frac{3}{2}\frac{G_c}{h * f'_c} \quad (3\text{-}7)$$

At present, there are no firm recommendations about the compressive fracture energy (Gc), due to the scarcity of experimental data pertaining to the softening regime of the uniaxial compressive response of concrete and masonry. Regarding concrete, Feenstra (1993) suggests that the compressive fracture energy (Gc) ranges from 15-25 [N.mm/mm^2] which is about 50 to 100 times the tensile fracture energy (Gf^I). Nakamura and Yoshimura (2002) have proposed an expression providing the compressive fracture energy (Gc) (equation 3-8) as a function of the compressive strength (f'c).

$$G_c = 8.8\sqrt{f'c(Mpa)} \qquad \text{(N/mm)} \quad (3\text{-}8)$$

Furthermore, compressive response can be affected by the presence of lateral confinement, and the presence of lateral cracking. The following sections cover those topics briefly; additional information can be found at the pointed references.

3.4.3. Effect of the Confinement on the Material Compressive Response

Concrete and masonry units exhibit a pressure-dependent response. Strength and ductility increase when the effect of lateral confinement on the compressive behavior is introduced. As a consequence, the compressive stress-strain function needs to be adjusted as a function of the computed stresses in the lateral directions. The increase of the strength with increasing isotropic stress can be modeled with the four parameter proposed by Hsieh et al. (1982). **Figure 3-6** depicts the influence of the lateral confinement on the compressive behavior

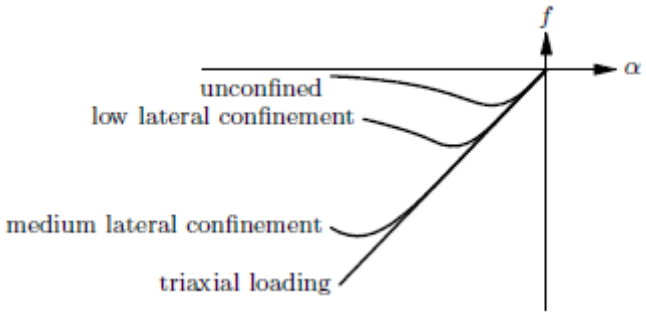

Figure 3-6. Influence of lateral confinement on the compressive stress-strain curve. (from Reference Manual DIANA (2014)).

3.4.4. Effect of Transverse Tension on Material Compressive Response

Vecchio and Collins (1986) have proven that the compressive behavior is also influenced by lateral cracking. Specifically, the occurrence of large tensile strains and cracking perpendicular to the direction of the principal compressive stresses lead to a reduction of the magnitude of the compressive stresses. To account for this effect, the employed material law for the continuum elements multiplies the obtained stress by a reduction coefficient, $\beta_{\sigma\,cr}$ as shown in **Figure 3-7**. The reduction coefficient depends on the transverse strains.

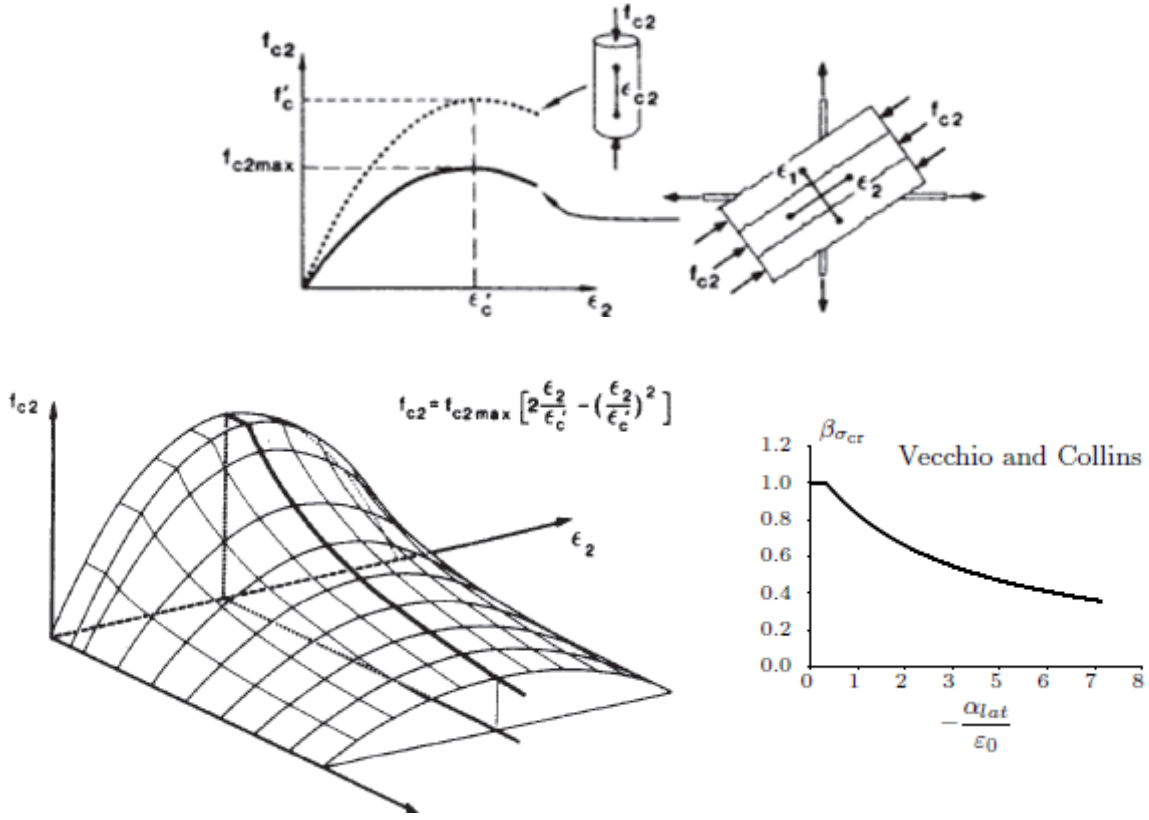

Figure 3-7. Influence of lateral cracking on the compressive stress-strain curve. (Adapted from Vecchio and Collins (1986))

3.5. Discrete-Cohesive Crack Interface Models

As explained in Section 3.3, the finite element analysis of non-ductile infilled frames requires the use of cohesive-crack interface elements, to properly capture the effect of strongly localized cracks such as shear cracks and also the localized deformations along the mortar joints. The elements pursued herein are based on a four-node formulation, as shown in **Figure 3-8**. The constitutive law of an interface relates the traction vector, (t), to the relative displacement vector, (Δu).

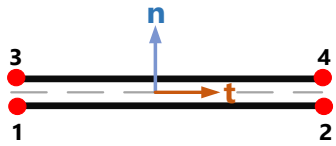

Figure 3-8. 2D interface element configuration.

For two-dimensional analysis, the traction vector (t) is defined as presented in equation 3-9. Note that the subscripts "n" and "t" refers to the normal direction and transverse direction respectively.

$$t = \begin{Bmatrix} t_n \\ t_t \end{Bmatrix} \tag{3-9}$$

The relative displacements can be written as:

$$\Delta u = \begin{Bmatrix} \Delta u_n \\ d_t \end{Bmatrix} \tag{3-10}$$

For a linearly elastic interface, the traction vector is related to the relative displacement vector in accordance with the following expression.

$$\begin{Bmatrix} t_n \\ t_t \end{Bmatrix} = \begin{bmatrix} k_n & 0 \\ 0 & k_t \end{bmatrix} \begin{Bmatrix} \Delta u_n \\ d_t \end{Bmatrix} \tag{3-11}$$

where, k_n and k_t are the normal and tangential stiffness, respectively. Usually these values require large penalty values to enforce a continuity of the displacement field. Equation 3-11 can be expressed in rate form, where the constitutive relation is assumed to be incrementally linear as is presented on equation 3-12.

$$\dot{t} = D\Delta\dot{u} \tag{3-12}$$

where $\dot{t}$ is the traction vector, $\Delta\dot{u}$ is the vector of the relative displacements, and D is the tangent stiffness matrix which depends on the constitutive model used to model the interface nonlinearities.

3.5.1. Combined Shear Crushing Interface (CSC) Model

The Combined Shear Crushing interface model is depicted in **Figure 3-9**. The inelasticity of the interface elements is described by the failure surface (Lourenco (1996)). This interface model is also known as the composite model. The specific surface consists of a Coulomb surface to account for shear sliding, a tension cutoff segment to capture tension-dominated fracture and a cap to capture crushing under large compressive stresses. The yield surface evolves by means of softening laws, to account for tensile softening and loss of shear cohesive strength. The stress update algorithm in the element uses an implicit Backward Euler scheme, accompanied by a Newton-Raphson iterative procedure. Additional details about this interface model and its implementation for 2D and 3D analysis can be found in Lourenco (1996).

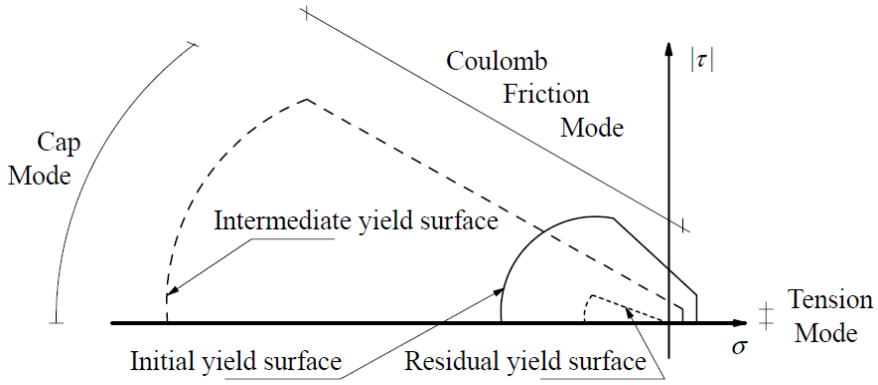

Figure 3-9. Combined shear crushing interface model. Lourenco (1996).

Tensile Behavior

Tensile behavior is modeled with a tension cut-off (i.e a tensile strength value used to limit the effective tensile stress) with exponential softening. This tension cut-off simulates the brittle failure of mortar joint under tensile force. The exponential softening idealization in tension is consistent with experimental results from Pluijm (1992).

Shear Behavior

The shear behavior of the interface element is modeled with the Coulomb friction yield surface, depicted in **Figure 3-9** and showed in Eq. 3-13.

$$f = |\tau| + \sigma.\tan(\varphi) - c \tag{3-13}$$

where φ is the friction angle, c is the cohesion, τ is shear stress, and σ is the normal stress. This interface material model considers exponential softening for both the cohesion and friction angle. The softening of the friction angle is assumed to be proportional to the softening of the cohesion Lourenco (1996). The dilatancy effect and strain softening behavior is also incorporated in this model. This interface model does not consider the cumulative damage due to the loss of mortar material (Al-Chaar and Mehrabi (2008)).

3.6. Nonlinear Finite Element Analysis of RCF with URM Infills Using DIANA

The previous sections described the material and element formulations used in the present study for nonlinear finite element analysis of infilled RC frames. The nonlinear finite element scheme has been validated using experimental data by Mehrabi et al. (1994). The goal of this section is not the creation of a novel material or analysis procedure but to obtain valuable insight into the behavior of RCF with URM infills subjected to monotonic in-plane lateral loads by: (1) conducting numerical simulations of large-scale tests described in the literature, and (2) performing a simplified sensitivity analysis of the parameters required to match both those experimental test results and the simulations conducted by other researchers. The objective is to gain an understanding of the effectiveness, inherit limitations and procedures of NLFEA. The author felt that this was an indispensable task as he had little experience with complex simulations of the type that will be conducted herein. Furthermore, the validated calibrations will become benchmarks for comparisons with the new approach presented in the next chapter. Finally, the new procedure will be used in further sections in the simulations where infilled frames are tested and no experimental results are available.

For the establishment of the NLFE models, Al-Chaar and Mehrabi (2008), Sattar (2013) recommendations are incorporated, but the starting point in all the simulations performed here were the original test data provided in Mehrabi et al. (1994).

3.6.1. Overview of Experimental Tests Used for Validation Analyses

Mehrabi et al. (1994) tested fourteen half-scale RC frames with URM infills for monotonic and cyclic loads with different geometric properties (i.e aspect ratio, hollow and solid bricks), different magnitude and distribution of axial load, and adjacent infilled bays on the structural performance. The specimens corresponded to a six-story, three-bay, prototype RC frame structure, representing a typical office building. They considered two alternative design solutions were pursued for the RC frames, were examined. One ''weak" frame, which was designed for a lateral wind pressure of 26 psf, corresponding to a basic wind speed of 100 mph. The other was a ''strong" frame, which was designed for a set of equivalent static forces stipulated for Seismic Zone 4 in the UBC. For this study only the weak frames are simulated.

This set of experiments is selected due to the comprehensive data available for the tests. It allows to validate the nonlinear finite element approach. **Table 3-1** presents the information related to the specimens selected in this section. Specimen 1 was a weak bare frame. Specimen 8 was the bare frame used in Specimen 1 which was repaired and strengthened with a weak infill panel laid with type S mortar. Specimen 9 corresponds to a weak bare frame infilled with solid units laid with S mortar. Specimen 8 and 9 different gravity load distribution was assumed accordingly **Figure 3-10** and **Table 3-1** Additional information can be found at Mehrabi et al. (1994).

Table 3-1 Test Specimens from Mehrabi et al. (1994).

Specimen	Type of Frame	Type of Masonry Units	Panel Aspect Ratio (h/L)	Lateral Load (P_1)	Vertical Load Distribution (Kips)	
					Columns (P_2)	Beam (P_3)
1	Weak	No infill	0.67	Monotonic	33	-
8	Weak - repaired	hollow			33	11
9	Weak - repaired	solid			22	11

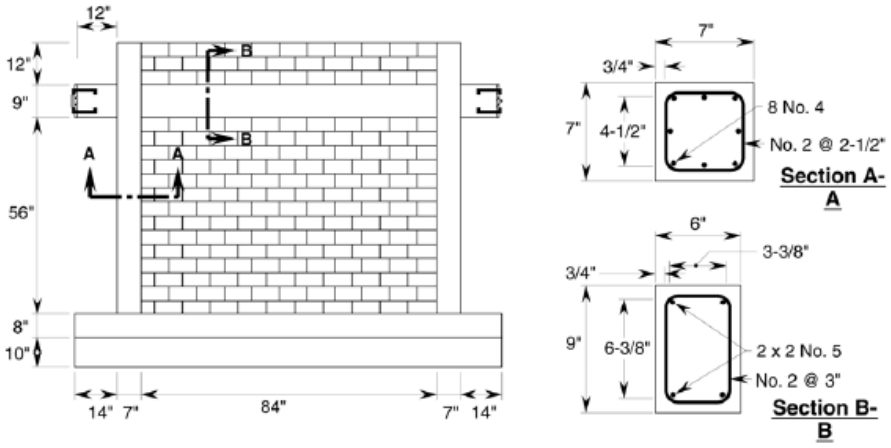

Figure 3-10. Test setup from Al-Chaar and Mehrabi (2008).

3.6.2. Nonlinear Finite Element Model

For the present study the Smeared Crack Model is used for modeling the RCF and the URM infills. The reinforcement is modeled by using Von Mises plasticity used with combined hardening (isotropic and kinematic hardening). The reinforcement is modeled with 1D elements, and perfect bond is assumed. Four integration points are used by all of the quadrilateral elements. For the nonlinear interface elements, two-dimensional, four-node two integration points were used for modeling mortar bed and head joints, and the frame-to-infill region. To avoid spurious effects from stress distributions in the computational model, elastic quadrilateral elements are used in the

vicinity of the nodal point where the displacement is applied. These elements can be thought of as a model of steel loading plates which are commonly used in experimental tests. In addition some rigid links are incorporated with multipoint constraints in order to mimic the applied test displacement (i.e. the nodes at the outer face of the beam, where the actuator is located are imposed to have the same horizontal displacement). The following sections describe the calibration process used for the finite element models.

3.6.3. Brick Calibration

In the NLFE model, the Total Strain Rotating Crack Model is applied to represent the behavior of the block unit. Compressive behavior of the block is modeled by using the parabolic option where three parameters are needed as input (peak compressive strength, fracture energy in compression and the bandwidth length). Thus, a 2D plane stress model for a single block of concrete (8" length x 4" width x 4" height) is created. The block is fixed at the base and a uniform compressive displacement is applied at the top. From Al-Chaar and Mehrabi (2008), a peak strength of 3 ksi and strain at peak stress of 0.0026 are given. **Figure 3-11** presents the result of the calibration process, highlighting the effect of different values of compressive fracture energy on the post-peak regime of the stress-strain law. For this model a value of 55 psi-in is selected as appropriate, to decrease the possibility of having compressive failure of the block unit which was not the case for the Specimens analyzed.

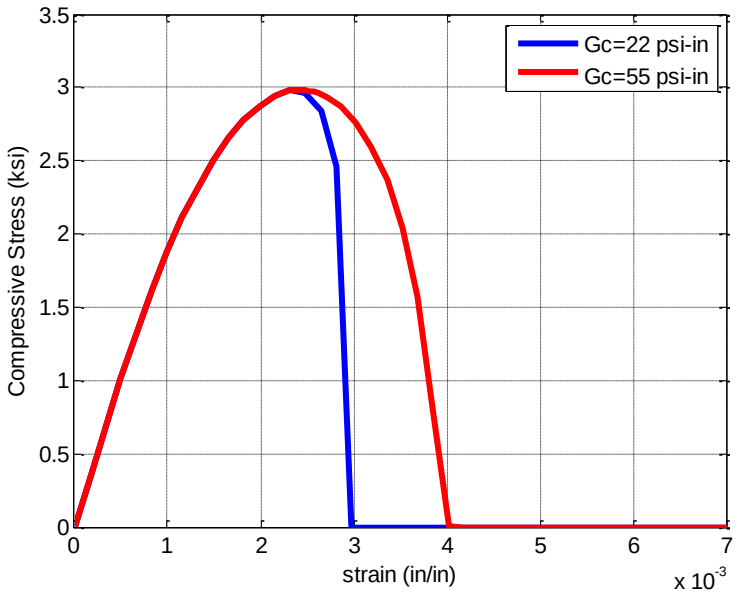

Figure 3-11. Effect of fracture energy in compression applied in brick calibration.

3.6.4. Calibration for Interface Elements

This section explains the calibration process of the mortar-brick interface. Linear elastic material is assumed for the brick behavior. For the mortar, zero thickness, two-dimensional, four-node two integration points were used. The interface was idealized with CSC (combined shear crushing) interface model.

To perform the calibration of the interface, two-brick elastic elements with a zero thickness interface element with CSC constitutive behavior are analyzed under pure tensile displacement, shear and cyclic behavior. The relevant material properties are presented in **Table 3-2**.

Table 3-2 Material properties used in the interface calibration.

Test	Knn (lb/in^3)	Kss (lb/in^3)	C (psi)	Φi	Ψ	Φr	σc (psi)	δ	ft (psi)	G_f^I (psi-in)	G_f^{II} (psi-in)	fc (psi)	Cs	G^c (psi-in)	κp (in)
				(Deg)											
Tensile	35000	28000	40	45.3	-	-	-	-	40	1.69	16.1	-	-	-	-
Shear			26	47	0.3	42	150	2				1500	1	22	0.006

Figure 3-12 depicts the variation of the tensile and shear stress of the interface Vs the vertical relative displacement (i.e. joint opening) and horizontal displacement (i.e. sliding). For the tensile behavior, the maximum reached value is 38.6 psi, and for the shear behavior the value of the cohesion stress was reached. For both cases, after reaching its maximum stresses, exponential softening was presented in accordance with the CSC interface model. It is noted that for both cases, some localized stress concentrations are presented. Further models will include a rigid elastic material at the displacement application point.

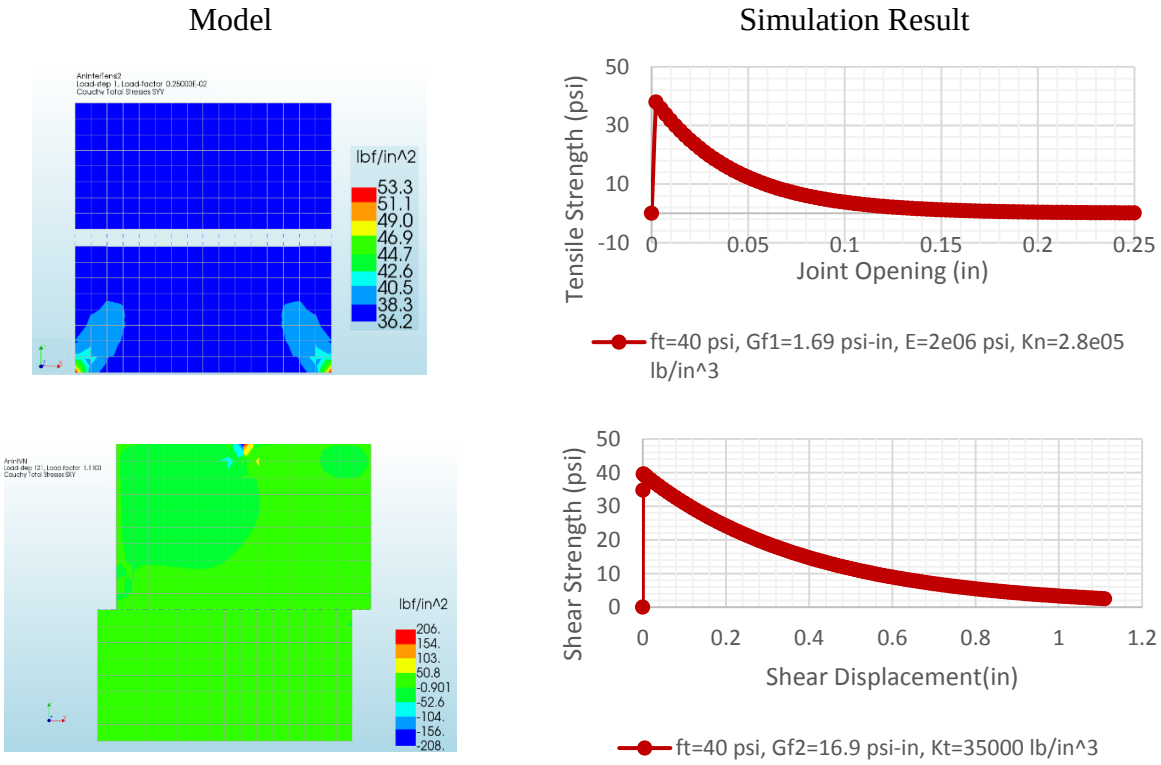

Figure 3-12. Tensile and shear calibration of the interface model.

Figure 3-13 presents the effect of pre-confined pressure on interface strength. A direct correlation between the applied pre-confined pressure and the shear strength of the interface is clear, they are almost directly proportional (i.e lateral strength increases as vertical pre-compression increases). This validated the capability of the CSC model in representing the pressure-dependent behavior of the mortar interface.

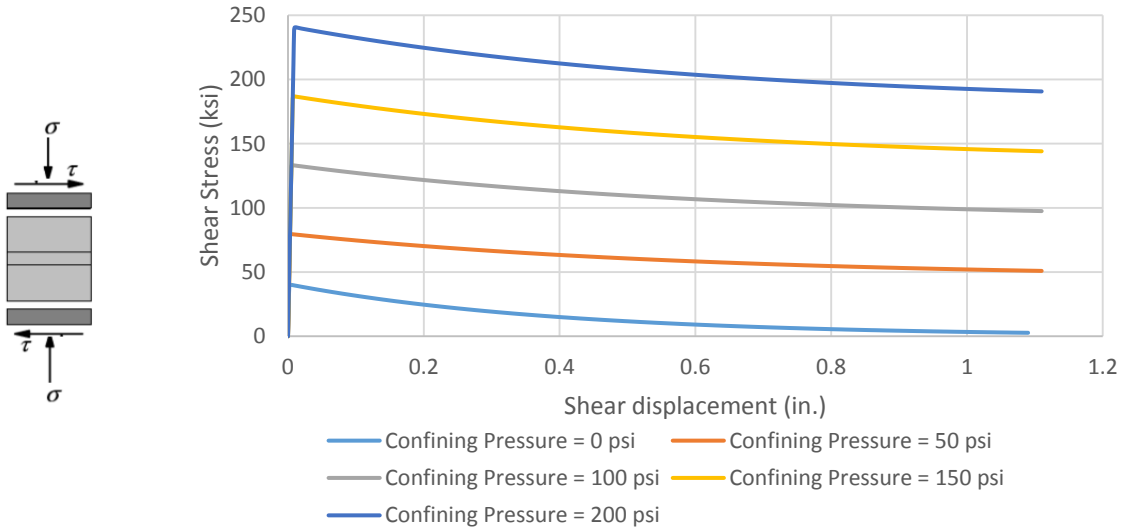

Figure 3-13. Effect of pre-confined pressure on interface strength.

The presented study is limited to the monotonic analysis, additional verification pertaining to cyclic behavior is not incorporated in this study.

3.6.5. Analysis of Specimen 1

This section is focused on the simulation of the specimen 1 from Mehrabi et al. (1994). It is a bare concrete frame with the same configuration and element dimensions as the frame presented in **Figure 3-14**. Two-dimensional, plane stress, four-node elements with four integration points were used for modeling the RCF. The Rotating Smeared Crack constitutive model was utilized for modeling the RCF as described previously. A constant axial load of 66 Kips was applied and kept constant during the analysis. Displacement control is applied to obtain the load displacement curve pushover curve).

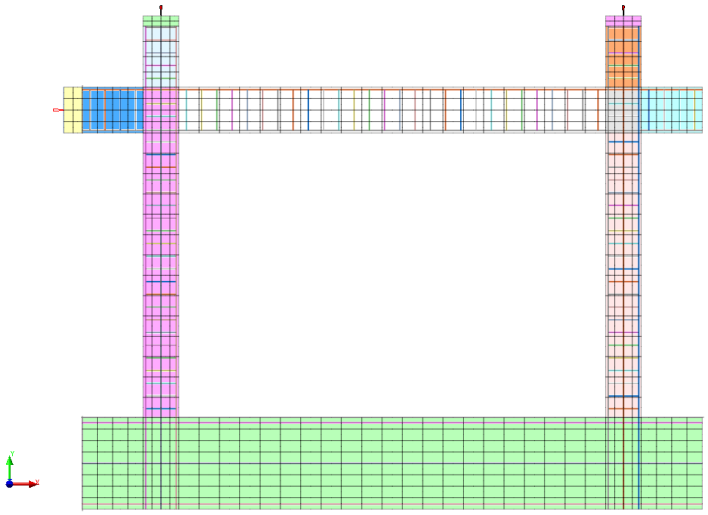

Figure 3-14. Finite element model for Specimen 1.

A similar study was conducted by Sattar (2013), but some differences were found compared with the original test results from Mehrabi et al. (1994). **Table 3-3** summarizes the main properties and the differences expressed above. For the present study, the original material properties reported

by Mehrabi et al. (1994) were used in the simulations, since the goal was to evaluate the predictive capabilities of the finite element modeling scheme.

Table 3-3 Material properties used for the analysis of Specimen 1.

Source	E (ksi)	f'c (ksi)	fy (ksi) $_{long}$	fu (ksi)$_{long}$
Mehrabi et al. (1994)	3180	4.48	61000	96000
Sattar (2013)	2800	4.00	70000	84100

Figure 3-15 shows the results of the NLFEA simulation of the Specimen 1. **Figure 3-15** (a) presents the reinforcing steel stresses where the first yielding of the longitudinal reinforcement is obtained. It can be appreciated a flexure-dominated behavior with yielding in tension at the bottom and inner part for both columns.

Figure 3-15 (b) presents the horizontal reinforcing steel stresses at the same time step in the analysis. It is noticed that the transverse steel still in the elastic regimen. **Figure 3-15** (c) depicts the principal stress contours for the concrete elements at the vertical and horizontal orientations.

In **Figure 3-15** (d) it is presented the shear stresses in the joint region, where large shear stresses are evident. **Figure 3-15** (e) shows the observed crack behavior at the expected locations based on the deformed shape of the structure. The crack pattern coincides with the tensile forces located at the outer part for both windward and leeward columns.

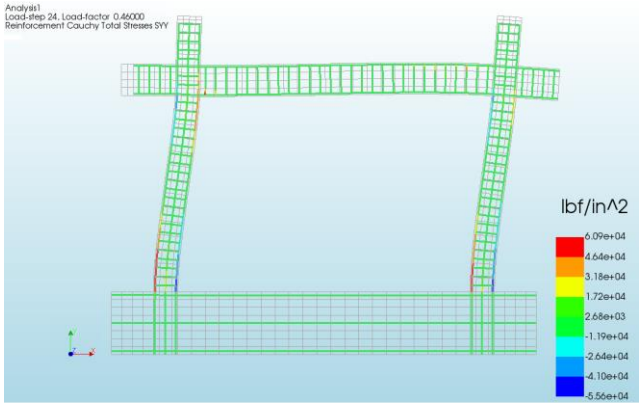

a) Cauchy total stresses SYY longitudinal reinforcement.

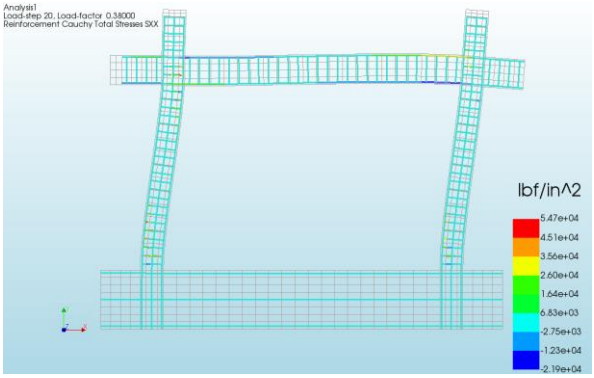

b) Cauchy total stresses transverse reinforcement

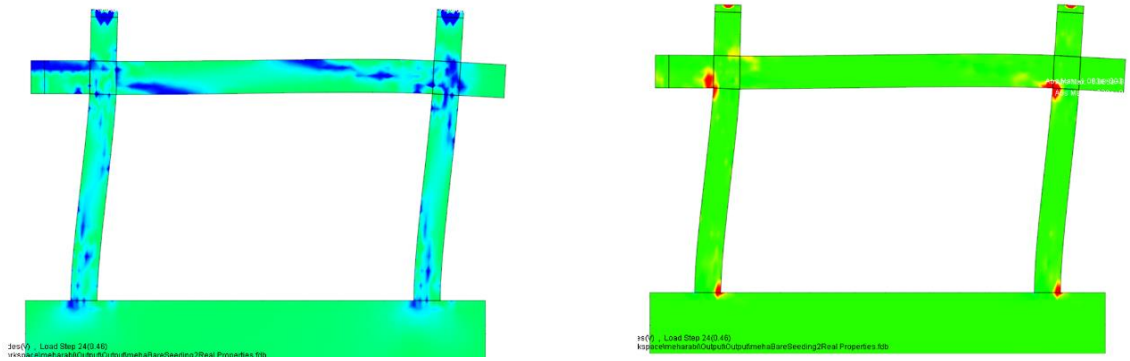

c) Principal S1, S2 stresses (@0.46 in.) concrete.

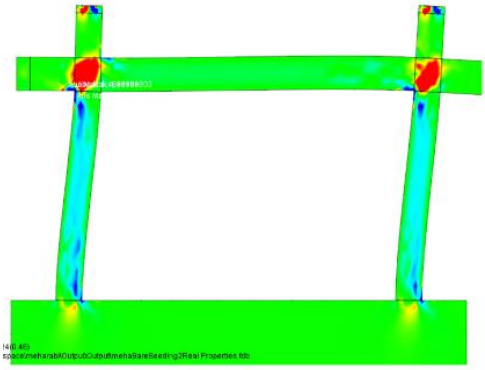

d) Principal Sxy stresses concrete

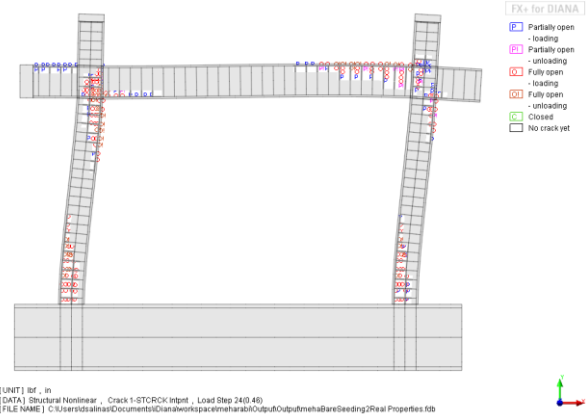

e) Crack behavior

Figure 3-15. Analysis results for Specimen 1 at 0.46 in. lateral displacement.

Figure 3-16 (a) depicts the pushover response obtained by Sattar (2013). This simulation was performed up to 2.0 in. lateral displacement. In a reasonable way, this adequately captures the initial stiffness and peak strength of the structural system.

Figure 3-16 (b) presents the result of the simulation obtained in this study using the un-calibrated material properties from by Mehrabi et al. (1994) and performed up to 3.0 in lateral displacement. Higher stiffness, underestimation of the displacement at peak stress, and an important softening after the peak stress were obtained. In the simulation by Sattar (2013), the post-peak behavior is unknown but it shows a tendency of having an important reduction.

The results presented in **Figure 3-16** (b) and **Figure 3-16** (c) have the same trends; i.e., high initial stiffness when they are compared with the test results (**Figure 3-16** (a) black line). This can be explained because Specimen 1 reported a flexure-dominated behavior, and none of the simulations presented in **Figure 3-16** included slip capabilities in the analysis. This supports the idea that using the given material properties provide reasonably good results. In addition, Specimen 1 was originally tested not with the idea to have a fully collapse, rather to obtain an initial estimate of the peak strength and initial stiffness of this system. This specimen was later repaired and this was infilled with URM wall.

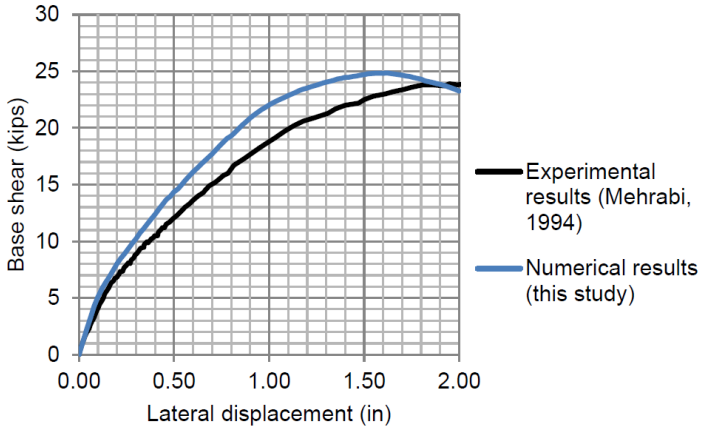

a) Pushover results from Sattar (2013)

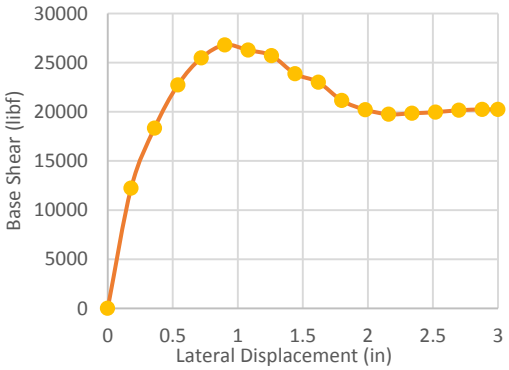

b) Pushover result in this study

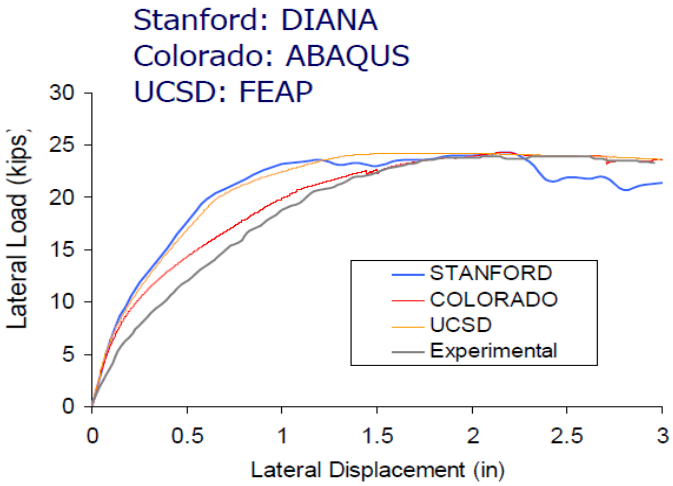

c) Pushover results from other researchers, from Shing et al. (2006).

Figure 3-16. Results of pushover analysis Specimen 1.

3.6.6. Analysis of Specimen 8

The mesh for the infilled frame, its geometry and details are shown in **Figure 3-17**. Two-dimensional, plane stress, four-node elements with four integration points were used for modeling the RCF and masonry units. The mortar bed, head joints and the mortar located at the perimeter of the infill wall (frame to infill interface) are modeled with interface elements as was presented

in Section 3.6. The remaining elements are identical to those used in the specimen 1. The URM infill bricks were discretized into two elements with an aspect ratio of 1. The gravity load was first applied in ten increments to the maximum and this was kept constant during the lateral displacement control loading.

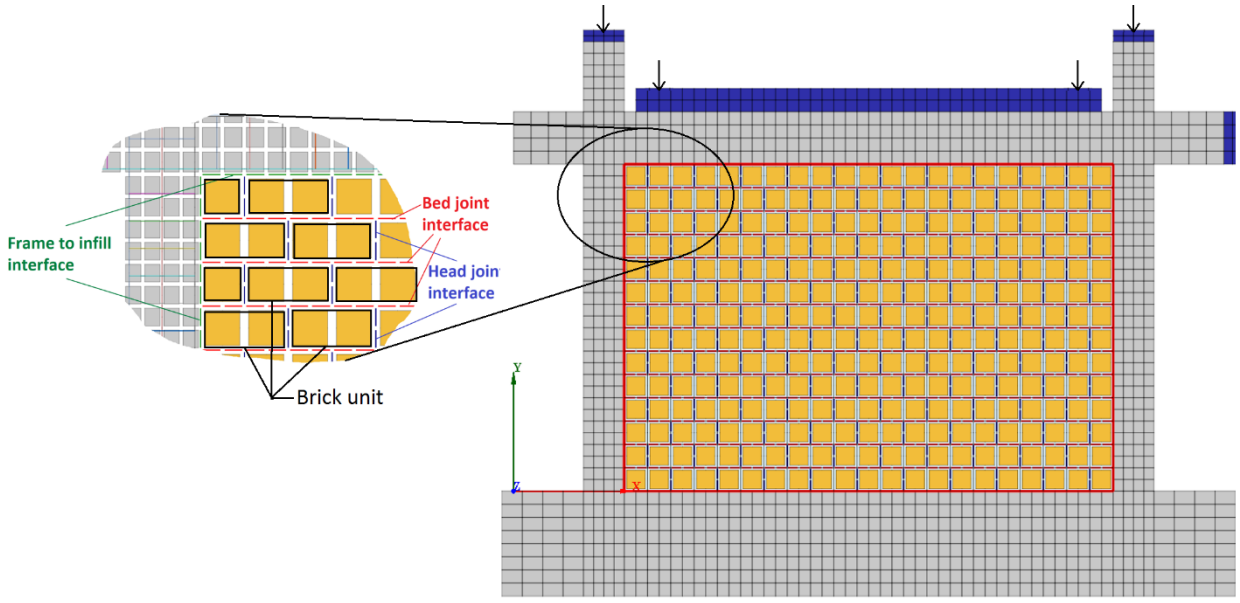

Figure 3-17. Mesh RCF with URM infill Specimen 8.

Al-Chaar and Mehrabi (2008) pointed out the need of adjusting the normal and shear stiffnesses of the mortar interface elements. The use of the stiffness values reported by Mehrabi et al. (1994) does not yield a good agreement between experimental and analytical responses. In fact, convergence problems are presented when the reported values are utilized. Thus the return mapping algorithm of the CSC model failed at the transitions zones between tension-shear or compression-shear corner zones Al-Chaar and Mehrabi (2008).

In order to overcome the convergence issues, trial analysis were performed using low normal stiffness. It was noticed that the vast majority of the gravity load was taken by the columns, since low normal stresses on the URM wall resulted in significantly lower lateral resistance for the infilled frame. Also, Al-Chaar and Mehrabi (2008) found that using lower shear stiffness for the mortar joints of the infill walls resulted to a significant underestimation of the initial stiffness of the specimen. Therefore, to find an agreement between analytical and experimental results, higher stiffness values need to be used in the calibration process Al-Chaar and Mehrabi (2008) decided to keep the stiffnesses at the lower values for all interfaces and to increase the theoretical width of joints to provide the higher overall stiffness required in order to match experimental results. However, to avoid unrealistic increase in the overall interface strength values it was necessary, to reduce the parameters affecting the strength (i.e., compressive strength, tensile strength, and cohesion) proportionally as the thicknesses are increased.

In general, it is considered unreasonable to artificially scale the stiffness and strength values for the objective of matching test results because: (1) for a desired target of strength and stiffness values there are many possible combinations of the parameters involved in the simulation which produce the desired output and, (2) the NLFEA simulations performed with those premises can be argued to lack physical meaning. When these studies were undertaken, the objective was to see if reasonable results could be obtained without resorting to artificial values like other researchers had done. This task proved impossible and provided impetus for the development of the nonlinear truss approach described in the next chapter; that approach eliminates the need of using artificial material properties or dimensions to obtain robust results.

Figure 3-18 shows the pushover curve for the specimen 8 compared with the NLFE model which includes the above recommendations. The lateral increasing displacement was carried out

to a maximum of 0.8 in. Despite that the results show a good agreement between the numerical and the experimental results, this required of an additional iterative calibration of the compressive fracture energy. The initial stiffness and peak stress were captured in a reasonable way, and the post-peak behavior was adequately represented.

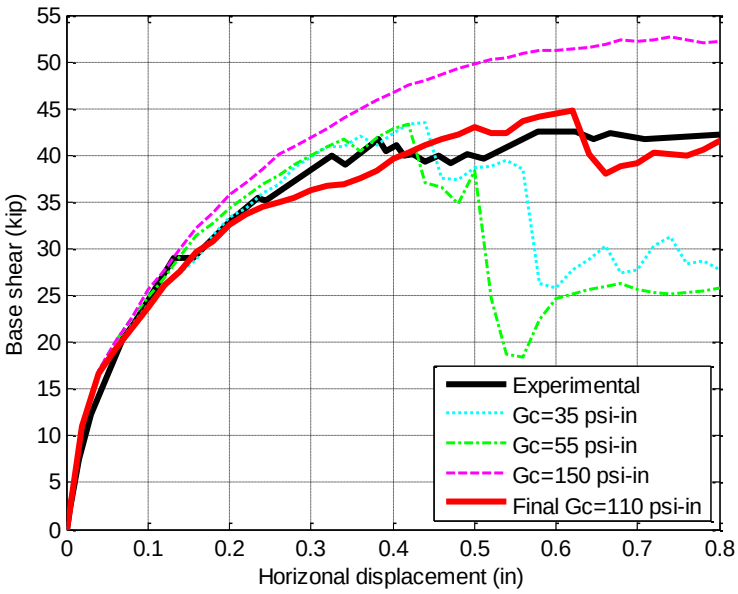

Figure 3-18. Pushover analysis Specimen 8.

To validate the lateral response obtained for Specimen 8, it is required to verify if the failure pattern match with the reported failure of this specimen. **Figure 3-19** (a) and (b) show a contour plot of the lateral displacement at loading step 32 (i.e. at 0.675 in. lateral displacement). It is depicted significant slip at bed and head joints (i.e. diagonal cracking). In fact, this behavior coincides with the type of failure reported for specimen 8. Mehrabi et al. (1994). Figure 6-30 (c) shows the stresses of the reinforcing bars aligned with the global "x" direction for the step 31 (i.e.

at 0.6 in. lateral displacement), this indicates yielding at the upper-inner part and external-bottom of the windward column, and the inner-bottom part of the leeward column.

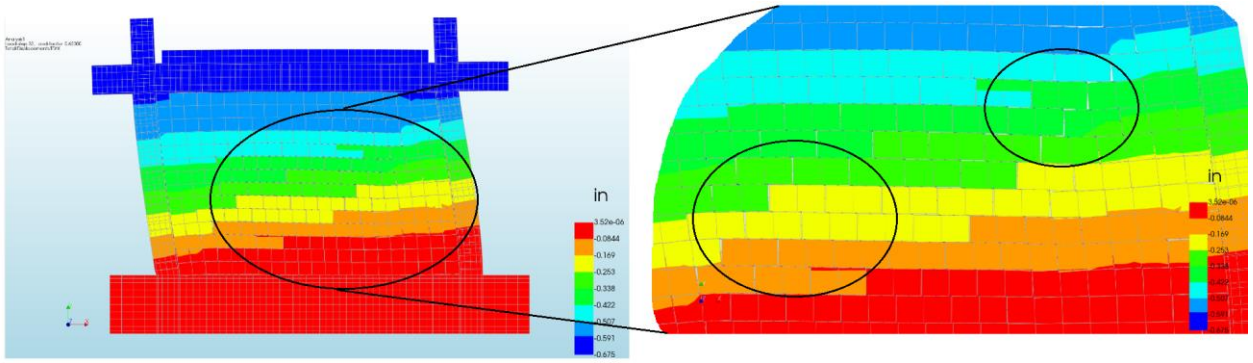

a) Lateral displacement at loading step 32 (0.675 in).

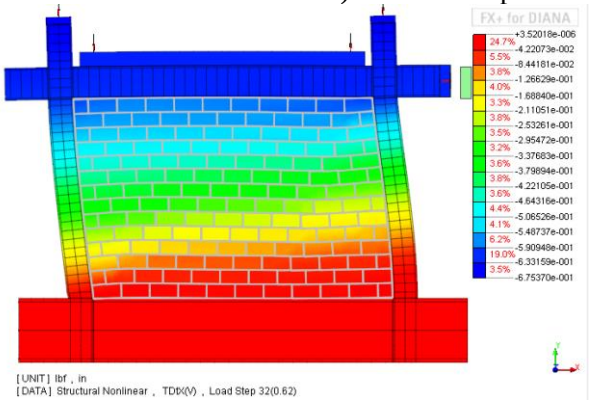

b) Lateral displacement at loading step 32 (0.675 in).

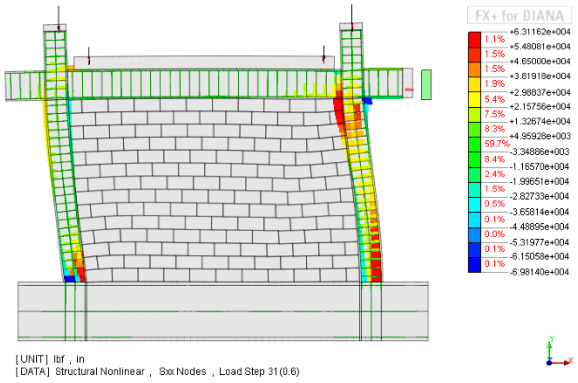

c) Reinforcement Sxx Stress Load step 31.

Figure 3-19. Mesh RCF with URM infill Specimen 8.

It is worth mentioning, the value of the mode-1 fracture energy recommended used by Al-Chaar and Mehrabi (2008) and Sattar, 2013 in their simulations seems to be too low when it is compared with the result obtained by Equation 3-2 (i.e about 5 times lower. GfI= 0.09 psi-in. used in the previous calibration process Vs GfI=0.48 psi-in.). Despite the acceptable results (**Figure 3-18**) obtained by using the lower value of mode-1 fracture energy the values of fracture energy,

tensile strength and element size "h" lead to a snapback in the stress-strain law after the peak tensile stress is reached. To prevent such snap-back behavior, (for a given fracture energy), it is necessary to increase the value of the ultimate tensile strain (ε_u).This can be accomplished by reducing the tensile strength of the material.

For completeness, the analysis has been repeated using the value of Gf^Iobtained from Eq. 3-2. **Figure 3-20** presents the results of the pushover analysis for Specimen 8. There is some discrepancy between the analytically obtained and the experimentally recorded force-displacement response. The discrepancy is attributed to the fact that the analysis does not account for the fact that the RCF had been initially tested and damaged as a bare frame, then repaired, provided with an infill wall and tested again. For this reason, the obtained results are deemed satisfactory.

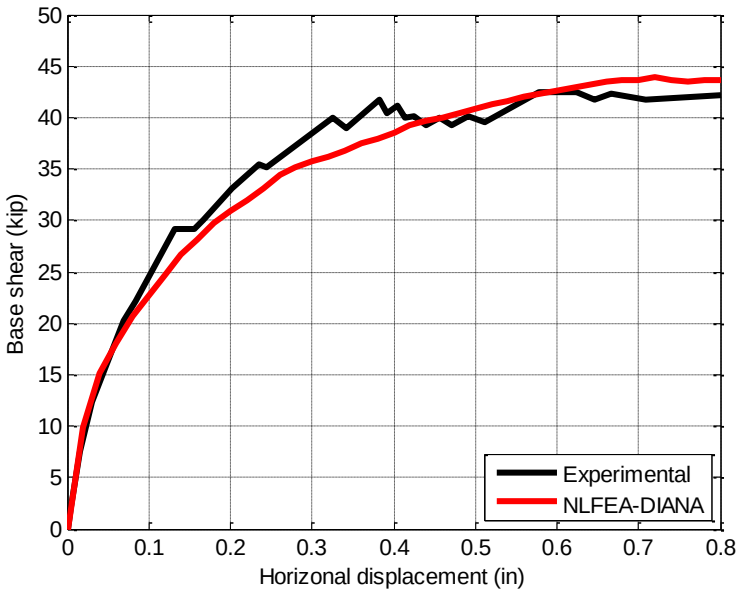

Figure 3-20. Pushover analysis Specimen 8.

3.7. Summary, and Comments

In this Chapter a brief background of nonlinear analysis of masonry-in filled RCF was presented. NLFEA procedures require complicated constitutive laws which involve many parameters to be calibrated and the use of special formulations such as those of cohesive crack interface elements to represent: (i) the complex behavior of mortar joints, (ii) the interaction between the frame and the infill walls, and (iii) to capture the displacement discontinuity presented in shear-critical elements. Lotfi and Shing (1991), Shing and Mehrabi (2002), Stavridis and Shing (2009), Koutromanos and Shing (2012) demonstrated that NLFE techniques can adequately represent: (i) the complex behavior, (ii) the failures modes, and (iii) the physical mechanisms leading to failure of reinforced concrete and masonry components.

The NLFEA simulations preformed in this chapter provided an invaluable insight about the implementation, overall complexity, strengths and shortcomings of this analytical technique. Indeed, NLFEA procedures require a high level of refinement, they are computational expensive, they involve elevated complexity and high level constitutive relationships that make them impractical to perform systematic parametric studies of multi-story, multi-bay structures. Next chapter, an innovative analysis technique is proposed and based on the concepts introduced in this chapter.

4. Nonlinear Truss Analogy (NLTA) Applied to RCF with URM Infills

As mentioned in the previous chapter, nonlinear finite element analysis can successfully capture the inelastic response and damage patterns of non-ductile, infilled RC frames. Still, finite element analyses are conceptually complicated, because they require the use of special formulations such as those of cohesive crack interface elements, and of complicated constitutive laws which involve many parameters to be calibrated. The fact that it is not possible to deduce all the values of the material parameters from material tests implies that the analytically obtained results will be governed by uncertainty. Furthermore, finite element analyses are computationally demanding, which means that it may be difficult – if at all possible – to conduct systematic parametric studies of prototype, multi-story structures.

An alternative to finite element analysis is the use of simplified models based on the equivalent strut concept. However, as mentioned in Section 2.3, strut models cannot realistically represent the interaction of the frame with the infill wall. Given the above, there is still a need for a computational tool which is accurate enough to capture the salient features of response, and computationally efficient to allow extensive parametric investigations. To address this need, the present Chapter describes an analysis technique for infilled frames, based on the nonlinear truss analogy.

4.1. State of the Art Review

Since the early 1900s, truss-oriented approaches have been using in the representation of RC components (Ritter (1899), Withey (1907), Morsch (1920)). More recently, many researchers have used successfully nonlinear truss models, also known as lattice models, for capturing the nonlinear response of two-dimensional and three-dimensional structures including: To et al. (2001), To et al. (2003), Park and Eom (2007), Panagiotou et al. (2012), Lu and Panagiotou (2014), Moharrami et al. (2015).

The idea for using strut-and-tie model was intended to address the design of structural members which have high irregularity in terms of internal stress and strain distributions. These make inapplicable traditional Bernoulli-type elements in analysis. These sections are known in the literature as disturbed stress and strain regions. Examples of disturbed regions include: deep beams, stepped beams, corbels, and anchor zones in posttensioning beams. The advantage of strut-and-tie models is their overall simplicity because they transform a complex problem into a truss analogy which relies on simplified uniaxial stress–strain laws. In the Nonlinear Truss Analogy (NLTA) applied in the analysis of RC elements, the elements areas are lumped into an arrangement of vertical, horizontal and diagonal elements. For the case of longitudinal and transverse rebar members, only a predefined set of vertical and horizontal elements is used. For the concrete portions, additional diagonal elements are placed with the idea of representing the diagonal compressive stress field of concrete.

Hrennikoff (1941) was the first in using truss models for solving problems in elasticity. Vallenas et al. (1979) used the truss analogy to calculate the shear deformation of a multistory wall structure subjected to monotonic loading. In this approach, each story was modeled with one

diagonal strut member to account for the concrete diagonal compression field whereas the tensile contribution was neglected. Hiraishi (1984), modified Vallena's work by adding a bottom truss cell comprised of non-prismatic truss elements with elastic-plastic material laws. The cross-sectional area of each truss element is calculated based on the stress along the height of the vertical truss elements. The inelastic activity was assumed to be located at the first story, so upper stories were modeled with rigid elements. The same idea used by Hrennikoff (1941) is used by Mazars et al. (2002). Whereas, Hrennikoff used elastic elements, Mazars used multiple truss cells comprised by vertical, horizontal and diagonal nonlinear elements.

Park and Eom (2007) refine the NLTA. In their formulation, the RC components are idealized as a composite element comprised by a vertical, horizontal and diagonal elements. The concrete element is idealized as a truss element subjected to cyclic compression and tension. Regarding the applied constitutive laws, the compressive and tensile envelope are defined accordingly Saenz (1964) and Mansour et al. (2001). The unconfined concrete is based on Foster and Gilbert (1996) while that for confined concrete is based on Mander et al. (1988) and Zhang and Hsu (1998). For the reinforcing steel, Brown and Jirsa (1971) was used. For the diagonal elements, the MCFT Vecchio and Collins (1986) was applied.

Panagiotou et al. (2012) enhanced NLTA. In this formulation, more advanced constitutive laws are applied for concrete and steel. The concrete model allows to capture the strength and stiffness degradation due to inelastic compressive and tensile strains. Its compressive envelope (confined or unconfined) is based on the Fujii concrete model Hoshikuma et al. (1997), and the softening in tension can be described by: (a) tri-linear or (b) nonlinear (based on the tension stiffening relation of Stevens et al. (1991). For the diagonal members, two additional nodes placed at the opposite diagonal members that comprise the truss cell that serve as virtual gauge to calculate the transverse

strain. This transverse strain is used to reduce the peak strength accordingly with the MCFT (Vecchio and Collins (1986)). The steel constitutive law is the one Menegotto and Pinto (1973) so this includes both a yield plateau and the Bauschinger effect capabilities. In addition, this approach proposes a way to account for the mesh-dependent behavior by regularizing the elements with the panel length used in derivation of the MCFT. This strength reduction and also the concrete model were implemented by Lu and Panagiotou (2014) in OpenSEES with the name of truss2 element and Concretebeta material, respectively, making easier its implementation in this platform.

Despite the fact that truss models add some extra complexity when compared to traditional beam models, the advantages are that truss models are conceptually simple, easy to understand and implement, computationally efficient, and easy to calibrate. They can inherently capture the axial-shear-flexure interaction and are not vulnerable to the stress locking effect. Furthermore, when they are used with or without other elements, they can capture not only strength and stiffness degradation in a satisfactory manner, but also the damage patterns. Finally, NLTA models are less computational expensive than NLFEA models. For all reasons NLTA is the selected approach for dealing with the NL Analysis of RCF with URM infills.

4.2. Description of the Model

In a truss model, the RC components are represented by an assemblage of horizontal, vertical, and diagonal truss elements. **Figure 4-1** depicts the idealization of the RCF and URM infill. Moharrami et al. (2015) have shown that the NLTA can capture the hysteretic response and strength degradation of shear-dominated RC columns. The present study combines the approach of Moharrami et al. (2015) with an approach to describe the masonry infills and the potential

localized damage in the mortar joints, as well as the infill-to-frame interfaces. The proposed methodology uses in the open-source software OpenSEES McKenna et al. (2000). Appendix D presents the most relevant aspects related with the implementation in OpenSEES.

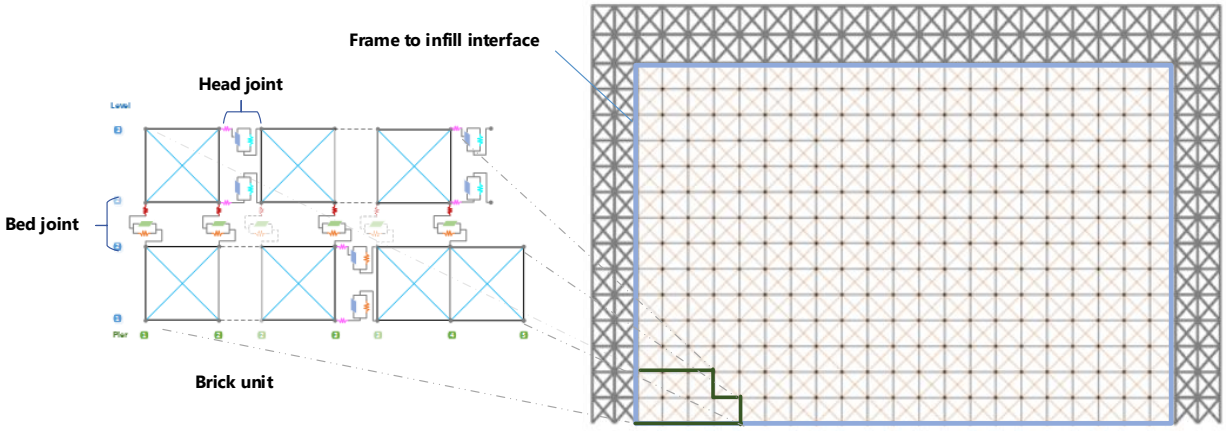

Figure 4-1. Schematic overview of truss modeling approach for masonry infill walls and infill-to-frame interfaces.

4.2.1. Determination of Truss Geometry

This section establishes a procedure to obtain the area of the truss elements representing the infill masonry and the RC frame members. **Figure 4-1** indicates that a truss model can be considered as the assemblage of multiple truss cells, each cell consisting of two horizontal, two vertical and two diagonal elements. The size of the cells in the analysis of infilled frames is governed by the dimensions of the infill masonry units. For this reason, the discretization of the masonry infill is described first. Appendix D.3.2 presents a guidance about these calculations.

4.2.1.1. Masonry Infill

In this study, it is proposed that every single brick be represented by an arrangement of vertical, horizontal and diagonal elements calculated according its tributary length as depicted in **Figure 4-2**. The cross-sectional area for vertical and horizontal element is calculated as the product of the tributary length and the thickness. For the diagonal elements, the equation proposed by Lu and Panagiotou (2014) is applied.

Once the infill mesh is defined, this mesh defines the path to be followed in terms of the amount of the beam discretization in the horizontal direction, and for the discretization of the column in the vertical direction. Eq. 4-1 to 4-5 are used to obtain the cross-sectional area of the truss elements to represent the brick unit.

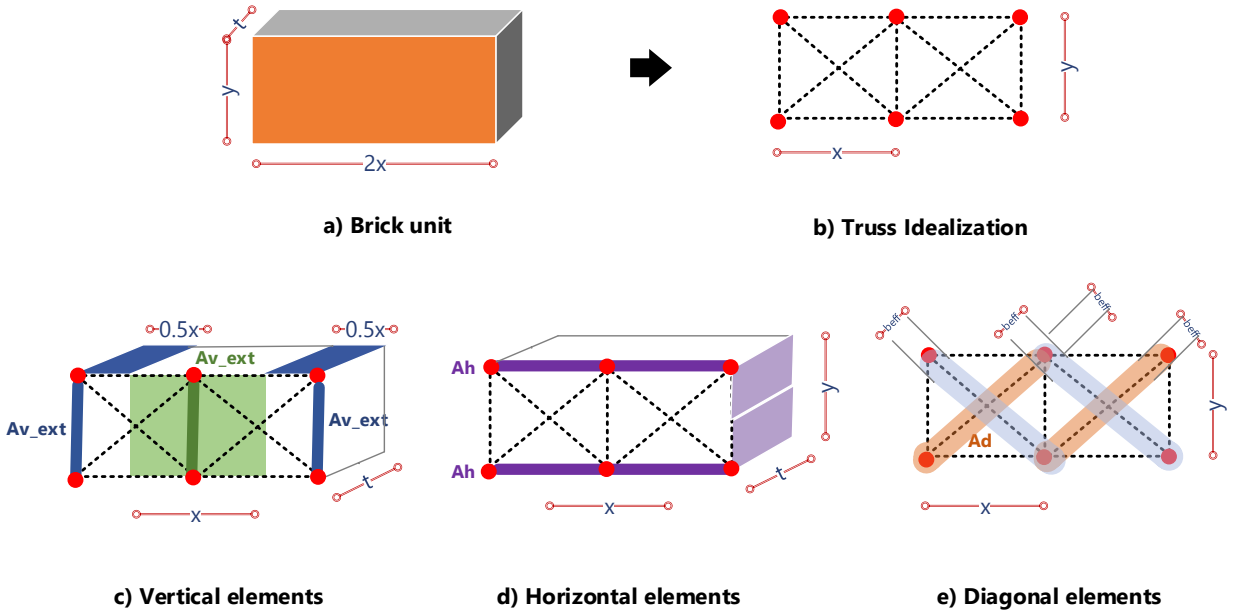

Figure 4-2. Schematic description of brick idealization in NLTA.

$$Av_{\_ext} = (0.5x)(t) \quad (4\text{-}1)$$

$$Av_{\_int} = (x)(t) \quad (4\text{-}2)$$

$$Ah = (0.5y)(t) \quad (4\text{-}3)$$

$$Ad = \left(b_{eff}\right)(t) \quad (4\text{-}4)$$

$$b_{eff} = (x)\sin\left(\operatorname{atan}\left(\frac{y}{x}\right)\right) \quad (4\text{-}5)$$

4.2.1.2. Beam and Column Elements

The cross-sectional areas of the truss elements are determined in accordance with the work of Moharrami et al. (2015) **Figure 4-3** (a) depicts the truss model idealization procedure involved in the determination of vertical, horizontal and diagonal cross-sectional areas of concrete and RC elements for a typical column. The discretization for the beam is applied in the same fashion. Again, the height of the vertical elements is determined by the brick height, and for the external vertical elements, those are placed at the location of the centroid of the external principal reinforcement. **Figure 4-3** (b) presents the graphical representation of the required calculations to calculate the cross-sectional area for the truss elements. This procedure is also applicable to the case of beam elements. It is worth mentioning that the study by Moharrami et al. (2015) had also established an expression to determine the inclination angle of the diagonal elements in truss models of RC columns. Such approach is not adopted herein; future studies can pursue an investigation of the effect of this inclination angle on the analytical results for infilled frames.

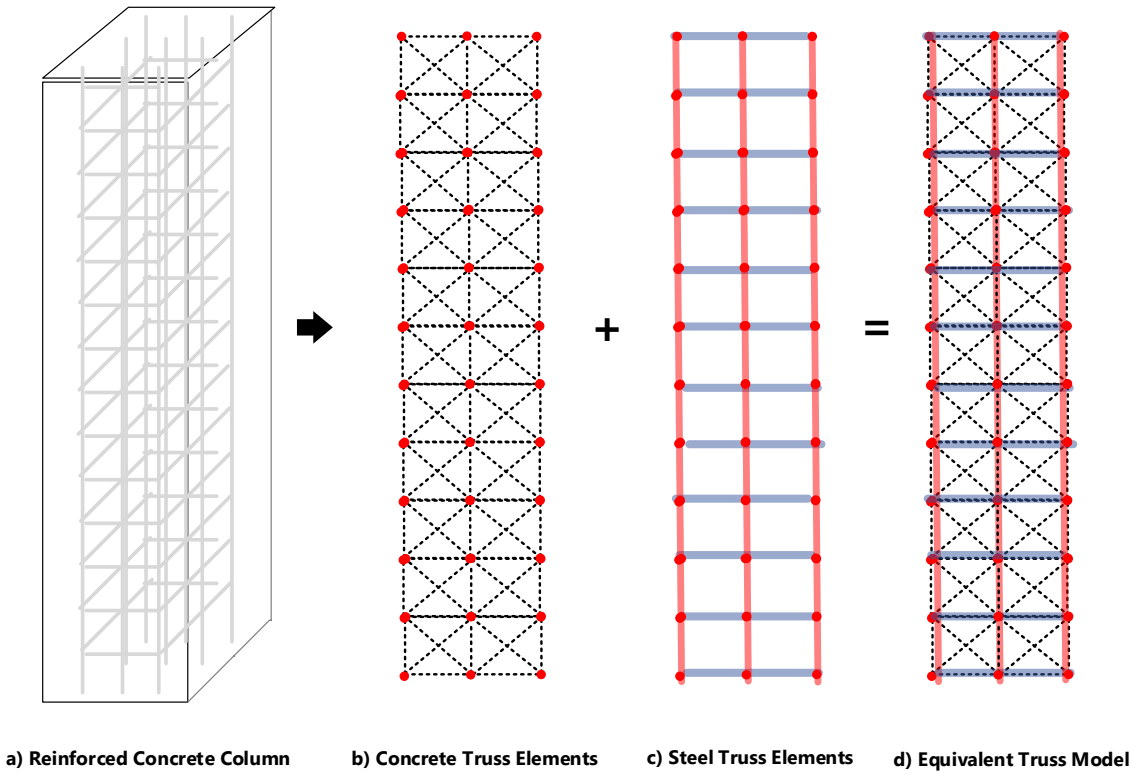

a) Truss model idealization.

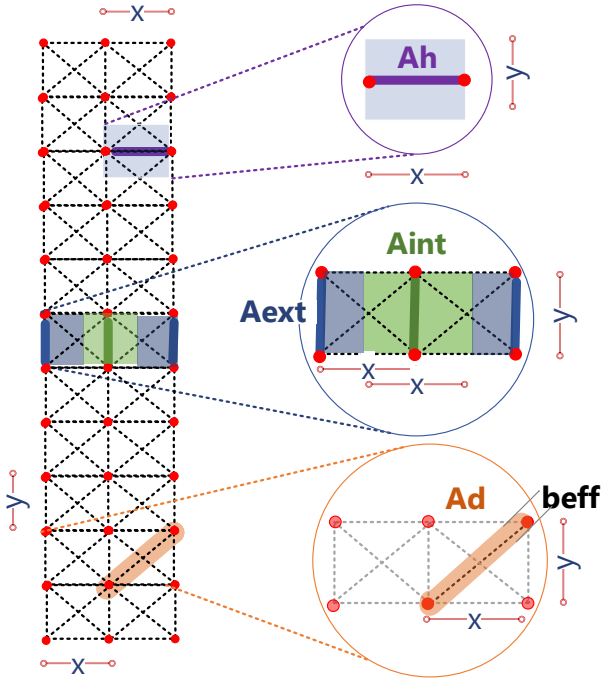

b) Cross-sectional areas for concrete in truss model.

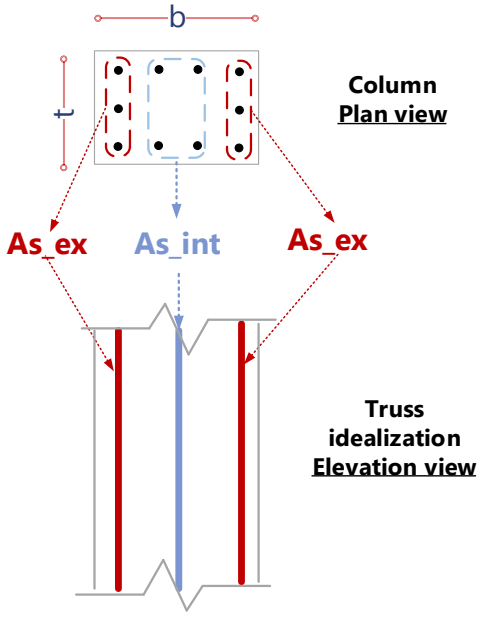

c) Cross-sectional areas for longitudinal steel in truss model.

Figure 4-3. Schematic description of column idealization in truss models.

4.2.2. Material Constitutive Stress-Strain Relationships

The nonlinear truss geometry is supplemented by constitutive models to capture the nonlinear response of concrete, masonry and steel reinforcement. This section provides an overview of the constitutive laws employed herein. Appendix D.2 presents an exemplification of the required input values and the calculations required to implement these constitutive models in OpenSEES.

4.2.2.1. Concrete and Masonry Units

The behavior of concrete and masonry is described using the stress-strain law of Panagiotou et al. (2012). This Material constitutive stress-strain relationship can capture the strength and stiffness degradation due to the development of inelastic compressive and tensile strains. The compressive envelope, up to the peak compressive strength either unconfined or confined is based on the Fujii concrete model Hoshikuma et al. (1997). **Figure 4-4** depicts this model. From zero stress to point "a" on **Figure 4-4**, a quadratic curve is presented. Then from point "a" to point "b," a cubic curve is used. At this point, a plateau region from the confined peak strain is presented (From point "b" to "c" on **Figure 4-4**), then linear softening to zero stress reaching the ultimate confined strain ε_{cu}. Unconfined concrete follows the same path up to the point "a" on **Figure 4-4** followed by a linear softening up to unconfined ultimate strain ε_{cu}. The unloading is made by using a nonlinear function until zero stress is reached. Then, a linear curve intercepts the point of maximum prior tensile strain. The softening in tension can be described by either a (a) tri-linear or (b) nonlinear relationship based on the tension stiffening relation of Stevens et al. (1991). Recalling that the tension stiffening phenomenon is the indirect increases in stiffness of a cracked RC member due to the restriction applied by the reinforcement. Once a RC member cracks, the

concrete located between the cracks tends to return to the unstressed state but it is restrained by the reinforcement. As a consequence, tensile stress is developed in the concrete which increases the reinforcement material stiffness.

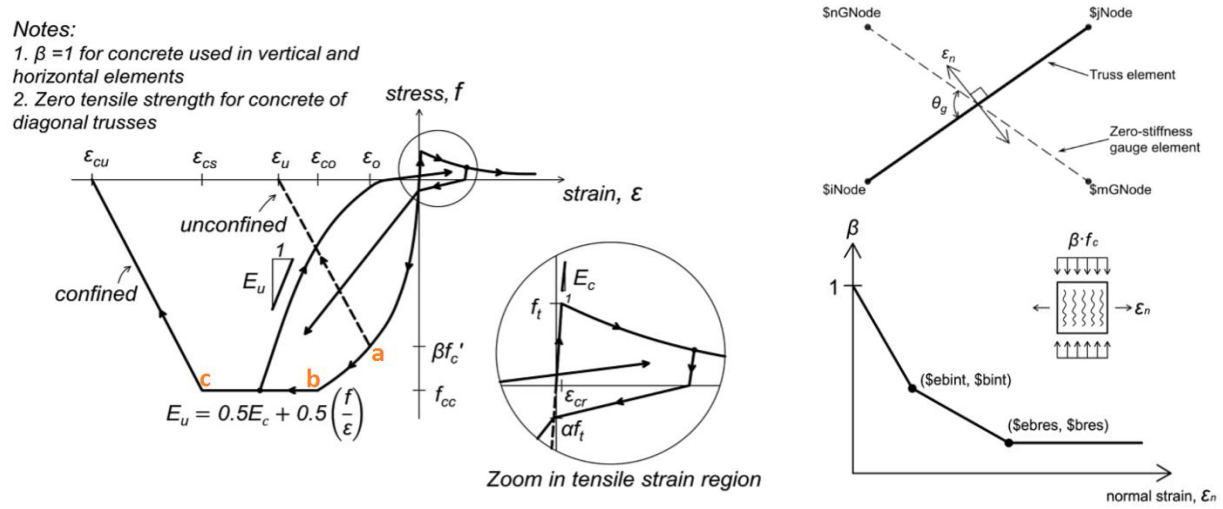

Figure 4-4. Constitutive model for concrete and brick units modified from Lu and Panagiotou (2014).

The specific constitutive law can also account for the effect of transverse tension on the concrete compressive behavior. To this end, an additional pair or nodes needs to be defined for each diagonal element to allow the computation of the transverse strain. The transverse strain is in turn used to calculate a reduction coefficient, β, that multiplies the compressive stresses of the diagonal elements and varies with the transverse strain as shown in (**Figure 4-4**). To prevent the occurrence of spurious mesh size effects on the analytical results, the softening portions of the constitutive models need to be regularized, i.e. adjusted with element size. The spurious mesh size effect is associated with localization of inelastic or fracturing strains (Bazant and Planas (1998),

Coleman and Spacone (2001), Panagiotou et al. (2012), and Lu and Panagiotou (2014). In the present study, the regularization is based on the assumption that the reference stress-strain laws which are defined correspond to an element size of 23.62 in. This value is based on the length over which average strains were measured in the concrete panel tests by Vecchio and Collins (1986).

4.2.2.2. Steel

The stress-strain relationship steel used here in the vertical, and horizontal elements is the Giuffré-Menegotto-Pinto model (GMP) Menegotto and Pinto (1973). The GMP is characterized by a monotonic envelope curve with linear hardening after yielding. **Figure 4-5** shows the model is described by a smooth curve asymptotic to the tangent lines at the point of stress reversal and at the point of the maximum/minimum strain in the loading history (Maekawa et al. (2003)).

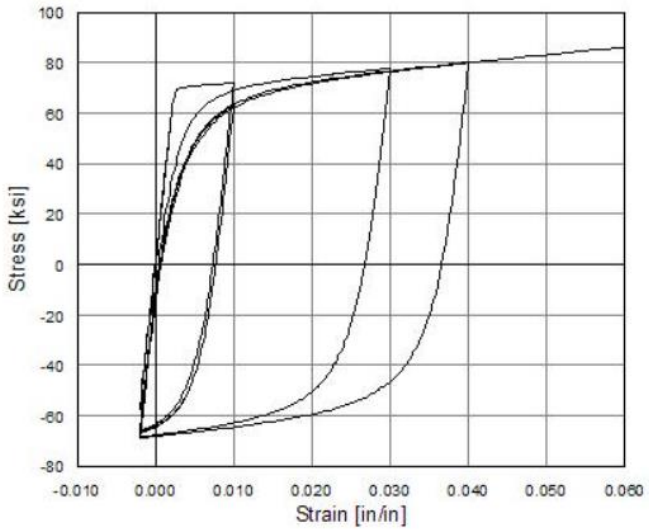

Figure 4-5. Constitutive model for steel. GMP model in OpenSEES McKenna et al. (2000)

The parameters controlling the transition between the elastic and plastic branches Filippou et al. (1983a) were as follows: c_{R0}=20, c_{R1}=0.925, c_{R2}=0.15 with isotropic strain hardening parameters of a_1=0.05, a_2=1.0, a_3=0 and a_4=1.0. The geometric nonlinearities such as bar buckling and bond slip, and strain penetration at the base were not considered in this study.

4.2.3. Accounting for the Mortar Joints in the Truss Models

The mortar joints and infill-to-frame interfaces need to be explicitly modeled in the analyses, since they constitute weak planes where localized tensile opening or shear sliding can occur. Additionally, it is necessary to capture the contact stress distribution along the infill-to-frame interface with adequate accuracy. A model for the mortar joints and infill-to-frame interfaces should be capable of capturing the following: (a) normal opening and closure, (b) shear sliding, and (c) the increase of shear sliding resistance due to normal compressive stress. As a consequence, **Figure 4-6** (a) presents a schematic representation of the bed joint zero-length mortar interface connecting two bricks prism idealized using the truss model. The nonlinear behavior associated to the interface is represented for an arrangement of zero-length elements intended to capture the behavior of the mortar joints. **Figure 4-6** (b) and (c) present the tensile and shear-slip behavior of the proposed interface model. The following sections explain the rational of the incorporated elements. Appendix D.3.3 presents an exemplification of the implementation of the interface in OpenSEES.

4.2.3.1. Tensile Behavior

The cohesive part of the normal resistance is modeled by zero-length element assemblages depicted in **Figure 4-6** (a). This is accounted for using the generic hysteretic material which is available in OpenSEES. The envelope curve in this model consists of multiple linear segments with no compressive resistance. The calibration used in the present study establishes an initial linear softening segment, up to a zero residual tensile strength as shown in **Figure 4-6** (b). The softening part is so calibrated that the area under the diagram equals the mode-I fracture energy of the interface. The cohesive part of the normal resistance is only important for tensile stresses, and the compressive resistance is contributed by the linear normal stiffness of the flat slider bearing elements. For this reason, the compressive resistance in the hysteretic material is set equal to zero.

4.2.3.2. Shear-Slip Behavior

The cohesive part of the shear resistance is comprised by two elements connected in parallel **Figure 4-6** (c). The first element is a zero-length element defined in the same fashion as the tensile spring with a bilinear softening forming a triangular shape with the cohesive stress defined as peak value and the area under the shear displacement diagram $(\tau - \delta_{shear})$ matching the mode-2 fracture energy. The second element is the flat slider bearing (FSB) element Schellenberg (2012). The FSB called "slider" **Figure 4-6** (c) is for accounting shear frictional-slipping deformations and for providing normal elastic stiffness to the system. This element requires the definition of a friction model which specifies the behavior of the coefficient of friction in terms of the absolute sliding velocity and the pressure on the contact area. In the proposed model, a Coulomb friction

models is used. In the model definition, the initial node represents the flat sliding surface and the end node represents the slider as is depicted in **Figure 4-7**.

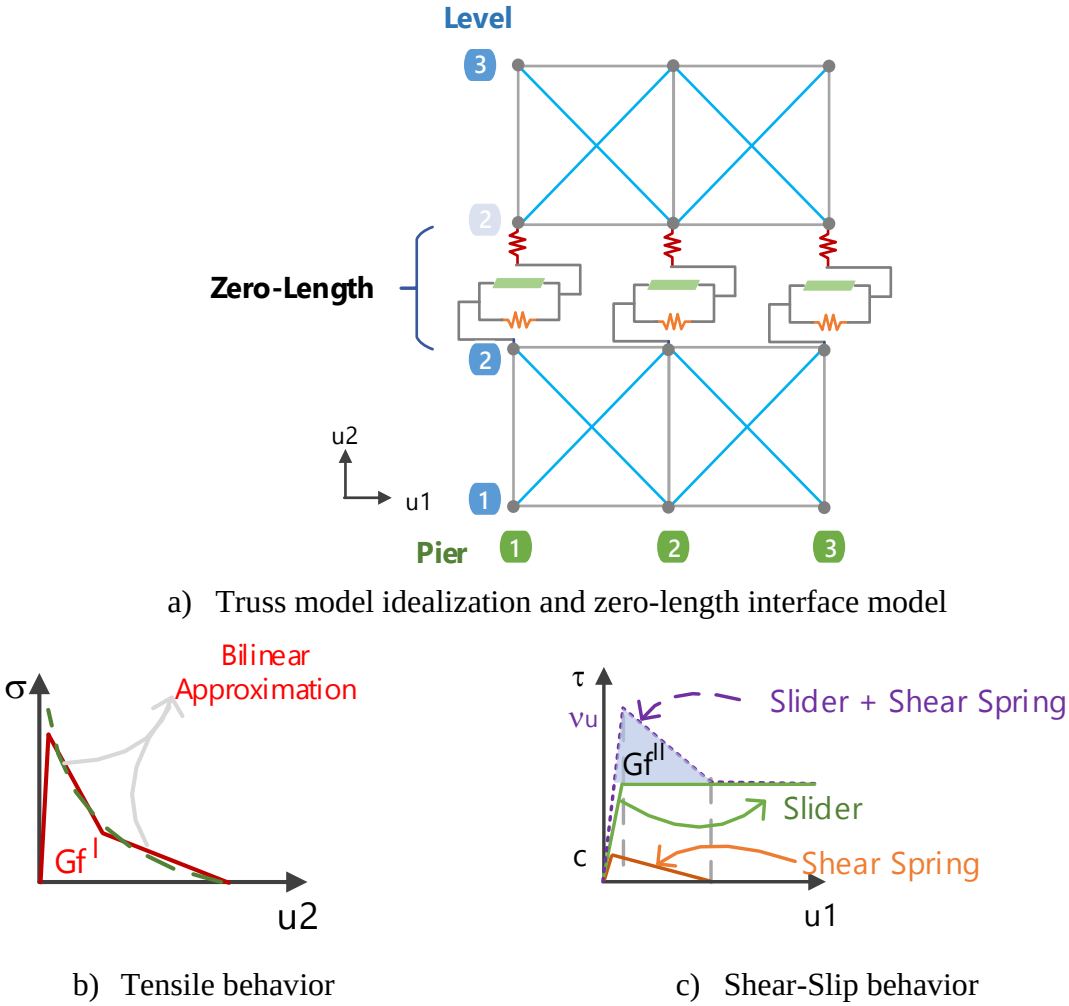

a) Truss model idealization and zero-length interface model

b) Tensile behavior

c) Shear-Slip behavior

Figure 4-6. Proposed modeling scheme for capturing mortar Interface.

Recall, the fracture energy mode II (Gf^{II}), is defined by the integral of the shear stress and the shear displacement diagram ($\tau - \delta_{shear}$) in the absence of confining pressure. The shear sliding resistance corresponding to zero normal compressive stress is commonly referred to as the cohesion, c. Typical values of cohesion range from 30 to 130 psi, and for the fracture energy mode

II, a common assumption is to set it as 10 times the value of the fracture energy mode I (Crisafull and Carr (2007, Sattar (2013, Mehrabi et al. (1994, Koutromanos (2011)).

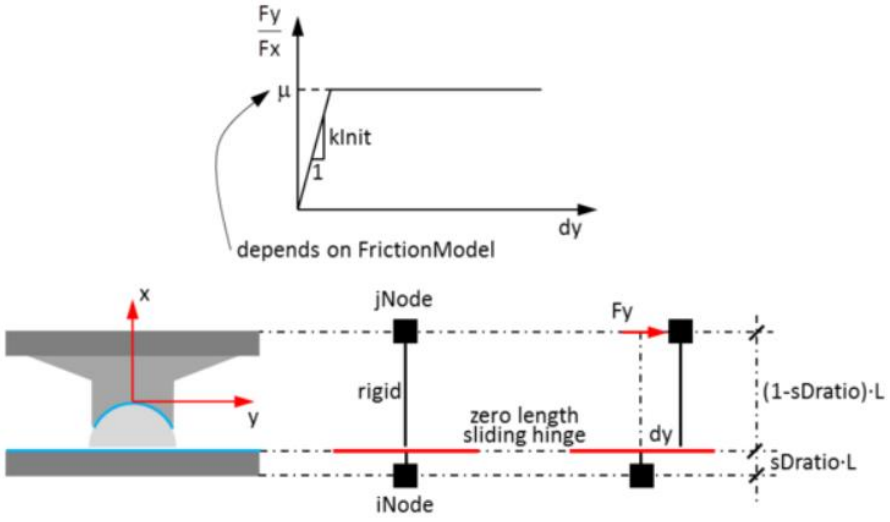

Figure 4-7. Flat slider bearing element with coulomb friction model from Schellenberg (2012).

To demonstrate the behavior of the flat slider element in OpenSEES, a single-element analysis is conducted for an element subjected to a cyclic shear displacement history under a constant applied vertical compressive force of 20 kips **Figure 4-8**(a).

Note that for those given properties the maximum shear load and the displacement at which sliding is presents are 17 kip and 0.034 in. respectively. First, a cycle with amplitude equal to 0.033 in. is applied **Figure 4-8** (b), followed by a cycle with an amplitude of 0.049 in. **Figure 4-8** (c).

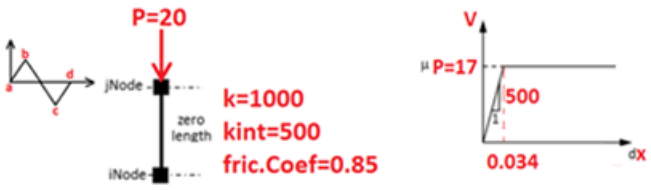

a) Slider input data

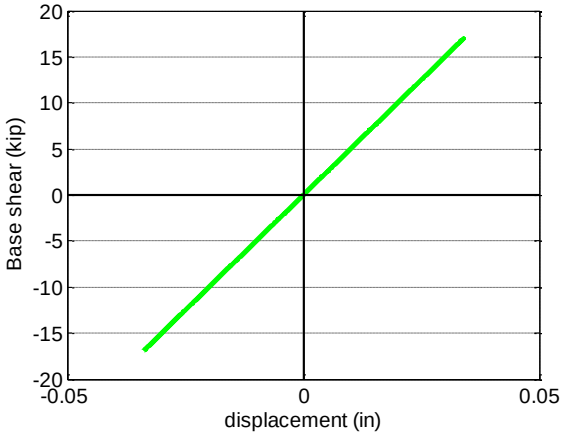

a) cycle with an amplitude of 0.033in

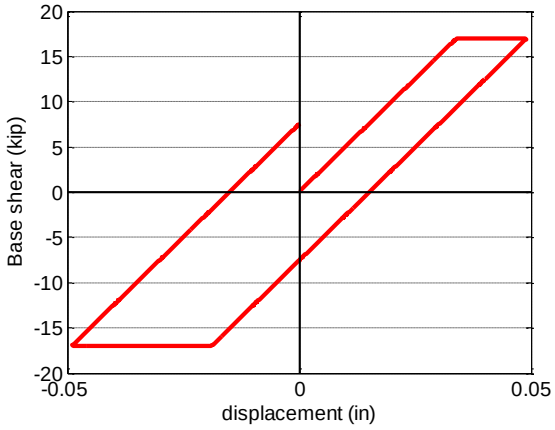

b) cycle with an amplitude of 0.049 in

Figure 4-8. Exemplification of flat slider bearing element with coulomb friction model.

Two important considerations with regard to the slider definition need to be clarified:

I. In the definition of the slider in conjunction of the NLTA, a predefined uniaxial material law in the axial direction is required. The elastic slope of the uniaxial law in the axial direction includes a penalty stiffness to ensure a stiff connection between the interboundary elements so as to mimic the contact condition. As is usual behavior in continuum interfaces, the proposed non-continuum version requires the definition of a dummy value for the constant "k" in **Figure 4-8**. This penalty stiffness value need to be large enough to limit the element interpenetration, but at the same time small enough to avoid numerical problems during the analysis. A recommended value can be

obtained by dividing the modulus of elasticity of the mortar joint by the height of the mortar joint, and

II. A consistent local axes definition is required. For the second consideration, in **Figure 4-9** presents the local axis definition applied for the frame infill interfaces. Note that it is very important to intuitively grasp the local axes definition in the force transfer mechanism. A non-consistent definition can cause element overlapping (i.e poor connectivity), and in some cases it can convert a well-condition problem into an ill-conditioned problem. If a poor definition of the local exes is applied and interpenetration is presented, the level of interpenetration has nothing to do with the value of the penalty stiffness used in the definition of the uniaxial law associated with the axial direction. For that reason, it is imperative that local axes definition be applied in a consistent manner.

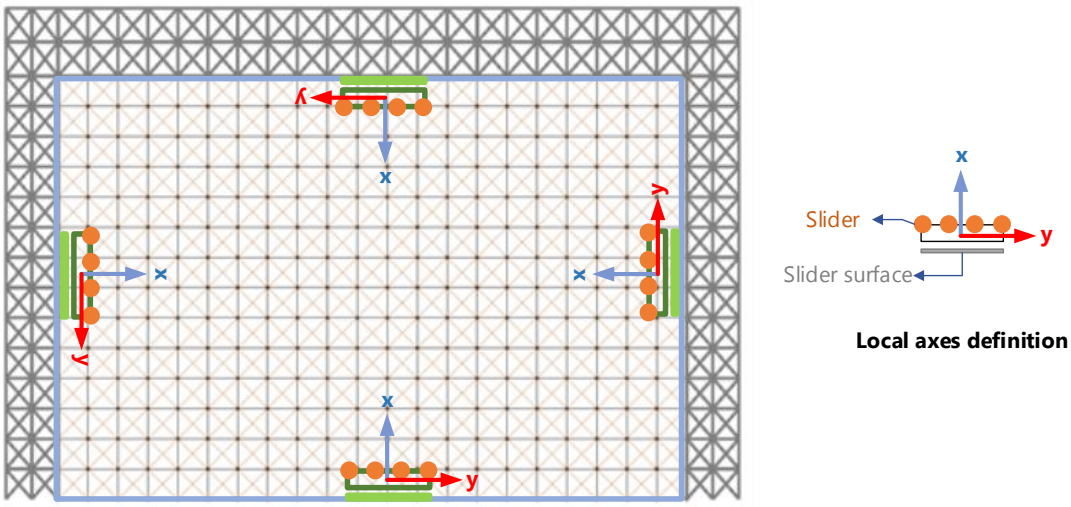

Figure 4-9. Definition of local axes for frame-to-infill interface elements.

4.3. Interface Verification and Calibration of Element Assemblages for Interfaces

This section presents several analyses to verify the capability of the element assemblages to describe the response of the joints and infill-to-frame interfaces for some simple loading scenarios.

Table 4-1 Material properties used in the interface calibration.

ft (psi)	Gf^{I} (psi-in)	C (psi)	Gf^{II} (psi-in)	Kint (kip-in)	k (kip-in)
40	0.5	40	5	110	10000

where: ft is the tensile resistant of the mortar interface, Gf^{I} is the fracture energy mode I, C is the cohesion of the mortar joint, Gf^{II} is the fracture energy mode II, and Kint and k are the slider stiffness and penalty stiffness. They were schematically presented in **Figure 4-8**.

4.3.1. Tensile Behavior

A first analysis is conducted for mode-I displacements, i.e., normal tensile opening, of a mortar interface. **Figure 4-10** (a) shows two-brick model subjected to a tensile displacement-controlled analysis applied at the top brick, name herein this section as OpenSEES NLTA. The results are compared with the FEA of the CSC model. **Figure 4-10** (b) shows the proposed interface model tested under uniaxial tensile displacements. The response indicates that the proposed interface model – if properly calibrated - can represent the tensile behavior of the interface in terms of peak tensile stress and softening.

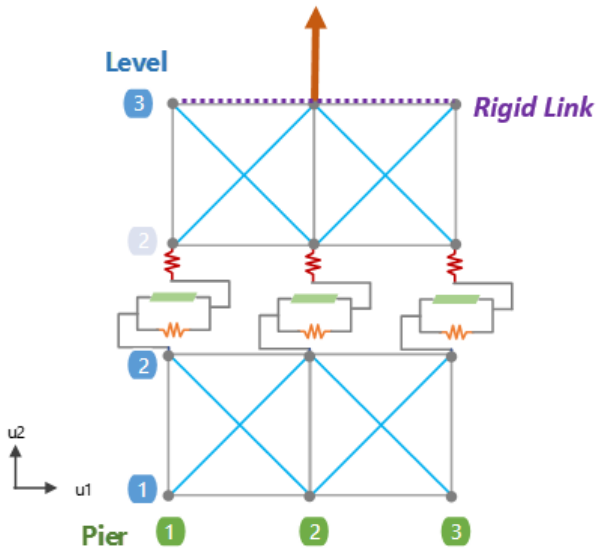

a) Proposed model.

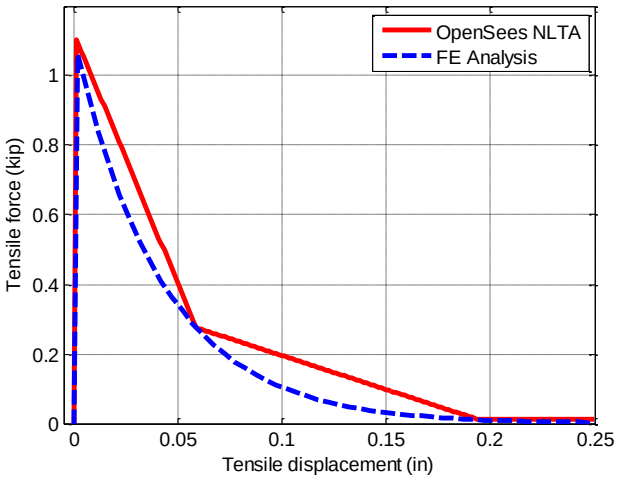

b) Comparison of NLFEA vs NLTA interface behavior in tension

Figure 4-10. Tensile interface model.

4.3.2. Monotonic Shear Behavior

In **Figure 4-11**, the shear-slip response of the proposed interface model is presented. **Figure 4-11** a) depicts a two-brick model subjected to a lateral displacement-controlled analysis applied uniformly at the top brick. **Figure 4-11** b) is shown the disaggregation of the shear-slip response. In this two brick model, the shear response is comprised of two parts:

I. the Slider (green dashed line) which: (a) controls the slip along the brick surface, (b) calculates the increasing in lateral strength due to the presence of the axial load based on the Coulomb friction model, (c) controls the level of interpenetration by the introduction of a penalty stiffness value, and (d) provides elastic compressive stiffness to the system, and

II. the cohesive part (solid red line) represented by a shear spring.

The total response (solid magenta line in **Figure 4-11** b)) represents the equivalent, or total shear-slip response. In **Figure 4-11** c) the shear monotonic versus the shear displacement response is presented. The figure indicates that the proposed interface model adequately represents the monotonic shear behavior of the interface in terms of initial stiffness, peak shear stress, and subsequent softening. Discrepancies result from the linear behavior assigned to the cohesive part whereas the FEA model incorporated an exponential softening.

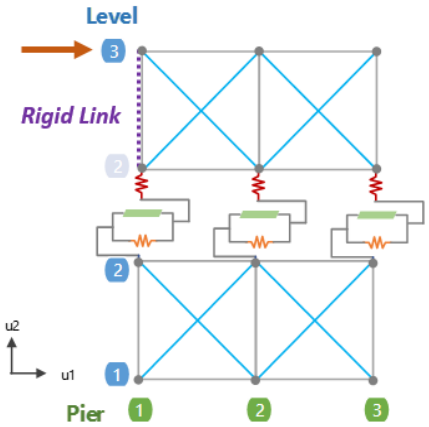

a) Shear model

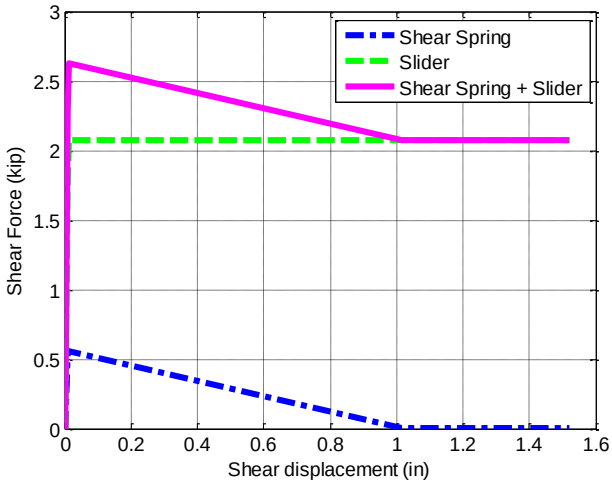

b) Slider plus Shear spring (cohesive force).

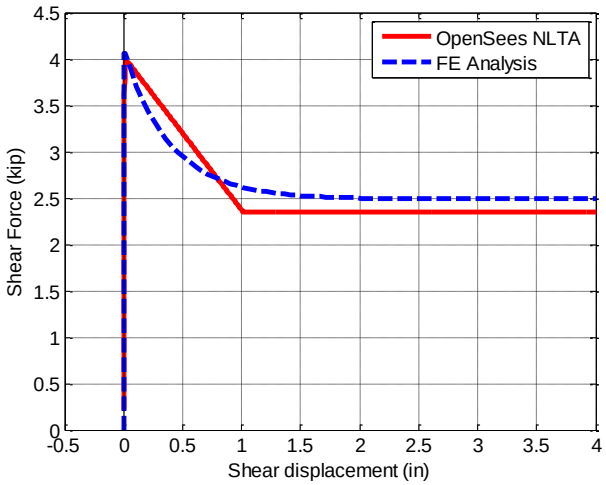

c) Monotonic response of the interface

Figure 4-11. Shear behavior of mortar joint of truss model.

4.3.3. Cyclic Shear Behavior

In this section the proposed model is used to verify the capability of the element assemblage for the interfaces to capture the cyclic under four different levels of normal compressive stress. As

shown in **Figure 4-12**, the proposed model can adequately capture the peak strength and cyclic shear stress-strain response for various levels of normal compressive stress.

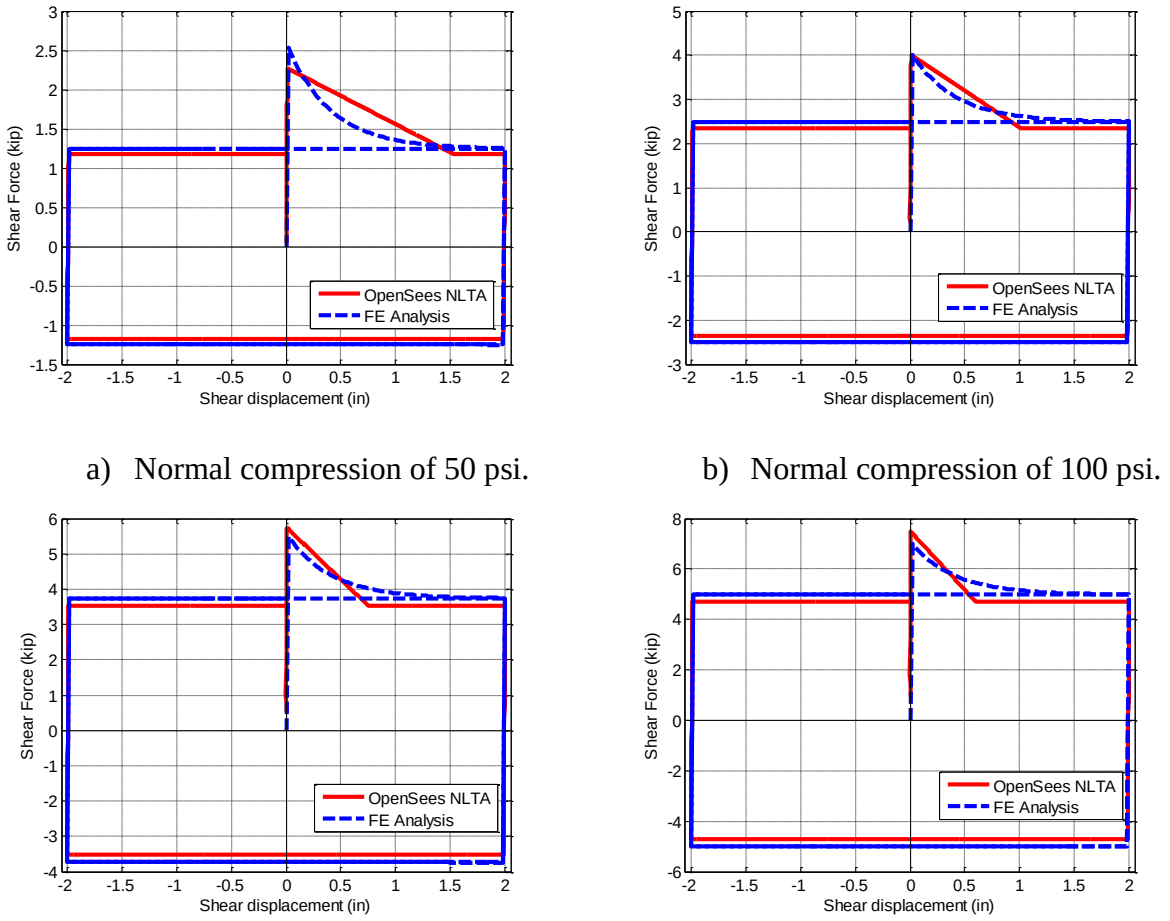

a) Normal compression of 50 psi.

b) Normal compression of 100 psi.

c) Normal compression of 150 psi.

d) Pre-compression of 200 psi.

Figure 4-12. Cyclic behavior of mortar joint of truss model.

4.4. Validation of Truss Modeling Approach for Infilled Frames

In this section, the proposed modeling approach and calibration procedures are evaluated through comparison of simulated NLFE and NLTA analyses for some of the RCF with URM infills

tested by Mehrabi et al. (1994). Some of the models compared in this sections were studied in section 3.6.5. Additional simulations were performed to test the model capabilities.

Numerical models implemented in OpenSEES were developed to simulate the response of the RCF with URM masonry infills tested in the laboratory. The numerical models are comprised of:

a) an arrangement of vertical horizontal and diagonal elements that model the nonlinear RCF elements and URM infill, and
b) the proposed non-continuum version of the 2D cohesive interface model, similar to the model presented in **Figure 4-1** to model the mortar joint as shown in Section 4.2.

The numerical models were calibrated on the basis of the following assumptions:

1. the general calibrations were made at the material level.
2. bilinear and linear softening were applied for tensile and shear behavior respectively.
3. bar slip and strain penetration effects were not included in the model.
4. only incremental monotonic analyses were used.

4.4.1. Specimen 1 Mehrabi et al. (1994)

The first analysis using the truss modeling approach is conducted for a bare RC frame, namely, for specimen 1 tested by Mehrabi et al. (1994). The specific frame was flexure-dominated, and it exhibited a fairly ductile behavior with inelastic flexural hinges developing in the columns. **Figure 4-13** (a) presents the deform shape of the NLTA model and is labelled as the Truss Analysis. **Figure 4-13** (b) shows the pushover curve of this specimens compared with the FE Analysis model simulated in DIANA. Other simulations made by other researchers for the same specimen are also

shown. **Table 4-1** presents the principal input parameters used in the Truss Analysis model. Note that the comparison of simulated and the experimental results for all cases fail to properly capture the initial stiffness, but the NLTA is the approach that exhibit the largest difference in terms of stiffness. This can be explained by the fact that the mode of failure of this specimen was flexural-dominated, and neither of the Truss Analysis and FE Analysis models incorporate slip capabilities, which are required to properly model flexural failures. In addition, as was presented in Mehrabi et al. (1994) for this specimen slip had a significant impact on the lateral response. It can be appreciated that while some of the other researchers have included some refinement it terms of slip, they also fail in capturing the initial stiffness.

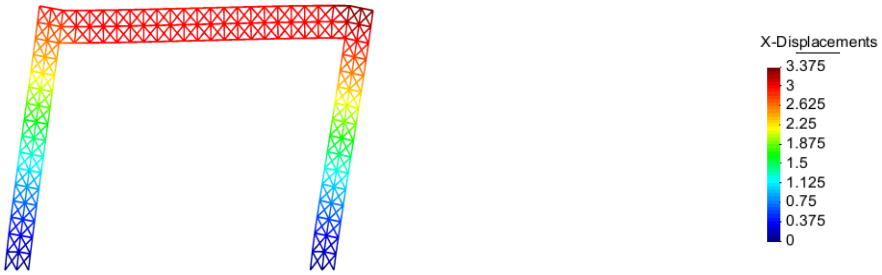

a) Deformed shape for specimen 1.

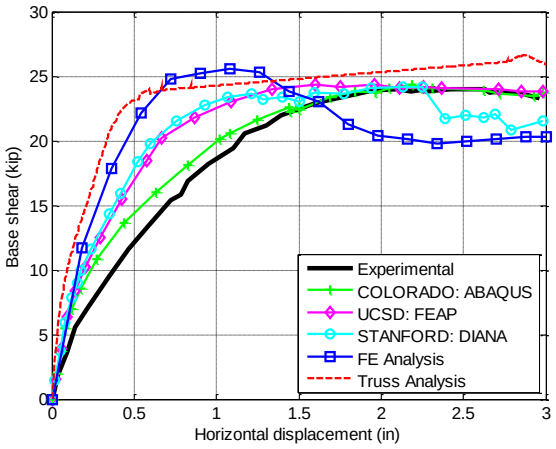

b) Pushover Analysis Specimen 1.

Figure 4-13. Comparison pushover analysis for Specimen 1 by Mehrabi et al. (1994).

In terms of peak strength all researchers make a good estimate. In addition, it is important to recall at this point that for the Truss Analysis and the FE Analysis models, the given materials properties were used to calculate the input parameters with no adjustments This was done because the principal objective in this research is to adequately capture the lateral response of the RCF with the presence of URM infill, Thus the lack of good stiffness matching for the bare frame is of no great concern as the infills will control the stiffness of other specimens.

4.4.2. Analysis of Specimen 8 by Mehrabi et al. (1994)

The NLFEA of this specimen was presented in Section 3.6.6. **Table 4-2** and **Table 4-3** present the principal input parameters used in the truss model.

Table 4-2 Material properties used for the interface.

ft (psi)	Gf^{I} (psi-in)	C (psi)	Gf^{II} (psi-in)	Kint (kip-in)	k (kip-in)
31	0.49	31	4.9	110	1000

Table 4-3 Material properties used in the NLTA.

Material	Concrete								Steel				
element	f'c (ksi)	εo	ft (ksi)	Ec (Ksi)	Av_ext (in^2)	Av_int (in^2)	Ah (in^2)	Ad (in^2)	Av_ext (in^2)	Av_int (in^2)	Ah (in^2)	fy_lg (ksi)	fy_tv (ksi)
Columns	3.89	0.0027	0.389	2852.7	12.25	24.5	28	18.44	0.60	0.40	0.16	61	53.3
beam					14	28	21	20.93	0.07	0.13	0.41		
Infill	2.39	0.0018	0.239	2629	3.7	7.4	7.4	5.23	-				

At Figures, **Figure 4-14** (a) through **Figure 4-14** (f) can be observed the obtained failure pattern. It is observed the sliding pattern and damage evolution from the contour plots of the lateral displacement and strain at different lateral displacement values. It can be observed the slip in the bed joints of the infill, that coincides with the mode of failure reported. **Figure 4-14** (g) depicts

the experimentally observed cracking pattern Mehrabi et al. (1994) to the pattern obtained from the truss model **Figure 4-14** (g). It is conclude that the truss model is capable of reproducing the failure pattern observed in the test.

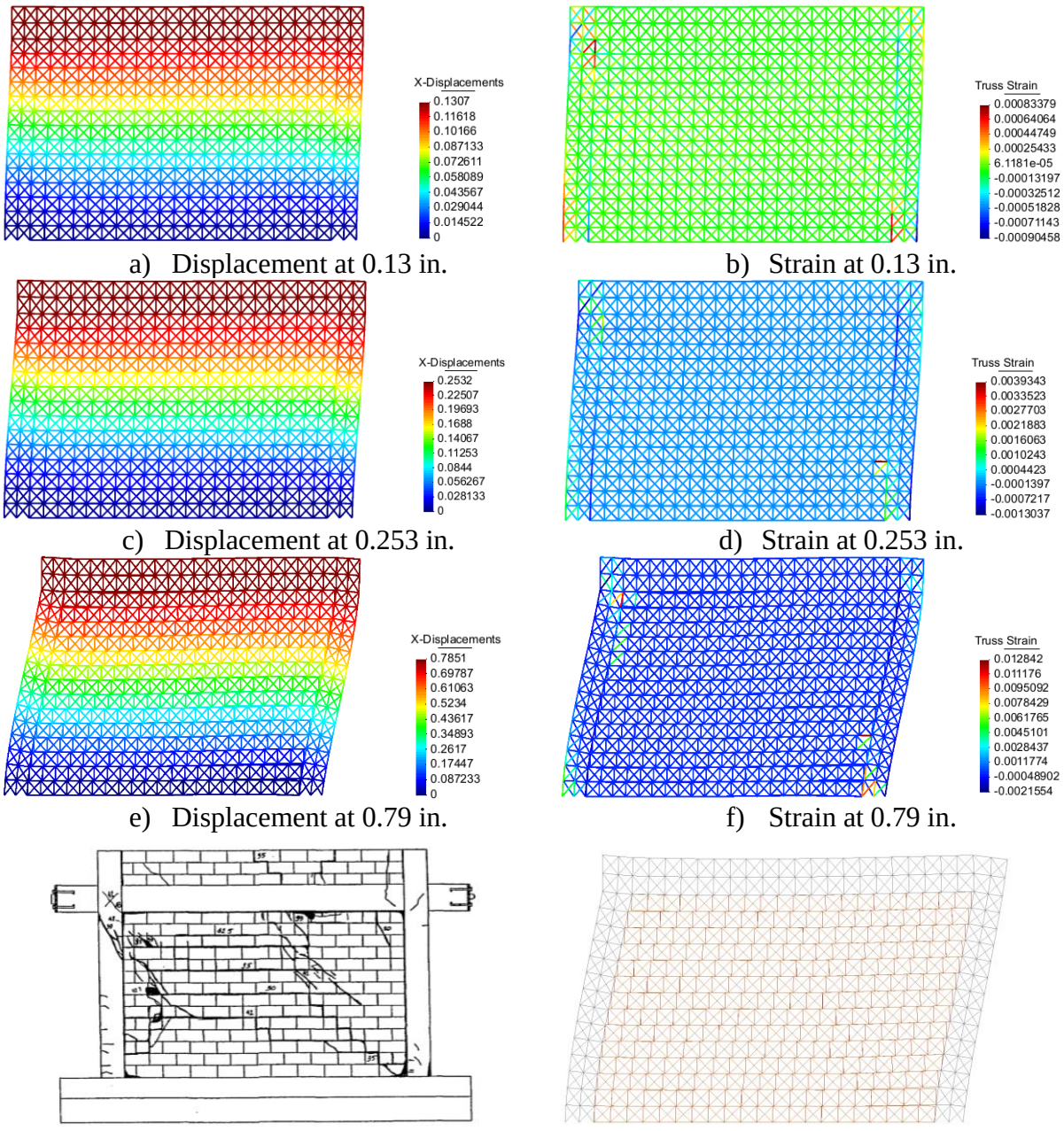

Figure 4-14. Deformations and damage pattern obtained for the analysis of specimen for Specimen 8 by Mehrabi et al. (1994).

Figure 4-15 shows the analytically obtained load-displacement curve for specimen 8 and the corresponding curves from the experimental test and the finite element analysis presented in section 6.7.6. The results show a good agreement between the curve obtained with the truss model and the experimentally recorded curve. The initial stiffness and peak stress from the models reasonably matched the experimental data and the post-peak behavior was also adequately captured.

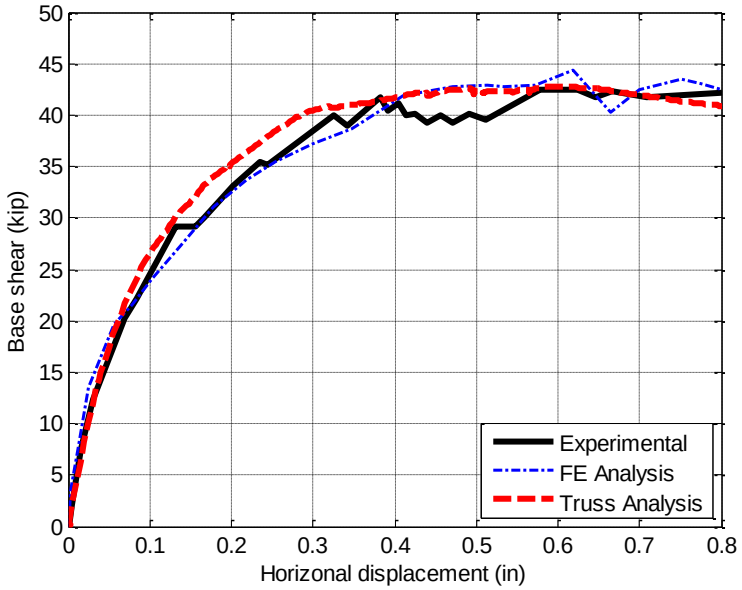

Figure 4-15. Load-displacement curve obtained for Specimen 8 by Mehrabi et al. (1994).

The comparison of the computational time for the FEA model (running time ≈30 min) versus the truss model (running time ≈10 minutes) indicates superior performance particularly when one considers that: (i) the convergence norm was far stricter for the NLTA model (i.e., the FEA model used an energy norm of $1x10^{-4}$ while the truss model had a tolerance of $1\ x10^{-8}$), and (ii) larger number of points calculated in the lateral load response for the NLTA, which for this example was

on a ratio of about 1:100. Thus as the model gets more complex, the difference in terms of computational time is expected to shift considerably towards the truss models, since the computational time of the NLFEA depends on how many elements become nonlinear, and the required number of iterations in the stress update algorithm will dramatically increase the computational time.

4.4.3. Analysis of Specimen 9 by Mehrabi et al. (1994)

The RCF used in Specimen 8 was repaired again and infilled with solid blocks and it was tested as Specimen 9. The effective width of the URM wall was set to 3.625 in. **Table 4-4** and **Table 4-5** present the principal input parameters used in the truss model. The presence of solid masonry units will lead to higher contact and bonding stresses between the mortar and the brick. This is accounted in the model by higher tensile stresses, higher cohesion of the interface and larger truss areas of the infill compared with its hollow counterpart.

Table 4-4 Material properties used for the interface.

ft (psi)	Gf^{I} (psi-in)	C (psi)	Gf^{II} (psi-in)	Kint (kip-in)	k (kip-in)
115	0.39	115	3.9	110	10000

Table 4-5 Material properties used in the NLTA.

Material	Concrete Properties and truss element Areas								Steel Properties and truss element Areas				
element	f'c (ksi)	εo	ft (ksi)	Ec (Ksi)	Av_ext (in^2)	Av_int (in^2)	Ah (in^2)	Ad (in^2)	Av_ext (in^2)	Av_int (in^2)	Ah (in^2)	fy_lg (ksi)	fy_tv (ksi)
Columns	3.89	0.0027	0.389	2852.67	12.25	24.5	28	18.44	0.60	0.40	0.16	61	53.3
beam					14	28	21	20.93	0.07	0.13	0.41		
Infill	2.26	0.0018	0.226	2486	7.25	14.5	14.5	10.25	-				

Figure 4-16 shows the load-displacement curve obtained from the analysis and compared this curve with the experimentally recorded one. The results show a satisfactory agreement with the experimental results. Initial stiffness, peak stress, and post-peak behavior were adequately captured well by the models. It is convenient to mention, that for this specimen, no comparison with a NLFEA model is shown. This is due to the fact that the solid panels induced a shear failure in the upper part of the windward column, and this failure mode was not considered in the previous chapter. In fact, this particular truss model was further than previous researches which mainly focus on the calibration process performed up to 0.8 in.

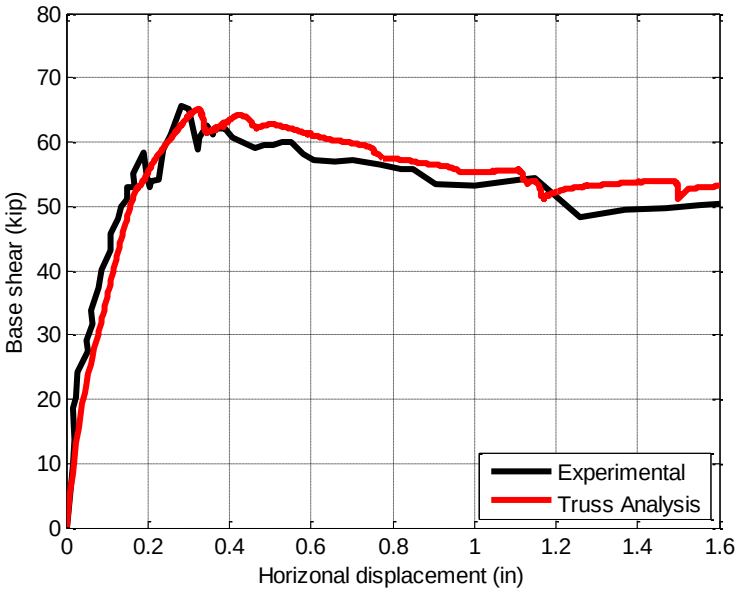

Figure 4-16. Load-displacement curve obtained for Specimen 9 by Mehrabi et al. (1994).

At Figures **Figure 4-17** (a) through **Figure 4-17** (f) can be observed the sliding pattern and damage evolution from the contour plots of the lateral displacement and strain at different loading steps. From the contours plots in **Figure 4-17** one can observed that the damage was concentrated in the principal diagonal in the direction of the analysis. **Figure 4-17** (g) shows the analytical failure pattern while **Figure 4-17** (h) depicts the experimental failure pattern; a very good

agreement in terms of the mode of failure is clear. In addition to initial sliding along both the bed and head joints, the ultimate strength is controlled by a diagonal failure pattern concentrated along the principal diagonal of the infill

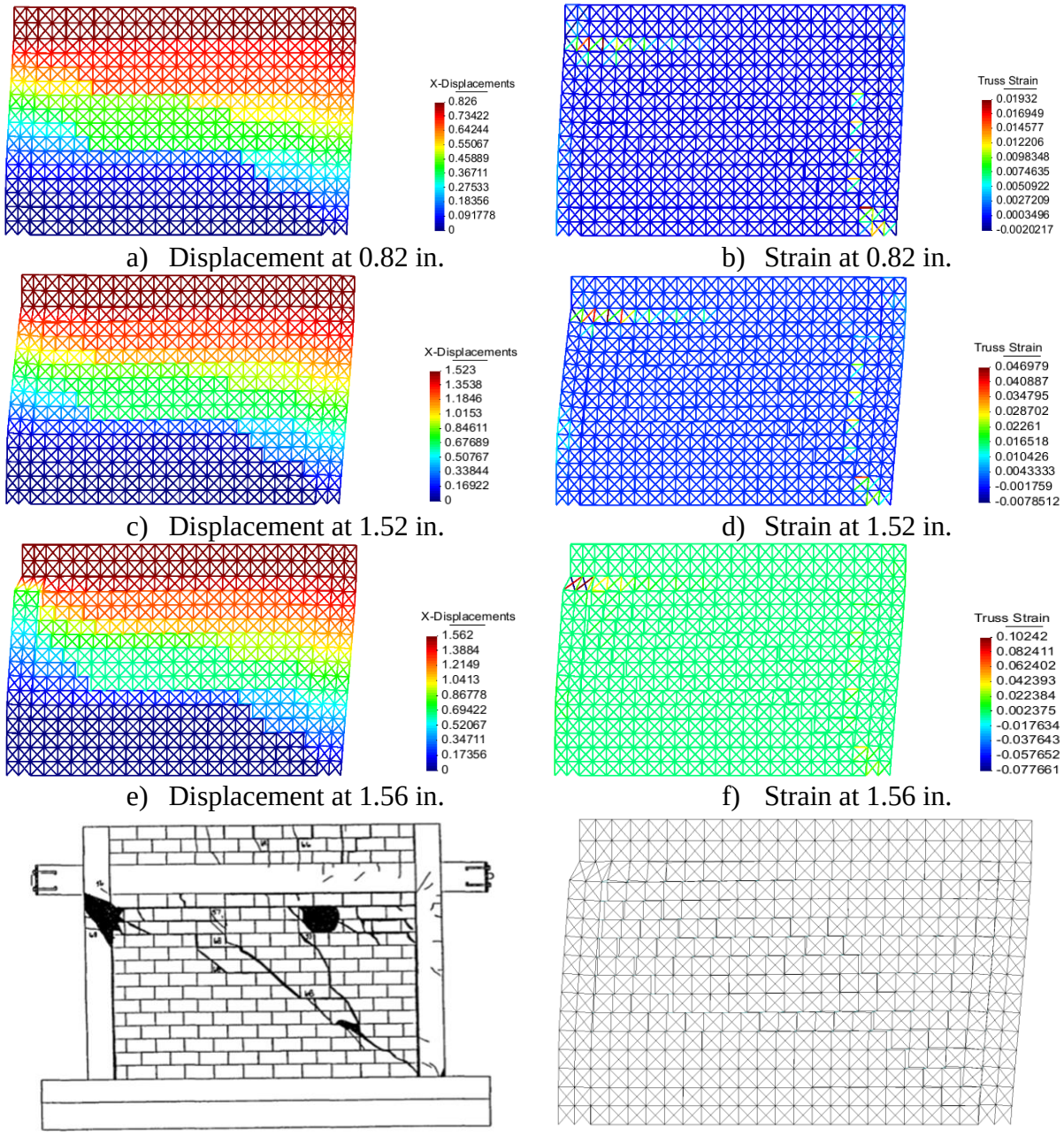

a) Displacement at 0.82 in.

b) Strain at 0.82 in.

c) Displacement at 1.52 in.

d) Strain at 1.52 in.

e) Displacement at 1.56 in.

f) Strain at 1.56 in.

g) Reported failure pattern.

h) Obtained failure pattern

Figure 4-17. Deformations and damage pattern obtained for Specimen 9 by Mehrabi et al. (1994).

4.4.4. Specimen 14 by Mehrabi et al. (1994)

This specimen is a two-bay frame with a weak-frame design infilled with solid brick units. Each panel had an aspect ratio of 0.67. A total vertical load of 99 kips was applied and it was equally distributed among the columns. This specimen was subjected to fully reversed displacement cycles. Regarding the failure mode, it can be appreciated in **Figure 4-18** a reasonable agreement is presented in terms of calculating the initial stiffness and the expected monotonic peak strength. Discrepancies result from the type of loading applied in the test compared with the monotonic response obtained with the NLTA. Since Specimen 14 was infilled with solid units, this explains the source of the severe degradation observed in **Figure 4-18**. The NLTA model experienced some degradation about 0.47 in. **Table 4-6** and **Table 4-7** present the principal input parameters used in the truss analysis model for the interface and the truss elements.

Table 4-6 Material properties used for the interface.

ft (psi)	Gf^{I} (psi-in)	C (psi)	Gf^{II} (psi-in)	Kint (kip-in)	k (kip-in)
40	0.5	40	5	110	10000

Table 4-7 Material properties used in the NLTA.

Material	Concrete Properties and truss element Areas								Steel Properties and truss element Areas				
element	f'c (ksi)	εo	ft (ksi)	Ec (Ksi)	Av_ext (in^2)	Av_int (in^2)	Ah (in^2)	Ad (in^2)	Av_ext (in^2)	Av_int (in^2)	Ah (in^2)	fy_lg (ksi)	fy_tv (ksi)
Columns	3.95	0.0027	0.395	2896.7	12.25	24.5	28	18.44	0.60	0.40	0.64	61	53.3
beam					14	28	21	20.93	0.07	0.13	0.41		
Infill	2.39	0.0018	0.239	2629	3.7	7.4	7.4	5.23	-				

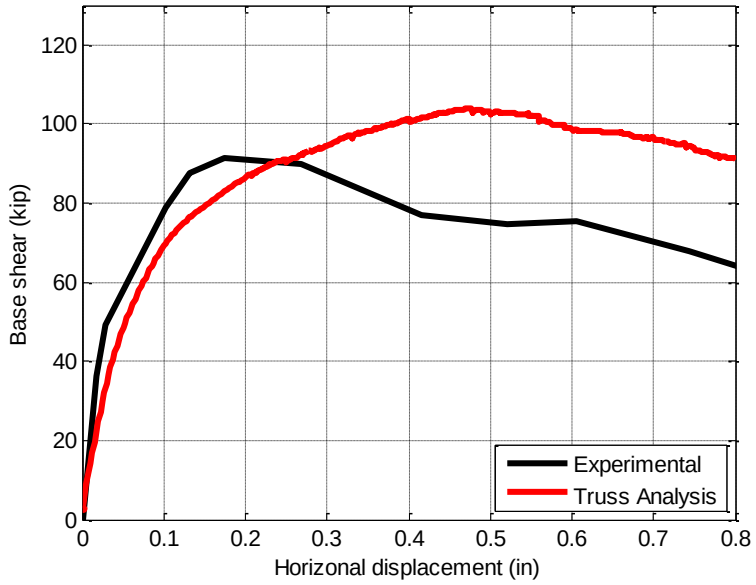

Figure 4-18. Comparison pushover analysis Specimen 14.

Figure 4-19 (a) to **Figure 4-19** (d) present contour plots of the lateral displacement and strain at different loading steps. The nonlinear activity was concentrated at the upper part of the windward column and vicinity and a preamble of the shear failure is presented. Additional nonlinear behavior is presented at the lower part of the windward column. For illustration purposes, **Figure 4-20** (a) depicts the reported failure pattern and **Figure 4-20** (b) depicts the obtained monotonic load pattern. Notice the importance of the damage in the other direction of the analysis. This help in explains why the post peak behavior is not adequately captured by the NLTA model.

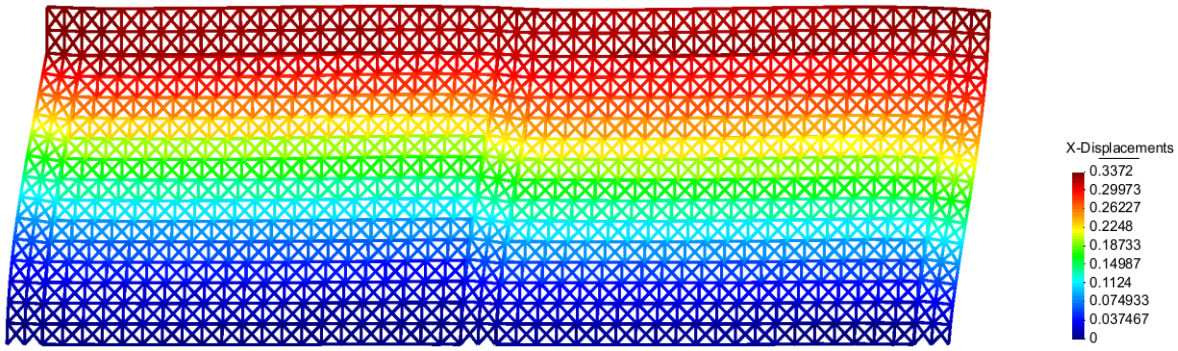

a) Displacement at 0.34 in.

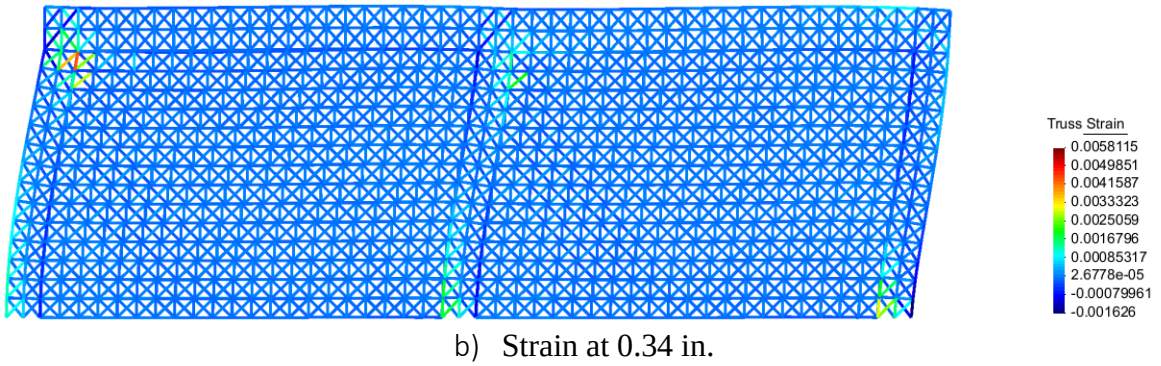

b) Strain at 0.34 in.

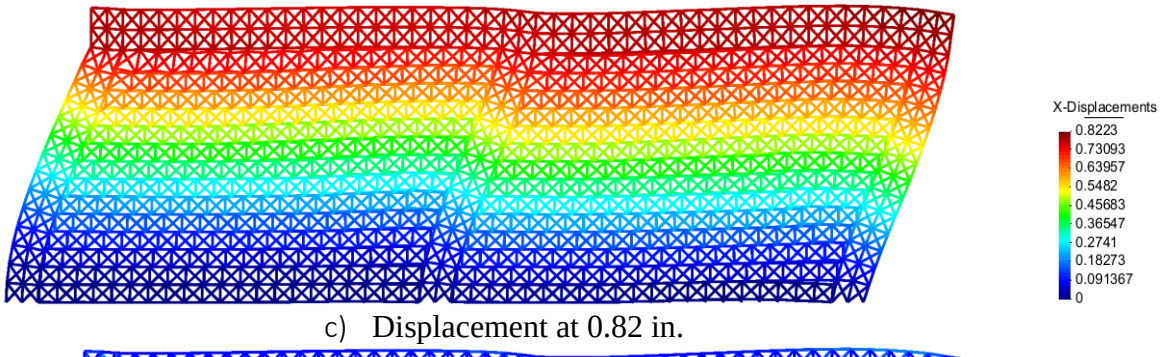

c) Displacement at 0.82 in.

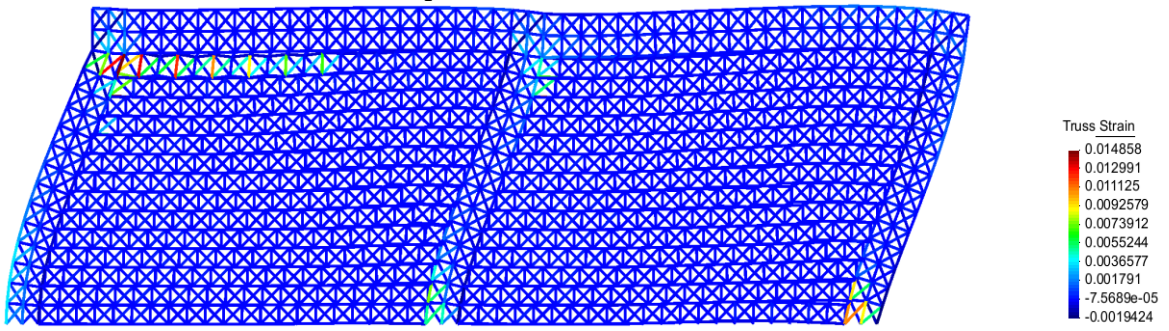

d) Strain at 0.82 in.

Figure 4-19. Strain contour plots for the truss model for Specimen 14 by Mehrabi et al. (1994).

.

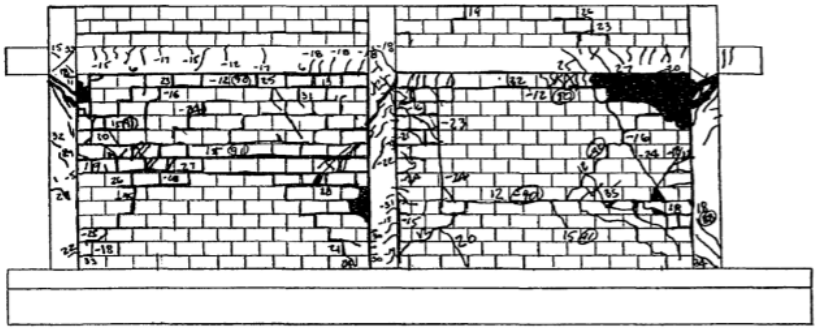

a) Reported failure pattern (Cyclic test) by Mehrabi et al. (1994).

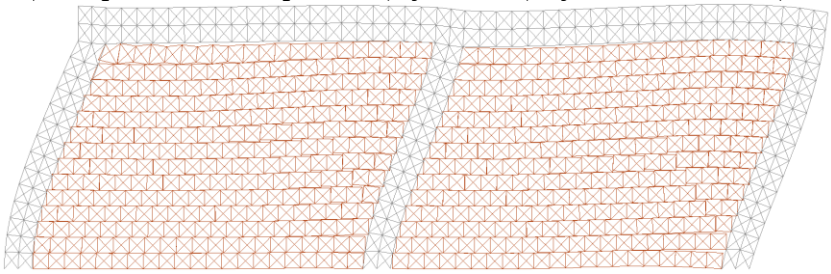

b) Obtained failure pattern (Pushover test).

Figure 4-20. Reported Vs obtained failure pattern for Specimen 14 by Mehrabi et al. (1994).

4.4.5. Three-story Specimen by Stavridis (2009)

Stavridis (2009) tested the largest structure of this type ever tested on a shake table shake-table. This corresponded to a 2/3-scale model of a three-story, two-bay RCF with URM infills presented in **Figure 4-21** (a). **Figure 4-21** (b) and (c) presents the front view and side view of the specimen. Additional details can be found in Stavridis (2009).

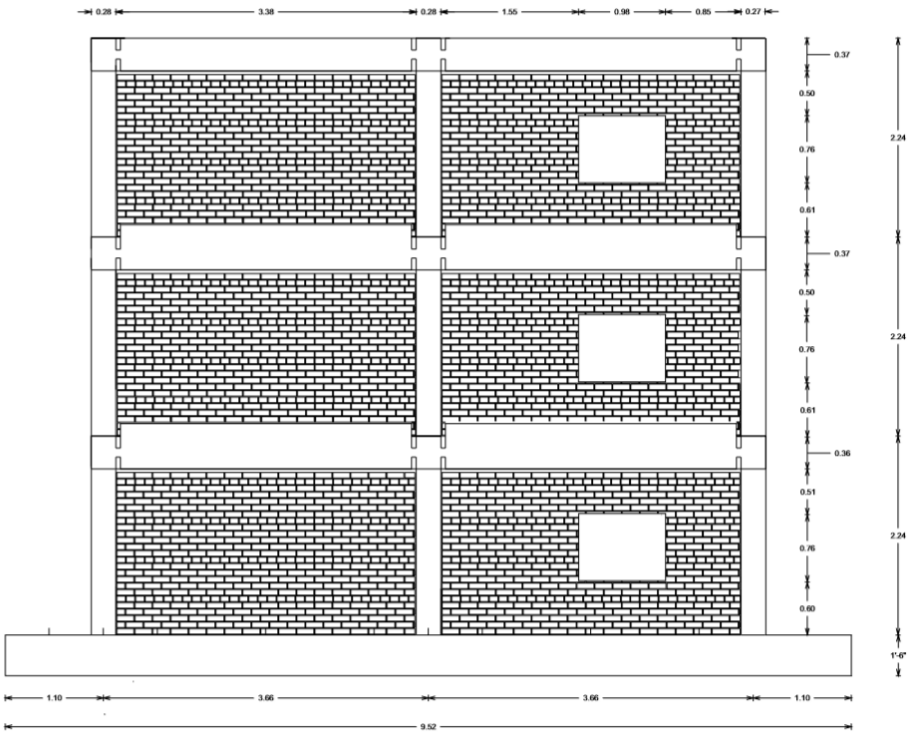

a) Three-story test specimen (dimensions in meters). from Stavridis (2009).

b) Front view from Stavridis (2009)

c) Side view fromStavridis (2009).

Figure 4-21. Three-Story specimen from Stavridis (2009).

Up to this point single and double bays specimens have been analyzed monolithically using the NLTA. This test will be used to test the suitability of the model to handle a more complicated structure. The proposed approach is used here as a blind predictor. In other words, the model is fed with the exact material properties reported by Stavridis (2009) and a monotonic pushover analysis is performed. No attempt was made to "calibrate" the results by varying material and other parameters. **Table 4-8** and **Table 4-9** present the principal data used in the NLTA simulations.

Table 4-8 Material properties.

Story	Concrete				Mortar		Brick units	
	E(ksi)	f'c(ksi)	εo	f'c(ksi)	f'c(ksi)	f't(ksi)	f'c(ksi)	f't(ksi)
1	2195	5.51	0.0032	0.5	0.58	0.065	7.10	0.71
2	2528	6.08	0.0033	0.57	0.59	0.080	7.10	0.71
3	2463	5.68	0.0032	0.568	0.62	0.072	7.10	0.71

Table 4-9 Material properties used in the NLTA.

Story	Elem.	Concrete / Infill				Steel				
		Av_ext (in^2)	Av_int (in^2)	Ah (in^2)	Ad (in^2)	Av_ext (in^2)	Av_int (in^2)	Ah (in^2)	fy_lg (ksi)	fy_tv (ksi)
1	Column	30.16	60.33	33.71	29.43	0.93	0.62	0.03	68.50	62.50
	Beam	23.58	47.17	53.19	40.60	-	-	1.05		
	Infill	16.37	32.74	23.40	19.04	-	-	-	-	-
2	Column	30.16	60.33	33.71	29.43	0.93	0.40	0.03	68.50	62.50
	Beam	23.58	47.17	53.19	40.60	-	-	1.05		
	Infill	16.37	32.74	23.40	19.04	-	-	-	-	-
3	Column	30.16	60.33	33.71	29.43	0.60	0.22	0.03	68.50	62.50
	Beam	23.58	47.17	53.19	40.60	-	-	1.05		
	Infill	16.37	32.74	23.40	19.04	-	-	-	-	-

Figure 4-22 (a) presents the deformed shape from Open SEES using GID. The tendency for a first story mechanism is obvious. **Figure 4-22** (b) depicts a close-up where one can appreciate the detachment of the infill from the frame on the bottom right of the figure.

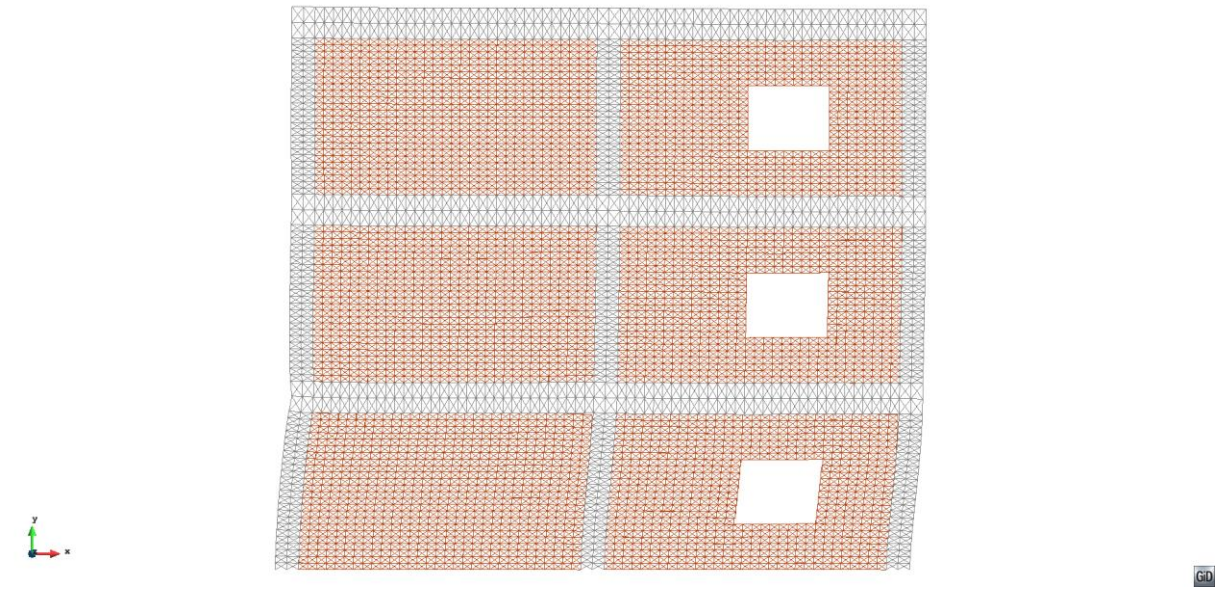

a) Deform shape three-story model.

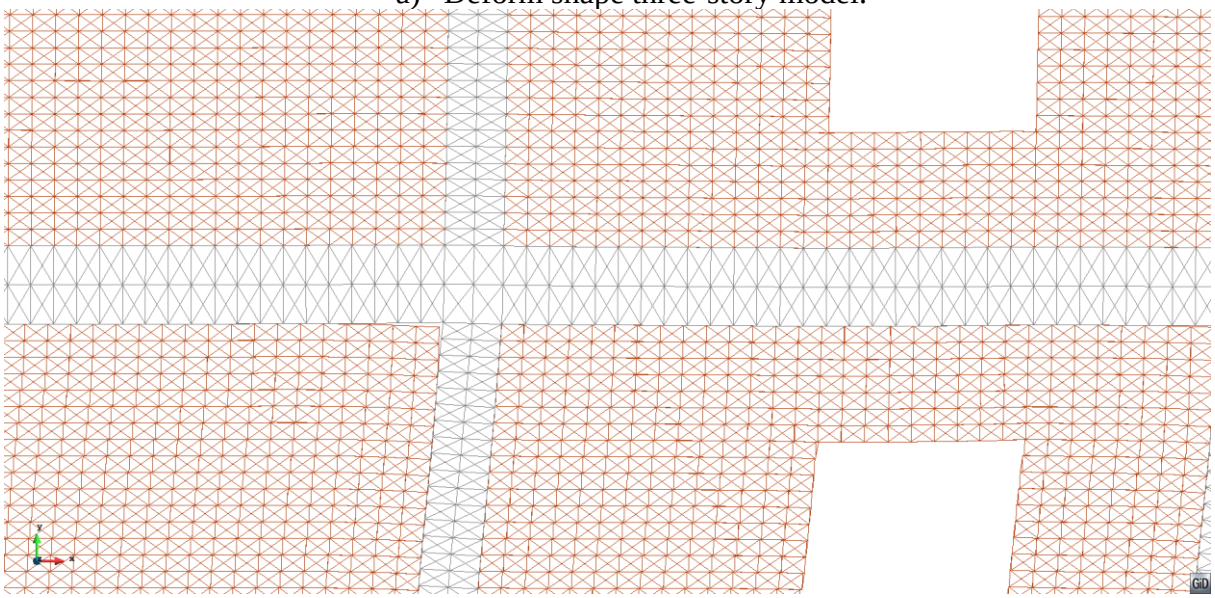

b) Deformed shape zoom

Figure 4-22. NLTA deformed shape for three-story model.

Figure 4-23 presents the shake table test Stavridis (2009), the monotonic response from Stavridis (2009) using the FEAP software, and the monotonic response using the NLTA. From this can be concluded that the NLTA approach adequately captures the initial stiffness and peak strength in both directions. This simulation was executed with the energy tolerance of 10e8, and the total running time was 22 hours for both directions, performed in a 8GB laptop with an Intel core i5, 2.6 GHz processor

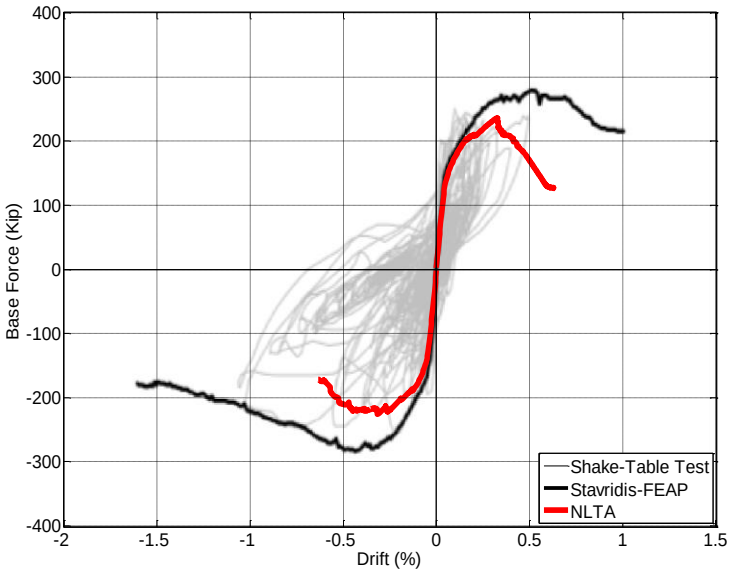

Figure 4-23. Results for the three-story model by Stavridis (2009).

Figure 4-24 (a) and (b) depict the contour displacement plots for the monotonic pushover analysis performed in the possitive and negative directions. From these, a high displacemnt gradient is evident in story 1. This is consistent with the tipical tendency to concentrate the maximun drifts at the first story.

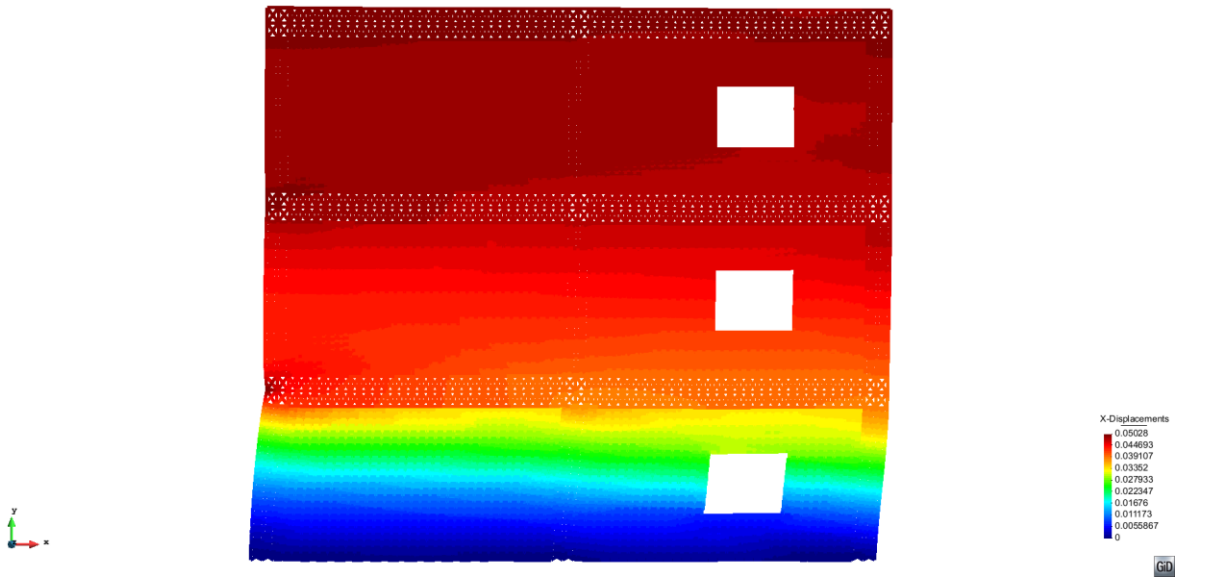

a) Monotonic analysis for the possitive direction of loading.

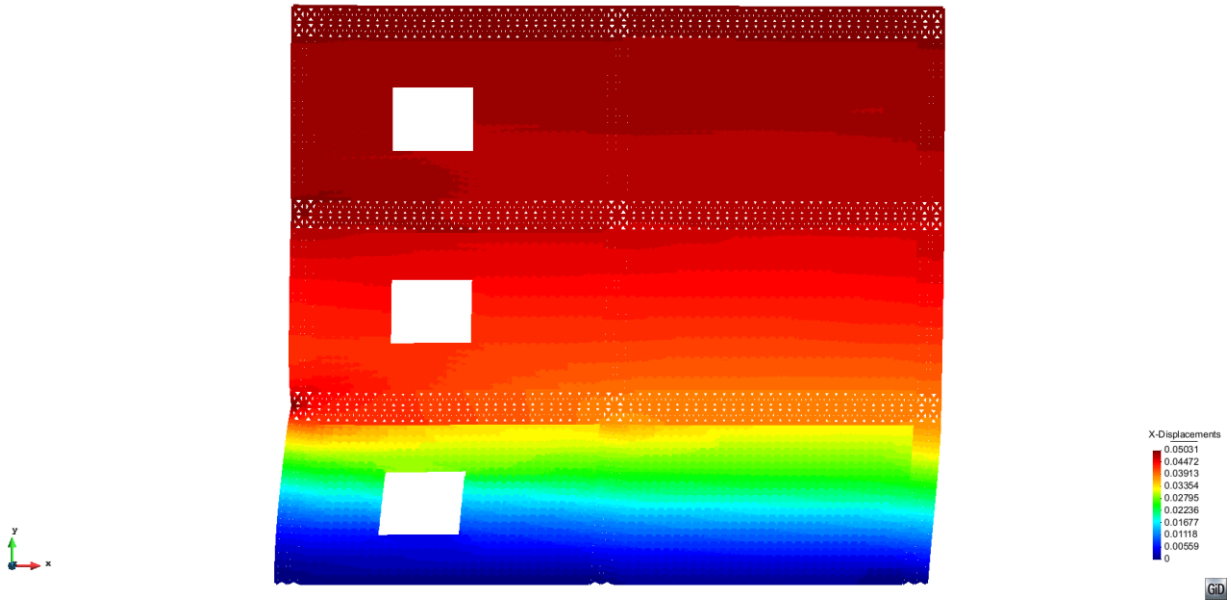

b) Monotonic analysis for the negative direction of loading.

Figure 4-24. Contour displacement plots for three-story model by Stavridis (2009).

Conclusions

This Chapter describes a novel method for analyzing planar RCF with URM infills subjected to monotonic uniaxial loading. The main conclusions of the present chapter are provided below.

- For single-bay, single-story frames infilled with either hollow (i.e weak) or solid (i.e strong) infills, the proposed approach was shown to adequately capture the initial stiffness and peak strength and their subsequent degradation. In addition, the obtained damage patterns are similar to the damage patterns reported from test results. The robustness of the proposed method was demonstrated by its ability to capture the shear-critical behavior reported for the case of RCF with URMI (Specimen 9 Mehrabi et al. (1994)) without resorting to any additional refinements.
- For one-story, double-bay test specimen that was subjected to fully reversed displacement cycles, comparison was made between its cyclic envelopes and the monotonic response from the proposed NLTA approach. For this case, good agreement between the test results was found in terms of initial stiffness. After reaching the peak strength, only minor degradation was present for the proposed model, whereas severe degradation was reported in the test due to the cyclic loading. Logically one would expect that cyclic damage will play a major role in the response of this structural system. Extension of the model to the cyclic case will probably significantly improve the post-peak strength comparison.
- For the three-story test, good agreement was found in the lateral load vs drift response. This comparison shows that the proposed approach can handle complex models such multi-bay, multi-story bay models.

5. Parametric Study of RCF with URM Infills

5.1. Introduction

The previous Chapter explained a novel method for the nonlinear analysis of infilled RC frames. This method provides the simplicity of the Nonlinear Truss Analogy (NLTA) and retains satisfactory accuracy when compared to refined NLFEA.

As described in Appendix A.3, the Colombian inventory it too broad. Even today, depending on the location of the project (i.e urban vs rural), local practices are commonly imposed with no intervention of the local authorities. As can be inferred from **Figure 5-1** (b), due to the construction sequence, this structure was unintentionally stiffened for vertical and lateral loads. Therefore, since the presence of the infills are commonly neglected in the design phase, it is highly probable that in case of a seismic event, this structure will attract forces for which this system might not be designed for.

The present chapter presents a parametric study to assess the effect of selected parameters on the nonlinear response of infilled RC frames subjected to monotonic, in-plane lateral loads. The prototype structures for the analyses have been selected to represent the building inventory in Colombia; however, the results of the parametric study are valid for infilled frames in general. In all analyses, a baseline configuration is selected; all baseline configurations are those of experimentally tested specimens.

The analyses elucidate the influence on the response of the several parameters, namely: (a) axial load variation and its vertical distribution, (b) amount of longitudinal reinforcement ratio in

the columns, (c) amount of transverse reinforcement in the columns, (d) presence of a mortar overlay on infill's face, and (e) presence of openings in the URM infills.

5.2. Effect of Axial Load

The amount of vertical load carried by the infill walls depends on several factors such as the construction sequence, the relative stiffness of the vertical RC members and the masonry walls, and the construction quality of the mortar interface between the RC beams and the infill walls, and long term deformations, such as creep in concrete and moisture expansion in masonry. A first series of parametric analyses has focused on the effect of vertical load distribution. The configuration of specimen 9 tested by Mehrabi et al. (1994) is taken as baseline case. Both the magnitude of the total vertical force (carried by the infill walls and the frame columns), and the percentage of vertical force carried by the infill and the frame members have been varied.

Table 5-1 summarizes the various analyses which are grouped into two general cases. Case 1 examines the effect of the relative distribution of a total vertical load of 66 kips. Case 2 is focused on varying levels of total vertical force, for a fixed distribution of the force to the infills and the frame members.

Figure 5-1 (a) shows a typical RCF with URM infills found in Colombia. It can be noticed that this structural system carries a considerable amount of gravity load due to the presence of the infills and layout. In addition, in **Figure 5-1** (b) one can observe that due to this particular construction sequence, infills are taking an important part of the gravity load. At this point, it is worth mentioning that this construction practice is not commonly found in Colombia. Instead, columns and beams are cast first, then as the construction evolves, infills are placed. The reasons

to conduct this parametric study are mainly to (1) study the influence of different parameters on the lateral response of the monotonic response of RCF with URM infills under lateral in-plane loading, and (2) to test the proposed approach under different conditions.

Table 5-1 Cases considered for axial load.

Case 1. (Axial load distribution)			Case 2. (Axial load variation)		
Id	**Axial Load in Columns (Kip)**	**Axial Load in Infill (Kip)**	**Id**	**Axial Load in Columns (Kip)**	**Axial Load in Infill (Kip)**
C1-33-67	44	22	C1-33-67	44	22
C1-0-100	0	66	C2-7.5-15	5	10
C1-15-85	10	56	C2-50-100	33	66
C1-30-70	20	46	C2-75-150	50	100
C1-44-55	30	36	C2-115-230	75	150
C1-60-40	40	26	C2-150-300	100	200
C1-75-25	50	16			
C1-90-10	60	6			
C1-100-0	66	0			

a) Typical RCF with URM infills.

b) Side view of a RCF with URM infills

Figure 5-1. Examples of RCF with URM. (Duitama, Boyacá Colombia).

Figure 5-2 presents the lateral force-vs.-displacements relations for the nine (9) configurations listed under Case 1 in **Table 5-1**. It is observed the larger the proportion of the axial force distributed to the wall, the greater its strength and the initial stiffness. The analysis where the entire vertical load is carried by the infill wall gives a peak strength value which is about 15% higher than that of the baseline case. The same type of damage pattern, that is shear failure at the top of the windward column, was obtained in all analyses. The displacement corresponding to the peak lateral strength did not significantly change in the various analyses.

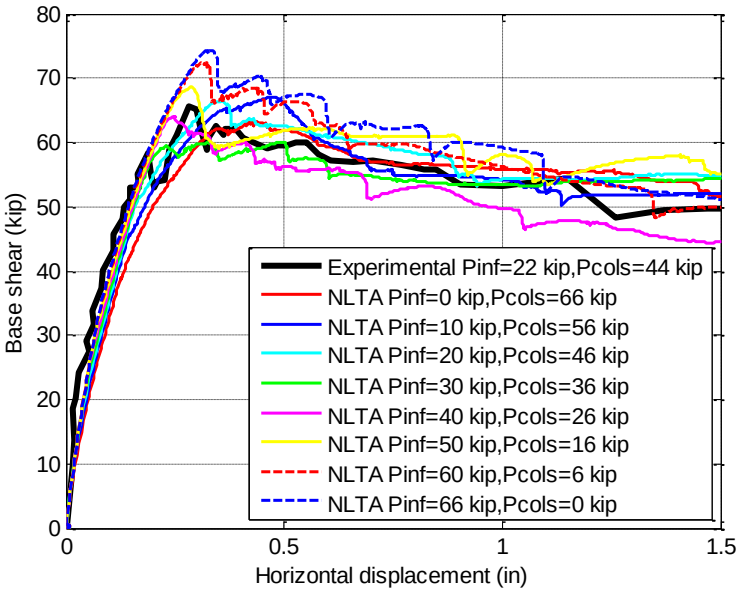

Figure 5-2. Pushover Analysis Specimen 9 under different axial load distribution.

Figure 5-3 depicts the lateral force-vs.-displacement relations for the analyses of Case 2, where the total vertical force is varied while the proportions of force carried by the frame and infill wall are kept fixed. An increase in vertical force increases the strength and secant stiffness at the peak strength for the infilled frame. Lower ductility can be expected for specimens heavily loaded

axially. The increase in axial load is translated into increased lateral strength due to the frictional resistance along the mortar joints and an increased overall strength of the system, but lower ductility.

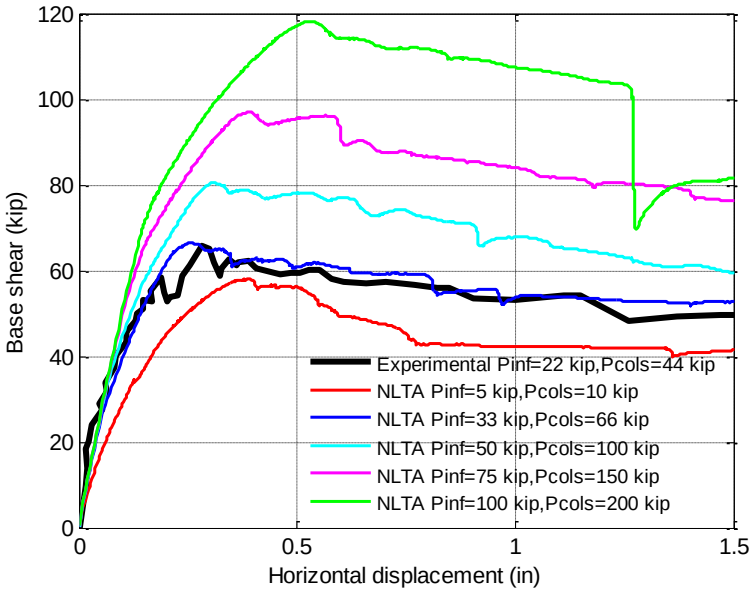

Figure 5-3. Pushover analysis Specimen 9 under different axial load levels.

5.3. Effect of Longitudinal Reinforcement at the Columns

The longitudinal reinforcement ratio considered in this study range from 1% to 3.5% of the column gross section. **Figure 5-4** shows the force-displacement curves for ratios considered for this study. It is observed that the amount of longitudinal reinforcement in the columns has an insignificant effect in terms of the variation of the initial stiffness for all cases studied here. Furthermore, for this specimen, the increase of longitudinal reinforcement brings additional strength to the system with an approximate 20% peak strength gain. The higher longitudinal

strength ratios increase the tensile resistance and, as a consequence, higher shear forces are developed in the section, thus increasing the peak strength of the system.

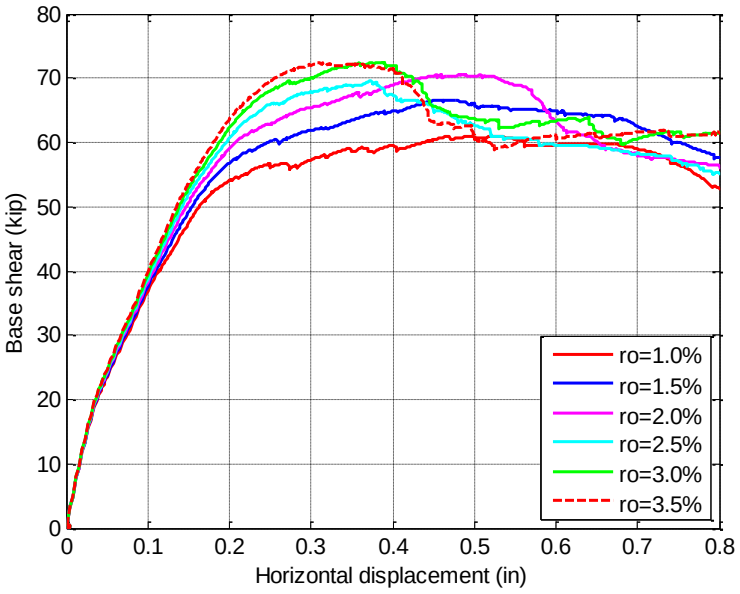

Figure 5-4. Pushover analysis Specimen 9 for different longitudinal reinforcement ratios.

5.4. Effect of Transverse Reinforcement at the Columns

This study considers transverse area ranging from 0.15 in^2 spaced at 4.5 in. to 0.93 in^2 spaced at 4.5 in. **Figure 5-5** depicts the lateral force-vs.-displacement relations for the five (5) cases considered on Specimen 9. For this particular specimen, increasing the amount of transverse reinforcement has virtually no effect on stiffness and strength, with the post-peak behavior almost identical for all cases. This can be explained by the fact that for this particular specimen the solid infill induces larger shear demands than the transverse reinforcement is unable to carry. The displacement at peak strength remains practically identical for all cases. In terms of the failure mechanisms, all specimens reported the same failure reported in Mehrabi et al. (1994) for

Specimen 9. The effect of considering different transverse spacing is implicitly considered in this study because the cross-sectional area of the horizontal elements used to represent the shear reinforcement are calculated based on the amount of transverse reinforcement and the spacing. Then this steel area is distributed equally into the total number of horizontal truss elements. Adoption of this approach implies that – for the analyses presented herein - an increase in the area of the transverse bars would have the same impact as an equal decrease in the spacing of the transverse reinforcement.

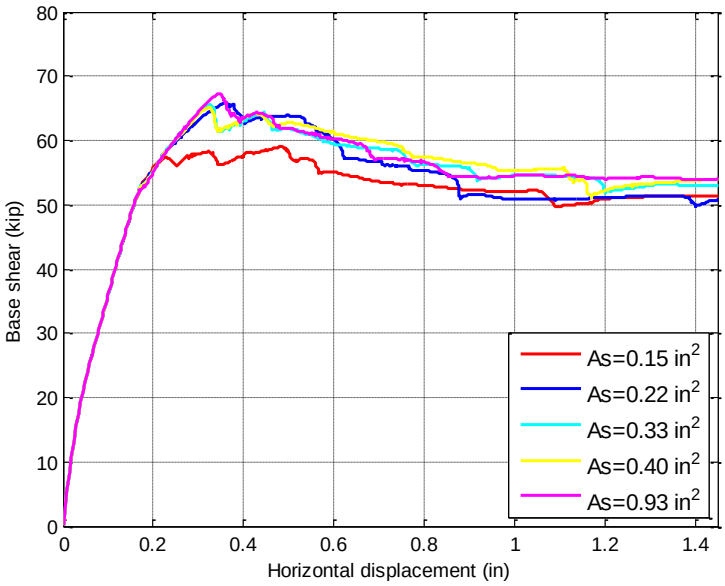

Figure 5-5. Pushover Analysis Specimen 9 for different transverse reinforcement areas.

5.5. Effect of Mortar Overlay

One common characteristic of RCF with URM infills in Colombia is the presence of a mortar overlay applied on each or just one of the infill's face. Such mortar overlay constitutes a cost-effective finish, which creates a water-resistant surface and increases the strength of the infill.

Post-earthquake reconnaissance after the Popayan earthquake in 1983 (Garcia, 1986) identified cases where the presence of a mortar overlay prevented the collapse of infilled frames (Garcia, 1986). **Figure 5-6** presents the application process for a mortar overlay on a brick masonry infill wall.

a) URM infill wall
b) Mortar overlay application
c) Mortar overlay close-up
d) URM infill with mortar overlay

Figure 5-6. URM infill with mortar overlay construction sequence.

The effect of the mortar overlay on RCF with URM infills is incorporated in the analysis by superimposing additional elements on the part of the model representing the infill wall. The arrangement of the superimposed elements is identical to that employed for the infill wall. The effect of the mortar overlay on the mortar joints was accounted by adding 50% of the mortar overlay thickness to the mortar joint thickness. For the mortar overlay, a typical mortar mix ratio used in Colombia is 1:3 by volume (1 part cement, and 3 parts fine sand) with W/C=0.5. For the

models, the compressive strength was assumed to be either 1.79 ksi or 2.25 ksi, taken a typical range for the mortar used. The strain value at peak stress was taken as 0.002 and the tensile strength was estimated as 10% of the compressive strength. The thickness of this mortar overlay was assumed to vary between 0.5 in and 2 in. For completeness, the presence of this mortar overlay was studied for the case of weak infill (Specimen 8) and strong infill (Specimen 9) by Mehrabi et al. (1994).

Figure 5-7 and **Figure 5-8** depict the load- displacement response for different mortar overlay characteristics. **Figure 5-7** (a) and **Figure 5-7** (b) present the pushover response of specimen 8 for a compressive mortar overlay of 1.78 ksi and 2.2 ksi respectively for different mortar overlays thicknesses. As expected, both the initial stiffness and the strength increases due to the additional thicknesses. When it comes to the post-capping behavior, the mortar overlay seems to enhance the ductility of Specimen 8 which had weak infills. Furthermore, the increases of compressive strength of the mortar overlay did not affect considerably the lateral response. This can be explained due to the fact that the tensile resistance of the mortar overlay incorporates the 10% of its compressive strength. Thus, the effective difference in terms of tensile strength for **Figure 5-7** (a) and **Figure 5-7** (b) is about 42 psi. One exception occurs when the mortar thickness is equal to 2.0 in. This can be attributed to the sensitivity of the parameters involved in the analysis. In general terms, both responses can be considered as similar.

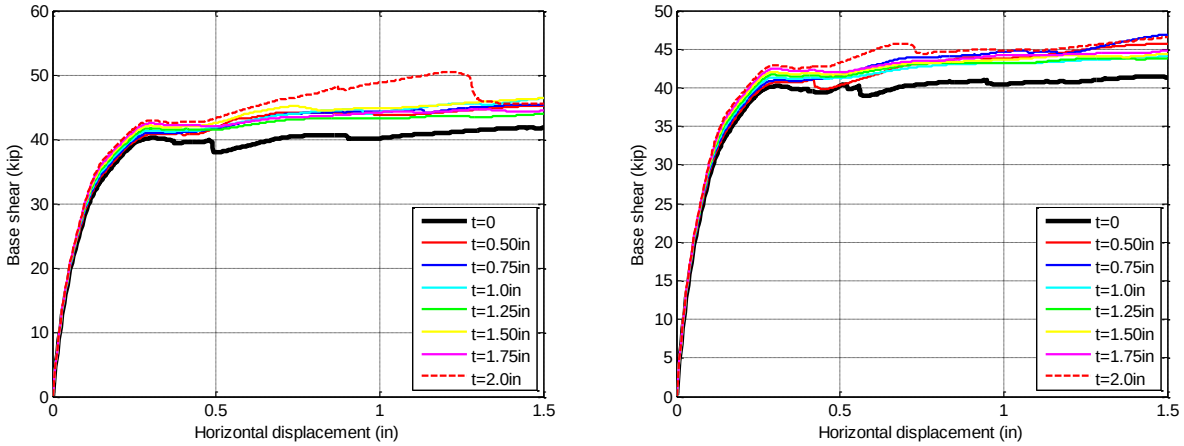

a) $f'c_{mortar}$=1.78 ksi b) $f'c_{mortar}$=2.2 ksi

Figure 5-7. Pushover curve for Specimen 8 under different mortar overlay parameters.

Figure 5-8 (a) and **Figure 5-8** (b) present the pushover response of Specimen 9 for a compressive mortar overlay of 1.78 ksi and 2.20 ksi respectively for different mortar overlays thicknesses. The mortar overlay keeps the same trends reported for specimen 8, with the initial stiffness and the strength increasing due to the presence of the mortar overlay. In terms of the peak strength, the presence of the mortar overlay increase the tensile resistance, and thus higher shear forces are developed in the section. As a consequence, the peak strength of the system is increased. Notice that for Specimen 9, with strong infills, a shear failure was reported. For lower displacement levels, the mortar overlay helps to increase the shear capacity of the section. For the strong infill of Specimen 9, the mortar overlay makes it even stronger, resulting in a 50% reduction of the strength of the system in the post-peak regimen for some of the analyses presented. For the case of higher compressive strength, a sudden drop of strength persists, this time at larger displacement demands.

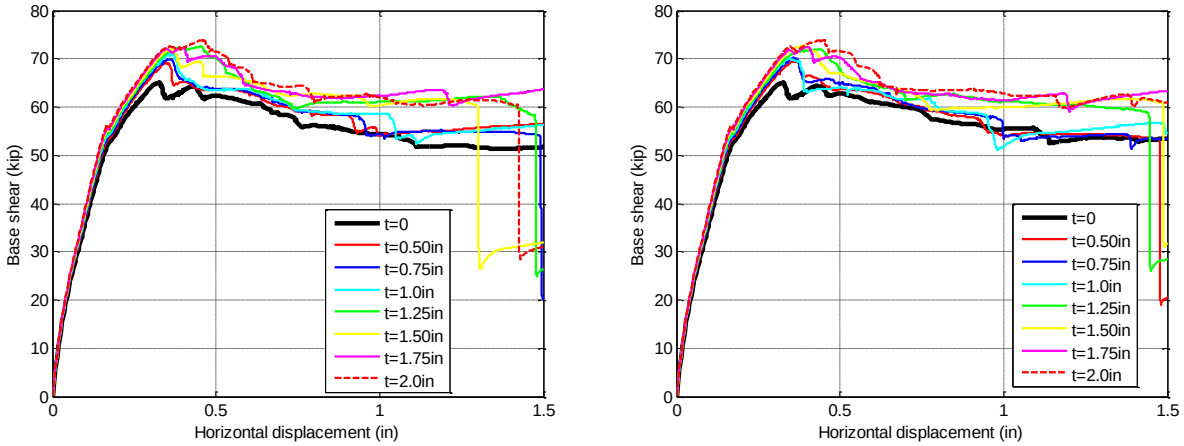

a) $f'c_{mortar}$=1.78 ksi b) $f'c_{mortar}$=2.2 ksi

Figure 5-8. Pushover curve for Specimen 9 under different mortar overlay parameters.

An additional set of analyses is conducted, using a different procedure to account for the mortar overlay similar to the approach used by Koutromanos (2011). The specific analyses have been conducted using the configuration of specimen 9 by Mehrabi et al. (1994) as the baseline case. **Figure 5-9** shows both approaches.

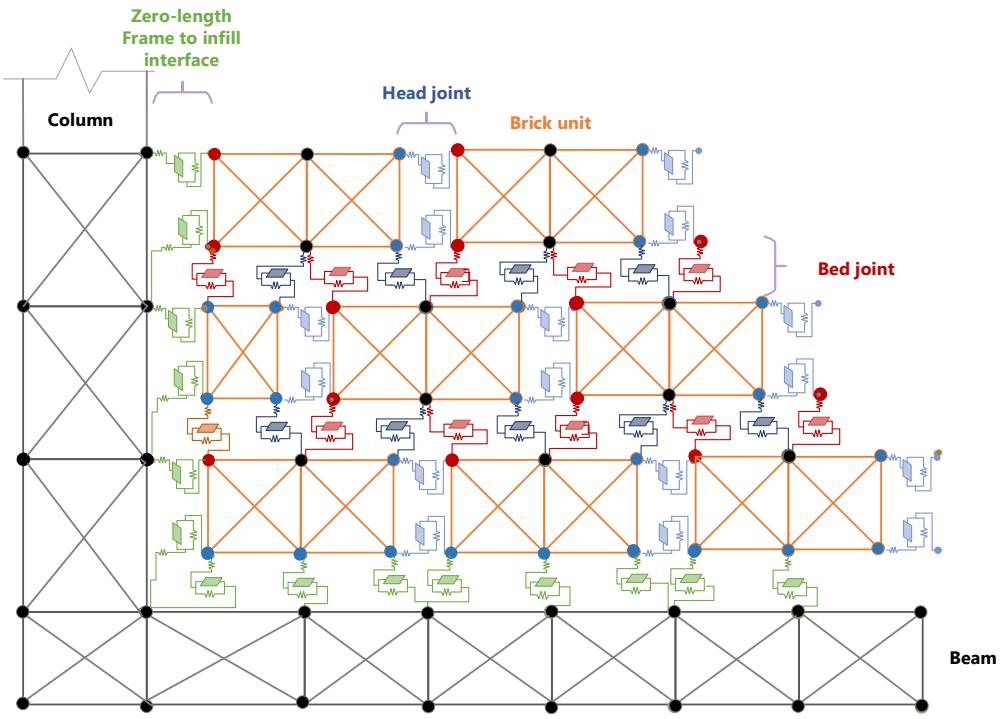

a) Simplified mortar overlays idealization (same as brick layout).

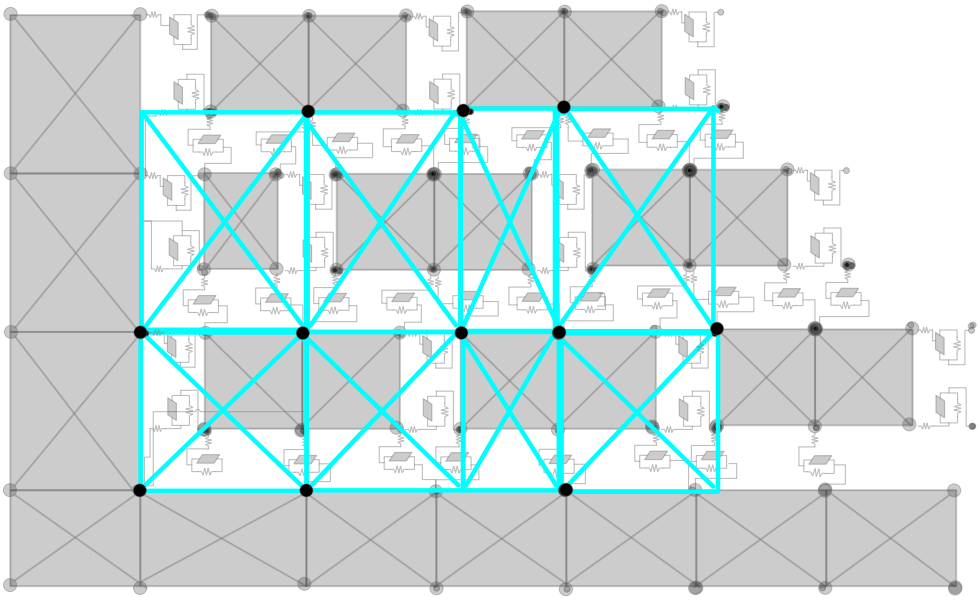

b) Mortar overlay with no localized sliding based on Koutromanos (2011).

Figure 5-9. Mortar overlay model approaches.

Figure 5-10 (a), depicts the lateral force-vs.-displacement relations for the nine (8) configurations studied before in **Figure 5-8** (a) and the contour plot for the case of 2 in. thickness. Generally speaking, both approaches reflect an improvement of the overall behavior of the system, but the latter reflects a considerable increase of the initial stiffness and strength but the capacity of deformation is decreased significantly.

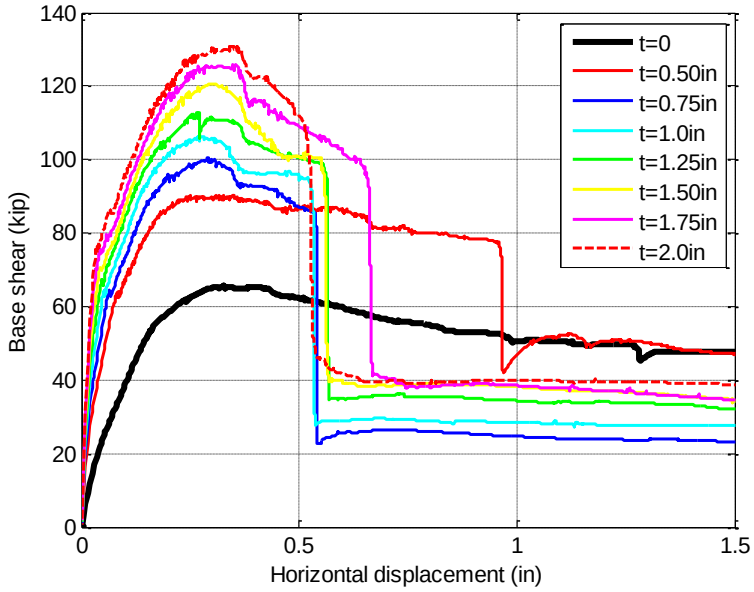

a) Specimen 9 f'c_{mortar}=1.78 ksi

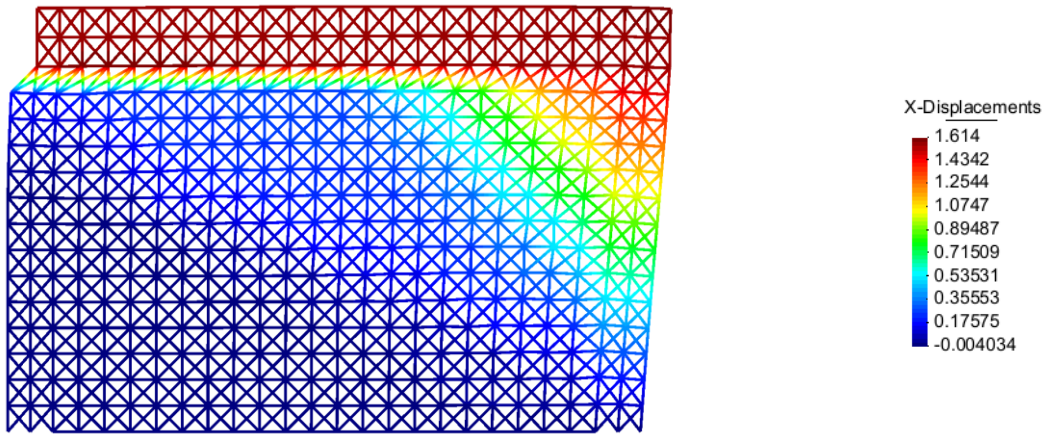

Contour displacement plot t=2 in.

Figure 5-10. Mortar overlay with no localized sliding.

Based on the models studied here it is concluded that the presence of the mortar overlay leads to a significantly increase in terms of strength and stiffness. The simplified approach of artificially increasing the mortar joint thickness due to the presence of the mortar overlay underestimates the benefit of the mortar overlay itself in the lateral response of the system. Despite that the mortar overlay increases the mass of the system, its beneficial contribution in terms of adding ductility is arguable. For older-type construction this layer of material can be decisive in delaying the structural collapse and incorporating an additional amount of damping as it fractures. For the case of Specimen 9, the presence of the mortar overlay contributed to slightly delay the shear failure of the top of the windward column, but in some cases a sudden drop in strength was seen. It can be concluded that the presence of the mortar overlay produces a similar effect to that of an increase in the strength of the infill wall. Thus the stronger the infill, the higher the probability of having shear failures in the frame columns. It is interesting to note that ductile-type of layers applied on the infill's face have been studied as retrofit schemes, with promising results Kyriakides and Billington (2008), Koutromanos (2011). In this study, only the effect of non-ductile mortar overlay was studied, but the proposed methodology can be used to perform this analysis.

It can be concluded that the presence of the mortar overlay produces a comparable effect as increasing the compressive strength of the infills similar effect to that of an increase in the strength of the infill wall. Thus the stronger the infill, the higher the probability of inducing a shear type of failure in the columns having shear failures in the frame columns. It is interesting to note that ductile-type of layers applied on the infill's face have been studied as retrofit schemes, with promising results Koutromanos (2011). In this study, only the effect of non-ductile mortar overlay was studied, but the proposed methodology can be used to perform this analysis.

5.6. Effect of Openings.

This section studies the effect of openings in the lateral force-vs.-displacement behavior of RCF with URM infills. The baseline configuration is a two-bay frame RCF with infills made of hollow units. A total of 36 configurations have been analyzed, as summarized in **Table 5-2**. The configurations corresponded to a variety of types and locations of openings, as shown in **Figure 5-11**. The parametric study presented here was expanded to two-bay frames with the idea to study different configurations in one single model.

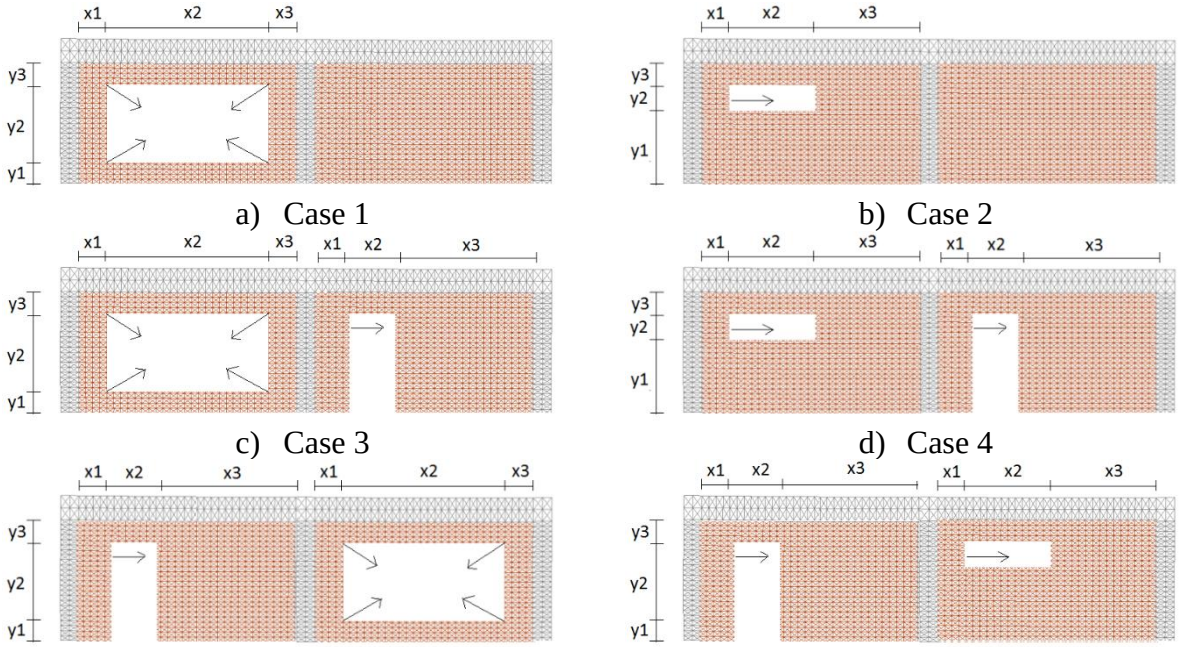

Figure 5-11. Openings configurations.

Table 5-2 Configurations considered for a two-bay frame RCF specimen.

Id	Bay	X1 (in)	X2 (in)	X3 (in)	Y1 (in)	Y2 (in)	Y3 (in)	Ah/ Ain	Id	Bay	X1 (in)	X2 (in)	X3 (in)	Y1 (in)	Y2 (in)	Y3 (in)	Ah/ Ain
H1	L	4	76	4	4	48	4	0.776	**H19**	L	4	36	44	36	8	12	0.06
	R	-	-	-	-	-	-	-		R	24	36	24	4	40	12	0.31
H2	L	8	68	8	8	40	8	0.578	**H20**	L	12	36	36	36	8	12	0.06
	R	-	-	-	-	-	-	-		R	28	36	20	4	40	12	0.31
H3	L	12	60	12	12	32	12	0.408	**H21**	L	20	36	28	36	8	12	0.06
	R	-	-	-	-	-	-	-		R	32	36	16	4	40	12	0.31
H4	L	16	52	16	16	24	16	0.265	**H22**	L	28	36	20	36	8	12	0.06
	R	-	-	-	-	-	-	-		R	36	36	12	4	40	12	0.31
H5	L	20	44	20	20	16	20	0.150	**H23**	L	36	36	12	36	8	12	0.06
	R	-	-	-	-	-	-	-		R	40	36	8	4	40	12	0.31
H6	L	24	36	24	24	8	24	0.061	**H24**	L	44	36	4	36	8	12	0.06
	R	-	-	-	-	-	-	-		R	44	36	4	4	40	12	0.31
H7	L	4	36	44	36	8	12	0.061	**H25**	L	12	36	36	4	44	8	0.34
	R	-	-	-	-	-	-	-		R	4	76	4	4	48	4	0.78
H8	L	8	36	40	36	16	4	0.061	**H26**	L	4	36	44	4	40	12	0.31
	R	-	-	-	-	-	-	-		R	8	68	8	8	40	8	0.58
H9	L	20	36	28	36	8	12	0.061	**H27**	L	12	36	36	4	40	12	0.31
	R	-	-	-	-	-	-	-		R	12	52	20	12	24	20	0.27
H10	L	28	36	20	36	8	12	0.061	**H28**	L	12	36	36	4	40	12	0.31
	R	-	-	-	-	-	-	-		R	16	52	16	16	24	16	0.27
H11	L	36	36	12	36	8	12	0.061	**H29**	L	12	36	36	4	40	12	0.31
	R	-	-	-	-	-	-	-		R	20	44	20	20	16	20	0.15
H12	L	44	36	4	36	8	12	0.061	**H30**	L	20	36	28	4	40	12	0.31
	R	-	-	-	-	-	-	-		R	24	36	24	24	8	24	0.06
H13	L	4	76	4	4	48	4	0.776	**H31**	L	24	36	24	4	40	12	0.31
	R	4	36	44	4	48	4	0.367		R	4	36	44	36	8	12	0.06
H14	L	8	68	8	8	40	8	0.578	**H32**	L	28	36	20	4	40	12	0.31
	R	4	36	44	4	40	12	0.306		R	12	36	36	36	8	12	0.06
H15	L	12	60	12	12	32	12	0.408	**H33**	L	32	36	16	4	40	12	0.31
	R	8	36	40	4	40	12	0.306		R	20	36	28	36	8	12	0.06
H16	L	16	52	16	16	24	16	0.265	**H34**	L	36	36	12	4	40	12	0.31
	R	12	36	36	4	40	12	0.306		R	28	36	20	36	8	12	0.06
H17	L	20	48	16	20	20	16	0.204	**H35**	L	40	36	8	4	40	12	0.31
	R	16	36	32	4	40	12	0.306		R	36	36	12	36	8	12	0.06
H18	L	24	36	24	24	8	24	0.061	**H36**	L	44	36	4	4	36	16	0.28
	R	20	36	28	4	40	12	0.306		R	44	36	4	36	8	12	0.06

Ah = Area of hole, Ain= Area of Infill, L=Left bay infill, R=Right bay infill.

Figure 5-12 presents the load-displacement response for the prototype structure under different representing possible locations for window or doors. **Figure 5-12** (a) depicts the pushover response of the two-bay specimen having different windows on the left bay whereas no opening is present in the right bay. It is noticed that strength and the stiffness vary as a direct function of the window size. For the cases analyzed, larger openings produce significant stiffness, strength and ductility

reductions, but small windows (less than 10% of the infill wall) produce negligible variations of strength (less than 4%) and stiffness (less than 20%) as shown in **Figure 5-13**.

Figure 5-12 (b) presents the pushover curve for the case of fixed window size with different locations along bay 1. For this case, no important variations were reported when the different configurations are compared with the baseline case. **Figure 5-12** (c) depicts the pushover curve for Case 3 in **Figure 5-11**. The left bay is similar to Case 1 whereas at the same time a door opening is located at the right bay in accordance with **Table 5-2**. A considerable reduction in terms of initial stiffness (≈ (35%-80%)) and strength is evident (≈ (15%-42%)) as shown in **Figure 5-13**. Up to this point, the failure pattern was the same for all models. (i.e sliding at the bed joints).

Figure 5-12 (d) depicts the pushover curve for Case 4. Most of the models analyzed here present a defined peak strength at about 0.55 in. lateral displacement. In the right bay, the wall slides and bends due to the reduction of resistance from the presence of the door opening. Some variation in terms of initial stiffness (50% reduction) and strength behavior (≈ (4%-18%)) is evident due to the different configurations studied here. **Figure 5-12** (e) presents the pushover curve for Case 5. The analysis results shows that both the initial stiffness and strength drop significantly, (≈ (35%-80%)) and (≈ (12%-42%)) respectively, due to the particular combination of door and windows openings.

Finally, **Figure 5-12** (f) presents the results obtained for Case 6. This model is similar to Case 5. The difference is that now a fixed size window opening present in the right bay instead of a window opening changing size. Compared with Case 5, the effect of the position of the fixed size window is less important. The most unfavorable behavior was present for the model which has the door closest to the windward column and the window opening closest to the middle column. This can be explained by (1) the lower resistance attributed to the reduction of the compressive force at

the windward column due to the overturning moment and (2) the adverse effects of the concentration of stresses in the vicinity of the frame infill elements due to the presence of the hole.

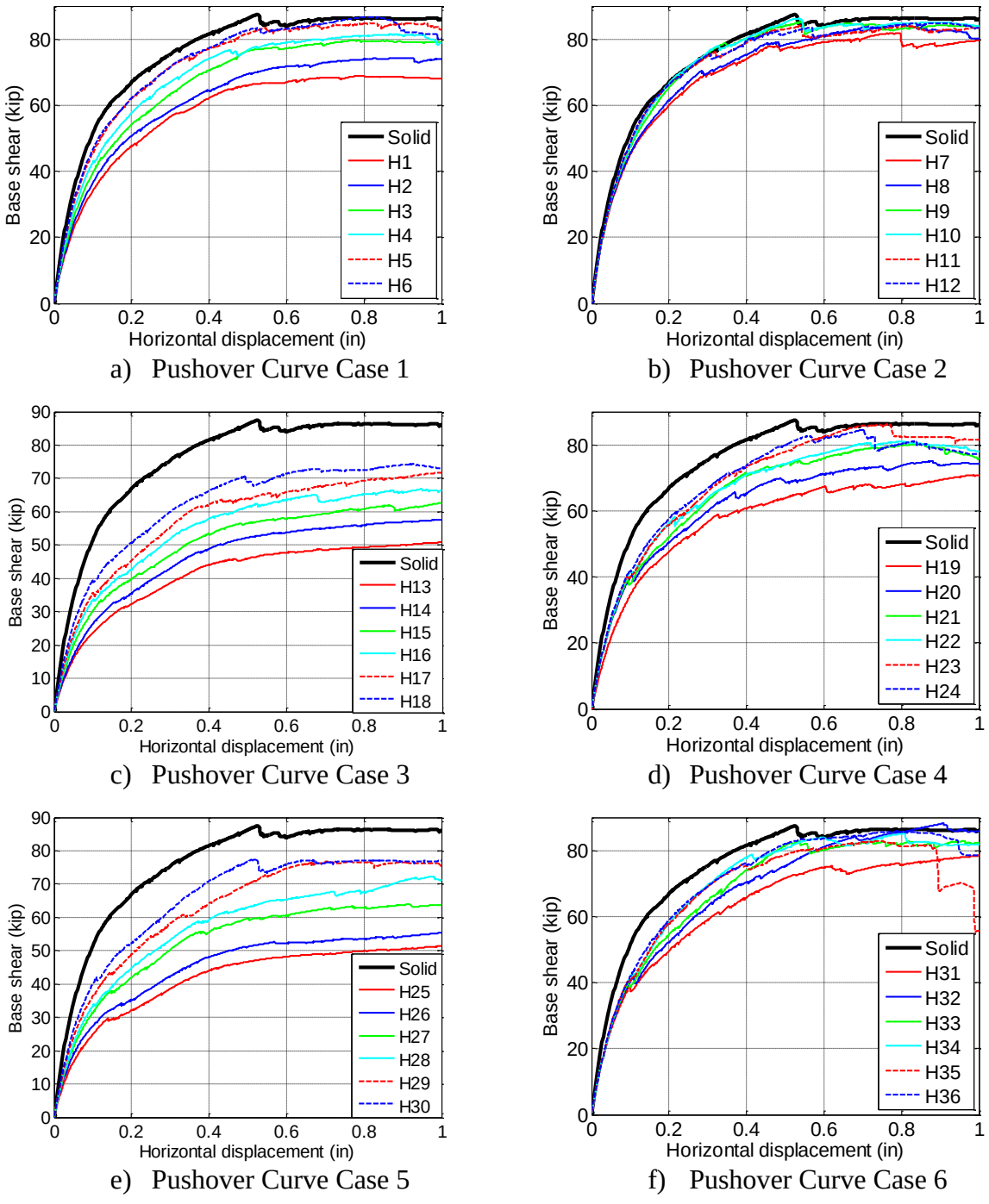

Figure 5-12. Pushover curve for two-bay specimen under different openings configurations.

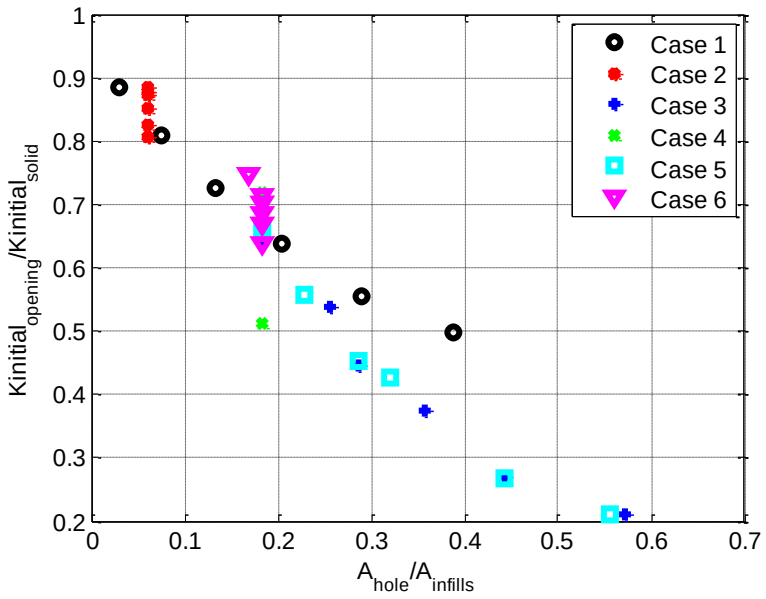

a) Stiffness variation calculated at 40% of the peak strength of the baseline case

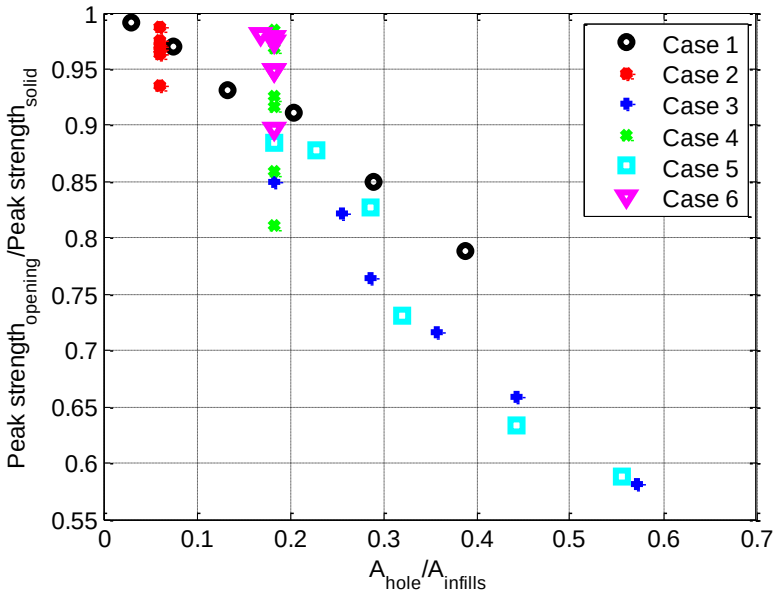

b) Strength variation

Figure 5-13. Stiffness and stress variation under different openings configurations.

Summary of findings

This chapter presented parametric analyses on infilled RC frames, to evaluate the significance of various parameters. The main conclusions of the analyses pursued are provided below.

- Axial load variation and distribution among the columns and infill play a major role in the strength and stiffness of the RCF with URM infills. The increase of compressive forces enhances the lateral resistance due to the additional frictional resistance. It was proved that a larger axial load level helps to increase the initial stiffness and strength but may result in a lower ductility, characterized by sudden failure.

- Longitudinal reinforcement and transverse reinforcement ratios of the column have an insignificant effect in terms of the variation of the initial stiffness of the system. The reported failure of this Specimen was a shear-critical failure. Therefore, for older-type construction, the increase of longitudinal reinforcement brings additional strength to the system due the fact that higher longitudinal strength ratios increase the tensile resistance. Thus higher shear forces can be developed in the section and the peak strength of the system is naturally increased. The increase of transverse steel area was unable to prevent the failure at the top of the windward column. For that reason, **Figure 5-5** depicts small variations for the cases analyzed, which included reasonable ranges for both longitudinal and transverse steel. A significant increase in the column size will be necessary before the effects of the variables becomes relevant.

- Mortar overlay applied on infill faces can be beneficial in terms of strength and ductility for RCF with URM infills, especially for older type construction with the presence of weak infills.
- The presence and location of openings significantly affect the strength and the initial stiffness in infilled frames. The larger the opening, the larger the reduction of in strength and initial stiffness. Small openings located at the middle of the infills result in almost identical strength and initial stiffness as its solid counterpart due to efficiency of the transfer force mechanism before reaching the opening area.

6. Nonlinear Truss Analysis of Prototype Building in Colombia

6.1. Introduction

In Chapter 4, a new method for performing nonlinear analysis of RCF with URM infills subjected to monotonic in-plane lateral was introduced. It was proved that this method retains satisfactory accuracy when compared to test results and refined NLFEA. In Chapter 5, this method revealed useful findings with regard to the structural response of specimens which have different conditions and configurations, and for which no experimental results are available. The only remaining aspect is to evaluate the suitability of the proposed method for a prototype building in Colombia. This Chapter is intended to address this last requirement.

The unbraced RCF is the most popular structural system in Colombia and the presence of the URM infills is a common practice even today. Experience has shown the vulnerability of the Colombian non-ductile structures (see Appendix A). Therefore, considering the fact that a gross percentage of Colombian buildings still remain without any structural intervention, this section presents an attempt to model the soft-story mechanism extensively reported after the Popayan earthquake in 1983. Despite that the most recent seismic events in Colombia can be characterized as having foci and/or epicenters located far away from the populated urban areas, an important number of buildings in the Colombian inventory can experience a soft-story collapse mechanism. This type of failure can be attributed to (1) the presence of wide openings in the bottom story, (2) the presence of slender columns at the base, and (3) the discontinuity of the infills walls for architectural considerations. Due to the sudden change in the vertical stiffness between consecutive

stories, this mechanism is characterized by an excessive localized drift that causes heavy damage in the bottom columns. The above facts are the rationale to propose the prototype building.

6.2. Description of the Prototype Colombian Building

A three-story two-bay non-ductile building with a plan layout as shown in **Figure 6-1** was used as prototype building in this study. This corresponds to a RCF with URM infills. The building was symmetric about both principal axes with uniform story heights of 9’ 10” feet. Customary loads, for building in Colombia were assumed. The uniformly distributed gravity factored load used for the gravity case in the 2D analysis was 1.32 kip/ft.

Square columns sections were used for the columns and beams. The cross-sectional area used was (11.8x11.8 in.) for both columns and beams. For the columns, 1.26% longitudinal reinforcement ratio was used, with transverse reinforcement area of 0.22 in^2 at 6 in. (#3 at 6 in.). For the beam, a longitudinal reinforcement ratio of 0.0033 and a transverse reinforcement area of 0.22 in^2 at 6 in. (#3 at 6 in.). Grade 60 and Grade 40 steel were assumed for the longitudinal and transverse reinforcement respectively.

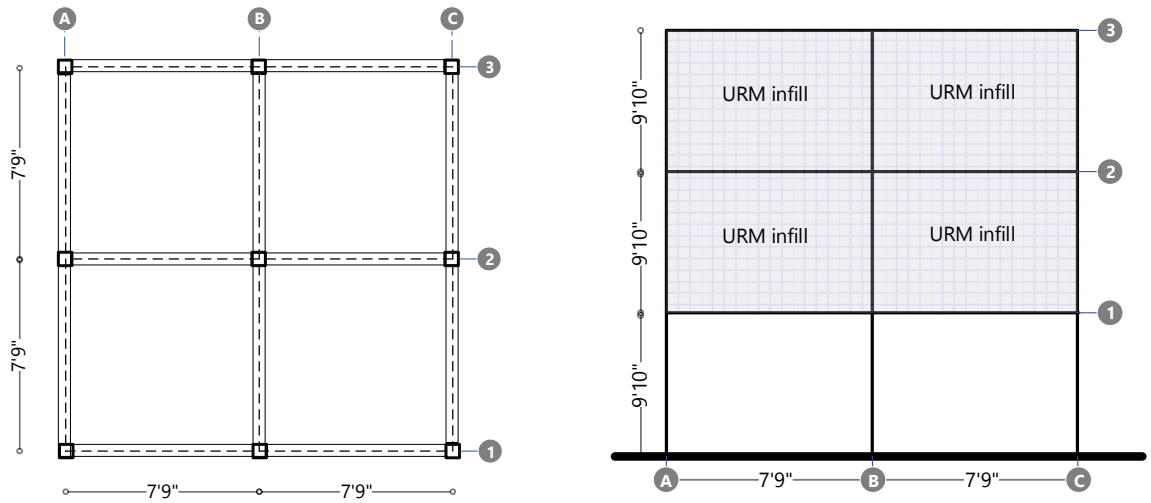

a) Plan view. b) Elevation view.

Figure 6-1. Prototype building.

6.3. Methodology

The prototype building was subject to nonlinear static pushover analyses conducted with the factored gravity load and a monotonic force-controlled lateral load pattern. A unit point load applied at each story level was used to emulate the fundamental mode shape during the lateral load application. OpenSEES McKenna et al. (2000) was selected as software platform to perform the simulation of the prototype building. This software includes the modeling capabilities to perform the simulation such as: material properties (concretebeta, steel02), element model (truss, truss2, zerolength), and several numerical algorithms for solving the nonlinear systems of equations. The main goal of this section is to extend the approach presented Chapter 4 to the nonlinear analysis of a prototype (multi-bay, multi-story) building in Colombia. At this time, the baseline comparison kept in previous simulations (i.e. test results NLFE simulations) vanishes. As a consequence, this

section presents two modeling approaches including: (1) a simplified lumped plasticity model concept using the modified Ibarra-Medina_Krawinkler-Lignos deterioration model with peak oriented hysteretic response Lignos and Krawinkler (2012.) in conjunction with the predictive regressions equations presented in Haselton and Deierlein (2008) and explained in Appendix B, and (2) the truss model in accordance with Chapter 4. The following sections describe both modeling approaches.

6.3.1. Simplified Analysis

The simplified model depicted in **Figure 6-2** is comprised of linear elastic beam-column elements for the beams and columns of the second and third story. Since the inelastic activity is expected only at the bottom story, this allows to represent the infill walls by linear elastic truss elements in the prototype building. The first-story columns are modeled by combination of elastic and inelastic zero-length elements placed at the two element ends. In Appendix B.2, a brief description and a validation example of this schematic procedure is presented. It is worth mentioning that due to the fact that the expected failure will generate considerable flexural deterioration concentrated at the first-story columns, the proposed phenomenological-oriented approach is a reasonable choice. If infill walls were placed at the bottom story, this simplified assumption will not be longer valid, due to the brittle type of failure induced by the presence of the infills and the reasons explained in Section 2.3. The lumped plasticity model requires using empirical equations relating the design parameters the column to the modeling parameters. The only parameter that demands a priori calculation is the estimation of the yielding moment of the section.

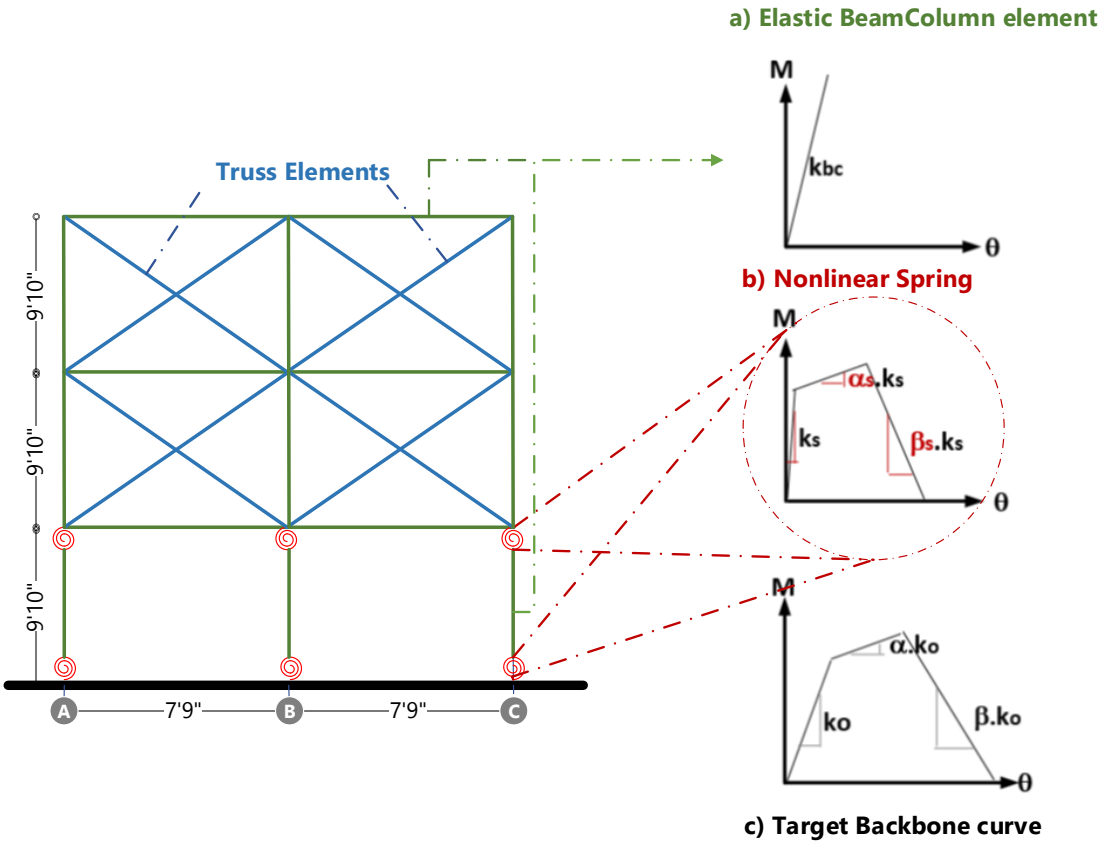

Figure 6-2. Approximate building model.

Figure 6-3 shows the lateral load vs drift response of the prototype building. Based on the results of the simplified model, yielding occurs at about 0.3% story drift ratio. The maximum strength obtained was 28 kips, and was followed by the onset of negative stiffness at a story drift ratio of 2.2%. For this approach, the post-capping rotation capacity was reduced by 50% to account for the low ductility expected in this model.

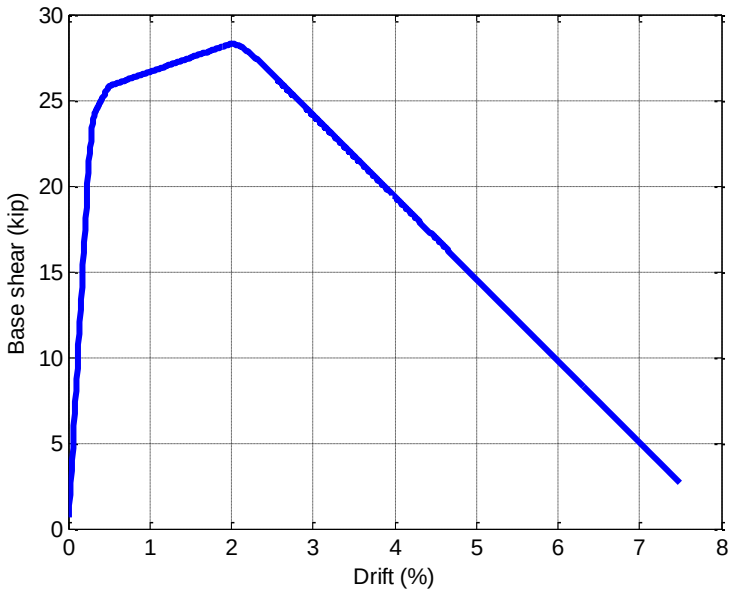

Figure 6-3. Lateral load vs drift response for the approximate building model.

6.3.2. Truss Model Simulation for the Prototype Building

This section presents the simulation results of the prototype building by using the truss model. The two-cases analyzed include: (a) the prototype building in absence of infill walls at the base, referred as "Truss Model NI", and (b) the prototype building with URM infills at the base and the presence of two openings, labelled as "Truss Model PI".

6.3.2.1. Truss Model for the Prototype Building with No Infills

The "Truss Model NI" model is intended to study the structural performance of the prototype non-ductile RC frame with infill walls totally omitted at the bottom-story. As shown in **Figure 6-6**, this structure displayed typical non-ductile frame behavior. The system response is

characterized by low values for initial stiffness, strength and ductility. Due to the concentration of inelastic deformation at the bottom elements, the first story is prone to have large drifts. The peak strength of the prototype structure is 18.7 kip and the drift at peak displacement was 0.75%. After this point, a considerable deterioration of the system was presented up to a residual value of about 10 kips.

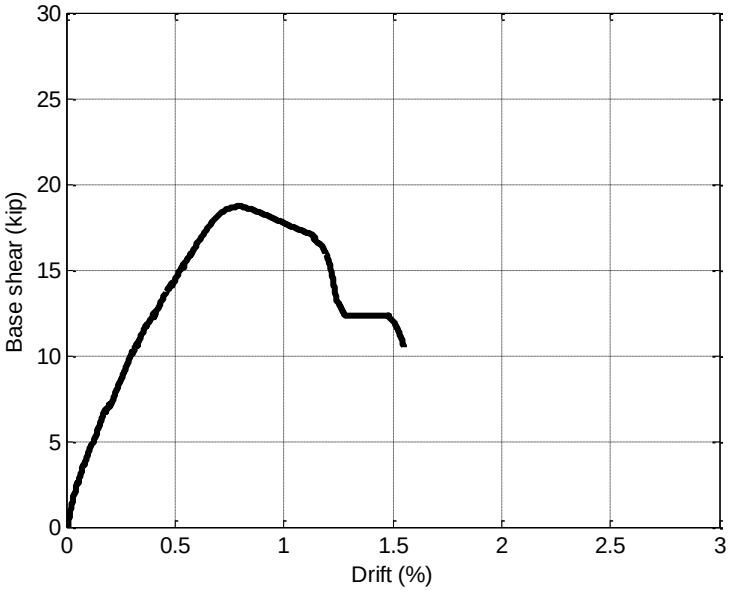

Figure 6-4. Geometry model for "Truss Model NI".

6.3.2.2. Truss Model for the Prototype Building with Infills

One additional case, "Truss Model PI" model is analyzed as a direct consequence of the data obtained from the parametric study in Section 5.6. It was demonstrated that presence of openings in the infills affect drastically the behavior of this structural system. In this model, the bottom-story of the prototype building is infilled. A door and a window opening, representing 19% and 16% of the wall area, are placed in accordance with **Figure 6-5** (b). For

simplicity, the infill material properties are kept the same for all stories. **Figure 6-5** (b) shows the significant contribution of the infills in terms of initial stiffness, strength and ductility. The peak strength obtained was 106 kip, and the drift at peak strength was presented at 1.1 %. The post-peak behavior is characterized by considerable softening up to a residual value of 60 kips.

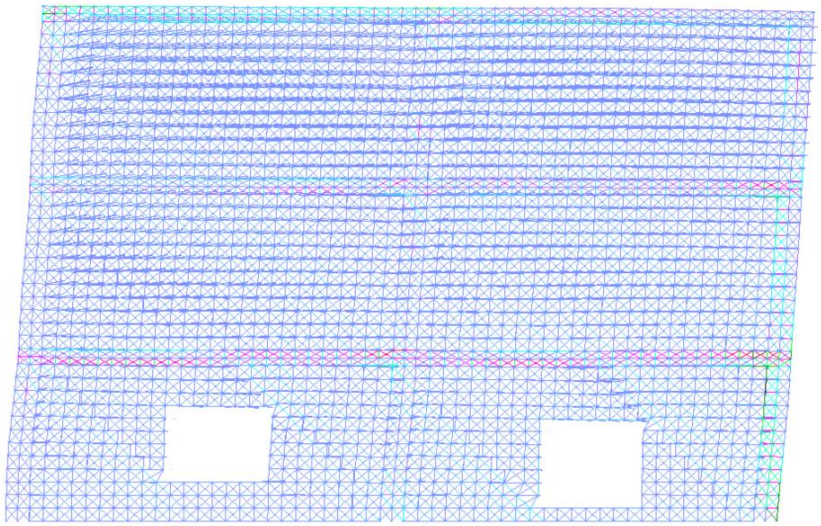

a) Deformed Shape "Truss Model PI" model at 1.0 in lateral displacement.

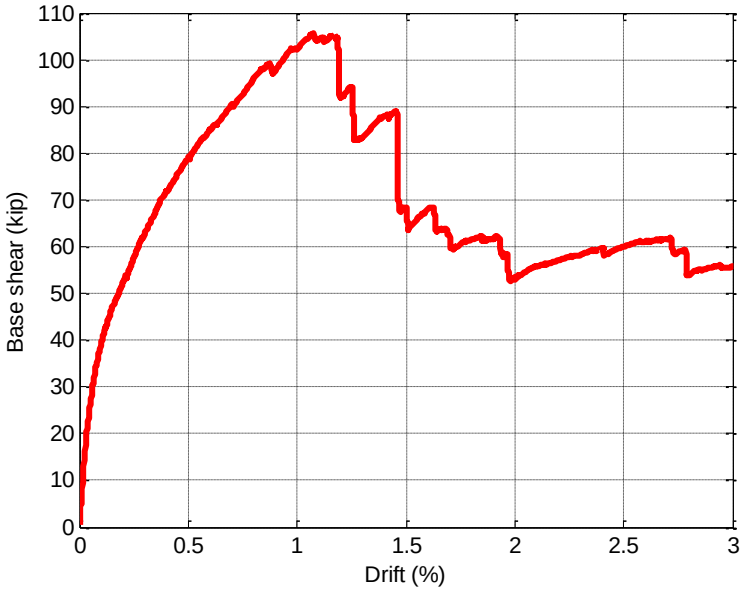

b) Pushover curve for the "Truss Model PI" model

Figure 6-5. Deformed shape and lateral load vs drift response for the "Truss Model PI" model.

The results of the three analysis, are presented in **Figure 6-6** and can be summarized as follows:

- Despite the rationality applied in the approximate analysis, it significantly overestimates the initial stiffness, strength and ductility of the prototype building. This can be explained by: (1) the over-simplification of the approximate approach, and (2) the fact that the regression equations were calibrated using cyclic and monotonic tests of 255 rectangular reinforced concrete elements with few of them representing non-ductile elements. The regression equations and the overall model approach presented in Appendix B.2 were validated mostly for code-conforming reinforced concrete moment frames. It is clear that the calibration of the parameters need to be validated with local tests in Colombia; unfortunately this data is not available at this time.
- The simulation of the prototype building resulted in a soft-story collapse mechanism at about 1.5% drift. Compared with the simplified model, the strength and ductility are considerable lower, which indicates the overall limitation of the approximate model. However, in terms of peak strength, both approaches provide relatively close values.
- The inclusion of the URM infill with openings results in higher strength and ductility due to the distribution of damage of the infill wall. However, the after the peak strength a substantial softening took place. The drift at peak strength was about 1.5 % drift. Despite the notorious benefits in term of strength and stiffness additions, the weak nature of the Colombian URM infill studied here implies that those benefits can be accrued just for low drift levels only. For that reason, for an

adequate response of the RC frame with weak URM infills, the frame itself must be rely in its ability to dissipate the energy and must avoid dependence on the additional ductility that the infill can provide.

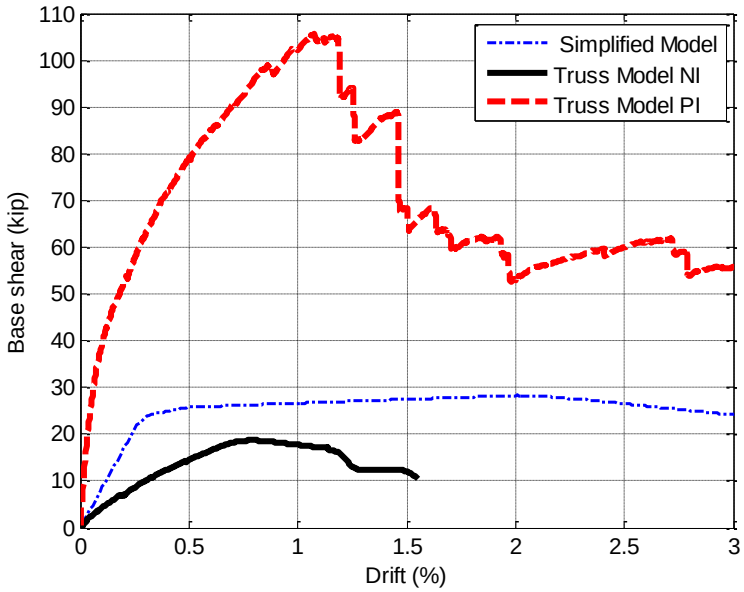

Figure 6-6. Lateral load vs drift responses for the prototype building.

Conclusions

This section demonstrated the suitability of the proposed model to handle a more complicated structure. Despite that an extensively validation of the model under different building configurations is still required, the proposed analytical approach has consistently given promising results. It is believed that the proposed approach is one step forward in bridging the gap between overly crude equivalent strut models and computationally expensive NLFEA.

7. Summary and Conclusions

7.1. Summary

Non-ductile Reinforced Concrete Frames (RCF) with and without Unreinforced Masonry (URM) infills can be found in many places around the world including the Western United States, Eastern Europe, Asia and Latin America. The vulnerability of such structures, to complete collapse and associated human and economic losses may have serious implications for the resilience of built communities.

The above facts indicate the need for the systematic, quantitative characterization of the performance and vulnerability of non-ductile reinforced concrete frames. A significant number of previous research efforts have relied on experimental tests to elucidate the hysteretic behavior and failure modes of such structures. While experimental research is always indispensable to provide real-life observations of the physical behavior, the size of the specimens and the range of possible configurations that can be tested are inherently limited by constraints associated with the capabilities of testing equipment and economic. Therefore, computational simulation is deemed necessary to allow systematic parametric studies which can focus on entire structural systems and also examine a sufficient range of possible configurations.

This study introduced a simplified modeling approach for non-ductile RCF with URM infills that combines the simplicity of strut-and-tie models with the accuracy of advanced finite element implementations. Experience, tests results and computational simulations have shown that the presence of infill walls in reinforced concrete frame construction may significantly affect the

behavior of such structures under lateral loading. Unfortunately the presence of the infills is commonly neglected in the design phase, possible due to the absence of practical models which can capture all the features of its response, such as the contact between the frame members and masonry infills and the localized damage at the mortar joints of the masonry. The proposed method is expected to solve this limitation, at the same time it is expected to bridge the gap between overly crude equivalent strut models and computationally expensive NLFEA.

7.2. Original Contributions

As a first step in this study, a comprehensive review of the literature related with some of the most relevant aspects associated with RCF in Colombia was conducted. Due to the complexity of the nonlinear problem (i.e frame-infill interaction, cracking of concrete and infill, failure patterns) NLFEA background was studied. Understanding the deficiencies of the simplified Strut-approaches and the capabilities of the NLFEA formulations of capturing the physical mechanisms leading to failure of reinforced concrete and masonry components, it was possible to develop a new analysis methodology for infilled frames, based on the nonlinear truss analogy (NLTA).

The proposed methodology uses the NLTA to describe the behavior of RC elements, and masonry infill units. The mortar joints and infill-to-frame interfaces are explicitly modeled in the analyses, since they constitute weak planes where localized tensile opening or shear sliding can occur. Additionally, the proposed interface model can capture the contact stress distribution along the infill-to-frame interface with adequate accuracy.

7.3. Conclusions

Masonry infills have been widely used as nonstructural elements (partitions, facades). However, its importance is not always recognized in analysis and design. Experience, test results and simulations have shown that its participation may be favorable in some cases, and on others it may be adverse. In fact, while the forces produced by the frame-infill-interaction are commonly neglected, this interaction can result in an unexpected brittle behavior in the elements of the structural system. Infills have heavy weight with low ductility, they can attract large seismic inertial forces, and their contributions to the strength and stiffness of the system will begin to deteriorate rapidly at low drift values. Furthermore, infills have low tensile and shear strength, and they can contribute to have local type of failures such as shear failure or captive column behavior, or they can influence soft story mechanism and trigger global collapse. Despite all these negative aspects, infills can be a source of additional lateral stiffness and overstrength to the building resulting in lower seismic deformation demands. As they fracture, infills can significantly contribute to the global energy dissipation capacity of the structural system while they remain confined by the frame. For the Colombian case, it is believed, based on Appendix C, that the probability of inducing brittle type of failure to the surrounding elements is low due to its low compressive strength> However as it was shown in Chapter 5, if infills are placed in particular locations or, as shown in Chapter 6, wide openings are concentrated at the bottom –story, infills can induce soft story mechanism.

Nonlinear analysis of RCF is particularly challenging, especially because the seismic response is likely to be highly non-linear due to factors such as rebar buckling, concrete cracking, and concrete crushing. The problem gains complexity once the presence of the infill is considered,

especially when considering the frame infill interaction and the infill mode of failure. Refined NLFEA can adequately represent the structural behavior and damage patter presented in such structural system. Unfortunately, the elevated complexity of these rational tools have been determinant in their lack of widespread use to determine structural behavior.

In general, the experimental and analytical results have indicated that the addition of infill panels has a profound influence on the behavior of RCF. The following conclusion arise from the present study:

- From the parametric study in Chapter 5, it was concluded that axial load variation and distribution among the columns and infill play a major role in the strength and stiffness of the RCF with URM infills. In addition, mortar overlay applied on infill faces can be beneficial in terms of strength and ductility for RCF with URM infills, especially for older type construction with the presence of weak infills. Nevertheless, mortar overlays are harmful if they induce a shear critical failure at the columns.
- The presence and location of openings have a deep effect on the strength and the initial stiffness of the RCF with URMI. The larger the opening, the larger the reduction of in strength and initial stiffness. Small openings located at the middle of the infills result in almost identical strength and initial stiffness as its solid counterpart due to efficiency of the transfer force mechanism before reaching the opening area interestingly, the deformation and ductility can be enhanced by these openings.
- Finite element analyses are conceptually complicated, as they require the use of both special formulations, such as those of cohesive crack interface elements, and of complicated constitutive laws which involve many parameters in their definitions. NLFEA

are computational expensive, which implies the limitation to conduct systematic parametric studies of prototype, multi-story structures.

- The proposed approach was validated and used to study the behavior of multi-bay and multistory buildings (with results from NLFEA simulations). The analysis of the prototype building confirmed that despite the notorious benefits in terms of strength and stiffness additions, the weak nature of the Colombian URM infill studied here implies that those benefits can only be assumed for low drift levels. For that reason, it is imperative that for an adequate response of the RC frame with weak URM infills, the frame itself must perform well, avoiding the dependence on the additional ductility that the infill can provide.
- The proposed modeling approach can adequately capture the strength and stiffness degradation and the damage patterns, while entailing a lower computational cost compared to finite element models. This method is conceptually simple, easy to understand and implement, computationally efficient, and easy to calibrate. It accounts for axial, flexure and shear interaction, and is not vulnerable to stress locking, an effect present in most NLFEA simulations which rely on smeared-crack formulations. It is believed that the proposed method can be used for the systematic performance assessment of non-ductile, infilled RC frames.

7.4. Recommendations Future Research

The contribution presented in this doctoral dissertation is a step towards the accurate and practical-oriented assessment RCF with URM infills. This section includes some suggestions of future research, which may involve:

- Further validation of the proposed method compared with test results, including the presence of the openings, and test its accuracy when this approach is used as blind predictor in assessing the effectiveness of retrofit schemes.
- Studying the P-Delta effects in the analysis of RCF with URMI especially for the cases with large openings.
- Enhancement of the spring idealizations to account for normal and transverse stiffness which better represent the interface behavior.
- Validation of the accuracy of the model with local tests carried out in Colombia to take into account some specific case of studies and local practices.
- Study the effect of the strut inclination angle on the analytical results of RCF with URM infills.
- Extension of the proposed approach to allow the simulation of RCF with URMI under cyclic pushover, nonlinear dynamic, and three dimensional analyses.

A. Appendix A

A.1. Colombia's Background

Colombia is located in the northern part of South America **Figure A-1**, one of the most seismically active zones in the world. The Circum-Pacific belt, also known as "ring of fire," contributes about 90% of the world's earthquakes. The Nazca, Cocos, and Pacific Plates all join off the northwest Colombian coast. The Nazca plate is believed to move from west to east at about 2.4 inches per year. The South-America plate moves from east to west at a relative velocity of 0.4 to 0.8 inches per year. The Caribbean plate moves in the WE direction at a relatively smaller velocity (Pujol et al. (2000)).

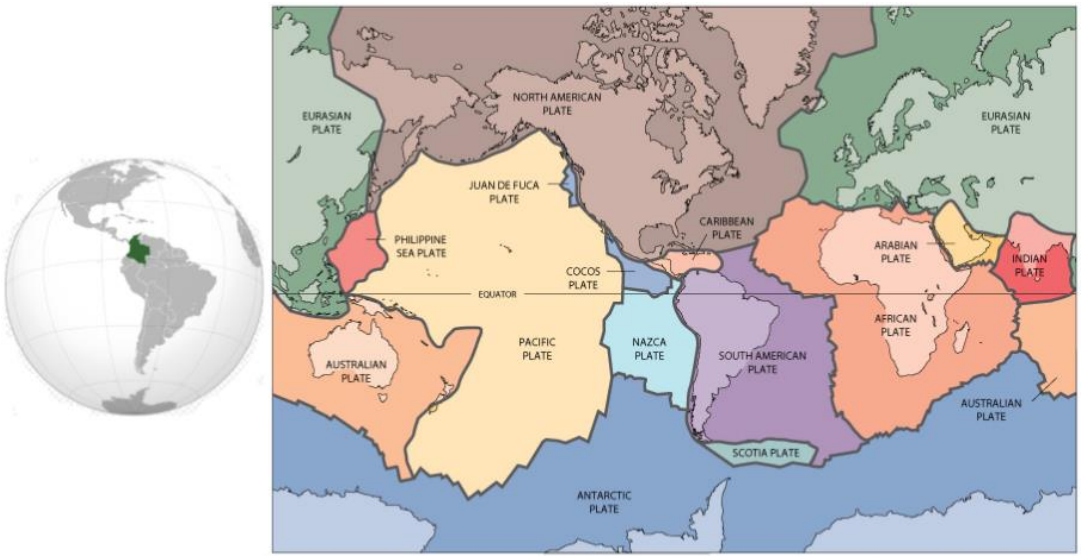

Figure A-1 Location of Colombia and its tectonic setting (Adapted from www.usgs.gov).

The vast majority of Colombia's inhabitants live on the Andes Mountains, geologically characterized by many active fault systems as depicted in **Figure A-2**. For instance, the Romeral fault system extends 1600 km from Barranquilla, Colombia to Talara, Peru.

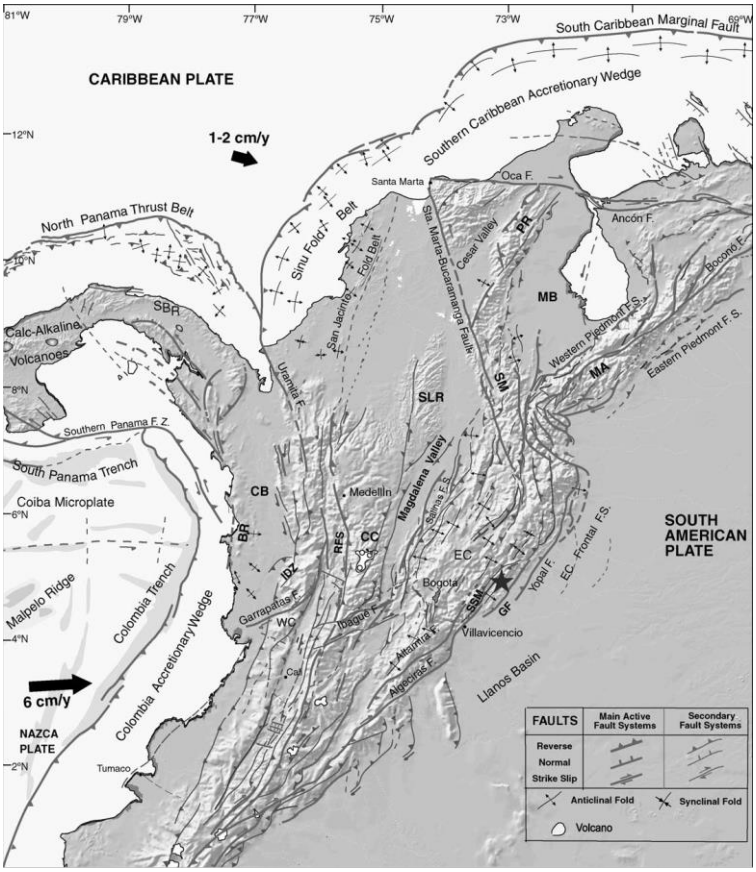

Figure A-2 Andes and Caribbean tectonic setting Taboada et al. (2000).

In addition, the Bucaramanga Nest is located in the mid-eastern part of this country. The Bucaramanga Nest represents the most intense concentration of intermediate-depth earthquakes in the world (see **Figure A-3** b). Despite the high risk clearly present, Colombia's infrastructure does not correspond to this reality. In the past 30 years, moderate earthquakes have destroyed several cities, killed thousands of people, and have produced significant infrastructure losses. The lack of economic resources for strengthening these structures provides a challenge to those attempting to

propose efficient retrofitting solutions that address those needs. **Table A-1** presents some of the most relevant earthquakes that have occurred in Colombia since 1906.

Table A-1 Major earthquakes in Colombia adapted from Restrepo (2008).

Date	Magnitude M.s	Location	Type
31st January 1906	Ms = 8.2	Tumaco	Subduction
31st August 1917	Ms = 7.3	Bogota	Eastern Frontal fault system
5th February 1938	Ms = 7.0	Coffee zone	Subduction
9th July 1950	Ms = 7.0	North of Santander	Local deep seismicity
19th January 1958	Ms =7.8	Limits with Ecuador	Subduction
20th December 1961	Ms = 6.7	Coffee zone	Subduction
30th July 1962	Ms = 6.7	Coffee zone	Subduction
9th February 1967	Ms = 6.8	Huila	Local deep seismicity
26th September 1970	Ms = 7.0	Chocó	Subduction
13th July 1974	mb = 6.4	Juradó	Shallow activity
23rd November 1979	Ms = 6.7	Coffee zone	Local deep seismicity
12th December 1979	Ms = 7.7	Pacific	coast Subduction
31st March 1983	Ms = 5.0	Popayan	Shallow activity
19th November 1991	Ms = 7.1	Buenaventura	Subduction
17th October 1992	Ms = 6.8	Murindó	
18th October 1992	Ms = 7.3	Murindó	
22nd July 1993	Ms = 5.9	Arauca Shallow activity	22nd July 1993
6th June 1994	Ms = 6.6	Paez	
19th January 1995	Ms = 6.6	Tauramena	19th January 1995
8th February 1995	Ms = 6.8	Calima	Local deep seism
25th January 1999	Ml = 6.1	Coffee zone	zone Shallow activity
15th November 2004	Mw = 7.2	Chocó	Subduction
13th August 2014	Mw = 6.5	Chocó	Subduction

According to the 2005 Colombian national census DANE (2006), the resident population of Colombia is 42 million and the rate of growth is 1.8% per year. The Colombian Seismic Standard NSR (2010), determined that about 86% of the Colombians live on moderate or high seismic hazard zones. Building construction in Colombia is mostly characterized by low-rise buildings (less or equal to five stories high). The predominant structural system of buildings with three-stories or higher is Reinforced Concrete Frames (RCF). Despite the elevated seismic risk, most

structures were designed and built without regard to seismic loads and today represent high risks for human life.

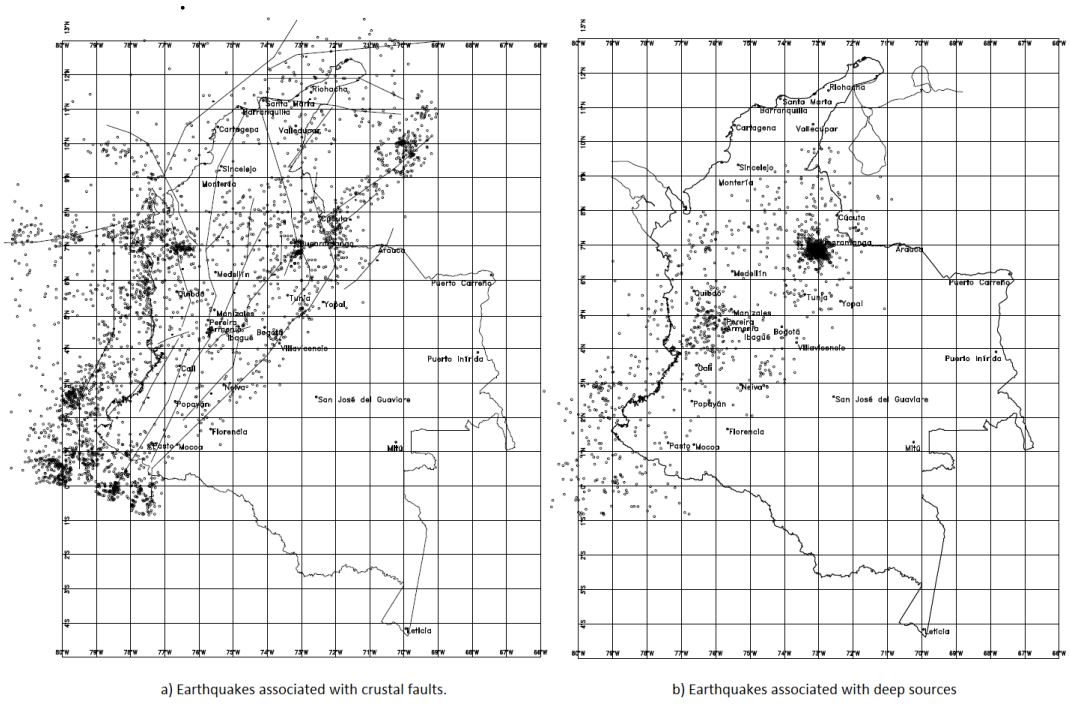

a) Earthquakes associated with crustal faults.

b) Earthquakes associated with deep sources

Figure A-3 Colombia seismic hazard map Salgado et al. (2010).

The 1999 Quindio Earthquake exposed the high vulnerability of the Colombian infrastructure. On Monday, January 25th, 1999, Colombia experienced a quake of magnitude 6.2 on the Richter scale. It devastated the cities of Quindío, as well as neighboring Pereira. According to the USGS, at least 1,185 people were killed; there were over 700 people missing, presumably dead. Additionally, there were over 4,750 injured, and about 250,000 were left homeless (Sanchez-Silva et al. (2000)). It was the strongest earthquake to strike Colombia for 16 years. **Figure A-4** depicts the three components of this ground motion. Much of the damage occurred because significant portions of the structures in this area were not built according to earthquake safety standards.

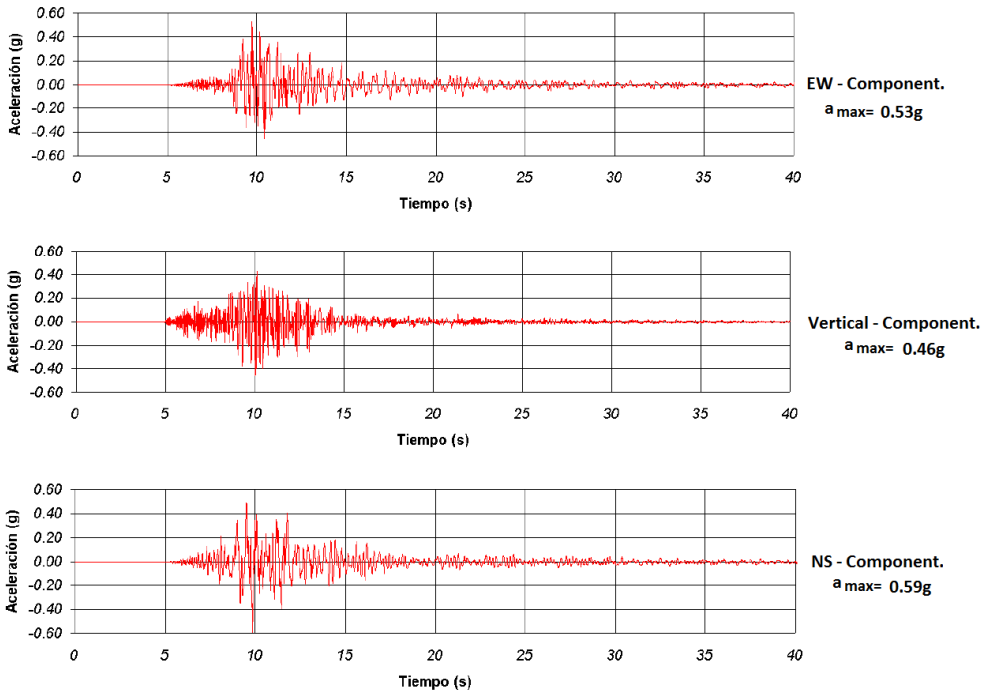

Figure A-4 El Quindio ground motion recorded at Universidad del Quindío in Armenia. Adapted from Garcia (2000).

The 1999 Quindio Earthquake was recorded by 31 recording stations located in different types of soil deposits. The University of Quindio recording station was the closest station that registered the ground motion. This station is located just 14 KM north to the epicenter. This station is located in a deposit of 30 meters of volcanic slimy argillaceous soils with shear waves speeds between 150 and 200 m/sec. This deposit, in turn, overlies a conglomerate with shear wave speeds between 600 and 1000 m/sec. The maximum acceleration recorded in this station was 0.59g in N-S direction, 0.53g in the E-W direction, and 0.46 in the vertical direction. **Figure A-5** depicts the two horizontal components plotted together with the corresponding vertical acceleration using a color code. It is possible to observe that in some instances the two horizontal peaks occur simultaneously, and are accompanied by a very strong vertical acceleration. **Figure A-6** (a), b), c) and d)) presents the

acceleration, displacement, energy and Fourier spectrums calculated from the University of Quindio recording station.

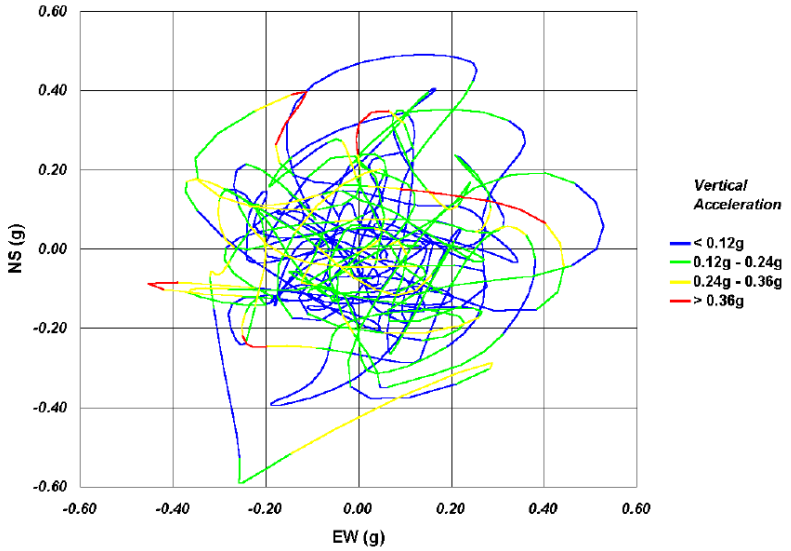

Figure A-5 El Quindio site accelerograph shown in plan view. Adapted from Garcia (2000).

The Castañares recording station was located in the city of Pereira, it is located approximately 48 km from the epicenter. This station rests in a 6 m deep man-made fill. Peak ground accelerations recorded in this station were 0.21g EW, 0.10g vertical, and 0.14g NS. In the town of Filandia, located about 33 KM from the epicenter, the soil profile consists of approximately 20 m of volcanic ash fill. The peak ground accelerations recorded were 0.57g EW, 0.19g vertical, and 0.49g NS. The soil profile consists of approximately 20 m of volcanic ash fill. **Figure A-6** (e), and (f) presents the acceleration response spectrum calculated from the Castañares and Finlandia recording stations respectively.

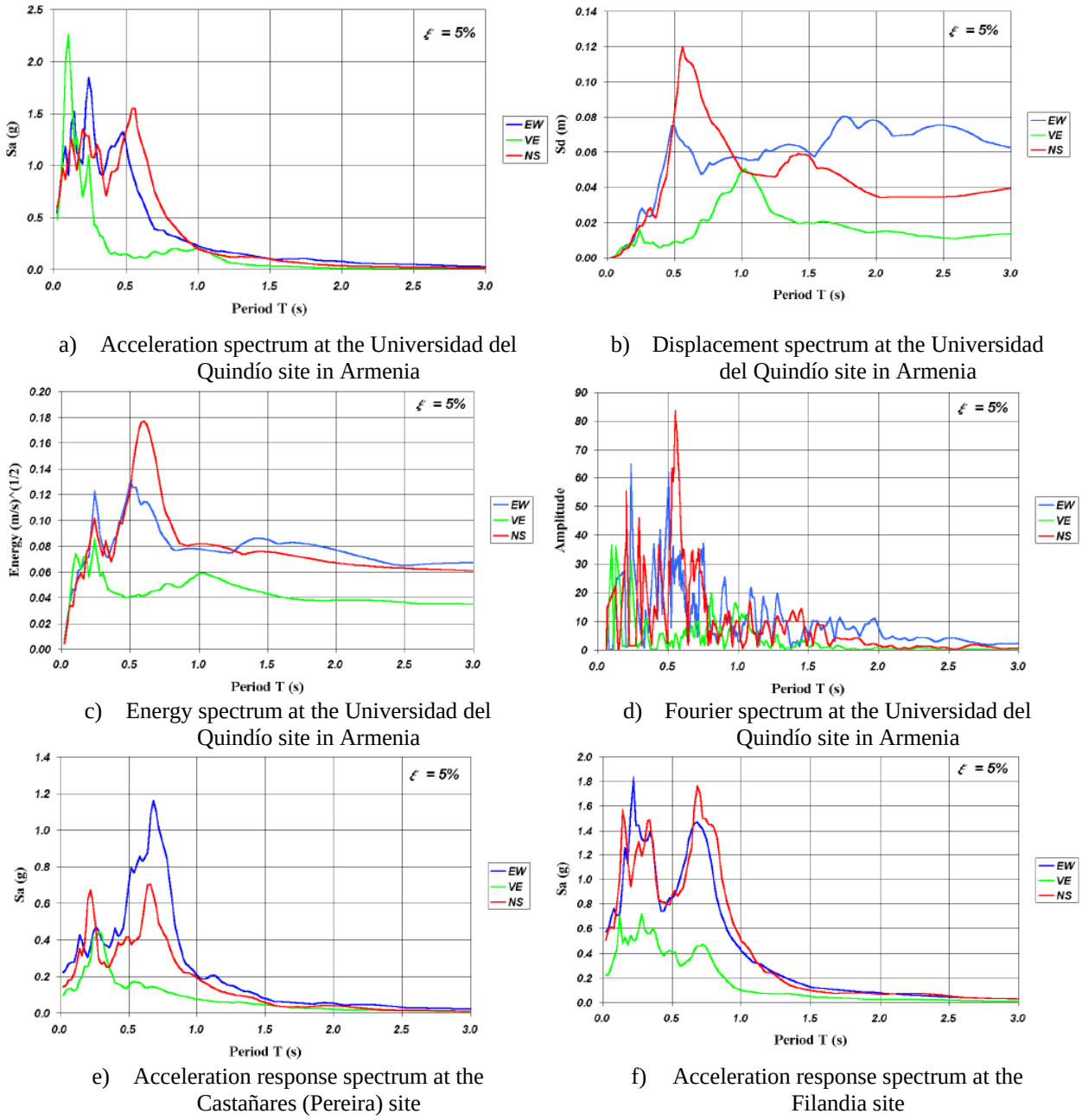

a) Acceleration spectrum at the Universidad del Quindío site in Armenia

b) Displacement spectrum at the Universidad del Quindío site in Armenia

c) Energy spectrum at the Universidad del Quindío site in Armenia

d) Fourier spectrum at the Universidad del Quindío site in Armenia

e) Acceleration response spectrum at the Castañares (Pereira) site

f) Acceleration response spectrum at the Filandia site

Figure A-6 El Quindio earthquake response spectrums from different recording stations. Adapted from Garcia (2000).

A.2. Historic Seismicity

The first seismic event recorded in Colombia was the 1566 earthquake that presumably had its epicenter in the southwest part of the country. This earthquake produced a lot of damage in the cities of Cali and Popayan (Baquero et al. (2004)). In 1923, the Jesuit order installed the first net of seismographs. They were later operated by the Geophysical Institute of Andes, and today are run by Javeriana University (attached to the Jesuit order).

The collection of the Colombian historical seismicity started with the studies of Jesús Emilio Ramírez, a geophysicist and Jesuit priest. In 1933 he published an "Earthquake History of Colombia". From 1933 to 1980 Ramirez was a very active researcher, and he developed more than seventeen reports that are still quoted today. In 1975 he published the first earthquake catalogue of Colombia (Ramirez (1975)). It covers the seismicity from 1566 to 1974. The catalogue includes 1256 seismic events with some information about the location, intensity, estimated epicenter, depth and description of damage. New catalogues have taken his work as starting point. However, there are other catalogues, such as those by the Regional Seismological Center for South America CERESIS (2013), and The Colombian Geological Survey CGS (2013), formerly the National Institute of Geology and Mining (INGEOMINAS). They also contain a history of Colombian seismicity. It is important to mention that in the CIRESIS catalogue of 1982, the number of events was raised to 4784 events, of which 1026 are considered as historic. In 1908 the ground motions were registered by five or less stations and in 1950 they were registered by six stations or more. These data provide a sense about the quality and reliability level of the information presented in the catalogues. **Figure A-7** presents the seismic event map for Colombia up to January 2013.

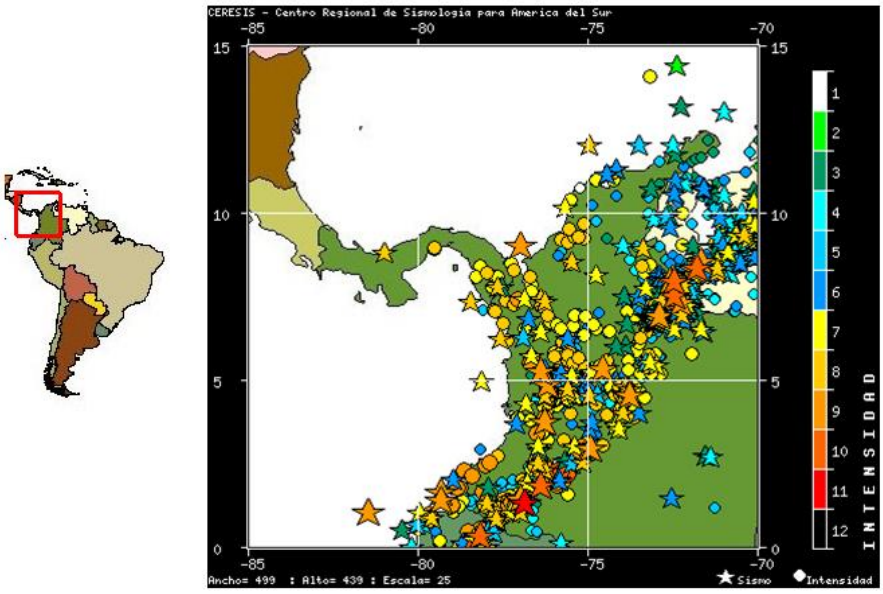

Figure A-7 Colombian seismic activity from 1566 to January 2013, based on MMI equivalence. (www.ceresis.org).

After the negative effects of the Popayan earthquake of March 31, 1983, and the mudflow of El Ruiz volcano that killed about 20,000 people on November 13, 1985, the Colombian government decided to invest resources in a new seismological network. The United Nations (UN) and the Canadian Agency for International Development (CAID) helped with important resources and training to modernize the Colombian Seismic Network (RSNC) that is today managed by INGEOMINAS. At the end of 1991 RSNC became operational. Currently the RSNC has 120 strong motion digital accelerographs located mainly in the Andes Mountains which cover all Colombian territory. The catalogue that is presented in the RSNC webpage covers the period of time from June 1, 1993 to today. As of February 15, 2013, there were 104,223 events. **Table A-2** and **Figure A-8** summarize the information presented in this catalogue.

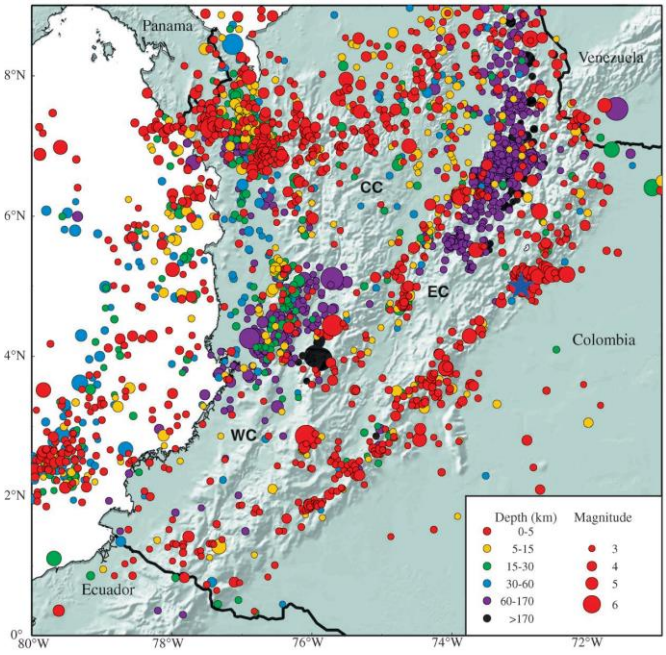

Figure A-8 Seismicity of Colombia from June 1993 to December 1999 CGS (2013).

Table A-2 Colombian seismic catalogue from June 1 1993 to February 15, 2013 CGS (2013).

Magnitude	Depth					
	0-60 Km	**60-100 Km**	**100-200 Km**	**200-400 Km**	**> 400Km**	**Total**
0-3	23074	3682	58876	23	0	85655
3-4	4318	449	11269	24	2	16062
4-5	739	57	1424	3	9	2232
5-6	98	7	143	3	2	253
6-7	16	1	11	2	2	32
7-8						0
Total						104234

Despite advances in the collection and analysis of seismic information in Colombia, especially during the past 20 years, the current catalogue is limited in terms of the number of strong ground motions to perform a reliable seismic collapse analysis. The quality of available information for the period before 1993 cannot be established based on the instrumentation installed. As a proof of

that is that the RSNC avoids presentation of any ground motion information for events before their network became fully operational.

A.3. Colombian Seismic Standards, Trends and Challenges

Colombian seismic standards are relatively new. In 1981, the Colombian Association for Earthquake Engineering (AIS) published a first draft of what became the first Colombian seismic code in 1984. This first document was based on the translation into Spanish of two documents: "The Recommended Lateral Force Requirements and Commentary" by the Structural Engineers Association of California (SEAOC) written in 1974 (SEAOC (1974)) and known as the "Blue Book", and the Applied Technology Council ATC 3-06 written in 1978 (3-06 (1980)), which became the basis for all modern seismic American codes.

After the Popayan earthquake on March 31, 1983, the Colombian Institute for Technical Standards (ICONTEC) adjusted the first draft made by the AIS into the format of ACI 318-83. This document covered both reinforced concrete and steel. Some authors who actively contributed to the American Standards also assisted with this new document, including luminaries such as Dr. Nathan Newmark and Dr. Mete A. Sozen. The Colombian Standards for Seismic Resistant Design and Construction was enacted by decree 1400 of June 7, 1984. Since then, the Colombian seismic code has been upgraded on two occasions, in 1998 and in 2010. It is important to highlight the fact that the first code was written with the idea to avoid introducing strict rules in a country that was not familiar with a seismic code. Fifteen years later, in 1998, the code was upgraded for the first

time. During this period, a considerable number of buildings were designed and constructed using the 1984, less strict guidelines. For example, up to 1998 the allowable lateral drift limit was 1.5% of the inter-story height. In order to check the story drift evaluation, a response modification factor ***R*** is selected based on the structural system used. Then, the structural analysis is perform for a lateral loads divided by ***R***, and the displacements from the structural analysis are multiplied by a displacement amplification factor ***Cd***. Finally, with the amplified displacements, the inter-story drift is calculated. The 1.5% drift limit was assigned in response to the excessive lateral drift problems characteristic of the buildings constructed without following any seismic standard. In 1998, drift limit was lowered to 1% of the inter-story height for RC and 0.5% for masonry structures. Today, these limits remain the same.

Another consideration is that even after 1984, and in some recent cases, it is common to find discrepancies between the design and construction process, primarily with evidence of a lack of adequate construction supervision. Construction QA/QC in Colombia, as elsewhere, varies considerably with the jurisdiction and the inspection agency. Therefore newly constructed structures may not behave as expected. For instance, on October 2013 in Medellin, Colombia's second biggest city, a brand new building suffered a gravity-collapse killing 12 people and resulted in the demolition of the final four towers of the "Space" residential building. As can be appreciated, this introduces additional complexity and uncertainty to the problem of seismic vulnerability and performance evaluation.

In addition, the lack of enforceability of construction permitting, especially in Latin America, increases the complexity at the time of evaluating seismic vulnerability. For instance, it has been estimated that from the 700,000 housing units built today in Mexico every year, at least 300,000 units have been built without construction permits, without compliance seismic standards and

without the participation of qualified professionals (Meli & Ordaz, 2004). There is probably a very large number of structures designed only for gravity loads that have been built in the past 20 years in Colombia, especially in rural areas. Although structures designed for gravity loads have some inherent lateral strength, it is not enough for them to perform properly under seismic events. This weakness has been proven directly by the tragic results presented in the recent Colombian seismic history.

B. Appendix B

In Chapter 2, a list of key vulnerabilities commonly present in non-ductile RCF was introduced. At the same time and based on the evidence presented in post-earthquake reconnaissance in Colombia, a subset of these vulnerabilities was selected and studied in some detail. As a result, this Appendix presents a practical-oriented approaches to address some of these key vulnerabilities in modeling non-ductile RCF. The validation process is performed by comparing their output results with some test or examples provided in the literature.

B.1. Approach to Modeling Unreinforced Beam-Column Joint

The simplest approach to performing nonlinear analysis of BCJ is by using a nonlinear spring at the intersection of the beam-column line elements with the inclusion of rigid offsets to define a physical size of the joint. **Figure B-1** depicts this beam column joint representation. Even though it is required more refinement in order to represent the true geometry and complex kinematic behavior of the BCJ, it is assumed that the procedures presented here consider that the BCJ will not to be the first critical element that will drive the behavior of RCF. This approach uses the concentrated plasticity concept in conjunction with a set of elements including: (a) rigid links to represent the joint geometry (b) in the middle point of the rigid links, a nonlinear rotational spring is created by using a zero length element and (c) nonlinear beam column elements to represent the BCJ subassembly. This approach is easily implemented in the OpenSEES platform and due to its overall simplicity, lack of numerical problems and perceived accuracy, has been used by many

researchers in the past few years. (Celik and Ellingwood (2010), Hassan (2011), Jeon et al. (2012), Park and Mosalam (2013)).

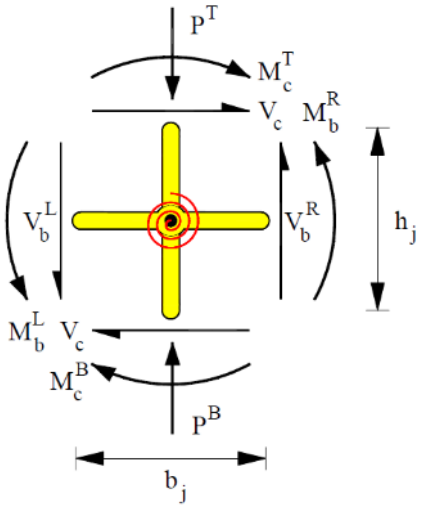

Figure B-1 Free body diagram of the scissors model from Celik (2007)

The suggested formulation for the scissors model is a force formulation, which implies that a definition of the plastic hinge length is not required. Distributed plasticity elements are modeled with fiber elements and five integration points are used in columns and beams to capture the material nonlinearity of the elements that frame into the joint. The advantage of the fiber formulation is to facilitate the specification of unconfined and confined concrete to account for the effects of confinement and ductility. The joint region is represented by rigid link elements. The constitutive relationship for the joint is assigned to a zero length element located in the center of the joint. The quad-linear backbone curve and the semi-empirical joint shear capacity proposed by Park and Mosalam (2012a) is implemented in this study. Once these variables are defined, a centerline analysis is applied. The main features of this methodology, as applied herein, are summarized on **Figure B-2**. The first step is to define the RCF geometry (i.e Beam-colum

elements, BCJ, rigid links, and rotational springs) using centerline analysis, inflections points are assumed to be located at midpoint of the beam and column elements, see **Figure B-2** (a). In **Figure B-2** (b), the joint shear strength is selected in accordance of ACI 352. Finally the strength modification factor is calculated, thus the joint shear capacity, backbone curve and the moment rotation behavior of the nonlinear spring can be determined. **Figure B-2** (c) to **Figure B-2** (f) depicts the above procedure.

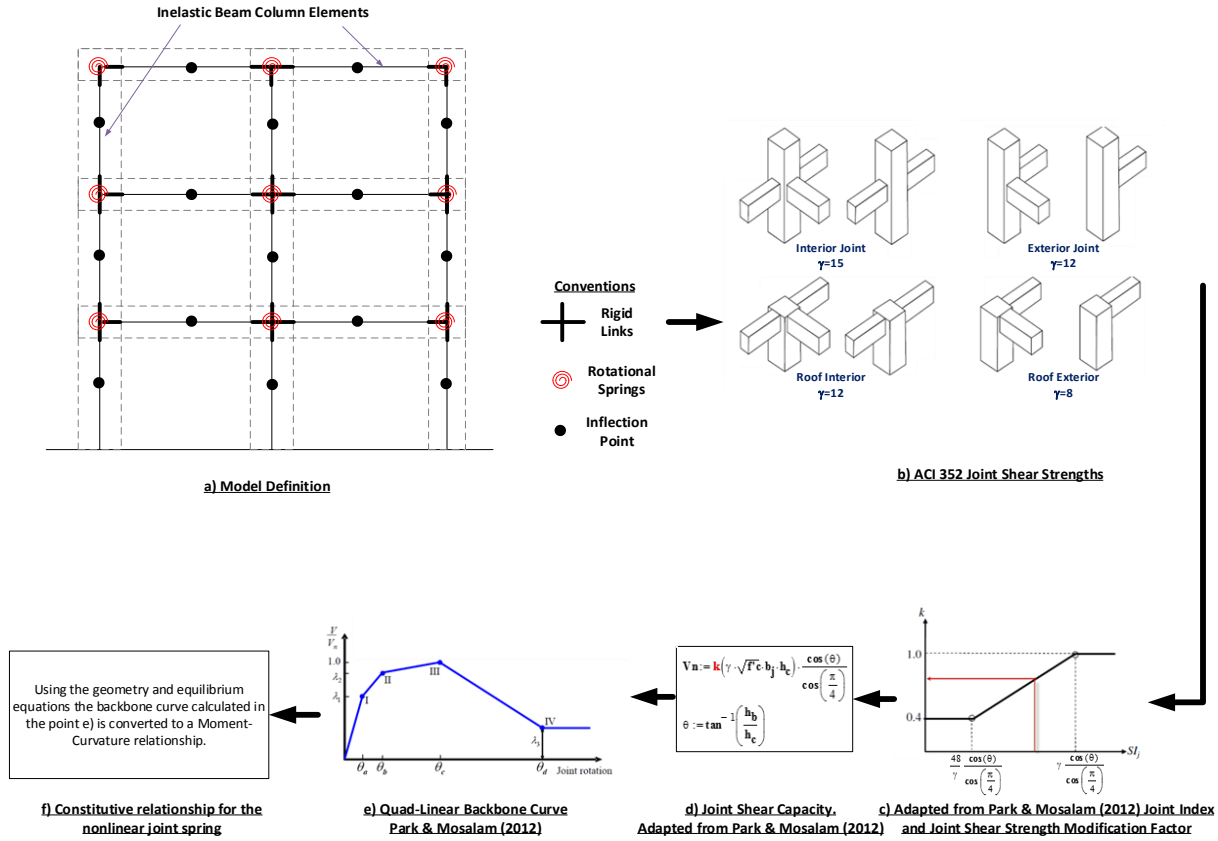

Figure B-2 Procedure outline proposed for modeling unreinforced BCJ.

The moment-rotation backbone relationship depicted in **Figure B-2** f) is calculated using the geometry and equilibrium equations applied to the isolated subassemblies. Similar procedures can be found in Charney and Johnson (1986), Celik (2007), Birely et al. (2012), and Park and Mosalam (2012b). Once the moment-rotation relationships are calculated, they can be implemented with the Pinching04 Lowes and Altoontash (2003) model in OpenSEES.

Figure B-3 depicts the displacement response for the specimen SP1 EW Park and Mosalam (2013). Note that the Pinching4 model compares satisfactorily to the experimental results. For this specimen, the EW yielded first in the downward direction. Thus, in this direction the envelope, initial stiffness, strength degradation, reloading stiffness, pre-capping, and post-capping capacity match satisfactorily the test results. For the upward loading, the results indicate a minor discrepancy which can be attributed to the previous yielding in the negative direction, and is also due to the degradation produced for the loading in the NS direction as the SP1 specimen was tested as a 3D BCJ. Despite that the unloading stiffness parameters are fixed based on the recommendations made in Park (2010), it appears that after the five cycles the unloading degradation stiffness is in some way mismatched, but other parameters are in satisfactory agreement with the test results. While recognizing some of these inherent limitations, the Pinching4 model is selected to represent the cyclic degradation of the joint shear spring.

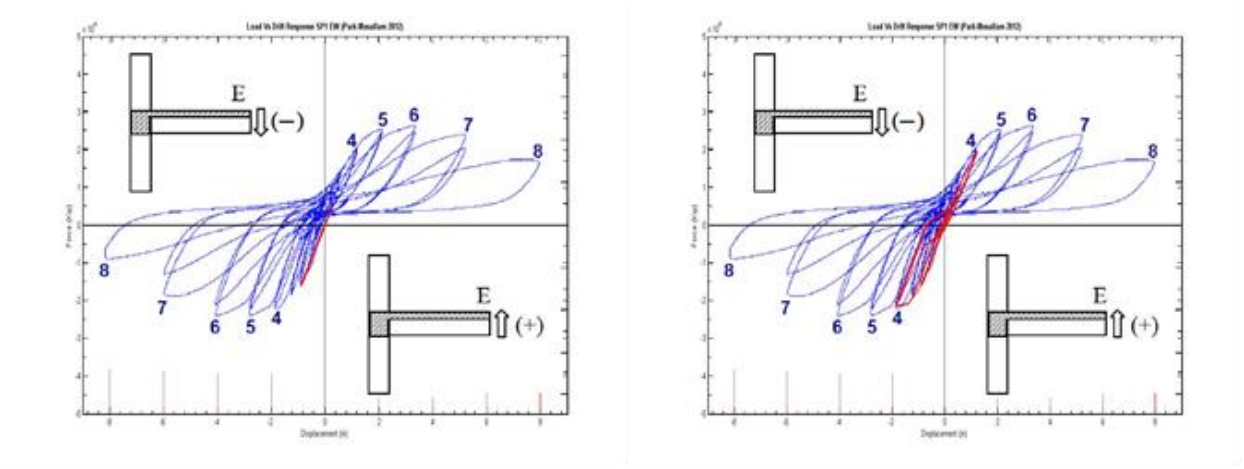

Cycle 3. Cycle 4.

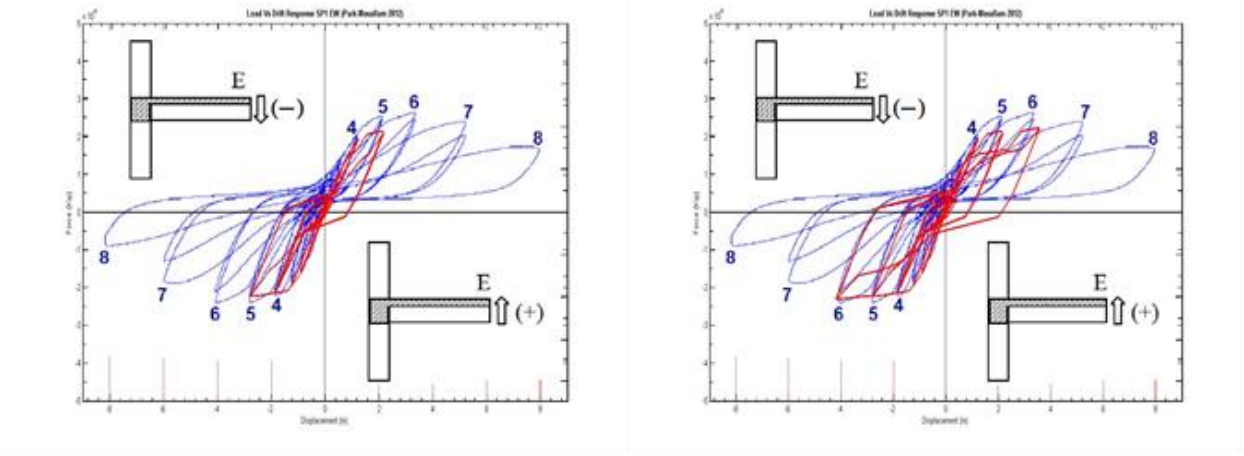

Cycle 5. Cycle 6.

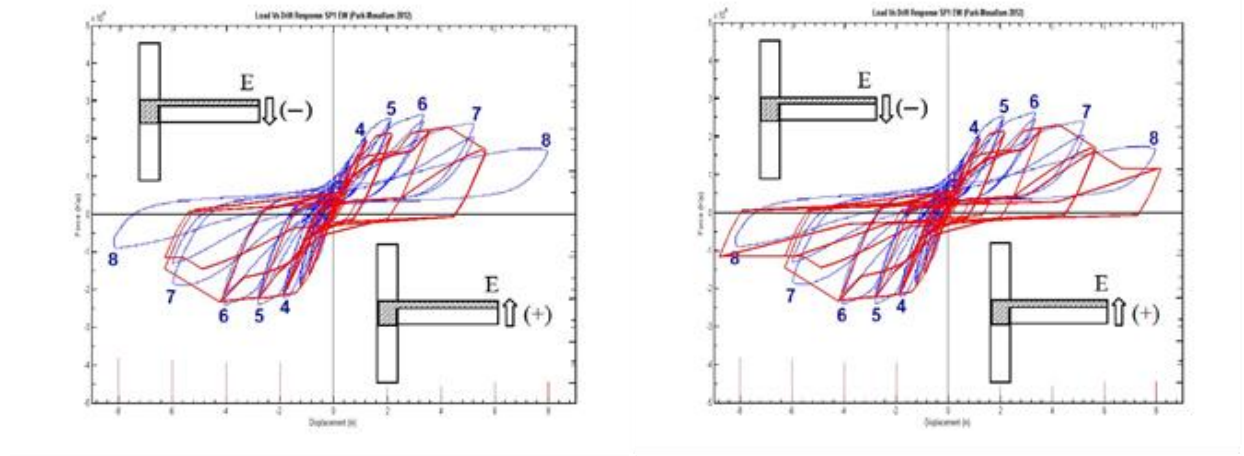

Cycle 7. Cycle 8.

Figure B-3 Obtained load-displacement response SP1 EW for Pinching4 model.

For defining the backbone curve for the nonlinear spring and its constitutive relationship, the model presented here is almost identical to the model presented in Park and Mosalam (2013). In essence, the model was modified to follow the same nomenclature of the ACI-352 (1991). The major modifications are:

1. The term Γ was omitted, instead it is proposed to use γ from ACI 352.2.
2. In equation (3) of the referenced paper, the nominal shear force is expressed in terms of the exterior shear strength coefficient (γ=12). This equation was expressed in a more general way as presented later on in this document (see **Figure B-2** (d)). This change was also applied because if equation (3) is applied directly, the nominal shear for the specimen SP1 EW would be overestimated by 20% because there is another beam framing into the joint in the perpendicular direction.

Incorporating the above modifications, the proposed model was applied to some tests found in the literature. **Table B-1** summarizes the comparison between the prediction equation and the test result. For the test results analyzed, the method proposed presents satisfactory agreement with the test results analyzed. The average value obtained indicated a 2% difference and a standard deviation of about 11% for the Park (2010) specimens. The effect of the slab reinforcement was not incorporated in the calculation of the shear index in order to be consistent with the other test results analyzed by Wong (2005). It is important to mention that taking into account the uncertainties associated with the materials, test measurements, test setup, and the tolerances, this method can satisfactorily predict the joint shear capacity.

Table B-1 Comparison between proposed joint model and some tests in the literature.

Reference	Specimen	f'c (ksi)	fy (ksi)	Vj Test (kip)	S*Ij*	θ	x1	x2	k	γ	Vn Calc (kip)	Vcalc / Vtest	Vn ASCE 41-06	Vcalc / Vn_{ASCE} 41-06
Wong (2005)	BS-U	4.5	75.4	76.70	11.08	0.98	3.14	9.41	1.16	12	95.06	***1.24***	52.24	***0.68***
	BS-L-LS	4.58	75.4	77.50	10.99	0.98	3.14	9.41	1.15	12	95.13	***1.23***	52.71	***0.68***
	BS-L-300	4.94	75.4	113.50	11.07	0.79	4.00	12.00	0.93	12	101.88	***0.90***	54.74	***0.48***
	BS-L-600	5.28	75.4	63.80	9.75	1.11	2.53	7.59	1.00	12	71.58	***1.12***	56.59	***0.89***
	BS-L-V2T10	4.73	75.4	89.70	10.81	0.98	3.14	9.41	1.13	12	95.27	***1.06***	53.56	***0.60***
	BS-L-V4T10	4.1	75.4	90.60	11.61	0.98	3.14	9.41	1.21	12	94.69	***1.05***	49.87	***0.55***
	JA-NN03	6.5	75.4	68.90	6.22	0.93	3.40	10.20	0.65	12	69.30	***1.01***	62.79	***0.91***
	JA-NN15	6.67	75.4	69.90	6.14	0.93	3.40	10.20	0.64	12	69.44	***0.99***	63.60	***0.91***
	JB-NN03	6.87	75.4	70.40	6.24	0.79	4.00	12.00	0.57	12	73.32	***1.04***	64.55	***0.92***
Park-Mosalam (2010)	SP1	3.5	68	155.70	5.91	0.79	3.20	15.00	0.54	15	146.08	***0.94***	108.62	***0.70***
	SP2	3.53	68	228.70	10.57	0.79	3.20	15.00	0.77	15	211.31	***0.92***	109.08	***0.48***
	SP3	3.6	68	131.30	5.37	1.03	2.33	15.00	0.54	15	109.03	***0.83***	110.16	***0.84***
	SP4	3.96	68	167.60	9.20	1.03	2.33	15.00	0.73	15	152.41	***0.91***	115.54	***0.69***
Average												***1.02***		***0.72***
Standard Deviation												***0.11***		***0.156***

On the other hand, the ASCE 41 (2006) provisions tend to underestimate the joint strength by about 30% with a standard deviation of 15.6%. Figure **Figure B-4** (a) presents the ASCE 41-06 backbone curve. As can be observed, ASCE 41-06 provisions tend to have a high level of conservatism and have little success in representing the true behavior of the BCJ. The model presented in this Appendix is shown in **Figure B-4** (b).

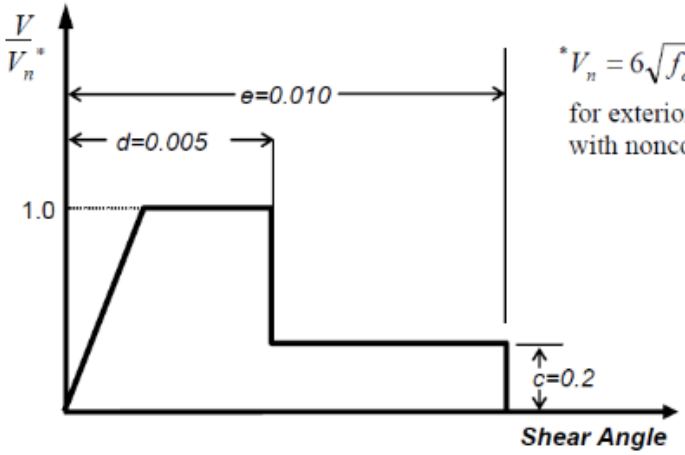

a) ASCE 41-06 Backbone

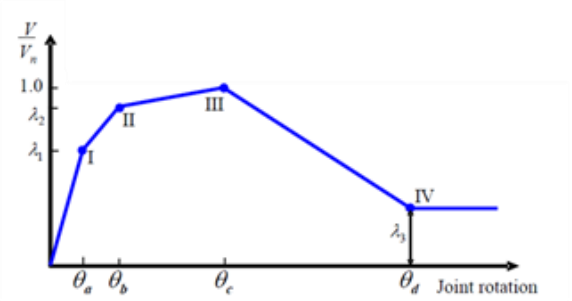

Joint type	θ_a	θ_b	θ_c	θ_d
Exterior	0.0025	0.005	$0.0325 - 0.0125\,(h_b/h_c)$	$\theta_c + 0.03$
Roof exterior				
Interior	0.0050	0.010		
Roof interior				

b) Backbone applied in this study (Park & Mosalam 2010).

Figure B-4 Comparison backbone ASCE 41-06, and backbone proposed by Park and Mosalam (2013).

B.2. Approach to Modeling Beam-Column Element

In order to model behavior associated with flexural deterioration, either fiber or lumped plasticity (concentrated plasticity) models could be used for modeling beam-columns elements. In this Appendix, the lumped plasticity approach is selected. While lumped plasticity models lack the capabilities of fiber models, they can be calibrated to capture the deterioration associated with

rebar buckling and stirrup fracture leading to loss of confinement (Ibarra and Krawinkler (2004), Haselton (2007)). At the present time, there is no available steel material model in OpenSEES that is able to mimic the behavior of rebar as it buckles and/or fractures Liel (2008). The lumped plasticity model requires using empirical equations relating the design parameters of a beam or column to the modeling parameters. The best calibration process available is based on 255 experimental tests of RC columns included in the PEER Structural Performance Database Berry et al. (2004). The database includes RC columns with both ductile and non-ductile detailing, and varying levels of axial load and geometries and, for each, reports of force-displacement history and other relevant data Berry et al. (2004). This process was based on mean values, unlike the conservative values given in the FEMA 356/ASCE 41 documents. A full report on the calibration study is available in Haselton (2007).

These models also account for bond-slip but do not account for the possibility of rebar pull-out and the resulting loss in strength. **Figure B-5** shows the lumped-plasticity model used for modeling beam-column elements. The element model is composed of an elastic element attached in series with two zero-lengths at each end. The elastic stiffness of the plastic hinge is arbitrarily modified by a factor of 11, and the elastic element stiffness of the beam-column element is increased by 10%. The previous modifications factors are applied following the recommendations presented in Ibarra and Krawinkler (2004). An adjustment, involving the above modifications are applied for the pre-capping and post-capping slope assigned to the backbone spring curve.

Previous researchers such as Haselton (2007), Liel (2008), Galanis and Moehle (2012) used mainly the above approach but with a major difference in the material model applied. They used a tri-linear moment-rotation diagram implemented in the Clough model in OpenSEES. This model was implemented into OpenSEES by Altoontash (2004). Note that the name “Clough” is a

misnomer, as the actual model as it is implemented in OpenSEES is based on the work by Ibarra and Krawinkler (2004). It is important to point out that the Clough model is not documented in the OpenSEES user manual or in OpenSEES wiki documentation. In addition the available model won't handle an asymmetric behavior present when the composite action of the beam and slab is included in the analysis. Because of the lack of complete documentation and its lack of asymmetry capabilities, the Clough model was discarded and another peak-oriented material was selected. In 2011, a new set of IMK materials were proposed (IMK peak-oriented, and IMK pinched-oriented hysteretic response) by Lignos and Krawinkler (2011). The new IMK materials are able to simulate a bilinear, peak-oriented, and pinched hysteretic response. These models have been used to calibrate the hysteretic response of a number of steel and RC components subjected to reverse cyclic loading. Further details about the original and modified IMK model can be found in Ibarra and Krawinkler (2004) and Lignos and Krawinkler (2011). The modified IMK peak oriented hysteretic response is chosen herein because it is capable of capturing the important modes of deterioration that precipitate sidesway collapse of RC frames. Non-ductile RCF are more likely to exhibit gravity load collapse rather than sidesway collapse, but for completeness, background information and the possibility in having ductile behavior after the retrofitting process, this approach is presented in some detail. **Figure B-5** shows the tri-linear monotonic backbone curve, which together with associated hysteretic rules of the model, permit versatile modeling of cyclic behavior. For simulating sidesway collapse, the most important aspect of this model is the post-peak response, which enables modeling the strain softening behavior associated with concrete crushing, rebar buckling and fracture, and/or bond failure. The model also captures four modes of cyclic deterioration: strength deterioration of the inelastic strain hardening branch, strength deterioration of the post-peak strain softening branch, accelerated reloading stiffness deterioration,

and unloading stiffness deterioration. Cyclic deterioration is based on an energy index that has two parameters: normalized energy dissipation capacity and an exponent term to describe how the rate of cyclic deterioration changes with accumulation of damage. In total, the model requires the specification of seven parameters to control the monotonic and cyclic behavior. The model can also be assigned a residual strength, as a function of the ultimate strength, which is not shown on **Figure B-5**. It is recommended to take 1% as residual strength for all beams and columns to avoid problems with numerical convergence. It is likely that RC beams and columns actually have higher residual strength such that the model is quite conservative, but it is difficult to quantify on the basis of available experimental data. The IMK model was modified to account for composite action, residual strength, and ultimate deformation capacity Lignos and Krawinkler (2011). The IMKL model is based on the evaluation of experimental data from tests that have been conducted over 40 years.

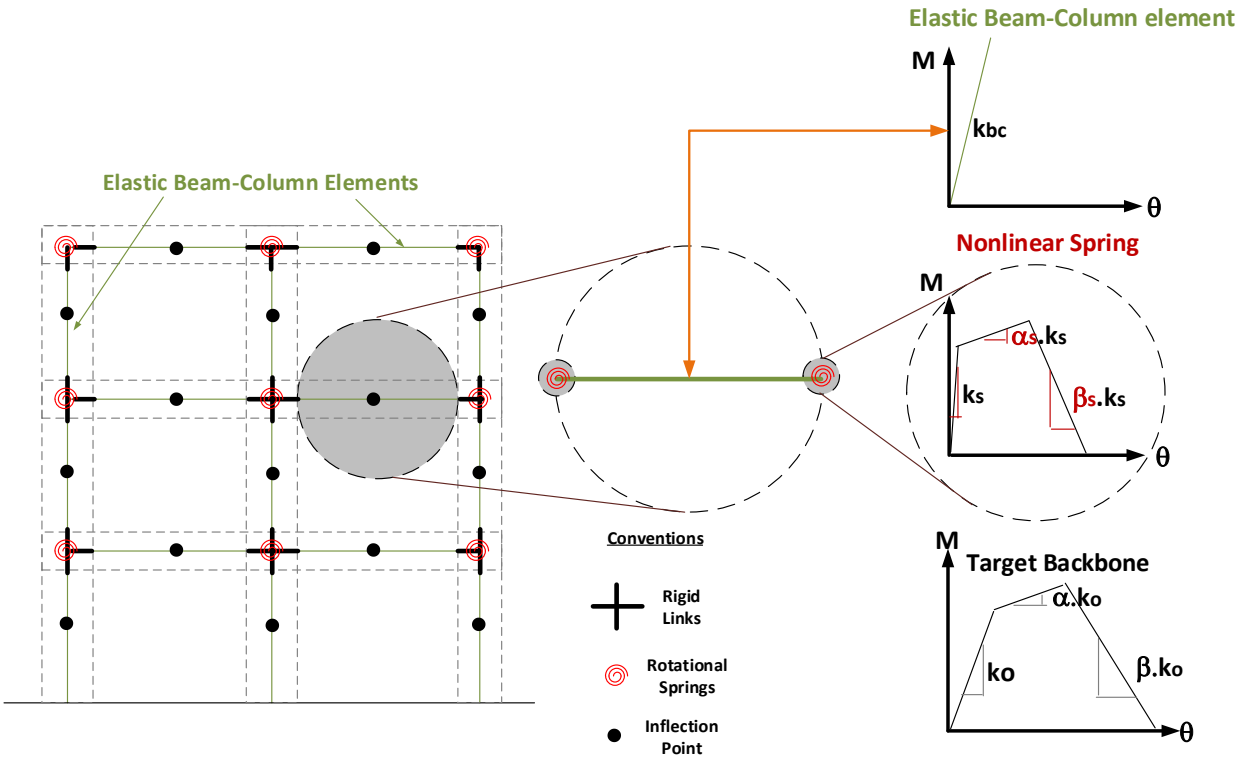

Figure B-5 Flexural beam-column element.

From **Figure B-5**, the spring properties for matching the target envelope, can be calculated as follows: (n=10 can be assumed).

Elastic stiffness for the rotational spring:

$$k_s = n.k_{bc} = (n+1)k_o \tag{B-1}$$

Pre-capping stiffness for the rotational spring:

$$\alpha_s = \frac{\alpha}{(n+1)-(\alpha * n)} \tag{B-2}$$

Post-capping stiffness for the rotational spring:

$$\beta_s = \frac{\beta}{(n+1)+(\beta * n)} \tag{B-3}$$

The defining parameters of the moment-rotation relationship are the elastic stiffness, yield moment, ultimate moment, capping rotation, and the post-capping rotation. The empirical regression equations are presented here, further details are presented in Haselton (2007). (OpenSEES commands: ModIMKPeakOriented material, Elastic element).

The secant stiffness to yielding is given as:

$$\frac{EI_y}{EI_g} = -0.07 + 0.59\left[\frac{P}{A_g f'_c}\right] + 0.07\left[\frac{L_s}{H}\right] \qquad 0.2 \leq \frac{EI_y}{EI_g} \leq 0.6 \tag{B-4}$$

The initial stiffness is given as:

$$\frac{EI_{stf40}}{EI_g} = -0.02 + 0.98\left[\frac{P}{A_g f'_c}\right] + 0.09\left[\frac{L_s}{H}\right] \qquad 0.35 \leq \frac{EI_{stf}}{EI_g} \leq 0.8 \tag{B-5}$$

The plastic rotation capacity is given by:

$$\theta_{cap,pl} = 0.12(1 + 0.55a_{sl})(0.16)^{\nu}(0.02 + 40\rho_{sh})^{0.43}(0.54)^{0.01c_{units}f'_c}(0.66)^{0.1s_n}(2.27)^{10\rho} \tag{B-6}$$

The total rotation capacity is given by:

$$\theta_{cap,tot} = 0.12(1 + 0.4a_{sl})(0.20)^{\nu}(0.02 + 40\rho_{sh})^{0.52}(0.56)^{0.01c_{units}f'_c}(2.37)^{10\rho} \tag{B-7}$$

An equation for correcting in case of having unbalanced reinforcement (applicable to the two previous equations) is given as:

$$FardisTerm = \left[\frac{max\left[0.01, \frac{\rho' f_y}{f'_c}\right]}{min\left[0.01, \frac{\rho f_y}{f'_c}\right]}\right]^{0.175} \tag{B-8}$$

The post-capping rotation capacity is given as:

$$\theta_{pc} = (0.76)(0.031)^{v}(0.02 + 40\rho_{sh})^{1.02} \leq 0.10 \quad \text{(B-9)}$$

The post-yielding hardening stiffness is given as:

$$\frac{M_c}{M_y} = (1.25)(0.89)^{v}(0.91)^{0.01 c_{units} f'_c} \quad \text{(B-10)}$$

The cyclic strength and stiffness degradation is given as:

$$\lambda = (127.2)(0.19)^{v}(0.24)^{s/d}(0.595)^{V_p/V_n}\ (4.25)^{\rho_{sh,eff}} \quad \text{(B-11)}$$

where $v = \frac{P}{A_g f'_c}$ (axial load ratio), $\rho_{sh=}$ lateral confinement ratio, $P_{b=}$ balanced axial load, $a_{sl=}$ bond slip indicator (1= possible 0=not possible), $\frac{L_s}{H}$ = column aspect ratio, $\rho_{sh,eff} = \rho_{sh} f_{y,sh} / f'_c$ is the confinement effectiveness factor, $s_{n=} \frac{s}{d_b} \sqrt{\frac{f_y(Mpa)}{100}}$ is the rebar buckling coefficient; $\rho =$ longitudinal reinforcement ratio, $\frac{s}{d}$ = ratio of transverse tie spacing to column depth, and $\frac{V_p}{V_n} =$ ratio of shear at flexural yielding to shear strength. **Table *B-2*** *Statistical analysis of predictive equations by Haselton (2007).* presents the statistical analysis for the predictive equations developed by Haselton (2007).

Table B-2 Statistical analysis of predictive equations by Haselton (2007).

Predictive equation.	Median (Predictive/observed)	Mean (Predictive/observed)	Standard deviation.
Secant to yielding stiffness. (equation B.4).	1.05	1.23	0.28
Initial stiffness. (equation B.5).	0.98	1.52	0.33
Plastic rotation capacity. (equation B.6).	1.03	1.00	0.30
Total rotation capacity. (equation B.7).	0.98	1.07	0.45
Post-capping rotation capacity. (equation B.9).	1.00	1.20	0.72
Post-yielding hardening stiffness. (equation B.10).	0.97	1.01	0.10
Cyclic strength and stiffness degradation. (equation B.11).	1.01	1.25	0.49

B.2.1. Validation of Beam-Column Element

In order to validate the equations presented in section B.2, the pushover example presented in the section 9.2 of the FEMA P695 (2009) methodology is analyzed here. The main difference is that Clough hysteretic material was used in the FEMA P695 (2009), here it is used the IMKLPeakOrientedHystereticResponse in accordance with section B.2.

Figure B-6 (a) presents the input parameters required to use the regression equations introduced in section B.2. Furthermore, **Figure B-6** (b) shows the required input parameters to define the beam and columns hinges. **Figure B-7** depicts the sequence of yielding. Notice that red dots represent yielding points and black dots represents the capping point. In **Figure B-8** is depicted the obtained pushover response.

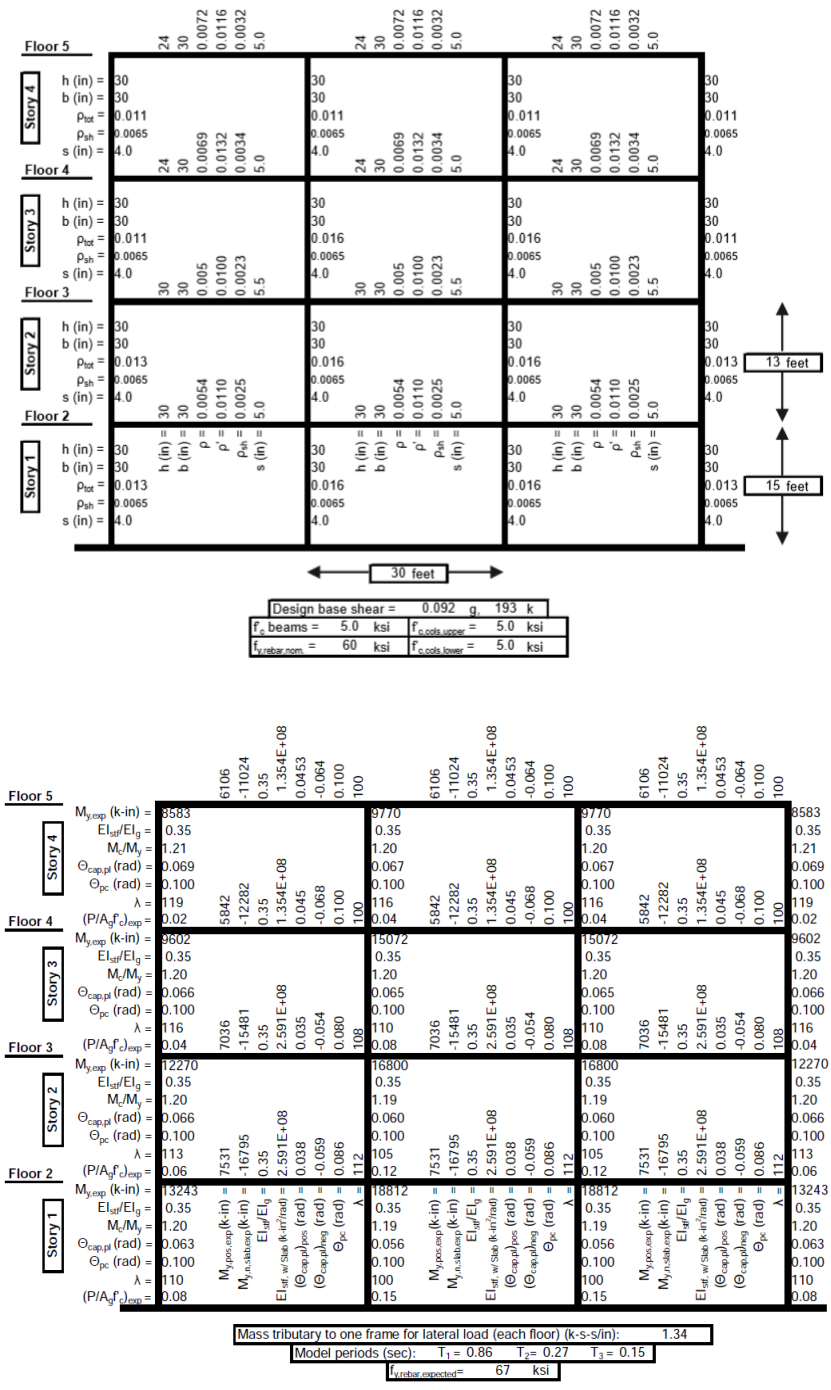

Figure B-6 RCF Example 9.2 FEMA P695 (2009).

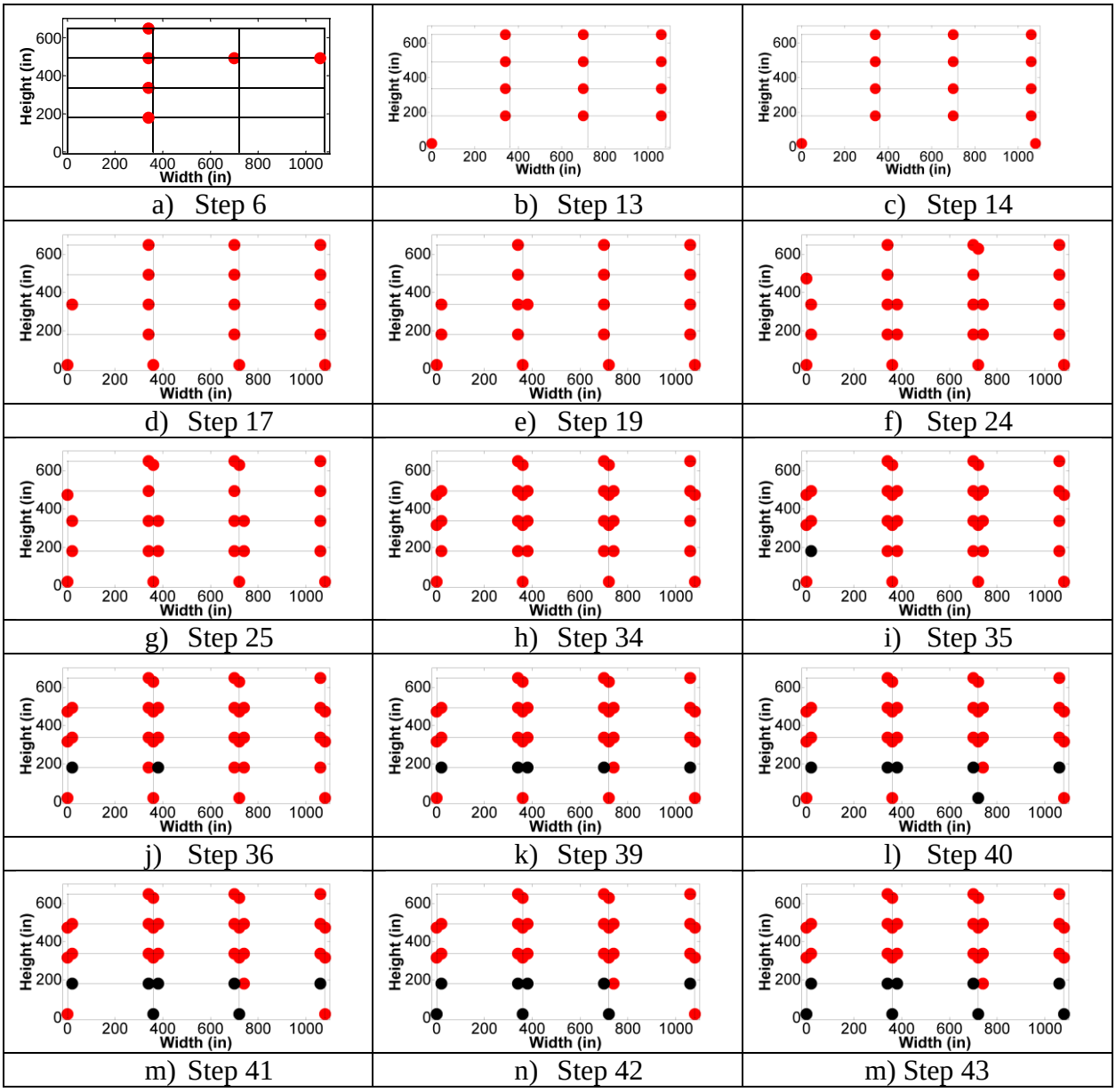

Figure B-7 Obtained sequence of yielding example 9.2 FEMA P695 (2009).

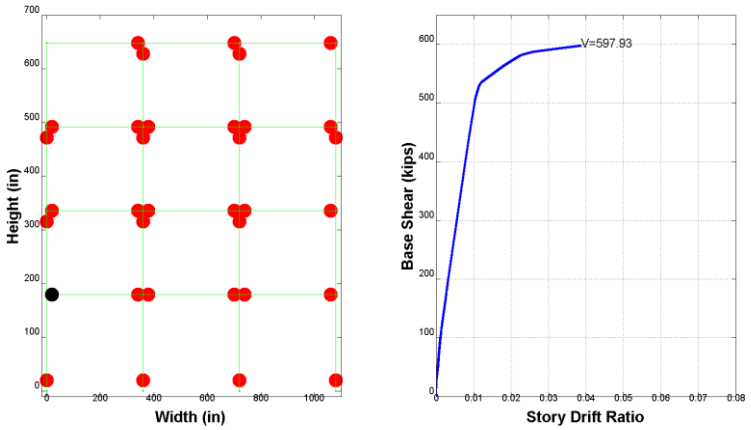

a) Step 35

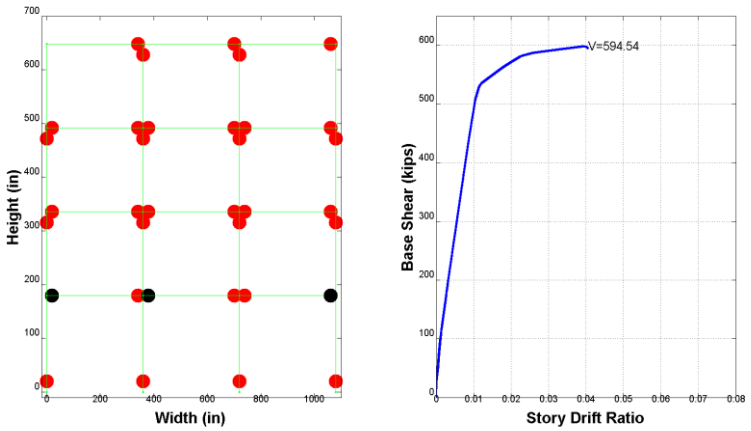

b) Step 37

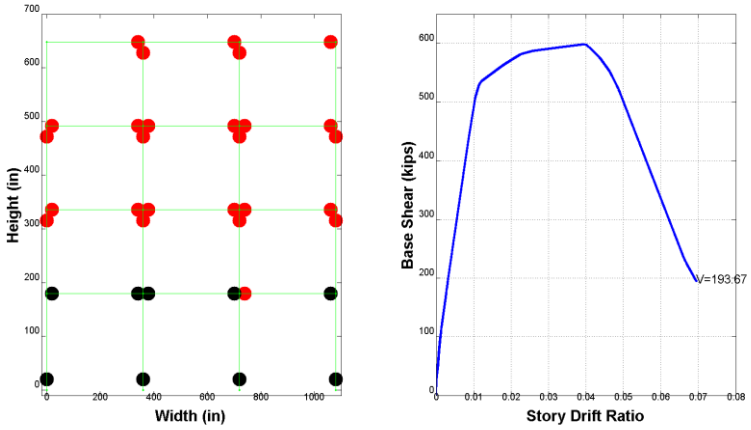

c) Step 43

Figure B-8 Obtained pushover analysis example 9.2 FEMA P695 (2009).

In **Figure B-9** is presented the comparison between the results from the Example 9.2 FEMA P695 (2009) and the analytical response obtained. A close math is founded so the predicted equations and the hysteretic model can be used to determine the lateral increasing monotonic capacity of the RCF. Notice that the collapse mechanism obtained for this example is the desired for any given RCF and is the intended collapse mode for the new RC codes. In terms of older type construction, this procedure is particular useful when a collapse assessment is required or for the cases when a retrofit technique is applied and a sidesway is expected to control. In this case, the validity of regression equations must be validated with a complete test data.

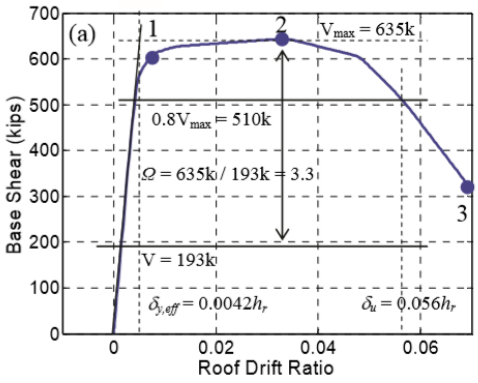

a) Pushover Analysis Example 9.2 Fema p695.

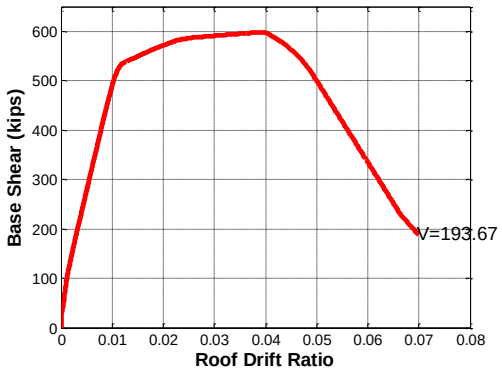

b) Obtained Pushover Analysis

Figure B-9 Obtained pushover analysis example 9.2 FEMA P695 (2009)

B.3. Explicit Beam-Column Joints Models

Model	Model	Description	Joint Shear	Bond slip	Constitutive relationships	Cyclic Deterioration
Biddah and Ghobarah (1999) from Mitra (2007)	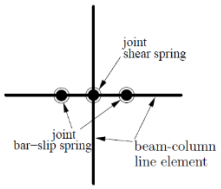	Two spring joint element. One spring represented the inelastic shear response of the joint and the other represented bond-slip	Tri-linear idealization based on a softening truss model (Hsu (1988)).	Bilinear model based on previous analytical and experimental data. (Kaku and Morita (1978)).	MCFT Vecchio and Collins (1986).	Chung et al. (1987)
Elmorsi et al. (2000) from Mitra (2007)	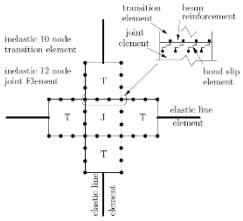	Panel zone represented by a 12 node inelastic plane stress element. 10 elastic elements connected to the joint through the interposition of non-linear transitional elements.	Plane stress element.	Contact elements were introduced in between the nodes of the flexural reinforcement and the adjacent plane stress elements. The bondslip model by Eligehausen et al. (1983) with modifications proposed by Filippou (1986)		Hysteretic relationship with no pinching effect.
Youssef and Ghobarah (2001) from Mitra (2007)	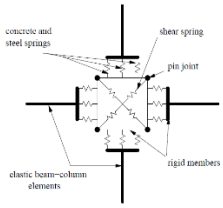	Two diagonal translational springs connecting the opposite corners of the panel zone simulate the joint shear deformation. 12 translational springs located at the panel zone interface.	MCFT (Vecchio and Collins (1986)) was utilized to define the backbone envelope of the curve.	Analytical material model by Giuriani et al. (1969).	Kent and Park (1971).	Biddah and Ghobarah (1999)
Lowes and Altoontash (2003) from Mitra (2007)	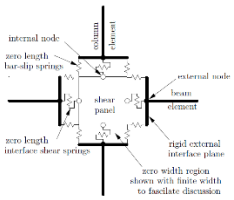	Four node 12 DOFs joint element. 8 zero-length translational springs simulate the bond–slip response of beam and column longitudinal reinforcement. Joint region modeled with one zero-length rotational spring. 4 zero-length shear springs simulate the interface-shear deformations.	Three linear backbone curve using MCFT (Vecchio and Collins (1986)).	Eligehausen et al. (1983)	Kent and Park (1971).	Adjusted from Park and Ang (1985). Lowes and Altoontash (2003)

Altoontash (2004) from Mitra (2007)	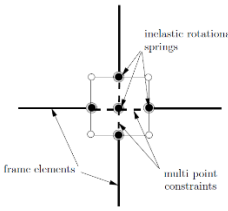	Four exterior nodes, constrained to a central node by multi-point constraints. One rotational spring to emulate shear response of the joint.	Three linear backbone by using modified Newton Raphson iteration curve using MCFT (Vecchio and Collins (1986)).	Eligehausen et al. (1983)	Kent and Park (1971).	Rahnama and Krawinkler (1993) Park and Ang (1985)
LaFave and Shin (2005) from Mitra (2007)	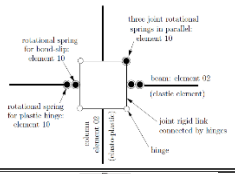	Rigid elements located along the edges of the panel zone. Rotational springs embedded in one of the four hinges linking adjacent rigid elements	Three linear backbone curve using MCFT (Vecchio and Collins (1986)).	The bond-slip rotational springs were calibrated using the formulation proposed by Morita and Kaku (1975)	Park et al. (1982)	Adjusted by test results.
Tajiri et al. (2006) from Mitra (2007)	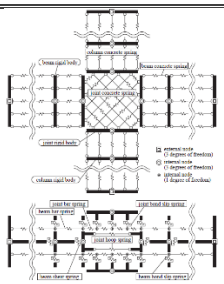	Four nodes, twelve degree of freedom element.	Axial springs connecting rigid bodies	The model proposed by Morita and Kaku (1975).	Park et al. (1982)	Morita and Kaku (1975)
Saito and Kikuchi (2012)	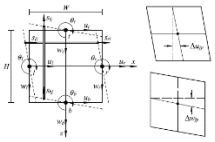	Beam element and a column element	MCFT (Vecchio and Collins (1986)).	The model proposed by Morita and Kaku (1975).	Saenz eq.	Morita and Kaku (1975)

Figure B-10 Examples of explicit BCJ.

C. Appendix C

C.1. Masonry Properties in Colombia

One of the major construction systems in Colombia, and in general throughout Latin America, consists of RCF filled with unreinforced masonry (URM) walls. These infill walls are conventionally built using clay tiles and type M or S mortar (Bastidas et al. (2002)). URM walls are prone to failure when subjected to in-plane and out-of-plane excitations. Seismic reconnaissance survey carried out after the earthquakes of Popayan 1982, Murindo 1992, Tauramena 1995, and Quindío 1999, have validated their vulnerability. For more than 20 years, researchers at the University of the Andes in Bogota, Colombia AIS (1982), Yamin and Garcia (1994a), Yamin and Garcia (1994b), Yamin and Garcia (1997), Gallego (2001.), Bastidas et al. (2002), Gutierrez (2003.) and others have studied the mechanical properties and behavior of Colombian masonry structures and their response under seismic excitations. The present section address the mechanical properties of the mortar, pieces and masonry units commonly found in Colombia. From the works cited above, the following mechanical properties can be ascribed to Colombian construction:

a) Mortar.

Type	f'_{cp} (Mpa)	Minimum water retentivity (%)	Minimum Flow (%)	Composition		
				Portland Cement	Hydrated lime	Sand/ cementitious material
M	17.5	75	120	1	0.25	2.25 to 3.00
S	12.5	75	115	1	0.25 to 0.50	2.50 to 3.50
N	7.5	75	7.5	1	0.50 to 1.25	3.00 to 4.50

b) Masonry units.

Type	IRA (grs/min)	Absorption (%)	Gross compression strength (Mpa)	Flexural Strength (Mpa)
Solid clay	30-40	10-15	19-22	4-6
Hollow clay	18-30	8-16	3-5	~2

c) Relation masonry compression strength (f'_m) with piece compression strength (f_p) (efficiency).

Type of Piece	f'_m
Clay + weak mortar	$0.25f_p$
Clay + strong mortar	$0.50f_p$
Concrete	$0.35f_p$ - $0.55f_p$

d) Masonry Modulus of elasticity.

Type of Piece	E_m
Confined Masonry	$600f'_m$
Typical Masonry	$750f'_m$

e) Clay masonry units.

Type	Compression Resistance (Mpa)	
	Single unit	Average of 5 units
Hollow clay (Horizontal holes)	3.5	5
Hollow clay (Vertical holes)	15	18
Solid clay	15	20

As was mentioned earlier, tension, shear, and flexural strengths of masonry unites are usually correlated with its compressive strength (f'_m). For that reason, it will be convenient to use simple relationships to determine the masonry compressive strength based of the compressive strength of its materials. (i.e. piece and mortar). In this section, a regression equation developed by Kaushik et al. (2007) is presented. It is accepted for the Masonry Standards Joint Committee that the uniaxial monotonic compressive stress-strain behavior for the masonry is adequately represented by the analogy of the Kent and Park constitutive model in reinforced concrete Paulay and Priestley

(1992). For the reference presented here require six intermediate points to define the performance limit states of the masonry material or member. This approach requires as an input the compressive strengths of bricks and mortar. The model is briefly presented in **Figure C-1**, Equations C.1 through C-3, and **Table C-1**.

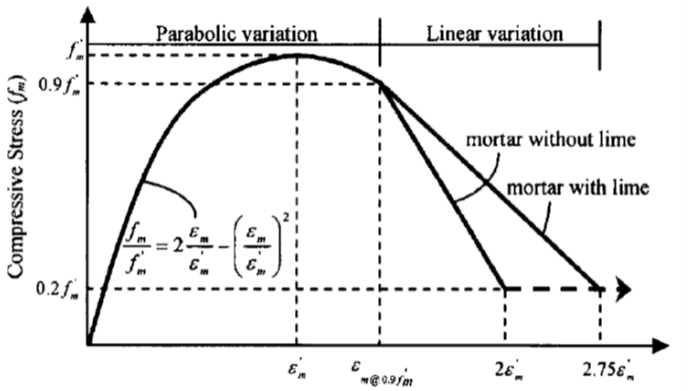

Figure C-1 Idealized stress-strain relationship for masonry Kaushik et al. (2007).

$$f'_m = 0.63 {f_p}^{0.49} {f_{cp}}^{0.32} \text{ (all values in Mpa)} \quad \text{(C-1)}$$

$$\varepsilon'_m = \frac{0.27}{{f_{cp}}^{0.25}} \frac{f'_m}{{E_m}^{0.7}} \quad \text{(C.2)}$$

$$\frac{f_m}{f'_m} = 2\frac{\varepsilon_m}{\varepsilon'_m} - \left[\frac{\varepsilon_m}{\varepsilon'_m}\right]^2 \quad \text{(C-3)}$$

Table C-1 Stress-strain control points proposed for masonry Kaushik et al. (2007).

Location on the curve	Control Point	Performance limit stages
Ascending branch	0.33 f'm	Point up to which the stress-strain curve remains linear.
	0.75 f'm	Vertical splitting cracks in bricks start developing. However masonry still resists loads without much deterioration.
	0.9 f'm	Represents the stress level in masonry just before the failure when the vertical splitting cracks propagate excessively throughout the masonry
	f'm	Ultimate stress level in masonry after which the masonry begins to drop the load and exhibits sudden increase in the strains.
Descending branch	0.5 f'm	This may be considered as the maximum dependable compressive strength of masonry.
	0.2 f'm	Maximum residual compressive stress and corresponding failure strain observed in masonry.

D. Appendix D

D.1. Implementation of the NLTA in OpenSEES

The present appendix covers implementation in OpenSEES of the approach introduced in Chapter 4. **Figure D-1** depicts the schematic representation of the steps required for the establishment of the Nonlinear Truss Analogy (NLTA) applied to RCF with URM infills. Specimen 8 by Mehrabi et al. (1994) is used to demonstrate the procedure and the most relevant calculations.

D.2. Determination of Constitutive Materials

In Section 4.2.2 the constitutive material relationships used for the concrete elements, brick units and steel were presented. The following sections address the implementation of the constitutive equations in the OpenSEES model for the concrete, brick units, steel, and zero-length elements.

D.2.1. Concrete and Brick Units

The ConcretewBeta material in OpenSEES is used to define the constitutive material for the concrete elements and brick units. This constitutive material explicitly accounts for the effect of normal tensile strains on the peak concrete compressive stress when used with the "Truss2" material. The required input parameters are presented in ***Table D-1*** and the calculation for the vertical concrete elements is presented in ***Table D-2***.

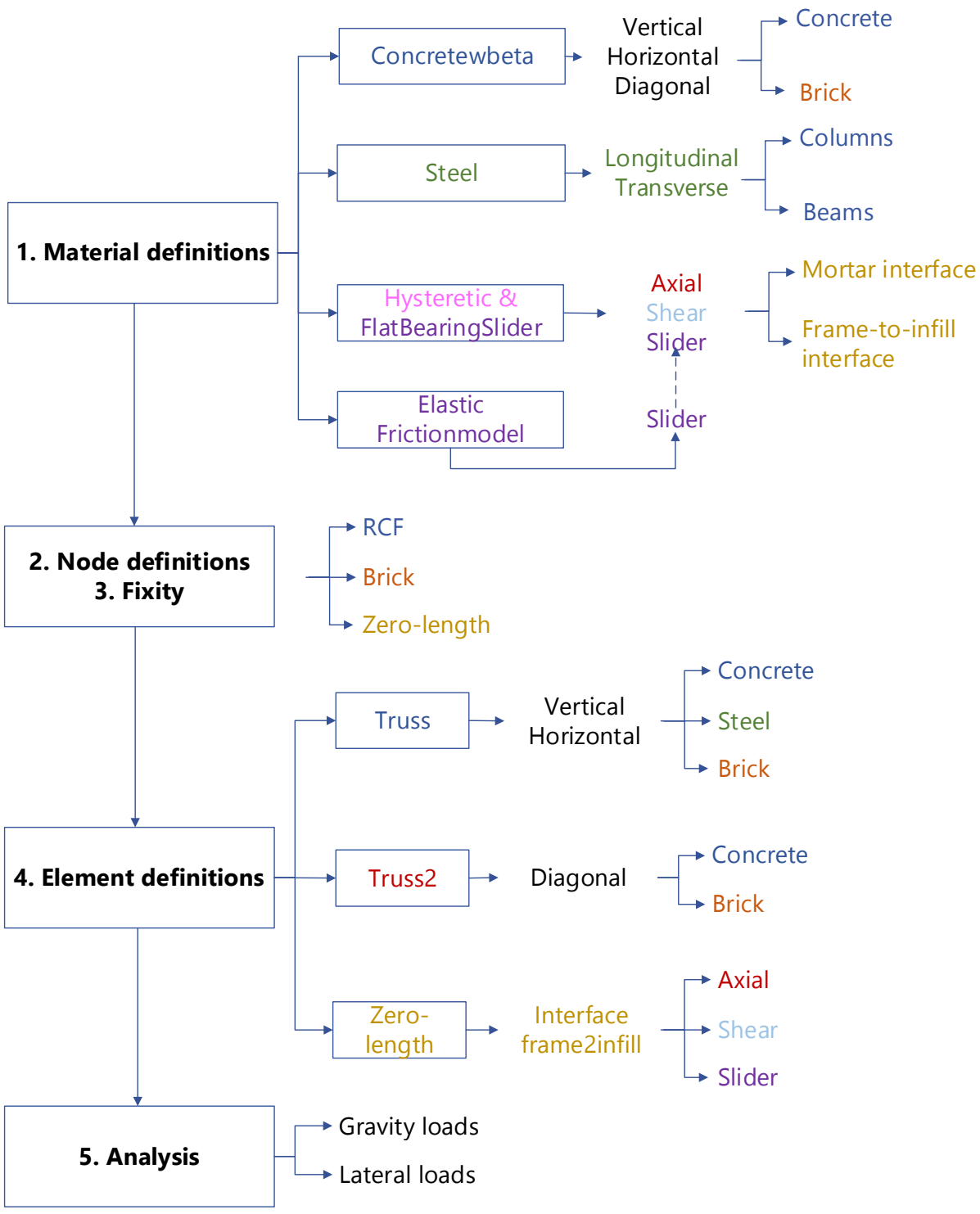

Figure D-1 Schematic representation of the implementation in OpenSEES of the NLTA.

Table D-1 Test results for Specimen 8 by Mehrabi et al. (1994).

Spec. No.	Frame Concrete					Three-Course Masonry Prisms			Compressive Strength of Masonry Units (ksi)	Compressive Strength of Mortar Cylinders (ksi)
	Secant Modulus * (ksi)	Compressive Strength (ksi)	Strain at Peak Stress	Modulus of Rupture (ksi)	Tensile Strength (Split-Cylinder Test) (ksi)	Secant Modulus * (ksi)	Compressive Strength (ksi)	Strain at Peak Stress		
8	2500	3.89	0.0027	0.705	0.401	740	1.38	0.0027	2.39	2.25

* At 45% of the Compressive Strength

a) Average Strengths of Concrete and Masonry Materials

Bar Size	Type of Bar	Nominal Diameter (in.)	Yield Stress (ksi)	Ultimate Stress (ksi)
No. 2	Plain	0.250	53.3	65.2
No. 4	Deformed	0.500	61.0	96.0
No. 5	Deformed	0.625	60.0	96.0

b) Average Tensile Strengths of Reinforcing Steel.

Table D-2 Calculation for the definition of vertical concrete elements.

Parameter	Value	Calculation	Parameter	Value	Calculation
matTag	2	user input	ftint	0.0897	((ftres-ft)/(etres-ecr))*(etint-ecr)+ft
f'_c	-3.89	from test	etint	0.00090	ecr+(etres-ecr)/2
e0	-0.013	from test	ftres	0.0201	0.05(ft)
fcint	-1.945	((fcres- f'_c)/(ecres-e0))*(ecint-e0)+ f'_c	etres	0.00166	1.2*ecr/(Lg/1000.0)
ecint	0.10	ec0+(ecres-ec0)/2	E	2852.67	2 f'_c /ec0
fcres	0	recommended	alpha	1.0	default
ecres	0.0234	(1.0-Omega)*e0+(LR/Lg)*(-0.2/100+Omega*e0)	lamda	0.5	default
Ft	0.401	from test	Where:	LR Omega Lg	23.63 in. fc/(0.5*(Ec*e0+fc)) Element length (4in.)

The required input parameters for the concretewbeta material in OpenSEES are presented below along with the numerical values for the vertical concrete elements.

uniaxialMaterial ConcretewBeta $matTag $fpc $ec0 $fcint $ecint $fcres $ecres $ft $ftint $etint $ftres $etres <-lambda $lambda> <-alpha $alpha> <-beta $bint $ebint $bres $ebres> <-M $M> <-E $Ec> <-conf $fcc $ecc>

uniaxialMaterial ConcretewBeta $ConcVertMat -3.89000000 -0.00270000 -1.94500000 -0.01305010 -0.00000000 -0.02340021 0.40100000 0.08966633 0.00090042 0.02005000 0.00166028 -E 2852.67 -alpha 0.50000000 -lambda 0.75000000

The above calculations must be are repeated for the remaining elements for concrete and brick elements using the appropriate truss element length for performing the regularization process mentioned in Section 4.2.2.1.

D.2.2. Steel

The GMP model is used for the longitudinal and transverse reinforcement. Steel02 is used to construct a uniaxial Giuffre-Menegotto-Pinto steel material object with isotropic strain hardening. With the information reported in **Table D-1**, ***Table D-3*** is constructed to exemplify the values used in the steel material definition in OpenSEES.

Table D-3 Data input for steel elements.

Element	Mat_tag	fy(ksi)	E(ksi)	b	R0	cR1	cR2
Longitudinal	1	61	29000	0.01	20	0.925	0.15
Transverse	6	53.3					
Source:		(test results)	(assumed)	(recommended values)			

The GMP model requires the following input in OpenSEES.

uniaxialMaterial Steel02 $SteelMat 61.0 $Es 0.01 $R0 $cR1 $cR2

uniaxialMaterial Steel02 $SteelMat2 53.3 $Es 0.01 $R0 $cR1 $cR2

D.2.3. Zero-length Interface

The cohesive part of the tensile and shear-slip behavior of the mortar interface is implemented by zero-length assemblages and a slider. For the tensile and shear zero-length elements, the generic hysteretic material in OpenSEES is used in accordance with Section 4.2.3. **Table D-4** presents the values used for Specimen 8. From Section **Accounting for the Mortar Joints in the Truss Models**4.2.3, and taking into account that the mortar unit for this specimen corresponds to a hollow unit (i.e. reduced contact area), 31 psi is assumed for tensile resistance and cohesion. Recall that typical values range from 30 to 130 psi. The mode-1 fracture energy was calculated in accordance with Eq. 3.2. The obtained value was 0.086 N/mm (0.49 psi/in), and the mode-2 fracture energy is calculated as 10 times the value of mode-1 fracture energy. The recommended values of the elastic slope of the slider and the penalty stiffness to ensure contact condition are 110 and 2000 (kip-in.), respectively.

Table D-4 Data input Specimen 8 for zero-length interface.

ft (psi)	Gf^{I} (psi-in)	C (psi)	Gf^{II} (psi-in)	Kint (kip-in)	k (kip-in)	Thickness (in)
31	0.49	31	4.9	110	1000	1.85

With the above data, it is possible to construct the stress displacement relationships depicted in **Figure 4-6.** Proposed modeling scheme for capturing mortar Interface. **Figure 4-6**. To obtain the force-displacement envelope, the stresses are multiplied by their corresponding areas (i.e. (tributary length) x (out-of-plane- thickness)). For instance, the tributary length for the bed joint is measured horizontally between neighboring zero-length elements, whereas for the head joint, this length corresponds to half brick height. The next step is to use the hysteretic material in OpenSEES

to create the positive envelopes. **Figure D-2** depicts the force displacement relationships for the tensile and shear springs. It is clear that the peak value is obtained as (31psi/1000)x1.85in.x(4in./2) =0.1175 kips. Note that no compressive backbone is defined due ttohe fact that the slider provides the normal elastic stiffness to the system.

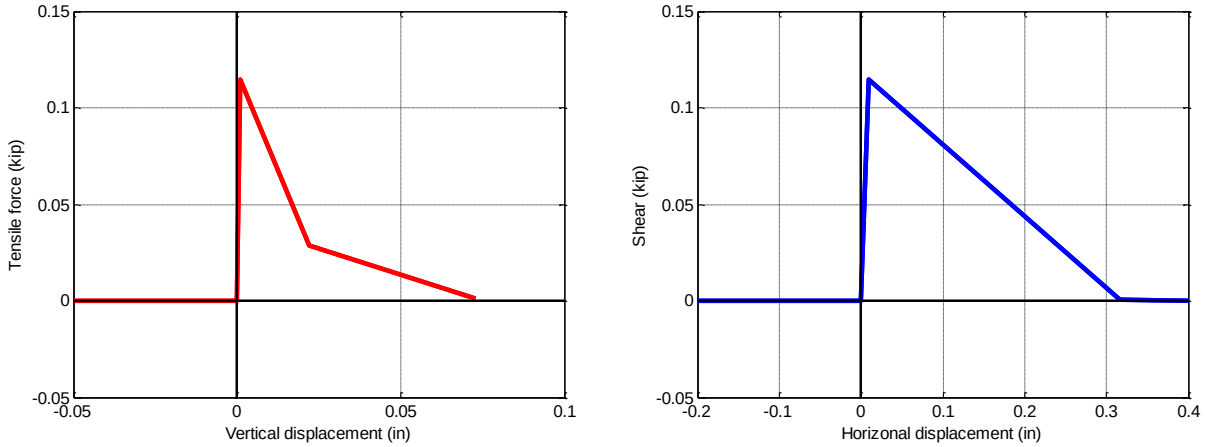

a) Tensile spring b) Shear Spring

Figure D-2 Force-displacement relationship for head joint definitions.

Once the force displacements relationships are defined, they are implemented in OpenSEES by using the generic hysteretic materials. The input parameters and values associated with the head joints are presented below.

Tensile spring:

uniaxialMaterial Hysteretic 41 0.11470 0.0010 0.0286750 0.0219124 0.0011470 0.0727914 -0.0000000010 -100.0 -0.000000001 -101.0 -0.0000000010 -102.0 0.50 0.50 0 0 0 ;

Shear spring:

uniaxialMaterial Hysteretic 40 0.11470 0.010 0.00050 0.3161290323 0.00005 0.4742 -0.0001 -100.0 -0.0002 -101.0 -0.0003 -102.0 0.50 0.50 0 0 0 ;

Regarding the slider, two material definitions are required including (1) the uniaxial law in the axial direction to provide the penalty stiffness value to establish the contact condition (i.e. Column 6 in **Table D-4**), and (2) a friction model capable of increasing in lateral strength due to the presence of vertical compressive forces. These definitions are introduced in OpenSEES as presented below:

Slider:

```
frictionModel Coulomb 10 0.85;
uniaxialMaterial Elastic 20 [expr $k];
```

D.3. Determination of Truss Geometry

In section 4.2.1 a procedure was established to obtain the area of the truss elements representing the URM infill masonry and the RCF members. Therefore, a truss model can be considered as the assemblage of multiple truss cells, each cell consisting of two horizontal, two vertical and two diagonal elements. The size of the cells in the analysis of infilled frames is governed by the dimensions of the infill masonry units. Based on the above, this section presents the required aspects to perform the definition of the model including: nodal definitions (coordinates and fixity) for RCF, URMI, and zero-length elements. In **Figure D-3** shows a close up view of a bottom left part of the NLTA model. Three different color nodes are shown including black, blue and red. For the definitions of RCF elements, only "black" nodes are used whereas for the infill definitions all three color nodes are used. For the frame-to-infill interface elements, all starting nodes are "black" nodes and the end node can be either "blue" or "red" as it is depicted in **Figure D-3**.

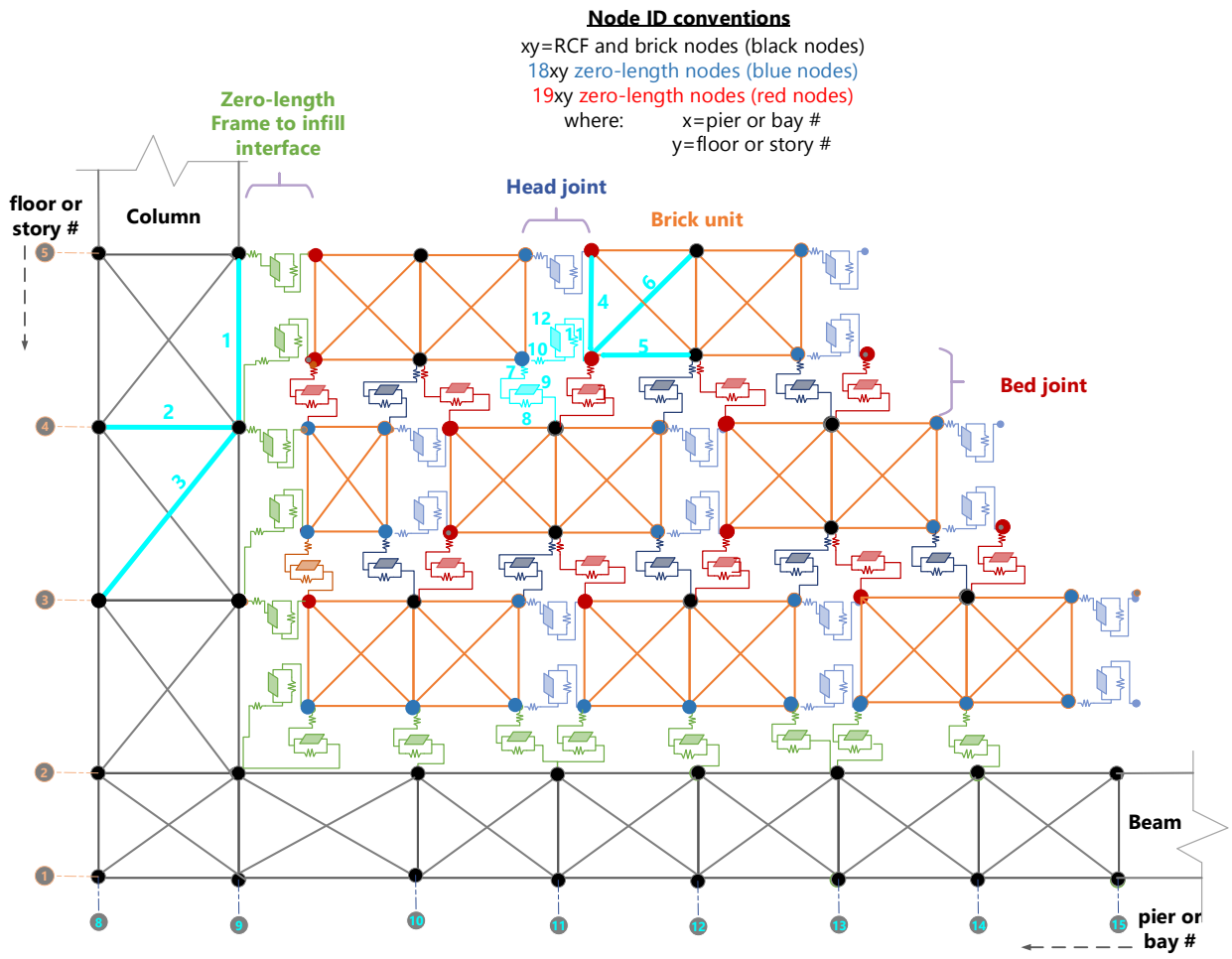

Figure D-3 close up view of a bottom left part of the NLTA model.

D.3.1. Nodal Definitions

The node ID conventions in the NLTA model are schematically depicted in **Figure D-3**. For instance, the tag node number 19112 corresponds with a zero-length "red" node located in pier (i.e., x coordinate) 11 and level (i.e., y coordinate) 2. It was found that the above convention has some benefits including: (1) it facilitates the element definitions, (2) it provides a better feeling about the location of a node, and (3) it allows a quick way to verify

element connectivity. It is convenient to highlight that depending of the size of the model, it'll be required to start either the pier numbering or story numbering from a number different to one in order to avoid node tags dupliciation.

D.3.2. Truss Elements

There are two types of truss elements including: generic ***truss*** elements and ***truss2*** elements. The former are used for horizontal and vertical elements for both RCF and brick units, whereas the latter allows to reduce the compressive peak strength based on the transverse cracking (i.e transverse strains) monitored by the virtual gauge nodes in conjunction with the constitutive law. The ***truss2*** element is used for the diagonal elements of both RCF and brick units with no tensile behavior definition. The required input parameters in OpenSEES and the calculation are schematically depicted in

Figure 4-2 and **Figure 4-3**. This section exemplify the calculation of the input parameters for the truss elements labeled from [**1-6**] in **Figure D-3**.

Table D-5 Cross-sectional calculations sample for truss elements.

Material	**Concrete** (x=3.5 in., y=4.0 in. d=5.32 in.) see **Figure 4-3** **Brick** (x=4.0 in., y=4.0 in. d=5.66 in.) see **Figure 4-2**			**Steel** $(8\ \#\ 4)_{longitudinal}$ $(\#2\ @2.5)_{transverse}$		
element	**Av_ext (in^2)**	**Ah (in^2)**	**Ad (in^2)**	**element**	**Av_ext (in^2)**	**Ah (in^2)**
1	12.25	-	-	**1,1**	0.60	-
2	-	28	-	**2,1**	-	0.16
3	-	-	18.44		-	-
4	3.7	-	-		-	-
5	-	3.7	-		-	-
6	-	-	5.23		-	-
Calculation	(Eq. 4-1)	(Eq. 4-3)	(Eq. 4-4)	Calc.	(3x0.2)	(0.05x2x4/2.5)

Input values in OpenSEES for regular ***truss*** elements.

Element	Type	Tag	Node i	Node j	Area (in^2)	Material
element	truss	**1**	94	95	12.25	Concrete_vertical_col
element	truss	**1,1**	94	95	0.60	Steel_longitudinal_col
element	truss	**2**	84	94	28	Concrete_horizontal_col
element	truss	**2,1**	84	94	0.16	Steel_transverse_col
element	truss	**4**	19114	19115	3.7	Brick_vertical
element	truss	**5**	19114	124	3.7	Brick_horizontal

Input values in OpenSEES for ***truss2*** elements.

Element	Type	Tag	Node i	Node j	mgNode	ngNode	Area (in^2)	Material
element	truss2	**3**	83	94	93	84	18.44	Con_diag_col
element	truss2	**6**	19114	125	124	19115	5.23	Brick_diag

D.3.3. Zero-length Elements

There are three types of zero-length elements. This section present an example of the OpenSEES definition for elements labeled [**7-12**] in **Figure D-3**, i.e., the axial, shear and slider for bed and head joint, respectively. The material and envelopes defined in Section **Zero-length Interface**D.2.3 for the head joint calculations are used consistently in these definitions. The required input is based in Section 4.2.3.1 and Section 4.2.3.2.

element zeroLength tag, node i, node j, mat_tag, global direction

element zeroLength **7** 18114 114 -mat 30 -dir 1;

element zeroLength **8** 18114 114 -mat 31 -dir 2;

element zeroLength **10** 19114 18114 -mat 41 -dir 1;

element zeroLength **11** 19114 18114 -mat 40 -dir 2;

```
element flatSliderBearing     tag, node i, node j, mat_tag, kint, add. mat. definitions, orientation.
element flatSliderBearing     9 18114     114     10  110.0 -P 20 -Mz 20  -orient 0. 1. 0. 1. 0. 0.;
element flatSliderBearing     12 19114 18114    10   110.0 -P 21 -Mz 21  -orient -1. 0. 0. 0. 1. 0.;
```

E. Appendix E

E.1. OpenSEES Script Specimen 8 by Mehrabi et al. (1994)

The present appendix is available on an "as-is" basis with no warranty as to its correctness or completeness. This appendix provides guidance in the implementation of the NLTA in OpenSEES by McKenna et al. (2000). It is believed that a motived reader with the information presented in this appendix, in combination with the previous appendix, and the rationale expressed in Chapter 4, can implement the NLTA in the analysis of RCF with URMI.

```
# NLTA Specimen 8 by (Mehrabi et al., 1994).
# by Daniel Salinas
# March 18, 2016
wipe all;                                                    # clear memory of past model definitions
model BasicBuilder -ndm 2 -ndf 3; # Define the model builder, ndm = #dimension, ndf = #dofs
set tcl_precision 16;


# --- DEFINE MATERIAL MODELS
set SteelMat 1;
set SteelMat2 6;
set ConcVertMat 2;
set ConcHorizMat 3;
set ConcDiagMat 4;
set ConcVertMat_beam 7;
set ConcHorizMat_beam 8;
set ConcDiagMat_beam 9;
set ElasticMat 5;


# Steel02
set fy     60.00000
set fu          65.20000
# Steel02 2
set fy2         53.30000
set fu2         96.00000
set esh         0.002;
set eult   0.12;
set Es          29000.00000
set Esh         4000.;


set R0 20.;
set cR1 0.925;
set cR2 0.15;
set a1 0.05
set a2 1.
set a3 0.
set a4 1.


uniaxialMaterial Steel02 $SteelMat $fy $Es 0.01 $R0 $cR1 $cR2


uniaxialMaterial Steel02 $SteelMat2 $fy2 $Es 0.01 $R0 $cR1 $cR2


# ConcretewBeta Concrete Columns
set dx     3.50000
set dy     4.00000
set dz     5.31507
set eo     -0.00270
set alpha0.50000
set lambda      0.75000

```

```
set fpc   -3.89000
set ec0   -0.00270
set Ec              2564.51852


#uniaxialMaterial ConcretewBeta $ConcVertMat          fpc       ec0       fcint     ecint     fcres     ecres     ft
ftint     etint     ftres     etres     -E 2564.51851852 -alpha 5.000000e-01 -lambda 7.500000e-01
uniaxialMaterial ConcretewBeta $ConcVertMat       -3.89000000 -0.00270000 -1.94500000 -0.01336986 -
0.00000000 -0.02403972 0.40100000 0.08966633 0.00100160 0.02005000 0.00184683 -E 2564.51851852 -alpha
0.50000000 -lambda 0.75000000
uniaxialMaterial ConcretewBeta $ConcHorizMat      -3.89000000 -0.00270000 -1.94500000 -0.01503287 -
0.00000000 -0.02736574 0.40100000 0.08966633 0.00113351 0.02005000 0.00211066 -E 2564.51851852 -alpha
0.50000000 -lambda 0.75000000


uniaxialMaterial ConcretewBeta $ConcDiagMat       -3.89000000 -0.00270000 -1.96445000 -0.01048958 -
0.03890000 -0.01827917 0.00000401 0.00000090 0.00077312 0.00000020 0.00138988 -E 2564.51851852 -beta
0.30000000 0.04444351 0.10000000 0.11110876


# ConcretewBeta Concrete Columns
set dx    4.00000
set dy    4.50000
set dz    6.02080
set eo    -0.00270
set alpha0.50000
set lambda          0.75000


set fpc   -3.89000
set ec0   -0.00270
set Ec              2564.51852


#uniaxialMaterial ConcretewBeta $ConcVertMat_beam          fpc       ec0       fcint     ecint     fcres     ecres
ft        ftint     etint     ftres     etres     -E 2564.51851852 -alpha 5.000000e-01 -lambda 7.500000e-01
uniaxialMaterial ConcretewBeta $ConcVertMat_beam       -3.89000000 -0.00270000 -1.94500000 -0.01207640
-0.00000000 -0.02145281 0.40100000 0.08966633 0.00089899 0.02005000 0.00164162 -E 2564.51851852 -alpha
0.50000000 -lambda 0.75000000
uniaxialMaterial ConcretewBeta $ConcHorizMat_beam       -3.89000000 -0.00270000 -1.94500000 -0.01336986
-0.00000000 -0.02403972 0.40100000 0.08966633 0.00100160 0.02005000 0.00184683 -E 2564.51851852 -alpha
0.50000000 -lambda 0.75000000


uniaxialMaterial ConcretewBeta $ConcDiagMat_beam       -3.89000000 -0.00270000 -1.96445000 -0.00946269
-0.03890000 -0.01622538 0.00000401 0.00000090 0.00069166 0.00000020 0.00122696 -E 2564.51851852 -beta
0.30000000 0.03923408 0.10000000 0.09808521


uniaxialMaterial Elastic $ElasticMat $Ec


#Nodes

```

```
111
112
113
114 # Materials Definitions Infill
115 set ConcVertMatinf 12
116 set ConcHorizMatinf 13
117 set ConcDiagMatinf 14
118
119
120 # ConcretewBeta
121 set dxinf 4.00000
122 set dyinf 4.00000
123 set dzinf 5.65685
124 set eoinf -0.00180
125 set alpha 0.50000
126 set lambda 0.75000
127
128
129 set fpcinf -2.39000
130 set ec0inf -0.00180
131 set Ecinf 2629.00000
132
133
134 uniaxialMaterial ConcretewBeta $ConcVertMatinf -2.39000000 -0.00180000 -1.19500000 -0.01066857 -
135 0.00000000 -0.01953715 0.23900000 0.05344202 0.00058232 0.01195000 0.00107373 -E 2629.00000000 -alpha
136 0.50000000 -lambda 0.75000000
137 uniaxialMaterial ConcretewBeta $ConcHorizMatinf -2.39000000 -0.00180000 -1.19500000 -0.01066857 -
138 0.00000000 -0.01953715 0.23900000 0.05344202 0.00058232 0.01195000 0.00107373 -E 2629.00000000 -alpha
139 0.50000000 -lambda 0.75000000
140
141
142 uniaxialMaterial ConcretewBeta $ConcDiagMatinf -2.39000000 -0.00180000 -1.20695000 -0.00789411 -
143 0.02390000 -0.01398822 0.00000239 0.00000053 0.00042508 0.00000012 0.00075924 -E 2629.00000000 -beta
144 0.30000000 0.04175827 0.10000000 0.10439569
145 set k1 1000.00000
146 frictionModel Coulomb 10 0.85;
147 frictionModel Coulomb 11 0.85;
148 frictionModel Coulomb 100 0.85;
149
150
151 uniaxialMaterial Elastic 20 716.10000
152 uniaxialMaterial Elastic 21 716.10000
153 uniaxialMaterial Hysteretic 30 0.0573500000 0.0100000000 0.0005000000 0.3161290323 0.0000500000
154 0.4741935484 -0.0001000000 -100.0000000000 -0.0002000000 -101.0000000000 -0.0003000000 -102.0000000000
155 0.50 0.50 0 0 0 ;
156 uniaxialMaterial Hysteretic 31 0.0573500000 0.0010000000 0.0143375000 0.0219123947 0.0005735000
157 0.0727913997 -0.0000000010 -100.0000000000 -0.0000000010 -101.0000000000 -0.0000000010 -102.0000000000
158 0.50 0.50 0 0 0 ;
159 uniaxialMaterial Hysteretic 40 0.1147000000 0.0100000000 0.0005000000 0.3161290323 0.0000500000
160 0.4741935484 -0.0001000000 -100.0000000000 -0.0002000000 -101.0000000000 -0.0003000000 -102.0000000000
161 0.50 0.50 0 0 0 ;
162 uniaxialMaterial Hysteretic 41 0.1147000000 0.0010000000 0.0286750000 0.0219123947 0.0011470000
163 0.0727913997 -0.0000000010 -100.0000000000 -0.0000000010 -101.0000000000 -0.0000000010 -102.0000000000
164 0.50 0.50 0 0 0 ;
165
```

```
166
167 # Define Nodal Coordinates for RCMF elements
168 node 71 0.0000 0.0000
169 node 72 0.0000 4.0000
170 node 73 0.0000 8.0000
171 node 74 0.0000 12.0000
172 node 75 0.0000 16.0000
173 node 76 0.0000 20.0000
174 node 77 0.0000 24.0000
175 node 78 0.0000 28.0000
176 node 79 0.0000 32.0000
177 node 710 0.0000 36.0000
178 node 711 0.0000 40.0000
179 node 712 0.0000 44.0000
180 node 713 0.0000 48.0000
181 node 714 0.0000 52.0000
182 node 715 0.0000 56.0000
183 node 716 0.0000 60.5000
184 node 717 0.0000 65.0000
185 node 81 3.5000 0.0000
186 node 82 3.5000 4.0000
187 node 83 3.5000 8.0000
188 node 84 3.5000 12.0000
189 node 85 3.5000 16.0000
190 node 86 3.5000 20.0000
191 node 87 3.5000 24.0000
192 node 88 3.5000 28.0000
193 node 89 3.5000 32.0000
194 node 810 3.5000 36.0000
195 node 811 3.5000 40.0000
196 node 812 3.5000 44.0000
197 node 813 3.5000 48.0000
198 node 814 3.5000 52.0000
199 node 815 3.5000 56.0000
200 node 816 3.5000 60.5000
201 node 817 3.5000 65.0000
202 node 91 7.0000 0.0000
203 node 92 7.0000 4.0000
204 node 93 7.0000 8.0000
205 node 94 7.0000 12.0000
206 node 95 7.0000 16.0000
207 node 96 7.0000 20.0000
208 node 97 7.0000 24.0000
209 node 98 7.0000 28.0000
210 node 99 7.0000 32.0000
211 node 910 7.0000 36.0000
212 node 911 7.0000 40.0000
213 node 912 7.0000 44.0000
214 node 913 7.0000 48.0000
215 node 914 7.0000 52.0000
216 node 915 7.0000 56.0000
217 node 916 7.0000 60.5000
218 node 917 7.0000 65.0000
219 node 301 91.0000 0.0000
220 node 302 91.0000 4.0000
```

```
node    303 91.0000 8.0000
node    304 91.0000 12.0000
node    305 91.0000 16.0000
node    306 91.0000 20.0000
node    307 91.0000 24.0000
node    308 91.0000 28.0000
node    309 91.0000 32.0000
node    3010 91.0000 36.0000
node    3011 91.0000 40.0000
node    3012 91.0000 44.0000
node    3013 91.0000 48.0000
node    3014 91.0000 52.0000
node    3015 91.0000 56.0000
node    3016 91.0000 60.5000
node    3017 91.0000 65.0000
node    311 94.5000 0.0000
node    312 94.5000 4.0000
node    313 94.5000 8.0000
node    314 94.5000 12.0000
node    315 94.5000 16.0000
node    316 94.5000 20.0000
node    317 94.5000 24.0000
node    318 94.5000 28.0000
node    319 94.5000 32.0000
node    3110 94.5000 36.0000
node    3111 94.5000 40.0000
node    3112 94.5000 44.0000
node    3113 94.5000 48.0000
node    3114 94.5000 52.0000
node    3115 94.5000 56.0000
node    3116 94.5000 60.5000
node    3117 94.5000 65.0000
node    321 98.0000 0.0000
node    322 98.0000 4.0000
node    323 98.0000 8.0000
node    324 98.0000 12.0000
node    325 98.0000 16.0000
node    326 98.0000 20.0000
node    327 98.0000 24.0000
node    328 98.0000 28.0000
node    329 98.0000 32.0000
node    3210 98.0000 36.0000
node    3211 98.0000 40.0000
node    3212 98.0000 44.0000
node    3213 98.0000 48.0000
node    3214 98.0000 52.0000
node    3215 98.0000 56.0000
node    3216 98.0000 60.5000
node    3217 98.0000 65.0000
node    1015 11.0000 56.0000
node    1016 11.0000 60.5000
node    1017 11.0000 65.0000
node    1115 15.0000 56.0000
node    1116 15.0000 60.5000
node    1117 15.0000 65.0000
```

```
node    1215 19.0000 56.0000
node    1216 19.0000 60.5000
node    1217 19.0000 65.0000
node    1315 23.0000 56.0000
node    1316 23.0000 60.5000
node    1317 23.0000 65.0000
node    1415 27.0000 56.0000
node    1416 27.0000 60.5000
node    1417 27.0000 65.0000
node    1515 31.0000 56.0000
node    1516 31.0000 60.5000
node    1517 31.0000 65.0000
node    1615 35.0000 56.0000
node    1616 35.0000 60.5000
node    1617 35.0000 65.0000
node    1715 39.0000 56.0000
node    1716 39.0000 60.5000
node    1717 39.0000 65.0000
node    1815 43.0000 56.0000
node    1816 43.0000 60.5000
node    1817 43.0000 65.0000
node    1915 47.0000 56.0000
node    1916 47.0000 60.5000
node    1917 47.0000 65.0000
node    2015 51.0000 56.0000
node    2016 51.0000 60.5000
node    2017 51.0000 65.0000
node    2115 55.0000 56.0000
node    2116 55.0000 60.5000
node    2117 55.0000 65.0000
node    2215 59.0000 56.0000
node    2216 59.0000 60.5000
node    2217 59.0000 65.0000
node    2315 63.0000 56.0000
node    2316 63.0000 60.5000
node    2317 63.0000 65.0000
node    2415 67.0000 56.0000
node    2416 67.0000 60.5000
node    2417 67.0000 65.0000
node    2515 71.0000 56.0000
node    2516 71.0000 60.5000
node    2517 71.0000 65.0000
node    2615 75.0000 56.0000
node    2616 75.0000 60.5000
node    2617 75.0000 65.0000
node    2715 79.0000 56.0000
node    2716 79.0000 60.5000
node    2717 79.0000 65.0000
node    2815 83.0000 56.0000
node    2816 83.0000 60.5000
node    2817 83.0000 65.0000
node    2915 87.0000 56.0000
node    2916 87.0000 60.5000
node    2917 87.0000 65.0000
# Define Nodal Coordinates for infill elements
```

```
node    101 11.0000 0.0000
node    102 11.0000 4.0000
node    103 11.0000 8.0000
node    104 11.0000 12.0000
node    105 11.0000 16.0000
node    106 11.0000 20.0000
node    107 11.0000 24.0000
node    108 11.0000 28.0000
node    109 11.0000 32.0000
node    1010 11.0000 36.0000
node    1011 11.0000 40.0000
node    1012 11.0000 44.0000
node    1013 11.0000 48.0000
node    1014 11.0000 52.0000
node    111 15.0000 0.0000
node    112 15.0000 4.0000
node    113 15.0000 8.0000
node    114 15.0000 12.0000
node    115 15.0000 16.0000
node    116 15.0000 20.0000
node    117 15.0000 24.0000
node    118 15.0000 28.0000
node    119 15.0000 32.0000
node    1110 15.0000 36.0000
node    1111 15.0000 40.0000
node    1112 15.0000 44.0000
node    1113 15.0000 48.0000
node    1114 15.0000 52.0000
node    121 19.0000 0.0000
node    122 19.0000 4.0000
node    123 19.0000 8.0000
node    124 19.0000 12.0000
node    125 19.0000 16.0000
node    126 19.0000 20.0000
node    127 19.0000 24.0000
node    128 19.0000 28.0000
node    129 19.0000 32.0000
node    1210 19.0000 36.0000
node    1211 19.0000 40.0000
node    1212 19.0000 44.0000
node    1213 19.0000 48.0000
node    1214 19.0000 52.0000
node    131 23.0000 0.0000
node    132 23.0000 4.0000
node    133 23.0000 8.0000
node    134 23.0000 12.0000
node    135 23.0000 16.0000
node    136 23.0000 20.0000
node    137 23.0000 24.0000
node    138 23.0000 28.0000
node    139 23.0000 32.0000
node    1310 23.0000 36.0000
node    1311 23.0000 40.0000
```

```
node    1312 23.0000 44.0000
node    1313 23.0000 48.0000
node    1314 23.0000 52.0000
node    141 27.0000 0.0000
node    142 27.0000 4.0000
node    143 27.0000 8.0000
node    144 27.0000 12.0000
node    145 27.0000 16.0000
node    146 27.0000 20.0000
node    147 27.0000 24.0000
node    148 27.0000 28.0000
node    149 27.0000 32.0000
node    1410 27.0000 36.0000
node    1411 27.0000 40.0000
node    1412 27.0000 44.0000
node    1413 27.0000 48.0000
node    1414 27.0000 52.0000
node    151 31.0000 0.0000
node    152 31.0000 4.0000
node    153 31.0000 8.0000
node    154 31.0000 12.0000
node    155 31.0000 16.0000
node    156 31.0000 20.0000
node    157 31.0000 24.0000
node    158 31.0000 28.0000
node    159 31.0000 32.0000
node    1510 31.0000 36.0000
node    1511 31.0000 40.0000
node    1512 31.0000 44.0000
node    1513 31.0000 48.0000
node    1514 31.0000 52.0000
node    161 35.0000 0.0000
node    162 35.0000 4.0000
node    163 35.0000 8.0000
node    164 35.0000 12.0000
node    165 35.0000 16.0000
node    166 35.0000 20.0000
node    167 35.0000 24.0000
node    168 35.0000 28.0000
node    169 35.0000 32.0000
node    1610 35.0000 36.0000
node    1611 35.0000 40.0000
node    1612 35.0000 44.0000
node    1613 35.0000 48.0000
node    1614 35.0000 52.0000
node    171 39.0000 0.0000
node    172 39.0000 4.0000
node    173 39.0000 8.0000
node    174 39.0000 12.0000
node    175 39.0000 16.0000
node    176 39.0000 20.0000
node    177 39.0000 24.0000
node    178 39.0000 28.0000
node    179 39.0000 32.0000
node    1710 39.0000 36.0000
```

```
node    1711 39.0000 40.0000
node    1712 39.0000 44.0000
node    1713 39.0000 48.0000
node    1714 39.0000 52.0000
node    181 43.0000 0.0000
node    182 43.0000 4.0000
node    183 43.0000 8.0000
node    184 43.0000 12.0000
node    185 43.0000 16.0000
node    186 43.0000 20.0000
node    187 43.0000 24.0000
node    188 43.0000 28.0000
node    189 43.0000 32.0000
node    1810 43.0000 36.0000
node    1811 43.0000 40.0000
node    1812 43.0000 44.0000
node    1813 43.0000 48.0000
node    1814 43.0000 52.0000
node    191 47.0000 0.0000
node    192 47.0000 4.0000
node    193 47.0000 8.0000
node    194 47.0000 12.0000
node    195 47.0000 16.0000
node    196 47.0000 20.0000
node    197 47.0000 24.0000
node    198 47.0000 28.0000
node    199 47.0000 32.0000
node    1910 47.0000 36.0000
node    1911 47.0000 40.0000
node    1912 47.0000 44.0000
node    1913 47.0000 48.0000
node    1914 47.0000 52.0000
node    201 51.0000 0.0000
node    202 51.0000 4.0000
node    203 51.0000 8.0000
node    204 51.0000 12.0000
node    205 51.0000 16.0000
node    206 51.0000 20.0000
node    207 51.0000 24.0000
node    208 51.0000 28.0000
node    209 51.0000 32.0000
node    2010 51.0000 36.0000
node    2011 51.0000 40.0000
node    2012 51.0000 44.0000
node    2013 51.0000 48.0000
node    2014 51.0000 52.0000
node    211 55.0000 0.0000
node    212 55.0000 4.0000
node    213 55.0000 8.0000
node    214 55.0000 12.0000
node    215 55.0000 16.0000
node    216 55.0000 20.0000
node    217 55.0000 24.0000
node    218 55.0000 28.0000
node    219 55.0000 32.0000
```

```
node    2110 55.0000 36.0000
node    2111 55.0000 40.0000
node    2112 55.0000 44.0000
node    2113 55.0000 48.0000
node    2114 55.0000 52.0000
node    221 59.0000 0.0000
node    222 59.0000 4.0000
node    223 59.0000 8.0000
node    224 59.0000 12.0000
node    225 59.0000 16.0000
node    226 59.0000 20.0000
node    227 59.0000 24.0000
node    228 59.0000 28.0000
node    229 59.0000 32.0000
node    2210 59.0000 36.0000
node    2211 59.0000 40.0000
node    2212 59.0000 44.0000
node    2213 59.0000 48.0000
node    2214 59.0000 52.0000
node    231 63.0000 0.0000
node    232 63.0000 4.0000
node    233 63.0000 8.0000
node    234 63.0000 12.0000
node    235 63.0000 16.0000
node    236 63.0000 20.0000
node    237 63.0000 24.0000
node    238 63.0000 28.0000
node    239 63.0000 32.0000
node    2310 63.0000 36.0000
node    2311 63.0000 40.0000
node    2312 63.0000 44.0000
node    2313 63.0000 48.0000
node    2314 63.0000 52.0000
node    241 67.0000 0.0000
node    242 67.0000 4.0000
node    243 67.0000 8.0000
node    244 67.0000 12.0000
node    245 67.0000 16.0000
node    246 67.0000 20.0000
node    247 67.0000 24.0000
node    248 67.0000 28.0000
node    249 67.0000 32.0000
node    2410 67.0000 36.0000
node    2411 67.0000 40.0000
node    2412 67.0000 44.0000
node    2413 67.0000 48.0000
node    2414 67.0000 52.0000
node    251 71.0000 0.0000
node    252 71.0000 4.0000
node    253 71.0000 8.0000
node    254 71.0000 12.0000
node    255 71.0000 16.0000
node    256 71.0000 20.0000
node    257 71.0000 24.0000
node    258 71.0000 28.0000
```

```
node     259 71.0000 32.0000
node     2510 71.0000 36.0000
node     2511 71.0000 40.0000
node     2512 71.0000 44.0000
node     2513 71.0000 48.0000
node     2514 71.0000 52.0000
node     261 75.0000 0.0000
node     262 75.0000 4.0000
node     263 75.0000 8.0000
node     264 75.0000 12.0000
node     265 75.0000 16.0000
node     266 75.0000 20.0000
node     267 75.0000 24.0000
node     268 75.0000 28.0000
node     269 75.0000 32.0000
node     2610 75.0000 36.0000
node     2611 75.0000 40.0000
node     2612 75.0000 44.0000
node     2613 75.0000 48.0000
node     2614 75.0000 52.0000
node     271 79.0000 0.0000
node     272 79.0000 4.0000
node     273 79.0000 8.0000
node     274 79.0000 12.0000
node     275 79.0000 16.0000
node     276 79.0000 20.0000
node     277 79.0000 24.0000
node     278 79.0000 28.0000
node     279 79.0000 32.0000
node     2710 79.0000 36.0000
node     2711 79.0000 40.0000
node     2712 79.0000 44.0000
node     2713 79.0000 48.0000
node     2714 79.0000 52.0000
node     281 83.0000 0.0000
node     282 83.0000 4.0000
node     283 83.0000 8.0000
node     284 83.0000 12.0000
node     285 83.0000 16.0000
node     286 83.0000 20.0000
node     287 83.0000 24.0000
node     288 83.0000 28.0000
node     289 83.0000 32.0000
node     2810 83.0000 36.0000
node     2811 83.0000 40.0000
node     2812 83.0000 44.0000
node     2813 83.0000 48.0000
node     2814 83.0000 52.0000
node     291 87.0000 0.0000
node     292 87.0000 4.0000
node     293 87.0000 8.0000
node     294 87.0000 12.0000
node     295 87.0000 16.0000
node     296 87.0000 20.0000
node     297 87.0000 24.0000
```

```
node    298 87.0000 28.0000
node    299 87.0000 32.0000
node    2910 87.0000 36.0000
node    2911 87.0000 40.0000
node    2912 87.0000 44.0000
node    2913 87.0000 48.0000
node    2914 87.0000 52.0000


#Fixity


# Fixity RCMF elements
fix     71 1 1 1
fix     72 0 0 1
fix     73 0 0 1
fix     74 0 0 1
fix     75 0 0 1
fix     76 0 0 1
fix     77 0 0 1
fix     78 0 0 1
fix     79 0 0 1
fix     710 0 0 1
fix     711 0 0 1
fix     712 0 0 1
fix     713 0 0 1
fix     714 0 0 1
fix     715 0 0 1
fix     716 0 0 1
fix     717 0 0 1
fix     81 1 1 1
fix     82 0 0 1
fix     83 0 0 1
fix     84 0 0 1
fix     85 0 0 1
fix     86 0 0 1
fix     87 0 0 1
fix     88 0 0 1
fix     89 0 0 1
fix     810 0 0 1
fix     811 0 0 1
fix     812 0 0 1
fix     813 0 0 1
fix     814 0 0 1
fix     815 0 0 1
fix     816 0 0 1
fix     817 0 0 1
fix     91 1 1 1
fix     92 0 0 1
fix     93 0 0 1
fix     94 0 0 1
fix     95 0 0 1
fix     96 0 0 1
fix     97 0 0 1
fix     98 0 0 1
```

```
fix     99 0 0 1
fix     910 0 0 1
fix     911 0 0 1
fix     912 0 0 1
fix     913 0 0 1
fix     914 0 0 1
fix     915 0 0 1
fix     916 0 0 1
fix     917 0 0 1
fix     301 1 1 1
fix     302 0 0 1
fix     303 0 0 1
fix     304 0 0 1
fix     305 0 0 1
fix     306 0 0 1
fix     307 0 0 1
fix     308 0 0 1
fix     309 0 0 1
fix     3010 0 0 1
fix     3011 0 0 1
fix     3012 0 0 1
fix     3013 0 0 1
fix     3014 0 0 1
fix     3015 0 0 1
fix     3016 0 0 1
fix     3017 0 0 1
fix     311 1 1 1
fix     312 0 0 1
fix     313 0 0 1
fix     314 0 0 1
fix     315 0 0 1
fix     316 0 0 1
fix     317 0 0 1
fix     318 0 0 1
fix     319 0 0 1
fix     3110 0 0 1
fix     3111 0 0 1
fix     3112 0 0 1
fix     3113 0 0 1
fix     3114 0 0 1
fix     3115 0 0 1
fix     3116 0 0 1
fix     3117 0 0 1
fix     321 1 1 1
fix     322 0 0 1
fix     323 0 0 1
fix     324 0 0 1
fix     325 0 0 1
fix     326 0 0 1
fix     327 0 0 1
fix     328 0 0 1
fix     329 0 0 1
fix     3210 0 0 1
fix     3211 0 0 1
fix     3212 0 0 1
```

```
fix     3213 0 0 1
fix     3214 0 0 1
fix     3215 0 0 1
fix     3216 0 0 1
fix     3217 0 0 1
fix     1015 0 0 1
fix     1016 0 0 1
fix     1017 0 0 1
fix     1115 0 0 1
fix     1116 0 0 1
fix     1117 0 0 1
fix     1215 0 0 1
fix     1216 0 0 1
fix     1217 0 0 1
fix     1315 0 0 1
fix     1316 0 0 1
fix     1317 0 0 1
fix     1415 0 0 1
fix     1416 0 0 1
fix     1417 0 0 1
fix     1515 0 0 1
fix     1516 0 0 1
fix     1517 0 0 1
fix     1615 0 0 1
fix     1616 0 0 1
fix     1617 0 0 1
fix     1715 0 0 1
fix     1716 0 0 1
fix     1717 0 0 1
fix     1815 0 0 1
fix     1816 0 0 1
fix     1817 0 0 1
fix     1915 0 0 1
fix     1916 0 0 1
fix     1917 0 0 1
fix     2015 0 0 1
fix     2016 0 0 1
fix     2017 0 0 1
fix     2115 0 0 1
fix     2116 0 0 1
fix     2117 0 0 1
fix     2215 0 0 1
fix     2216 0 0 1
fix     2217 0 0 1
fix     2315 0 0 1
fix     2316 0 0 1
fix     2317 0 0 1
fix     2415 0 0 1
fix     2416 0 0 1
fix     2417 0 0 1
fix     2515 0 0 1
fix     2516 0 0 1
fix     2517 0 0 1
fix     2615 0 0 1
fix     2616 0 0 1
```

```
fix 2617 0 0 1
fix 2715 0 0 1
fix 2716 0 0 1
fix 2717 0 0 1
fix 2815 0 0 1
fix 2816 0 0 1
fix 2817 0 0 1
fix 2915 0 0 1
fix 2916 0 0 1
fix 2917 0 0 1
# Fixity Infill elements
fix 101 1 1 1
fix 102 0 0 1
fix 103 0 0 1
fix 104 0 0 1
fix 105 0 0 1
fix 106 0 0 1
fix 107 0 0 1
fix 108 0 0 1
fix 109 0 0 1
fix 1010 0 0 1
fix 1011 0 0 1
fix 1012 0 0 1
fix 1013 0 0 1
fix 1014 0 0 1
fix 111 1 1 1
fix 112 0 0 1
fix 113 0 0 1
fix 114 0 0 1
fix 115 0 0 1
fix 116 0 0 1
fix 117 0 0 1
fix 118 0 0 1
fix 119 0 0 1
fix 1110 0 0 1
fix 1111 0 0 1
fix 1112 0 0 1
fix 1113 0 0 1
fix 1114 0 0 1
fix 121 1 1 1
fix 122 0 0 1
fix 123 0 0 1
fix 124 0 0 1
fix 125 0 0 1
fix 126 0 0 1
fix 127 0 0 1
fix 128 0 0 1
fix 129 0 0 1
fix 1210 0 0 1
fix 1211 0 0 1
fix 1212 0 0 1
fix 1213 0 0 1
fix 1214 0 0 1
fix 131 1 1 1
fix 132 0 0 1
```

```
fix     133 0 0 1
fix     134 0 0 1
fix     135 0 0 1
fix     136 0 0 1
fix     137 0 0 1
fix     138 0 0 1
fix     139 0 0 1
fix     1310 0 0 1
fix     1311 0 0 1
fix     1312 0 0 1
fix     1313 0 0 1
fix     1314 0 0 1
fix     141 1 1 1
fix     142 0 0 1
fix     143 0 0 1
fix     144 0 0 1
fix     145 0 0 1
fix     146 0 0 1
fix     147 0 0 1
fix     148 0 0 1
fix     149 0 0 1
fix     1410 0 0 1
fix     1411 0 0 1
fix     1412 0 0 1
fix     1413 0 0 1
fix     1414 0 0 1
fix     151 1 1 1
fix     152 0 0 1
fix     153 0 0 1
fix     154 0 0 1
fix     155 0 0 1
fix     156 0 0 1
fix     157 0 0 1
fix     158 0 0 1
fix     159 0 0 1
fix     1510 0 0 1
fix     1511 0 0 1
fix     1512 0 0 1
fix     1513 0 0 1
fix     1514 0 0 1
fix     161 1 1 1
fix     162 0 0 1
fix     163 0 0 1
fix     164 0 0 1
fix     165 0 0 1
fix     166 0 0 1
fix     167 0 0 1
fix     168 0 0 1
fix     169 0 0 1
fix     1610 0 0 1
fix     1611 0 0 1
fix     1612 0 0 1
fix     1613 0 0 1
fix     1614 0 0 1
fix     171 1 1 1
```

```
fix 172 0 0 1
fix 173 0 0 1
fix 174 0 0 1
fix 175 0 0 1
fix 176 0 0 1
fix 177 0 0 1
fix 178 0 0 1
fix 179 0 0 1
fix 1710 0 0 1
fix 1711 0 0 1
fix 1712 0 0 1
fix 1713 0 0 1
fix 1714 0 0 1
fix 181 1 1 1
fix 182 0 0 1
fix 183 0 0 1
fix 184 0 0 1
fix 185 0 0 1
fix 186 0 0 1
fix 187 0 0 1
fix 188 0 0 1
fix 189 0 0 1
fix 1810 0 0 1
fix 1811 0 0 1
fix 1812 0 0 1
fix 1813 0 0 1
fix 1814 0 0 1
fix 191 1 1 1
fix 192 0 0 1
fix 193 0 0 1
fix 194 0 0 1
fix 195 0 0 1
fix 196 0 0 1
fix 197 0 0 1
fix 198 0 0 1
fix 199 0 0 1
fix 1910 0 0 1
fix 1911 0 0 1
fix 1912 0 0 1
fix 1913 0 0 1
fix 1914 0 0 1
fix 201 1 1 1
fix 202 0 0 1
fix 203 0 0 1
fix 204 0 0 1
fix 205 0 0 1
fix 206 0 0 1
fix 207 0 0 1
fix 208 0 0 1
fix 209 0 0 1
fix 2010 0 0 1
fix 2011 0 0 1
fix 2012 0 0 1
fix 2013 0 0 1
fix 2014 0 0 1
```

```
fix     211 1 1 1
fix     212 0 0 1
fix     213 0 0 1
fix     214 0 0 1
fix     215 0 0 1
fix     216 0 0 1
fix     217 0 0 1
fix     218 0 0 1
fix     219 0 0 1
fix     2110 0 0 1
fix     2111 0 0 1
fix     2112 0 0 1
fix     2113 0 0 1
fix     2114 0 0 1
fix     221 1 1 1
fix     222 0 0 1
fix     223 0 0 1
fix     224 0 0 1
fix     225 0 0 1
fix     226 0 0 1
fix     227 0 0 1
fix     228 0 0 1
fix     229 0 0 1
fix     2210 0 0 1
fix     2211 0 0 1
fix     2212 0 0 1
fix     2213 0 0 1
fix     2214 0 0 1
fix     231 1 1 1
fix     232 0 0 1
fix     233 0 0 1
fix     234 0 0 1
fix     235 0 0 1
fix     236 0 0 1
fix     237 0 0 1
fix     238 0 0 1
fix     239 0 0 1
fix     2310 0 0 1
fix     2311 0 0 1
fix     2312 0 0 1
fix     2313 0 0 1
fix     2314 0 0 1
fix     241 1 1 1
fix     242 0 0 1
fix     243 0 0 1
fix     244 0 0 1
fix     245 0 0 1
fix     246 0 0 1
fix     247 0 0 1
fix     248 0 0 1
fix     249 0 0 1
fix     2410 0 0 1
fix     2411 0 0 1
fix     2412 0 0 1
fix     2413 0 0 1
```

```
991  fix  2414 0 0 1
992  fix  251 1 1 1
993  fix  252 0 0 1
994  fix  253 0 0 1
995  fix  254 0 0 1
996  fix  255 0 0 1
997  fix  256 0 0 1
998  fix  257 0 0 1
999  fix  258 0 0 1
1000 fix  259 0 0 1
1001 fix  2510 0 0 1
1002 fix  2511 0 0 1
1003 fix  2512 0 0 1
1004 fix  2513 0 0 1
1005 fix  2514 0 0 1
1006 fix  261 1 1 1
1007 fix  262 0 0 1
1008 fix  263 0 0 1
1009 fix  264 0 0 1
1010 fix  265 0 0 1
1011 fix  266 0 0 1
1012 fix  267 0 0 1
1013 fix  268 0 0 1
1014 fix  269 0 0 1
1015 fix  2610 0 0 1
1016 fix  2611 0 0 1
1017 fix  2612 0 0 1
1018 fix  2613 0 0 1
1019 fix  2614 0 0 1
1020 fix  271 1 1 1
1021 fix  272 0 0 1
1022 fix  273 0 0 1
1023 fix  274 0 0 1
1024 fix  275 0 0 1
1025 fix  276 0 0 1
1026 fix  277 0 0 1
1027 fix  278 0 0 1
1028 fix  279 0 0 1
1029 fix  2710 0 0 1
1030 fix  2711 0 0 1
1031 fix  2712 0 0 1
1032 fix  2713 0 0 1
1033 fix  2714 0 0 1
1034 fix  281 1 1 1
1035 fix  282 0 0 1
1036 fix  283 0 0 1
1037 fix  284 0 0 1
1038 fix  285 0 0 1
1039 fix  286 0 0 1
1040 fix  287 0 0 1
1041 fix  288 0 0 1
1042 fix  289 0 0 1
1043 fix  2810 0 0 1
1044 fix  2811 0 0 1
1045 fix  2812 0 0 1
```

```
fix     2813 0 0 1
fix     2814 0 0 1
fix     291 1 1 1
fix     292 0 0 1
fix     293 0 0 1
fix     294 0 0 1
fix     295 0 0 1
fix     296 0 0 1
fix     297 0 0 1
fix     298 0 0 1
fix     299 0 0 1
fix     2910 0 0 1
fix     2911 0 0 1
fix     2912 0 0 1
fix     2913 0 0 1
fix     2914 0 0 1


# Define Nodal Coordinates for Zero length elements


# Frame 1 tag=18
node    1891 7.0000 0.0000
node    1892 7.0000 4.0000
node    1893 7.0000 8.0000
node    1894 7.0000 12.0000
node    1895 7.0000 16.0000
node    1896 7.0000 20.0000
node    1897 7.0000 24.0000
node    1898 7.0000 28.0000
node    1899 7.0000 32.0000
node    18910 7.0000 36.0000
node    18911 7.0000 40.0000
node    18912 7.0000 44.0000
node    18913 7.0000 48.0000
node    18914 7.0000 52.0000
node    18915 7.0000 56.0000
node    18101 11.0000 0.0000
node    18102 11.0000 4.0000
node    18103 11.0000 8.0000
node    18104 11.0000 12.0000
node    18105 11.0000 16.0000
node    18106 11.0000 20.0000
node    18107 11.0000 24.0000
node    18108 11.0000 28.0000
node    18109 11.0000 32.0000
node    181010 11.0000 36.0000
node    181011 11.0000 40.0000
node    181012 11.0000 44.0000
node    181013 11.0000 48.0000
node    181014 11.0000 52.0000
node    181015 11.0000 56.0000
node    18111 15.0000 0.0000
node    18112 15.0000 4.0000
node    18113 15.0000 8.0000
```

```
node      18114 15.0000 12.0000
node      18115 15.0000 16.0000
node      18116 15.0000 20.0000
node      18117 15.0000 24.0000
node      18118 15.0000 28.0000
node      18119 15.0000 32.0000
node      181110 15.0000 36.0000
node      181111 15.0000 40.0000
node      181112 15.0000 44.0000
node      181113 15.0000 48.0000
node      181114 15.0000 52.0000
node      181115 15.0000 56.0000
node      18121 19.0000 0.0000
node      18122 19.0000 4.0000
node      18123 19.0000 8.0000
node      18124 19.0000 12.0000
node      18125 19.0000 16.0000
node      18126 19.0000 20.0000
node      18127 19.0000 24.0000
node      18128 19.0000 28.0000
node      18129 19.0000 32.0000
node      181210 19.0000 36.0000
node      181211 19.0000 40.0000
node      181212 19.0000 44.0000
node      181213 19.0000 48.0000
node      181214 19.0000 52.0000
node      181215 19.0000 56.0000
node      18131 23.0000 0.0000
node      18132 23.0000 4.0000
node      18133 23.0000 8.0000
node      18134 23.0000 12.0000
node      18135 23.0000 16.0000
node      18136 23.0000 20.0000
node      18137 23.0000 24.0000
node      18138 23.0000 28.0000
node      18139 23.0000 32.0000
node      181310 23.0000 36.0000
node      181311 23.0000 40.0000
node      181312 23.0000 44.0000
node      181313 23.0000 48.0000
node      181314 23.0000 52.0000
node      181315 23.0000 56.0000
node      18141 27.0000 0.0000
node      18142 27.0000 4.0000
node      18143 27.0000 8.0000
node      18144 27.0000 12.0000
node      18145 27.0000 16.0000
node      18146 27.0000 20.0000
node      18147 27.0000 24.0000
node      18148 27.0000 28.0000
node      18149 27.0000 32.0000
node      181410 27.0000 36.0000
node      181411 27.0000 40.0000
node      181412 27.0000 44.0000
node      181413 27.0000 48.0000
```

```
node    181414 27.0000 52.0000
node    181415 27.0000 56.0000
node    18151 31.0000 0.0000
node    18152 31.0000 4.0000
node    18153 31.0000 8.0000
node    18154 31.0000 12.0000
node    18155 31.0000 16.0000
node    18156 31.0000 20.0000
node    18157 31.0000 24.0000
node    18158 31.0000 28.0000
node    18159 31.0000 32.0000
node    181510 31.0000 36.0000
node    181511 31.0000 40.0000
node    181512 31.0000 44.0000
node    181513 31.0000 48.0000
node    181514 31.0000 52.0000
node    181515 31.0000 56.0000
node    18161 35.0000 0.0000
node    18162 35.0000 4.0000
node    18163 35.0000 8.0000
node    18164 35.0000 12.0000
node    18165 35.0000 16.0000
node    18166 35.0000 20.0000
node    18167 35.0000 24.0000
node    18168 35.0000 28.0000
node    18169 35.0000 32.0000
node    181610 35.0000 36.0000
node    181611 35.0000 40.0000
node    181612 35.0000 44.0000
node    181613 35.0000 48.0000
node    181614 35.0000 52.0000
node    181615 35.0000 56.0000
node    18171 39.0000 0.0000
node    18172 39.0000 4.0000
node    18173 39.0000 8.0000
node    18174 39.0000 12.0000
node    18175 39.0000 16.0000
node    18176 39.0000 20.0000
node    18177 39.0000 24.0000
node    18178 39.0000 28.0000
node    18179 39.0000 32.0000
node    181710 39.0000 36.0000
node    181711 39.0000 40.0000
node    181712 39.0000 44.0000
node    181713 39.0000 48.0000
node    181714 39.0000 52.0000
node    181715 39.0000 56.0000
node    18181 43.0000 0.0000
node    18182 43.0000 4.0000
node    18183 43.0000 8.0000
node    18184 43.0000 12.0000
node    18185 43.0000 16.0000
node    18186 43.0000 20.0000
node    18187 43.0000 24.0000
node    18188 43.0000 28.0000
```

```
node      18189 43.0000 32.0000
node      181810 43.0000 36.0000
node      181811 43.0000 40.0000
node      181812 43.0000 44.0000
node      181813 43.0000 48.0000
node      181814 43.0000 52.0000
node      181815 43.0000 56.0000
node      18191 47.0000 0.0000
node      18192 47.0000 4.0000
node      18193 47.0000 8.0000
node      18194 47.0000 12.0000
node      18195 47.0000 16.0000
node      18196 47.0000 20.0000
node      18197 47.0000 24.0000
node      18198 47.0000 28.0000
node      18199 47.0000 32.0000
node      181910 47.0000 36.0000
node      181911 47.0000 40.0000
node      181912 47.0000 44.0000
node      181913 47.0000 48.0000
node      181914 47.0000 52.0000
node      181915 47.0000 56.0000
node      18201 51.0000 0.0000
node      18202 51.0000 4.0000
node      18203 51.0000 8.0000
node      18204 51.0000 12.0000
node      18205 51.0000 16.0000
node      18206 51.0000 20.0000
node      18207 51.0000 24.0000
node      18208 51.0000 28.0000
node      18209 51.0000 32.0000
node      182010 51.0000 36.0000
node      182011 51.0000 40.0000
node      182012 51.0000 44.0000
node      182013 51.0000 48.0000
node      182014 51.0000 52.0000
node      182015 51.0000 56.0000
node      18211 55.0000 0.0000
node      18212 55.0000 4.0000
node      18213 55.0000 8.0000
node      18214 55.0000 12.0000
node      18215 55.0000 16.0000
node      18216 55.0000 20.0000
node      18217 55.0000 24.0000
node      18218 55.0000 28.0000
node      18219 55.0000 32.0000
node      182110 55.0000 36.0000
node      182111 55.0000 40.0000
node      182112 55.0000 44.0000
node      182113 55.0000 48.0000
node      182114 55.0000 52.0000
node      182115 55.0000 56.0000
node      18221 59.0000 0.0000
node      18222 59.0000 4.0000
node      18223 59.0000 8.0000
```

```
node    18224 59.0000 12.0000
node    18225 59.0000 16.0000
node    18226 59.0000 20.0000
node    18227 59.0000 24.0000
node    18228 59.0000 28.0000
node    18229 59.0000 32.0000
node    182210 59.0000 36.0000
node    182211 59.0000 40.0000
node    182212 59.0000 44.0000
node    182213 59.0000 48.0000
node    182214 59.0000 52.0000
node    182215 59.0000 56.0000
node    18231 63.0000 0.0000
node    18232 63.0000 4.0000
node    18233 63.0000 8.0000
node    18234 63.0000 12.0000
node    18235 63.0000 16.0000
node    18236 63.0000 20.0000
node    18237 63.0000 24.0000
node    18238 63.0000 28.0000
node    18239 63.0000 32.0000
node    182310 63.0000 36.0000
node    182311 63.0000 40.0000
node    182312 63.0000 44.0000
node    182313 63.0000 48.0000
node    182314 63.0000 52.0000
node    182315 63.0000 56.0000
node    18241 67.0000 0.0000
node    18242 67.0000 4.0000
node    18243 67.0000 8.0000
node    18244 67.0000 12.0000
node    18245 67.0000 16.0000
node    18246 67.0000 20.0000
node    18247 67.0000 24.0000
node    18248 67.0000 28.0000
node    18249 67.0000 32.0000
node    182410 67.0000 36.0000
node    182411 67.0000 40.0000
node    182412 67.0000 44.0000
node    182413 67.0000 48.0000
node    182414 67.0000 52.0000
node    182415 67.0000 56.0000
node    18251 71.0000 0.0000
node    18252 71.0000 4.0000
node    18253 71.0000 8.0000
node    18254 71.0000 12.0000
node    18255 71.0000 16.0000
node    18256 71.0000 20.0000
node    18257 71.0000 24.0000
node    18258 71.0000 28.0000
node    18259 71.0000 32.0000
node    182510 71.0000 36.0000
node    182511 71.0000 40.0000
node    182512 71.0000 44.0000
node    182513 71.0000 48.0000
```

```
node      182514 71.0000 52.0000
node      182515 71.0000 56.0000
node      18261 75.0000 0.0000
node      18262 75.0000 4.0000
node      18263 75.0000 8.0000
node      18264 75.0000 12.0000
node      18265 75.0000 16.0000
node      18266 75.0000 20.0000
node      18267 75.0000 24.0000
node      18268 75.0000 28.0000
node      18269 75.0000 32.0000
node      182610 75.0000 36.0000
node      182611 75.0000 40.0000
node      182612 75.0000 44.0000
node      182613 75.0000 48.0000
node      182614 75.0000 52.0000
node      182615 75.0000 56.0000
node      18271 79.0000 0.0000
node      18272 79.0000 4.0000
node      18273 79.0000 8.0000
node      18274 79.0000 12.0000
node      18275 79.0000 16.0000
node      18276 79.0000 20.0000
node      18277 79.0000 24.0000
node      18278 79.0000 28.0000
node      18279 79.0000 32.0000
node      182710 79.0000 36.0000
node      182711 79.0000 40.0000
node      182712 79.0000 44.0000
node      182713 79.0000 48.0000
node      182714 79.0000 52.0000
node      182715 79.0000 56.0000
node      18281 83.0000 0.0000
node      18282 83.0000 4.0000
node      18283 83.0000 8.0000
node      18284 83.0000 12.0000
node      18285 83.0000 16.0000
node      18286 83.0000 20.0000
node      18287 83.0000 24.0000
node      18288 83.0000 28.0000
node      18289 83.0000 32.0000
node      182810 83.0000 36.0000
node      182811 83.0000 40.0000
node      182812 83.0000 44.0000
node      182813 83.0000 48.0000
node      182814 83.0000 52.0000
node      182815 83.0000 56.0000
node      18291 87.0000 0.0000
node      18292 87.0000 4.0000
node      18293 87.0000 8.0000
node      18294 87.0000 12.0000
node      18295 87.0000 16.0000
node      18296 87.0000 20.0000
node      18297 87.0000 24.0000
node      18298 87.0000 28.0000
```

```
node      18299 87.0000 32.0000
node      182910 87.0000 36.0000
node      182911 87.0000 40.0000
node      182912 87.0000 44.0000
node      182913 87.0000 48.0000
node      182914 87.0000 52.0000
node      182915 87.0000 56.0000
node      18302 91.0000 4.0000
node      18303 91.0000 8.0000
node      18304 91.0000 12.0000
node      18305 91.0000 16.0000
node      18306 91.0000 20.0000
node      18307 91.0000 24.0000
node      18308 91.0000 28.0000
node      18309 91.0000 32.0000
node      183010 91.0000 36.0000
node      183011 91.0000 40.0000
node      183012 91.0000 44.0000
node      183013 91.0000 48.0000
node      183014 91.0000 52.0000
node      183015 91.0000 56.0000
# Frame 1 tag=19
node      1992 7.0000 4.0000
node      1993 7.0000 8.0000
node      1994 7.0000 12.0000
node      1995 7.0000 16.0000
node      1996 7.0000 20.0000
node      1997 7.0000 24.0000
node      1998 7.0000 28.0000
node      1999 7.0000 32.0000
node      19910 7.0000 36.0000
node      19911 7.0000 40.0000
node      19912 7.0000 44.0000
node      19913 7.0000 48.0000
node      19914 7.0000 52.0000
node      19102 11.0000 4.0000
node      19103 11.0000 8.0000
node      19104 11.0000 12.0000
node      19105 11.0000 16.0000
node      19106 11.0000 20.0000
node      19107 11.0000 24.0000
node      19108 11.0000 28.0000
node      19109 11.0000 32.0000
node      191010 11.0000 36.0000
node      191011 11.0000 40.0000
node      191012 11.0000 44.0000
node      191013 11.0000 48.0000
node      191014 11.0000 52.0000
node      191015 11.0000 56.0000
node      19111 15.0000 0.0000
node      19112 15.0000 4.0000
node      19113 15.0000 8.0000
node      19114 15.0000 12.0000
node      19115 15.0000 16.0000
node      19116 15.0000 20.0000
```

```
node     19117 15.0000 24.0000
node     19118 15.0000 28.0000
node     19119 15.0000 32.0000
node     191110 15.0000 36.0000
node     191111 15.0000 40.0000
node     191112 15.0000 44.0000
node     191113 15.0000 48.0000
node     191114 15.0000 52.0000
node     19122 19.0000 4.0000
node     19123 19.0000 8.0000
node     19124 19.0000 12.0000
node     19125 19.0000 16.0000
node     19126 19.0000 20.0000
node     19127 19.0000 24.0000
node     19128 19.0000 28.0000
node     19129 19.0000 32.0000
node     191210 19.0000 36.0000
node     191211 19.0000 40.0000
node     191212 19.0000 44.0000
node     191213 19.0000 48.0000
node     191214 19.0000 52.0000
node     191215 19.0000 56.0000
node     19131 23.0000 0.0000
node     19132 23.0000 4.0000
node     19133 23.0000 8.0000
node     19134 23.0000 12.0000
node     19135 23.0000 16.0000
node     19136 23.0000 20.0000
node     19137 23.0000 24.0000
node     19138 23.0000 28.0000
node     19139 23.0000 32.0000
node     191310 23.0000 36.0000
node     191311 23.0000 40.0000
node     191312 23.0000 44.0000
node     191313 23.0000 48.0000
node     191314 23.0000 52.0000
node     19142 27.0000 4.0000
node     19143 27.0000 8.0000
node     19144 27.0000 12.0000
node     19145 27.0000 16.0000
node     19146 27.0000 20.0000
node     19147 27.0000 24.0000
node     19148 27.0000 28.0000
node     19149 27.0000 32.0000
node     191410 27.0000 36.0000
node     191411 27.0000 40.0000
node     191412 27.0000 44.0000
node     191413 27.0000 48.0000
node     191414 27.0000 52.0000
node     191415 27.0000 56.0000
node     19151 31.0000 0.0000
node     19152 31.0000 4.0000
node     19153 31.0000 8.0000
node     19154 31.0000 12.0000
node     19155 31.0000 16.0000
```

```
node     19156 31.0000 20.0000
node     19157 31.0000 24.0000
node     19158 31.0000 28.0000
node     19159 31.0000 32.0000
node     191510 31.0000 36.0000
node     191511 31.0000 40.0000
node     191512 31.0000 44.0000
node     191513 31.0000 48.0000
node     191514 31.0000 52.0000
node     19162 35.0000 4.0000
node     19163 35.0000 8.0000
node     19164 35.0000 12.0000
node     19165 35.0000 16.0000
node     19166 35.0000 20.0000
node     19167 35.0000 24.0000
node     19168 35.0000 28.0000
node     19169 35.0000 32.0000
node     191610 35.0000 36.0000
node     191611 35.0000 40.0000
node     191612 35.0000 44.0000
node     191613 35.0000 48.0000
node     191614 35.0000 52.0000
node     191615 35.0000 56.0000
node     19171 39.0000 0.0000
node     19172 39.0000 4.0000
node     19173 39.0000 8.0000
node     19174 39.0000 12.0000
node     19175 39.0000 16.0000
node     19176 39.0000 20.0000
node     19177 39.0000 24.0000
node     19178 39.0000 28.0000
node     19179 39.0000 32.0000
node     191710 39.0000 36.0000
node     191711 39.0000 40.0000
node     191712 39.0000 44.0000
node     191713 39.0000 48.0000
node     191714 39.0000 52.0000
node     19182 43.0000 4.0000
node     19183 43.0000 8.0000
node     19184 43.0000 12.0000
node     19185 43.0000 16.0000
node     19186 43.0000 20.0000
node     19187 43.0000 24.0000
node     19188 43.0000 28.0000
node     19189 43.0000 32.0000
node     191810 43.0000 36.0000
node     191811 43.0000 40.0000
node     191812 43.0000 44.0000
node     191813 43.0000 48.0000
node     191814 43.0000 52.0000
node     191815 43.0000 56.0000
node     19191 47.0000 0.0000
node     19192 47.0000 4.0000
node     19193 47.0000 8.0000
node     19194 47.0000 12.0000
```

```
node     19195 47.0000 16.0000
node     19196 47.0000 20.0000
node     19197 47.0000 24.0000
node     19198 47.0000 28.0000
node     19199 47.0000 32.0000
node     191910 47.0000 36.0000
node     191911 47.0000 40.0000
node     191912 47.0000 44.0000
node     191913 47.0000 48.0000
node     191914 47.0000 52.0000
node     19202 51.0000 4.0000
node     19203 51.0000 8.0000
node     19204 51.0000 12.0000
node     19205 51.0000 16.0000
node     19206 51.0000 20.0000
node     19207 51.0000 24.0000
node     19208 51.0000 28.0000
node     19209 51.0000 32.0000
node     192010 51.0000 36.0000
node     192011 51.0000 40.0000
node     192012 51.0000 44.0000
node     192013 51.0000 48.0000
node     192014 51.0000 52.0000
node     192015 51.0000 56.0000
node     19211 55.0000 0.0000
node     19212 55.0000 4.0000
node     19213 55.0000 8.0000
node     19214 55.0000 12.0000
node     19215 55.0000 16.0000
node     19216 55.0000 20.0000
node     19217 55.0000 24.0000
node     19218 55.0000 28.0000
node     19219 55.0000 32.0000
node     192110 55.0000 36.0000
node     192111 55.0000 40.0000
node     192112 55.0000 44.0000
node     192113 55.0000 48.0000
node     192114 55.0000 52.0000
node     19222 59.0000 4.0000
node     19223 59.0000 8.0000
node     19224 59.0000 12.0000
node     19225 59.0000 16.0000
node     19226 59.0000 20.0000
node     19227 59.0000 24.0000
node     19228 59.0000 28.0000
node     19229 59.0000 32.0000
node     192210 59.0000 36.0000
node     192211 59.0000 40.0000
node     192212 59.0000 44.0000
node     192213 59.0000 48.0000
node     192214 59.0000 52.0000
node     192215 59.0000 56.0000
node     19231 63.0000 0.0000
node     19232 63.0000 4.0000
node     19233 63.0000 8.0000
```

```
node     19234 63.0000 12.0000
node     19235 63.0000 16.0000
node     19236 63.0000 20.0000
node     19237 63.0000 24.0000
node     19238 63.0000 28.0000
node     19239 63.0000 32.0000
node     192310 63.0000 36.0000
node     192311 63.0000 40.0000
node     192312 63.0000 44.0000
node     192313 63.0000 48.0000
node     192314 63.0000 52.0000
node     19242 67.0000 4.0000
node     19243 67.0000 8.0000
node     19244 67.0000 12.0000
node     19245 67.0000 16.0000
node     19246 67.0000 20.0000
node     19247 67.0000 24.0000
node     19248 67.0000 28.0000
node     19249 67.0000 32.0000
node     192410 67.0000 36.0000
node     192411 67.0000 40.0000
node     192412 67.0000 44.0000
node     192413 67.0000 48.0000
node     192414 67.0000 52.0000
node     192415 67.0000 56.0000
node     19251 71.0000 0.0000
node     19252 71.0000 4.0000
node     19253 71.0000 8.0000
node     19254 71.0000 12.0000
node     19255 71.0000 16.0000
node     19256 71.0000 20.0000
node     19257 71.0000 24.0000
node     19258 71.0000 28.0000
node     19259 71.0000 32.0000
node     192510 71.0000 36.0000
node     192511 71.0000 40.0000
node     192512 71.0000 44.0000
node     192513 71.0000 48.0000
node     192514 71.0000 52.0000
node     19262 75.0000 4.0000
node     19263 75.0000 8.0000
node     19264 75.0000 12.0000
node     19265 75.0000 16.0000
node     19266 75.0000 20.0000
node     19267 75.0000 24.0000
node     19268 75.0000 28.0000
node     19269 75.0000 32.0000
node     192610 75.0000 36.0000
node     192611 75.0000 40.0000
node     192612 75.0000 44.0000
node     192613 75.0000 48.0000
node     192614 75.0000 52.0000
node     192615 75.0000 56.0000
node     19271 79.0000 0.0000
node     19272 79.0000 4.0000
```

```
node      19273 79.0000 8.0000
node      19274 79.0000 12.0000
node      19275 79.0000 16.0000
node      19276 79.0000 20.0000
node      19277 79.0000 24.0000
node      19278 79.0000 28.0000
node      19279 79.0000 32.0000
node      192710 79.0000 36.0000
node      192711 79.0000 40.0000
node      192712 79.0000 44.0000
node      192713 79.0000 48.0000
node      192714 79.0000 52.0000
node      19282 83.0000 4.0000
node      19283 83.0000 8.0000
node      19284 83.0000 12.0000
node      19285 83.0000 16.0000
node      19286 83.0000 20.0000
node      19287 83.0000 24.0000
node      19288 83.0000 28.0000
node      19289 83.0000 32.0000
node      192810 83.0000 36.0000
node      192811 83.0000 40.0000
node      192812 83.0000 44.0000
node      192813 83.0000 48.0000
node      192814 83.0000 52.0000
node      192815 83.0000 56.0000
node      19291 87.0000 0.0000
node      19292 87.0000 4.0000
node      19293 87.0000 8.0000
node      19294 87.0000 12.0000
node      19295 87.0000 16.0000
node      19296 87.0000 20.0000
node      19297 87.0000 24.0000
node      19298 87.0000 28.0000
node      19299 87.0000 32.0000
node      192910 87.0000 36.0000
node      192911 87.0000 40.0000
node      192912 87.0000 44.0000
node      192913 87.0000 48.0000
node      192914 87.0000 52.0000
node      19301 91.0000 0.0000
node      19302 91.0000 4.0000
node      19303 91.0000 8.0000
node      19304 91.0000 12.0000
node      19305 91.0000 16.0000
node      19306 91.0000 20.0000
node      19307 91.0000 24.0000
node      19308 91.0000 28.0000
node      19309 91.0000 32.0000
node      193010 91.0000 36.0000
node      193011 91.0000 40.0000
node      193012 91.0000 44.0000
node      193013 91.0000 48.0000
node      193014 91.0000 52.0000
```

```
#Fixity Zerolength elements


# Frame 1 Tag = 18
fix     1891 0 0 1
fix     1892 0 0 1
fix     1893 0 0 1
fix     1894 0 0 1
fix     1895 0 0 1
fix     1896 0 0 1
fix     1897 0 0 1
fix     1898 0 0 1
fix     1899 0 0 1
fix     18910 0 0 1
fix     18911 0 0 1
fix     18912 0 0 1
fix     18913 0 0 1
fix     18914 0 0 1
fix     18915 0 0 1
fix     18101 0 0 1
fix     18102 0 0 1
fix     18103 0 0 1
fix     18104 0 0 1
fix     18105 0 0 1
fix     18106 0 0 1
fix     18107 0 0 1
fix     18108 0 0 1
fix     18109 0 0 1
fix     181010 0 0 1
fix     181011 0 0 1
fix     181012 0 0 1
fix     181013 0 0 1
fix     181014 0 0 1
fix     181015 0 0 1
fix     18111 0 0 1
fix     18112 0 0 1
fix     18113 0 0 1
fix     18114 0 0 1
fix     18115 0 0 1
fix     18116 0 0 1
fix     18117 0 0 1
fix     18118 0 0 1
fix     18119 0 0 1
fix     181110 0 0 1
fix     181111 0 0 1
fix     181112 0 0 1
fix     181113 0 0 1
fix     181114 0 0 1
fix     181115 0 0 1
fix     18121 0 0 1
fix     18122 0 0 1
fix     18123 0 0 1
fix     18124 0 0 1
fix     18125 0 0 1
```

```
fix 18126 0 0 1
fix 18127 0 0 1
fix 18128 0 0 1
fix 18129 0 0 1
fix 181210 0 0 1
fix 181211 0 0 1
fix 181212 0 0 1
fix 181213 0 0 1
fix 181214 0 0 1
fix 181215 0 0 1
fix 18131 0 0 1
fix 18132 0 0 1
fix 18133 0 0 1
fix 18134 0 0 1
fix 18135 0 0 1
fix 18136 0 0 1
fix 18137 0 0 1
fix 18138 0 0 1
fix 18139 0 0 1
fix 181310 0 0 1
fix 181311 0 0 1
fix 181312 0 0 1
fix 181313 0 0 1
fix 181314 0 0 1
fix 181315 0 0 1
fix 18141 0 0 1
fix 18142 0 0 1
fix 18143 0 0 1
fix 18144 0 0 1
fix 18145 0 0 1
fix 18146 0 0 1
fix 18147 0 0 1
fix 18148 0 0 1
fix 18149 0 0 1
fix 181410 0 0 1
fix 181411 0 0 1
fix 181412 0 0 1
fix 181413 0 0 1
fix 181414 0 0 1
fix 181415 0 0 1
fix 18151 0 0 1
fix 18152 0 0 1
fix 18153 0 0 1
fix 18154 0 0 1
fix 18155 0 0 1
fix 18156 0 0 1
fix 18157 0 0 1
fix 18158 0 0 1
fix 18159 0 0 1
fix 181510 0 0 1
fix 181511 0 0 1
fix 181512 0 0 1
fix 181513 0 0 1
fix 181514 0 0 1
fix 181515 0 0 1
```

```
fix 18161 0 0 1
fix 18162 0 0 1
fix 18163 0 0 1
fix 18164 0 0 1
fix 18165 0 0 1
fix 18166 0 0 1
fix 18167 0 0 1
fix 18168 0 0 1
fix 18169 0 0 1
fix 181610 0 0 1
fix 181611 0 0 1
fix 181612 0 0 1
fix 181613 0 0 1
fix 181614 0 0 1
fix 181615 0 0 1
fix 18171 0 0 1
fix 18172 0 0 1
fix 18173 0 0 1
fix 18174 0 0 1
fix 18175 0 0 1
fix 18176 0 0 1
fix 18177 0 0 1
fix 18178 0 0 1
fix 18179 0 0 1
fix 181710 0 0 1
fix 181711 0 0 1
fix 181712 0 0 1
fix 181713 0 0 1
fix 181714 0 0 1
fix 181715 0 0 1
fix 18181 0 0 1
fix 18182 0 0 1
fix 18183 0 0 1
fix 18184 0 0 1
fix 18185 0 0 1
fix 18186 0 0 1
fix 18187 0 0 1
fix 18188 0 0 1
fix 18189 0 0 1
fix 181810 0 0 1
fix 181811 0 0 1
fix 181812 0 0 1
fix 181813 0 0 1
fix 181814 0 0 1
fix 181815 0 0 1
fix 18191 0 0 1
fix 18192 0 0 1
fix 18193 0 0 1
fix 18194 0 0 1
fix 18195 0 0 1
fix 18196 0 0 1
fix 18197 0 0 1
fix 18198 0 0 1
fix 18199 0 0 1
fix 181910 0 0 1
```

```
fix     181911 0 0 1
fix     181912 0 0 1
fix     181913 0 0 1
fix     181914 0 0 1
fix     181915 0 0 1
fix     18201 0 0 1
fix     18202 0 0 1
fix     18203 0 0 1
fix     18204 0 0 1
fix     18205 0 0 1
fix     18206 0 0 1
fix     18207 0 0 1
fix     18208 0 0 1
fix     18209 0 0 1
fix     182010 0 0 1
fix     182011 0 0 1
fix     182012 0 0 1
fix     182013 0 0 1
fix     182014 0 0 1
fix     182015 0 0 1
fix     18211 0 0 1
fix     18212 0 0 1
fix     18213 0 0 1
fix     18214 0 0 1
fix     18215 0 0 1
fix     18216 0 0 1
fix     18217 0 0 1
fix     18218 0 0 1
fix     18219 0 0 1
fix     182110 0 0 1
fix     182111 0 0 1
fix     182112 0 0 1
fix     182113 0 0 1
fix     182114 0 0 1
fix     182115 0 0 1
fix     18221 0 0 1
fix     18222 0 0 1
fix     18223 0 0 1
fix     18224 0 0 1
fix     18225 0 0 1
fix     18226 0 0 1
fix     18227 0 0 1
fix     18228 0 0 1
fix     18229 0 0 1
fix     182210 0 0 1
fix     182211 0 0 1
fix     182212 0 0 1
fix     182213 0 0 1
fix     182214 0 0 1
fix     182215 0 0 1
fix     18231 0 0 1
fix     18232 0 0 1
fix     18233 0 0 1
fix     18234 0 0 1
fix     18235 0 0 1
```

```
1926 fix 18236 0 0 1
1927 fix 18237 0 0 1
1928 fix 18238 0 0 1
1929 fix 18239 0 0 1
1930 fix 182310 0 0 1
1931 fix 182311 0 0 1
1932 fix 182312 0 0 1
1933 fix 182313 0 0 1
1934 fix 182314 0 0 1
1935 fix 182315 0 0 1
1936 fix 18241 0 0 1
1937 fix 18242 0 0 1
1938 fix 18243 0 0 1
1939 fix 18244 0 0 1
1940 fix 18245 0 0 1
1941 fix 18246 0 0 1
1942 fix 18247 0 0 1
1943 fix 18248 0 0 1
1944 fix 18249 0 0 1
1945 fix 182410 0 0 1
1946 fix 182411 0 0 1
1947 fix 182412 0 0 1
1948 fix 182413 0 0 1
1949 fix 182414 0 0 1
1950 fix 182415 0 0 1
1951 fix 18251 0 0 1
1952 fix 18252 0 0 1
1953 fix 18253 0 0 1
1954 fix 18254 0 0 1
1955 fix 18255 0 0 1
1956 fix 18256 0 0 1
1957 fix 18257 0 0 1
1958 fix 18258 0 0 1
1959 fix 18259 0 0 1
1960 fix 182510 0 0 1
1961 fix 182511 0 0 1
1962 fix 182512 0 0 1
1963 fix 182513 0 0 1
1964 fix 182514 0 0 1
1965 fix 182515 0 0 1
1966 fix 18261 0 0 1
1967 fix 18262 0 0 1
1968 fix 18263 0 0 1
1969 fix 18264 0 0 1
1970 fix 18265 0 0 1
1971 fix 18266 0 0 1
1972 fix 18267 0 0 1
1973 fix 18268 0 0 1
1974 fix 18269 0 0 1
1975 fix 182610 0 0 1
1976 fix 182611 0 0 1
1977 fix 182612 0 0 1
1978 fix 182613 0 0 1
1979 fix 182614 0 0 1
1980 fix 182615 0 0 1
```

```
1981    fix     18271 0 0 1
1982    fix     18272 0 0 1
1983    fix     18273 0 0 1
1984    fix     18274 0 0 1
1985    fix     18275 0 0 1
1986    fix     18276 0 0 1
1987    fix     18277 0 0 1
1988    fix     18278 0 0 1
1989    fix     18279 0 0 1
1990    fix     182710 0 0 1
1991    fix     182711 0 0 1
1992    fix     182712 0 0 1
1993    fix     182713 0 0 1
1994    fix     182714 0 0 1
1995    fix     182715 0 0 1
1996    fix     18281 0 0 1
1997    fix     18282 0 0 1
1998    fix     18283 0 0 1
1999    fix     18284 0 0 1
2000    fix     18285 0 0 1
2001    fix     18286 0 0 1
2002    fix     18287 0 0 1
2003    fix     18288 0 0 1
2004    fix     18289 0 0 1
2005    fix     182810 0 0 1
2006    fix     182811 0 0 1
2007    fix     182812 0 0 1
2008    fix     182813 0 0 1
2009    fix     182814 0 0 1
2010    fix     182815 0 0 1
2011    fix     18291 0 0 1
2012    fix     18292 0 0 1
2013    fix     18293 0 0 1
2014    fix     18294 0 0 1
2015    fix     18295 0 0 1
2016    fix     18296 0 0 1
2017    fix     18297 0 0 1
2018    fix     18298 0 0 1
2019    fix     18299 0 0 1
2020    fix     182910 0 0 1
2021    fix     182911 0 0 1
2022    fix     182912 0 0 1
2023    fix     182913 0 0 1
2024    fix     182914 0 0 1
2025    fix     182915 0 0 1
2026    fix     18302 0 0 1
2027    fix     18303 0 0 1
2028    fix     18304 0 0 1
2029    fix     18305 0 0 1
2030    fix     18306 0 0 1
2031    fix     18307 0 0 1
2032    fix     18308 0 0 1
2033    fix     18309 0 0 1
2034    fix     183010 0 0 1
2035    fix     183011 0 0 1
```

```
fix 183012 0 0 1
fix 183013 0 0 1
fix 183014 0 0 1
fix 183015 0 0 1


# Frame 1 Tag = 19
fix 1992 0 0 1
fix 1993 0 0 1
fix 1994 0 0 1
fix 1995 0 0 1
fix 1996 0 0 1
fix 1997 0 0 1
fix 1998 0 0 1
fix 1999 0 0 1
fix 19910 0 0 1
fix 19911 0 0 1
fix 19912 0 0 1
fix 19913 0 0 1
fix 19914 0 0 1
fix 19102 0 0 1
fix 19103 0 0 1
fix 19104 0 0 1
fix 19105 0 0 1
fix 19106 0 0 1
fix 19107 0 0 1
fix 19108 0 0 1
fix 19109 0 0 1
fix 191010 0 0 1
fix 191011 0 0 1
fix 191012 0 0 1
fix 191013 0 0 1
fix 191014 0 0 1
fix 191015 0 0 1
fix 19111 0 0 1
fix 19112 0 0 1
fix 19113 0 0 1
fix 19114 0 0 1
fix 19115 0 0 1
fix 19116 0 0 1
fix 19117 0 0 1
fix 19118 0 0 1
fix 19119 0 0 1
fix 191110 0 0 1
fix 191111 0 0 1
fix 191112 0 0 1
fix 191113 0 0 1
fix 191114 0 0 1
fix 19122 0 0 1
fix 19123 0 0 1
fix 19124 0 0 1
fix 19125 0 0 1
fix 19126 0 0 1
fix 19127 0 0 1
fix 19128 0 0 1
```

```
2091  fix     19129 0 0 1
2092  fix     191210 0 0 1
2093  fix     191211 0 0 1
2094  fix     191212 0 0 1
2095  fix     191213 0 0 1
2096  fix     191214 0 0 1
2097  fix     191215 0 0 1
2098  fix     19131 0 0 1
2099  fix     19132 0 0 1
2100  fix     19133 0 0 1
2101  fix     19134 0 0 1
2102  fix     19135 0 0 1
2103  fix     19136 0 0 1
2104  fix     19137 0 0 1
2105  fix     19138 0 0 1
2106  fix     19139 0 0 1
2107  fix     191310 0 0 1
2108  fix     191311 0 0 1
2109  fix     191312 0 0 1
2110  fix     191313 0 0 1
2111  fix     191314 0 0 1
2112  fix     19142 0 0 1
2113  fix     19143 0 0 1
2114  fix     19144 0 0 1
2115  fix     19145 0 0 1
2116  fix     19146 0 0 1
2117  fix     19147 0 0 1
2118  fix     19148 0 0 1
2119  fix     19149 0 0 1
2120  fix     191410 0 0 1
2121  fix     191411 0 0 1
2122  fix     191412 0 0 1
2123  fix     191413 0 0 1
2124  fix     191414 0 0 1
2125  fix     191415 0 0 1
2126  fix     19151 0 0 1
2127  fix     19152 0 0 1
2128  fix     19153 0 0 1
2129  fix     19154 0 0 1
2130  fix     19155 0 0 1
2131  fix     19156 0 0 1
2132  fix     19157 0 0 1
2133  fix     19158 0 0 1
2134  fix     19159 0 0 1
2135  fix     191510 0 0 1
2136  fix     191511 0 0 1
2137  fix     191512 0 0 1
2138  fix     191513 0 0 1
2139  fix     191514 0 0 1
2140  fix     19162 0 0 1
2141  fix     19163 0 0 1
2142  fix     19164 0 0 1
2143  fix     19165 0 0 1
2144  fix     19166 0 0 1
2145  fix     19167 0 0 1
```

```
fix 19168 0 0 1
fix 19169 0 0 1
fix 191610 0 0 1
fix 191611 0 0 1
fix 191612 0 0 1
fix 191613 0 0 1
fix 191614 0 0 1
fix 191615 0 0 1
fix 19171 0 0 1
fix 19172 0 0 1
fix 19173 0 0 1
fix 19174 0 0 1
fix 19175 0 0 1
fix 19176 0 0 1
fix 19177 0 0 1
fix 19178 0 0 1
fix 19179 0 0 1
fix 191710 0 0 1
fix 191711 0 0 1
fix 191712 0 0 1
fix 191713 0 0 1
fix 191714 0 0 1
fix 19182 0 0 1
fix 19183 0 0 1
fix 19184 0 0 1
fix 19185 0 0 1
fix 19186 0 0 1
fix 19187 0 0 1
fix 19188 0 0 1
fix 19189 0 0 1
fix 191810 0 0 1
fix 191811 0 0 1
fix 191812 0 0 1
fix 191813 0 0 1
fix 191814 0 0 1
fix 191815 0 0 1
fix 19191 0 0 1
fix 19192 0 0 1
fix 19193 0 0 1
fix 19194 0 0 1
fix 19195 0 0 1
fix 19196 0 0 1
fix 19197 0 0 1
fix 19198 0 0 1
fix 19199 0 0 1
fix 191910 0 0 1
fix 191911 0 0 1
fix 191912 0 0 1
fix 191913 0 0 1
fix 191914 0 0 1
fix 19202 0 0 1
fix 19203 0 0 1
fix 19204 0 0 1
fix 19205 0 0 1
fix 19206 0 0 1
```

```
2201  fix     19207 0 0 1
2202  fix     19208 0 0 1
2203  fix     19209 0 0 1
2204  fix     192010 0 0 1
2205  fix     192011 0 0 1
2206  fix     192012 0 0 1
2207  fix     192013 0 0 1
2208  fix     192014 0 0 1
2209  fix     192015 0 0 1
2210  fix     19211 0 0 1
2211  fix     19212 0 0 1
2212  fix     19213 0 0 1
2213  fix     19214 0 0 1
2214  fix     19215 0 0 1
2215  fix     19216 0 0 1
2216  fix     19217 0 0 1
2217  fix     19218 0 0 1
2218  fix     19219 0 0 1
2219  fix     192110 0 0 1
2220  fix     192111 0 0 1
2221  fix     192112 0 0 1
2222  fix     192113 0 0 1
2223  fix     192114 0 0 1
2224  fix     19222 0 0 1
2225  fix     19223 0 0 1
2226  fix     19224 0 0 1
2227  fix     19225 0 0 1
2228  fix     19226 0 0 1
2229  fix     19227 0 0 1
2230  fix     19228 0 0 1
2231  fix     19229 0 0 1
2232  fix     192210 0 0 1
2233  fix     192211 0 0 1
2234  fix     192212 0 0 1
2235  fix     192213 0 0 1
2236  fix     192214 0 0 1
2237  fix     192215 0 0 1
2238  fix     19231 0 0 1
2239  fix     19232 0 0 1
2240  fix     19233 0 0 1
2241  fix     19234 0 0 1
2242  fix     19235 0 0 1
2243  fix     19236 0 0 1
2244  fix     19237 0 0 1
2245  fix     19238 0 0 1
2246  fix     19239 0 0 1
2247  fix     192310 0 0 1
2248  fix     192311 0 0 1
2249  fix     192312 0 0 1
2250  fix     192313 0 0 1
2251  fix     192314 0 0 1
2252  fix     19242 0 0 1
2253  fix     19243 0 0 1
2254  fix     19244 0 0 1
2255  fix     19245 0 0 1
```

```
fix 19246 0 0 1
fix 19247 0 0 1
fix 19248 0 0 1
fix 19249 0 0 1
fix 192410 0 0 1
fix 192411 0 0 1
fix 192412 0 0 1
fix 192413 0 0 1
fix 192414 0 0 1
fix 192415 0 0 1
fix 19251 0 0 1
fix 19252 0 0 1
fix 19253 0 0 1
fix 19254 0 0 1
fix 19255 0 0 1
fix 19256 0 0 1
fix 19257 0 0 1
fix 19258 0 0 1
fix 19259 0 0 1
fix 192510 0 0 1
fix 192511 0 0 1
fix 192512 0 0 1
fix 192513 0 0 1
fix 192514 0 0 1
fix 19262 0 0 1
fix 19263 0 0 1
fix 19264 0 0 1
fix 19265 0 0 1
fix 19266 0 0 1
fix 19267 0 0 1
fix 19268 0 0 1
fix 19269 0 0 1
fix 192610 0 0 1
fix 192611 0 0 1
fix 192612 0 0 1
fix 192613 0 0 1
fix 192614 0 0 1
fix 192615 0 0 1
fix 19271 0 0 1
fix 19272 0 0 1
fix 19273 0 0 1
fix 19274 0 0 1
fix 19275 0 0 1
fix 19276 0 0 1
fix 19277 0 0 1
fix 19278 0 0 1
fix 19279 0 0 1
fix 192710 0 0 1
fix 192711 0 0 1
fix 192712 0 0 1
fix 192713 0 0 1
fix 192714 0 0 1
fix 19282 0 0 1
fix 19283 0 0 1
fix 19284 0 0 1
```

```
fix 19285 0 0 1
fix 19286 0 0 1
fix 19287 0 0 1
fix 19288 0 0 1
fix 19289 0 0 1
fix 192810 0 0 1
fix 192811 0 0 1
fix 192812 0 0 1
fix 192813 0 0 1
fix 192814 0 0 1
fix 192815 0 0 1
fix 19291 0 0 1
fix 19292 0 0 1
fix 19293 0 0 1
fix 19294 0 0 1
fix 19295 0 0 1
fix 19296 0 0 1
fix 19297 0 0 1
fix 19298 0 0 1
fix 19299 0 0 1
fix 192910 0 0 1
fix 192911 0 0 1
fix 192912 0 0 1
fix 192913 0 0 1
fix 192914 0 0 1
fix 19301 0 0 1
fix 19302 0 0 1
fix 19303 0 0 1
fix 19304 0 0 1
fix 19305 0 0 1
fix 19306 0 0 1
fix 19307 0 0 1
fix 19308 0 0 1
fix 19309 0 0 1
fix 193010 0 0 1
fix 193011 0 0 1
fix 193012 0 0 1
fix 193013 0 0 1
fix 193014 0 0 1


equalDOF 716 717 1 ;

equalDOF 716 715 1 ;
# Elements Definitions RCMF


#Vertical concrete col 1 Frame 1


element truss 1 71 72 12.25000 2
element truss 2 72 73 12.25000 2
element truss 3 73 74 12.25000 2
element truss 4 74 75 12.25000 2
element truss 5 75 76 12.25000 2
```

```
element truss      6 76 77 12.25000 2
element truss      7 77 78 12.25000 2
element truss      8 78 79 12.25000 2
element truss      9 79 710 12.25000 2
element truss      10 710 711 12.25000 2
element truss      11 711 712 12.25000 2
element truss      12 712 713 12.25000 2
element truss      13 713 714 12.25000 2
element truss      14 714 715 12.25000 2
element truss      15 715 716 12.25000 2
element truss      16 716 717 12.25000 2
element truss      17 81 82 24.50000 2
element truss      18 82 83 24.50000 2
element truss      19 83 84 24.50000 2
element truss      20 84 85 24.50000 2
element truss      21 85 86 24.50000 2
element truss      22 86 87 24.50000 2
element truss      23 87 88 24.50000 2
element truss      24 88 89 24.50000 2
element truss      25 89 810 24.50000 2
element truss      26 810 811 24.50000 2
element truss      27 811 812 24.50000 2
element truss      28 812 813 24.50000 2
element truss      29 813 814 24.50000 2
element truss      30 814 815 24.50000 2
element truss      31 815 816 24.50000 2
element truss      32 816 817 24.50000 2
element truss      33 91 92 12.25000 2
element truss      34 92 93 12.25000 2
element truss      35 93 94 12.25000 2
element truss      36 94 95 12.25000 2
element truss      37 95 96 12.25000 2
element truss      38 96 97 12.25000 2
element truss      39 97 98 12.25000 2
element truss      40 98 99 12.25000 2
element truss      41 99 910 12.25000 2
element truss      42 910 911 12.25000 2
element truss      43 911 912 12.25000 2
element truss      44 912 913 12.25000 2
element truss      45 913 914 12.25000 2
element truss      46 914 915 12.25000 2
element truss      47 915 916 12.25000 2
element truss      48 916 917 12.25000 2


#Vertical concrete col 2 Frame 1


element truss      49 301 302 12.25000 2
element truss      50 302 303 12.25000 2
element truss      51 303 304 12.25000 2
element truss      52 304 305 12.25000 2
element truss      53 305 306 12.25000 2
element truss      54 306 307 12.25000 2
element truss      55 307 308 12.25000 2
```

```
element truss      56 308 309 12.25000 2
element truss      57 309 3010 12.25000 2
element truss      58 3010 3011 12.25000 2
element truss      59 3011 3012 12.25000 2
element truss      60 3012 3013 12.25000 2
element truss      61 3013 3014 12.25000 2
element truss      62 3014 3015 12.25000 2
element truss      63 3015 3016 12.25000 2
element truss      64 3016 3017 12.25000 2
element truss      65 311 312 24.50000 2
element truss      66 312 313 24.50000 2
element truss      67 313 314 24.50000 2
element truss      68 314 315 24.50000 2
element truss      69 315 316 24.50000 2
element truss      70 316 317 24.50000 2
element truss      71 317 318 24.50000 2
element truss      72 318 319 24.50000 2
element truss      73 319 3110 24.50000 2
element truss      74 3110 3111 24.50000 2
element truss      75 3111 3112 24.50000 2
element truss      76 3112 3113 24.50000 2
element truss      77 3113 3114 24.50000 2
element truss      78 3114 3115 24.50000 2
element truss      79 3115 3116 24.50000 2
element truss      80 3116 3117 24.50000 2
element truss      81 321 322 12.25000 2
element truss      82 322 323 12.25000 2
element truss      83 323 324 12.25000 2
element truss      84 324 325 12.25000 2
element truss      85 325 326 12.25000 2
element truss      86 326 327 12.25000 2
element truss      87 327 328 12.25000 2
element truss      88 328 329 12.25000 2
element truss      89 329 3210 12.25000 2
element truss      90 3210 3211 12.25000 2
element truss      91 3211 3212 12.25000 2
element truss      92 3212 3213 12.25000 2
element truss      93 3213 3214 12.25000 2
element truss      94 3214 3215 12.25000 2
element truss      95 3215 3216 12.25000 2
element truss      96 3216 3217 12.25000 2


#Vertical concrete beam Frame 1


element truss      97 915 916 14.00000 5
element truss      98 916 917 14.00000 5
element truss      99 1015 1016 28.00000 5
element truss      100 1016 1017 28.00000 5
element truss      101 1115 1116 28.00000 5
element truss      102 1116 1117 28.00000 5
element truss      103 1215 1216 28.00000 5
element truss      104 1216 1217 28.00000 5
element truss      105 1315 1316 28.00000 5
```

```
element truss      106 1316 1317 28.00000 5
element truss      107 1415 1416 28.00000 5
element truss      108 1416 1417 28.00000 5
element truss      109 1515 1516 28.00000 5
element truss      110 1516 1517 28.00000 5
element truss      111 1615 1616 28.00000 5
element truss      112 1616 1617 28.00000 5
element truss      113 1715 1716 28.00000 5
element truss      114 1716 1717 28.00000 5
element truss      115 1815 1816 28.00000 5
element truss      116 1816 1817 28.00000 5
element truss      117 1915 1916 28.00000 5
element truss      118 1916 1917 28.00000 5
element truss      119 2015 2016 28.00000 5
element truss      120 2016 2017 28.00000 5
element truss      121 2115 2116 28.00000 5
element truss      122 2116 2117 28.00000 5
element truss      123 2215 2216 28.00000 5
element truss      124 2216 2217 28.00000 5
element truss      125 2315 2316 28.00000 5
element truss      126 2316 2317 28.00000 5
element truss      127 2415 2416 28.00000 5
element truss      128 2416 2417 28.00000 5
element truss      129 2515 2516 28.00000 5
element truss      130 2516 2517 28.00000 5
element truss      131 2615 2616 28.00000 5
element truss      132 2616 2617 28.00000 5
element truss      133 2715 2716 28.00000 5
element truss      134 2716 2717 28.00000 5
element truss      135 2815 2816 28.00000 5
element truss      136 2816 2817 28.00000 5
element truss      137 2915 2916 28.00000 5
element truss      138 2916 2917 28.00000 5
element truss      139 3015 3016 14.00000 5
element truss      140 3016 3017 14.00000 5


#Vertical steel col 1 Frame 1


element truss      141 71 72 0.60000 1
element truss      142 72 73 0.60000 1
element truss      143 73 74 0.60000 1
element truss      144 74 75 0.60000 1
element truss      145 75 76 0.60000 1
element truss      146 76 77 0.60000 1
element truss      147 77 78 0.60000 1
element truss      148 78 79 0.60000 1
element truss      149 79 710 0.60000 1
element truss      150 710 711 0.60000 1
element truss      151 711 712 0.60000 1
element truss      152 712 713 0.60000 1
element truss      153 713 714 0.60000 1
element truss      154 714 715 0.60000 1
element truss      155 715 716 0.60000 1
```

```
element truss      156 716 717 0.60000 1
element truss      157 81 82 0.40000 1
element truss      158 82 83 0.40000 1
element truss      159 83 84 0.40000 1
element truss      160 84 85 0.40000 1
element truss      161 85 86 0.40000 1
element truss      162 86 87 0.40000 1
element truss      163 87 88 0.40000 1
element truss      164 88 89 0.40000 1
element truss      165 89 810 0.40000 1
element truss      166 810 811 0.40000 1
element truss      167 811 812 0.40000 1
element truss      168 812 813 0.40000 1
element truss      169 813 814 0.40000 1
element truss      170 814 815 0.40000 1
element truss      171 815 816 0.40000 1
element truss      172 816 817 0.40000 1
element truss      173 91 92 0.60000 1
element truss      174 92 93 0.60000 1
element truss      175 93 94 0.60000 1
element truss      176 94 95 0.60000 1
element truss      177 95 96 0.60000 1
element truss      178 96 97 0.60000 1
element truss      179 97 98 0.60000 1
element truss      180 98 99 0.60000 1
element truss      181 99 910 0.60000 1
element truss      182 910 911 0.60000 1
element truss      183 911 912 0.60000 1
element truss      184 912 913 0.60000 1
element truss      185 913 914 0.60000 1
element truss      186 914 915 0.60000 1
element truss      187 915 916 0.60000 1
element truss      188 916 917 0.60000 1


#Vertical steel col 2 Frame 1


element truss      189 301 302 0.60000 1
element truss      190 302 303 0.60000 1
element truss      191 303 304 0.60000 1
element truss      192 304 305 0.60000 1
element truss      193 305 306 0.60000 1
element truss      194 306 307 0.60000 1
element truss      195 307 308 0.60000 1
element truss      196 308 309 0.60000 1
element truss      197 309 3010 0.60000 1
element truss      198 3010 3011 0.60000 1
element truss      199 3011 3012 0.60000 1
element truss      200 3012 3013 0.60000 1
element truss      201 3013 3014 0.60000 1
element truss      202 3014 3015 0.60000 1
element truss      203 3015 3016 0.60000 1
element truss      204 3016 3017 0.60000 1
element truss      205 311 312 0.40000 1
```

```
element truss     206 312 313 0.40000 1
element truss     207 313 314 0.40000 1
element truss     208 314 315 0.40000 1
element truss     209 315 316 0.40000 1
element truss     210 316 317 0.40000 1
element truss     211 317 318 0.40000 1
element truss     212 318 319 0.40000 1
element truss     213 319 3110 0.40000 1
element truss     214 3110 3111 0.40000 1
element truss     215 3111 3112 0.40000 1
element truss     216 3112 3113 0.40000 1
element truss     217 3113 3114 0.40000 1
element truss     218 3114 3115 0.40000 1
element truss     219 3115 3116 0.40000 1
element truss     220 3116 3117 0.40000 1
element truss     221 321 322 0.60000 1
element truss     222 322 323 0.60000 1
element truss     223 323 324 0.60000 1
element truss     224 324 325 0.60000 1
element truss     225 325 326 0.60000 1
element truss     226 326 327 0.60000 1
element truss     227 327 328 0.60000 1
element truss     228 328 329 0.60000 1
element truss     229 329 3210 0.60000 1
element truss     230 3210 3211 0.60000 1
element truss     231 3211 3212 0.60000 1
element truss     232 3212 3213 0.60000 1
element truss     233 3213 3214 0.60000 1
element truss     234 3214 3215 0.60000 1
element truss     235 3215 3216 0.60000 1
element truss     236 3216 3217 0.60000 1


#Vertical steel beam Frame 1


element truss     237 915 916 0.06667 6
element truss     238 916 917 0.06667 6
element truss     239 1015 1016 0.13333 6
element truss     240 1016 1017 0.13333 6
element truss     241 1115 1116 0.13333 6
element truss     242 1116 1117 0.13333 6
element truss     243 1215 1216 0.13333 6
element truss     244 1216 1217 0.13333 6
element truss     245 1315 1316 0.13333 6
element truss     246 1316 1317 0.13333 6
element truss     247 1415 1416 0.13333 6
element truss     248 1416 1417 0.13333 6
element truss     249 1515 1516 0.13333 6
element truss     250 1516 1517 0.13333 6
element truss     251 1615 1616 0.13333 6
element truss     252 1616 1617 0.13333 6
element truss     253 1715 1716 0.13333 6
element truss     254 1716 1717 0.13333 6
element truss     255 1815 1816 0.13333 6
```

```
element truss      256 1816 1817 0.13333 6
element truss      257 1915 1916 0.13333 6
element truss      258 1916 1917 0.13333 6
element truss      259 2015 2016 0.13333 6
element truss      260 2016 2017 0.13333 6
element truss      261 2115 2116 0.13333 6
element truss      262 2116 2117 0.13333 6
element truss      263 2215 2216 0.13333 6
element truss      264 2216 2217 0.13333 6
element truss      265 2315 2316 0.13333 6
element truss      266 2316 2317 0.13333 6
element truss      267 2415 2416 0.13333 6
element truss      268 2416 2417 0.13333 6
element truss      269 2515 2516 0.13333 6
element truss      270 2516 2517 0.13333 6
element truss      271 2615 2616 0.13333 6
element truss      272 2616 2617 0.13333 6
element truss      273 2715 2716 0.13333 6
element truss      274 2716 2717 0.13333 6
element truss      275 2815 2816 0.13333 6
element truss      276 2816 2817 0.13333 6
element truss      277 2915 2916 0.13333 6
element truss      278 2916 2917 0.13333 6
element truss      279 3015 3016 0.06667 6
element truss      280 3016 3017 0.06667 6


#horizontal concrete Frame 1




#Horizontal concrete col 1 Frame 1


#element truss     281 71 81 28.00000 3
element truss      282 72 82 28.00000 3
element truss      283 73 83 28.00000 3
element truss      284 74 84 28.00000 3
element truss      285 75 85 28.00000 3
element truss      286 76 86 28.00000 3
element truss      287 77 87 28.00000 3
element truss      288 78 88 28.00000 3
element truss      289 79 89 28.00000 3
element truss      290 710 810 28.00000 3
element truss      291 711 811 28.00000 3
element truss      292 712 812 28.00000 3
element truss      293 713 813 28.00000 3
element truss      294 714 814 28.00000 3
element truss      295 715 815 28.00000 3
element truss      296 716 816 28.00000 3
element truss      297 717 817 28.00000 3
#element truss     298 81 91 28.00000 3
element truss      299 82 92 28.00000 3
element truss      300 83 93 28.00000 3
```

```
element truss      301 84 94 28.00000 3
element truss      302 85 95 28.00000 3
element truss      303 86 96 28.00000 3
element truss      304 87 97 28.00000 3
element truss      305 88 98 28.00000 3
element truss      306 89 99 28.00000 3
element truss      307 810 910 28.00000 3
element truss      308 811 911 28.00000 3
element truss      309 812 912 28.00000 3
element truss      310 813 913 28.00000 3
element truss      311 814 914 28.00000 3
element truss      312 815 915 28.00000 3
element truss      313 816 916 28.00000 3
element truss      314 817 917 28.00000 3


#Horizontal concrete col 2 Frame 1


#element truss     315 301 311 28.00000 3
element truss      316 302 312 28.00000 3
element truss      317 303 313 28.00000 3
element truss      318 304 314 28.00000 3
element truss      319 305 315 28.00000 3
element truss      320 306 316 28.00000 3
element truss      321 307 317 28.00000 3
element truss      322 308 318 28.00000 3
element truss      323 309 319 28.00000 3
element truss      324 3010 3110 28.00000 3
element truss      325 3011 3111 28.00000 3
element truss      326 3012 3112 28.00000 3
element truss      327 3013 3113 28.00000 3
element truss      328 3014 3114 28.00000 3
element truss      329 3015 3115 28.00000 3
element truss      330 3016 3116 28.00000 3
element truss      331 3017 3117 28.00000 3
#element truss     332 311 321 28.00000 3
element truss      333 312 322 28.00000 3
element truss      334 313 323 28.00000 3
element truss      335 314 324 28.00000 3
element truss      336 315 325 28.00000 3
element truss      337 316 326 28.00000 3
element truss      338 317 327 28.00000 3
element truss      339 318 328 28.00000 3
element truss      340 319 329 28.00000 3
element truss      341 3110 3210 28.00000 3
element truss      342 3111 3211 28.00000 3
element truss      343 3112 3212 28.00000 3
element truss      344 3113 3213 28.00000 3
element truss      345 3114 3214 28.00000 3
element truss      346 3115 3215 28.00000 3
element truss      347 3116 3216 28.00000 3
element truss      348 3117 3217 28.00000 3
```

```
#Horizontal concrete beam Frame 1


element truss      349 915 1015 21.00000 5
element truss      350 916 1016 21.00000 5
element truss      351 917 1017 21.00000 5
element truss      352 1015 1115 21.00000 5
element truss      353 1016 1116 21.00000 5
element truss      354 1017 1117 21.00000 5
element truss      355 1115 1215 21.00000 5
element truss      356 1116 1216 21.00000 5
element truss      357 1117 1217 21.00000 5
element truss      358 1215 1315 21.00000 5
element truss      359 1216 1316 21.00000 5
element truss      360 1217 1317 21.00000 5
element truss      361 1315 1415 21.00000 5
element truss      362 1316 1416 21.00000 5
element truss      363 1317 1417 21.00000 5
element truss      364 1415 1515 21.00000 5
element truss      365 1416 1516 21.00000 5
element truss      366 1417 1517 21.00000 5
element truss      367 1515 1615 21.00000 5
element truss      368 1516 1616 21.00000 5
element truss      369 1517 1617 21.00000 5
element truss      370 1615 1715 21.00000 5
element truss      371 1616 1716 21.00000 5
element truss      372 1617 1717 21.00000 5
element truss      373 1715 1815 21.00000 5
element truss      374 1716 1816 21.00000 5
element truss      375 1717 1817 21.00000 5
element truss      376 1815 1915 21.00000 5
element truss      377 1816 1916 21.00000 5
element truss      378 1817 1917 21.00000 5
element truss      379 1915 2015 21.00000 5
element truss      380 1916 2016 21.00000 5
element truss      381 1917 2017 21.00000 5
element truss      382 2015 2115 21.00000 5
element truss      383 2016 2116 21.00000 5
element truss      384 2017 2117 21.00000 5
element truss      385 2115 2215 21.00000 5
element truss      386 2116 2216 21.00000 5
element truss      387 2117 2217 21.00000 5
element truss      388 2215 2315 21.00000 5
element truss      389 2216 2316 21.00000 5
element truss      390 2217 2317 21.00000 5
element truss      391 2315 2415 21.00000 5
element truss      392 2316 2416 21.00000 5
element truss      393 2317 2417 21.00000 5
element truss      394 2415 2515 21.00000 5
element truss      395 2416 2516 21.00000 5
element truss      396 2417 2517 21.00000 5
element truss      397 2515 2615 21.00000 5
element truss      398 2516 2616 21.00000 5
element truss      399 2517 2617 21.00000 5
element truss      400 2615 2715 21.00000 5
```

```
element truss      401 2616 2716 21.00000 5
element truss      402 2617 2717 21.00000 5
element truss      403 2715 2815 21.00000 5
element truss      404 2716 2816 21.00000 5
element truss      405 2717 2817 21.00000 5
element truss      406 2815 2915 21.00000 5
element truss      407 2816 2916 21.00000 5
element truss      408 2817 2917 21.00000 5
element truss      409 2915 3015 21.00000 5
element truss      410 2916 3016 21.00000 5
element truss      411 2917 3017 21.00000 5


#horizontal steel col 1 Frame 1


#element truss     412 71 81 0.16000 6
element truss      413 72 82 0.16000 6
element truss      414 73 83 0.16000 6
element truss      415 74 84 0.16000 6
element truss      416 75 85 0.16000 6
element truss      417 76 86 0.16000 6
element truss      418 77 87 0.16000 6
element truss      419 78 88 0.16000 6
element truss      420 79 89 0.16000 6
element truss      421 710 810 0.16000 6
element truss      422 711 811 0.16000 6
element truss      423 712 812 0.16000 6
element truss      424 713 813 0.16000 6
element truss      425 714 814 0.16000 6
element truss      426 715 815 0.16000 6
element truss      427 716 816 0.16000 6
element truss      428 717 817 0.16000 6
#element truss     429 81 91 0.16000 6
element truss      430 82 92 0.16000 6
element truss      431 83 93 0.16000 6
element truss      432 84 94 0.16000 6
element truss      433 85 95 0.16000 6
element truss      434 86 96 0.16000 6
element truss      435 87 97 0.16000 6
element truss      436 88 98 0.16000 6
element truss      437 89 99 0.16000 6
element truss      438 810 910 0.16000 6
element truss      439 811 911 0.16000 6
element truss      440 812 912 0.16000 6
element truss      441 813 913 0.16000 6
element truss      442 814 914 0.16000 6
element truss      443 815 915 0.16000 6
element truss      444 816 916 0.16000 6
element truss      445 817 917 0.16000 6


#horizontal steel col 2 Frame 1


```

```
#element truss      446 301 311 0.16000 6
element truss       447 302 312 0.16000 6
element truss       448 303 313 0.16000 6
element truss       449 304 314 0.16000 6
element truss       450 305 315 0.16000 6
element truss       451 306 316 0.16000 6
element truss       452 307 317 0.16000 6
element truss       453 308 318 0.16000 6
element truss       454 309 319 0.16000 6
element truss       455 3010 3110 0.16000 6
element truss       456 3011 3111 0.16000 6
element truss       457 3012 3112 0.16000 6
element truss       458 3013 3113 0.16000 6
element truss       459 3014 3114 0.16000 6
element truss       460 3015 3115 0.16000 6
element truss       461 3016 3116 0.16000 6
element truss       462 3017 3117 0.16000 6
#element truss      463 311 321 0.16000 6
element truss       464 312 322 0.16000 6
element truss       465 313 323 0.16000 6
element truss       466 314 324 0.16000 6
element truss       467 315 325 0.16000 6
element truss       468 316 326 0.16000 6
element truss       469 317 327 0.16000 6
element truss       470 318 328 0.16000 6
element truss       471 319 329 0.16000 6
element truss       472 3110 3210 0.16000 6
element truss       473 3111 3211 0.16000 6
element truss       474 3112 3212 0.16000 6
element truss       475 3113 3213 0.16000 6
element truss       476 3114 3214 0.16000 6
element truss       477 3115 3215 0.16000 6
element truss       478 3116 3216 0.16000 6
element truss       479 3117 3217 0.16000 6


#horizontal steel beam Frame 1


element truss       480 915 1015 0.41333 1
element truss       481 916 1016 0.41333 1
element truss       482 917 1017 0.41333 1
element truss       483 1015 1115 0.41333 1
element truss       484 1016 1116 0.41333 1
element truss       485 1017 1117 0.41333 1
element truss       486 1115 1215 0.41333 1
element truss       487 1116 1216 0.41333 1
element truss       488 1117 1217 0.41333 1
element truss       489 1215 1315 0.41333 1
element truss       490 1216 1316 0.41333 1
element truss       491 1217 1317 0.41333 1
element truss       492 1315 1415 0.41333 1
element truss       493 1316 1416 0.41333 1
element truss       494 1317 1417 0.41333 1
element truss       495 1415 1515 0.41333 1
```

```
element truss      496 1416 1516 0.41333 1
element truss      497 1417 1517 0.41333 1
element truss      498 1515 1615 0.41333 1
element truss      499 1516 1616 0.41333 1
element truss      500 1517 1617 0.41333 1
element truss      501 1615 1715 0.41333 1
element truss      502 1616 1716 0.41333 1
element truss      503 1617 1717 0.41333 1
element truss      504 1715 1815 0.41333 1
element truss      505 1716 1816 0.41333 1
element truss      506 1717 1817 0.41333 1
element truss      507 1815 1915 0.41333 1
element truss      508 1816 1916 0.41333 1
element truss      509 1817 1917 0.41333 1
element truss      510 1915 2015 0.41333 1
element truss      511 1916 2016 0.41333 1
element truss      512 1917 2017 0.41333 1
element truss      513 2015 2115 0.41333 1
element truss      514 2016 2116 0.41333 1
element truss      515 2017 2117 0.41333 1
element truss      516 2115 2215 0.41333 1
element truss      517 2116 2216 0.41333 1
element truss      518 2117 2217 0.41333 1
element truss      519 2215 2315 0.41333 1
element truss      520 2216 2316 0.41333 1
element truss      521 2217 2317 0.41333 1
element truss      522 2315 2415 0.41333 1
element truss      523 2316 2416 0.41333 1
element truss      524 2317 2417 0.41333 1
element truss      525 2415 2515 0.41333 1
element truss      526 2416 2516 0.41333 1
element truss      527 2417 2517 0.41333 1
element truss      528 2515 2615 0.41333 1
element truss      529 2516 2616 0.41333 1
element truss      530 2517 2617 0.41333 1
element truss      531 2615 2715 0.41333 1
element truss      532 2616 2716 0.41333 1
element truss      533 2617 2717 0.41333 1
element truss      534 2715 2815 0.41333 1
element truss      535 2716 2816 0.41333 1
element truss      536 2717 2817 0.41333 1
element truss      537 2815 2915 0.41333 1
element truss      538 2816 2916 0.41333 1
element truss      539 2817 2917 0.41333 1
element truss      540 2915 3015 0.41333 1
element truss      541 2916 3016 0.41333 1
element truss      542 2917 3017 0.41333 1


#diagonal concrete col 1 Frame 1


element Truss2     543 71 82 81 72 18.43813 4
element Truss2     544 81 72 71 82 18.43813 4
element Truss2     545 72 83 82 73 18.43813 4
```

```
element Truss2  546 82 73 72 83 18.43813 4
element Truss2  547 73 84 83 74 18.43813 4
element Truss2  548 83 74 73 84 18.43813 4
element Truss2  549 74 85 84 75 18.43813 4
element Truss2  550 84 75 74 85 18.43813 4
element Truss2  551 75 86 85 76 18.43813 4
element Truss2  552 85 76 75 86 18.43813 4
element Truss2  553 76 87 86 77 18.43813 4
element Truss2  554 86 77 76 87 18.43813 4
element Truss2  555 77 88 87 78 18.43813 4
element Truss2  556 87 78 77 88 18.43813 4
element Truss2  557 78 89 88 79 18.43813 4
element Truss2  558 88 79 78 89 18.43813 4
element Truss2  559 79 810 89 710 18.43813 4
element Truss2  560 89 710 79 810 18.43813 4
element Truss2  561 710 811 810 711 18.43813 4
element Truss2  562 810 711 710 811 18.43813 4
element Truss2  563 711 812 811 712 18.43813 4
element Truss2  564 811 712 711 812 18.43813 4
element Truss2  565 712 813 812 713 18.43813 4
element Truss2  566 812 713 712 813 18.43813 4
element Truss2  567 713 814 813 714 18.43813 4
element Truss2  568 813 714 713 814 18.43813 4
element Truss2  569 714 815 814 715 18.43813 4
element Truss2  570 814 715 714 815 18.43813 4
element Truss2  571 715 816 815 716 18.43813 4
element Truss2  572 815 716 715 816 18.43813 4
element Truss2  573 716 817 816 717 18.43813 4
element Truss2  574 816 717 716 817 18.43813 4
element Truss2  575 81 92 91 82 18.43813 4
element Truss2  576 91 82 81 92 18.43813 4
element Truss2  577 82 93 92 83 18.43813 4
element Truss2  578 92 83 82 93 18.43813 4
element Truss2  579 83 94 93 84 18.43813 4
element Truss2  580 93 84 83 94 18.43813 4
element Truss2  581 84 95 94 85 18.43813 4
element Truss2  582 94 85 84 95 18.43813 4
element Truss2  583 85 96 95 86 18.43813 4
element Truss2  584 95 86 85 96 18.43813 4
element Truss2  585 86 97 96 87 18.43813 4
element Truss2  586 96 87 86 97 18.43813 4
element Truss2  587 87 98 97 88 18.43813 4
element Truss2  588 97 88 87 98 18.43813 4
element Truss2  589 88 99 98 89 18.43813 4
element Truss2  590 98 89 88 99 18.43813 4
element Truss2  591 89 910 99 810 18.43813 4
element Truss2  592 99 810 89 910 18.43813 4
element Truss2  593 810 911 910 811 18.43813 4
element Truss2  594 910 811 810 911 18.43813 4
element Truss2  595 811 912 911 812 18.43813 4
element Truss2  596 911 812 811 912 18.43813 4
element Truss2  597 812 913 912 813 18.43813 4
element Truss2  598 912 813 812 913 18.43813 4
element Truss2  599 813 914 913 814 18.43813 4
element Truss2  600 913 814 813 914 18.43813 4
```

```
element Truss2    601 814 915 914 815 18.43813 4
element Truss2    602 914 815 814 915 18.43813 4
element Truss2    603 815 916 915 816 18.43813 4
element Truss2    604 915 816 815 916 18.43813 4
element Truss2    605 816 917 916 817 18.43813 4
element Truss2    606 916 817 816 917 18.43813 4



#diagonal concrete col 2 Frame 1


element Truss2    607 301 312 311 302 18.43813 4
element Truss2    608 311 302 301 312 18.43813 4
element Truss2    609 302 313 312 303 18.43813 4
element Truss2    610 312 303 302 313 18.43813 4
element Truss2    611 303 314 313 304 18.43813 4
element Truss2    612 313 304 303 314 18.43813 4
element Truss2    613 304 315 314 305 18.43813 4
element Truss2    614 314 305 304 315 18.43813 4
element Truss2    615 305 316 315 306 18.43813 4
element Truss2    616 315 306 305 316 18.43813 4
element Truss2    617 306 317 316 307 18.43813 4
element Truss2    618 316 307 306 317 18.43813 4
element Truss2    619 307 318 317 308 18.43813 4
element Truss2    620 317 308 307 318 18.43813 4
element Truss2    621 308 319 318 309 18.43813 4
element Truss2    622 318 309 308 319 18.43813 4
element Truss2    623 309 3110 319 3010 18.43813 4
element Truss2    624 319 3010 309 3110 18.43813 4
element Truss2    625 3010 3111 3110 3011 18.43813 4
element Truss2    626 3110 3011 3010 3111 18.43813 4
element Truss2    627 3011 3112 3111 3012 18.43813 4
element Truss2    628 3111 3012 3011 3112 18.43813 4
element Truss2    629 3012 3113 3112 3013 18.43813 4
element Truss2    630 3112 3013 3012 3113 18.43813 4
element Truss2    631 3013 3114 3113 3014 18.43813 4
element Truss2    632 3113 3014 3013 3114 18.43813 4
element Truss2    633 3014 3115 3114 3015 18.43813 4
element Truss2    634 3114 3015 3014 3115 18.43813 4
element Truss2    635 3015 3116 3115 3016 18.43813 4
element Truss2    636 3115 3016 3015 3116 18.43813 4
element Truss2    637 3016 3117 3116 3017 18.43813 4
element Truss2    638 3116 3017 3016 3117 18.43813 4
element Truss2    639 311 322 321 312 18.43813 4
element Truss2    640 321 312 311 322 18.43813 4
element Truss2    641 312 323 322 313 18.43813 4
element Truss2    642 322 313 312 323 18.43813 4
element Truss2    643 313 324 323 314 18.43813 4
element Truss2    644 323 314 313 324 18.43813 4
element Truss2    645 314 325 324 315 18.43813 4
element Truss2    646 324 315 314 325 18.43813 4
element Truss2    647 315 326 325 316 18.43813 4
element Truss2    648 325 316 315 326 18.43813 4
```

```
element Truss2    649 316 327 326 317 18.43813 4
element Truss2    650 326 317 316 327 18.43813 4
element Truss2    651 317 328 327 318 18.43813 4
element Truss2    652 327 318 317 328 18.43813 4
element Truss2    653 318 329 328 319 18.43813 4
element Truss2    654 328 319 318 329 18.43813 4
element Truss2    655 319 3210 329 3110 18.43813 4
element Truss2    656 329 3110 319 3210 18.43813 4
element Truss2    657 3110 3211 3210 3111 18.43813 4
element Truss2    658 3210 3111 3110 3211 18.43813 4
element Truss2    659 3111 3212 3211 3112 18.43813 4
element Truss2    660 3211 3112 3111 3212 18.43813 4
element Truss2    661 3112 3213 3212 3113 18.43813 4
element Truss2    662 3212 3113 3112 3213 18.43813 4
element Truss2    663 3113 3214 3213 3114 18.43813 4
element Truss2    664 3213 3114 3113 3214 18.43813 4
element Truss2    665 3114 3215 3214 3115 18.43813 4
element Truss2    666 3214 3115 3114 3215 18.43813 4
element Truss2    667 3115 3216 3215 3116 18.43813 4
element Truss2    668 3215 3116 3115 3216 18.43813 4
element Truss2    669 3116 3217 3216 3117 18.43813 4
element Truss2    670 3216 3117 3116 3217 18.43813 4



#diagonal concrete beam Frame 1


element Truss2    671 915 1016 1015 916 20.92746 5
element Truss2    672 1015 916 915 1016 20.92746 5
element Truss2    673 916 1017 1016 917 20.92746 5
element Truss2    674 1016 917 916 1017 20.92746 5
element Truss2    675 1015 1116 1115 1016 20.92746 5
element Truss2    676 1115 1016 1015 1116 20.92746 5
element Truss2    677 1016 1117 1116 1017 20.92746 5
element Truss2    678 1116 1017 1016 1117 20.92746 5
element Truss2    679 1115 1216 1215 1116 20.92746 5
element Truss2    680 1215 1116 1115 1216 20.92746 5
element Truss2    681 1116 1217 1216 1117 20.92746 5
element Truss2    682 1216 1117 1116 1217 20.92746 5
element Truss2    683 1215 1316 1315 1216 20.92746 5
element Truss2    684 1315 1216 1215 1316 20.92746 5
element Truss2    685 1216 1317 1316 1217 20.92746 5
element Truss2    686 1316 1217 1216 1317 20.92746 5
element Truss2    687 1315 1416 1415 1316 20.92746 5
element Truss2    688 1415 1316 1315 1416 20.92746 5
element Truss2    689 1316 1417 1416 1317 20.92746 5
element Truss2    690 1416 1317 1316 1417 20.92746 5
element Truss2    691 1415 1516 1515 1416 20.92746 5
element Truss2    692 1515 1416 1415 1516 20.92746 5
element Truss2    693 1416 1517 1516 1417 20.92746 5
element Truss2    694 1516 1417 1416 1517 20.92746 5
element Truss2    695 1515 1616 1615 1516 20.92746 5
element Truss2    696 1615 1516 1515 1616 20.92746 5
```

```
element Truss2  697 1516 1617 1616 1517 20.92746 5
element Truss2  698 1616 1517 1516 1617 20.92746 5
element Truss2  699 1615 1716 1715 1616 20.92746 5
element Truss2  700 1715 1616 1615 1716 20.92746 5
element Truss2  701 1616 1717 1716 1617 20.92746 5
element Truss2  702 1716 1617 1616 1717 20.92746 5
element Truss2  703 1715 1816 1815 1716 20.92746 5
element Truss2  704 1815 1716 1715 1816 20.92746 5
element Truss2  705 1716 1817 1816 1717 20.92746 5
element Truss2  706 1816 1717 1716 1817 20.92746 5
element Truss2  707 1815 1916 1915 1816 20.92746 5
element Truss2  708 1915 1816 1815 1916 20.92746 5
element Truss2  709 1816 1917 1916 1817 20.92746 5
element Truss2  710 1916 1817 1816 1917 20.92746 5
element Truss2  711 1915 2016 2015 1916 20.92746 5
element Truss2  712 2015 1916 1915 2016 20.92746 5
element Truss2  713 1916 2017 2016 1917 20.92746 5
element Truss2  714 2016 1917 1916 2017 20.92746 5
element Truss2  715 2015 2116 2115 2016 20.92746 5
element Truss2  716 2115 2016 2015 2116 20.92746 5
element Truss2  717 2016 2117 2116 2017 20.92746 5
element Truss2  718 2116 2017 2016 2117 20.92746 5
element Truss2  719 2115 2216 2215 2116 20.92746 5
element Truss2  720 2215 2116 2115 2216 20.92746 5
element Truss2  721 2116 2217 2216 2117 20.92746 5
element Truss2  722 2216 2117 2116 2217 20.92746 5
element Truss2  723 2215 2316 2315 2216 20.92746 5
element Truss2  724 2315 2216 2215 2316 20.92746 5
element Truss2  725 2216 2317 2316 2217 20.92746 5
element Truss2  726 2316 2217 2216 2317 20.92746 5
element Truss2  727 2315 2416 2415 2316 20.92746 5
element Truss2  728 2415 2316 2315 2416 20.92746 5
element Truss2  729 2316 2417 2416 2317 20.92746 5
element Truss2  730 2416 2317 2316 2417 20.92746 5
element Truss2  731 2415 2516 2515 2416 20.92746 5
element Truss2  732 2515 2416 2415 2516 20.92746 5
element Truss2  733 2416 2517 2516 2417 20.92746 5
element Truss2  734 2516 2417 2416 2517 20.92746 5
element Truss2  735 2515 2616 2615 2516 20.92746 5
element Truss2  736 2615 2516 2515 2616 20.92746 5
element Truss2  737 2516 2617 2616 2517 20.92746 5
element Truss2  738 2616 2517 2516 2617 20.92746 5
element Truss2  739 2615 2716 2715 2616 20.92746 5
element Truss2  740 2715 2616 2615 2716 20.92746 5
element Truss2  741 2616 2717 2716 2617 20.92746 5
element Truss2  742 2716 2617 2616 2717 20.92746 5
element Truss2  743 2715 2816 2815 2716 20.92746 5
element Truss2  744 2815 2716 2715 2816 20.92746 5
element Truss2  745 2716 2817 2816 2717 20.92746 5
element Truss2  746 2816 2717 2716 2817 20.92746 5
element Truss2  747 2815 2916 2915 2816 20.92746 5
element Truss2  748 2915 2816 2815 2916 20.92746 5
element Truss2  749 2816 2917 2916 2817 20.92746 5
element Truss2  750 2916 2817 2816 2917 20.92746 5
element Truss2  751 2915 3016 3015 2916 20.92746 5
```

```
element Truss2    752 3015 2916 2915 3016 20.92746 5
element Truss2    753 2916 3017 3016 2917 20.92746 5
element Truss2    754 3016 2917 2916 3017 20.92746 5


#INFILL


#Vertical Elements Infill Frame 1


#Vertical Elements Infill Frame 1


element truss     755 1891 1992 3.70000 12
element truss     756 1892 1893 3.70000 12
element truss     757 1993 1994 3.70000 12
element truss     758 1894 1895 3.70000 12
element truss     759 1995 1996 3.70000 12
element truss     760 1896 1897 3.70000 12
element truss     761 1997 1998 3.70000 12
element truss     762 1898 1899 3.70000 12
element truss     763 1999 19910 3.70000 12
element truss     764 18910 18911 3.70000 12
element truss     765 19911 19912 3.70000 12
element truss     766 18912 18913 3.70000 12
element truss     767 19913 19914 3.70000 12
element truss     768 18914 18915 3.70000 12
element truss     769 18101 102 7.40000 12
element truss     770 18102 18103 3.70000 12
element truss     771 19102 19103 3.70000 12
element truss     772 103 104 7.40000 12
element truss     773 18104 18105 3.70000 12
element truss     774 19104 19105 3.70000 12
element truss     775 105 106 7.40000 12
element truss     776 18106 18107 3.70000 12
element truss     777 19106 19107 3.70000 12
element truss     778 107 108 7.40000 12
element truss     779 18108 18109 3.70000 12
element truss     780 19108 19109 3.70000 12
element truss     781 109 1010 7.40000 12
element truss     782 181010 181011 3.70000 12
element truss     783 191010 191011 3.70000 12
element truss     784 1011 1012 7.40000 12
element truss     785 181012 181013 3.70000 12
element truss     786 191012 191013 3.70000 12
element truss     787 1013 1014 7.40000 12
element truss     788 181014 181015 3.70000 12
element truss     789 191014 191015 3.70000 12
element truss     790 18111 18112 3.70000 12
element truss     791 19111 19112 3.70000 12
element truss     792 112 113 7.40000 12
element truss     793 18113 18114 3.70000 12
element truss     794 19113 19114 3.70000 12
element truss     795 114 115 7.40000 12
```

```
element truss 796 18115 18116 3.70000 12
element truss 797 19115 19116 3.70000 12
element truss 798 116 117 7.40000 12
element truss 799 18117 18118 3.70000 12
element truss 800 19117 19118 3.70000 12
element truss 801 118 119 7.40000 12
element truss 802 18119 181110 3.70000 12
element truss 803 19119 191110 3.70000 12
element truss 804 1110 1111 7.40000 12
element truss 805 181111 181112 3.70000 12
element truss 806 191111 191112 3.70000 12
element truss 807 1112 1113 7.40000 12
element truss 808 181113 181114 3.70000 12
element truss 809 191113 191114 3.70000 12
element truss 810 1114 181115 7.40000 12
element truss 811 18121 122 7.40000 12
element truss 812 18122 18123 3.70000 12
element truss 813 19122 19123 3.70000 12
element truss 814 123 124 7.40000 12
element truss 815 18124 18125 3.70000 12
element truss 816 19124 19125 3.70000 12
element truss 817 125 126 7.40000 12
element truss 818 18126 18127 3.70000 12
element truss 819 19126 19127 3.70000 12
element truss 820 127 128 7.40000 12
element truss 821 18128 18129 3.70000 12
element truss 822 19128 19129 3.70000 12
element truss 823 129 1210 7.40000 12
element truss 824 181210 181211 3.70000 12
element truss 825 191210 191211 3.70000 12
element truss 826 1211 1212 7.40000 12
element truss 827 181212 181213 3.70000 12
element truss 828 191212 191213 3.70000 12
element truss 829 1213 1214 7.40000 12
element truss 830 181214 181215 3.70000 12
element truss 831 191214 191215 3.70000 12
element truss 832 18131 18132 3.70000 12
element truss 833 19131 19132 3.70000 12
element truss 834 132 133 7.40000 12
element truss 835 18133 18134 3.70000 12
element truss 836 19133 19134 3.70000 12
element truss 837 134 135 7.40000 12
element truss 838 18135 18136 3.70000 12
element truss 839 19135 19136 3.70000 12
element truss 840 136 137 7.40000 12
element truss 841 18137 18138 3.70000 12
element truss 842 19137 19138 3.70000 12
element truss 843 138 139 7.40000 12
element truss 844 18139 181310 3.70000 12
element truss 845 19139 191310 3.70000 12
element truss 846 1310 1311 7.40000 12
element truss 847 181311 181312 3.70000 12
element truss 848 191311 191312 3.70000 12
element truss 849 1312 1313 7.40000 12
element truss 850 181313 181314 3.70000 12
```

```
element truss 851 191313 191314 3.70000 12
element truss 852 1314 181315 7.40000 12
element truss 853 18141 142 7.40000 12
element truss 854 18142 18143 3.70000 12
element truss 855 19142 19143 3.70000 12
element truss 856 143 144 7.40000 12
element truss 857 18144 18145 3.70000 12
element truss 858 19144 19145 3.70000 12
element truss 859 145 146 7.40000 12
element truss 860 18146 18147 3.70000 12
element truss 861 19146 19147 3.70000 12
element truss 862 147 148 7.40000 12
element truss 863 18148 18149 3.70000 12
element truss 864 19148 19149 3.70000 12
element truss 865 149 1410 7.40000 12
element truss 866 181410 181411 3.70000 12
element truss 867 191410 191411 3.70000 12
element truss 868 1411 1412 7.40000 12
element truss 869 181412 181413 3.70000 12
element truss 870 191412 191413 3.70000 12
element truss 871 1413 1414 7.40000 12
element truss 872 181414 181415 3.70000 12
element truss 873 191414 191415 3.70000 12
element truss 874 18151 18152 3.70000 12
element truss 875 19151 19152 3.70000 12
element truss 876 152 153 7.40000 12
element truss 877 18153 18154 3.70000 12
element truss 878 19153 19154 3.70000 12
element truss 879 154 155 7.40000 12
element truss 880 18155 18156 3.70000 12
element truss 881 19155 19156 3.70000 12
element truss 882 156 157 7.40000 12
element truss 883 18157 18158 3.70000 12
element truss 884 19157 19158 3.70000 12
element truss 885 158 159 7.40000 12
element truss 886 18159 181510 3.70000 12
element truss 887 19159 191510 3.70000 12
element truss 888 1510 1511 7.40000 12
element truss 889 181511 181512 3.70000 12
element truss 890 191511 191512 3.70000 12
element truss 891 1512 1513 7.40000 12
element truss 892 181513 181514 3.70000 12
element truss 893 191513 191514 3.70000 12
element truss 894 1514 181515 7.40000 12
element truss 895 18161 162 7.40000 12
element truss 896 18162 18163 3.70000 12
element truss 897 19162 19163 3.70000 12
element truss 898 163 164 7.40000 12
element truss 899 18164 18165 3.70000 12
element truss 900 19164 19165 3.70000 12
element truss 901 165 166 7.40000 12
element truss 902 18166 18167 3.70000 12
element truss 903 19166 19167 3.70000 12
element truss 904 167 168 7.40000 12
element truss 905 18168 18169 3.70000 12
```

```
element truss 906 19168 19169 3.70000 12
element truss 907 169 1610 7.40000 12
element truss 908 181610 181611 3.70000 12
element truss 909 191610 191611 3.70000 12
element truss 910 1611 1612 7.40000 12
element truss 911 181612 181613 3.70000 12
element truss 912 191612 191613 3.70000 12
element truss 913 1613 1614 7.40000 12
element truss 914 181614 181615 3.70000 12
element truss 915 191614 191615 3.70000 12
element truss 916 18171 18172 3.70000 12
element truss 917 19171 19172 3.70000 12
element truss 918 172 173 7.40000 12
element truss 919 18173 18174 3.70000 12
element truss 920 19173 19174 3.70000 12
element truss 921 174 175 7.40000 12
element truss 922 18175 18176 3.70000 12
element truss 923 19175 19176 3.70000 12
element truss 924 176 177 7.40000 12
element truss 925 18177 18178 3.70000 12
element truss 926 19177 19178 3.70000 12
element truss 927 178 179 7.40000 12
element truss 928 18179 181710 3.70000 12
element truss 929 19179 191710 3.70000 12
element truss 930 1710 1711 7.40000 12
element truss 931 181711 181712 3.70000 12
element truss 932 191711 191712 3.70000 12
element truss 933 1712 1713 7.40000 12
element truss 934 181713 181714 3.70000 12
element truss 935 191713 191714 3.70000 12
element truss 936 1714 181715 7.40000 12
element truss 937 18181 182 7.40000 12
element truss 938 18182 18183 3.70000 12
element truss 939 19182 19183 3.70000 12
element truss 940 183 184 7.40000 12
element truss 941 18184 18185 3.70000 12
element truss 942 19184 19185 3.70000 12
element truss 943 185 186 7.40000 12
element truss 944 18186 18187 3.70000 12
element truss 945 19186 19187 3.70000 12
element truss 946 187 188 7.40000 12
element truss 947 18188 18189 3.70000 12
element truss 948 19188 19189 3.70000 12
element truss 949 189 1810 7.40000 12
element truss 950 181810 181811 3.70000 12
element truss 951 191810 191811 3.70000 12
element truss 952 1811 1812 7.40000 12
element truss 953 181812 181813 3.70000 12
element truss 954 191812 191813 3.70000 12
element truss 955 1813 1814 7.40000 12
element truss 956 181814 181815 3.70000 12
element truss 957 191814 191815 3.70000 12
element truss 958 18191 18192 3.70000 12
element truss 959 19191 19192 3.70000 12
element truss 960 192 193 7.40000 12
```

```
element truss 961 18193 18194 3.70000 12
element truss 962 19193 19194 3.70000 12
element truss 963 194 195 7.40000 12
element truss 964 18195 18196 3.70000 12
element truss 965 19195 19196 3.70000 12
element truss 966 196 197 7.40000 12
element truss 967 18197 18198 3.70000 12
element truss 968 19197 19198 3.70000 12
element truss 969 198 199 7.40000 12
element truss 970 18199 181910 3.70000 12
element truss 971 19199 191910 3.70000 12
element truss 972 1910 1911 7.40000 12
element truss 973 181911 181912 3.70000 12
element truss 974 191911 191912 3.70000 12
element truss 975 1912 1913 7.40000 12
element truss 976 181913 181914 3.70000 12
element truss 977 191913 191914 3.70000 12
element truss 978 1914 181915 7.40000 12
element truss 979 18201 202 7.40000 12
element truss 980 18202 18203 3.70000 12
element truss 981 19202 19203 3.70000 12
element truss 982 203 204 7.40000 12
element truss 983 18204 18205 3.70000 12
element truss 984 19204 19205 3.70000 12
element truss 985 205 206 7.40000 12
element truss 986 18206 18207 3.70000 12
element truss 987 19206 19207 3.70000 12
element truss 988 207 208 7.40000 12
element truss 989 18208 18209 3.70000 12
element truss 990 19208 19209 3.70000 12
element truss 991 209 2010 7.40000 12
element truss 992 182010 182011 3.70000 12
element truss 993 192010 192011 3.70000 12
element truss 994 2011 2012 7.40000 12
element truss 995 182012 182013 3.70000 12
element truss 996 192012 192013 3.70000 12
element truss 997 2013 2014 7.40000 12
element truss 998 182014 182015 3.70000 12
element truss 999 192014 192015 3.70000 12
element truss 1000 18211 18212 3.70000 12
element truss 1001 19211 19212 3.70000 12
element truss 1002 212 213 7.40000 12
element truss 1003 18213 18214 3.70000 12
element truss 1004 19213 19214 3.70000 12
element truss 1005 214 215 7.40000 12
element truss 1006 18215 18216 3.70000 12
element truss 1007 19215 19216 3.70000 12
element truss 1008 216 217 7.40000 12
element truss 1009 18217 18218 3.70000 12
element truss 1010 19217 19218 3.70000 12
element truss 1011 218 219 7.40000 12
element truss 1012 18219 182110 3.70000 12
element truss 1013 19219 192110 3.70000 12
element truss 1014 2110 2111 7.40000 12
element truss 1015 182111 182112 3.70000 12
```

```
element truss 1016 192111 192112 3.70000 12
element truss 1017 2112 2113 7.40000 12
element truss 1018 182113 182114 3.70000 12
element truss 1019 192113 192114 3.70000 12
element truss 1020 2114 182115 7.40000 12
element truss 1021 18221 222 7.40000 12
element truss 1022 18222 18223 3.70000 12
element truss 1023 19222 19223 3.70000 12
element truss 1024 223 224 7.40000 12
element truss 1025 18224 18225 3.70000 12
element truss 1026 19224 19225 3.70000 12
element truss 1027 225 226 7.40000 12
element truss 1028 18226 18227 3.70000 12
element truss 1029 19226 19227 3.70000 12
element truss 1030 227 228 7.40000 12
element truss 1031 18228 18229 3.70000 12
element truss 1032 19228 19229 3.70000 12
element truss 1033 229 2210 7.40000 12
element truss 1034 182210 182211 3.70000 12
element truss 1035 192210 192211 3.70000 12
element truss 1036 2211 2212 7.40000 12
element truss 1037 182212 182213 3.70000 12
element truss 1038 192212 192213 3.70000 12
element truss 1039 2213 2214 7.40000 12
element truss 1040 182214 182215 3.70000 12
element truss 1041 192214 192215 3.70000 12
element truss 1042 18231 18232 3.70000 12
element truss 1043 19231 19232 3.70000 12
element truss 1044 232 233 7.40000 12
element truss 1045 18233 18234 3.70000 12
element truss 1046 19233 19234 3.70000 12
element truss 1047 234 235 7.40000 12
element truss 1048 18235 18236 3.70000 12
element truss 1049 19235 19236 3.70000 12
element truss 1050 236 237 7.40000 12
element truss 1051 18237 18238 3.70000 12
element truss 1052 19237 19238 3.70000 12
element truss 1053 238 239 7.40000 12
element truss 1054 18239 182310 3.70000 12
element truss 1055 19239 192310 3.70000 12
element truss 1056 2310 2311 7.40000 12
element truss 1057 182311 182312 3.70000 12
element truss 1058 192311 192312 3.70000 12
element truss 1059 2312 2313 7.40000 12
element truss 1060 182313 182314 3.70000 12
element truss 1061 192313 192314 3.70000 12
element truss 1062 2314 182315 7.40000 12
element truss 1063 18241 242 7.40000 12
element truss 1064 18242 18243 3.70000 12
element truss 1065 19242 19243 3.70000 12
element truss 1066 243 244 7.40000 12
element truss 1067 18244 18245 3.70000 12
element truss 1068 19244 19245 3.70000 12
element truss 1069 245 246 7.40000 12
element truss 1070 18246 18247 3.70000 12
```

```
element truss 1071 19246 19247 3.70000 12
element truss 1072 247 248 7.40000 12
element truss 1073 18248 18249 3.70000 12
element truss 1074 19248 19249 3.70000 12
element truss 1075 249 2410 7.40000 12
element truss 1076 182410 182411 3.70000 12
element truss 1077 192410 192411 3.70000 12
element truss 1078 2411 2412 7.40000 12
element truss 1079 182412 182413 3.70000 12
element truss 1080 192412 192413 3.70000 12
element truss 1081 2413 2414 7.40000 12
element truss 1082 182414 182415 3.70000 12
element truss 1083 192414 192415 3.70000 12
element truss 1084 18251 18252 3.70000 12
element truss 1085 19251 19252 3.70000 12
element truss 1086 252 253 7.40000 12
element truss 1087 18253 18254 3.70000 12
element truss 1088 19253 19254 3.70000 12
element truss 1089 254 255 7.40000 12
element truss 1090 18255 18256 3.70000 12
element truss 1091 19255 19256 3.70000 12
element truss 1092 256 257 7.40000 12
element truss 1093 18257 18258 3.70000 12
element truss 1094 19257 19258 3.70000 12
element truss 1095 258 259 7.40000 12
element truss 1096 18259 182510 3.70000 12
element truss 1097 19259 192510 3.70000 12
element truss 1098 2510 2511 7.40000 12
element truss 1099 182511 182512 3.70000 12
element truss 1100 192511 192512 3.70000 12
element truss 1101 2512 2513 7.40000 12
element truss 1102 182513 182514 3.70000 12
element truss 1103 192513 192514 3.70000 12
element truss 1104 2514 182515 7.40000 12
element truss 1105 18261 262 7.40000 12
element truss 1106 18262 18263 3.70000 12
element truss 1107 19262 19263 3.70000 12
element truss 1108 263 264 7.40000 12
element truss 1109 18264 18265 3.70000 12
element truss 1110 19264 19265 3.70000 12
element truss 1111 265 266 7.40000 12
element truss 1112 18266 18267 3.70000 12
element truss 1113 19266 19267 3.70000 12
element truss 1114 267 268 7.40000 12
element truss 1115 18268 18269 3.70000 12
element truss 1116 19268 19269 3.70000 12
element truss 1117 269 2610 7.40000 12
element truss 1118 182610 182611 3.70000 12
element truss 1119 192610 192611 3.70000 12
element truss 1120 2611 2612 7.40000 12
element truss 1121 182612 182613 3.70000 12
element truss 1122 192612 192613 3.70000 12
element truss 1123 2613 2614 7.40000 12
element truss 1124 182614 182615 3.70000 12
element truss 1125 192614 192615 3.70000 12
```

```
element truss 1126 18271 18272 3.70000 12
element truss 1127 19271 19272 3.70000 12
element truss 1128 272 273 7.40000 12
element truss 1129 18273 18274 3.70000 12
element truss 1130 19273 19274 3.70000 12
element truss 1131 274 275 7.40000 12
element truss 1132 18275 18276 3.70000 12
element truss 1133 19275 19276 3.70000 12
element truss 1134 276 277 7.40000 12
element truss 1135 18277 18278 3.70000 12
element truss 1136 19277 19278 3.70000 12
element truss 1137 278 279 7.40000 12
element truss 1138 18279 182710 3.70000 12
element truss 1139 19279 192710 3.70000 12
element truss 1140 2710 2711 7.40000 12
element truss 1141 182711 182712 3.70000 12
element truss 1142 192711 192712 3.70000 12
element truss 1143 2712 2713 7.40000 12
element truss 1144 182713 182714 3.70000 12
element truss 1145 192713 192714 3.70000 12
element truss 1146 2714 182715 7.40000 12
element truss 1147 18281 282 7.40000 12
element truss 1148 18282 18283 3.70000 12
element truss 1149 19282 19283 3.70000 12
element truss 1150 283 284 7.40000 12
element truss 1151 18284 18285 3.70000 12
element truss 1152 19284 19285 3.70000 12
element truss 1153 285 286 7.40000 12
element truss 1154 18286 18287 3.70000 12
element truss 1155 19286 19287 3.70000 12
element truss 1156 287 288 7.40000 12
element truss 1157 18288 18289 3.70000 12
element truss 1158 19288 19289 3.70000 12
element truss 1159 289 2810 7.40000 12
element truss 1160 182810 182811 3.70000 12
element truss 1161 192810 192811 3.70000 12
element truss 1162 2811 2812 7.40000 12
element truss 1163 182812 182813 3.70000 12
element truss 1164 192812 192813 3.70000 12
element truss 1165 2813 2814 7.40000 12
element truss 1166 182814 182815 3.70000 12
element truss 1167 192814 192815 3.70000 12
element truss 1168 18291 18292 3.70000 12
element truss 1169 19291 19292 3.70000 12
element truss 1170 292 293 7.40000 12
element truss 1171 18293 18294 3.70000 12
element truss 1172 19293 19294 3.70000 12
element truss 1173 294 295 7.40000 12
element truss 1174 18295 18296 3.70000 12
element truss 1175 19295 19296 3.70000 12
element truss 1176 296 297 7.40000 12
element truss 1177 18297 18298 3.70000 12
element truss 1178 19297 19298 3.70000 12
element truss 1179 298 299 7.40000 12
element truss 1180 18299 182910 3.70000 12
```

```
element truss 1181 19299 192910 3.70000 12
element truss 1182 2910 2911 7.40000 12
element truss 1183 182911 182912 3.70000 12
element truss 1184 192911 192912 3.70000 12
element truss 1185 2912 2913 7.40000 12
element truss 1186 182913 182914 3.70000 12
element truss 1187 192913 192914 3.70000 12
element truss 1188 2914 182915 7.40000 12
element truss 1189 19301 19302 3.70000 12
element truss 1190 18302 18303 3.70000 12
element truss 1191 19303 19304 3.70000 12
element truss 1192 18304 18305 3.70000 12
element truss 1193 19305 19306 3.70000 12
element truss 1194 18306 18307 3.70000 12
element truss 1195 19307 19308 3.70000 12
element truss 1196 18308 18309 3.70000 12
element truss 1197 19309 193010 3.70000 12
element truss 1198 183010 183011 3.70000 12
element truss 1199 193011 193012 3.70000 12
element truss 1200 183012 183013 3.70000 12
element truss 1201 193013 193014 3.70000 12
element truss 1202 183014 183015 3.70000 12


#Horizontal elements Infill Frame 1
element truss 1203 1891 18101 3.70000 13
element truss 1204 1992 102 3.70000 13
element truss 1205 1892 18102 3.70000 13
element truss 1206 1893 18103 3.70000 13
element truss 1207 1993 103 3.70000 13
element truss 1208 1994 104 3.70000 13
element truss 1209 1894 18104 3.70000 13
element truss 1210 1895 18105 3.70000 13
element truss 1211 1995 105 3.70000 13
element truss 1212 1996 106 3.70000 13
element truss 1213 1896 18106 3.70000 13
element truss 1214 1897 18107 3.70000 13
element truss 1215 1997 107 3.70000 13
element truss 1216 1998 108 3.70000 13
element truss 1217 1898 18108 3.70000 13
element truss 1218 1899 18109 3.70000 13
element truss 1219 1999 109 3.70000 13
element truss 1220 19910 1010 3.70000 13
element truss 1221 18910 181010 3.70000 13
element truss 1222 18911 181011 3.70000 13
element truss 1223 19911 1011 3.70000 13
element truss 1224 19912 1012 3.70000 13
element truss 1225 18912 181012 3.70000 13
element truss 1226 18913 181013 3.70000 13
element truss 1227 19913 1013 3.70000 13
element truss 1228 19914 1014 3.70000 13
element truss 1229 18914 181014 3.70000 13
element truss 1230 18915 181015 3.70000 13
element truss 1231 18101 18111 3.70000 13
element truss 1232 102 18112 3.70000 13
```

```
element truss 1233 19102 112 3.70000 13
element truss 1234 19103 113 3.70000 13
element truss 1235 103 18113 3.70000 13
element truss 1236 104 18114 3.70000 13
element truss 1237 19104 114 3.70000 13
element truss 1238 19105 115 3.70000 13
element truss 1239 105 18115 3.70000 13
element truss 1240 106 18116 3.70000 13
element truss 1241 19106 116 3.70000 13
element truss 1242 19107 117 3.70000 13
element truss 1243 107 18117 3.70000 13
element truss 1244 108 18118 3.70000 13
element truss 1245 19108 118 3.70000 13
element truss 1246 19109 119 3.70000 13
element truss 1247 109 18119 3.70000 13
element truss 1248 1010 181110 3.70000 13
element truss 1249 191010 1110 3.70000 13
element truss 1250 191011 1111 3.70000 13
element truss 1251 1011 181111 3.70000 13
element truss 1252 1012 181112 3.70000 13
element truss 1253 191012 1112 3.70000 13
element truss 1254 191013 1113 3.70000 13
element truss 1255 1013 181113 3.70000 13
element truss 1256 1014 181114 3.70000 13
element truss 1257 191014 1114 3.70000 13
element truss 1258 191015 181115 3.70000 13
element truss 1259 19111 18121 3.70000 13
element truss 1260 19112 122 3.70000 13
element truss 1261 112 18122 3.70000 13
element truss 1262 113 18123 3.70000 13
element truss 1263 19113 123 3.70000 13
element truss 1264 19114 124 3.70000 13
element truss 1265 114 18124 3.70000 13
element truss 1266 115 18125 3.70000 13
element truss 1267 19115 125 3.70000 13
element truss 1268 19116 126 3.70000 13
element truss 1269 116 18126 3.70000 13
element truss 1270 117 18127 3.70000 13
element truss 1271 19117 127 3.70000 13
element truss 1272 19118 128 3.70000 13
element truss 1273 118 18128 3.70000 13
element truss 1274 119 18129 3.70000 13
element truss 1275 19119 129 3.70000 13
element truss 1276 191110 1210 3.70000 13
element truss 1277 1110 181210 3.70000 13
element truss 1278 1111 181211 3.70000 13
element truss 1279 191111 1211 3.70000 13
element truss 1280 191112 1212 3.70000 13
element truss 1281 1112 181212 3.70000 13
element truss 1282 1113 181213 3.70000 13
element truss 1283 191113 1213 3.70000 13
element truss 1284 191114 1214 3.70000 13
element truss 1285 1114 181214 3.70000 13
element truss 1286 181115 181215 3.70000 13
element truss 1287 18121 18131 3.70000 13
```

```
element truss 1288 122 18132 3.70000 13
element truss 1289 19122 132 3.70000 13
element truss 1290 19123 133 3.70000 13
element truss 1291 123 18133 3.70000 13
element truss 1292 124 18134 3.70000 13
element truss 1293 19124 134 3.70000 13
element truss 1294 19125 135 3.70000 13
element truss 1295 125 18135 3.70000 13
element truss 1296 126 18136 3.70000 13
element truss 1297 19126 136 3.70000 13
element truss 1298 19127 137 3.70000 13
element truss 1299 127 18137 3.70000 13
element truss 1300 128 18138 3.70000 13
element truss 1301 19128 138 3.70000 13
element truss 1302 19129 139 3.70000 13
element truss 1303 129 18139 3.70000 13
element truss 1304 1210 181310 3.70000 13
element truss 1305 191210 1310 3.70000 13
element truss 1306 191211 1311 3.70000 13
element truss 1307 1211 181311 3.70000 13
element truss 1308 1212 181312 3.70000 13
element truss 1309 191212 1312 3.70000 13
element truss 1310 191213 1313 3.70000 13
element truss 1311 1213 181313 3.70000 13
element truss 1312 1214 181314 3.70000 13
element truss 1313 191214 1314 3.70000 13
element truss 1314 191215 181315 3.70000 13
element truss 1315 19131 18141 3.70000 13
element truss 1316 19132 142 3.70000 13
element truss 1317 132 18142 3.70000 13
element truss 1318 133 18143 3.70000 13
element truss 1319 19133 143 3.70000 13
element truss 1320 19134 144 3.70000 13
element truss 1321 134 18144 3.70000 13
element truss 1322 135 18145 3.70000 13
element truss 1323 19135 145 3.70000 13
element truss 1324 19136 146 3.70000 13
element truss 1325 136 18146 3.70000 13
element truss 1326 137 18147 3.70000 13
element truss 1327 19137 147 3.70000 13
element truss 1328 19138 148 3.70000 13
element truss 1329 138 18148 3.70000 13
element truss 1330 139 18149 3.70000 13
element truss 1331 19139 149 3.70000 13
element truss 1332 191310 1410 3.70000 13
element truss 1333 1310 181410 3.70000 13
element truss 1334 1311 181411 3.70000 13
element truss 1335 191311 1411 3.70000 13
element truss 1336 191312 1412 3.70000 13
element truss 1337 1312 181412 3.70000 13
element truss 1338 1313 181413 3.70000 13
element truss 1339 191313 1413 3.70000 13
element truss 1340 191314 1414 3.70000 13
element truss 1341 1314 181414 3.70000 13
element truss 1342 181315 181415 3.70000 13
```

```
3796  element truss  1343 18141 18151 3.70000 13
3797  element truss  1344 142 18152 3.70000 13
3798  element truss  1345 19142 152 3.70000 13
3799  element truss  1346 19143 153 3.70000 13
3800  element truss  1347 143 18153 3.70000 13
3801  element truss  1348 144 18154 3.70000 13
3802  element truss  1349 19144 154 3.70000 13
3803  element truss  1350 19145 155 3.70000 13
3804  element truss  1351 145 18155 3.70000 13
3805  element truss  1352 146 18156 3.70000 13
3806  element truss  1353 19146 156 3.70000 13
3807  element truss  1354 19147 157 3.70000 13
3808  element truss  1355 147 18157 3.70000 13
3809  element truss  1356 148 18158 3.70000 13
3810  element truss  1357 19148 158 3.70000 13
3811  element truss  1358 19149 159 3.70000 13
3812  element truss  1359 149 18159 3.70000 13
3813  element truss  1360 1410 181510 3.70000 13
3814  element truss  1361 191410 1510 3.70000 13
3815  element truss  1362 191411 1511 3.70000 13
3816  element truss  1363 1411 181511 3.70000 13
3817  element truss  1364 1412 181512 3.70000 13
3818  element truss  1365 191412 1512 3.70000 13
3819  element truss  1366 191413 1513 3.70000 13
3820  element truss  1367 1413 181513 3.70000 13
3821  element truss  1368 1414 181514 3.70000 13
3822  element truss  1369 191414 1514 3.70000 13
3823  element truss  1370 191415 181515 3.70000 13
3824  element truss  1371 19151 18161 3.70000 13
3825  element truss  1372 19152 162 3.70000 13
3826  element truss  1373 152 18162 3.70000 13
3827  element truss  1374 153 18163 3.70000 13
3828  element truss  1375 19153 163 3.70000 13
3829  element truss  1376 19154 164 3.70000 13
3830  element truss  1377 154 18164 3.70000 13
3831  element truss  1378 155 18165 3.70000 13
3832  element truss  1379 19155 165 3.70000 13
3833  element truss  1380 19156 166 3.70000 13
3834  element truss  1381 156 18166 3.70000 13
3835  element truss  1382 157 18167 3.70000 13
3836  element truss  1383 19157 167 3.70000 13
3837  element truss  1384 19158 168 3.70000 13
3838  element truss  1385 158 18168 3.70000 13
3839  element truss  1386 159 18169 3.70000 13
3840  element truss  1387 19159 169 3.70000 13
3841  element truss  1388 191510 1610 3.70000 13
3842  element truss  1389 1510 181610 3.70000 13
3843  element truss  1390 1511 181611 3.70000 13
3844  element truss  1391 191511 1611 3.70000 13
3845  element truss  1392 191512 1612 3.70000 13
3846  element truss  1393 1512 181612 3.70000 13
3847  element truss  1394 1513 181613 3.70000 13
3848  element truss  1395 191513 1613 3.70000 13
3849  element truss  1396 191514 1614 3.70000 13
3850  element truss  1397 1514 181614 3.70000 13
```

```
element truss 1398 181515 181615 3.70000 13
element truss 1399 18161 18171 3.70000 13
element truss 1400 162 18172 3.70000 13
element truss 1401 19162 172 3.70000 13
element truss 1402 19163 173 3.70000 13
element truss 1403 163 18173 3.70000 13
element truss 1404 164 18174 3.70000 13
element truss 1405 19164 174 3.70000 13
element truss 1406 19165 175 3.70000 13
element truss 1407 165 18175 3.70000 13
element truss 1408 166 18176 3.70000 13
element truss 1409 19166 176 3.70000 13
element truss 1410 19167 177 3.70000 13
element truss 1411 167 18177 3.70000 13
element truss 1412 168 18178 3.70000 13
element truss 1413 19168 178 3.70000 13
element truss 1414 19169 179 3.70000 13
element truss 1415 169 18179 3.70000 13
element truss 1416 1610 181710 3.70000 13
element truss 1417 191610 1710 3.70000 13
element truss 1418 191611 1711 3.70000 13
element truss 1419 1611 181711 3.70000 13
element truss 1420 1612 181712 3.70000 13
element truss 1421 191612 1712 3.70000 13
element truss 1422 191613 1713 3.70000 13
element truss 1423 1613 181713 3.70000 13
element truss 1424 1614 181714 3.70000 13
element truss 1425 191614 1714 3.70000 13
element truss 1426 191615 181715 3.70000 13
element truss 1427 19171 18181 3.70000 13
element truss 1428 19172 182 3.70000 13
element truss 1429 172 18182 3.70000 13
element truss 1430 173 18183 3.70000 13
element truss 1431 19173 183 3.70000 13
element truss 1432 19174 184 3.70000 13
element truss 1433 174 18184 3.70000 13
element truss 1434 175 18185 3.70000 13
element truss 1435 19175 185 3.70000 13
element truss 1436 19176 186 3.70000 13
element truss 1437 176 18186 3.70000 13
element truss 1438 177 18187 3.70000 13
element truss 1439 19177 187 3.70000 13
element truss 1440 19178 188 3.70000 13
element truss 1441 178 18188 3.70000 13
element truss 1442 179 18189 3.70000 13
element truss 1443 19179 189 3.70000 13
element truss 1444 191710 1810 3.70000 13
element truss 1445 1710 181810 3.70000 13
element truss 1446 1711 181811 3.70000 13
element truss 1447 191711 1811 3.70000 13
element truss 1448 191712 1812 3.70000 13
element truss 1449 1712 181812 3.70000 13
element truss 1450 1713 181813 3.70000 13
element truss 1451 191713 1813 3.70000 13
element truss 1452 191714 1814 3.70000 13
```

```
element truss 1453 1714 181814 3.70000 13
element truss 1454 181715 181815 3.70000 13
element truss 1455 18181 18191 3.70000 13
element truss 1456 182 18192 3.70000 13
element truss 1457 19182 192 3.70000 13
element truss 1458 19183 193 3.70000 13
element truss 1459 183 18193 3.70000 13
element truss 1460 184 18194 3.70000 13
element truss 1461 19184 194 3.70000 13
element truss 1462 19185 195 3.70000 13
element truss 1463 185 18195 3.70000 13
element truss 1464 186 18196 3.70000 13
element truss 1465 19186 196 3.70000 13
element truss 1466 19187 197 3.70000 13
element truss 1467 187 18197 3.70000 13
element truss 1468 188 18198 3.70000 13
element truss 1469 19188 198 3.70000 13
element truss 1470 19189 199 3.70000 13
element truss 1471 189 18199 3.70000 13
element truss 1472 1810 181910 3.70000 13
element truss 1473 191810 1910 3.70000 13
element truss 1474 191811 1911 3.70000 13
element truss 1475 1811 181911 3.70000 13
element truss 1476 1812 181912 3.70000 13
element truss 1477 191812 1912 3.70000 13
element truss 1478 191813 1913 3.70000 13
element truss 1479 1813 181913 3.70000 13
element truss 1480 1814 181914 3.70000 13
element truss 1481 191814 1914 3.70000 13
element truss 1482 191815 181915 3.70000 13
element truss 1483 19191 18201 3.70000 13
element truss 1484 19192 202 3.70000 13
element truss 1485 192 18202 3.70000 13
element truss 1486 193 18203 3.70000 13
element truss 1487 19193 203 3.70000 13
element truss 1488 19194 204 3.70000 13
element truss 1489 194 18204 3.70000 13
element truss 1490 195 18205 3.70000 13
element truss 1491 19195 205 3.70000 13
element truss 1492 19196 206 3.70000 13
element truss 1493 196 18206 3.70000 13
element truss 1494 197 18207 3.70000 13
element truss 1495 19197 207 3.70000 13
element truss 1496 19198 208 3.70000 13
element truss 1497 198 18208 3.70000 13
element truss 1498 199 18209 3.70000 13
element truss 1499 19199 209 3.70000 13
element truss 1500 191910 2010 3.70000 13
element truss 1501 1910 182010 3.70000 13
element truss 1502 1911 182011 3.70000 13
element truss 1503 191911 2011 3.70000 13
element truss 1504 191912 2012 3.70000 13
element truss 1505 1912 182012 3.70000 13
element truss 1506 1913 182013 3.70000 13
element truss 1507 191913 2013 3.70000 13
```

```
element truss 1508 191914 2014 3.70000 13
element truss 1509 1914 182014 3.70000 13
element truss 1510 181915 182015 3.70000 13
element truss 1511 18201 18211 3.70000 13
element truss 1512 202 18212 3.70000 13
element truss 1513 19202 212 3.70000 13
element truss 1514 19203 213 3.70000 13
element truss 1515 203 18213 3.70000 13
element truss 1516 204 18214 3.70000 13
element truss 1517 19204 214 3.70000 13
element truss 1518 19205 215 3.70000 13
element truss 1519 205 18215 3.70000 13
element truss 1520 206 18216 3.70000 13
element truss 1521 19206 216 3.70000 13
element truss 1522 19207 217 3.70000 13
element truss 1523 207 18217 3.70000 13
element truss 1524 208 18218 3.70000 13
element truss 1525 19208 218 3.70000 13
element truss 1526 19209 219 3.70000 13
element truss 1527 209 18219 3.70000 13
element truss 1528 2010 182110 3.70000 13
element truss 1529 192010 2110 3.70000 13
element truss 1530 192011 2111 3.70000 13
element truss 1531 2011 182111 3.70000 13
element truss 1532 2012 182112 3.70000 13
element truss 1533 192012 2112 3.70000 13
element truss 1534 192013 2113 3.70000 13
element truss 1535 2013 182113 3.70000 13
element truss 1536 2014 182114 3.70000 13
element truss 1537 192014 2114 3.70000 13
element truss 1538 192015 182115 3.70000 13
element truss 1539 19211 18221 3.70000 13
element truss 1540 19212 222 3.70000 13
element truss 1541 212 18222 3.70000 13
element truss 1542 213 18223 3.70000 13
element truss 1543 19213 223 3.70000 13
element truss 1544 19214 224 3.70000 13
element truss 1545 214 18224 3.70000 13
element truss 1546 215 18225 3.70000 13
element truss 1547 19215 225 3.70000 13
element truss 1548 19216 226 3.70000 13
element truss 1549 216 18226 3.70000 13
element truss 1550 217 18227 3.70000 13
element truss 1551 19217 227 3.70000 13
element truss 1552 19218 228 3.70000 13
element truss 1553 218 18228 3.70000 13
element truss 1554 219 18229 3.70000 13
element truss 1555 19219 229 3.70000 13
element truss 1556 192110 2210 3.70000 13
element truss 1557 2110 182210 3.70000 13
element truss 1558 2111 182211 3.70000 13
element truss 1559 192111 2211 3.70000 13
element truss 1560 192112 2212 3.70000 13
element truss 1561 2112 182212 3.70000 13
element truss 1562 2113 182213 3.70000 13
```

```
element truss 1563 192113 2213 3.70000 13
element truss 1564 192114 2214 3.70000 13
element truss 1565 2114 182214 3.70000 13
element truss 1566 182115 182215 3.70000 13
element truss 1567 18221 18231 3.70000 13
element truss 1568 222 18232 3.70000 13
element truss 1569 19222 232 3.70000 13
element truss 1570 19223 233 3.70000 13
element truss 1571 223 18233 3.70000 13
element truss 1572 224 18234 3.70000 13
element truss 1573 19224 234 3.70000 13
element truss 1574 19225 235 3.70000 13
element truss 1575 225 18235 3.70000 13
element truss 1576 226 18236 3.70000 13
element truss 1577 19226 236 3.70000 13
element truss 1578 19227 237 3.70000 13
element truss 1579 227 18237 3.70000 13
element truss 1580 228 18238 3.70000 13
element truss 1581 19228 238 3.70000 13
element truss 1582 19229 239 3.70000 13
element truss 1583 229 18239 3.70000 13
element truss 1584 2210 182310 3.70000 13
element truss 1585 192210 2310 3.70000 13
element truss 1586 192211 2311 3.70000 13
element truss 1587 2211 182311 3.70000 13
element truss 1588 2212 182312 3.70000 13
element truss 1589 192212 2312 3.70000 13
element truss 1590 192213 2313 3.70000 13
element truss 1591 2213 182313 3.70000 13
element truss 1592 2214 182314 3.70000 13
element truss 1593 192214 2314 3.70000 13
element truss 1594 192215 182315 3.70000 13
element truss 1595 19231 18241 3.70000 13
element truss 1596 19232 242 3.70000 13
element truss 1597 232 18242 3.70000 13
element truss 1598 233 18243 3.70000 13
element truss 1599 19233 243 3.70000 13
element truss 1600 19234 244 3.70000 13
element truss 1601 234 18244 3.70000 13
element truss 1602 235 18245 3.70000 13
element truss 1603 19235 245 3.70000 13
element truss 1604 19236 246 3.70000 13
element truss 1605 236 18246 3.70000 13
element truss 1606 237 18247 3.70000 13
element truss 1607 19237 247 3.70000 13
element truss 1608 19238 248 3.70000 13
element truss 1609 238 18248 3.70000 13
element truss 1610 239 18249 3.70000 13
element truss 1611 19239 249 3.70000 13
element truss 1612 192310 2410 3.70000 13
element truss 1613 2310 182410 3.70000 13
element truss 1614 2311 182411 3.70000 13
element truss 1615 192311 2411 3.70000 13
element truss 1616 192312 2412 3.70000 13
element truss 1617 2312 182412 3.70000 13
```

```
element truss 1618 2313 182413 3.70000 13
element truss 1619 192313 2413 3.70000 13
element truss 1620 192314 2414 3.70000 13
element truss 1621 2314 182414 3.70000 13
element truss 1622 182315 182415 3.70000 13
element truss 1623 18241 18251 3.70000 13
element truss 1624 242 18252 3.70000 13
element truss 1625 19242 252 3.70000 13
element truss 1626 19243 253 3.70000 13
element truss 1627 243 18253 3.70000 13
element truss 1628 244 18254 3.70000 13
element truss 1629 19244 254 3.70000 13
element truss 1630 19245 255 3.70000 13
element truss 1631 245 18255 3.70000 13
element truss 1632 246 18256 3.70000 13
element truss 1633 19246 256 3.70000 13
element truss 1634 19247 257 3.70000 13
element truss 1635 247 18257 3.70000 13
element truss 1636 248 18258 3.70000 13
element truss 1637 19248 258 3.70000 13
element truss 1638 19249 259 3.70000 13
element truss 1639 249 18259 3.70000 13
element truss 1640 2410 182510 3.70000 13
element truss 1641 192410 2510 3.70000 13
element truss 1642 192411 2511 3.70000 13
element truss 1643 2411 182511 3.70000 13
element truss 1644 2412 182512 3.70000 13
element truss 1645 192412 2512 3.70000 13
element truss 1646 192413 2513 3.70000 13
element truss 1647 2413 182513 3.70000 13
element truss 1648 2414 182514 3.70000 13
element truss 1649 192414 2514 3.70000 13
element truss 1650 192415 182515 3.70000 13
element truss 1651 19251 18261 3.70000 13
element truss 1652 19252 262 3.70000 13
element truss 1653 252 18262 3.70000 13
element truss 1654 253 18263 3.70000 13
element truss 1655 19253 263 3.70000 13
element truss 1656 19254 264 3.70000 13
element truss 1657 254 18264 3.70000 13
element truss 1658 255 18265 3.70000 13
element truss 1659 19255 265 3.70000 13
element truss 1660 19256 266 3.70000 13
element truss 1661 256 18266 3.70000 13
element truss 1662 257 18267 3.70000 13
element truss 1663 19257 267 3.70000 13
element truss 1664 19258 268 3.70000 13
element truss 1665 258 18268 3.70000 13
element truss 1666 259 18269 3.70000 13
element truss 1667 19259 269 3.70000 13
element truss 1668 192510 2610 3.70000 13
element truss 1669 2510 182610 3.70000 13
element truss 1670 2511 182611 3.70000 13
element truss 1671 192511 2611 3.70000 13
element truss 1672 192512 2612 3.70000 13
```

```
element truss 1673 2512 182612 3.70000 13
element truss 1674 2513 182613 3.70000 13
element truss 1675 192513 2613 3.70000 13
element truss 1676 192514 2614 3.70000 13
element truss 1677 2514 182614 3.70000 13
element truss 1678 182515 182615 3.70000 13
element truss 1679 18261 18271 3.70000 13
element truss 1680 262 18272 3.70000 13
element truss 1681 19262 272 3.70000 13
element truss 1682 19263 273 3.70000 13
element truss 1683 263 18273 3.70000 13
element truss 1684 264 18274 3.70000 13
element truss 1685 19264 274 3.70000 13
element truss 1686 19265 275 3.70000 13
element truss 1687 265 18275 3.70000 13
element truss 1688 266 18276 3.70000 13
element truss 1689 19266 276 3.70000 13
element truss 1690 19267 277 3.70000 13
element truss 1691 267 18277 3.70000 13
element truss 1692 268 18278 3.70000 13
element truss 1693 19268 278 3.70000 13
element truss 1694 19269 279 3.70000 13
element truss 1695 269 18279 3.70000 13
element truss 1696 2610 182710 3.70000 13
element truss 1697 192610 2710 3.70000 13
element truss 1698 192611 2711 3.70000 13
element truss 1699 2611 182711 3.70000 13
element truss 1700 2612 182712 3.70000 13
element truss 1701 192612 2712 3.70000 13
element truss 1702 192613 2713 3.70000 13
element truss 1703 2613 182713 3.70000 13
element truss 1704 2614 182714 3.70000 13
element truss 1705 192614 2714 3.70000 13
element truss 1706 192615 182715 3.70000 13
element truss 1707 19271 18281 3.70000 13
element truss 1708 19272 282 3.70000 13
element truss 1709 272 18282 3.70000 13
element truss 1710 273 18283 3.70000 13
element truss 1711 19273 283 3.70000 13
element truss 1712 19274 284 3.70000 13
element truss 1713 274 18284 3.70000 13
element truss 1714 275 18285 3.70000 13
element truss 1715 19275 285 3.70000 13
element truss 1716 19276 286 3.70000 13
element truss 1717 276 18286 3.70000 13
element truss 1718 277 18287 3.70000 13
element truss 1719 19277 287 3.70000 13
element truss 1720 19278 288 3.70000 13
element truss 1721 278 18288 3.70000 13
element truss 1722 279 18289 3.70000 13
element truss 1723 19279 289 3.70000 13
element truss 1724 192710 2810 3.70000 13
element truss 1725 2710 182810 3.70000 13
element truss 1726 2711 182811 3.70000 13
element truss 1727 192711 2811 3.70000 13
```

```
element truss 1728 192712 2812 3.70000 13
element truss 1729 2712 182812 3.70000 13
element truss 1730 2713 182813 3.70000 13
element truss 1731 192713 2813 3.70000 13
element truss 1732 192714 2814 3.70000 13
element truss 1733 2714 182814 3.70000 13
element truss 1734 182715 182815 3.70000 13
element truss 1735 18281 18291 3.70000 13
element truss 1736 282 18292 3.70000 13
element truss 1737 19282 292 3.70000 13
element truss 1738 19283 293 3.70000 13
element truss 1739 283 18293 3.70000 13
element truss 1740 284 18294 3.70000 13
element truss 1741 19284 294 3.70000 13
element truss 1742 19285 295 3.70000 13
element truss 1743 285 18295 3.70000 13
element truss 1744 286 18296 3.70000 13
element truss 1745 19286 296 3.70000 13
element truss 1746 19287 297 3.70000 13
element truss 1747 287 18297 3.70000 13
element truss 1748 288 18298 3.70000 13
element truss 1749 19288 298 3.70000 13
element truss 1750 19289 299 3.70000 13
element truss 1751 289 18299 3.70000 13
element truss 1752 2810 182910 3.70000 13
element truss 1753 192810 2910 3.70000 13
element truss 1754 192811 2911 3.70000 13
element truss 1755 2811 182911 3.70000 13
element truss 1756 2812 182912 3.70000 13
element truss 1757 192812 2912 3.70000 13
element truss 1758 192813 2913 3.70000 13
element truss 1759 2813 182913 3.70000 13
element truss 1760 2814 182914 3.70000 13
element truss 1761 192814 2914 3.70000 13
element truss 1762 192815 182915 3.70000 13
element truss 1763 19291 19301 3.70000 13
element truss 1764 19292 19302 3.70000 13
element truss 1765 292 18302 3.70000 13
element truss 1766 293 18303 3.70000 13
element truss 1767 19293 19303 3.70000 13
element truss 1768 19294 19304 3.70000 13
element truss 1769 294 18304 3.70000 13
element truss 1770 295 18305 3.70000 13
element truss 1771 19295 19305 3.70000 13
element truss 1772 19296 19306 3.70000 13
element truss 1773 296 18306 3.70000 13
element truss 1774 297 18307 3.70000 13
element truss 1775 19297 19307 3.70000 13
element truss 1776 19298 19308 3.70000 13
element truss 1777 298 18308 3.70000 13
element truss 1778 299 18309 3.70000 13
element truss 1779 19299 19309 3.70000 13
element truss 1780 192910 193010 3.70000 13
element truss 1781 2910 183010 3.70000 13
element truss 1782 2911 183011 3.70000 13
```

```
element truss      1783 192911 193011 3.70000 13
element truss      1784 192912 193012 3.70000 13
element truss      1785 2912 183012 3.70000 13
element truss      1786 2913 183013 3.70000 13
element truss      1787 192913 193013 3.70000 13
element truss      1788 192914 193014 3.70000 13
element truss      1789 2914 183014 3.70000 13
element truss      1790 182915 183015 3.70000 13


#Diagonal elements Infill Frame 1
element truss      1791 1891 102 5.23259 14
element truss      1792 18101 1992 5.23259 14
element truss      1793 1892 18103 5.23259 14
element truss      1794 18102 1893 5.23259 14
element truss      1795 1993 104 5.23259 14
element truss      1796 103 1994 5.23259 14
element truss      1797 1894 18105 5.23259 14
element truss      1798 18104 1895 5.23259 14
element truss      1799 1995 106 5.23259 14
element truss      1800 105 1996 5.23259 14
element truss      1801 1896 18107 5.23259 14
element truss      1802 18106 1897 5.23259 14
element truss      1803 1997 108 5.23259 14
element truss      1804 107 1998 5.23259 14
element truss      1805 1898 18109 5.23259 14
element truss      1806 18108 1899 5.23259 14
element truss      1807 1999 1010 5.23259 14
element truss      1808 109 19910 5.23259 14
element truss      1809 18910 181011 5.23259 14
element truss      1810 181010 18911 5.23259 14
element truss      1811 19911 1012 5.23259 14
element truss      1812 1011 19912 5.23259 14
element truss      1813 18912 181013 5.23259 14
element truss      1814 181012 18913 5.23259 14
element truss      1815 19913 1014 5.23259 14
element truss      1816 1013 19914 5.23259 14
element truss      1817 18914 181015 5.23259 14
element truss      1818 181014 18915 5.23259 14
element truss      1819 18101 18112 5.23259 14
element truss      1820 18111 102 5.23259 14
element truss      1821 19102 113 5.23259 14
element truss      1822 112 19103 5.23259 14
element truss      1823 103 18114 5.23259 14
element truss      1824 18113 104 5.23259 14
element truss      1825 19104 115 5.23259 14
element truss      1826 114 19105 5.23259 14
element truss      1827 105 18116 5.23259 14
element truss      1828 18115 106 5.23259 14
element truss      1829 19106 117 5.23259 14
element truss      1830 116 19107 5.23259 14
element truss      1831 107 18118 5.23259 14
element truss      1832 18117 108 5.23259 14
element truss      1833 19108 119 5.23259 14
element truss      1834 118 19109 5.23259 14
```

```
element truss 1835 109 181110 5.23259 14
element truss 1836 18119 1010 5.23259 14
element truss 1837 191010 1111 5.23259 14
element truss 1838 1110 191011 5.23259 14
element truss 1839 1011 181112 5.23259 14
element truss 1840 181111 1012 5.23259 14
element truss 1841 191012 1113 5.23259 14
element truss 1842 1112 191013 5.23259 14
element truss 1843 1013 181114 5.23259 14
element truss 1844 181113 1014 5.23259 14
element truss 1845 191014 181115 5.23259 14
element truss 1846 1114 191015 5.23259 14
element truss 1847 19111 122 5.23259 14
element truss 1848 18121 19112 5.23259 14
element truss 1849 112 18123 5.23259 14
element truss 1850 18122 113 5.23259 14
element truss 1851 19113 124 5.23259 14
element truss 1852 123 19114 5.23259 14
element truss 1853 114 18125 5.23259 14
element truss 1854 18124 115 5.23259 14
element truss 1855 19115 126 5.23259 14
element truss 1856 125 19116 5.23259 14
element truss 1857 116 18127 5.23259 14
element truss 1858 18126 117 5.23259 14
element truss 1859 19117 128 5.23259 14
element truss 1860 127 19118 5.23259 14
element truss 1861 118 18129 5.23259 14
element truss 1862 18128 119 5.23259 14
element truss 1863 19119 1210 5.23259 14
element truss 1864 129 191110 5.23259 14
element truss 1865 1110 181211 5.23259 14
element truss 1866 181210 1111 5.23259 14
element truss 1867 191111 1212 5.23259 14
element truss 1868 1211 191112 5.23259 14
element truss 1869 1112 181213 5.23259 14
element truss 1870 181212 1113 5.23259 14
element truss 1871 191113 1214 5.23259 14
element truss 1872 1213 191114 5.23259 14
element truss 1873 1114 181215 5.23259 14
element truss 1874 181214 181115 5.23259 14
element truss 1875 18121 18132 5.23259 14
element truss 1876 18131 122 5.23259 14
element truss 1877 19122 133 5.23259 14
element truss 1878 132 19123 5.23259 14
element truss 1879 123 18134 5.23259 14
element truss 1880 18133 124 5.23259 14
element truss 1881 19124 135 5.23259 14
element truss 1882 134 19125 5.23259 14
element truss 1883 125 18136 5.23259 14
element truss 1884 18135 126 5.23259 14
element truss 1885 19126 137 5.23259 14
element truss 1886 136 19127 5.23259 14
element truss 1887 127 18138 5.23259 14
element truss 1888 18137 128 5.23259 14
element truss 1889 19128 139 5.23259 14
```

```
element truss 1890 138 19129 5.23259 14
element truss 1891 129 181310 5.23259 14
element truss 1892 18139 1210 5.23259 14
element truss 1893 191210 1311 5.23259 14
element truss 1894 1310 191211 5.23259 14
element truss 1895 1211 181312 5.23259 14
element truss 1896 181311 1212 5.23259 14
element truss 1897 191212 1313 5.23259 14
element truss 1898 1312 191213 5.23259 14
element truss 1899 1213 181314 5.23259 14
element truss 1900 181313 1214 5.23259 14
element truss 1901 191214 181315 5.23259 14
element truss 1902 1314 191215 5.23259 14
element truss 1903 19131 142 5.23259 14
element truss 1904 18141 19132 5.23259 14
element truss 1905 132 18143 5.23259 14
element truss 1906 18142 133 5.23259 14
element truss 1907 19133 144 5.23259 14
element truss 1908 143 19134 5.23259 14
element truss 1909 134 18145 5.23259 14
element truss 1910 18144 135 5.23259 14
element truss 1911 19135 146 5.23259 14
element truss 1912 145 19136 5.23259 14
element truss 1913 136 18147 5.23259 14
element truss 1914 18146 137 5.23259 14
element truss 1915 19137 148 5.23259 14
element truss 1916 147 19138 5.23259 14
element truss 1917 138 18149 5.23259 14
element truss 1918 18148 139 5.23259 14
element truss 1919 19139 1410 5.23259 14
element truss 1920 149 191310 5.23259 14
element truss 1921 1310 181411 5.23259 14
element truss 1922 181410 1311 5.23259 14
element truss 1923 191311 1412 5.23259 14
element truss 1924 1411 191312 5.23259 14
element truss 1925 1312 181413 5.23259 14
element truss 1926 181412 1313 5.23259 14
element truss 1927 191313 1414 5.23259 14
element truss 1928 1413 191314 5.23259 14
element truss 1929 1314 181415 5.23259 14
element truss 1930 181414 181315 5.23259 14
element truss 1931 18141 18152 5.23259 14
element truss 1932 18151 142 5.23259 14
element truss 1933 19142 153 5.23259 14
element truss 1934 152 19143 5.23259 14
element truss 1935 143 18154 5.23259 14
element truss 1936 18153 144 5.23259 14
element truss 1937 19144 155 5.23259 14
element truss 1938 154 19145 5.23259 14
element truss 1939 145 18156 5.23259 14
element truss 1940 18155 146 5.23259 14
element truss 1941 19146 157 5.23259 14
element truss 1942 156 19147 5.23259 14
element truss 1943 147 18158 5.23259 14
element truss 1944 18157 148 5.23259 14
```

```
element truss 1945 19148 159 5.23259 14
element truss 1946 158 19149 5.23259 14
element truss 1947 149 181510 5.23259 14
element truss 1948 18159 1410 5.23259 14
element truss 1949 191410 1511 5.23259 14
element truss 1950 1510 191411 5.23259 14
element truss 1951 1411 181512 5.23259 14
element truss 1952 181511 1412 5.23259 14
element truss 1953 191412 1513 5.23259 14
element truss 1954 1512 191413 5.23259 14
element truss 1955 1413 181514 5.23259 14
element truss 1956 181513 1414 5.23259 14
element truss 1957 191414 181515 5.23259 14
element truss 1958 1514 191415 5.23259 14
element truss 1959 19151 162 5.23259 14
element truss 1960 18161 19152 5.23259 14
element truss 1961 152 18163 5.23259 14
element truss 1962 18162 153 5.23259 14
element truss 1963 19153 164 5.23259 14
element truss 1964 163 19154 5.23259 14
element truss 1965 154 18165 5.23259 14
element truss 1966 18164 155 5.23259 14
element truss 1967 19155 166 5.23259 14
element truss 1968 165 19156 5.23259 14
element truss 1969 156 18167 5.23259 14
element truss 1970 18166 157 5.23259 14
element truss 1971 19157 168 5.23259 14
element truss 1972 167 19158 5.23259 14
element truss 1973 158 18169 5.23259 14
element truss 1974 18168 159 5.23259 14
element truss 1975 19159 1610 5.23259 14
element truss 1976 169 191510 5.23259 14
element truss 1977 1510 181611 5.23259 14
element truss 1978 181610 1511 5.23259 14
element truss 1979 191511 1612 5.23259 14
element truss 1980 1611 191512 5.23259 14
element truss 1981 1512 181613 5.23259 14
element truss 1982 181612 1513 5.23259 14
element truss 1983 191513 1614 5.23259 14
element truss 1984 1613 191514 5.23259 14
element truss 1985 1514 181615 5.23259 14
element truss 1986 181614 181515 5.23259 14
element truss 1987 18161 18172 5.23259 14
element truss 1988 18171 162 5.23259 14
element truss 1989 19162 173 5.23259 14
element truss 1990 172 19163 5.23259 14
element truss 1991 163 18174 5.23259 14
element truss 1992 18173 164 5.23259 14
element truss 1993 19164 175 5.23259 14
element truss 1994 174 19165 5.23259 14
element truss 1995 165 18176 5.23259 14
element truss 1996 18175 166 5.23259 14
element truss 1997 19166 177 5.23259 14
element truss 1998 176 19167 5.23259 14
element truss 1999 167 18178 5.23259 14
```

```
element truss 2000 18177 168 5.23259 14
element truss 2001 19168 179 5.23259 14
element truss 2002 178 19169 5.23259 14
element truss 2003 169 181710 5.23259 14
element truss 2004 18179 1610 5.23259 14
element truss 2005 191610 1711 5.23259 14
element truss 2006 1710 191611 5.23259 14
element truss 2007 1611 181712 5.23259 14
element truss 2008 181711 1612 5.23259 14
element truss 2009 191612 1713 5.23259 14
element truss 2010 1712 191613 5.23259 14
element truss 2011 1613 181714 5.23259 14
element truss 2012 181713 1614 5.23259 14
element truss 2013 191614 181715 5.23259 14
element truss 2014 1714 191615 5.23259 14
element truss 2015 19171 182 5.23259 14
element truss 2016 18181 19172 5.23259 14
element truss 2017 172 18183 5.23259 14
element truss 2018 18182 173 5.23259 14
element truss 2019 19173 184 5.23259 14
element truss 2020 183 19174 5.23259 14
element truss 2021 174 18185 5.23259 14
element truss 2022 18184 175 5.23259 14
element truss 2023 19175 186 5.23259 14
element truss 2024 185 19176 5.23259 14
element truss 2025 176 18187 5.23259 14
element truss 2026 18186 177 5.23259 14
element truss 2027 19177 188 5.23259 14
element truss 2028 187 19178 5.23259 14
element truss 2029 178 18189 5.23259 14
element truss 2030 18188 179 5.23259 14
element truss 2031 19179 1810 5.23259 14
element truss 2032 189 191710 5.23259 14
element truss 2033 1710 181811 5.23259 14
element truss 2034 181810 1711 5.23259 14
element truss 2035 191711 1812 5.23259 14
element truss 2036 1811 191712 5.23259 14
element truss 2037 1712 181813 5.23259 14
element truss 2038 181812 1713 5.23259 14
element truss 2039 191713 1814 5.23259 14
element truss 2040 1813 191714 5.23259 14
element truss 2041 1714 181815 5.23259 14
element truss 2042 181814 181715 5.23259 14
element truss 2043 18181 18192 5.23259 14
element truss 2044 18191 182 5.23259 14
element truss 2045 19182 193 5.23259 14
element truss 2046 192 19183 5.23259 14
element truss 2047 183 18194 5.23259 14
element truss 2048 18193 184 5.23259 14
element truss 2049 19184 195 5.23259 14
element truss 2050 194 19185 5.23259 14
element truss 2051 185 18196 5.23259 14
element truss 2052 18195 186 5.23259 14
element truss 2053 19186 197 5.23259 14
element truss 2054 196 19187 5.23259 14
```

```
4511  element truss  2055 187 18198 5.23259 14
4512  element truss  2056 18197 188 5.23259 14
4513  element truss  2057 19188 199 5.23259 14
4514  element truss  2058 198 19189 5.23259 14
4515  element truss  2059 189 181910 5.23259 14
4516  element truss  2060 18199 1810 5.23259 14
4517  element truss  2061 191810 1911 5.23259 14
4518  element truss  2062 1910 191811 5.23259 14
4519  element truss  2063 1811 181912 5.23259 14
4520  element truss  2064 181911 1812 5.23259 14
4521  element truss  2065 191812 1913 5.23259 14
4522  element truss  2066 1912 191813 5.23259 14
4523  element truss  2067 1813 181914 5.23259 14
4524  element truss  2068 181913 1814 5.23259 14
4525  element truss  2069 191814 181915 5.23259 14
4526  element truss  2070 1914 191815 5.23259 14
4527  element truss  2071 19191 202 5.23259 14
4528  element truss  2072 18201 19192 5.23259 14
4529  element truss  2073 192 18203 5.23259 14
4530  element truss  2074 18202 193 5.23259 14
4531  element truss  2075 19193 204 5.23259 14
4532  element truss  2076 203 19194 5.23259 14
4533  element truss  2077 194 18205 5.23259 14
4534  element truss  2078 18204 195 5.23259 14
4535  element truss  2079 19195 206 5.23259 14
4536  element truss  2080 205 19196 5.23259 14
4537  element truss  2081 196 18207 5.23259 14
4538  element truss  2082 18206 197 5.23259 14
4539  element truss  2083 19197 208 5.23259 14
4540  element truss  2084 207 19198 5.23259 14
4541  element truss  2085 198 18209 5.23259 14
4542  element truss  2086 18208 199 5.23259 14
4543  element truss  2087 19199 2010 5.23259 14
4544  element truss  2088 209 191910 5.23259 14
4545  element truss  2089 1910 182011 5.23259 14
4546  element truss  2090 182010 1911 5.23259 14
4547  element truss  2091 191911 2012 5.23259 14
4548  element truss  2092 2011 191912 5.23259 14
4549  element truss  2093 1912 182013 5.23259 14
4550  element truss  2094 182012 1913 5.23259 14
4551  element truss  2095 191913 2014 5.23259 14
4552  element truss  2096 2013 191914 5.23259 14
4553  element truss  2097 1914 182015 5.23259 14
4554  element truss  2098 182014 181915 5.23259 14
4555  element truss  2099 18201 18212 5.23259 14
4556  element truss  2100 18211 202 5.23259 14
4557  element truss  2101 19202 213 5.23259 14
4558  element truss  2102 212 19203 5.23259 14
4559  element truss  2103 203 18214 5.23259 14
4560  element truss  2104 18213 204 5.23259 14
4561  element truss  2105 19204 215 5.23259 14
4562  element truss  2106 214 19205 5.23259 14
4563  element truss  2107 205 18216 5.23259 14
4564  element truss  2108 18215 206 5.23259 14
4565  element truss  2109 19206 217 5.23259 14
```

```
element truss 2110 216 19207 5.23259 14
element truss 2111 207 18218 5.23259 14
element truss 2112 18217 208 5.23259 14
element truss 2113 19208 219 5.23259 14
element truss 2114 218 19209 5.23259 14
element truss 2115 209 182110 5.23259 14
element truss 2116 18219 2010 5.23259 14
element truss 2117 192010 2111 5.23259 14
element truss 2118 2110 192011 5.23259 14
element truss 2119 2011 182112 5.23259 14
element truss 2120 182111 2012 5.23259 14
element truss 2121 192012 2113 5.23259 14
element truss 2122 2112 192013 5.23259 14
element truss 2123 2013 182114 5.23259 14
element truss 2124 182113 2014 5.23259 14
element truss 2125 192014 182115 5.23259 14
element truss 2126 2114 192015 5.23259 14
element truss 2127 19211 222 5.23259 14
element truss 2128 18221 19212 5.23259 14
element truss 2129 212 18223 5.23259 14
element truss 2130 18222 213 5.23259 14
element truss 2131 19213 224 5.23259 14
element truss 2132 223 19214 5.23259 14
element truss 2133 214 18225 5.23259 14
element truss 2134 18224 215 5.23259 14
element truss 2135 19215 226 5.23259 14
element truss 2136 225 19216 5.23259 14
element truss 2137 216 18227 5.23259 14
element truss 2138 18226 217 5.23259 14
element truss 2139 19217 228 5.23259 14
element truss 2140 227 19218 5.23259 14
element truss 2141 218 18229 5.23259 14
element truss 2142 18228 219 5.23259 14
element truss 2143 19219 2210 5.23259 14
element truss 2144 229 192110 5.23259 14
element truss 2145 2110 182211 5.23259 14
element truss 2146 182210 2111 5.23259 14
element truss 2147 192111 2212 5.23259 14
element truss 2148 2211 192112 5.23259 14
element truss 2149 2112 182213 5.23259 14
element truss 2150 182212 2113 5.23259 14
element truss 2151 192113 2214 5.23259 14
element truss 2152 2213 192114 5.23259 14
element truss 2153 2114 182215 5.23259 14
element truss 2154 182214 182115 5.23259 14
element truss 2155 18221 18232 5.23259 14
element truss 2156 18231 222 5.23259 14
element truss 2157 19222 233 5.23259 14
element truss 2158 232 19223 5.23259 14
element truss 2159 223 18234 5.23259 14
element truss 2160 18233 224 5.23259 14
element truss 2161 19224 235 5.23259 14
element truss 2162 234 19225 5.23259 14
element truss 2163 225 18236 5.23259 14
element truss 2164 18235 226 5.23259 14
```

```
element truss 2165 19226 237 5.23259 14
element truss 2166 236 19227 5.23259 14
element truss 2167 227 18238 5.23259 14
element truss 2168 18237 228 5.23259 14
element truss 2169 19228 239 5.23259 14
element truss 2170 238 19229 5.23259 14
element truss 2171 229 182310 5.23259 14
element truss 2172 18239 2210 5.23259 14
element truss 2173 192210 2311 5.23259 14
element truss 2174 2310 192211 5.23259 14
element truss 2175 2211 182312 5.23259 14
element truss 2176 182311 2212 5.23259 14
element truss 2177 192212 2313 5.23259 14
element truss 2178 2312 192213 5.23259 14
element truss 2179 2213 182314 5.23259 14
element truss 2180 182313 2214 5.23259 14
element truss 2181 192214 182315 5.23259 14
element truss 2182 2314 192215 5.23259 14
element truss 2183 19231 242 5.23259 14
element truss 2184 18241 19232 5.23259 14
element truss 2185 232 18243 5.23259 14
element truss 2186 18242 233 5.23259 14
element truss 2187 19233 244 5.23259 14
element truss 2188 243 19234 5.23259 14
element truss 2189 234 18245 5.23259 14
element truss 2190 18244 235 5.23259 14
element truss 2191 19235 246 5.23259 14
element truss 2192 245 19236 5.23259 14
element truss 2193 236 18247 5.23259 14
element truss 2194 18246 237 5.23259 14
element truss 2195 19237 248 5.23259 14
element truss 2196 247 19238 5.23259 14
element truss 2197 238 18249 5.23259 14
element truss 2198 18248 239 5.23259 14
element truss 2199 19239 2410 5.23259 14
element truss 2200 249 192310 5.23259 14
element truss 2201 2310 182411 5.23259 14
element truss 2202 182410 2311 5.23259 14
element truss 2203 192311 2412 5.23259 14
element truss 2204 2411 192312 5.23259 14
element truss 2205 2312 182413 5.23259 14
element truss 2206 182412 2313 5.23259 14
element truss 2207 192313 2414 5.23259 14
element truss 2208 2413 192314 5.23259 14
element truss 2209 2314 182415 5.23259 14
element truss 2210 182414 182315 5.23259 14
element truss 2211 18241 18252 5.23259 14
element truss 2212 18251 242 5.23259 14
element truss 2213 19242 253 5.23259 14
element truss 2214 252 19243 5.23259 14
element truss 2215 243 18254 5.23259 14
element truss 2216 18253 244 5.23259 14
element truss 2217 19244 255 5.23259 14
element truss 2218 254 19245 5.23259 14
element truss 2219 245 18256 5.23259 14
```

```
element truss 2220 18255 246 5.23259 14
element truss 2221 19246 257 5.23259 14
element truss 2222 256 19247 5.23259 14
element truss 2223 247 18258 5.23259 14
element truss 2224 18257 248 5.23259 14
element truss 2225 19248 259 5.23259 14
element truss 2226 258 19249 5.23259 14
element truss 2227 249 182510 5.23259 14
element truss 2228 18259 2410 5.23259 14
element truss 2229 192410 2511 5.23259 14
element truss 2230 2510 192411 5.23259 14
element truss 2231 2411 182512 5.23259 14
element truss 2232 182511 2412 5.23259 14
element truss 2233 192412 2513 5.23259 14
element truss 2234 2512 192413 5.23259 14
element truss 2235 2413 182514 5.23259 14
element truss 2236 182513 2414 5.23259 14
element truss 2237 192414 182515 5.23259 14
element truss 2238 2514 192415 5.23259 14
element truss 2239 19251 262 5.23259 14
element truss 2240 18261 19252 5.23259 14
element truss 2241 252 18263 5.23259 14
element truss 2242 18262 253 5.23259 14
element truss 2243 19253 264 5.23259 14
element truss 2244 263 19254 5.23259 14
element truss 2245 254 18265 5.23259 14
element truss 2246 18264 255 5.23259 14
element truss 2247 19255 266 5.23259 14
element truss 2248 265 19256 5.23259 14
element truss 2249 256 18267 5.23259 14
element truss 2250 18266 257 5.23259 14
element truss 2251 19257 268 5.23259 14
element truss 2252 267 19258 5.23259 14
element truss 2253 258 18269 5.23259 14
element truss 2254 18268 259 5.23259 14
element truss 2255 19259 2610 5.23259 14
element truss 2256 269 192510 5.23259 14
element truss 2257 2510 182611 5.23259 14
element truss 2258 182610 2511 5.23259 14
element truss 2259 192511 2612 5.23259 14
element truss 2260 2611 192512 5.23259 14
element truss 2261 2512 182613 5.23259 14
element truss 2262 182612 2513 5.23259 14
element truss 2263 192513 2614 5.23259 14
element truss 2264 2613 192514 5.23259 14
element truss 2265 2514 182615 5.23259 14
element truss 2266 182614 182515 5.23259 14
element truss 2267 18261 18272 5.23259 14
element truss 2268 18271 262 5.23259 14
element truss 2269 19262 273 5.23259 14
element truss 2270 272 19263 5.23259 14
element truss 2271 263 18274 5.23259 14
element truss 2272 18273 264 5.23259 14
element truss 2273 19264 275 5.23259 14
element truss 2274 274 19265 5.23259 14
```

```
4731  element truss  2275 265 18276 5.23259 14
4732  element truss  2276 18275 266 5.23259 14
4733  element truss  2277 19266 277 5.23259 14
4734  element truss  2278 276 19267 5.23259 14
4735  element truss  2279 267 18278 5.23259 14
4736  element truss  2280 18277 268 5.23259 14
4737  element truss  2281 19268 279 5.23259 14
4738  element truss  2282 278 19269 5.23259 14
4739  element truss  2283 269 182710 5.23259 14
4740  element truss  2284 18279 2610 5.23259 14
4741  element truss  2285 192610 2711 5.23259 14
4742  element truss  2286 2710 192611 5.23259 14
4743  element truss  2287 2611 182712 5.23259 14
4744  element truss  2288 182711 2612 5.23259 14
4745  element truss  2289 192612 2713 5.23259 14
4746  element truss  2290 2712 192613 5.23259 14
4747  element truss  2291 2613 182714 5.23259 14
4748  element truss  2292 182713 2614 5.23259 14
4749  element truss  2293 192614 182715 5.23259 14
4750  element truss  2294 2714 192615 5.23259 14
4751  element truss  2295 19271 282 5.23259 14
4752  element truss  2296 18281 19272 5.23259 14
4753  element truss  2297 272 18283 5.23259 14
4754  element truss  2298 18282 273 5.23259 14
4755  element truss  2299 19273 284 5.23259 14
4756  element truss  2300 283 19274 5.23259 14
4757  element truss  2301 274 18285 5.23259 14
4758  element truss  2302 18284 275 5.23259 14
4759  element truss  2303 19275 286 5.23259 14
4760  element truss  2304 285 19276 5.23259 14
4761  element truss  2305 276 18287 5.23259 14
4762  element truss  2306 18286 277 5.23259 14
4763  element truss  2307 19277 288 5.23259 14
4764  element truss  2308 287 19278 5.23259 14
4765  element truss  2309 278 18289 5.23259 14
4766  element truss  2310 18288 279 5.23259 14
4767  element truss  2311 19279 2810 5.23259 14
4768  element truss  2312 289 192710 5.23259 14
4769  element truss  2313 2710 182811 5.23259 14
4770  element truss  2314 182810 2711 5.23259 14
4771  element truss  2315 192711 2812 5.23259 14
4772  element truss  2316 2811 192712 5.23259 14
4773  element truss  2317 2712 182813 5.23259 14
4774  element truss  2318 182812 2713 5.23259 14
4775  element truss  2319 192713 2814 5.23259 14
4776  element truss  2320 2813 192714 5.23259 14
4777  element truss  2321 2714 182815 5.23259 14
4778  element truss  2322 182814 182715 5.23259 14
4779  element truss  2323 18281 18292 5.23259 14
4780  element truss  2324 18291 282 5.23259 14
4781  element truss  2325 19282 293 5.23259 14
4782  element truss  2326 292 19283 5.23259 14
4783  element truss  2327 283 18294 5.23259 14
4784  element truss  2328 18293 284 5.23259 14
4785  element truss  2329 19284 295 5.23259 14
```

```
element truss 2330 294 19285 5.23259 14
element truss 2331 285 18296 5.23259 14
element truss 2332 18295 286 5.23259 14
element truss 2333 19286 297 5.23259 14
element truss 2334 296 19287 5.23259 14
element truss 2335 287 18298 5.23259 14
element truss 2336 18297 288 5.23259 14
element truss 2337 19288 299 5.23259 14
element truss 2338 298 19289 5.23259 14
element truss 2339 289 182910 5.23259 14
element truss 2340 18299 2810 5.23259 14
element truss 2341 192810 2911 5.23259 14
element truss 2342 2910 192811 5.23259 14
element truss 2343 2811 182912 5.23259 14
element truss 2344 182911 2812 5.23259 14
element truss 2345 192812 2913 5.23259 14
element truss 2346 2912 192813 5.23259 14
element truss 2347 2813 182914 5.23259 14
element truss 2348 182913 2814 5.23259 14
element truss 2349 192814 182915 5.23259 14
element truss 2350 2914 192815 5.23259 14
element truss 2351 19291 19302 5.23259 14
element truss 2352 19301 19292 5.23259 14
element truss 2353 292 18303 5.23259 14
element truss 2354 18302 293 5.23259 14
element truss 2355 19293 19304 5.23259 14
element truss 2356 19303 19294 5.23259 14
element truss 2357 294 18305 5.23259 14
element truss 2358 18304 295 5.23259 14
element truss 2359 19295 19306 5.23259 14
element truss 2360 19305 19296 5.23259 14
element truss 2361 296 18307 5.23259 14
element truss 2362 18306 297 5.23259 14
element truss 2363 19297 19308 5.23259 14
element truss 2364 19307 19298 5.23259 14
element truss 2365 298 18309 5.23259 14
element truss 2366 18308 299 5.23259 14
element truss 2367 19299 193010 5.23259 14
element truss 2368 19309 192910 5.23259 14
element truss 2369 2910 183011 5.23259 14
element truss 2370 183010 2911 5.23259 14
element truss 2371 192911 193012 5.23259 14
element truss 2372 193011 192912 5.23259 14
element truss 2373 2912 183013 5.23259 14
element truss 2374 183012 2913 5.23259 14
element truss 2375 192913 193014 5.23259 14
element truss 2376 193013 192914 5.23259 14
element truss 2377 2914 183015 5.23259 14
element truss 2378 183014 182915 5.23259 14


#ZLE for discrete spring interfaces Frame 1


#ZLE Tag 18 Frame 1
```

```
element flatSliderBearing  2380 102 18102 10 110.000012345600 -P 20 -Mz 20  -orient 0. 1. 0. 1. 0. 0.;
element zeroLength         11321 102 18102 -mat  31 -dir 2;
element zeroLength         12641 102 18102 -mat  30 -dir 1;

element flatSliderBearing  2640 19102 18102 10 110.000012345600 -P 21 -Mz 21  -orient -1. 0. 0. 0. 1. 0.;
element zeroLength         11581 19102 18102 -mat  41 -dir 1;
element zeroLength         12901 19102 18102 -mat  40 -dir 2;

element flatSliderBearing  2381 18103 103 10 110.000012345600 -P 20 -Mz 20  -orient 0. 1. 0. 1. 0. 0.;
element zeroLength         11322 18103 103 -mat  31 -dir 2;
element zeroLength         12642 18103 103 -mat  30 -dir 1;

element flatSliderBearing  2641 19103 18103 10 110.000012345600 -P 21 -Mz 21  -orient -1. 0. 0. 0. 1. 0.;
element zeroLength         11582 19103 18103 -mat  41 -dir 1;
element zeroLength         12902 19103 18103 -mat  40 -dir 2;

element flatSliderBearing  2382 104 18104 10 110.000012345600 -P 20 -Mz 20  -orient 0. 1. 0. 1. 0. 0.;
element zeroLength         11323 104 18104 -mat  31 -dir 2;
element zeroLength         12643 104 18104 -mat  30 -dir 1;

element flatSliderBearing  2642 19104 18104 10 110.000012345600 -P 21 -Mz 21  -orient -1. 0. 0. 0. 1. 0.;
element zeroLength         11583 19104 18104 -mat  41 -dir 1;
element zeroLength         12903 19104 18104 -mat  40 -dir 2;

element flatSliderBearing  2383 18105 105 10 110.000012345600 -P 20 -Mz 20  -orient 0. 1. 0. 1. 0. 0.;
element zeroLength         11324 18105 105 -mat  31 -dir 2;
element zeroLength         12644 18105 105 -mat  30 -dir 1;

element flatSliderBearing  2643 19105 18105 10 110.000012345600 -P 21 -Mz 21  -orient -1. 0. 0. 0. 1. 0.;
element zeroLength         11584 19105 18105 -mat  41 -dir 1;
element zeroLength         12904 19105 18105 -mat  40 -dir 2;

element flatSliderBearing  2384 106 18106 10 110.000012345600 -P 20 -Mz 20  -orient 0. 1. 0. 1. 0. 0.;
element zeroLength         11325 106 18106 -mat  31 -dir 2;
element zeroLength         12645 106 18106 -mat  30 -dir 1;

element flatSliderBearing  2644 19106 18106 10 110.000012345600 -P 21 -Mz 21  -orient -1. 0. 0. 0. 1. 0.;
element zeroLength         11585 19106 18106 -mat  41 -dir 1;
element zeroLength         12905 19106 18106 -mat  40 -dir 2;

element flatSliderBearing  2385 18107 107 10 110.000012345600 -P 20 -Mz 20  -orient 0. 1. 0. 1. 0. 0.;
element zeroLength         11326 18107 107 -mat  31 -dir 2;
element zeroLength         12646 18107 107 -mat  30 -dir 1;

element flatSliderBearing  2645 19107 18107 10 110.000012345600 -P 21 -Mz 21  -orient -1. 0. 0. 0. 1. 0.;
element zeroLength         11586 19107 18107 -mat  41 -dir 1;
element zeroLength         12906 19107 18107 -mat  40 -dir 2;

element flatSliderBearing  2386 108 18108 10 110.000012345600 -P 20 -Mz 20  -orient 0. 1. 0. 1. 0. 0.;
element zeroLength         11327 108 18108 -mat  31 -dir 2;
element zeroLength         12647 108 18108 -mat  30 -dir 1;

element flatSliderBearing  2646 19108 18108 10 110.000012345600 -P 21 -Mz 21  -orient -1. 0. 0. 0. 1. 0.;
element zeroLength         11587 19108 18108 -mat  41 -dir 1;
```

```
element zeroLength          12907 19108 18108 -mat  40 -dir 2;

element flatSliderBearing   2387 18109 109 10 110.000012345600 -P 20 -Mz 20  -orient 0. 1. 0. 1. 0. 0.;
element zeroLength          11328 18109 109 -mat  31 -dir 2;
element zeroLength          12648 18109 109 -mat  30 -dir 1;

element flatSliderBearing   2647 19109 18109 10 110.000012345600 -P 21 -Mz 21  -orient -1. 0. 0. 0. 1. 0.;
element zeroLength          11588 19109 18109 -mat  41 -dir 1;
element zeroLength          12908 19109 18109 -mat  40 -dir 2;

element flatSliderBearing   2388 1010 181010 10 110.000012345600 -P 20 -Mz 20  -orient 0. 1. 0. 1. 0. 0.;
element zeroLength          11329 1010 181010 -mat  31 -dir 2;
element zeroLength          12649 1010 181010 -mat  30 -dir 1;

element flatSliderBearing   2648 191010 181010 10 110.000012345600 -P 21 -Mz 21  -orient -1. 0. 0. 0. 1. 0.;
element zeroLength          11589 191010 181010 -mat  41 -dir 1;
element zeroLength          12909 191010 181010 -mat  40 -dir 2;

element flatSliderBearing   2389 181011 1011 10 110.000012345600 -P 20 -Mz 20  -orient 0. 1. 0. 1. 0. 0.;
element zeroLength          11330 181011 1011 -mat  31 -dir 2;
element zeroLength          12650 181011 1011 -mat  30 -dir 1;

element flatSliderBearing   2649 191011 181011 10 110.000012345600 -P 21 -Mz 21  -orient -1. 0. 0. 0. 1. 0.;
element zeroLength          11590 191011 181011 -mat  41 -dir 1;
element zeroLength          12910 191011 181011 -mat  40 -dir 2;

element flatSliderBearing   2390 1012 181012 10 110.000012345600 -P 20 -Mz 20  -orient 0. 1. 0. 1. 0. 0.;
element zeroLength          11331 1012 181012 -mat  31 -dir 2;
element zeroLength          12651 1012 181012 -mat  30 -dir 1;

element flatSliderBearing   2650 191012 181012 10 110.000012345600 -P 21 -Mz 21  -orient -1. 0. 0. 0. 1. 0.;
element zeroLength          11591 191012 181012 -mat  41 -dir 1;
element zeroLength          12911 191012 181012 -mat  40 -dir 2;

element flatSliderBearing   2391 181013 1013 10 110.000012345600 -P 20 -Mz 20  -orient 0. 1. 0. 1. 0. 0.;
element zeroLength          11332 181013 1013 -mat  31 -dir 2;
element zeroLength          12652 181013 1013 -mat  30 -dir 1;

element flatSliderBearing   2651 191013 181013 10 110.000012345600 -P 21 -Mz 21  -orient -1. 0. 0. 0. 1. 0.;
element zeroLength          11592 191013 181013 -mat  41 -dir 1;
element zeroLength          12912 191013 181013 -mat  40 -dir 2;

element flatSliderBearing   2392 1014 181014 10 110.000012345600 -P 20 -Mz 20  -orient 0. 1. 0. 1. 0. 0.;
element zeroLength          11333 1014 181014 -mat  31 -dir 2;
element zeroLength          12653 1014 181014 -mat  30 -dir 1;

element flatSliderBearing   2652 191014 181014 10 110.000012345600 -P 21 -Mz 21  -orient -1. 0. 0. 0. 1. 0.;
element zeroLength          11593 191014 181014 -mat  41 -dir 1;
element zeroLength          12913 191014 181014 -mat  40 -dir 2;

element flatSliderBearing   2393 18112 112 10 110.000012345600 -P 20 -Mz 20  -orient 0. 1. 0. 1. 0. 0.;
element zeroLength          11334 18112 112 -mat  31 -dir 2;
element zeroLength          12654 18112 112 -mat  30 -dir 1;

element flatSliderBearing   2653 19112 18112 10 110.000012345600 -P 21 -Mz 21  -orient -1. 0. 0. 0. 1. 0.;
```

```
element zeroLength          11594 19112 18112 -mat  41 -dir 1;
element zeroLength          12914 19112 18112 -mat  40 -dir 2;

element flatSliderBearing   2394 113 18113 10 110.000012345600 -P 20 -Mz 20  -orient 0. 1. 0. 1. 0. 0.;
element zeroLength          11335 113 18113 -mat  31 -dir 2;
element zeroLength          12655 113 18113 -mat  30 -dir 1;

element flatSliderBearing   2654 19113 18113 10 110.000012345600 -P 21 -Mz 21  -orient -1. 0. 0. 0. 1. 0.;
element zeroLength          11595 19113 18113 -mat  41 -dir 1;
element zeroLength          12915 19113 18113 -mat  40 -dir 2;

element flatSliderBearing   2395 18114 114 10 110.000012345600 -P 20 -Mz 20  -orient 0. 1. 0. 1. 0. 0.;
element zeroLength          11336 18114 114 -mat  31 -dir 2;
element zeroLength          12656 18114 114 -mat  30 -dir 1;

element flatSliderBearing   2655 19114 18114 10 110.000012345600 -P 21 -Mz 21  -orient -1. 0. 0. 0. 1. 0.;
element zeroLength          11596 19114 18114 -mat  41 -dir 1;
element zeroLength          12916 19114 18114 -mat  40 -dir 2;

element flatSliderBearing   2396 115 18115 10 110.000012345600 -P 20 -Mz 20  -orient 0. 1. 0. 1. 0. 0.;
element zeroLength          11337 115 18115 -mat  31 -dir 2;
element zeroLength          12657 115 18115 -mat  30 -dir 1;

element flatSliderBearing   2656 19115 18115 10 110.000012345600 -P 21 -Mz 21  -orient -1. 0. 0. 0. 1. 0.;
element zeroLength          11597 19115 18115 -mat  41 -dir 1;
element zeroLength          12917 19115 18115 -mat  40 -dir 2;

element flatSliderBearing   2397 18116 116 10 110.000012345600 -P 20 -Mz 20  -orient 0. 1. 0. 1. 0. 0.;
element zeroLength          11338 18116 116 -mat  31 -dir 2;
element zeroLength          12658 18116 116 -mat  30 -dir 1;

element flatSliderBearing   2657 19116 18116 10 110.000012345600 -P 21 -Mz 21  -orient -1. 0. 0. 0. 1. 0.;
element zeroLength          11598 19116 18116 -mat  41 -dir 1;
element zeroLength          12918 19116 18116 -mat  40 -dir 2;

element flatSliderBearing   2398 117 18117 10 110.000012345600 -P 20 -Mz 20  -orient 0. 1. 0. 1. 0. 0.;
element zeroLength          11339 117 18117 -mat  31 -dir 2;
element zeroLength          12659 117 18117 -mat  30 -dir 1;

element flatSliderBearing   2658 19117 18117 10 110.000012345600 -P 21 -Mz 21  -orient -1. 0. 0. 0. 1. 0.;
element zeroLength          11599 19117 18117 -mat  41 -dir 1;
element zeroLength          12919 19117 18117 -mat  40 -dir 2;

element flatSliderBearing   2399 18118 118 10 110.000012345600 -P 20 -Mz 20  -orient 0. 1. 0. 1. 0. 0.;
element zeroLength          11340 18118 118 -mat  31 -dir 2;
element zeroLength          12660 18118 118 -mat  30 -dir 1;

element flatSliderBearing   2659 19118 18118 10 110.000012345600 -P 21 -Mz 21  -orient -1. 0. 0. 0. 1. 0.;
element zeroLength          11600 19118 18118 -mat  41 -dir 1;
element zeroLength          12920 19118 18118 -mat  40 -dir 2;

element flatSliderBearing   2400 119 18119 10 110.000012345600 -P 20 -Mz 20  -orient 0. 1. 0. 1. 0. 0.;
element zeroLength          11341 119 18119 -mat  31 -dir 2;
element zeroLength          12661 119 18119 -mat  30 -dir 1;
```

```
element flatSliderBearing  2660 19119 18119 10 110.000012345600 -P 21 -Mz 21  -orient -1. 0. 0. 0. 1. 0.;
element zeroLength         11601 19119 18119 -mat  41 -dir 1;
element zeroLength         12921 19119 18119 -mat  40 -dir 2;

element flatSliderBearing  2401 181110 1110 10 110.000012345600 -P 20 -Mz 20  -orient 0. 1. 0. 1. 0. 0.;
element zeroLength         11342 181110 1110 -mat  31 -dir 2;
element zeroLength         12662 181110 1110 -mat  30 -dir 1;

element flatSliderBearing  2661 191110 181110 10 110.000012345600 -P 21 -Mz 21  -orient -1. 0. 0. 0. 1. 0.;
element zeroLength         11602 191110 181110 -mat  41 -dir 1;
element zeroLength         12922 191110 181110 -mat  40 -dir 2;

element flatSliderBearing  2402 1111 181111 10 110.000012345600 -P 20 -Mz 20  -orient 0. 1. 0. 1. 0. 0.;
element zeroLength         11343 1111 181111 -mat  31 -dir 2;
element zeroLength         12663 1111 181111 -mat  30 -dir 1;

element flatSliderBearing  2662 191111 181111 10 110.000012345600 -P 21 -Mz 21  -orient -1. 0. 0. 0. 1. 0.;
element zeroLength         11603 191111 181111 -mat  41 -dir 1;
element zeroLength         12923 191111 181111 -mat  40 -dir 2;

element flatSliderBearing  2403 181112 1112 10 110.000012345600 -P 20 -Mz 20  -orient 0. 1. 0. 1. 0. 0.;
element zeroLength         11344 181112 1112 -mat  31 -dir 2;
element zeroLength         12664 181112 1112 -mat  30 -dir 1;

element flatSliderBearing  2663 191112 181112 10 110.000012345600 -P 21 -Mz 21  -orient -1. 0. 0. 0. 1. 0.;
element zeroLength         11604 191112 181112 -mat  41 -dir 1;
element zeroLength         12924 191112 181112 -mat  40 -dir 2;

element flatSliderBearing  2404 1113 181113 10 110.000012345600 -P 20 -Mz 20  -orient 0. 1. 0. 1. 0. 0.;
element zeroLength         11345 1113 181113 -mat  31 -dir 2;
element zeroLength         12665 1113 181113 -mat  30 -dir 1;

element flatSliderBearing  2664 191113 181113 10 110.000012345600 -P 21 -Mz 21  -orient -1. 0. 0. 0. 1. 0.;
element zeroLength         11605 191113 181113 -mat  41 -dir 1;
element zeroLength         12925 191113 181113 -mat  40 -dir 2;

element flatSliderBearing  2405 181114 1114 10 110.000012345600 -P 20 -Mz 20  -orient 0. 1. 0. 1. 0. 0.;
element zeroLength         11346 181114 1114 -mat  31 -dir 2;
element zeroLength         12666 181114 1114 -mat  30 -dir 1;

element flatSliderBearing  2665 191114 181114 10 110.000012345600 -P 21 -Mz 21  -orient -1. 0. 0. 0. 1. 0.;
element zeroLength         11606 191114 181114 -mat  41 -dir 1;
element zeroLength         12926 191114 181114 -mat  40 -dir 2;

element flatSliderBearing  2406 122 18122 10 110.000012345600 -P 20 -Mz 20  -orient 0. 1. 0. 1. 0. 0.;
element zeroLength         11347 122 18122 -mat  31 -dir 2;
element zeroLength         12667 122 18122 -mat  30 -dir 1;

element flatSliderBearing  2666 19122 18122 10 110.000012345600 -P 21 -Mz 21  -orient -1. 0. 0. 0. 1. 0.;
element zeroLength         11607 19122 18122 -mat  41 -dir 1;
element zeroLength         12927 19122 18122 -mat  40 -dir 2;

element flatSliderBearing  2407 18123 123 10 110.000012345600 -P 20 -Mz 20  -orient 0. 1. 0. 1. 0. 0.;
element zeroLength         11348 18123 123 -mat  31 -dir 2;
element zeroLength         12668 18123 123 -mat  30 -dir 1;
```

```
5061
5062  element flatSliderBearing  2667 19123 18123 10 110.000012345600 -P 21 -Mz 21  -orient -1. 0. 0. 0. 1. 0.;
5063  element zeroLength         11608 19123 18123 -mat  41 -dir 1;
5064  element zeroLength         12928 19123 18123 -mat  40 -dir 2;
5065
5066  element flatSliderBearing  2408 124 18124 10 110.000012345600 -P 20 -Mz 20  -orient 0. 1. 0. 1. 0. 0.;
5067  element zeroLength         11349 124 18124 -mat  31 -dir 2;
5068  element zeroLength         12669 124 18124 -mat  30 -dir 1;
5069
5070  element flatSliderBearing  2668 19124 18124 10 110.000012345600 -P 21 -Mz 21  -orient -1. 0. 0. 0. 1. 0.;
5071  element zeroLength         11609 19124 18124 -mat  41 -dir 1;
5072  element zeroLength         12929 19124 18124 -mat  40 -dir 2;
5073
5074  element flatSliderBearing  2409 18125 125 10 110.000012345600 -P 20 -Mz 20  -orient 0. 1. 0. 1. 0. 0.;
5075  element zeroLength         11350 18125 125 -mat  31 -dir 2;
5076  element zeroLength         12670 18125 125 -mat  30 -dir 1;
5077
5078  element flatSliderBearing  2669 19125 18125 10 110.000012345600 -P 21 -Mz 21  -orient -1. 0. 0. 0. 1. 0.;
5079  element zeroLength         11610 19125 18125 -mat  41 -dir 1;
5080  element zeroLength         12930 19125 18125 -mat  40 -dir 2;
5081
5082  element flatSliderBearing  2410 126 18126 10 110.000012345600 -P 20 -Mz 20  -orient 0. 1. 0. 1. 0. 0.;
5083  element zeroLength         11351 126 18126 -mat  31 -dir 2;
5084  element zeroLength         12671 126 18126 -mat  30 -dir 1;
5085
5086  element flatSliderBearing  2670 19126 18126 10 110.000012345600 -P 21 -Mz 21  -orient -1. 0. 0. 0. 1. 0.;
5087  element zeroLength         11611 19126 18126 -mat  41 -dir 1;
5088  element zeroLength         12931 19126 18126 -mat  40 -dir 2;
5089
5090  element flatSliderBearing  2411 18127 127 10 110.000012345600 -P 20 -Mz 20  -orient 0. 1. 0. 1. 0. 0.;
5091  element zeroLength         11352 18127 127 -mat  31 -dir 2;
5092  element zeroLength         12672 18127 127 -mat  30 -dir 1;
5093
5094  element flatSliderBearing  2671 19127 18127 10 110.000012345600 -P 21 -Mz 21  -orient -1. 0. 0. 0. 1. 0.;
5095  element zeroLength         11612 19127 18127 -mat  41 -dir 1;
5096  element zeroLength         12932 19127 18127 -mat  40 -dir 2;
5097
5098  element flatSliderBearing  2412 128 18128 10 110.000012345600 -P 20 -Mz 20  -orient 0. 1. 0. 1. 0. 0.;
5099  element zeroLength         11353 128 18128 -mat  31 -dir 2;
5100  element zeroLength         12673 128 18128 -mat  30 -dir 1;
5101
5102  element flatSliderBearing  2672 19128 18128 10 110.000012345600 -P 21 -Mz 21  -orient -1. 0. 0. 0. 1. 0.;
5103  element zeroLength         11613 19128 18128 -mat  41 -dir 1;
5104  element zeroLength         12933 19128 18128 -mat  40 -dir 2;
5105
5106  element flatSliderBearing  2413 18129 129 10 110.000012345600 -P 20 -Mz 20  -orient 0. 1. 0. 1. 0. 0.;
5107  element zeroLength         11354 18129 129 -mat  31 -dir 2;
5108  element zeroLength         12674 18129 129 -mat  30 -dir 1;
5109
5110  element flatSliderBearing  2673 19129 18129 10 110.000012345600 -P 21 -Mz 21  -orient -1. 0. 0. 0. 1. 0.;
5111  element zeroLength         11614 19129 18129 -mat  41 -dir 1;
5112  element zeroLength         12934 19129 18129 -mat  40 -dir 2;
5113
5114  element flatSliderBearing  2414 1210 181210 10 110.000012345600 -P 20 -Mz 20  -orient 0. 1. 0. 1. 0. 0.;
5115  element zeroLength         11355 1210 181210 -mat  31 -dir 2;
```

```
element zeroLength          12675 1210 181210 -mat  30 -dir 1;

element flatSliderBearing   2674 191210 181210 10 110.000012345600 -P 21 -Mz 21  -orient -1. 0. 0. 0. 1. 0.;
element zeroLength          11615 191210 181210 -mat  41 -dir 1;
element zeroLength          12935 191210 181210 -mat  40 -dir 2;

element flatSliderBearing   2415 181211 1211 10 110.000012345600 -P 20 -Mz 20  -orient 0. 1. 0. 1. 0. 0.;
element zeroLength          11356 181211 1211 -mat  31 -dir 2;
element zeroLength          12676 181211 1211 -mat  30 -dir 1;

element flatSliderBearing   2675 191211 181211 10 110.000012345600 -P 21 -Mz 21  -orient -1. 0. 0. 0. 1. 0.;
element zeroLength          11616 191211 181211 -mat  41 -dir 1;
element zeroLength          12936 191211 181211 -mat  40 -dir 2;

element flatSliderBearing   2416 1212 181212 10 110.000012345600 -P 20 -Mz 20  -orient 0. 1. 0. 1. 0. 0.;
element zeroLength          11357 1212 181212 -mat  31 -dir 2;
element zeroLength          12677 1212 181212 -mat  30 -dir 1;

element flatSliderBearing   2676 191212 181212 10 110.000012345600 -P 21 -Mz 21  -orient -1. 0. 0. 0. 1. 0.;
element zeroLength          11617 191212 181212 -mat  41 -dir 1;
element zeroLength          12937 191212 181212 -mat  40 -dir 2;

element flatSliderBearing   2417 181213 1213 10 110.000012345600 -P 20 -Mz 20  -orient 0. 1. 0. 1. 0. 0.;
element zeroLength          11358 181213 1213 -mat  31 -dir 2;
element zeroLength          12678 181213 1213 -mat  30 -dir 1;

element flatSliderBearing   2677 191213 181213 10 110.000012345600 -P 21 -Mz 21  -orient -1. 0. 0. 0. 1. 0.;
element zeroLength          11618 191213 181213 -mat  41 -dir 1;
element zeroLength          12938 191213 181213 -mat  40 -dir 2;

element flatSliderBearing   2418 1214 181214 10 110.000012345600 -P 20 -Mz 20  -orient 0. 1. 0. 1. 0. 0.;
element zeroLength          11359 1214 181214 -mat  31 -dir 2;
element zeroLength          12679 1214 181214 -mat  30 -dir 1;

element flatSliderBearing   2678 191214 181214 10 110.000012345600 -P 21 -Mz 21  -orient -1. 0. 0. 0. 1. 0.;
element zeroLength          11619 191214 181214 -mat  41 -dir 1;
element zeroLength          12939 191214 181214 -mat  40 -dir 2;

element flatSliderBearing   2419 18132 132 10 110.000012345600 -P 20 -Mz 20  -orient 0. 1. 0. 1. 0. 0.;
element zeroLength          11360 18132 132 -mat  31 -dir 2;
element zeroLength          12680 18132 132 -mat  30 -dir 1;

element flatSliderBearing   2679 19132 18132 10 110.000012345600 -P 21 -Mz 21  -orient -1. 0. 0. 0. 1. 0.;
element zeroLength          11620 19132 18132 -mat  41 -dir 1;
element zeroLength          12940 19132 18132 -mat  40 -dir 2;

element flatSliderBearing   2420 133 18133 10 110.000012345600 -P 20 -Mz 20  -orient 0. 1. 0. 1. 0. 0.;
element zeroLength          11361 133 18133 -mat  31 -dir 2;
element zeroLength          12681 133 18133 -mat  30 -dir 1;

element flatSliderBearing   2680 19133 18133 10 110.000012345600 -P 21 -Mz 21  -orient -1. 0. 0. 0. 1. 0.;
element zeroLength          11621 19133 18133 -mat  41 -dir 1;
element zeroLength          12941 19133 18133 -mat  40 -dir 2;

element flatSliderBearing   2421 18134 134 10 110.000012345600 -P 20 -Mz 20  -orient 0. 1. 0. 1. 0. 0.;
```

```
element zeroLength          11362 18134 134 -mat  31 -dir 2;
element zeroLength          12682 18134 134 -mat  30 -dir 1;

element flatSliderBearing   2681 19134 18134 10 110.000012345600 -P 21 -Mz 21  -orient -1. 0. 0. 0. 1. 0.;
element zeroLength          11622 19134 18134 -mat  41 -dir 1;
element zeroLength          12942 19134 18134 -mat  40 -dir 2;

element flatSliderBearing   2422 135 18135 10 110.000012345600 -P 20 -Mz 20  -orient 0. 1. 0. 1. 0. 0.;
element zeroLength          11363 135 18135 -mat  31 -dir 2;
element zeroLength          12683 135 18135 -mat  30 -dir 1;

element flatSliderBearing   2682 19135 18135 10 110.000012345600 -P 21 -Mz 21  -orient -1. 0. 0. 0. 1. 0.;
element zeroLength          11623 19135 18135 -mat  41 -dir 1;
element zeroLength          12943 19135 18135 -mat  40 -dir 2;

element flatSliderBearing   2423 18136 136 10 110.000012345600 -P 20 -Mz 20  -orient 0. 1. 0. 1. 0. 0.;
element zeroLength          11364 18136 136 -mat  31 -dir 2;
element zeroLength          12684 18136 136 -mat  30 -dir 1;

element flatSliderBearing   2683 19136 18136 10 110.000012345600 -P 21 -Mz 21  -orient -1. 0. 0. 0. 1. 0.;
element zeroLength          11624 19136 18136 -mat  41 -dir 1;
element zeroLength          12944 19136 18136 -mat  40 -dir 2;

element flatSliderBearing   2424 137 18137 10 110.000012345600 -P 20 -Mz 20  -orient 0. 1. 0. 1. 0. 0.;
element zeroLength          11365 137 18137 -mat  31 -dir 2;
element zeroLength          12685 137 18137 -mat  30 -dir 1;

element flatSliderBearing   2684 19137 18137 10 110.000012345600 -P 21 -Mz 21  -orient -1. 0. 0. 0. 1. 0.;
element zeroLength          11625 19137 18137 -mat  41 -dir 1;
element zeroLength          12945 19137 18137 -mat  40 -dir 2;

element flatSliderBearing   2425 18138 138 10 110.000012345600 -P 20 -Mz 20  -orient 0. 1. 0. 1. 0. 0.;
element zeroLength          11366 18138 138 -mat  31 -dir 2;
element zeroLength          12686 18138 138 -mat  30 -dir 1;

element flatSliderBearing   2685 19138 18138 10 110.000012345600 -P 21 -Mz 21  -orient -1. 0. 0. 0. 1. 0.;
element zeroLength          11626 19138 18138 -mat  41 -dir 1;
element zeroLength          12946 19138 18138 -mat  40 -dir 2;

element flatSliderBearing   2426 139 18139 10 110.000012345600 -P 20 -Mz 20  -orient 0. 1. 0. 1. 0. 0.;
element zeroLength          11367 139 18139 -mat  31 -dir 2;
element zeroLength          12687 139 18139 -mat  30 -dir 1;

element flatSliderBearing   2686 19139 18139 10 110.000012345600 -P 21 -Mz 21  -orient -1. 0. 0. 0. 1. 0.;
element zeroLength          11627 19139 18139 -mat  41 -dir 1;
element zeroLength          12947 19139 18139 -mat  40 -dir 2;

element flatSliderBearing   2427 181310 1310 10 110.000012345600 -P 20 -Mz 20  -orient 0. 1. 0. 1. 0. 0.;
element zeroLength          11368 181310 1310 -mat  31 -dir 2;
element zeroLength          12688 181310 1310 -mat  30 -dir 1;

element flatSliderBearing   2687 191310 181310 10 110.000012345600 -P 21 -Mz 21  -orient -1. 0. 0. 0. 1. 0.;
element zeroLength          11628 191310 181310 -mat  41 -dir 1;
element zeroLength          12948 191310 181310 -mat  40 -dir 2;
```

```
element flatSliderBearing  2428 1311 181311 10 110.000012345600 -P 20 -Mz 20  -orient 0. 1. 0. 1. 0. 0.;
element zeroLength         11369 1311 181311 -mat  31 -dir 2;
element zeroLength         12689 1311 181311 -mat  30 -dir 1;

element flatSliderBearing  2688 191311 181311 10 110.000012345600 -P 21 -Mz 21  -orient -1. 0. 0. 0. 1. 0.;
element zeroLength         11629 191311 181311 -mat  41 -dir 1;
element zeroLength         12949 191311 181311 -mat  40 -dir 2;

element flatSliderBearing  2429 181312 1312 10 110.000012345600 -P 20 -Mz 20  -orient 0. 1. 0. 1. 0. 0.;
element zeroLength         11370 181312 1312 -mat  31 -dir 2;
element zeroLength         12690 181312 1312 -mat  30 -dir 1;

element flatSliderBearing  2689 191312 181312 10 110.000012345600 -P 21 -Mz 21  -orient -1. 0. 0. 0. 1. 0.;
element zeroLength         11630 191312 181312 -mat  41 -dir 1;
element zeroLength         12950 191312 181312 -mat  40 -dir 2;

element flatSliderBearing  2430 1313 181313 10 110.000012345600 -P 20 -Mz 20  -orient 0. 1. 0. 1. 0. 0.;
element zeroLength         11371 1313 181313 -mat  31 -dir 2;
element zeroLength         12691 1313 181313 -mat  30 -dir 1;

element flatSliderBearing  2690 191313 181313 10 110.000012345600 -P 21 -Mz 21  -orient -1. 0. 0. 0. 1. 0.;
element zeroLength         11631 191313 181313 -mat  41 -dir 1;
element zeroLength         12951 191313 181313 -mat  40 -dir 2;

element flatSliderBearing  2431 181314 1314 10 110.000012345600 -P 20 -Mz 20  -orient 0. 1. 0. 1. 0. 0.;
element zeroLength         11372 181314 1314 -mat  31 -dir 2;
element zeroLength         12692 181314 1314 -mat  30 -dir 1;

element flatSliderBearing  2691 191314 181314 10 110.000012345600 -P 21 -Mz 21  -orient -1. 0. 0. 0. 1. 0.;
element zeroLength         11632 191314 181314 -mat  41 -dir 1;
element zeroLength         12952 191314 181314 -mat  40 -dir 2;

element flatSliderBearing  2432 142 18142 10 110.000012345600 -P 20 -Mz 20  -orient 0. 1. 0. 1. 0. 0.;
element zeroLength         11373 142 18142 -mat  31 -dir 2;
element zeroLength         12693 142 18142 -mat  30 -dir 1;

element flatSliderBearing  2692 19142 18142 10 110.000012345600 -P 21 -Mz 21  -orient -1. 0. 0. 0. 1. 0.;
element zeroLength         11633 19142 18142 -mat  41 -dir 1;
element zeroLength         12953 19142 18142 -mat  40 -dir 2;

element flatSliderBearing  2433 18143 143 10 110.000012345600 -P 20 -Mz 20  -orient 0. 1. 0. 1. 0. 0.;
element zeroLength         11374 18143 143 -mat  31 -dir 2;
element zeroLength         12694 18143 143 -mat  30 -dir 1;

element flatSliderBearing  2693 19143 18143 10 110.000012345600 -P 21 -Mz 21  -orient -1. 0. 0. 0. 1. 0.;
element zeroLength         11634 19143 18143 -mat  41 -dir 1;
element zeroLength         12954 19143 18143 -mat  40 -dir 2;

element flatSliderBearing  2434 144 18144 10 110.000012345600 -P 20 -Mz 20  -orient 0. 1. 0. 1. 0. 0.;
element zeroLength         11375 144 18144 -mat  31 -dir 2;
element zeroLength         12695 144 18144 -mat  30 -dir 1;

element flatSliderBearing  2694 19144 18144 10 110.000012345600 -P 21 -Mz 21  -orient -1. 0. 0. 0. 1. 0.;
element zeroLength         11635 19144 18144 -mat  41 -dir 1;
element zeroLength         12955 19144 18144 -mat  40 -dir 2;
```

```
element flatSliderBearing  2435 18145 145 10 110.000012345600 -P 20 -Mz 20  -orient 0. 1. 0. 1. 0. 0.;
element zeroLength         11376 18145 145 -mat  31 -dir 2;
element zeroLength         12696 18145 145 -mat  30 -dir 1;

element flatSliderBearing  2695 19145 18145 10 110.000012345600 -P 21 -Mz 21  -orient -1. 0. 0. 0. 1. 0.;
element zeroLength         11636 19145 18145 -mat  41 -dir 1;
element zeroLength         12956 19145 18145 -mat  40 -dir 2;

element flatSliderBearing  2436 146 18146 10 110.000012345600 -P 20 -Mz 20  -orient 0. 1. 0. 1. 0. 0.;
element zeroLength         11377 146 18146 -mat  31 -dir 2;
element zeroLength         12697 146 18146 -mat  30 -dir 1;

element flatSliderBearing  2696 19146 18146 10 110.000012345600 -P 21 -Mz 21  -orient -1. 0. 0. 0. 1. 0.;
element zeroLength         11637 19146 18146 -mat  41 -dir 1;
element zeroLength         12957 19146 18146 -mat  40 -dir 2;

element flatSliderBearing  2437 18147 147 10 110.000012345600 -P 20 -Mz 20  -orient 0. 1. 0. 1. 0. 0.;
element zeroLength         11378 18147 147 -mat  31 -dir 2;
element zeroLength         12698 18147 147 -mat  30 -dir 1;

element flatSliderBearing  2697 19147 18147 10 110.000012345600 -P 21 -Mz 21  -orient -1. 0. 0. 0. 1. 0.;
element zeroLength         11638 19147 18147 -mat  41 -dir 1;
element zeroLength         12958 19147 18147 -mat  40 -dir 2;

element flatSliderBearing  2438 148 18148 10 110.000012345600 -P 20 -Mz 20  -orient 0. 1. 0. 1. 0. 0.;
element zeroLength         11379 148 18148 -mat  31 -dir 2;
element zeroLength         12699 148 18148 -mat  30 -dir 1;

element flatSliderBearing  2698 19148 18148 10 110.000012345600 -P 21 -Mz 21  -orient -1. 0. 0. 0. 1. 0.;
element zeroLength         11639 19148 18148 -mat  41 -dir 1;
element zeroLength         12959 19148 18148 -mat  40 -dir 2;

element flatSliderBearing  2439 18149 149 10 110.000012345600 -P 20 -Mz 20  -orient 0. 1. 0. 1. 0. 0.;
element zeroLength         11380 18149 149 -mat  31 -dir 2;
element zeroLength         12700 18149 149 -mat  30 -dir 1;

element flatSliderBearing  2699 19149 18149 10 110.000012345600 -P 21 -Mz 21  -orient -1. 0. 0. 0. 1. 0.;
element zeroLength         11640 19149 18149 -mat  41 -dir 1;
element zeroLength         12960 19149 18149 -mat  40 -dir 2;

element flatSliderBearing  2440 1410 181410 10 110.000012345600 -P 20 -Mz 20  -orient 0. 1. 0. 1. 0. 0.;
element zeroLength         11381 1410 181410 -mat  31 -dir 2;
element zeroLength         12701 1410 181410 -mat  30 -dir 1;

element flatSliderBearing  2700 191410 181410 10 110.000012345600 -P 21 -Mz 21  -orient -1. 0. 0. 0. 1. 0.;
element zeroLength         11641 191410 181410 -mat  41 -dir 1;
element zeroLength         12961 191410 181410 -mat  40 -dir 2;

element flatSliderBearing  2441 181411 1411 10 110.000012345600 -P 20 -Mz 20  -orient 0. 1. 0. 1. 0. 0.;
element zeroLength         11382 181411 1411 -mat  31 -dir 2;
element zeroLength         12702 181411 1411 -mat  30 -dir 1;

element flatSliderBearing  2701 191411 181411 10 110.000012345600 -P 21 -Mz 21  -orient -1. 0. 0. 0. 1. 0.;
element zeroLength         11642 191411 181411 -mat  41 -dir 1;
```

```
element zeroLength          12962 191411 181411 -mat  40 -dir 2;

element flatSliderBearing   2442 1412 181412 10 110.000012345600 -P 20 -Mz 20  -orient 0. 1. 0. 1. 0. 0.;
element zeroLength          11383 1412 181412 -mat  31 -dir 2;
element zeroLength          12703 1412 181412 -mat  30 -dir 1;

element flatSliderBearing   2702 191412 181412 10 110.000012345600 -P 21 -Mz 21  -orient -1. 0. 0. 0. 1. 0.;
element zeroLength          11643 191412 181412 -mat  41 -dir 1;
element zeroLength          12963 191412 181412 -mat  40 -dir 2;

element flatSliderBearing   2443 181413 1413 10 110.000012345600 -P 20 -Mz 20  -orient 0. 1. 0. 1. 0. 0.;
element zeroLength          11384 181413 1413 -mat  31 -dir 2;
element zeroLength          12704 181413 1413 -mat  30 -dir 1;

element flatSliderBearing   2703 191413 181413 10 110.000012345600 -P 21 -Mz 21  -orient -1. 0. 0. 0. 1. 0.;
element zeroLength          11644 191413 181413 -mat  41 -dir 1;
element zeroLength          12964 191413 181413 -mat  40 -dir 2;

element flatSliderBearing   2444 1414 181414 10 110.000012345600 -P 20 -Mz 20  -orient 0. 1. 0. 1. 0. 0.;
element zeroLength          11385 1414 181414 -mat  31 -dir 2;
element zeroLength          12705 1414 181414 -mat  30 -dir 1;

element flatSliderBearing   2704 191414 181414 10 110.000012345600 -P 21 -Mz 21  -orient -1. 0. 0. 0. 1. 0.;
element zeroLength          11645 191414 181414 -mat  41 -dir 1;
element zeroLength          12965 191414 181414 -mat  40 -dir 2;

element flatSliderBearing   2445 18152 152 10 110.000012345600 -P 20 -Mz 20  -orient 0. 1. 0. 1. 0. 0.;
element zeroLength          11386 18152 152 -mat  31 -dir 2;
element zeroLength          12706 18152 152 -mat  30 -dir 1;

element flatSliderBearing   2705 19152 18152 10 110.000012345600 -P 21 -Mz 21  -orient -1. 0. 0. 0. 1. 0.;
element zeroLength          11646 19152 18152 -mat  41 -dir 1;
element zeroLength          12966 19152 18152 -mat  40 -dir 2;

element flatSliderBearing   2446 153 18153 10 110.000012345600 -P 20 -Mz 20  -orient 0. 1. 0. 1. 0. 0.;
element zeroLength          11387 153 18153 -mat  31 -dir 2;
element zeroLength          12707 153 18153 -mat  30 -dir 1;

element flatSliderBearing   2706 19153 18153 10 110.000012345600 -P 21 -Mz 21  -orient -1. 0. 0. 0. 1. 0.;
element zeroLength          11647 19153 18153 -mat  41 -dir 1;
element zeroLength          12967 19153 18153 -mat  40 -dir 2;

element flatSliderBearing   2447 18154 154 10 110.000012345600 -P 20 -Mz 20  -orient 0. 1. 0. 1. 0. 0.;
element zeroLength          11388 18154 154 -mat  31 -dir 2;
element zeroLength          12708 18154 154 -mat  30 -dir 1;

element flatSliderBearing   2707 19154 18154 10 110.000012345600 -P 21 -Mz 21  -orient -1. 0. 0. 0. 1. 0.;
element zeroLength          11648 19154 18154 -mat  41 -dir 1;
element zeroLength          12968 19154 18154 -mat  40 -dir 2;

element flatSliderBearing   2448 155 18155 10 110.000012345600 -P 20 -Mz 20  -orient 0. 1. 0. 1. 0. 0.;
element zeroLength          11389 155 18155 -mat  31 -dir 2;
element zeroLength          12709 155 18155 -mat  30 -dir 1;

element flatSliderBearing   2708 19155 18155 10 110.000012345600 -P 21 -Mz 21  -orient -1. 0. 0. 0. 1. 0.;
```

```
element zeroLength          11649 19155 18155 -mat  41 -dir 1;
element zeroLength          12969 19155 18155 -mat  40 -dir 2;

element flatSliderBearing   2449 18156 156 10 110.000012345600 -P 20 -Mz 20  -orient 0. 1. 0. 1. 0. 0.;
element zeroLength          11390 18156 156 -mat  31 -dir 2;
element zeroLength          12710 18156 156 -mat  30 -dir 1;

element flatSliderBearing   2709 19156 18156 10 110.000012345600 -P 21 -Mz 21  -orient -1. 0. 0. 0. 1. 0.;
element zeroLength          11650 19156 18156 -mat  41 -dir 1;
element zeroLength          12970 19156 18156 -mat  40 -dir 2;

element flatSliderBearing   2450 157 18157 10 110.000012345600 -P 20 -Mz 20  -orient 0. 1. 0. 1. 0. 0.;
element zeroLength          11391 157 18157 -mat  31 -dir 2;
element zeroLength          12711 157 18157 -mat  30 -dir 1;

element flatSliderBearing   2710 19157 18157 10 110.000012345600 -P 21 -Mz 21  -orient -1. 0. 0. 0. 1. 0.;
element zeroLength          11651 19157 18157 -mat  41 -dir 1;
element zeroLength          12971 19157 18157 -mat  40 -dir 2;

element flatSliderBearing   2451 18158 158 10 110.000012345600 -P 20 -Mz 20  -orient 0. 1. 0. 1. 0. 0.;
element zeroLength          11392 18158 158 -mat  31 -dir 2;
element zeroLength          12712 18158 158 -mat  30 -dir 1;

element flatSliderBearing   2711 19158 18158 10 110.000012345600 -P 21 -Mz 21  -orient -1. 0. 0. 0. 1. 0.;
element zeroLength          11652 19158 18158 -mat  41 -dir 1;
element zeroLength          12972 19158 18158 -mat  40 -dir 2;

element flatSliderBearing   2452 159 18159 10 110.000012345600 -P 20 -Mz 20  -orient 0. 1. 0. 1. 0. 0.;
element zeroLength          11393 159 18159 -mat  31 -dir 2;
element zeroLength          12713 159 18159 -mat  30 -dir 1;

element flatSliderBearing   2712 19159 18159 10 110.000012345600 -P 21 -Mz 21  -orient -1. 0. 0. 0. 1. 0.;
element zeroLength          11653 19159 18159 -mat  41 -dir 1;
element zeroLength          12973 19159 18159 -mat  40 -dir 2;

element flatSliderBearing   2453 181510 1510 10 110.000012345600 -P 20 -Mz 20  -orient 0. 1. 0. 1. 0. 0.;
element zeroLength          11394 181510 1510 -mat  31 -dir 2;
element zeroLength          12714 181510 1510 -mat  30 -dir 1;

element flatSliderBearing   2713 191510 181510 10 110.000012345600 -P 21 -Mz 21  -orient -1. 0. 0. 0. 1. 0.;
element zeroLength          11654 191510 181510 -mat  41 -dir 1;
element zeroLength          12974 191510 181510 -mat  40 -dir 2;

element flatSliderBearing   2454 1511 181511 10 110.000012345600 -P 20 -Mz 20  -orient 0. 1. 0. 1. 0. 0.;
element zeroLength          11395 1511 181511 -mat  31 -dir 2;
element zeroLength          12715 1511 181511 -mat  30 -dir 1;

element flatSliderBearing   2714 191511 181511 10 110.000012345600 -P 21 -Mz 21  -orient -1. 0. 0. 0. 1. 0.;
element zeroLength          11655 191511 181511 -mat  41 -dir 1;
element zeroLength          12975 191511 181511 -mat  40 -dir 2;

element flatSliderBearing   2455 181512 1512 10 110.000012345600 -P 20 -Mz 20  -orient 0. 1. 0. 1. 0. 0.;
element zeroLength          11396 181512 1512 -mat  31 -dir 2;
element zeroLength          12716 181512 1512 -mat  30 -dir 1;
```

```
element flatSliderBearing  2715 191512 181512 10 110.000012345600 -P 21 -Mz 21  -orient -1. 0. 0. 0. 1. 0.;
element zeroLength         11656 191512 181512 -mat  41 -dir 1;
element zeroLength         12976 191512 181512 -mat  40 -dir 2;

element flatSliderBearing  2456 1513 181513 10 110.000012345600 -P 20 -Mz 20  -orient 0. 1. 0. 1. 0. 0.;
element zeroLength         11397 1513 181513 -mat  31 -dir 2;
element zeroLength         12717 1513 181513 -mat  30 -dir 1;

element flatSliderBearing  2716 191513 181513 10 110.000012345600 -P 21 -Mz 21  -orient -1. 0. 0. 0. 1. 0.;
element zeroLength         11657 191513 181513 -mat  41 -dir 1;
element zeroLength         12977 191513 181513 -mat  40 -dir 2;

element flatSliderBearing  2457 181514 1514 10 110.000012345600 -P 20 -Mz 20  -orient 0. 1. 0. 1. 0. 0.;
element zeroLength         11398 181514 1514 -mat  31 -dir 2;
element zeroLength         12718 181514 1514 -mat  30 -dir 1;

element flatSliderBearing  2717 191514 181514 10 110.000012345600 -P 21 -Mz 21  -orient -1. 0. 0. 0. 1. 0.;
element zeroLength         11658 191514 181514 -mat  41 -dir 1;
element zeroLength         12978 191514 181514 -mat  40 -dir 2;

element flatSliderBearing  2458 162 18162 10 110.000012345600 -P 20 -Mz 20  -orient 0. 1. 0. 1. 0. 0.;
element zeroLength         11399 162 18162 -mat  31 -dir 2;
element zeroLength         12719 162 18162 -mat  30 -dir 1;

element flatSliderBearing  2718 19162 18162 10 110.000012345600 -P 21 -Mz 21  -orient -1. 0. 0. 0. 1. 0.;
element zeroLength         11659 19162 18162 -mat  41 -dir 1;
element zeroLength         12979 19162 18162 -mat  40 -dir 2;

element flatSliderBearing  2459 18163 163 10 110.000012345600 -P 20 -Mz 20  -orient 0. 1. 0. 1. 0. 0.;
element zeroLength         11400 18163 163 -mat  31 -dir 2;
element zeroLength         12720 18163 163 -mat  30 -dir 1;

element flatSliderBearing  2719 19163 18163 10 110.000012345600 -P 21 -Mz 21  -orient -1. 0. 0. 0. 1. 0.;
element zeroLength         11660 19163 18163 -mat  41 -dir 1;
element zeroLength         12980 19163 18163 -mat  40 -dir 2;

element flatSliderBearing  2460 164 18164 10 110.000012345600 -P 20 -Mz 20  -orient 0. 1. 0. 1. 0. 0.;
element zeroLength         11401 164 18164 -mat  31 -dir 2;
element zeroLength         12721 164 18164 -mat  30 -dir 1;

element flatSliderBearing  2720 19164 18164 10 110.000012345600 -P 21 -Mz 21  -orient -1. 0. 0. 0. 1. 0.;
element zeroLength         11661 19164 18164 -mat  41 -dir 1;
element zeroLength         12981 19164 18164 -mat  40 -dir 2;

element flatSliderBearing  2461 18165 165 10 110.000012345600 -P 20 -Mz 20  -orient 0. 1. 0. 1. 0. 0.;
element zeroLength         11402 18165 165 -mat  31 -dir 2;
element zeroLength         12722 18165 165 -mat  30 -dir 1;

element flatSliderBearing  2721 19165 18165 10 110.000012345600 -P 21 -Mz 21  -orient -1. 0. 0. 0. 1. 0.;
element zeroLength         11662 19165 18165 -mat  41 -dir 1;
element zeroLength         12982 19165 18165 -mat  40 -dir 2;

element flatSliderBearing  2462 166 18166 10 110.000012345600 -P 20 -Mz 20  -orient 0. 1. 0. 1. 0. 0.;
element zeroLength         11403 166 18166 -mat  31 -dir 2;
element zeroLength         12723 166 18166 -mat  30 -dir 1;
```

```
5501
5502  element flatSliderBearing  2722 19166 18166 10 110.000012345600 -P 21 -Mz 21  -orient -1. 0. 0. 0. 1. 0.;
5503  element zeroLength         11663 19166 18166 -mat  41 -dir 1;
5504  element zeroLength         12983 19166 18166 -mat  40 -dir 2;
5505
5506  element flatSliderBearing  2463 18167 167 10 110.000012345600 -P 20 -Mz 20  -orient 0. 1. 0. 1. 0. 0.;
5507  element zeroLength         11404 18167 167 -mat  31 -dir 2;
5508  element zeroLength         12724 18167 167 -mat  30 -dir 1;
5509
5510  element flatSliderBearing  2723 19167 18167 10 110.000012345600 -P 21 -Mz 21  -orient -1. 0. 0. 0. 1. 0.;
5511  element zeroLength         11664 19167 18167 -mat  41 -dir 1;
5512  element zeroLength         12984 19167 18167 -mat  40 -dir 2;
5513
5514  element flatSliderBearing  2464 168 18168 10 110.000012345600 -P 20 -Mz 20  -orient 0. 1. 0. 1. 0. 0.;
5515  element zeroLength         11405 168 18168 -mat  31 -dir 2;
5516  element zeroLength         12725 168 18168 -mat  30 -dir 1;
5517
5518  element flatSliderBearing  2724 19168 18168 10 110.000012345600 -P 21 -Mz 21  -orient -1. 0. 0. 0. 1. 0.;
5519  element zeroLength         11665 19168 18168 -mat  41 -dir 1;
5520  element zeroLength         12985 19168 18168 -mat  40 -dir 2;
5521
5522  element flatSliderBearing  2465 18169 169 10 110.000012345600 -P 20 -Mz 20  -orient 0. 1. 0. 1. 0. 0.;
5523  element zeroLength         11406 18169 169 -mat  31 -dir 2;
5524  element zeroLength         12726 18169 169 -mat  30 -dir 1;
5525
5526  element flatSliderBearing  2725 19169 18169 10 110.000012345600 -P 21 -Mz 21  -orient -1. 0. 0. 0. 1. 0.;
5527  element zeroLength         11666 19169 18169 -mat  41 -dir 1;
5528  element zeroLength         12986 19169 18169 -mat  40 -dir 2;
5529
5530  element flatSliderBearing  2466 1610 181610 10 110.000012345600 -P 20 -Mz 20  -orient 0. 1. 0. 1. 0. 0.;
5531  element zeroLength         11407 1610 181610 -mat  31 -dir 2;
5532  element zeroLength         12727 1610 181610 -mat  30 -dir 1;
5533
5534  element flatSliderBearing  2726 191610 181610 10 110.000012345600 -P 21 -Mz 21  -orient -1. 0. 0. 0. 1. 0.;
5535  element zeroLength         11667 191610 181610 -mat  41 -dir 1;
5536  element zeroLength         12987 191610 181610 -mat  40 -dir 2;
5537
5538  element flatSliderBearing  2467 181611 1611 10 110.000012345600 -P 20 -Mz 20  -orient 0. 1. 0. 1. 0. 0.;
5539  element zeroLength         11408 181611 1611 -mat  31 -dir 2;
5540  element zeroLength         12728 181611 1611 -mat  30 -dir 1;
5541
5542  element flatSliderBearing  2727 191611 181611 10 110.000012345600 -P 21 -Mz 21  -orient -1. 0. 0. 0. 1. 0.;
5543  element zeroLength         11668 191611 181611 -mat  41 -dir 1;
5544  element zeroLength         12988 191611 181611 -mat  40 -dir 2;
5545
5546  element flatSliderBearing  2468 1612 181612 10 110.000012345600 -P 20 -Mz 20  -orient 0. 1. 0. 1. 0. 0.;
5547  element zeroLength         11409 1612 181612 -mat  31 -dir 2;
5548  element zeroLength         12729 1612 181612 -mat  30 -dir 1;
5549
5550  element flatSliderBearing  2728 191612 181612 10 110.000012345600 -P 21 -Mz 21  -orient -1. 0. 0. 0. 1. 0.;
5551  element zeroLength         11669 191612 181612 -mat  41 -dir 1;
5552  element zeroLength         12989 191612 181612 -mat  40 -dir 2;
5553
5554  element flatSliderBearing  2469 181613 1613 10 110.000012345600 -P 20 -Mz 20  -orient 0. 1. 0. 1. 0. 0.;
5555  element zeroLength         11410 181613 1613 -mat  31 -dir 2;
```

```
element zeroLength          12730 181613 1613 -mat  30 -dir 1;

element flatSliderBearing   2729 191613 181613 10 110.000012345600 -P 21 -Mz 21  -orient -1. 0. 0. 0. 1. 0.;
element zeroLength          11670 191613 181613 -mat  41 -dir 1;
element zeroLength          12990 191613 181613 -mat  40 -dir 2;

element flatSliderBearing   2470 1614 181614 10 110.000012345600 -P 20 -Mz 20  -orient 0. 1. 0. 1. 0. 0.;
element zeroLength          11411 1614 181614 -mat  31 -dir 2;
element zeroLength          12731 1614 181614 -mat  30 -dir 1;

element flatSliderBearing   2730 191614 181614 10 110.000012345600 -P 21 -Mz 21  -orient -1. 0. 0. 0. 1. 0.;
element zeroLength          11671 191614 181614 -mat  41 -dir 1;
element zeroLength          12991 191614 181614 -mat  40 -dir 2;

element flatSliderBearing   2471 18172 172 10 110.000012345600 -P 20 -Mz 20  -orient 0. 1. 0. 1. 0. 0.;
element zeroLength          11412 18172 172 -mat  31 -dir 2;
element zeroLength          12732 18172 172 -mat  30 -dir 1;

element flatSliderBearing   2731 19172 18172 10 110.000012345600 -P 21 -Mz 21  -orient -1. 0. 0. 0. 1. 0.;
element zeroLength          11672 19172 18172 -mat  41 -dir 1;
element zeroLength          12992 19172 18172 -mat  40 -dir 2;

element flatSliderBearing   2472 173 18173 10 110.000012345600 -P 20 -Mz 20  -orient 0. 1. 0. 1. 0. 0.;
element zeroLength          11413 173 18173 -mat  31 -dir 2;
element zeroLength          12733 173 18173 -mat  30 -dir 1;

element flatSliderBearing   2732 19173 18173 10 110.000012345600 -P 21 -Mz 21  -orient -1. 0. 0. 0. 1. 0.;
element zeroLength          11673 19173 18173 -mat  41 -dir 1;
element zeroLength          12993 19173 18173 -mat  40 -dir 2;

element flatSliderBearing   2473 18174 174 10 110.000012345600 -P 20 -Mz 20  -orient 0. 1. 0. 1. 0. 0.;
element zeroLength          11414 18174 174 -mat  31 -dir 2;
element zeroLength          12734 18174 174 -mat  30 -dir 1;

element flatSliderBearing   2733 19174 18174 10 110.000012345600 -P 21 -Mz 21  -orient -1. 0. 0. 0. 1. 0.;
element zeroLength          11674 19174 18174 -mat  41 -dir 1;
element zeroLength          12994 19174 18174 -mat  40 -dir 2;

element flatSliderBearing   2474 175 18175 10 110.000012345600 -P 20 -Mz 20  -orient 0. 1. 0. 1. 0. 0.;
element zeroLength          11415 175 18175 -mat  31 -dir 2;
element zeroLength          12735 175 18175 -mat  30 -dir 1;

element flatSliderBearing   2734 19175 18175 10 110.000012345600 -P 21 -Mz 21  -orient -1. 0. 0. 0. 1. 0.;
element zeroLength          11675 19175 18175 -mat  41 -dir 1;
element zeroLength          12995 19175 18175 -mat  40 -dir 2;

element flatSliderBearing   2475 18176 176 10 110.000012345600 -P 20 -Mz 20  -orient 0. 1. 0. 1. 0. 0.;
element zeroLength          11416 18176 176 -mat  31 -dir 2;
element zeroLength          12736 18176 176 -mat  30 -dir 1;

element flatSliderBearing   2735 19176 18176 10 110.000012345600 -P 21 -Mz 21  -orient -1. 0. 0. 0. 1. 0.;
element zeroLength          11676 19176 18176 -mat  41 -dir 1;
element zeroLength          12996 19176 18176 -mat  40 -dir 2;

element flatSliderBearing   2476 177 18177 10 110.000012345600 -P 20 -Mz 20  -orient 0. 1. 0. 1. 0. 0.;
```

```
element zeroLength          11417 177 18177 -mat  31 -dir 2;
element zeroLength          12737 177 18177 -mat  30 -dir 1;

element flatSliderBearing   2736 19177 18177 10 110.000012345600 -P 21 -Mz 21  -orient -1. 0. 0. 0. 1. 0.;
element zeroLength          11677 19177 18177 -mat  41 -dir 1;
element zeroLength          12997 19177 18177 -mat  40 -dir 2;

element flatSliderBearing   2477 18178 178 10 110.000012345600 -P 20 -Mz 20  -orient 0. 1. 0. 1. 0. 0.;
element zeroLength          11418 18178 178 -mat  31 -dir 2;
element zeroLength          12738 18178 178 -mat  30 -dir 1;

element flatSliderBearing   2737 19178 18178 10 110.000012345600 -P 21 -Mz 21  -orient -1. 0. 0. 0. 1. 0.;
element zeroLength          11678 19178 18178 -mat  41 -dir 1;
element zeroLength          12998 19178 18178 -mat  40 -dir 2;

element flatSliderBearing   2478 179 18179 10 110.000012345600 -P 20 -Mz 20  -orient 0. 1. 0. 1. 0. 0.;
element zeroLength          11419 179 18179 -mat  31 -dir 2;
element zeroLength          12739 179 18179 -mat  30 -dir 1;

element flatSliderBearing   2738 19179 18179 10 110.000012345600 -P 21 -Mz 21  -orient -1. 0. 0. 0. 1. 0.;
element zeroLength          11679 19179 18179 -mat  41 -dir 1;
element zeroLength          12999 19179 18179 -mat  40 -dir 2;

element flatSliderBearing   2479 181710 1710 10 110.000012345600 -P 20 -Mz 20  -orient 0. 1. 0. 1. 0. 0.;
element zeroLength          11420 181710 1710 -mat  31 -dir 2;
element zeroLength          12740 181710 1710 -mat  30 -dir 1;

element flatSliderBearing   2739 191710 181710 10 110.000012345600 -P 21 -Mz 21  -orient -1. 0. 0. 0. 1. 0.;
element zeroLength          11680 191710 181710 -mat  41 -dir 1;
element zeroLength          13000 191710 181710 -mat  40 -dir 2;

element flatSliderBearing   2480 1711 181711 10 110.000012345600 -P 20 -Mz 20  -orient 0. 1. 0. 1. 0. 0.;
element zeroLength          11421 1711 181711 -mat  31 -dir 2;
element zeroLength          12741 1711 181711 -mat  30 -dir 1;

element flatSliderBearing   2740 191711 181711 10 110.000012345600 -P 21 -Mz 21  -orient -1. 0. 0. 0. 1. 0.;
element zeroLength          11681 191711 181711 -mat  41 -dir 1;
element zeroLength          13001 191711 181711 -mat  40 -dir 2;

element flatSliderBearing   2481 181712 1712 10 110.000012345600 -P 20 -Mz 20  -orient 0. 1. 0. 1. 0. 0.;
element zeroLength          11422 181712 1712 -mat  31 -dir 2;
element zeroLength          12742 181712 1712 -mat  30 -dir 1;

element flatSliderBearing   2741 191712 181712 10 110.000012345600 -P 21 -Mz 21  -orient -1. 0. 0. 0. 1. 0.;
element zeroLength          11682 191712 181712 -mat  41 -dir 1;
element zeroLength          13002 191712 181712 -mat  40 -dir 2;

element flatSliderBearing   2482 1713 181713 10 110.000012345600 -P 20 -Mz 20  -orient 0. 1. 0. 1. 0. 0.;
element zeroLength          11423 1713 181713 -mat  31 -dir 2;
element zeroLength          12743 1713 181713 -mat  30 -dir 1;

element flatSliderBearing   2742 191713 181713 10 110.000012345600 -P 21 -Mz 21  -orient -1. 0. 0. 0. 1. 0.;
element zeroLength          11683 191713 181713 -mat  41 -dir 1;
element zeroLength          13003 191713 181713 -mat  40 -dir 2;
```

```
element flatSliderBearing  2483 181714 1714 10 110.000012345600 -P 20 -Mz 20  -orient 0. 1. 0. 1. 0. 0.;
element zeroLength         11424 181714 1714 -mat  31 -dir 2;
element zeroLength         12744 181714 1714 -mat  30 -dir 1;

element flatSliderBearing  2743 191714 181714 10 110.000012345600 -P 21 -Mz 21  -orient -1. 0. 0. 0. 1. 0.;
element zeroLength         11684 191714 181714 -mat  41 -dir 1;
element zeroLength         13004 191714 181714 -mat  40 -dir 2;

element flatSliderBearing  2484 182 18182 10 110.000012345600 -P 20 -Mz 20  -orient 0. 1. 0. 1. 0. 0.;
element zeroLength         11425 182 18182 -mat  31 -dir 2;
element zeroLength         12745 182 18182 -mat  30 -dir 1;

element flatSliderBearing  2744 19182 18182 10 110.000012345600 -P 21 -Mz 21  -orient -1. 0. 0. 0. 1. 0.;
element zeroLength         11685 19182 18182 -mat  41 -dir 1;
element zeroLength         13005 19182 18182 -mat  40 -dir 2;

element flatSliderBearing  2485 18183 183 10 110.000012345600 -P 20 -Mz 20  -orient 0. 1. 0. 1. 0. 0.;
element zeroLength         11426 18183 183 -mat  31 -dir 2;
element zeroLength         12746 18183 183 -mat  30 -dir 1;

element flatSliderBearing  2745 19183 18183 10 110.000012345600 -P 21 -Mz 21  -orient -1. 0. 0. 0. 1. 0.;
element zeroLength         11686 19183 18183 -mat  41 -dir 1;
element zeroLength         13006 19183 18183 -mat  40 -dir 2;

element flatSliderBearing  2486 184 18184 10 110.000012345600 -P 20 -Mz 20  -orient 0. 1. 0. 1. 0. 0.;
element zeroLength         11427 184 18184 -mat  31 -dir 2;
element zeroLength         12747 184 18184 -mat  30 -dir 1;

element flatSliderBearing  2746 19184 18184 10 110.000012345600 -P 21 -Mz 21  -orient -1. 0. 0. 0. 1. 0.;
element zeroLength         11687 19184 18184 -mat  41 -dir 1;
element zeroLength         13007 19184 18184 -mat  40 -dir 2;

element flatSliderBearing  2487 18185 185 10 110.000012345600 -P 20 -Mz 20  -orient 0. 1. 0. 1. 0. 0.;
element zeroLength         11428 18185 185 -mat  31 -dir 2;
element zeroLength         12748 18185 185 -mat  30 -dir 1;

element flatSliderBearing  2747 19185 18185 10 110.000012345600 -P 21 -Mz 21  -orient -1. 0. 0. 0. 1. 0.;
element zeroLength         11688 19185 18185 -mat  41 -dir 1;
element zeroLength         13008 19185 18185 -mat  40 -dir 2;

element flatSliderBearing  2488 186 18186 10 110.000012345600 -P 20 -Mz 20  -orient 0. 1. 0. 1. 0. 0.;
element zeroLength         11429 186 18186 -mat  31 -dir 2;
element zeroLength         12749 186 18186 -mat  30 -dir 1;

element flatSliderBearing  2748 19186 18186 10 110.000012345600 -P 21 -Mz 21  -orient -1. 0. 0. 0. 1. 0.;
element zeroLength         11689 19186 18186 -mat  41 -dir 1;
element zeroLength         13009 19186 18186 -mat  40 -dir 2;

element flatSliderBearing  2489 18187 187 10 110.000012345600 -P 20 -Mz 20  -orient 0. 1. 0. 1. 0. 0.;
element zeroLength         11430 18187 187 -mat  31 -dir 2;
element zeroLength         12750 18187 187 -mat  30 -dir 1;

element flatSliderBearing  2749 19187 18187 10 110.000012345600 -P 21 -Mz 21  -orient -1. 0. 0. 0. 1. 0.;
element zeroLength         11690 19187 18187 -mat  41 -dir 1;
element zeroLength         13010 19187 18187 -mat  40 -dir 2;
```

```
5721
5722  element flatSliderBearing  2490 188 18188 10 110.000012345600 -P 20 -Mz 20  -orient 0. 1. 0. 1. 0. 0.;
5723  element zeroLength         11431 188 18188 -mat  31 -dir 2;
5724  element zeroLength         12751 188 18188 -mat  30 -dir 1;
5725
5726  element flatSliderBearing  2750 19188 18188 10 110.000012345600 -P 21 -Mz 21  -orient -1. 0. 0. 0. 1. 0.;
5727  element zeroLength         11691 19188 18188 -mat  41 -dir 1;
5728  element zeroLength         13011 19188 18188 -mat  40 -dir 2;
5729
5730  element flatSliderBearing  2491 18189 189 10 110.000012345600 -P 20 -Mz 20  -orient 0. 1. 0. 1. 0. 0.;
5731  element zeroLength         11432 18189 189 -mat  31 -dir 2;
5732  element zeroLength         12752 18189 189 -mat  30 -dir 1;
5733
5734  element flatSliderBearing  2751 19189 18189 10 110.000012345600 -P 21 -Mz 21  -orient -1. 0. 0. 0. 1. 0.;
5735  element zeroLength         11692 19189 18189 -mat  41 -dir 1;
5736  element zeroLength         13012 19189 18189 -mat  40 -dir 2;
5737
5738  element flatSliderBearing  2492 1810 181810 10 110.000012345600 -P 20 -Mz 20  -orient 0. 1. 0. 1. 0. 0.;
5739  element zeroLength         11433 1810 181810 -mat  31 -dir 2;
5740  element zeroLength         12753 1810 181810 -mat  30 -dir 1;
5741
5742  element flatSliderBearing  2752 191810 181810 10 110.000012345600 -P 21 -Mz 21  -orient -1. 0. 0. 0. 1. 0.;
5743  element zeroLength         11693 191810 181810 -mat  41 -dir 1;
5744  element zeroLength         13013 191810 181810 -mat  40 -dir 2;
5745
5746  element flatSliderBearing  2493 181811 1811 10 110.000012345600 -P 20 -Mz 20  -orient 0. 1. 0. 1. 0. 0.;
5747  element zeroLength         11434 181811 1811 -mat  31 -dir 2;
5748  element zeroLength         12754 181811 1811 -mat  30 -dir 1;
5749
5750  element flatSliderBearing  2753 191811 181811 10 110.000012345600 -P 21 -Mz 21  -orient -1. 0. 0. 0. 1. 0.;
5751  element zeroLength         11694 191811 181811 -mat  41 -dir 1;
5752  element zeroLength         13014 191811 181811 -mat  40 -dir 2;
5753
5754  element flatSliderBearing  2494 1812 181812 10 110.000012345600 -P 20 -Mz 20  -orient 0. 1. 0. 1. 0. 0.;
5755  element zeroLength         11435 1812 181812 -mat  31 -dir 2;
5756  element zeroLength         12755 1812 181812 -mat  30 -dir 1;
5757
5758  element flatSliderBearing  2754 191812 181812 10 110.000012345600 -P 21 -Mz 21  -orient -1. 0. 0. 0. 1. 0.;
5759  element zeroLength         11695 191812 181812 -mat  41 -dir 1;
5760  element zeroLength         13015 191812 181812 -mat  40 -dir 2;
5761
5762  element flatSliderBearing  2495 181813 1813 10 110.000012345600 -P 20 -Mz 20  -orient 0. 1. 0. 1. 0. 0.;
5763  element zeroLength         11436 181813 1813 -mat  31 -dir 2;
5764  element zeroLength         12756 181813 1813 -mat  30 -dir 1;
5765
5766  element flatSliderBearing  2755 191813 181813 10 110.000012345600 -P 21 -Mz 21  -orient -1. 0. 0. 0. 1. 0.;
5767  element zeroLength         11696 191813 181813 -mat  41 -dir 1;
5768  element zeroLength         13016 191813 181813 -mat  40 -dir 2;
5769
5770  element flatSliderBearing  2496 1814 181814 10 110.000012345600 -P 20 -Mz 20  -orient 0. 1. 0. 1. 0. 0.;
5771  element zeroLength         11437 1814 181814 -mat  31 -dir 2;
5772  element zeroLength         12757 1814 181814 -mat  30 -dir 1;
5773
5774  element flatSliderBearing  2756 191814 181814 10 110.000012345600 -P 21 -Mz 21  -orient -1. 0. 0. 0. 1. 0.;
5775  element zeroLength         11697 191814 181814 -mat  41 -dir 1;
```

```
element zeroLength          13017 191814 181814 -mat  40 -dir 2;

element flatSliderBearing   2497 18192 192 10 110.000012345600 -P 20 -Mz 20  -orient 0. 1. 0. 1. 0. 0.;
element zeroLength          11438 18192 192 -mat  31 -dir 2;
element zeroLength          12758 18192 192 -mat  30 -dir 1;

element flatSliderBearing   2757 19192 18192 10 110.000012345600 -P 21 -Mz 21  -orient -1. 0. 0. 0. 1. 0.;
element zeroLength          11698 19192 18192 -mat  41 -dir 1;
element zeroLength          13018 19192 18192 -mat  40 -dir 2;

element flatSliderBearing   2498 193 18193 10 110.000012345600 -P 20 -Mz 20  -orient 0. 1. 0. 1. 0. 0.;
element zeroLength          11439 193 18193 -mat  31 -dir 2;
element zeroLength          12759 193 18193 -mat  30 -dir 1;

element flatSliderBearing   2758 19193 18193 10 110.000012345600 -P 21 -Mz 21  -orient -1. 0. 0. 0. 1. 0.;
element zeroLength          11699 19193 18193 -mat  41 -dir 1;
element zeroLength          13019 19193 18193 -mat  40 -dir 2;

element flatSliderBearing   2499 18194 194 10 110.000012345600 -P 20 -Mz 20  -orient 0. 1. 0. 1. 0. 0.;
element zeroLength          11440 18194 194 -mat  31 -dir 2;
element zeroLength          12760 18194 194 -mat  30 -dir 1;

element flatSliderBearing   2759 19194 18194 10 110.000012345600 -P 21 -Mz 21  -orient -1. 0. 0. 0. 1. 0.;
element zeroLength          11700 19194 18194 -mat  41 -dir 1;
element zeroLength          13020 19194 18194 -mat  40 -dir 2;

element flatSliderBearing   2500 195 18195 10 110.000012345600 -P 20 -Mz 20  -orient 0. 1. 0. 1. 0. 0.;
element zeroLength          11441 195 18195 -mat  31 -dir 2;
element zeroLength          12761 195 18195 -mat  30 -dir 1;

element flatSliderBearing   2760 19195 18195 10 110.000012345600 -P 21 -Mz 21  -orient -1. 0. 0. 0. 1. 0.;
element zeroLength          11701 19195 18195 -mat  41 -dir 1;
element zeroLength          13021 19195 18195 -mat  40 -dir 2;

element flatSliderBearing   2501 18196 196 10 110.000012345600 -P 20 -Mz 20  -orient 0. 1. 0. 1. 0. 0.;
element zeroLength          11442 18196 196 -mat  31 -dir 2;
element zeroLength          12762 18196 196 -mat  30 -dir 1;

element flatSliderBearing   2761 19196 18196 10 110.000012345600 -P 21 -Mz 21  -orient -1. 0. 0. 0. 1. 0.;
element zeroLength          11702 19196 18196 -mat  41 -dir 1;
element zeroLength          13022 19196 18196 -mat  40 -dir 2;

element flatSliderBearing   2502 197 18197 10 110.000012345600 -P 20 -Mz 20  -orient 0. 1. 0. 1. 0. 0.;
element zeroLength          11443 197 18197 -mat  31 -dir 2;
element zeroLength          12763 197 18197 -mat  30 -dir 1;

element flatSliderBearing   2762 19197 18197 10 110.000012345600 -P 21 -Mz 21  -orient -1. 0. 0. 0. 1. 0.;
element zeroLength          11703 19197 18197 -mat  41 -dir 1;
element zeroLength          13023 19197 18197 -mat  40 -dir 2;

element flatSliderBearing   2503 18198 198 10 110.000012345600 -P 20 -Mz 20  -orient 0. 1. 0. 1. 0. 0.;
element zeroLength          11444 18198 198 -mat  31 -dir 2;
element zeroLength          12764 18198 198 -mat  30 -dir 1;

element flatSliderBearing   2763 19198 18198 10 110.000012345600 -P 21 -Mz 21  -orient -1. 0. 0. 0. 1. 0.;
```

```
element zeroLength          11704 19198 18198 -mat  41 -dir 1;
element zeroLength          13024 19198 18198 -mat  40 -dir 2;

element flatSliderBearing   2504 199 18199 10 110.000012345600 -P 20 -Mz 20  -orient 0. 1. 0. 1. 0. 0.;
element zeroLength          11445 199 18199 -mat  31 -dir 2;
element zeroLength          12765 199 18199 -mat  30 -dir 1;

element flatSliderBearing   2764 19199 18199 10 110.000012345600 -P 21 -Mz 21  -orient -1. 0. 0. 0. 1. 0.;
element zeroLength          11705 19199 18199 -mat  41 -dir 1;
element zeroLength          13025 19199 18199 -mat  40 -dir 2;

element flatSliderBearing   2505 181910 1910 10 110.000012345600 -P 20 -Mz 20  -orient 0. 1. 0. 1. 0. 0.;
element zeroLength          11446 181910 1910 -mat  31 -dir 2;
element zeroLength          12766 181910 1910 -mat  30 -dir 1;

element flatSliderBearing   2765 191910 181910 10 110.000012345600 -P 21 -Mz 21  -orient -1. 0. 0. 0. 1. 0.;
element zeroLength          11706 191910 181910 -mat  41 -dir 1;
element zeroLength          13026 191910 181910 -mat  40 -dir 2;

element flatSliderBearing   2506 1911 181911 10 110.000012345600 -P 20 -Mz 20  -orient 0. 1. 0. 1. 0. 0.;
element zeroLength          11447 1911 181911 -mat  31 -dir 2;
element zeroLength          12767 1911 181911 -mat  30 -dir 1;

element flatSliderBearing   2766 191911 181911 10 110.000012345600 -P 21 -Mz 21  -orient -1. 0. 0. 0. 1. 0.;
element zeroLength          11707 191911 181911 -mat  41 -dir 1;
element zeroLength          13027 191911 181911 -mat  40 -dir 2;

element flatSliderBearing   2507 181912 1912 10 110.000012345600 -P 20 -Mz 20  -orient 0. 1. 0. 1. 0. 0.;
element zeroLength          11448 181912 1912 -mat  31 -dir 2;
element zeroLength          12768 181912 1912 -mat  30 -dir 1;

element flatSliderBearing   2767 191912 181912 10 110.000012345600 -P 21 -Mz 21  -orient -1. 0. 0. 0. 1. 0.;
element zeroLength          11708 191912 181912 -mat  41 -dir 1;
element zeroLength          13028 191912 181912 -mat  40 -dir 2;

element flatSliderBearing   2508 1913 181913 10 110.000012345600 -P 20 -Mz 20  -orient 0. 1. 0. 1. 0. 0.;
element zeroLength          11449 1913 181913 -mat  31 -dir 2;
element zeroLength          12769 1913 181913 -mat  30 -dir 1;

element flatSliderBearing   2768 191913 181913 10 110.000012345600 -P 21 -Mz 21  -orient -1. 0. 0. 0. 1. 0.;
element zeroLength          11709 191913 181913 -mat  41 -dir 1;
element zeroLength          13029 191913 181913 -mat  40 -dir 2;

element flatSliderBearing   2509 181914 1914 10 110.000012345600 -P 20 -Mz 20  -orient 0. 1. 0. 1. 0. 0.;
element zeroLength          11450 181914 1914 -mat  31 -dir 2;
element zeroLength          12770 181914 1914 -mat  30 -dir 1;

element flatSliderBearing   2769 191914 181914 10 110.000012345600 -P 21 -Mz 21  -orient -1. 0. 0. 0. 1. 0.;
element zeroLength          11710 191914 181914 -mat  41 -dir 1;
element zeroLength          13030 191914 181914 -mat  40 -dir 2;

element flatSliderBearing   2510 202 18202 10 110.000012345600 -P 20 -Mz 20  -orient 0. 1. 0. 1. 0. 0.;
element zeroLength          11451 202 18202 -mat  31 -dir 2;
element zeroLength          12771 202 18202 -mat  30 -dir 1;
```

```
element flatSliderBearing  2770 19202 18202 10 110.000012345600 -P 21 -Mz 21  -orient -1. 0. 0. 0. 1. 0.;
element zeroLength         11711 19202 18202 -mat  41 -dir 1;
element zeroLength         13031 19202 18202 -mat  40 -dir 2;

element flatSliderBearing  2511 18203 203 10 110.000012345600 -P 20 -Mz 20  -orient 0. 1. 0. 1. 0. 0.;
element zeroLength         11452 18203 203 -mat  31 -dir 2;
element zeroLength         12772 18203 203 -mat  30 -dir 1;

element flatSliderBearing  2771 19203 18203 10 110.000012345600 -P 21 -Mz 21  -orient -1. 0. 0. 0. 1. 0.;
element zeroLength         11712 19203 18203 -mat  41 -dir 1;
element zeroLength         13032 19203 18203 -mat  40 -dir 2;

element flatSliderBearing  2512 204 18204 10 110.000012345600 -P 20 -Mz 20  -orient 0. 1. 0. 1. 0. 0.;
element zeroLength         11453 204 18204 -mat  31 -dir 2;
element zeroLength         12773 204 18204 -mat  30 -dir 1;

element flatSliderBearing  2772 19204 18204 10 110.000012345600 -P 21 -Mz 21  -orient -1. 0. 0. 0. 1. 0.;
element zeroLength         11713 19204 18204 -mat  41 -dir 1;
element zeroLength         13033 19204 18204 -mat  40 -dir 2;

element flatSliderBearing  2513 18205 205 10 110.000012345600 -P 20 -Mz 20  -orient 0. 1. 0. 1. 0. 0.;
element zeroLength         11454 18205 205 -mat  31 -dir 2;
element zeroLength         12774 18205 205 -mat  30 -dir 1;

element flatSliderBearing  2773 19205 18205 10 110.000012345600 -P 21 -Mz 21  -orient -1. 0. 0. 0. 1. 0.;
element zeroLength         11714 19205 18205 -mat  41 -dir 1;
element zeroLength         13034 19205 18205 -mat  40 -dir 2;

element flatSliderBearing  2514 206 18206 10 110.000012345600 -P 20 -Mz 20  -orient 0. 1. 0. 1. 0. 0.;
element zeroLength         11455 206 18206 -mat  31 -dir 2;
element zeroLength         12775 206 18206 -mat  30 -dir 1;

element flatSliderBearing  2774 19206 18206 10 110.000012345600 -P 21 -Mz 21  -orient -1. 0. 0. 0. 1. 0.;
element zeroLength         11715 19206 18206 -mat  41 -dir 1;
element zeroLength         13035 19206 18206 -mat  40 -dir 2;

element flatSliderBearing  2515 18207 207 10 110.000012345600 -P 20 -Mz 20  -orient 0. 1. 0. 1. 0. 0.;
element zeroLength         11456 18207 207 -mat  31 -dir 2;
element zeroLength         12776 18207 207 -mat  30 -dir 1;

element flatSliderBearing  2775 19207 18207 10 110.000012345600 -P 21 -Mz 21  -orient -1. 0. 0. 0. 1. 0.;
element zeroLength         11716 19207 18207 -mat  41 -dir 1;
element zeroLength         13036 19207 18207 -mat  40 -dir 2;

element flatSliderBearing  2516 208 18208 10 110.000012345600 -P 20 -Mz 20  -orient 0. 1. 0. 1. 0. 0.;
element zeroLength         11457 208 18208 -mat  31 -dir 2;
element zeroLength         12777 208 18208 -mat  30 -dir 1;

element flatSliderBearing  2776 19208 18208 10 110.000012345600 -P 21 -Mz 21  -orient -1. 0. 0. 0. 1. 0.;
element zeroLength         11717 19208 18208 -mat  41 -dir 1;
element zeroLength         13037 19208 18208 -mat  40 -dir 2;

element flatSliderBearing  2517 18209 209 10 110.000012345600 -P 20 -Mz 20  -orient 0. 1. 0. 1. 0. 0.;
element zeroLength         11458 18209 209 -mat  31 -dir 2;
element zeroLength         12778 18209 209 -mat  30 -dir 1;
```

```
5941
5942  element flatSliderBearing  2777 19209 18209 10 110.000012345600 -P 21 -Mz 21  -orient -1. 0. 0. 0. 1. 0.;
5943  element zeroLength         11718 19209 18209 -mat  41 -dir 1;
5944  element zeroLength         13038 19209 18209 -mat  40 -dir 2;
5945
5946  element flatSliderBearing  2518 2010 182010 10 110.000012345600 -P 20 -Mz 20  -orient 0. 1. 0. 1. 0. 0.;
5947  element zeroLength         11459 2010 182010 -mat  31 -dir 2;
5948  element zeroLength         12779 2010 182010 -mat  30 -dir 1;
5949
5950  element flatSliderBearing  2778 192010 182010 10 110.000012345600 -P 21 -Mz 21  -orient -1. 0. 0. 0. 1. 0.;
5951  element zeroLength         11719 192010 182010 -mat  41 -dir 1;
5952  element zeroLength         13039 192010 182010 -mat  40 -dir 2;
5953
5954  element flatSliderBearing  2519 182011 2011 10 110.000012345600 -P 20 -Mz 20  -orient 0. 1. 0. 1. 0. 0.;
5955  element zeroLength         11460 182011 2011 -mat  31 -dir 2;
5956  element zeroLength         12780 182011 2011 -mat  30 -dir 1;
5957
5958  element flatSliderBearing  2779 192011 182011 10 110.000012345600 -P 21 -Mz 21  -orient -1. 0. 0. 0. 1. 0.;
5959  element zeroLength         11720 192011 182011 -mat  41 -dir 1;
5960  element zeroLength         13040 192011 182011 -mat  40 -dir 2;
5961
5962  element flatSliderBearing  2520 2012 182012 10 110.000012345600 -P 20 -Mz 20  -orient 0. 1. 0. 1. 0. 0.;
5963  element zeroLength         11461 2012 182012 -mat  31 -dir 2;
5964  element zeroLength         12781 2012 182012 -mat  30 -dir 1;
5965
5966  element flatSliderBearing  2780 192012 182012 10 110.000012345600 -P 21 -Mz 21  -orient -1. 0. 0. 0. 1. 0.;
5967  element zeroLength         11721 192012 182012 -mat  41 -dir 1;
5968  element zeroLength         13041 192012 182012 -mat  40 -dir 2;
5969
5970  element flatSliderBearing  2521 182013 2013 10 110.000012345600 -P 20 -Mz 20  -orient 0. 1. 0. 1. 0. 0.;
5971  element zeroLength         11462 182013 2013 -mat  31 -dir 2;
5972  element zeroLength         12782 182013 2013 -mat  30 -dir 1;
5973
5974  element flatSliderBearing  2781 192013 182013 10 110.000012345600 -P 21 -Mz 21  -orient -1. 0. 0. 0. 1. 0.;
5975  element zeroLength         11722 192013 182013 -mat  41 -dir 1;
5976  element zeroLength         13042 192013 182013 -mat  40 -dir 2;
5977
5978  element flatSliderBearing  2522 2014 182014 10 110.000012345600 -P 20 -Mz 20  -orient 0. 1. 0. 1. 0. 0.;
5979  element zeroLength         11463 2014 182014 -mat  31 -dir 2;
5980  element zeroLength         12783 2014 182014 -mat  30 -dir 1;
5981
5982  element flatSliderBearing  2782 192014 182014 10 110.000012345600 -P 21 -Mz 21  -orient -1. 0. 0. 0. 1. 0.;
5983  element zeroLength         11723 192014 182014 -mat  41 -dir 1;
5984  element zeroLength         13043 192014 182014 -mat  40 -dir 2;
5985
5986  element flatSliderBearing  2523 18212 212 10 110.000012345600 -P 20 -Mz 20  -orient 0. 1. 0. 1. 0. 0.;
5987  element zeroLength         11464 18212 212 -mat  31 -dir 2;
5988  element zeroLength         12784 18212 212 -mat  30 -dir 1;
5989
5990  element flatSliderBearing  2783 19212 18212 10 110.000012345600 -P 21 -Mz 21  -orient -1. 0. 0. 0. 1. 0.;
5991  element zeroLength         11724 19212 18212 -mat  41 -dir 1;
5992  element zeroLength         13044 19212 18212 -mat  40 -dir 2;
5993
5994  element flatSliderBearing  2524 213 18213 10 110.000012345600 -P 20 -Mz 20  -orient 0. 1. 0. 1. 0. 0.;
5995  element zeroLength         11465 213 18213 -mat  31 -dir 2;
```

```
element zeroLength          12785 213 18213 -mat  30 -dir 1;

element flatSliderBearing   2784 19213 18213 10 110.000012345600 -P 21 -Mz 21  -orient -1. 0. 0. 0. 1. 0.;
element zeroLength          11725 19213 18213 -mat  41 -dir 1;
element zeroLength          13045 19213 18213 -mat  40 -dir 2;

element flatSliderBearing   2525 18214 214 10 110.000012345600 -P 20 -Mz 20  -orient 0. 1. 0. 1. 0. 0.;
element zeroLength          11466 18214 214 -mat  31 -dir 2;
element zeroLength          12786 18214 214 -mat  30 -dir 1;

element flatSliderBearing   2785 19214 18214 10 110.000012345600 -P 21 -Mz 21  -orient -1. 0. 0. 0. 1. 0.;
element zeroLength          11726 19214 18214 -mat  41 -dir 1;
element zeroLength          13046 19214 18214 -mat  40 -dir 2;

element flatSliderBearing   2526 215 18215 10 110.000012345600 -P 20 -Mz 20  -orient 0. 1. 0. 1. 0. 0.;
element zeroLength          11467 215 18215 -mat  31 -dir 2;
element zeroLength          12787 215 18215 -mat  30 -dir 1;

element flatSliderBearing   2786 19215 18215 10 110.000012345600 -P 21 -Mz 21  -orient -1. 0. 0. 0. 1. 0.;
element zeroLength          11727 19215 18215 -mat  41 -dir 1;
element zeroLength          13047 19215 18215 -mat  40 -dir 2;

element flatSliderBearing   2527 18216 216 10 110.000012345600 -P 20 -Mz 20  -orient 0. 1. 0. 1. 0. 0.;
element zeroLength          11468 18216 216 -mat  31 -dir 2;
element zeroLength          12788 18216 216 -mat  30 -dir 1;

element flatSliderBearing   2787 19216 18216 10 110.000012345600 -P 21 -Mz 21  -orient -1. 0. 0. 0. 1. 0.;
element zeroLength          11728 19216 18216 -mat  41 -dir 1;
element zeroLength          13048 19216 18216 -mat  40 -dir 2;

element flatSliderBearing   2528 217 18217 10 110.000012345600 -P 20 -Mz 20  -orient 0. 1. 0. 1. 0. 0.;
element zeroLength          11469 217 18217 -mat  31 -dir 2;
element zeroLength          12789 217 18217 -mat  30 -dir 1;

element flatSliderBearing   2788 19217 18217 10 110.000012345600 -P 21 -Mz 21  -orient -1. 0. 0. 0. 1. 0.;
element zeroLength          11729 19217 18217 -mat  41 -dir 1;
element zeroLength          13049 19217 18217 -mat  40 -dir 2;

element flatSliderBearing   2529 18218 218 10 110.000012345600 -P 20 -Mz 20  -orient 0. 1. 0. 1. 0. 0.;
element zeroLength          11470 18218 218 -mat  31 -dir 2;
element zeroLength          12790 18218 218 -mat  30 -dir 1;

element flatSliderBearing   2789 19218 18218 10 110.000012345600 -P 21 -Mz 21  -orient -1. 0. 0. 0. 1. 0.;
element zeroLength          11730 19218 18218 -mat  41 -dir 1;
element zeroLength          13050 19218 18218 -mat  40 -dir 2;

element flatSliderBearing   2530 219 18219 10 110.000012345600 -P 20 -Mz 20  -orient 0. 1. 0. 1. 0. 0.;
element zeroLength          11471 219 18219 -mat  31 -dir 2;
element zeroLength          12791 219 18219 -mat  30 -dir 1;

element flatSliderBearing   2790 19219 18219 10 110.000012345600 -P 21 -Mz 21  -orient -1. 0. 0. 0. 1. 0.;
element zeroLength          11731 19219 18219 -mat  41 -dir 1;
element zeroLength          13051 19219 18219 -mat  40 -dir 2;

element flatSliderBearing   2531 182110 2110 10 110.000012345600 -P 20 -Mz 20  -orient 0. 1. 0. 1. 0. 0.;
```

```
element zeroLength          11472 182110 2110 -mat  31 -dir 2;
element zeroLength          12792 182110 2110 -mat  30 -dir 1;

element flatSliderBearing   2791 192110 182110 10 110.000012345600 -P 21 -Mz 21  -orient -1. 0. 0. 0. 1. 0.;
element zeroLength          11732 192110 182110 -mat  41 -dir 1;
element zeroLength          13052 192110 182110 -mat  40 -dir 2;

element flatSliderBearing   2532 2111 182111 10 110.000012345600 -P 20 -Mz 20  -orient 0. 1. 0. 1. 0. 0.;
element zeroLength          11473 2111 182111 -mat  31 -dir 2;
element zeroLength          12793 2111 182111 -mat  30 -dir 1;

element flatSliderBearing   2792 192111 182111 10 110.000012345600 -P 21 -Mz 21  -orient -1. 0. 0. 0. 1. 0.;
element zeroLength          11733 192111 182111 -mat  41 -dir 1;
element zeroLength          13053 192111 182111 -mat  40 -dir 2;

element flatSliderBearing   2533 182112 2112 10 110.000012345600 -P 20 -Mz 20  -orient 0. 1. 0. 1. 0. 0.;
element zeroLength          11474 182112 2112 -mat  31 -dir 2;
element zeroLength          12794 182112 2112 -mat  30 -dir 1;

element flatSliderBearing   2793 192112 182112 10 110.000012345600 -P 21 -Mz 21  -orient -1. 0. 0. 0. 1. 0.;
element zeroLength          11734 192112 182112 -mat  41 -dir 1;
element zeroLength          13054 192112 182112 -mat  40 -dir 2;

element flatSliderBearing   2534 2113 182113 10 110.000012345600 -P 20 -Mz 20  -orient 0. 1. 0. 1. 0. 0.;
element zeroLength          11475 2113 182113 -mat  31 -dir 2;
element zeroLength          12795 2113 182113 -mat  30 -dir 1;

element flatSliderBearing   2794 192113 182113 10 110.000012345600 -P 21 -Mz 21  -orient -1. 0. 0. 0. 1. 0.;
element zeroLength          11735 192113 182113 -mat  41 -dir 1;
element zeroLength          13055 192113 182113 -mat  40 -dir 2;

element flatSliderBearing   2535 182114 2114 10 110.000012345600 -P 20 -Mz 20  -orient 0. 1. 0. 1. 0. 0.;
element zeroLength          11476 182114 2114 -mat  31 -dir 2;
element zeroLength          12796 182114 2114 -mat  30 -dir 1;

element flatSliderBearing   2795 192114 182114 10 110.000012345600 -P 21 -Mz 21  -orient -1. 0. 0. 0. 1. 0.;
element zeroLength          11736 192114 182114 -mat  41 -dir 1;
element zeroLength          13056 192114 182114 -mat  40 -dir 2;

element flatSliderBearing   2536 222 18222 10 110.000012345600 -P 20 -Mz 20  -orient 0. 1. 0. 1. 0. 0.;
element zeroLength          11477 222 18222 -mat  31 -dir 2;
element zeroLength          12797 222 18222 -mat  30 -dir 1;

element flatSliderBearing   2796 19222 18222 10 110.000012345600 -P 21 -Mz 21  -orient -1. 0. 0. 0. 1. 0.;
element zeroLength          11737 19222 18222 -mat  41 -dir 1;
element zeroLength          13057 19222 18222 -mat  40 -dir 2;

element flatSliderBearing   2537 18223 223 10 110.000012345600 -P 20 -Mz 20  -orient 0. 1. 0. 1. 0. 0.;
element zeroLength          11478 18223 223 -mat  31 -dir 2;
element zeroLength          12798 18223 223 -mat  30 -dir 1;

element flatSliderBearing   2797 19223 18223 10 110.000012345600 -P 21 -Mz 21  -orient -1. 0. 0. 0. 1. 0.;
element zeroLength          11738 19223 18223 -mat  41 -dir 1;
element zeroLength          13058 19223 18223 -mat  40 -dir 2;
```

```
element flatSliderBearing  2538 224 18224 10 110.000012345600 -P 20 -Mz 20  -orient 0. 1. 0. 1. 0. 0.;
element zeroLength         11479 224 18224 -mat  31 -dir 2;
element zeroLength         12799 224 18224 -mat  30 -dir 1;

element flatSliderBearing  2798 19224 18224 10 110.000012345600 -P 21 -Mz 21  -orient -1. 0. 0. 0. 1. 0.;
element zeroLength         11739 19224 18224 -mat  41 -dir 1;
element zeroLength         13059 19224 18224 -mat  40 -dir 2;

element flatSliderBearing  2539 18225 225 10 110.000012345600 -P 20 -Mz 20  -orient 0. 1. 0. 1. 0. 0.;
element zeroLength         11480 18225 225 -mat  31 -dir 2;
element zeroLength         12800 18225 225 -mat  30 -dir 1;

element flatSliderBearing  2799 19225 18225 10 110.000012345600 -P 21 -Mz 21  -orient -1. 0. 0. 0. 1. 0.;
element zeroLength         11740 19225 18225 -mat  41 -dir 1;
element zeroLength         13060 19225 18225 -mat  40 -dir 2;

element flatSliderBearing  2540 226 18226 10 110.000012345600 -P 20 -Mz 20  -orient 0. 1. 0. 1. 0. 0.;
element zeroLength         11481 226 18226 -mat  31 -dir 2;
element zeroLength         12801 226 18226 -mat  30 -dir 1;

element flatSliderBearing  2800 19226 18226 10 110.000012345600 -P 21 -Mz 21  -orient -1. 0. 0. 0. 1. 0.;
element zeroLength         11741 19226 18226 -mat  41 -dir 1;
element zeroLength         13061 19226 18226 -mat  40 -dir 2;

element flatSliderBearing  2541 18227 227 10 110.000012345600 -P 20 -Mz 20  -orient 0. 1. 0. 1. 0. 0.;
element zeroLength         11482 18227 227 -mat  31 -dir 2;
element zeroLength         12802 18227 227 -mat  30 -dir 1;

element flatSliderBearing  2801 19227 18227 10 110.000012345600 -P 21 -Mz 21  -orient -1. 0. 0. 0. 1. 0.;
element zeroLength         11742 19227 18227 -mat  41 -dir 1;
element zeroLength         13062 19227 18227 -mat  40 -dir 2;

element flatSliderBearing  2542 228 18228 10 110.000012345600 -P 20 -Mz 20  -orient 0. 1. 0. 1. 0. 0.;
element zeroLength         11483 228 18228 -mat  31 -dir 2;
element zeroLength         12803 228 18228 -mat  30 -dir 1;

element flatSliderBearing  2802 19228 18228 10 110.000012345600 -P 21 -Mz 21  -orient -1. 0. 0. 0. 1. 0.;
element zeroLength         11743 19228 18228 -mat  41 -dir 1;
element zeroLength         13063 19228 18228 -mat  40 -dir 2;

element flatSliderBearing  2543 18229 229 10 110.000012345600 -P 20 -Mz 20  -orient 0. 1. 0. 1. 0. 0.;
element zeroLength         11484 18229 229 -mat  31 -dir 2;
element zeroLength         12804 18229 229 -mat  30 -dir 1;

element flatSliderBearing  2803 19229 18229 10 110.000012345600 -P 21 -Mz 21  -orient -1. 0. 0. 0. 1. 0.;
element zeroLength         11744 19229 18229 -mat  41 -dir 1;
element zeroLength         13064 19229 18229 -mat  40 -dir 2;

element flatSliderBearing  2544 2210 182210 10 110.000012345600 -P 20 -Mz 20  -orient 0. 1. 0. 1. 0. 0.;
element zeroLength         11485 2210 182210 -mat  31 -dir 2;
element zeroLength         12805 2210 182210 -mat  30 -dir 1;

element flatSliderBearing  2804 192210 182210 10 110.000012345600 -P 21 -Mz 21  -orient -1. 0. 0. 0. 1. 0.;
element zeroLength         11745 192210 182210 -mat  41 -dir 1;
element zeroLength         13065 192210 182210 -mat  40 -dir 2;
```

```
element flatSliderBearing  2545 182211 2211 10 110.000012345600 -P 20 -Mz 20  -orient 0. 1. 0. 1. 0. 0.;
element zeroLength         11486 182211 2211 -mat  31 -dir 2;
element zeroLength         12806 182211 2211 -mat  30 -dir 1;

element flatSliderBearing  2805 192211 182211 10 110.000012345600 -P 21 -Mz 21  -orient -1. 0. 0. 0. 1. 0.;
element zeroLength         11746 192211 182211 -mat  41 -dir 1;
element zeroLength         13066 192211 182211 -mat  40 -dir 2;

element flatSliderBearing  2546 2212 182212 10 110.000012345600 -P 20 -Mz 20  -orient 0. 1. 0. 1. 0. 0.;
element zeroLength         11487 2212 182212 -mat  31 -dir 2;
element zeroLength         12807 2212 182212 -mat  30 -dir 1;

element flatSliderBearing  2806 192212 182212 10 110.000012345600 -P 21 -Mz 21  -orient -1. 0. 0. 0. 1. 0.;
element zeroLength         11747 192212 182212 -mat  41 -dir 1;
element zeroLength         13067 192212 182212 -mat  40 -dir 2;

element flatSliderBearing  2547 182213 2213 10 110.000012345600 -P 20 -Mz 20  -orient 0. 1. 0. 1. 0. 0.;
element zeroLength         11488 182213 2213 -mat  31 -dir 2;
element zeroLength         12808 182213 2213 -mat  30 -dir 1;

element flatSliderBearing  2807 192213 182213 10 110.000012345600 -P 21 -Mz 21  -orient -1. 0. 0. 0. 1. 0.;
element zeroLength         11748 192213 182213 -mat  41 -dir 1;
element zeroLength         13068 192213 182213 -mat  40 -dir 2;

element flatSliderBearing  2548 2214 182214 10 110.000012345600 -P 20 -Mz 20  -orient 0. 1. 0. 1. 0. 0.;
element zeroLength         11489 2214 182214 -mat  31 -dir 2;
element zeroLength         12809 2214 182214 -mat  30 -dir 1;

element flatSliderBearing  2808 192214 182214 10 110.000012345600 -P 21 -Mz 21  -orient -1. 0. 0. 0. 1. 0.;
element zeroLength         11749 192214 182214 -mat  41 -dir 1;
element zeroLength         13069 192214 182214 -mat  40 -dir 2;

element flatSliderBearing  2549 18232 232 10 110.000012345600 -P 20 -Mz 20  -orient 0. 1. 0. 1. 0. 0.;
element zeroLength         11490 18232 232 -mat  31 -dir 2;
element zeroLength         12810 18232 232 -mat  30 -dir 1;

element flatSliderBearing  2809 19232 18232 10 110.000012345600 -P 21 -Mz 21  -orient -1. 0. 0. 0. 1. 0.;
element zeroLength         11750 19232 18232 -mat  41 -dir 1;
element zeroLength         13070 19232 18232 -mat  40 -dir 2;

element flatSliderBearing  2550 233 18233 10 110.000012345600 -P 20 -Mz 20  -orient 0. 1. 0. 1. 0. 0.;
element zeroLength         11491 233 18233 -mat  31 -dir 2;
element zeroLength         12811 233 18233 -mat  30 -dir 1;

element flatSliderBearing  2810 19233 18233 10 110.000012345600 -P 21 -Mz 21  -orient -1. 0. 0. 0. 1. 0.;
element zeroLength         11751 19233 18233 -mat  41 -dir 1;
element zeroLength         13071 19233 18233 -mat  40 -dir 2;

element flatSliderBearing  2551 18234 234 10 110.000012345600 -P 20 -Mz 20  -orient 0. 1. 0. 1. 0. 0.;
element zeroLength         11492 18234 234 -mat  31 -dir 2;
element zeroLength         12812 18234 234 -mat  30 -dir 1;

element flatSliderBearing  2811 19234 18234 10 110.000012345600 -P 21 -Mz 21  -orient -1. 0. 0. 0. 1. 0.;
element zeroLength         11752 19234 18234 -mat  41 -dir 1;
```

```
element zeroLength          13072 19234 18234 -mat  40 -dir 2;

element flatSliderBearing   2552 235 18235 10 110.000012345600 -P 20 -Mz 20  -orient 0. 1. 0. 1. 0. 0.;
element zeroLength          11493 235 18235 -mat  31 -dir 2;
element zeroLength          12813 235 18235 -mat  30 -dir 1;

element flatSliderBearing   2812 19235 18235 10 110.000012345600 -P 21 -Mz 21  -orient -1. 0. 0. 0. 1. 0.;
element zeroLength          11753 19235 18235 -mat  41 -dir 1;
element zeroLength          13073 19235 18235 -mat  40 -dir 2;

element flatSliderBearing   2553 18236 236 10 110.000012345600 -P 20 -Mz 20  -orient 0. 1. 0. 1. 0. 0.;
element zeroLength          11494 18236 236 -mat  31 -dir 2;
element zeroLength          12814 18236 236 -mat  30 -dir 1;

element flatSliderBearing   2813 19236 18236 10 110.000012345600 -P 21 -Mz 21  -orient -1. 0. 0. 0. 1. 0.;
element zeroLength          11754 19236 18236 -mat  41 -dir 1;
element zeroLength          13074 19236 18236 -mat  40 -dir 2;

element flatSliderBearing   2554 237 18237 10 110.000012345600 -P 20 -Mz 20  -orient 0. 1. 0. 1. 0. 0.;
element zeroLength          11495 237 18237 -mat  31 -dir 2;
element zeroLength          12815 237 18237 -mat  30 -dir 1;

element flatSliderBearing   2814 19237 18237 10 110.000012345600 -P 21 -Mz 21  -orient -1. 0. 0. 0. 1. 0.;
element zeroLength          11755 19237 18237 -mat  41 -dir 1;
element zeroLength          13075 19237 18237 -mat  40 -dir 2;

element flatSliderBearing   2555 18238 238 10 110.000012345600 -P 20 -Mz 20  -orient 0. 1. 0. 1. 0. 0.;
element zeroLength          11496 18238 238 -mat  31 -dir 2;
element zeroLength          12816 18238 238 -mat  30 -dir 1;

element flatSliderBearing   2815 19238 18238 10 110.000012345600 -P 21 -Mz 21  -orient -1. 0. 0. 0. 1. 0.;
element zeroLength          11756 19238 18238 -mat  41 -dir 1;
element zeroLength          13076 19238 18238 -mat  40 -dir 2;

element flatSliderBearing   2556 239 18239 10 110.000012345600 -P 20 -Mz 20  -orient 0. 1. 0. 1. 0. 0.;
element zeroLength          11497 239 18239 -mat  31 -dir 2;
element zeroLength          12817 239 18239 -mat  30 -dir 1;

element flatSliderBearing   2816 19239 18239 10 110.000012345600 -P 21 -Mz 21  -orient -1. 0. 0. 0. 1. 0.;
element zeroLength          11757 19239 18239 -mat  41 -dir 1;
element zeroLength          13077 19239 18239 -mat  40 -dir 2;

element flatSliderBearing   2557 182310 2310 10 110.000012345600 -P 20 -Mz 20  -orient 0. 1. 0. 1. 0. 0.;
element zeroLength          11498 182310 2310 -mat  31 -dir 2;
element zeroLength          12818 182310 2310 -mat  30 -dir 1;

element flatSliderBearing   2817 192310 182310 10 110.000012345600 -P 21 -Mz 21  -orient -1. 0. 0. 0. 1. 0.;
element zeroLength          11758 192310 182310 -mat  41 -dir 1;
element zeroLength          13078 192310 182310 -mat  40 -dir 2;

element flatSliderBearing   2558 2311 182311 10 110.000012345600 -P 20 -Mz 20  -orient 0. 1. 0. 1. 0. 0.;
element zeroLength          11499 2311 182311 -mat  31 -dir 2;
element zeroLength          12819 2311 182311 -mat  30 -dir 1;

element flatSliderBearing   2818 192311 182311 10 110.000012345600 -P 21 -Mz 21  -orient -1. 0. 0. 0. 1. 0.;
```

```
element zeroLength          11759 192311 182311 -mat  41 -dir 1;
element zeroLength          13079 192311 182311 -mat  40 -dir 2;

element flatSliderBearing   2559 182312 2312 10 110.000012345600 -P 20 -Mz 20  -orient 0. 1. 0. 1. 0. 0.;
element zeroLength          11500 182312 2312 -mat  31 -dir 2;
element zeroLength          12820 182312 2312 -mat  30 -dir 1;

element flatSliderBearing   2819 192312 182312 10 110.000012345600 -P 21 -Mz 21  -orient -1. 0. 0. 0. 1. 0.;
element zeroLength          11760 192312 182312 -mat  41 -dir 1;
element zeroLength          13080 192312 182312 -mat  40 -dir 2;

element flatSliderBearing   2560 2313 182313 10 110.000012345600 -P 20 -Mz 20  -orient 0. 1. 0. 1. 0. 0.;
element zeroLength          11501 2313 182313 -mat  31 -dir 2;
element zeroLength          12821 2313 182313 -mat  30 -dir 1;

element flatSliderBearing   2820 192313 182313 10 110.000012345600 -P 21 -Mz 21  -orient -1. 0. 0. 0. 1. 0.;
element zeroLength          11761 192313 182313 -mat  41 -dir 1;
element zeroLength          13081 192313 182313 -mat  40 -dir 2;

element flatSliderBearing   2561 182314 2314 10 110.000012345600 -P 20 -Mz 20  -orient 0. 1. 0. 1. 0. 0.;
element zeroLength          11502 182314 2314 -mat  31 -dir 2;
element zeroLength          12822 182314 2314 -mat  30 -dir 1;

element flatSliderBearing   2821 192314 182314 10 110.000012345600 -P 21 -Mz 21  -orient -1. 0. 0. 0. 1. 0.;
element zeroLength          11762 192314 182314 -mat  41 -dir 1;
element zeroLength          13082 192314 182314 -mat  40 -dir 2;

element flatSliderBearing   2562 242 18242 10 110.000012345600 -P 20 -Mz 20  -orient 0. 1. 0. 1. 0. 0.;
element zeroLength          11503 242 18242 -mat  31 -dir 2;
element zeroLength          12823 242 18242 -mat  30 -dir 1;

element flatSliderBearing   2822 19242 18242 10 110.000012345600 -P 21 -Mz 21  -orient -1. 0. 0. 0. 1. 0.;
element zeroLength          11763 19242 18242 -mat  41 -dir 1;
element zeroLength          13083 19242 18242 -mat  40 -dir 2;

element flatSliderBearing   2563 18243 243 10 110.000012345600 -P 20 -Mz 20  -orient 0. 1. 0. 1. 0. 0.;
element zeroLength          11504 18243 243 -mat  31 -dir 2;
element zeroLength          12824 18243 243 -mat  30 -dir 1;

element flatSliderBearing   2823 19243 18243 10 110.000012345600 -P 21 -Mz 21  -orient -1. 0. 0. 0. 1. 0.;
element zeroLength          11764 19243 18243 -mat  41 -dir 1;
element zeroLength          13084 19243 18243 -mat  40 -dir 2;

element flatSliderBearing   2564 244 18244 10 110.000012345600 -P 20 -Mz 20  -orient 0. 1. 0. 1. 0. 0.;
element zeroLength          11505 244 18244 -mat  31 -dir 2;
element zeroLength          12825 244 18244 -mat  30 -dir 1;

element flatSliderBearing   2824 19244 18244 10 110.000012345600 -P 21 -Mz 21  -orient -1. 0. 0. 0. 1. 0.;
element zeroLength          11765 19244 18244 -mat  41 -dir 1;
element zeroLength          13085 19244 18244 -mat  40 -dir 2;

element flatSliderBearing   2565 18245 245 10 110.000012345600 -P 20 -Mz 20  -orient 0. 1. 0. 1. 0. 0.;
element zeroLength          11506 18245 245 -mat  31 -dir 2;
element zeroLength          12826 18245 245 -mat  30 -dir 1;
```

```
element flatSliderBearing  2825 19245 18245 10 110.000012345600 -P 21 -Mz 21  -orient -1. 0. 0. 0. 1. 0.;
element zeroLength         11766 19245 18245 -mat  41 -dir 1;
element zeroLength         13086 19245 18245 -mat  40 -dir 2;

element flatSliderBearing  2566 246 18246 10 110.000012345600 -P 20 -Mz 20  -orient 0. 1. 0. 1. 0. 0.;
element zeroLength         11507 246 18246 -mat  31 -dir 2;
element zeroLength         12827 246 18246 -mat  30 -dir 1;

element flatSliderBearing  2826 19246 18246 10 110.000012345600 -P 21 -Mz 21  -orient -1. 0. 0. 0. 1. 0.;
element zeroLength         11767 19246 18246 -mat  41 -dir 1;
element zeroLength         13087 19246 18246 -mat  40 -dir 2;

element flatSliderBearing  2567 18247 247 10 110.000012345600 -P 20 -Mz 20  -orient 0. 1. 0. 1. 0. 0.;
element zeroLength         11508 18247 247 -mat  31 -dir 2;
element zeroLength         12828 18247 247 -mat  30 -dir 1;

element flatSliderBearing  2827 19247 18247 10 110.000012345600 -P 21 -Mz 21  -orient -1. 0. 0. 0. 1. 0.;
element zeroLength         11768 19247 18247 -mat  41 -dir 1;
element zeroLength         13088 19247 18247 -mat  40 -dir 2;

element flatSliderBearing  2568 248 18248 10 110.000012345600 -P 20 -Mz 20  -orient 0. 1. 0. 1. 0. 0.;
element zeroLength         11509 248 18248 -mat  31 -dir 2;
element zeroLength         12829 248 18248 -mat  30 -dir 1;

element flatSliderBearing  2828 19248 18248 10 110.000012345600 -P 21 -Mz 21  -orient -1. 0. 0. 0. 1. 0.;
element zeroLength         11769 19248 18248 -mat  41 -dir 1;
element zeroLength         13089 19248 18248 -mat  40 -dir 2;

element flatSliderBearing  2569 18249 249 10 110.000012345600 -P 20 -Mz 20  -orient 0. 1. 0. 1. 0. 0.;
element zeroLength         11510 18249 249 -mat  31 -dir 2;
element zeroLength         12830 18249 249 -mat  30 -dir 1;

element flatSliderBearing  2829 19249 18249 10 110.000012345600 -P 21 -Mz 21  -orient -1. 0. 0. 0. 1. 0.;
element zeroLength         11770 19249 18249 -mat  41 -dir 1;
element zeroLength         13090 19249 18249 -mat  40 -dir 2;

element flatSliderBearing  2570 2410 182410 10 110.000012345600 -P 20 -Mz 20  -orient 0. 1. 0. 1. 0. 0.;
element zeroLength         11511 2410 182410 -mat  31 -dir 2;
element zeroLength         12831 2410 182410 -mat  30 -dir 1;

element flatSliderBearing  2830 192410 182410 10 110.000012345600 -P 21 -Mz 21  -orient -1. 0. 0. 0. 1. 0.;
element zeroLength         11771 192410 182410 -mat  41 -dir 1;
element zeroLength         13091 192410 182410 -mat  40 -dir 2;

element flatSliderBearing  2571 182411 2411 10 110.000012345600 -P 20 -Mz 20  -orient 0. 1. 0. 1. 0. 0.;
element zeroLength         11512 182411 2411 -mat  31 -dir 2;
element zeroLength         12832 182411 2411 -mat  30 -dir 1;

element flatSliderBearing  2831 192411 182411 10 110.000012345600 -P 21 -Mz 21  -orient -1. 0. 0. 0. 1. 0.;
element zeroLength         11772 192411 182411 -mat  41 -dir 1;
element zeroLength         13092 192411 182411 -mat  40 -dir 2;

element flatSliderBearing  2572 2412 182412 10 110.000012345600 -P 20 -Mz 20  -orient 0. 1. 0. 1. 0. 0.;
element zeroLength         11513 2412 182412 -mat  31 -dir 2;
element zeroLength         12833 2412 182412 -mat  30 -dir 1;
```

```
element flatSliderBearing  2832 192412 182412 10 110.000012345600 -P 21 -Mz 21  -orient -1. 0. 0. 0. 1. 0.;
element zeroLength         11773 192412 182412 -mat  41 -dir 1;
element zeroLength         13093 192412 182412 -mat  40 -dir 2;

element flatSliderBearing  2573 182413 2413 10 110.000012345600 -P 20 -Mz 20  -orient 0. 1. 0. 1. 0. 0.;
element zeroLength         11514 182413 2413 -mat  31 -dir 2;
element zeroLength         12834 182413 2413 -mat  30 -dir 1;

element flatSliderBearing  2833 192413 182413 10 110.000012345600 -P 21 -Mz 21  -orient -1. 0. 0. 0. 1. 0.;
element zeroLength         11774 192413 182413 -mat  41 -dir 1;
element zeroLength         13094 192413 182413 -mat  40 -dir 2;

element flatSliderBearing  2574 2414 182414 10 110.000012345600 -P 20 -Mz 20  -orient 0. 1. 0. 1. 0. 0.;
element zeroLength         11515 2414 182414 -mat  31 -dir 2;
element zeroLength         12835 2414 182414 -mat  30 -dir 1;

element flatSliderBearing  2834 192414 182414 10 110.000012345600 -P 21 -Mz 21  -orient -1. 0. 0. 0. 1. 0.;
element zeroLength         11775 192414 182414 -mat  41 -dir 1;
element zeroLength         13095 192414 182414 -mat  40 -dir 2;

element flatSliderBearing  2575 18252 252 10 110.000012345600 -P 20 -Mz 20  -orient 0. 1. 0. 1. 0. 0.;
element zeroLength         11516 18252 252 -mat  31 -dir 2;
element zeroLength         12836 18252 252 -mat  30 -dir 1;

element flatSliderBearing  2835 19252 18252 10 110.000012345600 -P 21 -Mz 21  -orient -1. 0. 0. 0. 1. 0.;
element zeroLength         11776 19252 18252 -mat  41 -dir 1;
element zeroLength         13096 19252 18252 -mat  40 -dir 2;

element flatSliderBearing  2576 253 18253 10 110.000012345600 -P 20 -Mz 20  -orient 0. 1. 0. 1. 0. 0.;
element zeroLength         11517 253 18253 -mat  31 -dir 2;
element zeroLength         12837 253 18253 -mat  30 -dir 1;

element flatSliderBearing  2836 19253 18253 10 110.000012345600 -P 21 -Mz 21  -orient -1. 0. 0. 0. 1. 0.;
element zeroLength         11777 19253 18253 -mat  41 -dir 1;
element zeroLength         13097 19253 18253 -mat  40 -dir 2;

element flatSliderBearing  2577 18254 254 10 110.000012345600 -P 20 -Mz 20  -orient 0. 1. 0. 1. 0. 0.;
element zeroLength         11518 18254 254 -mat  31 -dir 2;
element zeroLength         12838 18254 254 -mat  30 -dir 1;

element flatSliderBearing  2837 19254 18254 10 110.000012345600 -P 21 -Mz 21  -orient -1. 0. 0. 0. 1. 0.;
element zeroLength         11778 19254 18254 -mat  41 -dir 1;
element zeroLength         13098 19254 18254 -mat  40 -dir 2;

element flatSliderBearing  2578 255 18255 10 110.000012345600 -P 20 -Mz 20  -orient 0. 1. 0. 1. 0. 0.;
element zeroLength         11519 255 18255 -mat  31 -dir 2;
element zeroLength         12839 255 18255 -mat  30 -dir 1;

element flatSliderBearing  2838 19255 18255 10 110.000012345600 -P 21 -Mz 21  -orient -1. 0. 0. 0. 1. 0.;
element zeroLength         11779 19255 18255 -mat  41 -dir 1;
element zeroLength         13099 19255 18255 -mat  40 -dir 2;

element flatSliderBearing  2579 18256 256 10 110.000012345600 -P 20 -Mz 20  -orient 0. 1. 0. 1. 0. 0.;
element zeroLength         11520 18256 256 -mat  31 -dir 2;
```

```
element zeroLength          12840 18256 256 -mat  30 -dir 1;

element flatSliderBearing   2839 19256 18256 10 110.000012345600 -P 21 -Mz 21  -orient -1. 0. 0. 0. 1. 0.;
element zeroLength          11780 19256 18256 -mat  41 -dir 1;
element zeroLength          13100 19256 18256 -mat  40 -dir 2;

element flatSliderBearing   2580 257 18257 10 110.000012345600 -P 20 -Mz 20  -orient 0. 1. 0. 1. 0. 0.;
element zeroLength          11521 257 18257 -mat  31 -dir 2;
element zeroLength          12841 257 18257 -mat  30 -dir 1;

element flatSliderBearing   2840 19257 18257 10 110.000012345600 -P 21 -Mz 21  -orient -1. 0. 0. 0. 1. 0.;
element zeroLength          11781 19257 18257 -mat  41 -dir 1;
element zeroLength          13101 19257 18257 -mat  40 -dir 2;

element flatSliderBearing   2581 18258 258 10 110.000012345600 -P 20 -Mz 20  -orient 0. 1. 0. 1. 0. 0.;
element zeroLength          11522 18258 258 -mat  31 -dir 2;
element zeroLength          12842 18258 258 -mat  30 -dir 1;

element flatSliderBearing   2841 19258 18258 10 110.000012345600 -P 21 -Mz 21  -orient -1. 0. 0. 0. 1. 0.;
element zeroLength          11782 19258 18258 -mat  41 -dir 1;
element zeroLength          13102 19258 18258 -mat  40 -dir 2;

element flatSliderBearing   2582 259 18259 10 110.000012345600 -P 20 -Mz 20  -orient 0. 1. 0. 1. 0. 0.;
element zeroLength          11523 259 18259 -mat  31 -dir 2;
element zeroLength          12843 259 18259 -mat  30 -dir 1;

element flatSliderBearing   2842 19259 18259 10 110.000012345600 -P 21 -Mz 21  -orient -1. 0. 0. 0. 1. 0.;
element zeroLength          11783 19259 18259 -mat  41 -dir 1;
element zeroLength          13103 19259 18259 -mat  40 -dir 2;

element flatSliderBearing   2583 182510 2510 10 110.000012345600 -P 20 -Mz 20  -orient 0. 1. 0. 1. 0. 0.;
element zeroLength          11524 182510 2510 -mat  31 -dir 2;
element zeroLength          12844 182510 2510 -mat  30 -dir 1;

element flatSliderBearing   2843 192510 182510 10 110.000012345600 -P 21 -Mz 21  -orient -1. 0. 0. 0. 1. 0.;
element zeroLength          11784 192510 182510 -mat  41 -dir 1;
element zeroLength          13104 192510 182510 -mat  40 -dir 2;

element flatSliderBearing   2584 2511 182511 10 110.000012345600 -P 20 -Mz 20  -orient 0. 1. 0. 1. 0. 0.;
element zeroLength          11525 2511 182511 -mat  31 -dir 2;
element zeroLength          12845 2511 182511 -mat  30 -dir 1;

element flatSliderBearing   2844 192511 182511 10 110.000012345600 -P 21 -Mz 21  -orient -1. 0. 0. 0. 1. 0.;
element zeroLength          11785 192511 182511 -mat  41 -dir 1;
element zeroLength          13105 192511 182511 -mat  40 -dir 2;

element flatSliderBearing   2585 182512 2512 10 110.000012345600 -P 20 -Mz 20  -orient 0. 1. 0. 1. 0. 0.;
element zeroLength          11526 182512 2512 -mat  31 -dir 2;
element zeroLength          12846 182512 2512 -mat  30 -dir 1;

element flatSliderBearing   2845 192512 182512 10 110.000012345600 -P 21 -Mz 21  -orient -1. 0. 0. 0. 1. 0.;
element zeroLength          11786 192512 182512 -mat  41 -dir 1;
element zeroLength          13106 192512 182512 -mat  40 -dir 2;

element flatSliderBearing   2586 2513 182513 10 110.000012345600 -P 20 -Mz 20  -orient 0. 1. 0. 1. 0. 0.;
```

```
element zeroLength          11527 2513 182513 -mat  31 -dir 2;
element zeroLength          12847 2513 182513 -mat  30 -dir 1;

element flatSliderBearing   2846 192513 182513 10 110.000012345600 -P 21 -Mz 21  -orient -1. 0. 0. 0. 1. 0.;
element zeroLength          11787 192513 182513 -mat  41 -dir 1;
element zeroLength          13107 192513 182513 -mat  40 -dir 2;

element flatSliderBearing   2587 182514 2514 10 110.000012345600 -P 20 -Mz 20  -orient 0. 1. 0. 1. 0. 0.;
element zeroLength          11528 182514 2514 -mat  31 -dir 2;
element zeroLength          12848 182514 2514 -mat  30 -dir 1;

element flatSliderBearing   2847 192514 182514 10 110.000012345600 -P 21 -Mz 21  -orient -1. 0. 0. 0. 1. 0.;
element zeroLength          11788 192514 182514 -mat  41 -dir 1;
element zeroLength          13108 192514 182514 -mat  40 -dir 2;

element flatSliderBearing   2588 262 18262 10 110.000012345600 -P 20 -Mz 20  -orient 0. 1. 0. 1. 0. 0.;
element zeroLength          11529 262 18262 -mat  31 -dir 2;
element zeroLength          12849 262 18262 -mat  30 -dir 1;

element flatSliderBearing   2848 19262 18262 10 110.000012345600 -P 21 -Mz 21  -orient -1. 0. 0. 0. 1. 0.;
element zeroLength          11789 19262 18262 -mat  41 -dir 1;
element zeroLength          13109 19262 18262 -mat  40 -dir 2;

element flatSliderBearing   2589 18263 263 10 110.000012345600 -P 20 -Mz 20  -orient 0. 1. 0. 1. 0. 0.;
element zeroLength          11530 18263 263 -mat  31 -dir 2;
element zeroLength          12850 18263 263 -mat  30 -dir 1;

element flatSliderBearing   2849 19263 18263 10 110.000012345600 -P 21 -Mz 21  -orient -1. 0. 0. 0. 1. 0.;
element zeroLength          11790 19263 18263 -mat  41 -dir 1;
element zeroLength          13110 19263 18263 -mat  40 -dir 2;

element flatSliderBearing   2590 264 18264 10 110.000012345600 -P 20 -Mz 20  -orient 0. 1. 0. 1. 0. 0.;
element zeroLength          11531 264 18264 -mat  31 -dir 2;
element zeroLength          12851 264 18264 -mat  30 -dir 1;

element flatSliderBearing   2850 19264 18264 10 110.000012345600 -P 21 -Mz 21  -orient -1. 0. 0. 0. 1. 0.;
element zeroLength          11791 19264 18264 -mat  41 -dir 1;
element zeroLength          13111 19264 18264 -mat  40 -dir 2;

element flatSliderBearing   2591 18265 265 10 110.000012345600 -P 20 -Mz 20  -orient 0. 1. 0. 1. 0. 0.;
element zeroLength          11532 18265 265 -mat  31 -dir 2;
element zeroLength          12852 18265 265 -mat  30 -dir 1;

element flatSliderBearing   2851 19265 18265 10 110.000012345600 -P 21 -Mz 21  -orient -1. 0. 0. 0. 1. 0.;
element zeroLength          11792 19265 18265 -mat  41 -dir 1;
element zeroLength          13112 19265 18265 -mat  40 -dir 2;

element flatSliderBearing   2592 266 18266 10 110.000012345600 -P 20 -Mz 20  -orient 0. 1. 0. 1. 0. 0.;
element zeroLength          11533 266 18266 -mat  31 -dir 2;
element zeroLength          12853 266 18266 -mat  30 -dir 1;

element flatSliderBearing   2852 19266 18266 10 110.000012345600 -P 21 -Mz 21  -orient -1. 0. 0. 0. 1. 0.;
element zeroLength          11793 19266 18266 -mat  41 -dir 1;
element zeroLength          13113 19266 18266 -mat  40 -dir 2;
```

```
element flatSliderBearing  2593 18267 267 10 110.000012345600 -P 20 -Mz 20  -orient 0. 1. 0. 1. 0. 0.;
element zeroLength         11534 18267 267 -mat  31 -dir 2;
element zeroLength         12854 18267 267 -mat  30 -dir 1;

element flatSliderBearing  2853 19267 18267 10 110.000012345600 -P 21 -Mz 21  -orient -1. 0. 0. 0. 1. 0.;
element zeroLength         11794 19267 18267 -mat  41 -dir 1;
element zeroLength         13114 19267 18267 -mat  40 -dir 2;

element flatSliderBearing  2594 268 18268 10 110.000012345600 -P 20 -Mz 20  -orient 0. 1. 0. 1. 0. 0.;
element zeroLength         11535 268 18268 -mat  31 -dir 2;
element zeroLength         12855 268 18268 -mat  30 -dir 1;

element flatSliderBearing  2854 19268 18268 10 110.000012345600 -P 21 -Mz 21  -orient -1. 0. 0. 0. 1. 0.;
element zeroLength         11795 19268 18268 -mat  41 -dir 1;
element zeroLength         13115 19268 18268 -mat  40 -dir 2;

element flatSliderBearing  2595 18269 269 10 110.000012345600 -P 20 -Mz 20  -orient 0. 1. 0. 1. 0. 0.;
element zeroLength         11536 18269 269 -mat  31 -dir 2;
element zeroLength         12856 18269 269 -mat  30 -dir 1;

element flatSliderBearing  2855 19269 18269 10 110.000012345600 -P 21 -Mz 21  -orient -1. 0. 0. 0. 1. 0.;
element zeroLength         11796 19269 18269 -mat  41 -dir 1;
element zeroLength         13116 19269 18269 -mat  40 -dir 2;

element flatSliderBearing  2596 2610 182610 10 110.000012345600 -P 20 -Mz 20  -orient 0. 1. 0. 1. 0. 0.;
element zeroLength         11537 2610 182610 -mat  31 -dir 2;
element zeroLength         12857 2610 182610 -mat  30 -dir 1;

element flatSliderBearing  2856 192610 182610 10 110.000012345600 -P 21 -Mz 21  -orient -1. 0. 0. 0. 1. 0.;
element zeroLength         11797 192610 182610 -mat  41 -dir 1;
element zeroLength         13117 192610 182610 -mat  40 -dir 2;

element flatSliderBearing  2597 182611 2611 10 110.000012345600 -P 20 -Mz 20  -orient 0. 1. 0. 1. 0. 0.;
element zeroLength         11538 182611 2611 -mat  31 -dir 2;
element zeroLength         12858 182611 2611 -mat  30 -dir 1;

element flatSliderBearing  2857 192611 182611 10 110.000012345600 -P 21 -Mz 21  -orient -1. 0. 0. 0. 1. 0.;
element zeroLength         11798 192611 182611 -mat  41 -dir 1;
element zeroLength         13118 192611 182611 -mat  40 -dir 2;

element flatSliderBearing  2598 2612 182612 10 110.000012345600 -P 20 -Mz 20  -orient 0. 1. 0. 1. 0. 0.;
element zeroLength         11539 2612 182612 -mat  31 -dir 2;
element zeroLength         12859 2612 182612 -mat  30 -dir 1;

element flatSliderBearing  2858 192612 182612 10 110.000012345600 -P 21 -Mz 21  -orient -1. 0. 0. 0. 1. 0.;
element zeroLength         11799 192612 182612 -mat  41 -dir 1;
element zeroLength         13119 192612 182612 -mat  40 -dir 2;

element flatSliderBearing  2599 182613 2613 10 110.000012345600 -P 20 -Mz 20  -orient 0. 1. 0. 1. 0. 0.;
element zeroLength         11540 182613 2613 -mat  31 -dir 2;
element zeroLength         12860 182613 2613 -mat  30 -dir 1;

element flatSliderBearing  2859 192613 182613 10 110.000012345600 -P 21 -Mz 21  -orient -1. 0. 0. 0. 1. 0.;
element zeroLength         11800 192613 182613 -mat  41 -dir 1;
element zeroLength         13120 192613 182613 -mat  40 -dir 2;
```

```
element flatSliderBearing  2600 2614 182614 10 110.000012345600 -P 20 -Mz 20  -orient 0. 1. 0. 1. 0. 0.;
element zeroLength         11541 2614 182614 -mat  31 -dir 2;
element zeroLength         12861 2614 182614 -mat  30 -dir 1;

element flatSliderBearing  2860 192614 182614 10 110.000012345600 -P 21 -Mz 21  -orient -1. 0. 0. 0. 1. 0.;
element zeroLength         11801 192614 182614 -mat  41 -dir 1;
element zeroLength         13121 192614 182614 -mat  40 -dir 2;

element flatSliderBearing  2601 18272 272 10 110.000012345600 -P 20 -Mz 20  -orient 0. 1. 0. 1. 0. 0.;
element zeroLength         11542 18272 272 -mat  31 -dir 2;
element zeroLength         12862 18272 272 -mat  30 -dir 1;

element flatSliderBearing  2861 19272 18272 10 110.000012345600 -P 21 -Mz 21  -orient -1. 0. 0. 0. 1. 0.;
element zeroLength         11802 19272 18272 -mat  41 -dir 1;
element zeroLength         13122 19272 18272 -mat  40 -dir 2;

element flatSliderBearing  2602 273 18273 10 110.000012345600 -P 20 -Mz 20  -orient 0. 1. 0. 1. 0. 0.;
element zeroLength         11543 273 18273 -mat  31 -dir 2;
element zeroLength         12863 273 18273 -mat  30 -dir 1;

element flatSliderBearing  2862 19273 18273 10 110.000012345600 -P 21 -Mz 21  -orient -1. 0. 0. 0. 1. 0.;
element zeroLength         11803 19273 18273 -mat  41 -dir 1;
element zeroLength         13123 19273 18273 -mat  40 -dir 2;

element flatSliderBearing  2603 18274 274 10 110.000012345600 -P 20 -Mz 20  -orient 0. 1. 0. 1. 0. 0.;
element zeroLength         11544 18274 274 -mat  31 -dir 2;
element zeroLength         12864 18274 274 -mat  30 -dir 1;

element flatSliderBearing  2863 19274 18274 10 110.000012345600 -P 21 -Mz 21  -orient -1. 0. 0. 0. 1. 0.;
element zeroLength         11804 19274 18274 -mat  41 -dir 1;
element zeroLength         13124 19274 18274 -mat  40 -dir 2;

element flatSliderBearing  2604 275 18275 10 110.000012345600 -P 20 -Mz 20  -orient 0. 1. 0. 1. 0. 0.;
element zeroLength         11545 275 18275 -mat  31 -dir 2;
element zeroLength         12865 275 18275 -mat  30 -dir 1;

element flatSliderBearing  2864 19275 18275 10 110.000012345600 -P 21 -Mz 21  -orient -1. 0. 0. 0. 1. 0.;
element zeroLength         11805 19275 18275 -mat  41 -dir 1;
element zeroLength         13125 19275 18275 -mat  40 -dir 2;

element flatSliderBearing  2605 18276 276 10 110.000012345600 -P 20 -Mz 20  -orient 0. 1. 0. 1. 0. 0.;
element zeroLength         11546 18276 276 -mat  31 -dir 2;
element zeroLength         12866 18276 276 -mat  30 -dir 1;

element flatSliderBearing  2865 19276 18276 10 110.000012345600 -P 21 -Mz 21  -orient -1. 0. 0. 0. 1. 0.;
element zeroLength         11806 19276 18276 -mat  41 -dir 1;
element zeroLength         13126 19276 18276 -mat  40 -dir 2;

element flatSliderBearing  2606 277 18277 10 110.000012345600 -P 20 -Mz 20  -orient 0. 1. 0. 1. 0. 0.;
element zeroLength         11547 277 18277 -mat  31 -dir 2;
element zeroLength         12867 277 18277 -mat  30 -dir 1;

element flatSliderBearing  2866 19277 18277 10 110.000012345600 -P 21 -Mz 21  -orient -1. 0. 0. 0. 1. 0.;
element zeroLength         11807 19277 18277 -mat  41 -dir 1;
```

```
element zeroLength          13127 19277 18277 -mat  40 -dir 2;

element flatSliderBearing   2607 18278 278 10 110.000012345600 -P 20 -Mz 20  -orient 0. 1. 0. 1. 0. 0.;
element zeroLength          11548 18278 278 -mat  31 -dir 2;
element zeroLength          12868 18278 278 -mat  30 -dir 1;

element flatSliderBearing   2867 19278 18278 10 110.000012345600 -P 21 -Mz 21  -orient -1. 0. 0. 0. 1. 0.;
element zeroLength          11808 19278 18278 -mat  41 -dir 1;
element zeroLength          13128 19278 18278 -mat  40 -dir 2;

element flatSliderBearing   2608 279 18279 10 110.000012345600 -P 20 -Mz 20  -orient 0. 1. 0. 1. 0. 0.;
element zeroLength          11549 279 18279 -mat  31 -dir 2;
element zeroLength          12869 279 18279 -mat  30 -dir 1;

element flatSliderBearing   2868 19279 18279 10 110.000012345600 -P 21 -Mz 21  -orient -1. 0. 0. 0. 1. 0.;
element zeroLength          11809 19279 18279 -mat  41 -dir 1;
element zeroLength          13129 19279 18279 -mat  40 -dir 2;

element flatSliderBearing   2609 182710 2710 10 110.000012345600 -P 20 -Mz 20  -orient 0. 1. 0. 1. 0. 0.;
element zeroLength          11550 182710 2710 -mat  31 -dir 2;
element zeroLength          12870 182710 2710 -mat  30 -dir 1;

element flatSliderBearing   2869 192710 182710 10 110.000012345600 -P 21 -Mz 21  -orient -1. 0. 0. 0. 1. 0.;
element zeroLength          11810 192710 182710 -mat  41 -dir 1;
element zeroLength          13130 192710 182710 -mat  40 -dir 2;

element flatSliderBearing   2610 2711 182711 10 110.000012345600 -P 20 -Mz 20  -orient 0. 1. 0. 1. 0. 0.;
element zeroLength          11551 2711 182711 -mat  31 -dir 2;
element zeroLength          12871 2711 182711 -mat  30 -dir 1;

element flatSliderBearing   2870 192711 182711 10 110.000012345600 -P 21 -Mz 21  -orient -1. 0. 0. 0. 1. 0.;
element zeroLength          11811 192711 182711 -mat  41 -dir 1;
element zeroLength          13131 192711 182711 -mat  40 -dir 2;

element flatSliderBearing   2611 182712 2712 10 110.000012345600 -P 20 -Mz 20  -orient 0. 1. 0. 1. 0. 0.;
element zeroLength          11552 182712 2712 -mat  31 -dir 2;
element zeroLength          12872 182712 2712 -mat  30 -dir 1;

element flatSliderBearing   2871 192712 182712 10 110.000012345600 -P 21 -Mz 21  -orient -1. 0. 0. 0. 1. 0.;
element zeroLength          11812 192712 182712 -mat  41 -dir 1;
element zeroLength          13132 192712 182712 -mat  40 -dir 2;

element flatSliderBearing   2612 2713 182713 10 110.000012345600 -P 20 -Mz 20  -orient 0. 1. 0. 1. 0. 0.;
element zeroLength          11553 2713 182713 -mat  31 -dir 2;
element zeroLength          12873 2713 182713 -mat  30 -dir 1;

element flatSliderBearing   2872 192713 182713 10 110.000012345600 -P 21 -Mz 21  -orient -1. 0. 0. 0. 1. 0.;
element zeroLength          11813 192713 182713 -mat  41 -dir 1;
element zeroLength          13133 192713 182713 -mat  40 -dir 2;

element flatSliderBearing   2613 182714 2714 10 110.000012345600 -P 20 -Mz 20  -orient 0. 1. 0. 1. 0. 0.;
element zeroLength          11554 182714 2714 -mat  31 -dir 2;
element zeroLength          12874 182714 2714 -mat  30 -dir 1;

element flatSliderBearing   2873 192714 182714 10 110.000012345600 -P 21 -Mz 21  -orient -1. 0. 0. 0. 1. 0.;
```

```
element zeroLength          11814 192714 182714 -mat  41 -dir 1;
element zeroLength          13134 192714 182714 -mat  40 -dir 2;

element flatSliderBearing   2614 282 18282 10 110.000012345600 -P 20 -Mz 20  -orient 0. 1. 0. 1. 0. 0.;
element zeroLength          11555 282 18282 -mat  31 -dir 2;
element zeroLength          12875 282 18282 -mat  30 -dir 1;

element flatSliderBearing   2874 19282 18282 10 110.000012345600 -P 21 -Mz 21  -orient -1. 0. 0. 0. 1. 0.;
element zeroLength          11815 19282 18282 -mat  41 -dir 1;
element zeroLength          13135 19282 18282 -mat  40 -dir 2;

element flatSliderBearing   2615 18283 283 10 110.000012345600 -P 20 -Mz 20  -orient 0. 1. 0. 1. 0. 0.;
element zeroLength          11556 18283 283 -mat  31 -dir 2;
element zeroLength          12876 18283 283 -mat  30 -dir 1;

element flatSliderBearing   2875 19283 18283 10 110.000012345600 -P 21 -Mz 21  -orient -1. 0. 0. 0. 1. 0.;
element zeroLength          11816 19283 18283 -mat  41 -dir 1;
element zeroLength          13136 19283 18283 -mat  40 -dir 2;

element flatSliderBearing   2616 284 18284 10 110.000012345600 -P 20 -Mz 20  -orient 0. 1. 0. 1. 0. 0.;
element zeroLength          11557 284 18284 -mat  31 -dir 2;
element zeroLength          12877 284 18284 -mat  30 -dir 1;

element flatSliderBearing   2876 19284 18284 10 110.000012345600 -P 21 -Mz 21  -orient -1. 0. 0. 0. 1. 0.;
element zeroLength          11817 19284 18284 -mat  41 -dir 1;
element zeroLength          13137 19284 18284 -mat  40 -dir 2;

element flatSliderBearing   2617 18285 285 10 110.000012345600 -P 20 -Mz 20  -orient 0. 1. 0. 1. 0. 0.;
element zeroLength          11558 18285 285 -mat  31 -dir 2;
element zeroLength          12878 18285 285 -mat  30 -dir 1;

element flatSliderBearing   2877 19285 18285 10 110.000012345600 -P 21 -Mz 21  -orient -1. 0. 0. 0. 1. 0.;
element zeroLength          11818 19285 18285 -mat  41 -dir 1;
element zeroLength          13138 19285 18285 -mat  40 -dir 2;

element flatSliderBearing   2618 286 18286 10 110.000012345600 -P 20 -Mz 20  -orient 0. 1. 0. 1. 0. 0.;
element zeroLength          11559 286 18286 -mat  31 -dir 2;
element zeroLength          12879 286 18286 -mat  30 -dir 1;

element flatSliderBearing   2878 19286 18286 10 110.000012345600 -P 21 -Mz 21  -orient -1. 0. 0. 0. 1. 0.;
element zeroLength          11819 19286 18286 -mat  41 -dir 1;
element zeroLength          13139 19286 18286 -mat  40 -dir 2;

element flatSliderBearing   2619 18287 287 10 110.000012345600 -P 20 -Mz 20  -orient 0. 1. 0. 1. 0. 0.;
element zeroLength          11560 18287 287 -mat  31 -dir 2;
element zeroLength          12880 18287 287 -mat  30 -dir 1;

element flatSliderBearing   2879 19287 18287 10 110.000012345600 -P 21 -Mz 21  -orient -1. 0. 0. 0. 1. 0.;
element zeroLength          11820 19287 18287 -mat  41 -dir 1;
element zeroLength          13140 19287 18287 -mat  40 -dir 2;

element flatSliderBearing   2620 288 18288 10 110.000012345600 -P 20 -Mz 20  -orient 0. 1. 0. 1. 0. 0.;
element zeroLength          11561 288 18288 -mat  31 -dir 2;
element zeroLength          12881 288 18288 -mat  30 -dir 1;
```

```
element flatSliderBearing  2880 19288 18288 10 110.000012345600 -P 21 -Mz 21  -orient -1. 0. 0. 0. 1. 0.;
element zeroLength         11821 19288 18288 -mat  41 -dir 1;
element zeroLength         13141 19288 18288 -mat  40 -dir 2;

element flatSliderBearing  2621 18289 289 10 110.000012345600 -P 20 -Mz 20  -orient 0. 1. 0. 1. 0. 0.;
element zeroLength         11562 18289 289 -mat  31 -dir 2;
element zeroLength         12882 18289 289 -mat  30 -dir 1;

element flatSliderBearing  2881 19289 18289 10 110.000012345600 -P 21 -Mz 21  -orient -1. 0. 0. 0. 1. 0.;
element zeroLength         11822 19289 18289 -mat  41 -dir 1;
element zeroLength         13142 19289 18289 -mat  40 -dir 2;

element flatSliderBearing  2622 2810 182810 10 110.000012345600 -P 20 -Mz 20  -orient 0. 1. 0. 1. 0. 0.;
element zeroLength         11563 2810 182810 -mat  31 -dir 2;
element zeroLength         12883 2810 182810 -mat  30 -dir 1;

element flatSliderBearing  2882 192810 182810 10 110.000012345600 -P 21 -Mz 21  -orient -1. 0. 0. 0. 1. 0.;
element zeroLength         11823 192810 182810 -mat  41 -dir 1;
element zeroLength         13143 192810 182810 -mat  40 -dir 2;

element flatSliderBearing  2623 182811 2811 10 110.000012345600 -P 20 -Mz 20  -orient 0. 1. 0. 1. 0. 0.;
element zeroLength         11564 182811 2811 -mat  31 -dir 2;
element zeroLength         12884 182811 2811 -mat  30 -dir 1;

element flatSliderBearing  2883 192811 182811 10 110.000012345600 -P 21 -Mz 21  -orient -1. 0. 0. 0. 1. 0.;
element zeroLength         11824 192811 182811 -mat  41 -dir 1;
element zeroLength         13144 192811 182811 -mat  40 -dir 2;

element flatSliderBearing  2624 2812 182812 10 110.000012345600 -P 20 -Mz 20  -orient 0. 1. 0. 1. 0. 0.;
element zeroLength         11565 2812 182812 -mat  31 -dir 2;
element zeroLength         12885 2812 182812 -mat  30 -dir 1;

element flatSliderBearing  2884 192812 182812 10 110.000012345600 -P 21 -Mz 21  -orient -1. 0. 0. 0. 1. 0.;
element zeroLength         11825 192812 182812 -mat  41 -dir 1;
element zeroLength         13145 192812 182812 -mat  40 -dir 2;

element flatSliderBearing  2625 182813 2813 10 110.000012345600 -P 20 -Mz 20  -orient 0. 1. 0. 1. 0. 0.;
element zeroLength         11566 182813 2813 -mat  31 -dir 2;
element zeroLength         12886 182813 2813 -mat  30 -dir 1;

element flatSliderBearing  2885 192813 182813 10 110.000012345600 -P 21 -Mz 21  -orient -1. 0. 0. 0. 1. 0.;
element zeroLength         11826 192813 182813 -mat  41 -dir 1;
element zeroLength         13146 192813 182813 -mat  40 -dir 2;

element flatSliderBearing  2626 2814 182814 10 110.000012345600 -P 20 -Mz 20  -orient 0. 1. 0. 1. 0. 0.;
element zeroLength         11567 2814 182814 -mat  31 -dir 2;
element zeroLength         12887 2814 182814 -mat  30 -dir 1;

element flatSliderBearing  2886 192814 182814 10 110.000012345600 -P 21 -Mz 21  -orient -1. 0. 0. 0. 1. 0.;
element zeroLength         11827 192814 182814 -mat  41 -dir 1;
element zeroLength         13147 192814 182814 -mat  40 -dir 2;

element flatSliderBearing  2627 18292 292 10 110.000012345600 -P 20 -Mz 20  -orient 0. 1. 0. 1. 0. 0.;
element zeroLength         11568 18292 292 -mat  31 -dir 2;
element zeroLength         12888 18292 292 -mat  30 -dir 1;
```

```
element flatSliderBearing  2887 19292 18292 10 110.000012345600 -P 21 -Mz 21  -orient -1. 0. 0. 0. 1. 0.;
element zeroLength         11828 19292 18292 -mat  41 -dir 1;
element zeroLength         13148 19292 18292 -mat  40 -dir 2;

element flatSliderBearing  2628 293 18293 10 110.000012345600 -P 20 -Mz 20  -orient 0. 1. 0. 1. 0. 0.;
element zeroLength         11569 293 18293 -mat  31 -dir 2;
element zeroLength         12889 293 18293 -mat  30 -dir 1;

element flatSliderBearing  2888 19293 18293 10 110.000012345600 -P 21 -Mz 21  -orient -1. 0. 0. 0. 1. 0.;
element zeroLength         11829 19293 18293 -mat  41 -dir 1;
element zeroLength         13149 19293 18293 -mat  40 -dir 2;

element flatSliderBearing  2629 18294 294 10 110.000012345600 -P 20 -Mz 20  -orient 0. 1. 0. 1. 0. 0.;
element zeroLength         11570 18294 294 -mat  31 -dir 2;
element zeroLength         12890 18294 294 -mat  30 -dir 1;

element flatSliderBearing  2889 19294 18294 10 110.000012345600 -P 21 -Mz 21  -orient -1. 0. 0. 0. 1. 0.;
element zeroLength         11830 19294 18294 -mat  41 -dir 1;
element zeroLength         13150 19294 18294 -mat  40 -dir 2;

element flatSliderBearing  2630 295 18295 10 110.000012345600 -P 20 -Mz 20  -orient 0. 1. 0. 1. 0. 0.;
element zeroLength         11571 295 18295 -mat  31 -dir 2;
element zeroLength         12891 295 18295 -mat  30 -dir 1;

element flatSliderBearing  2890 19295 18295 10 110.000012345600 -P 21 -Mz 21  -orient -1. 0. 0. 0. 1. 0.;
element zeroLength         11831 19295 18295 -mat  41 -dir 1;
element zeroLength         13151 19295 18295 -mat  40 -dir 2;

element flatSliderBearing  2631 18296 296 10 110.000012345600 -P 20 -Mz 20  -orient 0. 1. 0. 1. 0. 0.;
element zeroLength         11572 18296 296 -mat  31 -dir 2;
element zeroLength         12892 18296 296 -mat  30 -dir 1;

element flatSliderBearing  2891 19296 18296 10 110.000012345600 -P 21 -Mz 21  -orient -1. 0. 0. 0. 1. 0.;
element zeroLength         11832 19296 18296 -mat  41 -dir 1;
element zeroLength         13152 19296 18296 -mat  40 -dir 2;

element flatSliderBearing  2632 297 18297 10 110.000012345600 -P 20 -Mz 20  -orient 0. 1. 0. 1. 0. 0.;
element zeroLength         11573 297 18297 -mat  31 -dir 2;
element zeroLength         12893 297 18297 -mat  30 -dir 1;

element flatSliderBearing  2892 19297 18297 10 110.000012345600 -P 21 -Mz 21  -orient -1. 0. 0. 0. 1. 0.;
element zeroLength         11833 19297 18297 -mat  41 -dir 1;
element zeroLength         13153 19297 18297 -mat  40 -dir 2;

element flatSliderBearing  2633 18298 298 10 110.000012345600 -P 20 -Mz 20  -orient 0. 1. 0. 1. 0. 0.;
element zeroLength         11574 18298 298 -mat  31 -dir 2;
element zeroLength         12894 18298 298 -mat  30 -dir 1;

element flatSliderBearing  2893 19298 18298 10 110.000012345600 -P 21 -Mz 21  -orient -1. 0. 0. 0. 1. 0.;
element zeroLength         11834 19298 18298 -mat  41 -dir 1;
element zeroLength         13154 19298 18298 -mat  40 -dir 2;

element flatSliderBearing  2634 299 18299 10 110.000012345600 -P 20 -Mz 20  -orient 0. 1. 0. 1. 0. 0.;
element zeroLength         11575 299 18299 -mat  31 -dir 2;
```

```
element zeroLength          12895 299 18299 -mat  30 -dir 1;

element flatSliderBearing   2894 19299 18299 10 110.000012345600 -P 21 -Mz 21  -orient -1. 0. 0. 0. 1. 0.;
element zeroLength          11835 19299 18299 -mat  41 -dir 1;
element zeroLength          13155 19299 18299 -mat  40 -dir 2;

element flatSliderBearing   2635 182910 2910 10 110.000012345600 -P 20 -Mz 20  -orient 0. 1. 0. 1. 0. 0.;
element zeroLength          11576 182910 2910 -mat  31 -dir 2;
element zeroLength          12896 182910 2910 -mat  30 -dir 1;

element flatSliderBearing   2895 192910 182910 10 110.000012345600 -P 21 -Mz 21  -orient -1. 0. 0. 0. 1. 0.;
element zeroLength          11836 192910 182910 -mat  41 -dir 1;
element zeroLength          13156 192910 182910 -mat  40 -dir 2;

element flatSliderBearing   2636 2911 182911 10 110.000012345600 -P 20 -Mz 20  -orient 0. 1. 0. 1. 0. 0.;
element zeroLength          11577 2911 182911 -mat  31 -dir 2;
element zeroLength          12897 2911 182911 -mat  30 -dir 1;

element flatSliderBearing   2896 192911 182911 10 110.000012345600 -P 21 -Mz 21  -orient -1. 0. 0. 0. 1. 0.;
element zeroLength          11837 192911 182911 -mat  41 -dir 1;
element zeroLength          13157 192911 182911 -mat  40 -dir 2;

element flatSliderBearing   2637 182912 2912 10 110.000012345600 -P 20 -Mz 20  -orient 0. 1. 0. 1. 0. 0.;
element zeroLength          11578 182912 2912 -mat  31 -dir 2;
element zeroLength          12898 182912 2912 -mat  30 -dir 1;

element flatSliderBearing   2897 192912 182912 10 110.000012345600 -P 21 -Mz 21  -orient -1. 0. 0. 0. 1. 0.;
element zeroLength          11838 192912 182912 -mat  41 -dir 1;
element zeroLength          13158 192912 182912 -mat  40 -dir 2;

element flatSliderBearing   2638 2913 182913 10 110.000012345600 -P 20 -Mz 20  -orient 0. 1. 0. 1. 0. 0.;
element zeroLength          11579 2913 182913 -mat  31 -dir 2;
element zeroLength          12899 2913 182913 -mat  30 -dir 1;

element flatSliderBearing   2898 192913 182913 10 110.000012345600 -P 21 -Mz 21  -orient -1. 0. 0. 0. 1. 0.;
element zeroLength          11839 192913 182913 -mat  41 -dir 1;
element zeroLength          13159 192913 182913 -mat  40 -dir 2;

element flatSliderBearing   2639 182914 2914 10 110.000012345600 -P 20 -Mz 20  -orient 0. 1. 0. 1. 0. 0.;
element zeroLength          11580 182914 2914 -mat  31 -dir 2;
element zeroLength          12900 182914 2914 -mat  30 -dir 1;

element flatSliderBearing   2899 192914 182914 10 110.000012345600 -P 21 -Mz 21  -orient -1. 0. 0. 0. 1. 0.;
element zeroLength          11840 192914 182914 -mat  41 -dir 1;
element zeroLength          13160 192914 182914 -mat  40 -dir 2;



#ZLE for discrete spring interfaces Frame 1  Tag 19 or AUX


element flatSliderBearing   2900 102 19102 10 110.000012345600 -P 20 -Mz 20  -orient 0. 1. 0. 1. 0. 0.;
element zeroLength          11841 102 19102 -mat  31 -dir 2;
element zeroLength          13161 102 19102 -mat  30 -dir 1;

```

```
element flatSliderBearing  2901 19103 103 10 110.000012345600 -P 20 -Mz 20  -orient 0. 1. 0. 1. 0. 0.;
element zeroLength         11842 19103 103 -mat  31 -dir 2;
element zeroLength         13162 19103 103 -mat  30 -dir 1;

element flatSliderBearing  2902 104 19104 10 110.000012345600 -P 20 -Mz 20  -orient 0. 1. 0. 1. 0. 0.;
element zeroLength         11843 104 19104 -mat  31 -dir 2;
element zeroLength         13163 104 19104 -mat  30 -dir 1;

element flatSliderBearing  2903 19105 105 10 110.000012345600 -P 20 -Mz 20  -orient 0. 1. 0. 1. 0. 0.;
element zeroLength         11844 19105 105 -mat  31 -dir 2;
element zeroLength         13164 19105 105 -mat  30 -dir 1;

element flatSliderBearing  2904 106 19106 10 110.000012345600 -P 20 -Mz 20  -orient 0. 1. 0. 1. 0. 0.;
element zeroLength         11845 106 19106 -mat  31 -dir 2;
element zeroLength         13165 106 19106 -mat  30 -dir 1;

element flatSliderBearing  2905 19107 107 10 110.000012345600 -P 20 -Mz 20  -orient 0. 1. 0. 1. 0. 0.;
element zeroLength         11846 19107 107 -mat  31 -dir 2;
element zeroLength         13166 19107 107 -mat  30 -dir 1;

element flatSliderBearing  2906 108 19108 10 110.000012345600 -P 20 -Mz 20  -orient 0. 1. 0. 1. 0. 0.;
element zeroLength         11847 108 19108 -mat  31 -dir 2;
element zeroLength         13167 108 19108 -mat  30 -dir 1;

element flatSliderBearing  2907 19109 109 10 110.000012345600 -P 20 -Mz 20  -orient 0. 1. 0. 1. 0. 0.;
element zeroLength         11848 19109 109 -mat  31 -dir 2;
element zeroLength         13168 19109 109 -mat  30 -dir 1;

element flatSliderBearing  2908 1010 191010 10 110.000012345600 -P 20 -Mz 20  -orient 0. 1. 0. 1. 0. 0.;
element zeroLength         11849 1010 191010 -mat  31 -dir 2;
element zeroLength         13169 1010 191010 -mat  30 -dir 1;

element flatSliderBearing  2909 191011 1011 10 110.000012345600 -P 20 -Mz 20  -orient 0. 1. 0. 1. 0. 0.;
element zeroLength         11850 191011 1011 -mat  31 -dir 2;
element zeroLength         13170 191011 1011 -mat  30 -dir 1;

element flatSliderBearing  2910 1012 191012 10 110.000012345600 -P 20 -Mz 20  -orient 0. 1. 0. 1. 0. 0.;
element zeroLength         11851 1012 191012 -mat  31 -dir 2;
element zeroLength         13171 1012 191012 -mat  30 -dir 1;

element flatSliderBearing  2911 191013 1013 10 110.000012345600 -P 20 -Mz 20  -orient 0. 1. 0. 1. 0. 0.;
element zeroLength         11852 191013 1013 -mat  31 -dir 2;
element zeroLength         13172 191013 1013 -mat  30 -dir 1;

element flatSliderBearing  2912 1014 191014 10 110.000012345600 -P 20 -Mz 20  -orient 0. 1. 0. 1. 0. 0.;
element zeroLength         11853 1014 191014 -mat  31 -dir 2;
element zeroLength         13173 1014 191014 -mat  30 -dir 1;

element flatSliderBearing  2913 19112 112 10 110.000012345600 -P 20 -Mz 20  -orient 0. 1. 0. 1. 0. 0.;
element zeroLength         11854 19112 112 -mat  31 -dir 2;
element zeroLength         13174 19112 112 -mat  30 -dir 1;

element flatSliderBearing  2914 113 19113 10 110.000012345600 -P 20 -Mz 20  -orient 0. 1. 0. 1. 0. 0.;
element zeroLength         11855 113 19113 -mat  31 -dir 2;
element zeroLength         13175 113 19113 -mat  30 -dir 1;
```

```
6986
6987  element flatSliderBearing  2915 19114 114 10 110.000012345600 -P 20 -Mz 20  -orient 0. 1. 0. 1. 0. 0.;
6988  element zeroLength         11856 19114 114 -mat  31 -dir 2;
6989  element zeroLength         13176 19114 114 -mat  30 -dir 1;
6990
6991  element flatSliderBearing  2916 115 19115 10 110.000012345600 -P 20 -Mz 20  -orient 0. 1. 0. 1. 0. 0.;
6992  element zeroLength         11857 115 19115 -mat  31 -dir 2;
6993  element zeroLength         13177 115 19115 -mat  30 -dir 1;
6994
6995  element flatSliderBearing  2917 19116 116 10 110.000012345600 -P 20 -Mz 20  -orient 0. 1. 0. 1. 0. 0.;
6996  element zeroLength         11858 19116 116 -mat  31 -dir 2;
6997  element zeroLength         13178 19116 116 -mat  30 -dir 1;
6998
6999  element flatSliderBearing  2918 117 19117 10 110.000012345600 -P 20 -Mz 20  -orient 0. 1. 0. 1. 0. 0.;
7000  element zeroLength         11859 117 19117 -mat  31 -dir 2;
7001  element zeroLength         13179 117 19117 -mat  30 -dir 1;
7002
7003  element flatSliderBearing  2919 19118 118 10 110.000012345600 -P 20 -Mz 20  -orient 0. 1. 0. 1. 0. 0.;
7004  element zeroLength         11860 19118 118 -mat  31 -dir 2;
7005  element zeroLength         13180 19118 118 -mat  30 -dir 1;
7006
7007  element flatSliderBearing  2920 119 19119 10 110.000012345600 -P 20 -Mz 20  -orient 0. 1. 0. 1. 0. 0.;
7008  element zeroLength         11861 119 19119 -mat  31 -dir 2;
7009  element zeroLength         13181 119 19119 -mat  30 -dir 1;
7010
7011  element flatSliderBearing  2921 191110 1110 10 110.000012345600 -P 20 -Mz 20  -orient 0. 1. 0. 1. 0. 0.;
7012  element zeroLength         11862 191110 1110 -mat  31 -dir 2;
7013  element zeroLength         13182 191110 1110 -mat  30 -dir 1;
7014
7015  element flatSliderBearing  2922 1111 191111 10 110.000012345600 -P 20 -Mz 20  -orient 0. 1. 0. 1. 0. 0.;
7016  element zeroLength         11863 1111 191111 -mat  31 -dir 2;
7017  element zeroLength         13183 1111 191111 -mat  30 -dir 1;
7018
7019  element flatSliderBearing  2923 191112 1112 10 110.000012345600 -P 20 -Mz 20  -orient 0. 1. 0. 1. 0. 0.;
7020  element zeroLength         11864 191112 1112 -mat  31 -dir 2;
7021  element zeroLength         13184 191112 1112 -mat  30 -dir 1;
7022
7023  element flatSliderBearing  2924 1113 191113 10 110.000012345600 -P 20 -Mz 20  -orient 0. 1. 0. 1. 0. 0.;
7024  element zeroLength         11865 1113 191113 -mat  31 -dir 2;
7025  element zeroLength         13185 1113 191113 -mat  30 -dir 1;
7026
7027  element flatSliderBearing  2925 191114 1114 10 110.000012345600 -P 20 -Mz 20  -orient 0. 1. 0. 1. 0. 0.;
7028  element zeroLength         11866 191114 1114 -mat  31 -dir 2;
7029  element zeroLength         13186 191114 1114 -mat  30 -dir 1;
7030
7031  element flatSliderBearing  2926 122 19122 10 110.000012345600 -P 20 -Mz 20  -orient 0. 1. 0. 1. 0. 0.;
7032  element zeroLength         11867 122 19122 -mat  31 -dir 2;
7033  element zeroLength         13187 122 19122 -mat  30 -dir 1;
7034
7035  element flatSliderBearing  2927 19123 123 10 110.000012345600 -P 20 -Mz 20  -orient 0. 1. 0. 1. 0. 0.;
7036  element zeroLength         11868 19123 123 -mat  31 -dir 2;
7037  element zeroLength         13188 19123 123 -mat  30 -dir 1;
7038
7039  element flatSliderBearing  2928 124 19124 10 110.000012345600 -P 20 -Mz 20  -orient 0. 1. 0. 1. 0. 0.;
7040  element zeroLength         11869 124 19124 -mat  31 -dir 2;
```

```
element zeroLength          13189 124 19124 -mat  30 -dir 1;

element flatSliderBearing   2929 19125 125 10 110.000012345600 -P 20 -Mz 20  -orient 0. 1. 0. 1. 0. 0.;
element zeroLength          11870 19125 125 -mat  31 -dir 2;
element zeroLength          13190 19125 125 -mat  30 -dir 1;

element flatSliderBearing   2930 126 19126 10 110.000012345600 -P 20 -Mz 20  -orient 0. 1. 0. 1. 0. 0.;
element zeroLength          11871 126 19126 -mat  31 -dir 2;
element zeroLength          13191 126 19126 -mat  30 -dir 1;

element flatSliderBearing   2931 19127 127 10 110.000012345600 -P 20 -Mz 20  -orient 0. 1. 0. 1. 0. 0.;
element zeroLength          11872 19127 127 -mat  31 -dir 2;
element zeroLength          13192 19127 127 -mat  30 -dir 1;

element flatSliderBearing   2932 128 19128 10 110.000012345600 -P 20 -Mz 20  -orient 0. 1. 0. 1. 0. 0.;
element zeroLength          11873 128 19128 -mat  31 -dir 2;
element zeroLength          13193 128 19128 -mat  30 -dir 1;

element flatSliderBearing   2933 19129 129 10 110.000012345600 -P 20 -Mz 20  -orient 0. 1. 0. 1. 0. 0.;
element zeroLength          11874 19129 129 -mat  31 -dir 2;
element zeroLength          13194 19129 129 -mat  30 -dir 1;

element flatSliderBearing   2934 1210 191210 10 110.000012345600 -P 20 -Mz 20  -orient 0. 1. 0. 1. 0. 0.;
element zeroLength          11875 1210 191210 -mat  31 -dir 2;
element zeroLength          13195 1210 191210 -mat  30 -dir 1;

element flatSliderBearing   2935 191211 1211 10 110.000012345600 -P 20 -Mz 20  -orient 0. 1. 0. 1. 0. 0.;
element zeroLength          11876 191211 1211 -mat  31 -dir 2;
element zeroLength          13196 191211 1211 -mat  30 -dir 1;

element flatSliderBearing   2936 1212 191212 10 110.000012345600 -P 20 -Mz 20  -orient 0. 1. 0. 1. 0. 0.;
element zeroLength          11877 1212 191212 -mat  31 -dir 2;
element zeroLength          13197 1212 191212 -mat  30 -dir 1;

element flatSliderBearing   2937 191213 1213 10 110.000012345600 -P 20 -Mz 20  -orient 0. 1. 0. 1. 0. 0.;
element zeroLength          11878 191213 1213 -mat  31 -dir 2;
element zeroLength          13198 191213 1213 -mat  30 -dir 1;

element flatSliderBearing   2938 1214 191214 10 110.000012345600 -P 20 -Mz 20  -orient 0. 1. 0. 1. 0. 0.;
element zeroLength          11879 1214 191214 -mat  31 -dir 2;
element zeroLength          13199 1214 191214 -mat  30 -dir 1;

element flatSliderBearing   2939 19132 132 10 110.000012345600 -P 20 -Mz 20  -orient 0. 1. 0. 1. 0. 0.;
element zeroLength          11880 19132 132 -mat  31 -dir 2;
element zeroLength          13200 19132 132 -mat  30 -dir 1;

element flatSliderBearing   2940 133 19133 10 110.000012345600 -P 20 -Mz 20  -orient 0. 1. 0. 1. 0. 0.;
element zeroLength          11881 133 19133 -mat  31 -dir 2;
element zeroLength          13201 133 19133 -mat  30 -dir 1;

element flatSliderBearing   2941 19134 134 10 110.000012345600 -P 20 -Mz 20  -orient 0. 1. 0. 1. 0. 0.;
element zeroLength          11882 19134 134 -mat  31 -dir 2;
element zeroLength          13202 19134 134 -mat  30 -dir 1;

element flatSliderBearing   2942 135 19135 10 110.000012345600 -P 20 -Mz 20  -orient 0. 1. 0. 1. 0. 0.;
```

```
element zeroLength          11883 135 19135 -mat  31 -dir 2;
element zeroLength          13203 135 19135 -mat  30 -dir 1;

element flatSliderBearing   2943 19136 136 10 110.000012345600 -P 20 -Mz 20  -orient 0. 1. 0. 1. 0. 0.;
element zeroLength          11884 19136 136 -mat  31 -dir 2;
element zeroLength          13204 19136 136 -mat  30 -dir 1;

element flatSliderBearing   2944 137 19137 10 110.000012345600 -P 20 -Mz 20  -orient 0. 1. 0. 1. 0. 0.;
element zeroLength          11885 137 19137 -mat  31 -dir 2;
element zeroLength          13205 137 19137 -mat  30 -dir 1;

element flatSliderBearing   2945 19138 138 10 110.000012345600 -P 20 -Mz 20  -orient 0. 1. 0. 1. 0. 0.;
element zeroLength          11886 19138 138 -mat  31 -dir 2;
element zeroLength          13206 19138 138 -mat  30 -dir 1;

element flatSliderBearing   2946 139 19139 10 110.000012345600 -P 20 -Mz 20  -orient 0. 1. 0. 1. 0. 0.;
element zeroLength          11887 139 19139 -mat  31 -dir 2;
element zeroLength          13207 139 19139 -mat  30 -dir 1;

element flatSliderBearing   2947 191310 1310 10 110.000012345600 -P 20 -Mz 20  -orient 0. 1. 0. 1. 0. 0.;
element zeroLength          11888 191310 1310 -mat  31 -dir 2;
element zeroLength          13208 191310 1310 -mat  30 -dir 1;

element flatSliderBearing   2948 1311 191311 10 110.000012345600 -P 20 -Mz 20  -orient 0. 1. 0. 1. 0. 0.;
element zeroLength          11889 1311 191311 -mat  31 -dir 2;
element zeroLength          13209 1311 191311 -mat  30 -dir 1;

element flatSliderBearing   2949 191312 1312 10 110.000012345600 -P 20 -Mz 20  -orient 0. 1. 0. 1. 0. 0.;
element zeroLength          11890 191312 1312 -mat  31 -dir 2;
element zeroLength          13210 191312 1312 -mat  30 -dir 1;

element flatSliderBearing   2950 1313 191313 10 110.000012345600 -P 20 -Mz 20  -orient 0. 1. 0. 1. 0. 0.;
element zeroLength          11891 1313 191313 -mat  31 -dir 2;
element zeroLength          13211 1313 191313 -mat  30 -dir 1;

element flatSliderBearing   2951 191314 1314 10 110.000012345600 -P 20 -Mz 20  -orient 0. 1. 0. 1. 0. 0.;
element zeroLength          11892 191314 1314 -mat  31 -dir 2;
element zeroLength          13212 191314 1314 -mat  30 -dir 1;

element flatSliderBearing   2952 142 19142 10 110.000012345600 -P 20 -Mz 20  -orient 0. 1. 0. 1. 0. 0.;
element zeroLength          11893 142 19142 -mat  31 -dir 2;
element zeroLength          13213 142 19142 -mat  30 -dir 1;

element flatSliderBearing   2953 19143 143 10 110.000012345600 -P 20 -Mz 20  -orient 0. 1. 0. 1. 0. 0.;
element zeroLength          11894 19143 143 -mat  31 -dir 2;
element zeroLength          13214 19143 143 -mat  30 -dir 1;

element flatSliderBearing   2954 144 19144 10 110.000012345600 -P 20 -Mz 20  -orient 0. 1. 0. 1. 0. 0.;
element zeroLength          11895 144 19144 -mat  31 -dir 2;
element zeroLength          13215 144 19144 -mat  30 -dir 1;

element flatSliderBearing   2955 19145 145 10 110.000012345600 -P 20 -Mz 20  -orient 0. 1. 0. 1. 0. 0.;
element zeroLength          11896 19145 145 -mat  31 -dir 2;
element zeroLength          13216 19145 145 -mat  30 -dir 1;
```

```
element flatSliderBearing  2956 146 19146 10 110.000012345600 -P 20 -Mz 20  -orient 0. 1. 0. 1. 0. 0.;
element zeroLength         11897 146 19146 -mat  31 -dir 2;
element zeroLength         13217 146 19146 -mat  30 -dir 1;

element flatSliderBearing  2957 19147 147 10 110.000012345600 -P 20 -Mz 20  -orient 0. 1. 0. 1. 0. 0.;
element zeroLength         11898 19147 147 -mat  31 -dir 2;
element zeroLength         13218 19147 147 -mat  30 -dir 1;

element flatSliderBearing  2958 148 19148 10 110.000012345600 -P 20 -Mz 20  -orient 0. 1. 0. 1. 0. 0.;
element zeroLength         11899 148 19148 -mat  31 -dir 2;
element zeroLength         13219 148 19148 -mat  30 -dir 1;

element flatSliderBearing  2959 19149 149 10 110.000012345600 -P 20 -Mz 20  -orient 0. 1. 0. 1. 0. 0.;
element zeroLength         11900 19149 149 -mat  31 -dir 2;
element zeroLength         13220 19149 149 -mat  30 -dir 1;

element flatSliderBearing  2960 1410 191410 10 110.000012345600 -P 20 -Mz 20  -orient 0. 1. 0. 1. 0. 0.;
element zeroLength         11901 1410 191410 -mat  31 -dir 2;
element zeroLength         13221 1410 191410 -mat  30 -dir 1;

element flatSliderBearing  2961 191411 1411 10 110.000012345600 -P 20 -Mz 20  -orient 0. 1. 0. 1. 0. 0.;
element zeroLength         11902 191411 1411 -mat  31 -dir 2;
element zeroLength         13222 191411 1411 -mat  30 -dir 1;

element flatSliderBearing  2962 1412 191412 10 110.000012345600 -P 20 -Mz 20  -orient 0. 1. 0. 1. 0. 0.;
element zeroLength         11903 1412 191412 -mat  31 -dir 2;
element zeroLength         13223 1412 191412 -mat  30 -dir 1;

element flatSliderBearing  2963 191413 1413 10 110.000012345600 -P 20 -Mz 20  -orient 0. 1. 0. 1. 0. 0.;
element zeroLength         11904 191413 1413 -mat  31 -dir 2;
element zeroLength         13224 191413 1413 -mat  30 -dir 1;

element flatSliderBearing  2964 1414 191414 10 110.000012345600 -P 20 -Mz 20  -orient 0. 1. 0. 1. 0. 0.;
element zeroLength         11905 1414 191414 -mat  31 -dir 2;
element zeroLength         13225 1414 191414 -mat  30 -dir 1;

element flatSliderBearing  2965 19152 152 10 110.000012345600 -P 20 -Mz 20  -orient 0. 1. 0. 1. 0. 0.;
element zeroLength         11906 19152 152 -mat  31 -dir 2;
element zeroLength         13226 19152 152 -mat  30 -dir 1;

element flatSliderBearing  2966 153 19153 10 110.000012345600 -P 20 -Mz 20  -orient 0. 1. 0. 1. 0. 0.;
element zeroLength         11907 153 19153 -mat  31 -dir 2;
element zeroLength         13227 153 19153 -mat  30 -dir 1;

element flatSliderBearing  2967 19154 154 10 110.000012345600 -P 20 -Mz 20  -orient 0. 1. 0. 1. 0. 0.;
element zeroLength         11908 19154 154 -mat  31 -dir 2;
element zeroLength         13228 19154 154 -mat  30 -dir 1;

element flatSliderBearing  2968 155 19155 10 110.000012345600 -P 20 -Mz 20  -orient 0. 1. 0. 1. 0. 0.;
element zeroLength         11909 155 19155 -mat  31 -dir 2;
element zeroLength         13229 155 19155 -mat  30 -dir 1;

element flatSliderBearing  2969 19156 156 10 110.000012345600 -P 20 -Mz 20  -orient 0. 1. 0. 1. 0. 0.;
element zeroLength         11910 19156 156 -mat  31 -dir 2;
element zeroLength         13230 19156 156 -mat  30 -dir 1;
```

```
7206
7207  element flatSliderBearing  2970 157 19157 10 110.000012345600 -P 20 -Mz 20  -orient 0. 1. 0. 1. 0. 0.;
7208  element zeroLength         11911 157 19157 -mat  31 -dir 2;
7209  element zeroLength         13231 157 19157 -mat  30 -dir 1;
7210
7211  element flatSliderBearing  2971 19158 158 10 110.000012345600 -P 20 -Mz 20  -orient 0. 1. 0. 1. 0. 0.;
7212  element zeroLength         11912 19158 158 -mat  31 -dir 2;
7213  element zeroLength         13232 19158 158 -mat  30 -dir 1;
7214
7215  element flatSliderBearing  2972 159 19159 10 110.000012345600 -P 20 -Mz 20  -orient 0. 1. 0. 1. 0. 0.;
7216  element zeroLength         11913 159 19159 -mat  31 -dir 2;
7217  element zeroLength         13233 159 19159 -mat  30 -dir 1;
7218
7219  element flatSliderBearing  2973 191510 1510 10 110.000012345600 -P 20 -Mz 20  -orient 0. 1. 0. 1. 0. 0.;
7220  element zeroLength         11914 191510 1510 -mat  31 -dir 2;
7221  element zeroLength         13234 191510 1510 -mat  30 -dir 1;
7222
7223  element flatSliderBearing  2974 1511 191511 10 110.000012345600 -P 20 -Mz 20  -orient 0. 1. 0. 1. 0. 0.;
7224  element zeroLength         11915 1511 191511 -mat  31 -dir 2;
7225  element zeroLength         13235 1511 191511 -mat  30 -dir 1;
7226
7227  element flatSliderBearing  2975 191512 1512 10 110.000012345600 -P 20 -Mz 20  -orient 0. 1. 0. 1. 0. 0.;
7228  element zeroLength         11916 191512 1512 -mat  31 -dir 2;
7229  element zeroLength         13236 191512 1512 -mat  30 -dir 1;
7230
7231  element flatSliderBearing  2976 1513 191513 10 110.000012345600 -P 20 -Mz 20  -orient 0. 1. 0. 1. 0. 0.;
7232  element zeroLength         11917 1513 191513 -mat  31 -dir 2;
7233  element zeroLength         13237 1513 191513 -mat  30 -dir 1;
7234
7235  element flatSliderBearing  2977 191514 1514 10 110.000012345600 -P 20 -Mz 20  -orient 0. 1. 0. 1. 0. 0.;
7236  element zeroLength         11918 191514 1514 -mat  31 -dir 2;
7237  element zeroLength         13238 191514 1514 -mat  30 -dir 1;
7238
7239  element flatSliderBearing  2978 162 19162 10 110.000012345600 -P 20 -Mz 20  -orient 0. 1. 0. 1. 0. 0.;
7240  element zeroLength         11919 162 19162 -mat  31 -dir 2;
7241  element zeroLength         13239 162 19162 -mat  30 -dir 1;
7242
7243  element flatSliderBearing  2979 19163 163 10 110.000012345600 -P 20 -Mz 20  -orient 0. 1. 0. 1. 0. 0.;
7244  element zeroLength         11920 19163 163 -mat  31 -dir 2;
7245  element zeroLength         13240 19163 163 -mat  30 -dir 1;
7246
7247  element flatSliderBearing  2980 164 19164 10 110.000012345600 -P 20 -Mz 20  -orient 0. 1. 0. 1. 0. 0.;
7248  element zeroLength         11921 164 19164 -mat  31 -dir 2;
7249  element zeroLength         13241 164 19164 -mat  30 -dir 1;
7250
7251  element flatSliderBearing  2981 19165 165 10 110.000012345600 -P 20 -Mz 20  -orient 0. 1. 0. 1. 0. 0.;
7252  element zeroLength         11922 19165 165 -mat  31 -dir 2;
7253  element zeroLength         13242 19165 165 -mat  30 -dir 1;
7254
7255  element flatSliderBearing  2982 166 19166 10 110.000012345600 -P 20 -Mz 20  -orient 0. 1. 0. 1. 0. 0.;
7256  element zeroLength         11923 166 19166 -mat  31 -dir 2;
7257  element zeroLength         13243 166 19166 -mat  30 -dir 1;
7258
7259  element flatSliderBearing  2983 19167 167 10 110.000012345600 -P 20 -Mz 20  -orient 0. 1. 0. 1. 0. 0.;
7260  element zeroLength         11924 19167 167 -mat  31 -dir 2;
```

```
element zeroLength          13244 19167 167 -mat  30 -dir 1;

element flatSliderBearing   2984 168 19168 10 110.000012345600 -P 20 -Mz 20  -orient 0. 1. 0. 1. 0. 0.;
element zeroLength          11925 168 19168 -mat  31 -dir 2;
element zeroLength          13245 168 19168 -mat  30 -dir 1;

element flatSliderBearing   2985 19169 169 10 110.000012345600 -P 20 -Mz 20  -orient 0. 1. 0. 1. 0. 0.;
element zeroLength          11926 19169 169 -mat  31 -dir 2;
element zeroLength          13246 19169 169 -mat  30 -dir 1;

element flatSliderBearing   2986 1610 191610 10 110.000012345600 -P 20 -Mz 20  -orient 0. 1. 0. 1. 0. 0.;
element zeroLength          11927 1610 191610 -mat  31 -dir 2;
element zeroLength          13247 1610 191610 -mat  30 -dir 1;

element flatSliderBearing   2987 191611 1611 10 110.000012345600 -P 20 -Mz 20  -orient 0. 1. 0. 1. 0. 0.;
element zeroLength          11928 191611 1611 -mat  31 -dir 2;
element zeroLength          13248 191611 1611 -mat  30 -dir 1;

element flatSliderBearing   2988 1612 191612 10 110.000012345600 -P 20 -Mz 20  -orient 0. 1. 0. 1. 0. 0.;
element zeroLength          11929 1612 191612 -mat  31 -dir 2;
element zeroLength          13249 1612 191612 -mat  30 -dir 1;

element flatSliderBearing   2989 191613 1613 10 110.000012345600 -P 20 -Mz 20  -orient 0. 1. 0. 1. 0. 0.;
element zeroLength          11930 191613 1613 -mat  31 -dir 2;
element zeroLength          13250 191613 1613 -mat  30 -dir 1;

element flatSliderBearing   2990 1614 191614 10 110.000012345600 -P 20 -Mz 20  -orient 0. 1. 0. 1. 0. 0.;
element zeroLength          11931 1614 191614 -mat  31 -dir 2;
element zeroLength          13251 1614 191614 -mat  30 -dir 1;

element flatSliderBearing   2991 19172 172 10 110.000012345600 -P 20 -Mz 20  -orient 0. 1. 0. 1. 0. 0.;
element zeroLength          11932 19172 172 -mat  31 -dir 2;
element zeroLength          13252 19172 172 -mat  30 -dir 1;

element flatSliderBearing   2992 173 19173 10 110.000012345600 -P 20 -Mz 20  -orient 0. 1. 0. 1. 0. 0.;
element zeroLength          11933 173 19173 -mat  31 -dir 2;
element zeroLength          13253 173 19173 -mat  30 -dir 1;

element flatSliderBearing   2993 19174 174 10 110.000012345600 -P 20 -Mz 20  -orient 0. 1. 0. 1. 0. 0.;
element zeroLength          11934 19174 174 -mat  31 -dir 2;
element zeroLength          13254 19174 174 -mat  30 -dir 1;

element flatSliderBearing   2994 175 19175 10 110.000012345600 -P 20 -Mz 20  -orient 0. 1. 0. 1. 0. 0.;
element zeroLength          11935 175 19175 -mat  31 -dir 2;
element zeroLength          13255 175 19175 -mat  30 -dir 1;

element flatSliderBearing   2995 19176 176 10 110.000012345600 -P 20 -Mz 20  -orient 0. 1. 0. 1. 0. 0.;
element zeroLength          11936 19176 176 -mat  31 -dir 2;
element zeroLength          13256 19176 176 -mat  30 -dir 1;

element flatSliderBearing   2996 177 19177 10 110.000012345600 -P 20 -Mz 20  -orient 0. 1. 0. 1. 0. 0.;
element zeroLength          11937 177 19177 -mat  31 -dir 2;
element zeroLength          13257 177 19177 -mat  30 -dir 1;

element flatSliderBearing   2997 19178 178 10 110.000012345600 -P 20 -Mz 20  -orient 0. 1. 0. 1. 0. 0.;
```

```
element zeroLength          11938 19178 178 -mat  31 -dir 2;
element zeroLength          13258 19178 178 -mat  30 -dir 1;

element flatSliderBearing   2998 179 19179 10 110.000012345600 -P 20 -Mz 20  -orient 0. 1. 0. 1. 0. 0.;
element zeroLength          11939 179 19179 -mat  31 -dir 2;
element zeroLength          13259 179 19179 -mat  30 -dir 1;

element flatSliderBearing   2999 191710 1710 10 110.000012345600 -P 20 -Mz 20  -orient 0. 1. 0. 1. 0. 0.;
element zeroLength          11940 191710 1710 -mat  31 -dir 2;
element zeroLength          13260 191710 1710 -mat  30 -dir 1;

element flatSliderBearing   3000 1711 191711 10 110.000012345600 -P 20 -Mz 20  -orient 0. 1. 0. 1. 0. 0.;
element zeroLength          11941 1711 191711 -mat  31 -dir 2;
element zeroLength          13261 1711 191711 -mat  30 -dir 1;

element flatSliderBearing   3001 191712 1712 10 110.000012345600 -P 20 -Mz 20  -orient 0. 1. 0. 1. 0. 0.;
element zeroLength          11942 191712 1712 -mat  31 -dir 2;
element zeroLength          13262 191712 1712 -mat  30 -dir 1;

element flatSliderBearing   3002 1713 191713 10 110.000012345600 -P 20 -Mz 20  -orient 0. 1. 0. 1. 0. 0.;
element zeroLength          11943 1713 191713 -mat  31 -dir 2;
element zeroLength          13263 1713 191713 -mat  30 -dir 1;

element flatSliderBearing   3003 191714 1714 10 110.000012345600 -P 20 -Mz 20  -orient 0. 1. 0. 1. 0. 0.;
element zeroLength          11944 191714 1714 -mat  31 -dir 2;
element zeroLength          13264 191714 1714 -mat  30 -dir 1;

element flatSliderBearing   3004 182 19182 10 110.000012345600 -P 20 -Mz 20  -orient 0. 1. 0. 1. 0. 0.;
element zeroLength          11945 182 19182 -mat  31 -dir 2;
element zeroLength          13265 182 19182 -mat  30 -dir 1;

element flatSliderBearing   3005 19183 183 10 110.000012345600 -P 20 -Mz 20  -orient 0. 1. 0. 1. 0. 0.;
element zeroLength          11946 19183 183 -mat  31 -dir 2;
element zeroLength          13266 19183 183 -mat  30 -dir 1;

element flatSliderBearing   3006 184 19184 10 110.000012345600 -P 20 -Mz 20  -orient 0. 1. 0. 1. 0. 0.;
element zeroLength          11947 184 19184 -mat  31 -dir 2;
element zeroLength          13267 184 19184 -mat  30 -dir 1;

element flatSliderBearing   3007 19185 185 10 110.000012345600 -P 20 -Mz 20  -orient 0. 1. 0. 1. 0. 0.;
element zeroLength          11948 19185 185 -mat  31 -dir 2;
element zeroLength          13268 19185 185 -mat  30 -dir 1;

element flatSliderBearing   3008 186 19186 10 110.000012345600 -P 20 -Mz 20  -orient 0. 1. 0. 1. 0. 0.;
element zeroLength          11949 186 19186 -mat  31 -dir 2;
element zeroLength          13269 186 19186 -mat  30 -dir 1;

element flatSliderBearing   3009 19187 187 10 110.000012345600 -P 20 -Mz 20  -orient 0. 1. 0. 1. 0. 0.;
element zeroLength          11950 19187 187 -mat  31 -dir 2;
element zeroLength          13270 19187 187 -mat  30 -dir 1;

element flatSliderBearing   3010 188 19188 10 110.000012345600 -P 20 -Mz 20  -orient 0. 1. 0. 1. 0. 0.;
element zeroLength          11951 188 19188 -mat  31 -dir 2;
element zeroLength          13271 188 19188 -mat  30 -dir 1;
```

```
element flatSliderBearing   3011 19189 189 10 110.000012345600 -P 20 -Mz 20  -orient 0. 1. 0. 1. 0. 0.;
element zeroLength          11952 19189 189 -mat  31 -dir 2;
element zeroLength          13272 19189 189 -mat  30 -dir 1;

element flatSliderBearing   3012 1810 191810 10 110.000012345600 -P 20 -Mz 20  -orient 0. 1. 0. 1. 0. 0.;
element zeroLength          11953 1810 191810 -mat  31 -dir 2;
element zeroLength          13273 1810 191810 -mat  30 -dir 1;

element flatSliderBearing   3013 191811 1811 10 110.000012345600 -P 20 -Mz 20  -orient 0. 1. 0. 1. 0. 0.;
element zeroLength          11954 191811 1811 -mat  31 -dir 2;
element zeroLength          13274 191811 1811 -mat  30 -dir 1;

element flatSliderBearing   3014 1812 191812 10 110.000012345600 -P 20 -Mz 20  -orient 0. 1. 0. 1. 0. 0.;
element zeroLength          11955 1812 191812 -mat  31 -dir 2;
element zeroLength          13275 1812 191812 -mat  30 -dir 1;

element flatSliderBearing   3015 191813 1813 10 110.000012345600 -P 20 -Mz 20  -orient 0. 1. 0. 1. 0. 0.;
element zeroLength          11956 191813 1813 -mat  31 -dir 2;
element zeroLength          13276 191813 1813 -mat  30 -dir 1;

element flatSliderBearing   3016 1814 191814 10 110.000012345600 -P 20 -Mz 20  -orient 0. 1. 0. 1. 0. 0.;
element zeroLength          11957 1814 191814 -mat  31 -dir 2;
element zeroLength          13277 1814 191814 -mat  30 -dir 1;

element flatSliderBearing   3017 19192 192 10 110.000012345600 -P 20 -Mz 20  -orient 0. 1. 0. 1. 0. 0.;
element zeroLength          11958 19192 192 -mat  31 -dir 2;
element zeroLength          13278 19192 192 -mat  30 -dir 1;

element flatSliderBearing   3018 193 19193 10 110.000012345600 -P 20 -Mz 20  -orient 0. 1. 0. 1. 0. 0.;
element zeroLength          11959 193 19193 -mat  31 -dir 2;
element zeroLength          13279 193 19193 -mat  30 -dir 1;

element flatSliderBearing   3019 19194 194 10 110.000012345600 -P 20 -Mz 20  -orient 0. 1. 0. 1. 0. 0.;
element zeroLength          11960 19194 194 -mat  31 -dir 2;
element zeroLength          13280 19194 194 -mat  30 -dir 1;

element flatSliderBearing   3020 195 19195 10 110.000012345600 -P 20 -Mz 20  -orient 0. 1. 0. 1. 0. 0.;
element zeroLength          11961 195 19195 -mat  31 -dir 2;
element zeroLength          13281 195 19195 -mat  30 -dir 1;

element flatSliderBearing   3021 19196 196 10 110.000012345600 -P 20 -Mz 20  -orient 0. 1. 0. 1. 0. 0.;
element zeroLength          11962 19196 196 -mat  31 -dir 2;
element zeroLength          13282 19196 196 -mat  30 -dir 1;

element flatSliderBearing   3022 197 19197 10 110.000012345600 -P 20 -Mz 20  -orient 0. 1. 0. 1. 0. 0.;
element zeroLength          11963 197 19197 -mat  31 -dir 2;
element zeroLength          13283 197 19197 -mat  30 -dir 1;

element flatSliderBearing   3023 19198 198 10 110.000012345600 -P 20 -Mz 20  -orient 0. 1. 0. 1. 0. 0.;
element zeroLength          11964 19198 198 -mat  31 -dir 2;
element zeroLength          13284 19198 198 -mat  30 -dir 1;

element flatSliderBearing   3024 199 19199 10 110.000012345600 -P 20 -Mz 20  -orient 0. 1. 0. 1. 0. 0.;
element zeroLength          11965 199 19199 -mat  31 -dir 2;
element zeroLength          13285 199 19199 -mat  30 -dir 1;
```

```
7426
7427  element flatSliderBearing  3025 191910 1910 10 110.000012345600 -P 20 -Mz 20  -orient 0. 1. 0. 1. 0. 0.;
7428  element zeroLength         11966 191910 1910 -mat  31 -dir 2;
7429  element zeroLength         13286 191910 1910 -mat  30 -dir 1;
7430
7431  element flatSliderBearing  3026 1911 191911 10 110.000012345600 -P 20 -Mz 20  -orient 0. 1. 0. 1. 0. 0.;
7432  element zeroLength         11967 1911 191911 -mat  31 -dir 2;
7433  element zeroLength         13287 1911 191911 -mat  30 -dir 1;
7434
7435  element flatSliderBearing  3027 191912 1912 10 110.000012345600 -P 20 -Mz 20  -orient 0. 1. 0. 1. 0. 0.;
7436  element zeroLength         11968 191912 1912 -mat  31 -dir 2;
7437  element zeroLength         13288 191912 1912 -mat  30 -dir 1;
7438
7439  element flatSliderBearing  3028 1913 191913 10 110.000012345600 -P 20 -Mz 20  -orient 0. 1. 0. 1. 0. 0.;
7440  element zeroLength         11969 1913 191913 -mat  31 -dir 2;
7441  element zeroLength         13289 1913 191913 -mat  30 -dir 1;
7442
7443  element flatSliderBearing  3029 191914 1914 10 110.000012345600 -P 20 -Mz 20  -orient 0. 1. 0. 1. 0. 0.;
7444  element zeroLength         11970 191914 1914 -mat  31 -dir 2;
7445  element zeroLength         13290 191914 1914 -mat  30 -dir 1;
7446
7447  element flatSliderBearing  3030 202 19202 10 110.000012345600 -P 20 -Mz 20  -orient 0. 1. 0. 1. 0. 0.;
7448  element zeroLength         11971 202 19202 -mat  31 -dir 2;
7449  element zeroLength         13291 202 19202 -mat  30 -dir 1;
7450
7451  element flatSliderBearing  3031 19203 203 10 110.000012345600 -P 20 -Mz 20  -orient 0. 1. 0. 1. 0. 0.;
7452  element zeroLength         11972 19203 203 -mat  31 -dir 2;
7453  element zeroLength         13292 19203 203 -mat  30 -dir 1;
7454
7455  element flatSliderBearing  3032 204 19204 10 110.000012345600 -P 20 -Mz 20  -orient 0. 1. 0. 1. 0. 0.;
7456  element zeroLength         11973 204 19204 -mat  31 -dir 2;
7457  element zeroLength         13293 204 19204 -mat  30 -dir 1;
7458
7459  element flatSliderBearing  3033 19205 205 10 110.000012345600 -P 20 -Mz 20  -orient 0. 1. 0. 1. 0. 0.;
7460  element zeroLength         11974 19205 205 -mat  31 -dir 2;
7461  element zeroLength         13294 19205 205 -mat  30 -dir 1;
7462
7463  element flatSliderBearing  3034 206 19206 10 110.000012345600 -P 20 -Mz 20  -orient 0. 1. 0. 1. 0. 0.;
7464  element zeroLength         11975 206 19206 -mat  31 -dir 2;
7465  element zeroLength         13295 206 19206 -mat  30 -dir 1;
7466
7467  element flatSliderBearing  3035 19207 207 10 110.000012345600 -P 20 -Mz 20  -orient 0. 1. 0. 1. 0. 0.;
7468  element zeroLength         11976 19207 207 -mat  31 -dir 2;
7469  element zeroLength         13296 19207 207 -mat  30 -dir 1;
7470
7471  element flatSliderBearing  3036 208 19208 10 110.000012345600 -P 20 -Mz 20  -orient 0. 1. 0. 1. 0. 0.;
7472  element zeroLength         11977 208 19208 -mat  31 -dir 2;
7473  element zeroLength         13297 208 19208 -mat  30 -dir 1;
7474
7475  element flatSliderBearing  3037 19209 209 10 110.000012345600 -P 20 -Mz 20  -orient 0. 1. 0. 1. 0. 0.;
7476  element zeroLength         11978 19209 209 -mat  31 -dir 2;
7477  element zeroLength         13298 19209 209 -mat  30 -dir 1;
7478
7479  element flatSliderBearing  3038 2010 192010 10 110.000012345600 -P 20 -Mz 20  -orient 0. 1. 0. 1. 0. 0.;
7480  element zeroLength         11979 2010 192010 -mat  31 -dir 2;
```

```
element zeroLength          13299 2010 192010 -mat  30 -dir 1;

element flatSliderBearing   3039 192011 2011 10 110.000012345600 -P 20 -Mz 20  -orient 0. 1. 0. 1. 0. 0.;
element zeroLength          11980 192011 2011 -mat  31 -dir 2;
element zeroLength          13300 192011 2011 -mat  30 -dir 1;

element flatSliderBearing   3040 2012 192012 10 110.000012345600 -P 20 -Mz 20  -orient 0. 1. 0. 1. 0. 0.;
element zeroLength          11981 2012 192012 -mat  31 -dir 2;
element zeroLength          13301 2012 192012 -mat  30 -dir 1;

element flatSliderBearing   3041 192013 2013 10 110.000012345600 -P 20 -Mz 20  -orient 0. 1. 0. 1. 0. 0.;
element zeroLength          11982 192013 2013 -mat  31 -dir 2;
element zeroLength          13302 192013 2013 -mat  30 -dir 1;

element flatSliderBearing   3042 2014 192014 10 110.000012345600 -P 20 -Mz 20  -orient 0. 1. 0. 1. 0. 0.;
element zeroLength          11983 2014 192014 -mat  31 -dir 2;
element zeroLength          13303 2014 192014 -mat  30 -dir 1;

element flatSliderBearing   3043 19212 212 10 110.000012345600 -P 20 -Mz 20  -orient 0. 1. 0. 1. 0. 0.;
element zeroLength          11984 19212 212 -mat  31 -dir 2;
element zeroLength          13304 19212 212 -mat  30 -dir 1;

element flatSliderBearing   3044 213 19213 10 110.000012345600 -P 20 -Mz 20  -orient 0. 1. 0. 1. 0. 0.;
element zeroLength          11985 213 19213 -mat  31 -dir 2;
element zeroLength          13305 213 19213 -mat  30 -dir 1;

element flatSliderBearing   3045 19214 214 10 110.000012345600 -P 20 -Mz 20  -orient 0. 1. 0. 1. 0. 0.;
element zeroLength          11986 19214 214 -mat  31 -dir 2;
element zeroLength          13306 19214 214 -mat  30 -dir 1;

element flatSliderBearing   3046 215 19215 10 110.000012345600 -P 20 -Mz 20  -orient 0. 1. 0. 1. 0. 0.;
element zeroLength          11987 215 19215 -mat  31 -dir 2;
element zeroLength          13307 215 19215 -mat  30 -dir 1;

element flatSliderBearing   3047 19216 216 10 110.000012345600 -P 20 -Mz 20  -orient 0. 1. 0. 1. 0. 0.;
element zeroLength          11988 19216 216 -mat  31 -dir 2;
element zeroLength          13308 19216 216 -mat  30 -dir 1;

element flatSliderBearing   3048 217 19217 10 110.000012345600 -P 20 -Mz 20  -orient 0. 1. 0. 1. 0. 0.;
element zeroLength          11989 217 19217 -mat  31 -dir 2;
element zeroLength          13309 217 19217 -mat  30 -dir 1;

element flatSliderBearing   3049 19218 218 10 110.000012345600 -P 20 -Mz 20  -orient 0. 1. 0. 1. 0. 0.;
element zeroLength          11990 19218 218 -mat  31 -dir 2;
element zeroLength          13310 19218 218 -mat  30 -dir 1;

element flatSliderBearing   3050 219 19219 10 110.000012345600 -P 20 -Mz 20  -orient 0. 1. 0. 1. 0. 0.;
element zeroLength          11991 219 19219 -mat  31 -dir 2;
element zeroLength          13311 219 19219 -mat  30 -dir 1;

element flatSliderBearing   3051 192110 2110 10 110.000012345600 -P 20 -Mz 20  -orient 0. 1. 0. 1. 0. 0.;
element zeroLength          11992 192110 2110 -mat  31 -dir 2;
element zeroLength          13312 192110 2110 -mat  30 -dir 1;

element flatSliderBearing   3052 2111 192111 10 110.000012345600 -P 20 -Mz 20  -orient 0. 1. 0. 1. 0. 0.;
```

```
element zeroLength          11993 2111 192111 -mat  31 -dir 2;
element zeroLength          13313 2111 192111 -mat  30 -dir 1;

element flatSliderBearing   3053 192112 2112 10 110.000012345600 -P 20 -Mz 20  -orient 0. 1. 0. 1. 0. 0.;
element zeroLength          11994 192112 2112 -mat  31 -dir 2;
element zeroLength          13314 192112 2112 -mat  30 -dir 1;

element flatSliderBearing   3054 2113 192113 10 110.000012345600 -P 20 -Mz 20  -orient 0. 1. 0. 1. 0. 0.;
element zeroLength          11995 2113 192113 -mat  31 -dir 2;
element zeroLength          13315 2113 192113 -mat  30 -dir 1;

element flatSliderBearing   3055 192114 2114 10 110.000012345600 -P 20 -Mz 20  -orient 0. 1. 0. 1. 0. 0.;
element zeroLength          11996 192114 2114 -mat  31 -dir 2;
element zeroLength          13316 192114 2114 -mat  30 -dir 1;

element flatSliderBearing   3056 222 19222 10 110.000012345600 -P 20 -Mz 20  -orient 0. 1. 0. 1. 0. 0.;
element zeroLength          11997 222 19222 -mat  31 -dir 2;
element zeroLength          13317 222 19222 -mat  30 -dir 1;

element flatSliderBearing   3057 19223 223 10 110.000012345600 -P 20 -Mz 20  -orient 0. 1. 0. 1. 0. 0.;
element zeroLength          11998 19223 223 -mat  31 -dir 2;
element zeroLength          13318 19223 223 -mat  30 -dir 1;

element flatSliderBearing   3058 224 19224 10 110.000012345600 -P 20 -Mz 20  -orient 0. 1. 0. 1. 0. 0.;
element zeroLength          11999 224 19224 -mat  31 -dir 2;
element zeroLength          13319 224 19224 -mat  30 -dir 1;

element flatSliderBearing   3059 19225 225 10 110.000012345600 -P 20 -Mz 20  -orient 0. 1. 0. 1. 0. 0.;
element zeroLength          12000 19225 225 -mat  31 -dir 2;
element zeroLength          13320 19225 225 -mat  30 -dir 1;

element flatSliderBearing   3060 226 19226 10 110.000012345600 -P 20 -Mz 20  -orient 0. 1. 0. 1. 0. 0.;
element zeroLength          12001 226 19226 -mat  31 -dir 2;
element zeroLength          13321 226 19226 -mat  30 -dir 1;

element flatSliderBearing   3061 19227 227 10 110.000012345600 -P 20 -Mz 20  -orient 0. 1. 0. 1. 0. 0.;
element zeroLength          12002 19227 227 -mat  31 -dir 2;
element zeroLength          13322 19227 227 -mat  30 -dir 1;

element flatSliderBearing   3062 228 19228 10 110.000012345600 -P 20 -Mz 20  -orient 0. 1. 0. 1. 0. 0.;
element zeroLength          12003 228 19228 -mat  31 -dir 2;
element zeroLength          13323 228 19228 -mat  30 -dir 1;

element flatSliderBearing   3063 19229 229 10 110.000012345600 -P 20 -Mz 20  -orient 0. 1. 0. 1. 0. 0.;
element zeroLength          12004 19229 229 -mat  31 -dir 2;
element zeroLength          13324 19229 229 -mat  30 -dir 1;

element flatSliderBearing   3064 2210 192210 10 110.000012345600 -P 20 -Mz 20  -orient 0. 1. 0. 1. 0. 0.;
element zeroLength          12005 2210 192210 -mat  31 -dir 2;
element zeroLength          13325 2210 192210 -mat  30 -dir 1;

element flatSliderBearing   3065 192211 2211 10 110.000012345600 -P 20 -Mz 20  -orient 0. 1. 0. 1. 0. 0.;
element zeroLength          12006 192211 2211 -mat  31 -dir 2;
element zeroLength          13326 192211 2211 -mat  30 -dir 1;
```

```
element flatSliderBearing   3066 2212 192212 10 110.000012345600 -P 20 -Mz 20  -orient 0. 1. 0. 1. 0. 0.;
element zeroLength          12007 2212 192212 -mat  31 -dir 2;
element zeroLength          13327 2212 192212 -mat  30 -dir 1;

element flatSliderBearing   3067 192213 2213 10 110.000012345600 -P 20 -Mz 20  -orient 0. 1. 0. 1. 0. 0.;
element zeroLength          12008 192213 2213 -mat  31 -dir 2;
element zeroLength          13328 192213 2213 -mat  30 -dir 1;

element flatSliderBearing   3068 2214 192214 10 110.000012345600 -P 20 -Mz 20  -orient 0. 1. 0. 1. 0. 0.;
element zeroLength          12009 2214 192214 -mat  31 -dir 2;
element zeroLength          13329 2214 192214 -mat  30 -dir 1;

element flatSliderBearing   3069 19232 232 10 110.000012345600 -P 20 -Mz 20  -orient 0. 1. 0. 1. 0. 0.;
element zeroLength          12010 19232 232 -mat  31 -dir 2;
element zeroLength          13330 19232 232 -mat  30 -dir 1;

element flatSliderBearing   3070 233 19233 10 110.000012345600 -P 20 -Mz 20  -orient 0. 1. 0. 1. 0. 0.;
element zeroLength          12011 233 19233 -mat  31 -dir 2;
element zeroLength          13331 233 19233 -mat  30 -dir 1;

element flatSliderBearing   3071 19234 234 10 110.000012345600 -P 20 -Mz 20  -orient 0. 1. 0. 1. 0. 0.;
element zeroLength          12012 19234 234 -mat  31 -dir 2;
element zeroLength          13332 19234 234 -mat  30 -dir 1;

element flatSliderBearing   3072 235 19235 10 110.000012345600 -P 20 -Mz 20  -orient 0. 1. 0. 1. 0. 0.;
element zeroLength          12013 235 19235 -mat  31 -dir 2;
element zeroLength          13333 235 19235 -mat  30 -dir 1;

element flatSliderBearing   3073 19236 236 10 110.000012345600 -P 20 -Mz 20  -orient 0. 1. 0. 1. 0. 0.;
element zeroLength          12014 19236 236 -mat  31 -dir 2;
element zeroLength          13334 19236 236 -mat  30 -dir 1;

element flatSliderBearing   3074 237 19237 10 110.000012345600 -P 20 -Mz 20  -orient 0. 1. 0. 1. 0. 0.;
element zeroLength          12015 237 19237 -mat  31 -dir 2;
element zeroLength          13335 237 19237 -mat  30 -dir 1;

element flatSliderBearing   3075 19238 238 10 110.000012345600 -P 20 -Mz 20  -orient 0. 1. 0. 1. 0. 0.;
element zeroLength          12016 19238 238 -mat  31 -dir 2;
element zeroLength          13336 19238 238 -mat  30 -dir 1;

element flatSliderBearing   3076 239 19239 10 110.000012345600 -P 20 -Mz 20  -orient 0. 1. 0. 1. 0. 0.;
element zeroLength          12017 239 19239 -mat  31 -dir 2;
element zeroLength          13337 239 19239 -mat  30 -dir 1;

element flatSliderBearing   3077 192310 2310 10 110.000012345600 -P 20 -Mz 20  -orient 0. 1. 0. 1. 0. 0.;
element zeroLength          12018 192310 2310 -mat  31 -dir 2;
element zeroLength          13338 192310 2310 -mat  30 -dir 1;

element flatSliderBearing   3078 2311 192311 10 110.000012345600 -P 20 -Mz 20  -orient 0. 1. 0. 1. 0. 0.;
element zeroLength          12019 2311 192311 -mat  31 -dir 2;
element zeroLength          13339 2311 192311 -mat  30 -dir 1;

element flatSliderBearing   3079 192312 2312 10 110.000012345600 -P 20 -Mz 20  -orient 0. 1. 0. 1. 0. 0.;
element zeroLength          12020 192312 2312 -mat  31 -dir 2;
element zeroLength          13340 192312 2312 -mat  30 -dir 1;
```

```
element flatSliderBearing   3080 2313 192313 10 110.000012345600 -P 20 -Mz 20  -orient 0. 1. 0. 1. 0. 0.;
element zeroLength          12021 2313 192313 -mat  31 -dir 2;
element zeroLength          13341 2313 192313 -mat  30 -dir 1;

element flatSliderBearing   3081 192314 2314 10 110.000012345600 -P 20 -Mz 20  -orient 0. 1. 0. 1. 0. 0.;
element zeroLength          12022 192314 2314 -mat  31 -dir 2;
element zeroLength          13342 192314 2314 -mat  30 -dir 1;

element flatSliderBearing   3082 242 19242 10 110.000012345600 -P 20 -Mz 20  -orient 0. 1. 0. 1. 0. 0.;
element zeroLength          12023 242 19242 -mat  31 -dir 2;
element zeroLength          13343 242 19242 -mat  30 -dir 1;

element flatSliderBearing   3083 19243 243 10 110.000012345600 -P 20 -Mz 20  -orient 0. 1. 0. 1. 0. 0.;
element zeroLength          12024 19243 243 -mat  31 -dir 2;
element zeroLength          13344 19243 243 -mat  30 -dir 1;

element flatSliderBearing   3084 244 19244 10 110.000012345600 -P 20 -Mz 20  -orient 0. 1. 0. 1. 0. 0.;
element zeroLength          12025 244 19244 -mat  31 -dir 2;
element zeroLength          13345 244 19244 -mat  30 -dir 1;

element flatSliderBearing   3085 19245 245 10 110.000012345600 -P 20 -Mz 20  -orient 0. 1. 0. 1. 0. 0.;
element zeroLength          12026 19245 245 -mat  31 -dir 2;
element zeroLength          13346 19245 245 -mat  30 -dir 1;

element flatSliderBearing   3086 246 19246 10 110.000012345600 -P 20 -Mz 20  -orient 0. 1. 0. 1. 0. 0.;
element zeroLength          12027 246 19246 -mat  31 -dir 2;
element zeroLength          13347 246 19246 -mat  30 -dir 1;

element flatSliderBearing   3087 19247 247 10 110.000012345600 -P 20 -Mz 20  -orient 0. 1. 0. 1. 0. 0.;
element zeroLength          12028 19247 247 -mat  31 -dir 2;
element zeroLength          13348 19247 247 -mat  30 -dir 1;

element flatSliderBearing   3088 248 19248 10 110.000012345600 -P 20 -Mz 20  -orient 0. 1. 0. 1. 0. 0.;
element zeroLength          12029 248 19248 -mat  31 -dir 2;
element zeroLength          13349 248 19248 -mat  30 -dir 1;

element flatSliderBearing   3089 19249 249 10 110.000012345600 -P 20 -Mz 20  -orient 0. 1. 0. 1. 0. 0.;
element zeroLength          12030 19249 249 -mat  31 -dir 2;
element zeroLength          13350 19249 249 -mat  30 -dir 1;

element flatSliderBearing   3090 2410 192410 10 110.000012345600 -P 20 -Mz 20  -orient 0. 1. 0. 1. 0. 0.;
element zeroLength          12031 2410 192410 -mat  31 -dir 2;
element zeroLength          13351 2410 192410 -mat  30 -dir 1;

element flatSliderBearing   3091 192411 2411 10 110.000012345600 -P 20 -Mz 20  -orient 0. 1. 0. 1. 0. 0.;
element zeroLength          12032 192411 2411 -mat  31 -dir 2;
element zeroLength          13352 192411 2411 -mat  30 -dir 1;

element flatSliderBearing   3092 2412 192412 10 110.000012345600 -P 20 -Mz 20  -orient 0. 1. 0. 1. 0. 0.;
element zeroLength          12033 2412 192412 -mat  31 -dir 2;
element zeroLength          13353 2412 192412 -mat  30 -dir 1;

element flatSliderBearing   3093 192413 2413 10 110.000012345600 -P 20 -Mz 20  -orient 0. 1. 0. 1. 0. 0.;
element zeroLength          12034 192413 2413 -mat  31 -dir 2;
```

```
element zeroLength          13354 192413 2413 -mat  30 -dir 1;

element flatSliderBearing   3094 2414 192414 10 110.000012345600 -P 20 -Mz 20  -orient 0. 1. 0. 1. 0. 0.;
element zeroLength          12035 2414 192414 -mat  31 -dir 2;
element zeroLength          13355 2414 192414 -mat  30 -dir 1;

element flatSliderBearing   3095 19252 252 10 110.000012345600 -P 20 -Mz 20  -orient 0. 1. 0. 1. 0. 0.;
element zeroLength          12036 19252 252 -mat  31 -dir 2;
element zeroLength          13356 19252 252 -mat  30 -dir 1;

element flatSliderBearing   3096 253 19253 10 110.000012345600 -P 20 -Mz 20  -orient 0. 1. 0. 1. 0. 0.;
element zeroLength          12037 253 19253 -mat  31 -dir 2;
element zeroLength          13357 253 19253 -mat  30 -dir 1;

element flatSliderBearing   3097 19254 254 10 110.000012345600 -P 20 -Mz 20  -orient 0. 1. 0. 1. 0. 0.;
element zeroLength          12038 19254 254 -mat  31 -dir 2;
element zeroLength          13358 19254 254 -mat  30 -dir 1;

element flatSliderBearing   3098 255 19255 10 110.000012345600 -P 20 -Mz 20  -orient 0. 1. 0. 1. 0. 0.;
element zeroLength          12039 255 19255 -mat  31 -dir 2;
element zeroLength          13359 255 19255 -mat  30 -dir 1;

element flatSliderBearing   3099 19256 256 10 110.000012345600 -P 20 -Mz 20  -orient 0. 1. 0. 1. 0. 0.;
element zeroLength          12040 19256 256 -mat  31 -dir 2;
element zeroLength          13360 19256 256 -mat  30 -dir 1;

element flatSliderBearing   3100 257 19257 10 110.000012345600 -P 20 -Mz 20  -orient 0. 1. 0. 1. 0. 0.;
element zeroLength          12041 257 19257 -mat  31 -dir 2;
element zeroLength          13361 257 19257 -mat  30 -dir 1;

element flatSliderBearing   3101 19258 258 10 110.000012345600 -P 20 -Mz 20  -orient 0. 1. 0. 1. 0. 0.;
element zeroLength          12042 19258 258 -mat  31 -dir 2;
element zeroLength          13362 19258 258 -mat  30 -dir 1;

element flatSliderBearing   3102 259 19259 10 110.000012345600 -P 20 -Mz 20  -orient 0. 1. 0. 1. 0. 0.;
element zeroLength          12043 259 19259 -mat  31 -dir 2;
element zeroLength          13363 259 19259 -mat  30 -dir 1;

element flatSliderBearing   3103 192510 2510 10 110.000012345600 -P 20 -Mz 20  -orient 0. 1. 0. 1. 0. 0.;
element zeroLength          12044 192510 2510 -mat  31 -dir 2;
element zeroLength          13364 192510 2510 -mat  30 -dir 1;

element flatSliderBearing   3104 2511 192511 10 110.000012345600 -P 20 -Mz 20  -orient 0. 1. 0. 1. 0. 0.;
element zeroLength          12045 2511 192511 -mat  31 -dir 2;
element zeroLength          13365 2511 192511 -mat  30 -dir 1;

element flatSliderBearing   3105 192512 2512 10 110.000012345600 -P 20 -Mz 20  -orient 0. 1. 0. 1. 0. 0.;
element zeroLength          12046 192512 2512 -mat  31 -dir 2;
element zeroLength          13366 192512 2512 -mat  30 -dir 1;

element flatSliderBearing   3106 2513 192513 10 110.000012345600 -P 20 -Mz 20  -orient 0. 1. 0. 1. 0. 0.;
element zeroLength          12047 2513 192513 -mat  31 -dir 2;
element zeroLength          13367 2513 192513 -mat  30 -dir 1;

element flatSliderBearing   3107 192514 2514 10 110.000012345600 -P 20 -Mz 20  -orient 0. 1. 0. 1. 0. 0.;
```

```
element zeroLength          12048 192514 2514 -mat  31 -dir 2;
element zeroLength          13368 192514 2514 -mat  30 -dir 1;

element flatSliderBearing   3108 262 19262 10 110.000012345600 -P 20 -Mz 20  -orient 0. 1. 0. 1. 0. 0.;
element zeroLength          12049 262 19262 -mat  31 -dir 2;
element zeroLength          13369 262 19262 -mat  30 -dir 1;

element flatSliderBearing   3109 19263 263 10 110.000012345600 -P 20 -Mz 20  -orient 0. 1. 0. 1. 0. 0.;
element zeroLength          12050 19263 263 -mat  31 -dir 2;
element zeroLength          13370 19263 263 -mat  30 -dir 1;

element flatSliderBearing   3110 264 19264 10 110.000012345600 -P 20 -Mz 20  -orient 0. 1. 0. 1. 0. 0.;
element zeroLength          12051 264 19264 -mat  31 -dir 2;
element zeroLength          13371 264 19264 -mat  30 -dir 1;

element flatSliderBearing   3111 19265 265 10 110.000012345600 -P 20 -Mz 20  -orient 0. 1. 0. 1. 0. 0.;
element zeroLength          12052 19265 265 -mat  31 -dir 2;
element zeroLength          13372 19265 265 -mat  30 -dir 1;

element flatSliderBearing   3112 266 19266 10 110.000012345600 -P 20 -Mz 20  -orient 0. 1. 0. 1. 0. 0.;
element zeroLength          12053 266 19266 -mat  31 -dir 2;
element zeroLength          13373 266 19266 -mat  30 -dir 1;

element flatSliderBearing   3113 19267 267 10 110.000012345600 -P 20 -Mz 20  -orient 0. 1. 0. 1. 0. 0.;
element zeroLength          12054 19267 267 -mat  31 -dir 2;
element zeroLength          13374 19267 267 -mat  30 -dir 1;

element flatSliderBearing   3114 268 19268 10 110.000012345600 -P 20 -Mz 20  -orient 0. 1. 0. 1. 0. 0.;
element zeroLength          12055 268 19268 -mat  31 -dir 2;
element zeroLength          13375 268 19268 -mat  30 -dir 1;

element flatSliderBearing   3115 19269 269 10 110.000012345600 -P 20 -Mz 20  -orient 0. 1. 0. 1. 0. 0.;
element zeroLength          12056 19269 269 -mat  31 -dir 2;
element zeroLength          13376 19269 269 -mat  30 -dir 1;

element flatSliderBearing   3116 2610 192610 10 110.000012345600 -P 20 -Mz 20  -orient 0. 1. 0. 1. 0. 0.;
element zeroLength          12057 2610 192610 -mat  31 -dir 2;
element zeroLength          13377 2610 192610 -mat  30 -dir 1;

element flatSliderBearing   3117 192611 2611 10 110.000012345600 -P 20 -Mz 20  -orient 0. 1. 0. 1. 0. 0.;
element zeroLength          12058 192611 2611 -mat  31 -dir 2;
element zeroLength          13378 192611 2611 -mat  30 -dir 1;

element flatSliderBearing   3118 2612 192612 10 110.000012345600 -P 20 -Mz 20  -orient 0. 1. 0. 1. 0. 0.;
element zeroLength          12059 2612 192612 -mat  31 -dir 2;
element zeroLength          13379 2612 192612 -mat  30 -dir 1;

element flatSliderBearing   3119 192613 2613 10 110.000012345600 -P 20 -Mz 20  -orient 0. 1. 0. 1. 0. 0.;
element zeroLength          12060 192613 2613 -mat  31 -dir 2;
element zeroLength          13380 192613 2613 -mat  30 -dir 1;

element flatSliderBearing   3120 2614 192614 10 110.000012345600 -P 20 -Mz 20  -orient 0. 1. 0. 1. 0. 0.;
element zeroLength          12061 2614 192614 -mat  31 -dir 2;
element zeroLength          13381 2614 192614 -mat  30 -dir 1;
```

```
element flatSliderBearing  3121 19272 272 10 110.000012345600 -P 20 -Mz 20  -orient 0. 1. 0. 1. 0. 0.;
element zeroLength         12062 19272 272 -mat  31 -dir 2;
element zeroLength         13382 19272 272 -mat  30 -dir 1;

element flatSliderBearing  3122 273 19273 10 110.000012345600 -P 20 -Mz 20  -orient 0. 1. 0. 1. 0. 0.;
element zeroLength         12063 273 19273 -mat  31 -dir 2;
element zeroLength         13383 273 19273 -mat  30 -dir 1;

element flatSliderBearing  3123 19274 274 10 110.000012345600 -P 20 -Mz 20  -orient 0. 1. 0. 1. 0. 0.;
element zeroLength         12064 19274 274 -mat  31 -dir 2;
element zeroLength         13384 19274 274 -mat  30 -dir 1;

element flatSliderBearing  3124 275 19275 10 110.000012345600 -P 20 -Mz 20  -orient 0. 1. 0. 1. 0. 0.;
element zeroLength         12065 275 19275 -mat  31 -dir 2;
element zeroLength         13385 275 19275 -mat  30 -dir 1;

element flatSliderBearing  3125 19276 276 10 110.000012345600 -P 20 -Mz 20  -orient 0. 1. 0. 1. 0. 0.;
element zeroLength         12066 19276 276 -mat  31 -dir 2;
element zeroLength         13386 19276 276 -mat  30 -dir 1;

element flatSliderBearing  3126 277 19277 10 110.000012345600 -P 20 -Mz 20  -orient 0. 1. 0. 1. 0. 0.;
element zeroLength         12067 277 19277 -mat  31 -dir 2;
element zeroLength         13387 277 19277 -mat  30 -dir 1;

element flatSliderBearing  3127 19278 278 10 110.000012345600 -P 20 -Mz 20  -orient 0. 1. 0. 1. 0. 0.;
element zeroLength         12068 19278 278 -mat  31 -dir 2;
element zeroLength         13388 19278 278 -mat  30 -dir 1;

element flatSliderBearing  3128 279 19279 10 110.000012345600 -P 20 -Mz 20  -orient 0. 1. 0. 1. 0. 0.;
element zeroLength         12069 279 19279 -mat  31 -dir 2;
element zeroLength         13389 279 19279 -mat  30 -dir 1;

element flatSliderBearing  3129 192710 2710 10 110.000012345600 -P 20 -Mz 20  -orient 0. 1. 0. 1. 0. 0.;
element zeroLength         12070 192710 2710 -mat  31 -dir 2;
element zeroLength         13390 192710 2710 -mat  30 -dir 1;

element flatSliderBearing  3130 2711 192711 10 110.000012345600 -P 20 -Mz 20  -orient 0. 1. 0. 1. 0. 0.;
element zeroLength         12071 2711 192711 -mat  31 -dir 2;
element zeroLength         13391 2711 192711 -mat  30 -dir 1;

element flatSliderBearing  3131 192712 2712 10 110.000012345600 -P 20 -Mz 20  -orient 0. 1. 0. 1. 0. 0.;
element zeroLength         12072 192712 2712 -mat  31 -dir 2;
element zeroLength         13392 192712 2712 -mat  30 -dir 1;

element flatSliderBearing  3132 2713 192713 10 110.000012345600 -P 20 -Mz 20  -orient 0. 1. 0. 1. 0. 0.;
element zeroLength         12073 2713 192713 -mat  31 -dir 2;
element zeroLength         13393 2713 192713 -mat  30 -dir 1;

element flatSliderBearing  3133 192714 2714 10 110.000012345600 -P 20 -Mz 20  -orient 0. 1. 0. 1. 0. 0.;
element zeroLength         12074 192714 2714 -mat  31 -dir 2;
element zeroLength         13394 192714 2714 -mat  30 -dir 1;

element flatSliderBearing  3134 282 19282 10 110.000012345600 -P 20 -Mz 20  -orient 0. 1. 0. 1. 0. 0.;
element zeroLength         12075 282 19282 -mat  31 -dir 2;
element zeroLength         13395 282 19282 -mat  30 -dir 1;
```

```
7866
7867  element flatSliderBearing  3135 19283 283 10 110.000012345600 -P 20 -Mz 20  -orient 0. 1. 0. 1. 0. 0.;
7868  element zeroLength         12076 19283 283 -mat  31 -dir 2;
7869  element zeroLength         13396 19283 283 -mat  30 -dir 1;
7870
7871  element flatSliderBearing  3136 284 19284 10 110.000012345600 -P 20 -Mz 20  -orient 0. 1. 0. 1. 0. 0.;
7872  element zeroLength         12077 284 19284 -mat  31 -dir 2;
7873  element zeroLength         13397 284 19284 -mat  30 -dir 1;
7874
7875  element flatSliderBearing  3137 19285 285 10 110.000012345600 -P 20 -Mz 20  -orient 0. 1. 0. 1. 0. 0.;
7876  element zeroLength         12078 19285 285 -mat  31 -dir 2;
7877  element zeroLength         13398 19285 285 -mat  30 -dir 1;
7878
7879  element flatSliderBearing  3138 286 19286 10 110.000012345600 -P 20 -Mz 20  -orient 0. 1. 0. 1. 0. 0.;
7880  element zeroLength         12079 286 19286 -mat  31 -dir 2;
7881  element zeroLength         13399 286 19286 -mat  30 -dir 1;
7882
7883  element flatSliderBearing  3139 19287 287 10 110.000012345600 -P 20 -Mz 20  -orient 0. 1. 0. 1. 0. 0.;
7884  element zeroLength         12080 19287 287 -mat  31 -dir 2;
7885  element zeroLength         13400 19287 287 -mat  30 -dir 1;
7886
7887  element flatSliderBearing  3140 288 19288 10 110.000012345600 -P 20 -Mz 20  -orient 0. 1. 0. 1. 0. 0.;
7888  element zeroLength         12081 288 19288 -mat  31 -dir 2;
7889  element zeroLength         13401 288 19288 -mat  30 -dir 1;
7890
7891  element flatSliderBearing  3141 19289 289 10 110.000012345600 -P 20 -Mz 20  -orient 0. 1. 0. 1. 0. 0.;
7892  element zeroLength         12082 19289 289 -mat  31 -dir 2;
7893  element zeroLength         13402 19289 289 -mat  30 -dir 1;
7894
7895  element flatSliderBearing  3142 2810 192810 10 110.000012345600 -P 20 -Mz 20  -orient 0. 1. 0. 1. 0. 0.;
7896  element zeroLength         12083 2810 192810 -mat  31 -dir 2;
7897  element zeroLength         13403 2810 192810 -mat  30 -dir 1;
7898
7899  element flatSliderBearing  3143 192811 2811 10 110.000012345600 -P 20 -Mz 20  -orient 0. 1. 0. 1. 0. 0.;
7900  element zeroLength         12084 192811 2811 -mat  31 -dir 2;
7901  element zeroLength         13404 192811 2811 -mat  30 -dir 1;
7902
7903  element flatSliderBearing  3144 2812 192812 10 110.000012345600 -P 20 -Mz 20  -orient 0. 1. 0. 1. 0. 0.;
7904  element zeroLength         12085 2812 192812 -mat  31 -dir 2;
7905  element zeroLength         13405 2812 192812 -mat  30 -dir 1;
7906
7907  element flatSliderBearing  3145 192813 2813 10 110.000012345600 -P 20 -Mz 20  -orient 0. 1. 0. 1. 0. 0.;
7908  element zeroLength         12086 192813 2813 -mat  31 -dir 2;
7909  element zeroLength         13406 192813 2813 -mat  30 -dir 1;
7910
7911  element flatSliderBearing  3146 2814 192814 10 110.000012345600 -P 20 -Mz 20  -orient 0. 1. 0. 1. 0. 0.;
7912  element zeroLength         12087 2814 192814 -mat  31 -dir 2;
7913  element zeroLength         13407 2814 192814 -mat  30 -dir 1;
7914
7915  element flatSliderBearing  3147 19292 292 10 110.000012345600 -P 20 -Mz 20  -orient 0. 1. 0. 1. 0. 0.;
7916  element zeroLength         12088 19292 292 -mat  31 -dir 2;
7917  element zeroLength         13408 19292 292 -mat  30 -dir 1;
7918
7919  element flatSliderBearing  3148 293 19293 10 110.000012345600 -P 20 -Mz 20  -orient 0. 1. 0. 1. 0. 0.;
7920  element zeroLength         12089 293 19293 -mat  31 -dir 2;
```

```
element zeroLength          13409 293 19293 -mat  30 -dir 1;

element flatSliderBearing   3149 19294 294 10 110.000012345600 -P 20 -Mz 20  -orient 0. 1. 0. 1. 0. 0.;
element zeroLength          12090 19294 294 -mat  31 -dir 2;
element zeroLength          13410 19294 294 -mat  30 -dir 1;

element flatSliderBearing   3150 295 19295 10 110.000012345600 -P 20 -Mz 20  -orient 0. 1. 0. 1. 0. 0.;
element zeroLength          12091 295 19295 -mat  31 -dir 2;
element zeroLength          13411 295 19295 -mat  30 -dir 1;

element flatSliderBearing   3151 19296 296 10 110.000012345600 -P 20 -Mz 20  -orient 0. 1. 0. 1. 0. 0.;
element zeroLength          12092 19296 296 -mat  31 -dir 2;
element zeroLength          13412 19296 296 -mat  30 -dir 1;

element flatSliderBearing   3152 297 19297 10 110.000012345600 -P 20 -Mz 20  -orient 0. 1. 0. 1. 0. 0.;
element zeroLength          12093 297 19297 -mat  31 -dir 2;
element zeroLength          13413 297 19297 -mat  30 -dir 1;

element flatSliderBearing   3153 19298 298 10 110.000012345600 -P 20 -Mz 20  -orient 0. 1. 0. 1. 0. 0.;
element zeroLength          12094 19298 298 -mat  31 -dir 2;
element zeroLength          13414 19298 298 -mat  30 -dir 1;

element flatSliderBearing   3154 299 19299 10 110.000012345600 -P 20 -Mz 20  -orient 0. 1. 0. 1. 0. 0.;
element zeroLength          12095 299 19299 -mat  31 -dir 2;
element zeroLength          13415 299 19299 -mat  30 -dir 1;

element flatSliderBearing   3155 192910 2910 10 110.000012345600 -P 20 -Mz 20  -orient 0. 1. 0. 1. 0. 0.;
element zeroLength          12096 192910 2910 -mat  31 -dir 2;
element zeroLength          13416 192910 2910 -mat  30 -dir 1;

element flatSliderBearing   3156 2911 192911 10 110.000012345600 -P 20 -Mz 20  -orient 0. 1. 0. 1. 0. 0.;
element zeroLength          12097 2911 192911 -mat  31 -dir 2;
element zeroLength          13417 2911 192911 -mat  30 -dir 1;

element flatSliderBearing   3157 192912 2912 10 110.000012345600 -P 20 -Mz 20  -orient 0. 1. 0. 1. 0. 0.;
element zeroLength          12098 192912 2912 -mat  31 -dir 2;
element zeroLength          13418 192912 2912 -mat  30 -dir 1;

element flatSliderBearing   3158 2913 192913 10 110.000012345600 -P 20 -Mz 20  -orient 0. 1. 0. 1. 0. 0.;
element zeroLength          12099 2913 192913 -mat  31 -dir 2;
element zeroLength          13419 2913 192913 -mat  30 -dir 1;

element flatSliderBearing   3159 192914 2914 10 110.000012345600 -P 20 -Mz 20  -orient 0. 1. 0. 1. 0. 0.;
element zeroLength          12100 192914 2914 -mat  31 -dir 2;
element zeroLength          13420 192914 2914 -mat  30 -dir 1;



#fRAME TO iNFILL Frame 1


#F2I Top and Bottom Frame 1


#Tag 18 Bottom
```

```
7976
7977  #for bed joints
7978  element flatSliderBearing   3420 91 1891 100 110.000012345600 -P 20 -Mz 20  -orient 0. 1. 0. 1. 0. 0.;
7979  element zeroLength          12361 91 1891 -mat  31 -dir 2;
7980  element zeroLength          13681 91 1891 -mat  30 -dir 1;
7981
7982  #for bed joints
7983  element flatSliderBearing   3421 101 18101 100 110.000012345600 -P 20 -Mz 20  -orient 0. 1. 0. 1. 0. 0.;
7984  element zeroLength          12362 101 18101 -mat  31 -dir 2;
7985  element zeroLength          13682 101 18101 -mat  30 -dir 1;
7986
7987  #for bed joints
7988  element flatSliderBearing   3422 111 18111 100 110.000012345600 -P 20 -Mz 20  -orient 0. 1. 0. 1. 0. 0.;
7989  element zeroLength          12363 111 18111 -mat  31 -dir 2;
7990  element zeroLength          13683 111 18111 -mat  30 -dir 1;
7991
7992  #for bed joints
7993  element flatSliderBearing   3423 121 18121 100 110.000012345600 -P 20 -Mz 20  -orient 0. 1. 0. 1. 0. 0.;
7994  element zeroLength          12364 121 18121 -mat  31 -dir 2;
7995  element zeroLength          13684 121 18121 -mat  30 -dir 1;
7996
7997  #for bed joints
7998  element flatSliderBearing   3424 131 18131 100 110.000012345600 -P 20 -Mz 20  -orient 0. 1. 0. 1. 0. 0.;
7999  element zeroLength          12365 131 18131 -mat  31 -dir 2;
8000  element zeroLength          13685 131 18131 -mat  30 -dir 1;
8001
8002  #for bed joints
8003  element flatSliderBearing   3425 141 18141 100 110.000012345600 -P 20 -Mz 20  -orient 0. 1. 0. 1. 0. 0.;
8004  element zeroLength          12366 141 18141 -mat  31 -dir 2;
8005  element zeroLength          13686 141 18141 -mat  30 -dir 1;
8006
8007  #for bed joints
8008  element flatSliderBearing   3426 151 18151 100 110.000012345600 -P 20 -Mz 20  -orient 0. 1. 0. 1. 0. 0.;
8009  element zeroLength          12367 151 18151 -mat  31 -dir 2;
8010  element zeroLength          13687 151 18151 -mat  30 -dir 1;
8011
8012  #for bed joints
8013  element flatSliderBearing   3427 161 18161 100 110.000012345600 -P 20 -Mz 20  -orient 0. 1. 0. 1. 0. 0.;
8014  element zeroLength          12368 161 18161 -mat  31 -dir 2;
8015  element zeroLength          13688 161 18161 -mat  30 -dir 1;
8016
8017  #for bed joints
8018  element flatSliderBearing   3428 171 18171 100 110.000012345600 -P 20 -Mz 20  -orient 0. 1. 0. 1. 0. 0.;
8019  element zeroLength          12369 171 18171 -mat  31 -dir 2;
8020  element zeroLength          13689 171 18171 -mat  30 -dir 1;
8021
8022  #for bed joints
8023  element flatSliderBearing   3429 181 18181 100 110.000012345600 -P 20 -Mz 20  -orient 0. 1. 0. 1. 0. 0.;
8024  element zeroLength          12370 181 18181 -mat  31 -dir 2;
8025  element zeroLength          13690 181 18181 -mat  30 -dir 1;
8026
8027  #for bed joints
8028  element flatSliderBearing   3430 191 18191 100 110.000012345600 -P 20 -Mz 20  -orient 0. 1. 0. 1. 0. 0.;
8029  element zeroLength          12371 191 18191 -mat  31 -dir 2;
8030  element zeroLength          13691 191 18191 -mat  30 -dir 1;
```

```
8031
8032  #for bed joints
8033  element flatSliderBearing   3431 201 18201 100 110.000012345600 -P 20 -Mz 20  -orient 0. 1. 0. 1. 0. 0.;
8034  element zeroLength          12372 201 18201 -mat  31 -dir 2;
8035  element zeroLength          13692 201 18201 -mat  30 -dir 1;
8036
8037  #for bed joints
8038  element flatSliderBearing   3432 211 18211 100 110.000012345600 -P 20 -Mz 20  -orient 0. 1. 0. 1. 0. 0.;
8039  element zeroLength          12373 211 18211 -mat  31 -dir 2;
8040  element zeroLength          13693 211 18211 -mat  30 -dir 1;
8041
8042  #for bed joints
8043  element flatSliderBearing   3433 221 18221 100 110.000012345600 -P 20 -Mz 20  -orient 0. 1. 0. 1. 0. 0.;
8044  element zeroLength          12374 221 18221 -mat  31 -dir 2;
8045  element zeroLength          13694 221 18221 -mat  30 -dir 1;
8046
8047  #for bed joints
8048  element flatSliderBearing   3434 231 18231 100 110.000012345600 -P 20 -Mz 20  -orient 0. 1. 0. 1. 0. 0.;
8049  element zeroLength          12375 231 18231 -mat  31 -dir 2;
8050  element zeroLength          13695 231 18231 -mat  30 -dir 1;
8051
8052  #for bed joints
8053  element flatSliderBearing   3435 241 18241 100 110.000012345600 -P 20 -Mz 20  -orient 0. 1. 0. 1. 0. 0.;
8054  element zeroLength          12376 241 18241 -mat  31 -dir 2;
8055  element zeroLength          13696 241 18241 -mat  30 -dir 1;
8056
8057  #for bed joints
8058  element flatSliderBearing   3436 251 18251 100 110.000012345600 -P 20 -Mz 20  -orient 0. 1. 0. 1. 0. 0.;
8059  element zeroLength          12377 251 18251 -mat  31 -dir 2;
8060  element zeroLength          13697 251 18251 -mat  30 -dir 1;
8061
8062  #for bed joints
8063  element flatSliderBearing   3437 261 18261 100 110.000012345600 -P 20 -Mz 20  -orient 0. 1. 0. 1. 0. 0.;
8064  element zeroLength          12378 261 18261 -mat  31 -dir 2;
8065  element zeroLength          13698 261 18261 -mat  30 -dir 1;
8066
8067  #for bed joints
8068  element flatSliderBearing   3438 271 18271 100 110.000012345600 -P 20 -Mz 20  -orient 0. 1. 0. 1. 0. 0.;
8069  element zeroLength          12379 271 18271 -mat  31 -dir 2;
8070  element zeroLength          13699 271 18271 -mat  30 -dir 1;
8071
8072  #for bed joints
8073  element flatSliderBearing   3439 281 18281 100 110.000012345600 -P 20 -Mz 20  -orient 0. 1. 0. 1. 0. 0.;
8074  element zeroLength          12380 281 18281 -mat  31 -dir 2;
8075  element zeroLength          13700 281 18281 -mat  30 -dir 1;
8076
8077  #for bed joints
8078  element flatSliderBearing   3440 291 18291 100 110.000012345600 -P 20 -Mz 20  -orient 0. 1. 0. 1. 0. 0.;
8079  element zeroLength          12381 291 18291 -mat  31 -dir 2;
8080  element zeroLength          13701 291 18291 -mat  30 -dir 1;
8081
8082
8083
8084  #Tag 18 top
8085  #for bed joints
```

```
element flatSliderBearing   3462 915 18915 100 110.000012345600 -P 20 -Mz 20  -orient 0. -1. 0. -1. 0. 0.;
element zeroLength          12403 915 18915 -mat  31 -dir 2;
element zeroLength          13723 915 18915 -mat  30 -dir 1;

#for bed joints
element flatSliderBearing   3463 1015 181015 100 110.000012345600 -P 20 -Mz 20  -orient 0. -1. 0. -1. 0. 0.;
element zeroLength          12404 1015 181015 -mat  31 -dir 2;
element zeroLength          13724 1015 181015 -mat  30 -dir 1;

#for bed joints
element flatSliderBearing   3464 1115 181115 100 110.000012345600 -P 20 -Mz 20  -orient 0. -1. 0. -1. 0. 0.;
element zeroLength          12405 1115 181115 -mat  31 -dir 2;
element zeroLength          13725 1115 181115 -mat  30 -dir 1;

#for bed joints
element flatSliderBearing   3465 1215 181215 100 110.000012345600 -P 20 -Mz 20  -orient 0. -1. 0. -1. 0. 0.;
element zeroLength          12406 1215 181215 -mat  31 -dir 2;
element zeroLength          13726 1215 181215 -mat  30 -dir 1;

#for bed joints
element flatSliderBearing   3466 1315 181315 100 110.000012345600 -P 20 -Mz 20  -orient 0. -1. 0. -1. 0. 0.;
element zeroLength          12407 1315 181315 -mat  31 -dir 2;
element zeroLength          13727 1315 181315 -mat  30 -dir 1;

#for bed joints
element flatSliderBearing   3467 1415 181415 100 110.000012345600 -P 20 -Mz 20  -orient 0. -1. 0. -1. 0. 0.;
element zeroLength          12408 1415 181415 -mat  31 -dir 2;
element zeroLength          13728 1415 181415 -mat  30 -dir 1;

#for bed joints
element flatSliderBearing   3468 1515 181515 100 110.000012345600 -P 20 -Mz 20  -orient 0. -1. 0. -1. 0. 0.;
element zeroLength          12409 1515 181515 -mat  31 -dir 2;
element zeroLength          13729 1515 181515 -mat  30 -dir 1;

#for bed joints
element flatSliderBearing   3469 1615 181615 100 110.000012345600 -P 20 -Mz 20  -orient 0. -1. 0. -1. 0. 0.;
element zeroLength          12410 1615 181615 -mat  31 -dir 2;
element zeroLength          13730 1615 181615 -mat  30 -dir 1;

#for bed joints
element flatSliderBearing   3470 1715 181715 100 110.000012345600 -P 20 -Mz 20  -orient 0. -1. 0. -1. 0. 0.;
element zeroLength          12411 1715 181715 -mat  31 -dir 2;
element zeroLength          13731 1715 181715 -mat  30 -dir 1;

#for bed joints
element flatSliderBearing   3471 1815 181815 100 110.000012345600 -P 20 -Mz 20  -orient 0. -1. 0. -1. 0. 0.;
element zeroLength          12412 1815 181815 -mat  31 -dir 2;
element zeroLength          13732 1815 181815 -mat  30 -dir 1;

#for bed joints
element flatSliderBearing   3472 1915 181915 100 110.000012345600 -P 20 -Mz 20  -orient 0. -1. 0. -1. 0. 0.;
element zeroLength          12413 1915 181915 -mat  31 -dir 2;
element zeroLength          13733 1915 181915 -mat  30 -dir 1;

#for bed joints
```

```
element flatSliderBearing   3473 2015 182015 100 110.000012345600 -P 20 -Mz 20  -orient 0. -1. 0. -1. 0. 0.;
element zeroLength          12414 2015 182015 -mat  31 -dir 2;
element zeroLength          13734 2015 182015 -mat  30 -dir 1;

#for bed joints
element flatSliderBearing   3474 2115 182115 100 110.000012345600 -P 20 -Mz 20  -orient 0. -1. 0. -1. 0. 0.;
element zeroLength          12415 2115 182115 -mat  31 -dir 2;
element zeroLength          13735 2115 182115 -mat  30 -dir 1;

#for bed joints
element flatSliderBearing   3475 2215 182215 100 110.000012345600 -P 20 -Mz 20  -orient 0. -1. 0. -1. 0. 0.;
element zeroLength          12416 2215 182215 -mat  31 -dir 2;
element zeroLength          13736 2215 182215 -mat  30 -dir 1;

#for bed joints
element flatSliderBearing   3476 2315 182315 100 110.000012345600 -P 20 -Mz 20  -orient 0. -1. 0. -1. 0. 0.;
element zeroLength          12417 2315 182315 -mat  31 -dir 2;
element zeroLength          13737 2315 182315 -mat  30 -dir 1;

#for bed joints
element flatSliderBearing   3477 2415 182415 100 110.000012345600 -P 20 -Mz 20  -orient 0. -1. 0. -1. 0. 0.;
element zeroLength          12418 2415 182415 -mat  31 -dir 2;
element zeroLength          13738 2415 182415 -mat  30 -dir 1;

#for bed joints
element flatSliderBearing   3478 2515 182515 100 110.000012345600 -P 20 -Mz 20  -orient 0. -1. 0. -1. 0. 0.;
element zeroLength          12419 2515 182515 -mat  31 -dir 2;
element zeroLength          13739 2515 182515 -mat  30 -dir 1;

#for bed joints
element flatSliderBearing   3479 2615 182615 100 110.000012345600 -P 20 -Mz 20  -orient 0. -1. 0. -1. 0. 0.;
element zeroLength          12420 2615 182615 -mat  31 -dir 2;
element zeroLength          13740 2615 182615 -mat  30 -dir 1;

#for bed joints
element flatSliderBearing   3480 2715 182715 100 110.000012345600 -P 20 -Mz 20  -orient 0. -1. 0. -1. 0. 0.;
element zeroLength          12421 2715 182715 -mat  31 -dir 2;
element zeroLength          13741 2715 182715 -mat  30 -dir 1;

#for bed joints
element flatSliderBearing   3481 2815 182815 100 110.000012345600 -P 20 -Mz 20  -orient 0. -1. 0. -1. 0. 0.;
element zeroLength          12422 2815 182815 -mat  31 -dir 2;
element zeroLength          13742 2815 182815 -mat  30 -dir 1;

#for bed joints
element flatSliderBearing   3482 2915 182915 100 110.000012345600 -P 20 -Mz 20  -orient 0. -1. 0. -1. 0. 0.;
element zeroLength          12423 2915 182915 -mat  31 -dir 2;
element zeroLength          13743 2915 182915 -mat  30 -dir 1;

#for bed joints
element flatSliderBearing   3483 3015 183015 100 110.000012345600 -P 20 -Mz 20  -orient 0. -1. 0. -1. 0. 0.;
element zeroLength          12424 3015 183015 -mat  31 -dir 2;
element zeroLength          13744 3015 183015 -mat  30 -dir 1;
```

```
#Tag 19 or AUX


#Tag 19 Bottom
#for bed joints
element flatSliderBearing   3484 111 19111 100 110.000012345600 -P 20 -Mz 20  -orient 0. 1. 0. 1. 0. 0.;
element zeroLength          12425 111 19111 -mat  31 -dir 2;
element zeroLength          13745 111 19111 -mat  30 -dir 1;

#for bed joints
element flatSliderBearing   3485 131 19131 100 110.000012345600 -P 20 -Mz 20  -orient 0. 1. 0. 1. 0. 0.;
element zeroLength          12426 131 19131 -mat  31 -dir 2;
element zeroLength          13746 131 19131 -mat  30 -dir 1;

#for bed joints
element flatSliderBearing   3486 151 19151 100 110.000012345600 -P 20 -Mz 20  -orient 0. 1. 0. 1. 0. 0.;
element zeroLength          12427 151 19151 -mat  31 -dir 2;
element zeroLength          13747 151 19151 -mat  30 -dir 1;

#for bed joints
element flatSliderBearing   3487 171 19171 100 110.000012345600 -P 20 -Mz 20  -orient 0. 1. 0. 1. 0. 0.;
element zeroLength          12428 171 19171 -mat  31 -dir 2;
element zeroLength          13748 171 19171 -mat  30 -dir 1;

#for bed joints
element flatSliderBearing   3488 191 19191 100 110.000012345600 -P 20 -Mz 20  -orient 0. 1. 0. 1. 0. 0.;
element zeroLength          12429 191 19191 -mat  31 -dir 2;
element zeroLength          13749 191 19191 -mat  30 -dir 1;

#for bed joints
element flatSliderBearing   3489 211 19211 100 110.000012345600 -P 20 -Mz 20  -orient 0. 1. 0. 1. 0. 0.;
element zeroLength          12430 211 19211 -mat  31 -dir 2;
element zeroLength          13750 211 19211 -mat  30 -dir 1;

#for bed joints
element flatSliderBearing   3490 231 19231 100 110.000012345600 -P 20 -Mz 20  -orient 0. 1. 0. 1. 0. 0.;
element zeroLength          12431 231 19231 -mat  31 -dir 2;
element zeroLength          13751 231 19231 -mat  30 -dir 1;

#for bed joints
element flatSliderBearing   3491 251 19251 100 110.000012345600 -P 20 -Mz 20  -orient 0. 1. 0. 1. 0. 0.;
element zeroLength          12432 251 19251 -mat  31 -dir 2;
element zeroLength          13752 251 19251 -mat  30 -dir 1;

#for bed joints
element flatSliderBearing   3492 271 19271 100 110.000012345600 -P 20 -Mz 20  -orient 0. 1. 0. 1. 0. 0.;
element zeroLength          12433 271 19271 -mat  31 -dir 2;
element zeroLength          13753 271 19271 -mat  30 -dir 1;

#for bed joints
element flatSliderBearing   3493 291 19291 100 110.000012345600 -P 20 -Mz 20  -orient 0. 1. 0. 1. 0. 0.;
element zeroLength          12434 291 19291 -mat  31 -dir 2;
```

```
element zeroLength          13754 291 19291 -mat  30 -dir 1;

#for bed joints
element flatSliderBearing   3494 301 19301 100 110.000012345600 -P 20 -Mz 20  -orient 0. 1. 0. 1. 0. 0.;
element zeroLength          12435 301 19301 -mat  31 -dir 2;
element zeroLength          13755 301 19301 -mat  30 -dir 1;




#Tag 19 top
#for bed joints
element flatSliderBearing   3506 1015 191015 100 110.000012345600 -P 20 -Mz 20  -orient 0. -1. 0. -1. 0. 0.;
element zeroLength          12447 1015 191015 -mat  31 -dir 2;
element zeroLength          13767 1015 191015 -mat  30 -dir 1;

#for bed joints
element flatSliderBearing   3507 1215 191215 100 110.000012345600 -P 20 -Mz 20  -orient 0. -1. 0. -1. 0. 0.;
element zeroLength          12448 1215 191215 -mat  31 -dir 2;
element zeroLength          13768 1215 191215 -mat  30 -dir 1;

#for bed joints
element flatSliderBearing   3508 1415 191415 100 110.000012345600 -P 20 -Mz 20  -orient 0. -1. 0. -1. 0. 0.;
element zeroLength          12449 1415 191415 -mat  31 -dir 2;
element zeroLength          13769 1415 191415 -mat  30 -dir 1;

#for bed joints
element flatSliderBearing   3509 1615 191615 100 110.000012345600 -P 20 -Mz 20  -orient 0. -1. 0. -1. 0. 0.;
element zeroLength          12450 1615 191615 -mat  31 -dir 2;
element zeroLength          13770 1615 191615 -mat  30 -dir 1;

#for bed joints
element flatSliderBearing   3510 1815 191815 100 110.000012345600 -P 20 -Mz 20  -orient 0. -1. 0. -1. 0. 0.;
element zeroLength          12451 1815 191815 -mat  31 -dir 2;
element zeroLength          13771 1815 191815 -mat  30 -dir 1;

#for bed joints
element flatSliderBearing   3511 2015 192015 100 110.000012345600 -P 20 -Mz 20  -orient 0. -1. 0. -1. 0. 0.;
element zeroLength          12452 2015 192015 -mat  31 -dir 2;
element zeroLength          13772 2015 192015 -mat  30 -dir 1;

#for bed joints
element flatSliderBearing   3512 2215 192215 100 110.000012345600 -P 20 -Mz 20  -orient 0. -1. 0. -1. 0. 0.;
element zeroLength          12453 2215 192215 -mat  31 -dir 2;
element zeroLength          13773 2215 192215 -mat  30 -dir 1;

#for bed joints
element flatSliderBearing   3513 2415 192415 100 110.000012345600 -P 20 -Mz 20  -orient 0. -1. 0. -1. 0. 0.;
element zeroLength          12454 2415 192415 -mat  31 -dir 2;
element zeroLength          13774 2415 192415 -mat  30 -dir 1;

#for bed joints
element flatSliderBearing   3514 2615 192615 100 110.000012345600 -P 20 -Mz 20  -orient 0. -1. 0. -1. 0. 0.;
element zeroLength          12455 2615 192615 -mat  31 -dir 2;
```

```
element zeroLength          13775 2615 192615 -mat  30 -dir 1;

#for bed joints
element flatSliderBearing   3515 2815 192815 100 110.000012345600 -P 20 -Mz 20  -orient 0. -1. 0. -1. 0. 0.;
element zeroLength          12456 2815 192815 -mat  31 -dir 2;
element zeroLength          13776 2815 192815 -mat  30 -dir 1;



#F2I Left and Right Frame 1


#Tag 18 left


#for bed joints
element flatSliderBearing   3516 92 1892 11 110.000012345600 -P 21 -Mz 21 -orient 1. 0. 0. 0. -1. 0.;
element zeroLength          12457 92 1892 -mat  41 -dir 1;
element zeroLength          13777 92 1892 -mat  40 -dir 2;

#for bed joints
element flatSliderBearing   3517 93 1893 11 110.000012345600 -P 21 -Mz 21 -orient 1. 0. 0. 0. -1. 0.;
element zeroLength          12458 93 1893 -mat  41 -dir 1;
element zeroLength          13778 93 1893 -mat  40 -dir 2;

#for bed joints
element flatSliderBearing   3518 94 1894 11 110.000012345600 -P 21 -Mz 21 -orient 1. 0. 0. 0. -1. 0.;
element zeroLength          12459 94 1894 -mat  41 -dir 1;
element zeroLength          13779 94 1894 -mat  40 -dir 2;

#for bed joints
element flatSliderBearing   3519 95 1895 11 110.000012345600 -P 21 -Mz 21 -orient 1. 0. 0. 0. -1. 0.;
element zeroLength          12460 95 1895 -mat  41 -dir 1;
element zeroLength          13780 95 1895 -mat  40 -dir 2;

#for bed joints
element flatSliderBearing   3520 96 1896 11 110.000012345600 -P 21 -Mz 21 -orient 1. 0. 0. 0. -1. 0.;
element zeroLength          12461 96 1896 -mat  41 -dir 1;
element zeroLength          13781 96 1896 -mat  40 -dir 2;

#for bed joints
element flatSliderBearing   3521 97 1897 11 110.000012345600 -P 21 -Mz 21 -orient 1. 0. 0. 0. -1. 0.;
element zeroLength          12462 97 1897 -mat  41 -dir 1;
element zeroLength          13782 97 1897 -mat  40 -dir 2;

#for bed joints
element flatSliderBearing   3522 98 1898 11 110.000012345600 -P 21 -Mz 21 -orient 1. 0. 0. 0. -1. 0.;
element zeroLength          12463 98 1898 -mat  41 -dir 1;
element zeroLength          13783 98 1898 -mat  40 -dir 2;

#for bed joints
element flatSliderBearing   3523 99 1899 11 110.000012345600 -P 21 -Mz 21 -orient 1. 0. 0. 0. -1. 0.;
element zeroLength          12464 99 1899 -mat  41 -dir 1;
element zeroLength          13784 99 1899 -mat  40 -dir 2;

```

```
#for bed joints
element flatSliderBearing  3524 910 18910 11 110.000012345600 -P 21 -Mz 21 -orient 1. 0. 0. 0. -1. 0.;
element zeroLength         12465 910 18910 -mat  41 -dir 1;
element zeroLength         13785 910 18910 -mat  40 -dir 2;

#for bed joints
element flatSliderBearing  3525 911 18911 11 110.000012345600 -P 21 -Mz 21 -orient 1. 0. 0. 0. -1. 0.;
element zeroLength         12466 911 18911 -mat  41 -dir 1;
element zeroLength         13786 911 18911 -mat  40 -dir 2;

#for bed joints
element flatSliderBearing  3526 912 18912 11 110.000012345600 -P 21 -Mz 21 -orient 1. 0. 0. 0. -1. 0.;
element zeroLength         12467 912 18912 -mat  41 -dir 1;
element zeroLength         13787 912 18912 -mat  40 -dir 2;

#for bed joints
element flatSliderBearing  3527 913 18913 11 110.000012345600 -P 21 -Mz 21 -orient 1. 0. 0. 0. -1. 0.;
element zeroLength         12468 913 18913 -mat  41 -dir 1;
element zeroLength         13788 913 18913 -mat  40 -dir 2;

#for bed joints
element flatSliderBearing  3528 914 18914 11 110.000012345600 -P 21 -Mz 21 -orient 1. 0. 0. 0. -1. 0.;
element zeroLength         12469 914 18914 -mat  41 -dir 1;
element zeroLength         13789 914 18914 -mat  40 -dir 2;









#Tag 18 right
#for bed joints
element flatSliderBearing  3542 302 18302 11 110.000012345600 -P 21 -Mz 21 -orient -1. 0. 0. 0. 1. 0.;
element zeroLength         12483 302 18302 -mat  41 -dir 1;
element zeroLength         13803 302 18302 -mat  40 -dir 2;

#for bed joints
element flatSliderBearing  3543 303 18303 11 110.000012345600 -P 21 -Mz 21 -orient -1. 0. 0. 0. 1. 0.;
element zeroLength         12484 303 18303 -mat  41 -dir 1;
element zeroLength         13804 303 18303 -mat  40 -dir 2;

#for bed joints
element flatSliderBearing  3544 304 18304 11 110.000012345600 -P 21 -Mz 21 -orient -1. 0. 0. 0. 1. 0.;
element zeroLength         12485 304 18304 -mat  41 -dir 1;
element zeroLength         13805 304 18304 -mat  40 -dir 2;

#for bed joints
element flatSliderBearing  3545 305 18305 11 110.000012345600 -P 21 -Mz 21 -orient -1. 0. 0. 0. 1. 0.;
element zeroLength         12486 305 18305 -mat  41 -dir 1;
element zeroLength         13806 305 18305 -mat  40 -dir 2;

#for bed joints
element flatSliderBearing  3546 306 18306 11 110.000012345600 -P 21 -Mz 21 -orient -1. 0. 0. 0. 1. 0.;
element zeroLength         12487 306 18306 -mat  41 -dir 1;
element zeroLength         13807 306 18306 -mat  40 -dir 2;
```

```
#for bed joints
element flatSliderBearing   3547 307 18307 11 110.000012345600 -P 21 -Mz 21 -orient -1. 0. 0. 0. 1. 0.;
element zeroLength          12488 307 18307 -mat  41 -dir 1;
element zeroLength          13808 307 18307 -mat  40 -dir 2;

#for bed joints
element flatSliderBearing   3548 308 18308 11 110.000012345600 -P 21 -Mz 21 -orient -1. 0. 0. 0. 1. 0.;
element zeroLength          12489 308 18308 -mat  41 -dir 1;
element zeroLength          13809 308 18308 -mat  40 -dir 2;

#for bed joints
element flatSliderBearing   3549 309 18309 11 110.000012345600 -P 21 -Mz 21 -orient -1. 0. 0. 0. 1. 0.;
element zeroLength          12490 309 18309 -mat  41 -dir 1;
element zeroLength          13810 309 18309 -mat  40 -dir 2;

#for bed joints
element flatSliderBearing   3550 3010 183010 11 110.000012345600 -P 21 -Mz 21 -orient -1. 0. 0. 0. 1. 0.;
element zeroLength          12491 3010 183010 -mat  41 -dir 1;
element zeroLength          13811 3010 183010 -mat  40 -dir 2;

#for bed joints
element flatSliderBearing   3551 3011 183011 11 110.000012345600 -P 21 -Mz 21 -orient -1. 0. 0. 0. 1. 0.;
element zeroLength          12492 3011 183011 -mat  41 -dir 1;
element zeroLength          13812 3011 183011 -mat  40 -dir 2;

#for bed joints
element flatSliderBearing   3552 3012 183012 11 110.000012345600 -P 21 -Mz 21 -orient -1. 0. 0. 0. 1. 0.;
element zeroLength          12493 3012 183012 -mat  41 -dir 1;
element zeroLength          13813 3012 183012 -mat  40 -dir 2;

#for bed joints
element flatSliderBearing   3553 3013 183013 11 110.000012345600 -P 21 -Mz 21 -orient -1. 0. 0. 0. 1. 0.;
element zeroLength          12494 3013 183013 -mat  41 -dir 1;
element zeroLength          13814 3013 183013 -mat  40 -dir 2;

#for bed joints
element flatSliderBearing   3554 3014 183014 11 110.000012345600 -P 21 -Mz 21 -orient -1. 0. 0. 0. 1. 0.;
element zeroLength          12495 3014 183014 -mat  41 -dir 1;
element zeroLength          13815 3014 183014 -mat  40 -dir 2;









#Tag 19 Left


#for bed joints
element flatSliderBearing   3555 92 1992 11 110.000012345600 -P 21 -Mz 21  -orient 1. 0. 0. 0. -1. 0.;
element zeroLength          12496 92 1992 -mat  41 -dir 1;
element zeroLength          13816 92 1992 -mat  40 -dir 2;

#for bed joints
element flatSliderBearing   3556 93 1993 11 110.000012345600 -P 21 -Mz 21  -orient 1. 0. 0. 0. -1. 0.;
element zeroLength          12497 93 1993 -mat  41 -dir 1;
```

```
element zeroLength          13817 93 1993 -mat  40 -dir 2;

#for bed joints
element flatSliderBearing   3557 94 1994 11 110.000012345600 -P 21 -Mz 21  -orient 1. 0. 0. 0. -1. 0.;
element zeroLength          12498 94 1994 -mat  41 -dir 1;
element zeroLength          13818 94 1994 -mat  40 -dir 2;

#for bed joints
element flatSliderBearing   3558 95 1995 11 110.000012345600 -P 21 -Mz 21  -orient 1. 0. 0. 0. -1. 0.;
element zeroLength          12499 95 1995 -mat  41 -dir 1;
element zeroLength          13819 95 1995 -mat  40 -dir 2;

#for bed joints
element flatSliderBearing   3559 96 1996 11 110.000012345600 -P 21 -Mz 21  -orient 1. 0. 0. 0. -1. 0.;
element zeroLength          12500 96 1996 -mat  41 -dir 1;
element zeroLength          13820 96 1996 -mat  40 -dir 2;

#for bed joints
element flatSliderBearing   3560 97 1997 11 110.000012345600 -P 21 -Mz 21  -orient 1. 0. 0. 0. -1. 0.;
element zeroLength          12501 97 1997 -mat  41 -dir 1;
element zeroLength          13821 97 1997 -mat  40 -dir 2;

#for bed joints
element flatSliderBearing   3561 98 1998 11 110.000012345600 -P 21 -Mz 21  -orient 1. 0. 0. 0. -1. 0.;
element zeroLength          12502 98 1998 -mat  41 -dir 1;
element zeroLength          13822 98 1998 -mat  40 -dir 2;

#for bed joints
element flatSliderBearing   3562 99 1999 11 110.000012345600 -P 21 -Mz 21  -orient 1. 0. 0. 0. -1. 0.;
element zeroLength          12503 99 1999 -mat  41 -dir 1;
element zeroLength          13823 99 1999 -mat  40 -dir 2;

#for bed joints
element flatSliderBearing   3563 910 19910 11 110.000012345600 -P 21 -Mz 21  -orient 1. 0. 0. 0. -1. 0.;
element zeroLength          12504 910 19910 -mat  41 -dir 1;
element zeroLength          13824 910 19910 -mat  40 -dir 2;

#for bed joints
element flatSliderBearing   3564 911 19911 11 110.000012345600 -P 21 -Mz 21  -orient 1. 0. 0. 0. -1. 0.;
element zeroLength          12505 911 19911 -mat  41 -dir 1;
element zeroLength          13825 911 19911 -mat  40 -dir 2;

#for bed joints
element flatSliderBearing   3565 912 19912 11 110.000012345600 -P 21 -Mz 21  -orient 1. 0. 0. 0. -1. 0.;
element zeroLength          12506 912 19912 -mat  41 -dir 1;
element zeroLength          13826 912 19912 -mat  40 -dir 2;

#for bed joints
element flatSliderBearing   3566 913 19913 11 110.000012345600 -P 21 -Mz 21  -orient 1. 0. 0. 0. -1. 0.;
element zeroLength          12507 913 19913 -mat  41 -dir 1;
element zeroLength          13827 913 19913 -mat  40 -dir 2;

#for bed joints
element flatSliderBearing   3567 914 19914 11 110.000012345600 -P 21 -Mz 21  -orient 1. 0. 0. 0. -1. 0.;
element zeroLength          12508 914 19914 -mat  41 -dir 1;
```

```
element zeroLength          13828 914 19914 -mat  40 -dir 2;


#Tag 19 right
#for bed joints
element flatSliderBearing   3581 302 19302 11 110.000012345600 -P 21 -Mz 21  -orient -1. 0. 0. 0. 1. 0.;
element zeroLength          12522 302 19302 -mat  41 -dir 1;
element zeroLength          13842 302 19302 -mat  40 -dir 2;

#for bed joints
element flatSliderBearing   3582 303 19303 11 110.000012345600 -P 21 -Mz 21  -orient -1. 0. 0. 0. 1. 0.;
element zeroLength          12523 303 19303 -mat  41 -dir 1;
element zeroLength          13843 303 19303 -mat  40 -dir 2;

#for bed joints
element flatSliderBearing   3583 304 19304 11 110.000012345600 -P 21 -Mz 21  -orient -1. 0. 0. 0. 1. 0.;
element zeroLength          12524 304 19304 -mat  41 -dir 1;
element zeroLength          13844 304 19304 -mat  40 -dir 2;

#for bed joints
element flatSliderBearing   3584 305 19305 11 110.000012345600 -P 21 -Mz 21  -orient -1. 0. 0. 0. 1. 0.;
element zeroLength          12525 305 19305 -mat  41 -dir 1;
element zeroLength          13845 305 19305 -mat  40 -dir 2;

#for bed joints
element flatSliderBearing   3585 306 19306 11 110.000012345600 -P 21 -Mz 21  -orient -1. 0. 0. 0. 1. 0.;
element zeroLength          12526 306 19306 -mat  41 -dir 1;
element zeroLength          13846 306 19306 -mat  40 -dir 2;

#for bed joints
element flatSliderBearing   3586 307 19307 11 110.000012345600 -P 21 -Mz 21  -orient -1. 0. 0. 0. 1. 0.;
element zeroLength          12527 307 19307 -mat  41 -dir 1;
element zeroLength          13847 307 19307 -mat  40 -dir 2;

#for bed joints
element flatSliderBearing   3587 308 19308 11 110.000012345600 -P 21 -Mz 21  -orient -1. 0. 0. 0. 1. 0.;
element zeroLength          12528 308 19308 -mat  41 -dir 1;
element zeroLength          13848 308 19308 -mat  40 -dir 2;

#for bed joints
element flatSliderBearing   3588 309 19309 11 110.000012345600 -P 21 -Mz 21  -orient -1. 0. 0. 0. 1. 0.;
element zeroLength          12529 309 19309 -mat  41 -dir 1;
element zeroLength          13849 309 19309 -mat  40 -dir 2;

#for bed joints
element flatSliderBearing   3589 3010 193010 11 110.000012345600 -P 21 -Mz 21  -orient -1. 0. 0. 0. 1. 0.;
element zeroLength          12530 3010 193010 -mat  41 -dir 1;
element zeroLength          13850 3010 193010 -mat  40 -dir 2;

#for bed joints
element flatSliderBearing   3590 3011 193011 11 110.000012345600 -P 21 -Mz 21  -orient -1. 0. 0. 0. 1. 0.;
element zeroLength          12531 3011 193011 -mat  41 -dir 1;
```

```
element zeroLength          13851 3011 193011 -mat  40 -dir 2;

#for bed joints
element flatSliderBearing   3591 3012 193012 11 110.000012345600 -P 21 -Mz 21  -orient -1. 0. 0. 0. 1. 0.;
element zeroLength          12532 3012 193012 -mat  41 -dir 1;
element zeroLength          13852 3012 193012 -mat  40 -dir 2;

#for bed joints
element flatSliderBearing   3592 3013 193013 11 110.000012345600 -P 21 -Mz 21  -orient -1. 0. 0. 0. 1. 0.;
element zeroLength          12533 3013 193013 -mat  41 -dir 1;
element zeroLength          13853 3013 193013 -mat  40 -dir 2;

#for bed joints
element flatSliderBearing   3593 3014 193014 11 110.000012345600 -P 21 -Mz 21  -orient -1. 0. 0. 0. 1. 0.;
element zeroLength          12534 3014 193014 -mat  41 -dir 1;
element zeroLength          13854 3014 193014 -mat  40 -dir 2;









#ORNER NODES LEFT
#for bed joints
element flatSliderBearing   3594 91 1891 11 110.000012345600 -P 21 -Mz 21  -orient 1. 0. 0. 0. -1. 0.;
element zeroLength          22535 91 1891 -mat  41 -dir 1;
element zeroLength          14855 91 1891 -mat  40 -dir 2;

#for bed joints
element flatSliderBearing   3595 915 18915 11 110.000012345600 -P 21 -Mz 21  -orient 1. 0. 0. 0. -1. 0.;
element zeroLength          22536 915 18915 -mat  41 -dir 1;
element zeroLength          14856 915 18915 -mat  40 -dir 2;









#ORNER NODES RIGHT
#for bed joints
element flatSliderBearing   3596 3015 183015 11 110.000012345600 -P 21 -Mz 21  -orient -1. 0. 0. 0. 1. 0.;
element zeroLength          32537 3015 183015 -mat  41 -dir 1;
element zeroLength          15857 3015 183015 -mat  40 -dir 2;

#for bed joints
element flatSliderBearing   3597 301 19301 11 110.000012345600 -P 21 -Mz 21  -orient -1. 0. 0. 0. 1. 0.;
element zeroLength          32538 301 19301 -mat  41 -dir 1;
element zeroLength          15858 301 19301 -mat  40 -dir 2;









#Additional ZLE f2I Bottom Tag from 18 to 19


#Bottom
```

```
element flatSliderBearing  3598 18111 19111 10 110.000012345600 -P 21 -Mz 21  -orient 1. 0. 0. 0. -1. 0.;
element zeroLength         42799 18111 19111 -mat  41 -dir 1;
element zeroLength         17119 18111 19111 -mat  40 -dir 2;

element flatSliderBearing  3599 18131 19131 10 110.000012345600 -P 21 -Mz 21  -orient 1. 0. 0. 0. -1. 0.;
element zeroLength         42800 18131 19131 -mat  41 -dir 1;
element zeroLength         17120 18131 19131 -mat  40 -dir 2;

element flatSliderBearing  3600 18151 19151 10 110.000012345600 -P 21 -Mz 21  -orient 1. 0. 0. 0. -1. 0.;
element zeroLength         42801 18151 19151 -mat  41 -dir 1;
element zeroLength         17121 18151 19151 -mat  40 -dir 2;

element flatSliderBearing  3601 18171 19171 10 110.000012345600 -P 21 -Mz 21  -orient 1. 0. 0. 0. -1. 0.;
element zeroLength         42802 18171 19171 -mat  41 -dir 1;
element zeroLength         17122 18171 19171 -mat  40 -dir 2;

element flatSliderBearing  3602 18191 19191 10 110.000012345600 -P 21 -Mz 21  -orient 1. 0. 0. 0. -1. 0.;
element zeroLength         42803 18191 19191 -mat  41 -dir 1;
element zeroLength         17123 18191 19191 -mat  40 -dir 2;

element flatSliderBearing  3603 18211 19211 10 110.000012345600 -P 21 -Mz 21  -orient 1. 0. 0. 0. -1. 0.;
element zeroLength         42804 18211 19211 -mat  41 -dir 1;
element zeroLength         17124 18211 19211 -mat  40 -dir 2;

element flatSliderBearing  3604 18231 19231 10 110.000012345600 -P 21 -Mz 21  -orient 1. 0. 0. 0. -1. 0.;
element zeroLength         42805 18231 19231 -mat  41 -dir 1;
element zeroLength         17125 18231 19231 -mat  40 -dir 2;

element flatSliderBearing  3605 18251 19251 10 110.000012345600 -P 21 -Mz 21  -orient 1. 0. 0. 0. -1. 0.;
element zeroLength         42806 18251 19251 -mat  41 -dir 1;
element zeroLength         17126 18251 19251 -mat  40 -dir 2;

element flatSliderBearing  3606 18271 19271 10 110.000012345600 -P 21 -Mz 21  -orient 1. 0. 0. 0. -1. 0.;
element zeroLength         42807 18271 19271 -mat  41 -dir 1;
element zeroLength         17127 18271 19271 -mat  40 -dir 2;

element flatSliderBearing  3607 18291 19291 10 110.000012345600 -P 21 -Mz 21  -orient 1. 0. 0. 0. -1. 0.;
element zeroLength         42808 18291 19291 -mat  41 -dir 1;
element zeroLength         17128 18291 19291 -mat  40 -dir 2;









#Additional ZLE f2I top Tag from 18 to 19


#Top
element flatSliderBearing  3608 181015 191015 10 110.000012345600 -P 21 -Mz 21  -orient 1. 0. 0. 0. -1. 0.;
element zeroLength         42809 181015 191015 -mat  41 -dir 1;
element zeroLength         17129 181015 191015 -mat  40 -dir 2;

element flatSliderBearing  3609 181215 191215 10 110.000012345600 -P 21 -Mz 21  -orient 1. 0. 0. 0. -1. 0.;
element zeroLength         42810 181215 191215 -mat  41 -dir 1;
element zeroLength         17130 181215 191215 -mat  40 -dir 2;
```

```
element flatSliderBearing  3610 181415 191415 10 110.000012345600 -P 21 -Mz 21  -orient 1. 0. 0. 0. -1. 0.;
element zeroLength         42811 181415 191415 -mat  41 -dir 1;
element zeroLength         17131 181415 191415 -mat  40 -dir 2;

element flatSliderBearing  3611 181615 191615 10 110.000012345600 -P 21 -Mz 21  -orient 1. 0. 0. 0. -1. 0.;
element zeroLength         42812 181615 191615 -mat  41 -dir 1;
element zeroLength         17132 181615 191615 -mat  40 -dir 2;

element flatSliderBearing  3612 181815 191815 10 110.000012345600 -P 21 -Mz 21  -orient 1. 0. 0. 0. -1. 0.;
element zeroLength         42813 181815 191815 -mat  41 -dir 1;
element zeroLength         17133 181815 191815 -mat  40 -dir 2;

element flatSliderBearing  3613 182015 192015 10 110.000012345600 -P 21 -Mz 21  -orient 1. 0. 0. 0. -1. 0.;
element zeroLength         42814 182015 192015 -mat  41 -dir 1;
element zeroLength         17134 182015 192015 -mat  40 -dir 2;

element flatSliderBearing  3614 182215 192215 10 110.000012345600 -P 21 -Mz 21  -orient 1. 0. 0. 0. -1. 0.;
element zeroLength         42815 182215 192215 -mat  41 -dir 1;
element zeroLength         17135 182215 192215 -mat  40 -dir 2;

element flatSliderBearing  3615 182415 192415 10 110.000012345600 -P 21 -Mz 21  -orient 1. 0. 0. 0. -1. 0.;
element zeroLength         42816 182415 192415 -mat  41 -dir 1;
element zeroLength         17136 182415 192415 -mat  40 -dir 2;

element flatSliderBearing  3616 182615 192615 10 110.000012345600 -P 21 -Mz 21  -orient 1. 0. 0. 0. -1. 0.;
element zeroLength         42817 182615 192615 -mat  41 -dir 1;
element zeroLength         17137 182615 192615 -mat  40 -dir 2;

element flatSliderBearing  3617 182815 192815 10 110.000012345600 -P 21 -Mz 21  -orient 1. 0. 0. 0. -1. 0.;
element zeroLength         42818 182815 192815 -mat  41 -dir 1;
element zeroLength         17138 182815 192815 -mat  40 -dir 2;



#Additional ZLE f2I left from 18 to 19


#Left
element flatSliderBearing  3618 1992 1892 10 110.000012345600 -P 20 -Mz 20  -orient 0. 1. 0. 1. 0. 0.;
element zeroLength         42559 1992 1892 -mat  31 -dir 2;
element zeroLength         16879 1992 1892 -mat  30 -dir 1;

element flatSliderBearing  3619 1893 1993 10 110.000012345600 -P 20 -Mz 20  -orient 0. 1. 0. 1. 0. 0.;
element zeroLength         42560 1893 1993 -mat  31 -dir 2;
element zeroLength         16880 1893 1993 -mat  30 -dir 1;

element flatSliderBearing  3620 1994 1894 10 110.000012345600 -P 20 -Mz 20  -orient 0. 1. 0. 1. 0. 0.;
element zeroLength         42561 1994 1894 -mat  31 -dir 2;
element zeroLength         16881 1994 1894 -mat  30 -dir 1;

element flatSliderBearing  3621 1895 1995 10 110.000012345600 -P 20 -Mz 20  -orient 0. 1. 0. 1. 0. 0.;
element zeroLength         42562 1895 1995 -mat  31 -dir 2;
```

```
element zeroLength          16882 1895 1995 -mat  30 -dir 1;

element flatSliderBearing   3622 1996 1896 10 110.000012345600 -P 20 -Mz 20  -orient 0. 1. 0. 1. 0. 0.;
element zeroLength          42563 1996 1896 -mat  31 -dir 2;
element zeroLength          16883 1996 1896 -mat  30 -dir 1;

element flatSliderBearing   3623 1897 1997 10 110.000012345600 -P 20 -Mz 20  -orient 0. 1. 0. 1. 0. 0.;
element zeroLength          42564 1897 1997 -mat  31 -dir 2;
element zeroLength          16884 1897 1997 -mat  30 -dir 1;

element flatSliderBearing   3624 1998 1898 10 110.000012345600 -P 20 -Mz 20  -orient 0. 1. 0. 1. 0. 0.;
element zeroLength          42565 1998 1898 -mat  31 -dir 2;
element zeroLength          16885 1998 1898 -mat  30 -dir 1;

element flatSliderBearing   3625 1899 1999 10 110.000012345600 -P 20 -Mz 20  -orient 0. 1. 0. 1. 0. 0.;
element zeroLength          42566 1899 1999 -mat  31 -dir 2;
element zeroLength          16886 1899 1999 -mat  30 -dir 1;

element flatSliderBearing   3626 19910 18910 10 110.000012345600 -P 20 -Mz 20  -orient 0. 1. 0. 1. 0. 0.;
element zeroLength          42567 19910 18910 -mat  31 -dir 2;
element zeroLength          16887 19910 18910 -mat  30 -dir 1;

element flatSliderBearing   3627 18911 19911 10 110.000012345600 -P 20 -Mz 20  -orient 0. 1. 0. 1. 0. 0.;
element zeroLength          42568 18911 19911 -mat  31 -dir 2;
element zeroLength          16888 18911 19911 -mat  30 -dir 1;

element flatSliderBearing   3628 19912 18912 10 110.000012345600 -P 20 -Mz 20  -orient 0. 1. 0. 1. 0. 0.;
element zeroLength          42569 19912 18912 -mat  31 -dir 2;
element zeroLength          16889 19912 18912 -mat  30 -dir 1;

element flatSliderBearing   3629 18913 19913 10 110.000012345600 -P 20 -Mz 20  -orient 0. 1. 0. 1. 0. 0.;
element zeroLength          42570 18913 19913 -mat  31 -dir 2;
element zeroLength          16890 18913 19913 -mat  30 -dir 1;

element flatSliderBearing   3630 19914 18914 10 110.000012345600 -P 20 -Mz 20  -orient 0. 1. 0. 1. 0. 0.;
element zeroLength          42571 19914 18914 -mat  31 -dir 2;
element zeroLength          16891 19914 18914 -mat  30 -dir 1;




#Additional ZLE f2I right from 18 to 19


#Right
element flatSliderBearing   3631 19302 18302 10 110.000012345600 -P 20 -Mz 20  -orient 0. 1. 0. 1. 0. 0.;
element zeroLength          42572 19302 18302 -mat  31 -dir 2;
element zeroLength          16892 19302 18302 -mat  30 -dir 1;

element flatSliderBearing   3632 18303 19303 10 110.000012345600 -P 20 -Mz 20  -orient 0. 1. 0. 1. 0. 0.;
element zeroLength          42573 18303 19303 -mat  31 -dir 2;
element zeroLength          16893 18303 19303 -mat  30 -dir 1;

element flatSliderBearing   3633 19304 18304 10 110.000012345600 -P 20 -Mz 20  -orient 0. 1. 0. 1. 0. 0.;
```

```
element zeroLength          42574 19304 18304 -mat  31 -dir 2;
element zeroLength          16894 19304 18304 -mat  30 -dir 1;

element flatSliderBearing   3634 18305 19305 10 110.000012345600 -P 20 -Mz 20  -orient 0. 1. 0. 1. 0. 0.;
element zeroLength          42575 18305 19305 -mat  31 -dir 2;
element zeroLength          16895 18305 19305 -mat  30 -dir 1;

element flatSliderBearing   3635 19306 18306 10 110.000012345600 -P 20 -Mz 20  -orient 0. 1. 0. 1. 0. 0.;
element zeroLength          42576 19306 18306 -mat  31 -dir 2;
element zeroLength          16896 19306 18306 -mat  30 -dir 1;

element flatSliderBearing   3636 18307 19307 10 110.000012345600 -P 20 -Mz 20  -orient 0. 1. 0. 1. 0. 0.;
element zeroLength          42577 18307 19307 -mat  31 -dir 2;
element zeroLength          16897 18307 19307 -mat  30 -dir 1;

element flatSliderBearing   3637 19308 18308 10 110.000012345600 -P 20 -Mz 20  -orient 0. 1. 0. 1. 0. 0.;
element zeroLength          42578 19308 18308 -mat  31 -dir 2;
element zeroLength          16898 19308 18308 -mat  30 -dir 1;

element flatSliderBearing   3638 18309 19309 10 110.000012345600 -P 20 -Mz 20  -orient 0. 1. 0. 1. 0. 0.;
element zeroLength          42579 18309 19309 -mat  31 -dir 2;
element zeroLength          16899 18309 19309 -mat  30 -dir 1;

element flatSliderBearing   3639 193010 183010 10 110.000012345600 -P 20 -Mz 20  -orient 0. 1. 0. 1. 0. 0.;
element zeroLength          42580 193010 183010 -mat  31 -dir 2;
element zeroLength          16900 193010 183010 -mat  30 -dir 1;

element flatSliderBearing   3640 183011 193011 10 110.000012345600 -P 20 -Mz 20  -orient 0. 1. 0. 1. 0. 0.;
element zeroLength          42581 183011 193011 -mat  31 -dir 2;
element zeroLength          16901 183011 193011 -mat  30 -dir 1;

element flatSliderBearing   3641 193012 183012 10 110.000012345600 -P 20 -Mz 20  -orient 0. 1. 0. 1. 0. 0.;
element zeroLength          42582 193012 183012 -mat  31 -dir 2;
element zeroLength          16902 193012 183012 -mat  30 -dir 1;

element flatSliderBearing   3642 183013 193013 10 110.000012345600 -P 20 -Mz 20  -orient 0. 1. 0. 1. 0. 0.;
element zeroLength          42583 183013 193013 -mat  31 -dir 2;
element zeroLength          16903 183013 193013 -mat  30 -dir 1;

element flatSliderBearing   3643 193014 183014 10 110.000012345600 -P 20 -Mz 20  -orient 0. 1. 0. 1. 0. 0.;
element zeroLength          42584 193014 183014 -mat  31 -dir 2;
element zeroLength          16904 193014 183014 -mat  30 -dir 1;
```

References

3-06, A. 1980. *Review and refinement of ATC 3-06 tentative seismic provisions, Report of Technical Committee 9: Regulatory Use*.

ACI-352 1991. Recommendations for design of beam-column connections in monolithic reinforced concrete structures. *Farmington Hills, Michigan. : American Concrete Institute, [1991]*.

AIS 1982. Estudio sobre la utilizacion estructural del ladrillo producido en el pais. . *Colombian Association for Earthquake Engineering. In Spanish.* , Boletín Técnico No. 15.

AIS 2009. Estudio General de Amenaza Sismica de Colombia 2009. *Colombian Association for Earthquake Engineering. In Spanish.*

AKIN, L. A. 2006. *Behavior of reinforced concrete frames with masonry infills in seismic regions.* Dissertation/Thesis, ProQuest, UMI Dissertations Publishing.

AL-CHAAR, G. 1998a. Non-Ductile Behavior of Reinforced Concrete Frames With Masonry Infill Panels Subjected to In-Plane Loading.

AL-CHAAR, G. K. 1998b. *Nonductile behavior of reinforced concrete frames with masonry infill panels subjected to in-plane loading.* Dissertation/Thesis, ProQuest, UMI Dissertations Publishing.

AL-CHAAR, G. L. & MEHRABI, A. B. 2008. Constitutive Models for Nonlinear Finite Element Analysis of Masonry Prisms and Infill Walls. *ENGINEER RESEARCH AND DEVELOPMENT CENTER CHAMPAIGN IL CONSTRUCTION ENGINEERING RESEARCH LAB.*

ALTOONTASH, A. 2004. *Simulation and damage models for performance assessment of reinforced concrete beam-column joints.* Dissertation/Thesis, ProQuest, UMI Dissertations Publishing.

ANDERSON, J. C. & TOWNSEND, W. H. 1977. Models for RC Frames with Degrading Stiffness. *Journal of the Structural Division.,* 103**,** 2361-2376.

ASCE 41 2006. Seismic Rehabilitation of Existing Buildings. *American Society of Civil Engineers. ASCE.*

ASFURA, A. P. & FLORES, P. J. 1999. *Quindio, Colombia earthquake of January 25, 1999 : reconnaissance report*.

ASTERIS, P. G., ANTONIOU, S. T., SOPHIANOPOULOS, D. S. & CHRYSOSTOMOU, C. Z. 2011. Mathematical Macromodeling of Infilled Frames: State of the Art. *Journal of Structural Engineering ASCE.,* 137**,** 1508-1517.

ASTM C67 2013a. Standard Test Methods for Sampling and Testing Brick and Structural Clay Tile. *ASTM International, West Conshohocken, PA, 2003, www.astm.org.*

ATC 2006. *Seismic Retrofitting Guidelines for Highway Bridges*, U.S. Department of Transportation. Federal Highway Administration.

BAQUERO, A. E., CAPERA, A. A. G. & HURTADO, E. D. S. 2004. State-of-the-art of the historical seismology in Colombia. *Annals of Geophysics,* 47**,** 437-449.

BASTIDAS, D., MOLINA, L., YAMIN, L. E., SARRIA, A. & ORTEGA, J. 2002. Non-Structural Masonry Walls Strengthened with GFRP Laminates. *Revista de Ingeniería Universidad de los Andes,* 16**,** 4-11.

BAZANT, Z. P. & PLANAS, J. 1998. Fracture and size effect in concrete and other quasibrittle materials. *CRC Press, Boca Raton, FL.*

BENJAMIN, J. R. & WILLIAMS, H. A. 1958. *The Behavior of One-Story Brick Shear Walls,* Reston, Va, ASCE Press.

BERRY, M., PARRISH, M. & EBERHARD, M. 2004. PEER Structural Performance Database User's Manual. *Pacific Engineering Research Center, University of California, Berkeley, California. Available at http://nisee.berkeley.edu/spd/ and http://maximus.ce.washington.edu/~peera1/.*

BERTERO, V. & BROKKEN, S. 1983. Infills in Seismic Resistant Building. *Journal of Structural Engineering,* 109**,** 1337-1361.

BIDDAH, A. & GHOBARAH, A. 1999. Modeling of shear deformation and bond slip in reinforced concrete joints. *Structural Engineering and Mechanics, 7(4):413–432.*

BIRELY, A. C., LOWES, L. N. & LEHMAN, D. E. 2012. A model for the practical nonlinear analysis of reinforced-concrete frames including joint flexibility. *Engineering Structures,* 34**,** 455-465.

BORST, D., R. & NAUTA, P. 1985. Non-orthogonal cracks in a smeared finite element model. *Engineering Computations 2***,** 35–46.

BRACCI, J. M. 1995. Seismic resistance of reinforced-concrete frame structures designed only for gravity loads - experimental performance of subassemblages. *ACI Structural Journal,* 92**,** 502-503.

BROWN, R. H. & JIRSA, J. O. 1971. Reinforced concrete beams under load reversals. *J. Am. Concr. Inst.***,** 380–390.

BUONOPANE, S. G. & WHITE, R. N. 1999. *Seismic evaluation of a masonry infilled reinforced concrete frame by pseudodynamic testing.*

C1314, A. 2014. Standard Test Method for Compressive Strength of Masonry Prisms. *AST International, West Conshohocken, Pa. www.astm.org*.

CALVI, G., MAGENES, G. & PAMPANIN, S. 2002. Experimental Test on a Three Storey RC Frame Designed for Gravity Only. *Proceedings o f the Twelfth European Conference on Earthquake Engineering, September 9-13, 2002, London, UK.*

CARDONA, O. D. & YAMIN, L. E. 1997. Seismic microzonation and estimation of earthquake loss scenarios: integrated risk mitigation project of Bogota, Colombia. *Earthquake Spectra,* 13**,** 795-814.

CELIK, O. C. 2007. *Probabilistic Assessment of Non-Ductile Reinforced Concrete Frames Susceptible to Mid-America Ground Motions.* Dissertation/Thesis, Georgia Institute of Technology.

CELIK, O. C. & ELLINGWOOD, B. R. 2010. Seismic fragilities for non-ductile reinforced concrete frames - Role of aleatoric and epistemic uncertainties. *Structural Safety,* 32**,** 1-12.

CENTENO, J., VENTURA, C. & FOO, S. Shake Table Testing of Gravity Load Designed Reinforced Concrete Frames with Unreinforced Masonry Infill Walls. 2008.

CERESIS 2013. Regional Seismological Center for South America. *http://www.ceresis.org*.

CGS 2013. RSNC Seismic Catalogue from June 1 1993 to February 15, 2013.

CHARNEY, F. & JOHNSON, R. 1986. The Effect of the Joint Deformations on the Drift of the Steel Frame Structures. *. KKBNA, Inc., Consulting Engineers. Colorado.*

CHUNG, Y. S., C., M. & SHINOZUKA, M. 1987. Seismic damage assessment of reinforced concrete members. *Technical Report NCEER-87-0022, State University of New-York at Buffalo.*

CLOUGH, R., BENUSKA, K. & WILSON, E. Inelastic earthquake response of tall buildings. 1965. II-68 to II-89.

CLOUGH, R. W. & JOHNSTON, S. B. 1966. *Effect of Stiffness Degradation on Earthquake Ductility Requirements*.

COLEMAN, J. & SPACONE, E. 2001. Localization issues in force-based frame elements. *J. Struct. Eng., 10.1061***,** 1422–1425.

CRISAFULL, F. J. & CARR, A. J. 2007. Proposed macro-model for the analysis of infilled frame structures. *Bulletin of the New Zealand Society for Earthquake Engineering,* 40**,** 69-77.

DANE 2006. Colombia General Census 2005-2006. (in Spanish). *National Administrative Department of Statistics (DANE).*

DEPAE. & JICA 2002. Estudio para la Prevención de Desastres en el Área Metropolitana de Bogotá, en la República de Colombia.

DIANA 2014. Release 9.5, TNO DIANA. *Delft, The Netherlands*.

EL-DAKHALCHNI, W. W., HAMID, A. A. & ELGAALY, M. 2004. In-Plane Strengthening of URM Infill Wall Assemblages Using GFRP Laminates. *Masonry Society Journal,* 22**,** 39-50.

EL-METWALLY, S. E. & CHEN, W. F. 1988. Moment-rotation modeling of reinforced concrete beam-column connections. *ACI Structural Journal,* 85**,** 384-394.

ELIGEHAUSEN, R., POPOV, E. & BERTERO, V. 1983. Local bond stress slip relationship of deformed bars under generalized excitations. *Technical Report UCB/EERC 83-23, Earthquake Engineering Research Center, University of California, Berkeley.*

ELMORSI, M., KIANOUSH, M. R. & TSO, W. K. 2000. Modeling bond-slip deformations in reinforced concrete beam-column joints. *Canadian Journal of Civil Engineering,* 27**,** 490-505.

ELWOOD, K. 2004. Modelling failures in existing reinforced concrete columns. *Canadian Journal of Civil Engineering,* 31**,** 846-846.

ELWOOD, K. & MOEHLE, J. 2005. Axial Capacity Model for Shear-Damaged Columns. *ACI Structural Journal,* 102**,** 578.

ELWOOD, K. J. & MOEHLE, J. P. 2008. Dynamic collapse analysis for a reinforced concrete frame sustaining shear and axial failures. *Earthquake Engineering & Structural Dynamics,* 37**,** 991-1012.

FARDIS, M. N. & PANAGIOTAKOS, T. B. 1997. Seismic design and response of bare and masonry-infilled reinforced concrete buildings. Part I: Bare structures. *Journal of Earthquake Engineering.,* 1**,** 219-256.

FEENSTRA, P. H. 1993. Computational aspects of biaxial stress in plain and reinforced concrete. *PhD Thesis, Department of Civil Engineering, TU Delft.*

FEGHALI, H. L. 1999. *Seismic performance of flexible concrete structures.* Dissertation/Thesis, ProQuest, UMI Dissertations Publishing.

FEMA P695 2009. Quantification of Building Seismic Performance Factors. *Federal Emergency Management Agency, Washington, D.C.*

FIB. 2013. State-of-art report "Code-type models for concrete behaviour" *fib Bulletin No. 70.*

FILIPPOU, F. 1986. A simple model for reinforcing bar anchorages under cyclic excitations. *Journal of Structural Engineering, ASCE, 112:1639–1659.*

FILIPPOU, F., POPOV, E. & BERTERO, V. 1983a. Effects of bond deterioration on hysteretic behavior of reinforced concrete joints. *Rep. EERC 83-19, Earthquake Engineering Research Center, Univ. of California, Berkeley.*

FILIPPOU, F. C., POPOV, E. P. & BERTERO, V. V. 1983b. Modeling of R/C Joints under Cyclic Excitations. *Journal of Structural Engineering,* 109**,** 2666-2684.

FIORATO, A., SOZEN, M. & GAMBLE, W. 1970. *An investigation of the interaction of reinforced concrete frames with masonry filler walls.*

FIORATO, A. E. 1971. *An investigation of the interaction of reinforced concrete frames with masonry filler walls.* Dissertation/Thesis, ProQuest, UMI Dissertations Publishing U6.

FOSTER, S. J. & GILBERT, R. I. 1996. The design of non-flexural members with normal and high-strength concrete. *ACI Struct. J.***,** 3–10.

GALANIS, P. & MOEHLE, J. 2012. Using OpenSEES for the seismic assessment of existing reinforced concrete buildings. *OpenSEES days 2012. University of California, Berkeley.*

GALLEGO, C. A. 2001. Sistemas de aislamiento sísmico para muros no estructurales. *Master Thesis. Civil and Environmental Engineering.*

GARCIA, L. E. 2000. The January 25, 1999, Earthquake in the Coffee Growing Region of Colombia: Accelerographic Records, Structural Response and Damage, and Code Compliance and Enforcement. *12 WCEE 2000 : 12th World Conference on Earthquake Engineering; Auckland, New Zeland.,* 2809.

GHANNOUM, W. M. & MOEHLE, J. P. 2012. Rotation-Based Shear Failure Model for Lightly Confined RC Columns. *Journal of Structural Engineering ASCE.,* 138**,** 1267-1278.

GHOBARAH, A. & BIDDAH, A. 1999. Dynamic analysis of reinforced concrete frames including joint shear deformation. *Engineering Structures,* 21**,** 971-987.

GIBERSON, M. F. 1969. *The response of nonlinear multi-story structures subjected to earthquake excitation.* Dissertation/Thesis.

GIURIANI, E., PLIZZARI, G. & C., S. 1969. Role of stirrups and residual tensile strength of cracked concrete on bond. *Journal of Structural Engineering, ASCE, 117(1):1–18.*

GUTIERREZ, O. J. 2003. Mamposteria Estructural. *Master Thesis. Civil and Environmental Engineering.*

HASELTON, C. 2007. *Assessing seismic collapse safety of modern reinforced concrete moment frame buildings.*

HASELTON, C. & DEIERLEIN, G. 2008. *Assessing seismic collapse safety of modern reinforced concrete moment-frame buildings.* Dissertation/Thesis, Pacific Earthquake Engineering Research Center. .

HASSAN, W. M. 2011. *Analytical and Experimental Assessment of Seismic Vulnerability of Beam-Column Joints without Transverse Reinforcement in Concrete Buildings.* Dissertation/Thesis.

HIRAISHI, H. 1984. Evaluation of Shear and Flexural Deformations of Flexural Type Shear Wall. *In Proc. Of 8th WCEE.,* 5.

HOLMES, M. 1961. Steel frames with brickwork and concrete infilling. . *ICE Proceedings.,* 19**,** 473-478.

HOLZER, T. L. & SAVAGE, J. C. 2013. Global Earthquake Fatalities and Population. *Earthquake Spectra,* 29**,** 155-175.

HORDIJK, D. A. 1991. Local approach to fatigue of concrete. *Dissertation, Delft University of Technology, Delft,The Netherlands.*

HOSHIKUMA, J., KAWASHIMA, K., NAGAYA, K. & TAYLOR, A. W. 1997. Stress-strain model for confined reinforced concrete in bridge piers. *J. Struct. Eng.***,** 624–633.

HOSSEIN, M. & TOSHIMI, K. 2007. Axial-Shear-Flexure Interaction Approach for Reinforced Concrete Columns. *ACI Materials Journal,* 104**,** 218.

HRENNIKOFF, A. 1941. Solution of Problems of Elasticity by the Framework Method. *Journal of Applied Mechanics,* 8**,** 169–175.

HSIEH, S. S., TING, E. C. & CHEN, W. F. 1982. A plasticity-fracture model for concrete. *Int. J. Solids Struct,* 18**,** 181–197.

HSU, T. 1988. Softened truss model theory for shear and torsion. *ACI Structural Journal, 85(6):624–634*.

IBARRA, L. & KRAWINKLER, H. 2004. *Global collapse of frame structures under seismic excitations.* Dissertation/Thesis.

IBARRA, L. F., MEDINA, R. A. & KRAWINKLER, H. 2005. Hysteretic models that incorporate strength and stiffness deterioration. *Earthquake Engineering & Structural Dynamics,* 34**,** 1489-1511.

ILKI, A. & KUMBASAR, N. 2000. Theoretical and experimental energy dissipation of reinforced concrete. *Proceedings of the Third Japan-Turkey Workshop on Earthquake Engineering, 21-25 February 2000, Istanbul,* 1**,** 167-177.

JEON, J. S., DESROCHES, R., BRILAKIS, I. & LOWES, L. 2012. Modeling and Fragility Analysis of Non-Ductile Reinforced Concrete Buildings in Low-to-Moderate Seismic Zones. *ASCE Structures Congress 2012.,* 2199.

KAKU & MORITA, S. 1978. Bond behavior of beam bars in the joint of reinforced concrete frames. *Annual Meeting of the Architectural Institute of Japan, AIJ, pages 1777–1778*.

KATO, D. & OHNISHI, K. Axial load carrying capacity of R/C columns under lateral load reversals. 2002. 247-255.

KAUSHIK, H. B., RAI, D. C. & JAIN, S. K. 2007. Stress-strain characteristics of clay brick masonry under uniaxial compression. *Journal of Materials in Civil Engineering,* 19**,** 728-739.

KENT, D. & PARK, R. 1971. Flexural members with confined concrete. *Journal of the Structural Division, ASCE 113(10):2160–2173.*

KLINGNER, R. E. 1997. Evaluation and analytical verification of shaking table data from infilled frames. *The Masonry Society Journal.,* 15**,** 33-41.

KLINGNER, R. E. & BERTERO, V. V. 1978. Earthquake Resistance of Infilled Frames. *Journal of the Structural Division.,* 104**,** 973-989.

KODUR, V. K. R., ERKI, M. A. & QUENNEVILLE, J. H. P. 1995. Seismic design and analysis of masonry-infilled frames. *Canadian Journal of Civil Engineering,* 22**,** 576-587.

KOUTROMANOS, I. 2011. *Numerical Analysis of Masonry-Infilled Reinforced Concrete Frames Subjected to Seismic Loads and Experimental Evaluation of Retrofit Techniques*.

KOUTROMANOS, I. 2014. Nonlinear Finite Element Analysis. Lecture Notes. *Virginia Polytechnic Institute and State University,* Department of Civil and Environmental Engineering. Blacksburg, Va 24060.

KOUTROMANOS, I. & SHING, P. B. 2012. Cohesive Crack Model to Simulate Cyclic Response of Concrete and Masonry Structures. *ACI Structural Journal,* 109**,** 349-358.

KOUTROMANOS, I. & SHING, P. B. 2013. Numerical modeling of masonry-infilled RC frame buildings. *Springer-Verlag Berlin Heidelberg,* 123.

KUSUHARA, F., SHIOHARA, H. & TAJIRI, S. A New Macro Element of Reinforced Concrete Beam-Column Joint for Elasto-Plastic Plane Frame Analysis. 2006 2006.

KYRIAKIDES, M. A. & BILLINGTON, S. L. Seismic retrofit of masonry-infilled non-ductile reinforced concrete frames using sprayable ductile fiber-reinforced cementitious composites., 2008 2008.

LAFAVE, J. & SHIN, M. 2005. Discussion of "Modeling reinforced concrete beam-column joints subjected to cyclic loading" by L. N. Lowes & A. Altoontash. *Journal of Structural Engineering, ASCE, 131(6):992–993.*

LEE, H.-S. & WOO, S.-W. 2002. Effect of masonry infills on seismic performance of a 3-storey R/C frame with non-seismic detailing. *Earthquake Engineering & Structural Dynamics,* 31**,** 353.

LIAUW, T. C. & KWAN, K. H. 1985. Unified Plastic Analysis for Infilled Frames. *Journal of Structural Engineering,* 111**,** 1427-1448.

LIEL, A. B. 2008. *Assessing the collapse risk of California's existing reinforced concrete frame structures: Metrics for seismic safety decisions.* Dissertation/Thesis.

LIGNOS, D. G. & KRAWINKLER, H. 2011. Deterioration Modeling of Steel Components in Support of Collapse Prediction of Steel Moment Frames under Earthquake Loading. *JOURNAL OF STRUCTURAL ENGINEERING-ASCE,* 137**,** 1291-1302.

LIGNOS, D. G. & KRAWINKLER, H. 2012. Development and Utilization of Structural Component Databases for Performance Based Earthquake Engineering. *Journal of Structural Engineering*.

LITTON, R. W. 1974. Contribution to the Analysis of Concrete Structures Under Cyclic Loading. *PhD thesis, University of California, Berkeley.*

LOTFI, H. R. & SHING, P. B. An appraisal of smeared crack models for masonry shear wall analysis. 1991. 413-425.

LOURENCO, P. J. B. B. 1996. *Computational strategies for masonry structures.* Dissertation/Thesis, ProQuest Dissertations Publishing.

LOWES, L. N. & ALTOONTASH, A. 2003. Modeling Reinforced-Concrete Beam-Column Joints Subjected to Cyclic Loading. *Journal of Structural Engineering,* 129**,** 1686-1697.

LOWES, L. N., ALTOONTASH, A. & MITRA, N. 2005. Closure to "Modeling Reinforced-Concrete Beam-Column Joints Subjected to Cyclic Loading" by Laura N. Lowes and Arash Altoontash. *Journal of Structural Engineering,* 131**,** 993-994.

LU, Y. & PANAGIOTOU, M. 2014. Three-Dimensional Cyclic Beam-Truss Model for Nonplanar Reinforced Concrete Walls. *Journal of Structural Engineering,* 140**,** 4013071.

LYNN, A. C. 2001. *Seismic evaluation of existing reinforced concrete building columns.* Dissertation/Thesis, ProQuest, UMI Dissertations Publishing.

MADAN, A., REINHORN, A. M., MANDER, J. B. & VALLES, R. E. 1997. Modeling of masonry infill panels for structural analysis. *Journal of Structural Engineering-ASCE,* 123**,** 1295-1302.

MAEKAWA, K., PIMANMAS, A. & OKAMURA, H. 2003. Nonlinear mechanics of reinforced concrete. *Spon Press, New York.*

MAINSTONE, R. J. 1971. On the Stiffness and Strengths of Infill Frames. *Proceedings, The Institution of Civil Engineers.,* 49**,** 230-230.

MANDER, J. B., PRIESTLEY, M. J. N. & PARK, R. 1988. Theoretical stress–strain model for confined concrete. *J. Struct. Eng.,* 114(8).

MANSOUR, M., LEE, J. & HSU, T. T. C. 2001. Cyclic stress–strain of concrete and steel bars in membrane elements. *J. Struct. Eng***,** 1402–1411.

MAZARS, J., P., KOTRONIS & L.., D. 2002. A New Modelling Strategy for the Behaviour of Shear Walls under Dynamic Loading. *Earthquake Engineering & Structural Dynamics,* 937–954.

MCKENNA, F. 2011. OpenSEES: A Framework for Earthquake Engineering Simulation. *Computing in Science&Engineering,* 13**,** 58-66.

MCKENNA, F., FENVES, G. L., SCOTT, M. H. & JEREMIC, B. 2000. OpenSEES Version 2.4.5 rev 5915. *Computer program. Berkeley, Univ. of California.*

MEHRABI, A. B., SHING, P. B., SCHULLER, M. P. & NOLAND, J. L. 1994. *Performance of masonry-infilled R/C frames under in-plane lateral loads,* University of Colorado at Boulder.

MENEGOTTO, M. & PINTO, P. E. 1973. Method of analysis for cyclically loaded reinforced concrete plane frames including changes in geometry and non-elastic behavior of elements under combined normal force and bending. *IABSE Symp. (Lisboa): Resistance and Ultimate Deformability of Structures Acted on by Well-Defined Repeated Loads,* 13**,** 15–22.

MITRA, N. 2007. An Analytical Study of Reinforced Concrete Beam-Column Joint Behavior Under Seismic Loading. *Dissertation/Thesis.*

MOHARRAMI, M., KOUTROMANOS, I., PANAGIOTOU, M. & GIRGIN, S. C. 2015. Analysis of shear-dominated RC columns using the nonlinear truss analogy. *Earthquake Engineering & Structural Dynamics,* 44**,** 677-694.

MORITA, S. & KAKU, T. 1975. Bond slip relationship under repeated loading. *Transactions of the AIJ, 229:15–24.*

MORSCH, E. 1920. Reinforced concrete construction - Theory and application. *5th Ed., Wittwer, Stuttgart, Vol. 1, Part 1.*

NAKAMURA, T. & YOSHIMURA, M. 2002. Gravity load collapse of reinforced concrete columns with brittle failure modes. *Journal of Asian Architecture and Building Engineering,* 1**,** 21-27.

NIST GCR 10-917-7 2010. Program Plan for the Development of Collapse Assessment and Mitigation Strategies for Existing Reinforced Concrete Buildings. *National Institute of Standards and Technology, NEHRP*

Consultants Joint Venture A partnership of the Applied Technology Council and the Consortium of Universities for Research in Earthquake Engineering.

NSR 2010. El Reglamento Colombiano de Construcción Sismo Resistente (NSR-10).

OTANI, S. 1973. *Behavior of Multistory Reinforced Concrete Frames During Earthquakes.* Dissertation/Thesis, ProQuest, UMI Dissertations.

OTANI, S. 1999. RC building damage statistics and SDF response with design seismic forces. *Earthquake Spectra,* 15**,** 485-501.

PANAGIOTOU, M., RESTREPO, J. I., SCHOETTLER, M. & KIM, G. 2012. Nonlinear Cyclic Truss Model for Reinforced Concrete Walls. *ACI Structural Journal,* 109**,** 205-214.

PARK, H. & EOM, T. 2007. Truss Model for Nonlinear Analysis of RC Members Subject to Cyclic Loading. *Journal of Structural Engineering,* 133**,** 1351-1363.

PARK, R., PRIESTLEY, M. & GILL, W. 1982. Ductility of square confined reinforced concrete columns. *Journal of the Structural Division, ASCE, 108(ST4):929–950.*

PARK, S. 2010. *Experimental and Analytical Studies on Old Reinforced Concrete Buildings with Seismically Vulnerable Beam-Column Joints.* Dissertation/Thesis, ProQuest, UMI Dissertations Publishing.

PARK, S. & MOSALAM, K. 2012a. Analytical Model for Predicting Shear Strength of Unreinforced Exterior Beam-Column Joints. *ACI Structural Journal,* 109**,** 149-159.

PARK, S. & MOSALAM, K. 2012b. Parameters for shear strength prediction of exterior beam–column joints without transverse reinforcement. *Engineering Structures,* 36**,** 198-209.

PARK, S. & MOSALAM, K. 2013. Simulation of Reinforced Concrete Frames with Nonductile Beam-Column Joints. *Earthquake Spectra,* 29**,** 233-257.

PARK, Y. & ANG, A. 1985. Seismic damage analysis of reinforced concrete buildings. *Journal o f Structural Engineering, Vol. 111,, pp. 740-757.*

PAULAY, T. & PRIESTLEY, M. J. N. 1992. *Seismic design of reinforced concrete and masonry buildings,* New York, N.Y, Wiley.

PINTO, A., VARUM, H. & MOLINA, J. 2002. Experimental Assessment and Retrofit of Full-Scale Models o f Existing RC Frames. *Proceedings o f the Twelfth European Conference on Earthquake Engineering, September 9-13, 2002, London, UK.*

PLUIJM, R. V. D. 1992. Material properties of masonry and its components under tension and shear. *Proc. 6th Canadian Masonry Symposium, eds. V.V. Neis, Saskatoon, Saskatchewan. Canada***,** 675-686.

POLYAKOV, S. V. 1960. On the Interaction Between Masonry Filler Walls and Enclosing Frame When Loaded in the Plane of the Wall. *Translations in Earthquake Engineering, Earthquake Engineering Research Institute. San Francisco.***,** 36-42.

PRIESTLEY, M., VERMA, R. & XIAO, Y. 1994. Seismic Shear Strength of Reinforced Concrete Columns. *Journal o f Structural Engineering, Vol. 120, No. 8, pp. 2310-2329.*

PUJOL, S. & FICK, D. 2010. The test of a full-scale three-story RC structure with masonry infill walls. *Engineering Structures,* 32**,** 3112-3121.

PUJOL, S., RAMIREZ, J. A. & SARRIA, A. 2000. Behavior of low-rise reinforced concrete buildings. *Concrete International,* 22**,** 40-44.

PUJOL, S., RAMIREZ, J. A. & SOZEN, M. A. Drift capacity of reinforced concrete columns subjected to cyclic shear reversals. 1999. 255-274.

RAHNAMA, M. & KRAWINKLER, H. 1993. Effects of soft soil and hysteresis model on seismic demands. *BLUME-108, John A. Blume Earthquake Engineering Center, Stanford, California, July 1993, 238 pages.*

RAMIREZ, J. E. 1975. Historia de los Terremotos en Colombia. *Instituto Geografico Agustin Codazzi.*

RESTREPO, J. 2008. Concrete frames designed with the Colombian seismic code (nsr-98) from a Displacement perspective *Istituto Universitario di Studi Superiori di Pavia. Master Thesis. Università degli Studi di Pavia*.

RITTER, W. 1899. Die bauweise hennebique. *Schweizerische Bauzeitung, 33(7), 59-61*.

RODRIGUES, H., VARUM, H. & COSTA, A. 2008. A non-linear masonry infill macro-model to represent the global behaviour of buildings under cyclic loading. *International Journal of Mechanics and Materials in Design,* 4**,** 123-135.

ROTS, J. G. 1988. Computational Modeling of Concrete Fracture. *PhD thesis, Delft University of Technology*.

ROTS, J. G. & BLAAUWENDRAAD, J. 1989. Crack Models for Concrete, Discrete or Smeared? Fixed, Multi-Directional or Rotating? *Delft University of Technology*

SAENZ, I. P. 1964. Discussion of 'Equation for the stress-strain curve of concrete by Desayi and Krishnan. *J. Am. Concr. Inst***,** 1229–1235.

SAIIDI, M. 1979. *Simple and complex models for nonlinear seismic response of reinforced concrete structures / by Mehdi Saiidi and Mete A. Sozen*.

SAITO, T. & KIKUCHI, M. 2012. A New Analytical Model for Reinforced Concrete Beam-Column Joints Subjected to Cyclic Loading *Proceedings Of The Fifthteenth World Conference On Earthquake Engineering Lisbon, Portugal, 2012*.

SALGADO, G., BERNAL, G., YAMÍN, L. & O., C. 2010. Seismic Hazard Assessment in Colombia. Updates and Useage in the New National Building Code NSR-10. (In Spanish). *Revista de Ingeniería. Universidad de los Andes.* , 32**,** 28-37.

SANCHEZ-SILVA, M., YAMIN, L. E. & CAICEDO, B. 2000. Lessons of the 25 January 1999 earthquake in central Colombia. *Earthquake Spectra,* 16**,** 493-510.

SANEINEJAD, A. & HOBBS, B. 1995. Inelastic design of infilled frames. *Journal of Structural Engineering-ASCE,* 121**,** 634-650.

SATTAR, S. 2013. *Influence of masonry infill walls and other building characteristics on seismic collapse of concrete frame buildings.* Dissertation/Thesis, ProQuest, UMI Dissertations Publishing.

SCHELLENBERG, A. 2012. Flat Slider Bearing Element. *OpenSEES.berkeley.edu/wiki,* University of California, Berkeley.

SEAOC 1974. Basic Design Criteria of the Recommended Lateral Force Requirements and Commentary. *Journal of the Structural Division.,* 98**,** 1913-1922.

SEZEN, H. 2002. *Seismic behavior and modeling of reinforced concrete building columns.* Dissertation/Thesis, ProQuest, UMI Dissertations.

SEZEN, H. & MOEHLE, J. P. 2004. Shear Strength Model for Lightly Reinforced Concrete Columns. *Journal of Structural Engineering,* 130**,** 1692-1703.

SHARMA, A., ELIGEHAUSEN, R. & REDDY, G. R. 2011. A New Model to Simulate Joint Shear Behavior of Poorly Detailed Beam–Column Connections in RC Structures Under Seismic Loads, Part I: Exterior Joints. . *Engineering Structures,* 33.

SHIN, P. & LAFAVE, J. 2004. Testing and Modeling For Cyclic Joint Shear Deformations in RC Beam-Column Connections. *13 th World Conference on Earthquake Engineering. Vancouver, B.C., Canada August 1-6, 2004. Paper No. 0301.* .

SHING, B., RESTREPO, J., A., S., KASPAR, W. I., SIVASELVAN, M., BLACKARD, B., BILLINGTON, S. & M., K. 2006. EESR NEESR-SG Seismic Performance Assessment and Retrofit of Non Non-Ductile RC Frames with Infill Walls. *NEES Annual Meeting*.

SHING, P. & SPENCER, B. 1999. Modeling of Shear Behavior of RC Bridge Structures. *Proc. of the US-Japan Seminar on Post-Peak Behavior of RC Structures Subjected to Seismic Loads - Recent Advances and Challenges of Analysis and Design, NSF-JSPS-JCI***,** 315-333.

SHING, P. B. & LOTFI, H. R. 1994. Interface Model Applied to Fracture of Masonry Structures. *Journal of Structural Engineering,* 120**,** 63-80.

SHING, P. B. & MEHRABI, A. B. 2002. Behaviour and analysis of masonry-infilled frames. *Progress in Structural Engineering and Materials,* 4**,** 320-331.

STAFFORD SMITH, B. 1967. Methods for predicting the lateral stiffness and strength of multi-storey infilled frames. *Building Science,* 2**,** 247-257.

STAVRIDIS, A. 2009. *Analytical and experimental study of seismic performance of reinforced concrete frames infilled with masonry walls*.

STAVRIDIS, A. & SHING, P. B. 2009. Finite Element Modeling of Nonlinear Behavior of Masonry-Infilled RC Frames. *Journal of Structural Engineering*.

STEVENS, N. J., UZUMERI, S. M. & COLLINS, M. P. 1991. REINFORCED-CONCRETE SUBJECTED TO REVERSED CYCLIC SHEAR - EXPERIMENTS AND CONSTITUTIVE MODEL. *ACI Structural Journal,* 88**,** 135-146.

TABOADA, A., RIVERA, L. A., FUENZALIDA, A., CISTERNAS, A., PHILIP, H., BIJWAARD, H., OLAYA, J. & RIVERA, C. 2000. Geodynamics of the northern Andes: Subductions and intracontinental deformation (Colombia). *TECTONICS,* 19**,** 787-813.

TAJIRI, S., SHIOHARA, H. & KUSUHARA, F. 2006. A new macroelement of reinforced concrete beam column joint for elasto-plastic plane frame analysis. *In Eighth National Conference of Earthquake Engineering, San Francisco, California, number 1*.

TAKEDA, T., SOZEN, M. A. & NIELSEN, N. N. 1970. *Reinforced concrete response to simulated earthquakes*.

TO, N. H. T., INGHAM, J. M. & SRITHARAN, S. 2001. Monotonic nonlinear strut-and-tie computer models. *New Zealand Nat. Soc. Earthquake Eng. Bull,* 34**,** 169–190.

TO, N. H. T., INGHAM, J. M. & SRITHARAN, S. 2003. Cyclic strut-and-tie modeling of reinforced concrete structures. *Pacific Conf. on Earthquake Engineering, Paper No. 102, Christchurch, New Zealand.*

TOMAŽEVIČ, M. 1999. *Earthquake-resistant design of masonry buildings,* London, Imperial College Press.

VALLENAS, J., BERTERO, V. & POPOV, E. 1979. Hysteric Behavior of Reinforced Concrete Structural Walls. *NASA STI/Recon Technical Report N 80: 27533.*

VECCHIO, F. J. & COLLINS, M. P. 1986. The modified compression-field theory for reinforced concrete elements subjected to shear. *ACI* 83**,** 219-231.

WATANABE, F. & ICHINOSE, T. 1991. Strength and ductility design of RC members subjected to combined bending and shear *Preliminary Proceedings Volume of International Workshop on Concrete Shear in Earthquake, January 13-16, 1991, University of Houston, authors retain copyright, 1991-01-16.*

WITHEY, M. O. 1907. Tests of plain and reinforced concrete series of 1906. *Bull. Univ. of Wis.• Engineering Series, 4(1), 1-66.*

WONG, H. F. 2005. *Shear strength and seismic performance of non-seismically designed reinforced concrete beam-column joints.* Dissertation/Thesis, ProQuest, UMI Dissertations Publishing.

WOOD, R. H. 1978. Plasticity, Composite Action and Collapse Design of Reinforced Shear Wall Panel in Frames. *Proceedings of Institute o f Civil Engineering Journal,* 65**,** 381-411.

YAMIN, L. & GARCIA, L. E. 1994a. Comportamiento Sísmico de Muros de Mampostería Confinada. *Asociación Colombiana de Ingeniería Sísmica, AIS.,* Boletín Técnico No. 45.

YAMIN, L. & GARCIA, L. E. 1994b. A review of Masonry Construction in Colombia. . *American Concrete Institute. ACI.,* SP-147.

YAMIN, L. & GARCIA, L. E. 1997. *Experimental development for earthquake resistance of low-cost housing systems in Colombia*.

YOUSSEF, M. & GHOBARAH, A. 2001. Modelling of RC beam-column joints and structural walls. *Journal of earthquake engineering,* 5**,** 93-111.

ZARNIC, R. & GOSTIC, S. Non-linear modelling of masonry infilled frames. 1998.

ZARNIC, R. & TOMAZEVIC, M. 1985. *Study of the behaviour of masonry infilled reinforced concrete frames subjected to seismic loading--Part Two*.

ZARNIC, R. & TOMAZEVIC, M. An experimentally obtained method for evaluation of the behaviour of masonry infilled R/C frames. 1989 1988. 163-168.

ZHANG, L. X. & HSU, T. T. C. 1998. Behavior and analysis of 100 MPa concrete membrane elements. *J. Struct. Eng*.**,** 24–34.